

UCSF

UC San Francisco Electronic Theses and Dissertations

Title

Development of cell-active irreversible inhibitors of the human centrosomal kinase Nek2

Permalink

<https://escholarship.org/uc/item/02858335>

Author

Henise, Jeff

Publication Date

2011

Peer reviewed|Thesis/dissertation

**Development of cell-active irreversible inhibitors of the human
centrosomal kinase Nek2**

by

Jeffrey C. Henise

DISSERTATION

Submitted in partial satisfaction of the requirements for the degree of

DOCTOR OF PHILOSOPHY

in

Chemistry and Chemical biology

in the

GRADUATE DIVISION

of the

UNIVERSITY OF CALIFORNIA, SAN FRANCISCO

Copyright 2011

by

Jeffrey C. Henise

Acknowledgements

I would like to thank Jack Taunton for countless hours of mentorship and guidance; current and former members of the Taunton lab, Mike Cohen, Jennifer Garrison, Carl Co, Nathan Gushwa, Derek Wong, Andrew Mackinnon, Iana Serafimova, Sarah Maifeld, Jesse McFarland, Ville Paavilainen, Rand Miller, Rebecca Maglathlin, and Shyam Krishnan for insightful discussion and help in the lab; my former rotation students, Mike Lopez, Jon Choy, Beatrice Wang, and Nicholas Hertz for help with this project; and the UCSF Mass Spectrometry Facility, in particular Katalin Medzihradzsky and Saida Patricia Salas for analysis of recombinant Nek2 phosphopeptides, and David Maltby for the acquisition of small molecule HRMS data.

Chapter 1 and parts of Chapter 2 of this dissertation are reproduced from a manuscript in preparation for the ACS Journal of Medicinal Chemistry with the following authors:

Henise, J. C.; and Taunton, J.

Development of cell-active irreversible inhibitors of the human centrosomal kinase Nek2

Jeffrey C. Henise

Jack Taunton, Ph.D.

Abstract

A structure-based design strategy was used to transform a promiscuous oxindole kinase inhibitor scaffold into the first cysteine-reactive, irreversible inhibitors of the human centrosomal kinase Nek2. These compounds achieve selective irreversible inhibition of Nek2 through alkylation of a key active-site cysteine (Cys22). This cysteine is found in the glycine-rich loop of a small subset (2%) of human kinases. Many of the irreversible Nek2 inhibitors that we developed turned out to also be potent (nM to pM affinity) inhibitors of the mitotic regulator Cdk1. Consistent with inhibition of Cdk1, these compounds rapidly triggered mitotic exit without cell division when added to cells arrested in mitosis. The induction of this dominant Cdk1-mediated phenotype limits the usefulness of these compounds with respect to studying the mitotic function of Nek2. However, our medicinal chemistry efforts led to the discovery of the propynamide oxindole compound **2** (JH295). Compound **2** contains a key ethyl group that destabilizes binding to Cdk1, resulting in 2,000-fold loss of potency, while retaining nanomolar potency toward Nek2. At concentrations that give full inhibition of Nek2 in cells, compound **2** does not prevent mitotic progression or cause major defects in spindle

assembly. These results suggest that compound **2** does not inhibit the mitotic regulatory kinases Cdk1, Aurora B, or Plk1 in cells.

The development of several chemical and biological tools for the study of the cellular roles of Nek2 is also presented. These include new leads into Nek2 inhibitor scaffolds, an *in vitro* kinase assay to measure the binding affinity and alkylation efficiency of irreversible inhibitors, Nek2 active site-directed probes, cell-based Nek2 inhibition assays, cell lines expressing an inhibitor-resistant Nek2 mutant, and control compounds designed to tease out nonspecific effects of the active Nek2 inhibitors in cells.

Table of Contents

Chapter 1: The development of our most specific Nek2 inhibitor: JH295 (2)	
1.1 Abstract	2
1.2 Introduction	3
1.3 Structure-based design of irreversible Nek2 inhibitors	6
1.4 Synthesis and <i>in vitro</i> characterization of lead Nek2 inhibitors	8
1.5 Synthesis and <i>in vitro</i> characterization of optimized Nek2 inhibitors	12
1.6 Synthesis and <i>in vitro</i> characterization of negative control compounds	18
1.7 Cell-based evaluation of Nek2 inhibitors	21
1.8 Inhibition of Nek2 in monastrol-arrested cells	24
1.9 Further analysis of our most selective Nek2 inhibitor	27
1.10 Inhibition of Nek2 at the G2/M transition	28
1.11 Conclusions	31
1.12 Experimental methods	32
- Mutagenesis and protein expression	32
- <i>In vitro</i> Nek2, Cdk1, Rsk2, and Plk1 kinase assays	32
- Mass spectrometry-based covalent binding assays	35
- General tissue culture	35
- Preparation of poly-L-lysine coated cover slips	35
- Generation of stable cell lines	36
- Immunoprecipitation kinase assays	37
- Western blot analysis	39
- Mitosis assays in A549 cells	40
- Immunofluorescence microscopy	41
Chapter 2: Synthesis of additional Nek2 inhibitors and oxindole scaffolds	
2.1 Abstract	43
2.2 Synthesis of 5-chloromethylketone oxindole Nek2 inhibitors	44

2.3	Synthesis of 5-substituted oxindoles	45
2.4	Synthesis of oxindole inhibitors substituted at the 5-position	46
2.5	Synthesis of 4-substituted oxindoles	47
2.6	Synthesis of oxindole inhibitors with electrophiles at the 4-position	48
2.7	Synthesis of 4,5-di-substituted oxindole inhibitor scaffolds	49
2.8	Synthesis of 5-acyl sunitinib analogs and chloromethylketone Nek2 active site-directed probes	51
2.9	Synthesis of propynamide and vinyl sulfonamide-based Nek2 probes, and sunitinib analogs	52
2.10	Synthesis of the 5-substituted 4-azaoxindole inhibitor scaffold	54
2.11	Experimental methods for the synthesis of all compounds	55
	- General chemical synthesis methodology	55
	- Synthesis of compounds 2-144	56

Chapter 3: Biochemical characterization of inhibitors and Nek2

3.1	Abstract	121
3.2	Electrophilic inhibitors in Nek2 kinase assays	122
3.3	Reversible inhibitors in Nek2 kinase assays	129
3.4	Oxindole compounds in Aurora B kinase assays	135
3.5	The kinetics of irreversible Nek2 inhibition	136
3.6	Nek2 active site-directed probes	139
3.7	Autophosphorylation of recombinant Nek2	143
3.8	Phosphorylation of Eg5 by Nek2A	147
3.9	Experimental methods	148
	- WT Nek2A Kinase assays	148
	- Aurora B kinase assays	148
	- Immobilized Nek2 kinase assay	149
	- Labeling of Nek2 with rhodamine-conjugated inhibitors	150
	- Labeling of Nek2 with “clickable” inhibitors	150
	- Mass spectrometry for Nek2A-T175A autophosphorylation	151

- Determination of ATP K_m values for Nek2 mutants	155
- Phosphorylation of Eg5 by Nek2A	155
Chapter 4: Cell-based characterization of inhibitors	
4.1 Abstract	158
4.2 Inhibition of Nek2 in Hek293 cells	159
4.3 Inhibition of Rsk2 and Msk1 in cells	162
4.4 Inhibitor-induced mitotic phenotypes	164
4.5 Inhibition of cell proliferation	173
4.6 Experimental methods	174
- Dot blot IP kinase assays of Nek2A-3HA	174
- Cell-based Rsk2 and Msk1 autophosphorylation assays	174
- Mitosis assays in A549, HeLa, and RPE cells	177
- Plk1 IP kinase assays	177
- Inhibition of Hek293 cell proliferation	178
Appendix A: Abbreviations	180
Appendix B: ^1H NMR spectra of compounds 2-144	181
Appendix C: References	249

List of Figures and Schemes

Figure 1-1 Structure based design of irreversible Nek2 inhibitors	7
Scheme 1-1 Synthesis of initial electrophilic Nek2 inhibitors 4 , 8 , 9 , and 14-17	9
Figure 1-2 <i>In vitro</i> characterization of the final compounds from Scheme 1-1	11
Scheme 1-2 Synthesis of imidazole-substituted Nek2 inhibitors 2 , 19-21 , 26 and 27	13
Figure 1-3 <i>In vitro</i> characterization of compounds 2 and 21	17
Scheme 1-3 Synthesis of negative control compounds 31 and 34	20
Scheme 1-4 Synthesis of negative control compounds 35 and 36	20
Figure 1-4 Kinase assays of HA-tagged Nek2A immunoprecipitates from cells treated with compound 2	23
Figure 1-5 Representative images of the induction of mitotic exit in monastrol-arrested A549 cells	26
Figure 1-6 The effects of Nek2 inhibition on the G2/M transition and mitotic spindle assembly	29
Figure 1-7 <i>In vitro</i> kinase assay dose-response curves	34
Figure 1-8 Endogenous Nek2 IP kinase assays from A549 cells	39
Scheme 2-1 Synthesis of 5-chloromethylketone oxindole Nek2 inhibitors	44

Scheme 2-2	45
Synthesis of 5-substituted oxindoles	
Scheme 2-3	46
Synthesis of oxindole inhibitors substituted at the 5-position	
Scheme 2-4	47
Synthesis of 4-substituted oxindoles	
Scheme 2-5	48
Synthesis of oxindole inhibitors with electrophiles at the 4-position	
Scheme 2-6	49
Synthesis of 4,5-di-substituted oxindole inhibitor scaffolds	
Scheme 2-7	49
Synthesis of oxindole inhibitor scaffolds with tertiary amines in the 4-position	
Scheme 2-8	50
Synthesis of oxindole inhibitor scaffolds with an alkyne in the 4-position	
Scheme 2-9	51
Synthesis of 5-acyl sunitinib analogs and chloromethylketone Nek2 active site-directed probes	
Scheme 2-10	52
Synthesis of 5-amino sunitinib analogs	
Scheme 2-11	53
Synthesis of propynamide and vinyl sulfonamide Nek2 active site-directed probes, and sunitinib analogs	
Scheme 2-12	54
Synthesis of the 5-substituted 4-azaoxindole inhibitor scaffold	
Figure 3-1	138
Immobilized Nek2 kinase assay at 25 °C	
Figure 3-2	140
Rhodamine labeling of recombinant Nek2 with rhodamine-conjugated inhibitors	
Figure 3-3	142
Rhodamine labeling of recombinant Nek2 with “clickable” inhibitors	

Figure 3-4	145
Discovery of Nek2A autophosphorylation sites and characterization of T13 phosphomimetic Nek2 mutants	
Figure 3-5	146
Partial glycine-rich-loop sequence alignment generated from the UCSF Shokat Lab Kinase Sequence Database ⁶² showing kinases that may have a phosphorylation-controlled salt bridge.	
Figure 3-6	147
WT Nek2A was used to phosphorylate recombinant full-length Eg5	
Figure 3-8	154
Annotated CID spectra for new Nek2 autophosphorylation sites	
Figure 4-1	161
Inhibition of Nek2A-3HA in tetracycline-inducible Hek293 cells using a dot blot IP kinase assay readout	
Figure 4-2	163
Inhibition of HA-tagged Rsk2 in Hek293 cells, and inhibition of HA-tagged Msk1 in Cos7 cells	
Figure 4-3	165
Cartoon depicting mitotic exit from monastrol-arrested cells due to AurB or Cdk1 inhibition	
Figure 4-4	166
Compounds that trigger mitotic exit in monastrol-arrested cells	
Figure 4-5	167
Representative images of monastrol-arrested A549 cells that have been treated with either VX680 or 20 for 80 min in the presence of the proteasome inhibitor MG132	
Figure 4-6	170
At concentrations higher than required to inhibit Nek2, compound 21 induces the formation of monopolar spindles	
Figure 4-7	172
Representative images of HeLa cells that have failed to align their chromosomes at the metaphase plate following treatment with oxindole Nek2 inhibitors during G2/M arrest	
Figure 4-8	173
EC ₅₀ values for the inhibition of Hek293 cell proliferation	

List of Tables

Table 1-1	16
Activity of inhibitors against Nek2 <i>in vitro</i> , Nek2 in cells, as inducers of mitotic exit, and against Cdk1 <i>in vitro</i>	
Table 2-1	44
5-Chloromethylketone inhibitors synthesized according to Scheme 2-1	
Table 3-1	124
Electrophilic oxindole inhibitors in Nek2 kinase assays	
Table 3-2	128
Nek2 kinase assays of 5-vinyl-4-aza-oxindoles	
Table 3-3	130
Oxindole reversible inhibitors in Nek2 kinase assays	
Table 3-4	132
Pyrimidine inhibitors in Nek2 kinase assays	
Table 3-5	135
Oxindole compounds in Aurora-B kinase assays	

Chapter 1

The development of our most specific Nek2 inhibitor: JH295 (2)

1.1 Abstract

A structure-based design approach was employed to develop the first irreversible, cysteine-targeted inhibitors of the human centrosomal kinase, Nek2. Systematic elaboration of an oxindole kinase inhibitor scaffold led to compounds with high selectivity for Nek2 over Cdk1. Potent inhibition of Nek2 kinase activity *in vitro* and in cells required a key cysteine (Cys22), located near the C-terminal end of the glycine-rich loop in a small subset of human kinases. Our most selective compound, oxindole propynamide **2** (JH295), inhibited cellular Nek2 without affecting the mitotic kinases, Cdk1, Aurora B, or Plk1, and without causing significant defects in mitotic spindle assembly. To our knowledge, JH295 is the first small molecule shown to inactivate Nek2 kinase activity in cells.

1.2 Introduction

Nek2 is a serine/threonine protein kinase that regulates several mitotic functions. Nek2 is expressed primarily as two splice variants that localize to the centrosome and contain identical N-terminal kinase domains: the full length form, Nek2A, and a C-terminally truncated form, Nek2B.¹ The C-terminus specific to Nek2A has been implicated in regulation of its nuclear translocation², its APC/C-mediated mitotic degradation,³ and binding to proteins that regulate its function at the centrosome.^{4,5} At the onset of mitosis Nek2A plays a role in centrosome disjunction through phosphorylation-mediated displacement of the inter-centrosome linker proteins C-Nap1 and rootletin.⁶⁻⁸ Though non-essential for metaphase bi-polar spindle assembly, this Nek2A mediated centrosome-separation pathway is complementary to the essential Eg5-kinesin driven spindle-assembly pathway.⁵ Consistent with a role in regulation of the spindle assembly checkpoint (SAC), knockdown of Nek2A through shRNA expression compromised the ability of cells to undergo SAC-dependent metaphase arrest.⁹ Furthermore, Nek2A has been shown to phosphorylate core components of the SAC, including Mad2 and Cdc20.¹⁰ Finally Nek2A has been implicated in regulation of kinetochore-microtubule attachment, and metaphase chromosome-congression through phosphorylation of the kinetochore proteins Hec1 and Sgo1.^{11,12} In contrast to Nek2A, little is known about the specific function of Nek2B, aside from its ability to dimerize with and presumably activate Nek2A through autophosphorylation.²

In addition to its roles in mitosis, recent studies support a role for Nek2 in tumorigenesis, and as a potential anti-cancer drug target. Nek2 siRNA has been shown to suppress the growth of breast and cholangiocarcinoma tumor xenografts, as well as

inhibit proliferation of their parent cell lines while having no effect on normal fibroblasts.^{13,14} Furthermore, overexpression of Nek2 at the mRNA and/or protein level has been documented in primary breast tumors,¹⁵ cholangiocarcinoma,¹³ testicular seminoma,¹⁶ and in diffuse large B-cell lymphoma where its expression correlates with oncogenic transformation.¹⁷ Ectopic overexpression of Nek2 in non-transformed breast epithelial cells leads to the formation of multinucleated cells with supernumerary centrosomes, a phenotype associated with the induction of mitotic errors, aneuploidy, and oncogenesis.¹⁵ Similarly, Nek2 expression is required for and upregulated in response to oncogenic H-Ras-G12V induced centrosome amplification.¹⁸

Small-molecule, cell-active Nek2 inhibitors will be required to directly test Nek2 inhibition as a viable means of tumor suppression. Furthermore, in contrast to siRNA, small-molecule inhibitors will provide a way to study the cellular function of endogenous Nek2 kinase activity *alone*. To date, several small-molecules have been reported to inhibit Nek2 kinase activity *in vitro*. However none of these compounds have been directly shown to target Nek2 in cells. The known Nek2 inhibitors include a series of aminopyrazines,¹⁹ a thiophene-based Plk1 inhibitor,²⁰ a set of toxoflavin and viridian analogs,²¹ and the generic kinase inhibitor **1** (SU11652, Figure 1-1A).²² So far, only two of the Nek2 active viridian analogs have been tested in cells. At 5 μ M these compounds caused a 50% reduction in the number of cells exhibiting centrosome-separation resulting from ectopic overexpression of Nek2A.²¹ Though proposed to be acting through inhibition of Nek2 kinase activity, the cellular mechanism of the viridian analogs remains to be determined. Here we report the development of **2** (JH295, Figure 1-1B), an

irreversible, oxindole-based Nek2 inhibitor, and the first demonstration of Nek2 inhibition in live cells through specific targeting of the ATP binding site.

The Nek2 active site contains a poorly conserved cysteine found in only 2% of the human kinome.²³ The selective alkylation of such cysteines has successfully been exploited as a means of enhancing the potency and specificity of kinase inhibitors.²⁴ The fungal polyketide natural product hypothemycin is one example that reacts selectively with kinases containing a different active-site cysteine conserved in less than 10% of the human kinome.²⁵ A synthetic polyketide related to hypothemycin is currently in clinical trials for the treatment of B-Raf mutant advanced solid tumors and psoriasis.²⁶ To date at least six other cysteine-reactive kinase inhibitors, developed through rational structure-based design approaches, have gone into clinical trials as anti-cancer agents.^{24,27} Previously our group employed a structural bioinformatic-based strategy to rationally design a highly specific, cysteine-directed inhibitor of the C-terminal kinase domain of p90Rsk2, and identified Nek2 as one of eleven kinases with an analogous cysteine (Figure 1-1C).²³ In this work, we apply similar methodology to the development of **2**, and demonstrate that Nek2 is irreversibly inhibited in cells through alkylation of that cysteine.

1.3 Structure-based design of irreversible Nek2 inhibitors

We examined a crystal structure of the Nek2 kinase domain bound to oxindole **1**²² to create a model for the development of our irreversible inhibitors (Figure 1-1D). The basic oxindole inhibitor model consists of a (Z)-3-((1*H*-pyrrol-2-yl)methylene)indolin-2-one core (Figure 1-1E), which is predicted to form three hydrogen bonds to the amide backbone of the hinge-region. This feature is predicted to be essential for inhibitor binding, and is common to ATP competitive kinase inhibitors.²⁸ Positions 6 and 7 of the oxindole ring form close hydrophobic contacts with the gatekeeper²⁹ residue Met86. Modification of these positions would likely produce a steric clash with Met86 leading to reduced binding affinity. Substituents at the pyrrole 3', 4', and 5' positions are predicted to form contacts with Nek2. These positions represent opportunities to tune the reversible binding affinity to Nek2, and destabilize binding to off-target kinases. We hypothesized that electrophilic substituents placed at the 5 position of the oxindole ring would be capable of alkylating Cys22, thereby achieving potent irreversible inhibition.

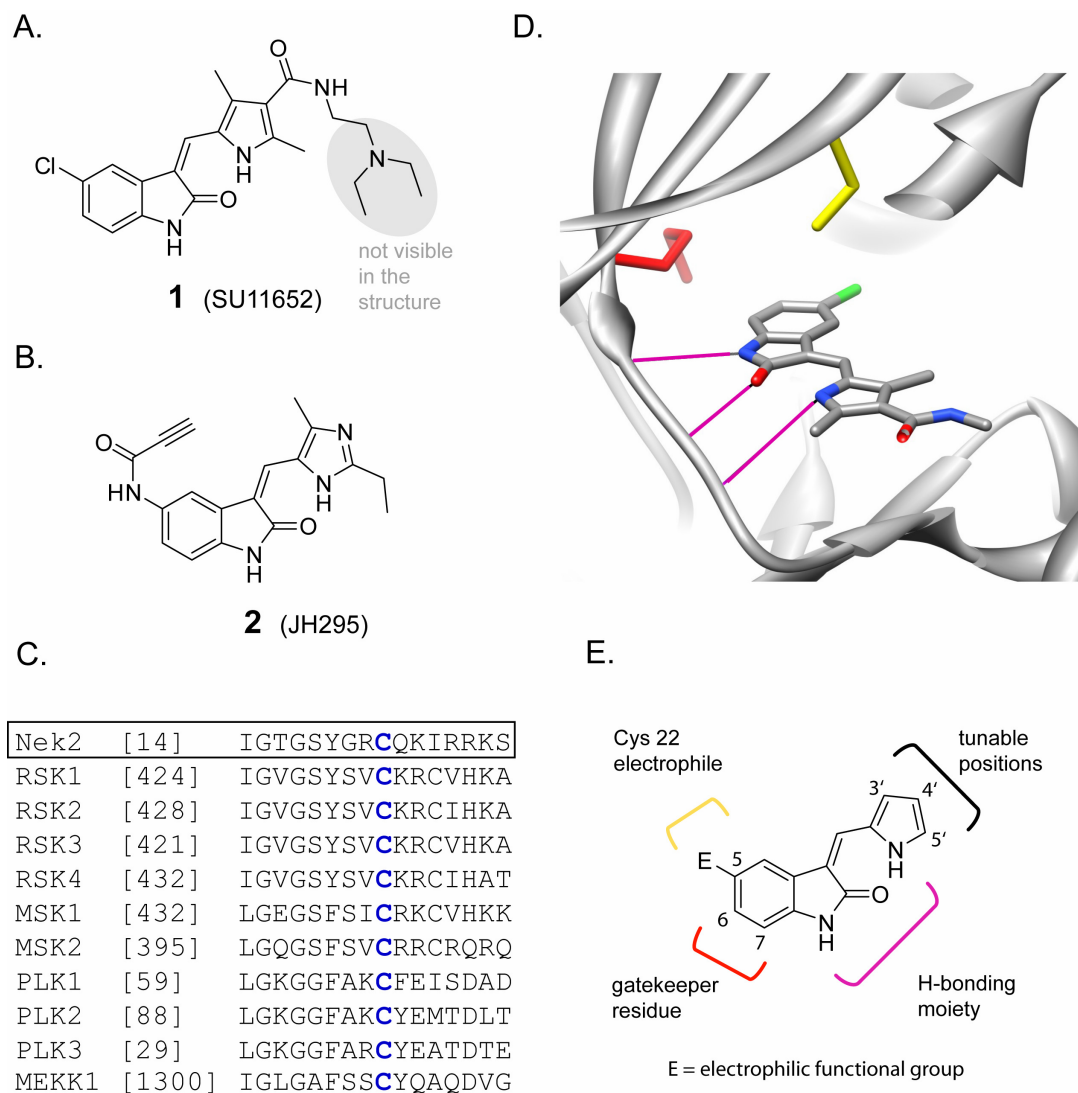
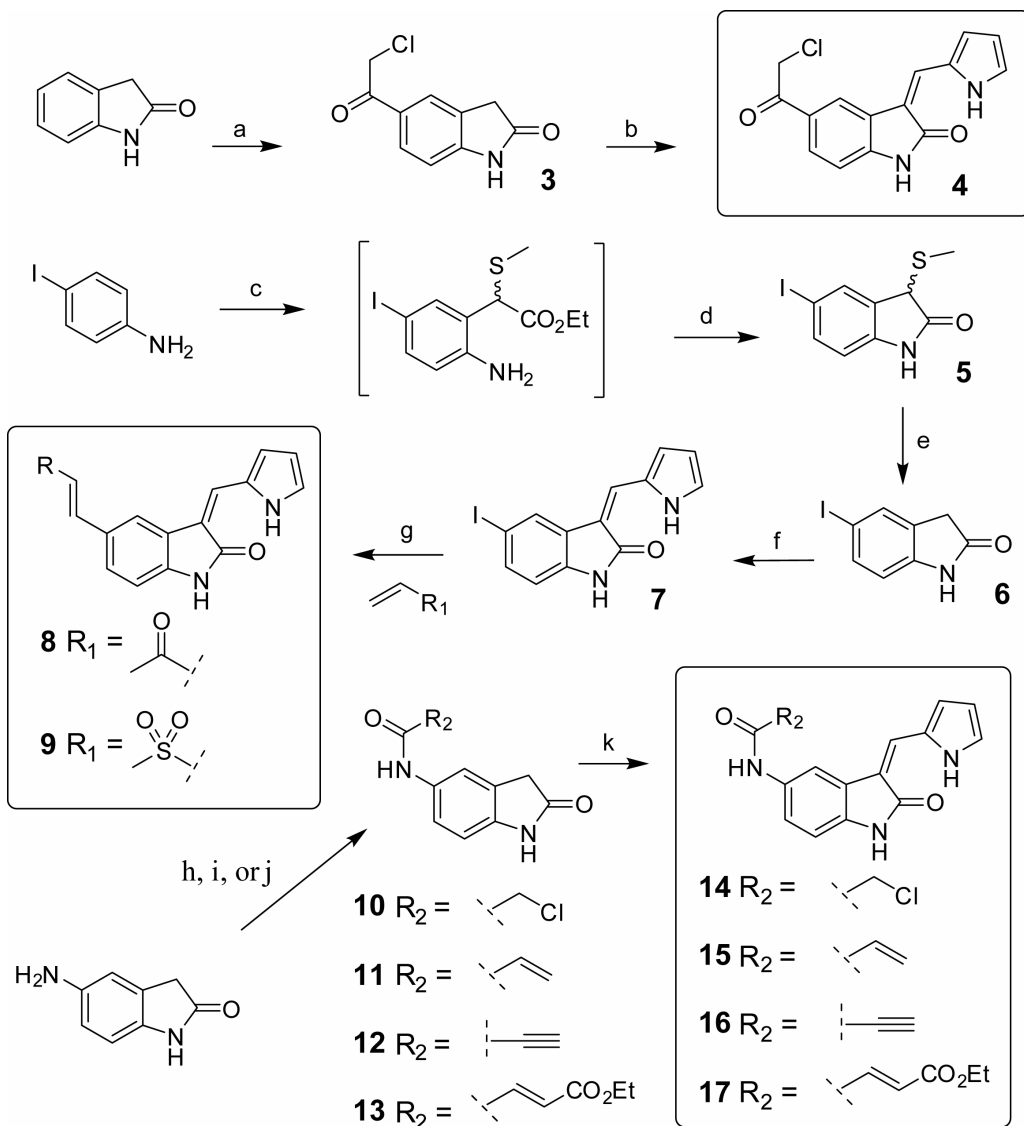


Figure 1-1. Structure based design of irreversible Nek2 inhibitors. (A) The chemical structure of **1**. (B) The chemical structure of **2**. (C) Sequence alignment of human kinases containing an active site cysteine analogous to Nek2. (D) Crystal structure of Nek2 bound to **1** (PDB ID 2JAV),²² showing hydrogen bonds to the amide backbone of the hinge-region (magenta), the position of the gate keeper residue Met86 (red), and the target Cys22 (yellow). (E) Minimal oxindole model for the design of our irreversible inhibitors.

1.4 Synthesis and *in vitro* characterization of lead Nek2 inhibitors

Based on the minimal oxindole model shown in Figure 1-1E, we designed a set of seven analogs substituted with different electrophiles at the oxindole 5-position (Scheme 1-1). The electrophilic functionalities include five Michael acceptors (**8**, **9** and **15-17**), a chloromethylketone (**4**), and a chloroacetamide (**14**). The synthesis of these compounds began with Friedel-Crafts acylation of oxindole, to give intermediate **3**, followed by Knoevenagel condensation onto pyrrole-2-carboxaldehyde to provide the chloromethylketone-based inhibitor **4**. The Gassman oxindole synthesis was employed to generate the 3-thiomethyl substituted oxindole intermediate **5**, starting from commercial 4-iodo-aniline. Cleavage of the thiomethyl group by zinc reduction, gave 5-iodo-oxindole **6**, followed by installation of the pyrrole ring by Knoevenagel condensation gave intermediate **7**. Finally, palladium-catalyzed cross coupling under Heck conditions provided the vinyl-oxindole based inhibitors **8** and **9**. Electrophilic oxindoles **10-13** were synthesized from 5-amino-oxindole using standard acid chloride or carbodiimide amide bond forming chemistry. Similar to **3**, these intermediates readily underwent Knoevenagel condensation onto pyrrole-2-carboxaldehyde to provide the electrophilic amide-linked inhibitors **14-17**.

Scheme 1-1. Synthesis of initial electrophilic Nek2 inhibitors **4**, **8**, **9**, and **14-17**.^a



^aReagents and conditions: (a) AlCl_3 (6 equiv), ClCH_2COCl (1.7 equiv), CS_2 , reflux 2.5 h (92%); (b) pyrrole-2-carboxaldehyde (10 equiv), piperidine (0.2 equiv), THF, 60 °C, 45 min (20%); (c) one pot: tBuOCl (1 equiv), DCM, -60 °C, 15 min, then $\text{CH}_3\text{SCH}_2\text{CO}_2\text{Et}$ (1 equiv), DCM, -60 °C, 1 h, then Et_3N (1 equiv), DCM, -60 °C to rt, 1 h; (d) aq. HCl , Et_2O , rt, 4 h (47%, yield over four steps); (e) Zn^0 (5 equiv), AcOH , 60 °C, 30 min (80%); (f) pyrrole-2-carboxaldehyde (1.1 equiv), piperidine (0.2 equiv), THF, 75 °C, 4 h (67%); (g) $\text{R}_1\text{-CH=CH}_2$ (4 equiv), Ph_3P (0.6 equiv), $\text{Pd}(\text{OAc})_2$ (0.3 equiv), Et_3N (5 equiv), DMF, 85 °C, 2 h (yield **8**, 48%, yield **9**, 34%); (h) ClCH_2COCl (1.3 equiv), pyridine (1.5 equiv), THF, 0 °C to rt, 30 min, (yield **10**, 45%); (i) $\text{CH}_2=\text{CHCOCl}$ (1.2 equiv), THF, 0 °C to rt, 10 min, (yield **11**, 41%); (j) $\text{R}_2\text{-CO}_2\text{H}$ (1.2 equiv), EDC (2 equiv), CH_3CN , rt, 30 min to 2 h, (yield **12**, 40%, yield **13**, 55%); (k) pyrrole-2-carboxaldehyde (5 to 10 equiv), piperidine (0.1 to 0.2 equiv), THF, 75 °C, 4 h to 20 h, (yield **14**, 63%, yield **15**, 56%, yield **16** 29%, yield **17**, 50%).

We first tested the final compounds from Scheme 1-1 against recombinant Nek2 in an *in vitro* kinase activity assay. Chloromethylketone **4** and propynamide **16** were the most potent inhibitors, giving greater than 80% inhibition after a 30 min incubation with the enzyme at 5 μ M (Figure 1-2A). To test the requirement of Cys22 for potent inhibition by **4** and **16** we expressed the C22V mutant of Nek2 where the target cysteine was replaced by the non-nucleophilic residue valine. Comparison of kinase assay dose response curves for **4** and **16** against WT and C22V Nek2 revealed a strong dependence on Cys22 for potent inhibition. Compounds **4** and **16** were greater than 2000 and 22-fold selective for WT Nek2 respectively (Figure 1-2B). The selectivity of these compounds for WT Nek2 supports the hypothesis that they function through alkylation of Cys22. However, these data do not rule out other possible mechanisms of selectivity such as steric occlusion by the bulkier valine side chain, or enhanced affinity of the C22V mutant for the competitive substrate ATP present in the kinase reactions.

To demonstrate Cys22 dependent alkylation of Nek2, we used a mass spectrometry-based binding assay capable of measuring the full mass of the Nek2 kinase domain (aa 1-271), plus that of any covalent adducts (Figure 1-2C). Importantly, this assay will not detect reversibly associated enzyme-inhibitor complexes as the protein is denatured in the LC conditions leading to disassociation. At physiological pH, a 10-fold excess of **4** or **16** selectively modified a single residue on the Nek2 kinase domain, giving the predicted increase in mass for the expected adducts. Importantly, the Nek2 Kinase domain contains five total cysteines serving as possible sites of modification. No modification of the corresponding C22V mutant was detected under identical conditions, consistent with the site of modification for WT Nek2 being Cys22.

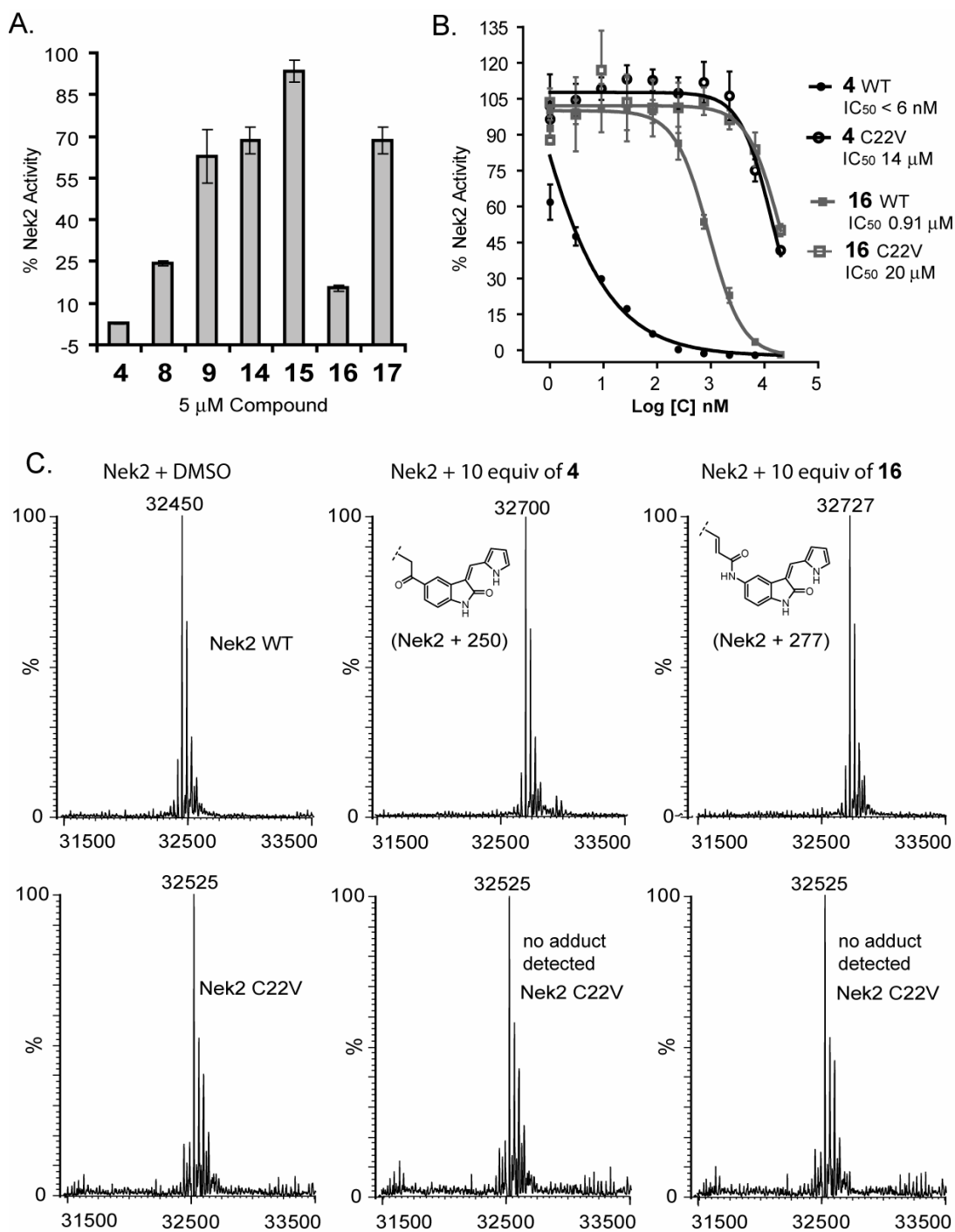
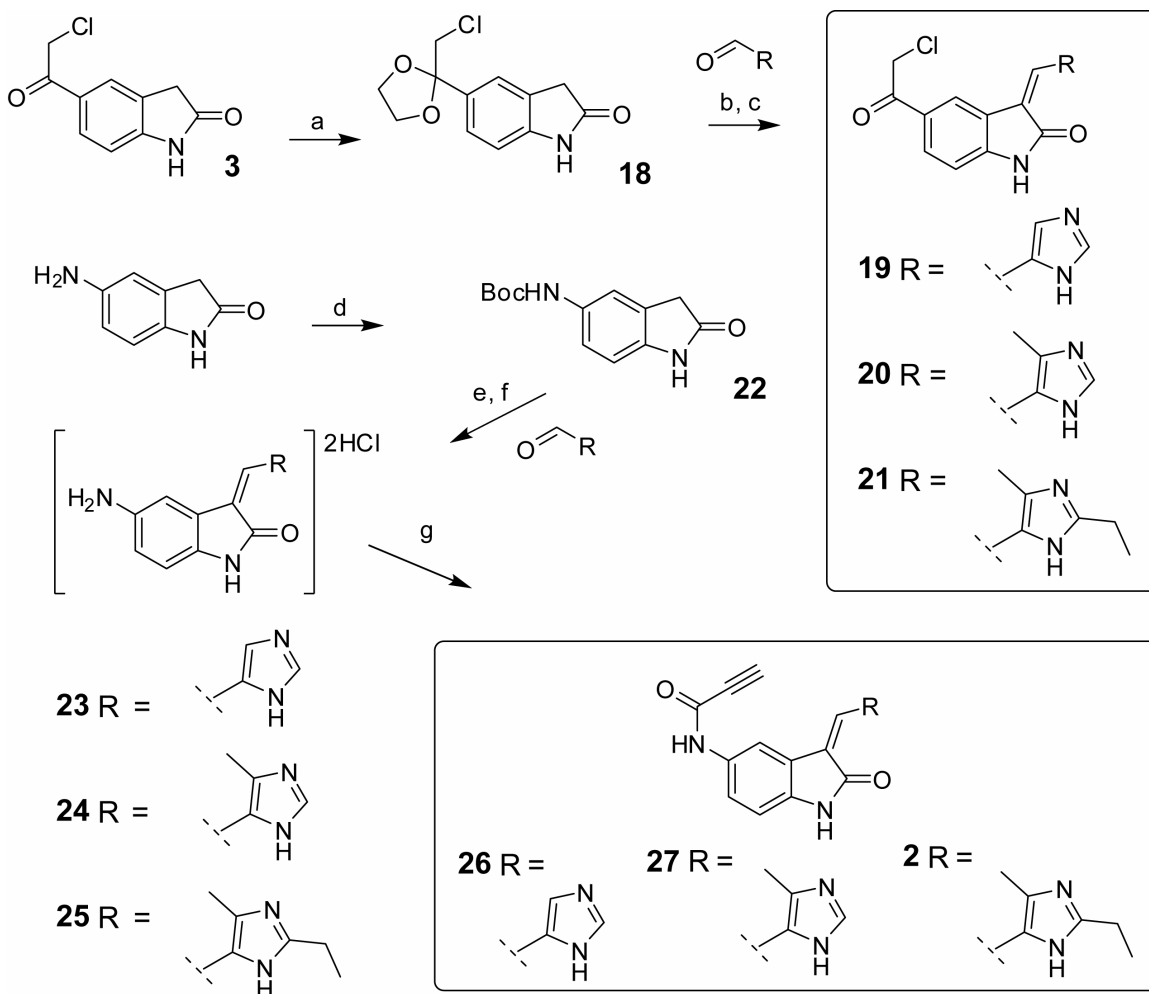


Figure 1-2. *In vitro* characterization of the final compounds from Scheme 1-1. (A) Kinase assay of the final compounds from Scheme 1-1 against Nek2. (B) Kinase assay showing the dependence on Cys22 for potent Nek2 inhibition by **4** and **16**. (C) Mass spectrometry-based covalent binding assay showing specific alkylation of Cys22 by **4** and **16**.

1.5 Synthesis and *in vitro* characterization of optimized Nek2 inhibitors

To test the effects of alkyl substitution and nitrogen insertion at the pyrrole ring, we synthesized a series of imidazole analogs with small alkyl groups in the 3' and 5' positions, while retaining the chloromethylketone or propynamide electrophiles at the oxindole 5 position (Scheme 1-2). To eliminate side reactions in the subsequent Knoevenagel condensations, the carbonyl group of **3** was protected as 1,3-dioxolane **18**, which was used to form the imidazole-substituted chloromethylketone-based inhibitors **19-21**. This one pot condensation/deprotection strategy starting from **18** produced twice the yield of **19-21**, compared to the direct Knoevenagel condensation of **3** used in the synthesis of chloromethylketone-based inhibitor **4**. A similar condensation/deprotection strategy starting from Boc-protected 5-amino-oxindole **22** was used to generate the imidazole-substituted 5-amino-oxindoles **23-25**. Boc-protection of the free amine was required to eliminate the competing formation of imines that otherwise occurred during the condensation reactions. Carbodiimide amide bond-forming chemistry was then used to make the imidazole-substituted propynamide-based inhibitors **2**, **26**, and **27**.

Scheme 1-2. Synthesis of imidazole-substituted Nek2 inhibitors **2**, **19-21**, **26** and **27**.^a



^aReagents and conditions: (a) Ethylene glycol (2 equiv), pTSA·H₂O (0.2 equiv), toluene, reflux Dean Stark, 12 h (100%); (b) R-CHO (1.1 to 1.2 equiv), piperidine (0.3 equiv), THF, 75 °C, 7 to 20 h; (c) aq. HCl (excess), THF, rt, 5 to 24 h (for two steps: yield **19**, 41%, yield **20**, 49%, yield **21**, 49%); (d) (Boc)₂O (2.8 equiv), DIPEA (4 equiv), THF, 25 h, rt (92%); (e) R-CHO (1.1 equiv), piperidine (0.2 equiv), THF, 75 °C, 20 h; (f) anhydrous HCl (excess), MeOH, rt, 23 to 48 h (for two steps: yield **23**, 83%, yield **24**, 83%, yield **25**, 72%); (g) propionic acid (1.5 to 6 equiv), DIPEA (2 equiv), EDC (2 equiv), DMF, 0 °C, 2 to 2.5 h (yield **26**, 8.2%, yield **27**, 32%, yield **2**, 44%).

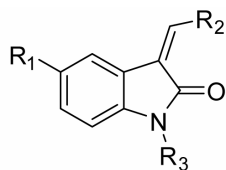
In vitro Nek2 kinase assays of the new imidazole-based chloromethylketone and propynamide inhibitors revealed different trends in potency depending on which electrophile was present (Table 1-1^a). For the chloromethylketone series, replacement of the pyrrole ring of **4** with the imidazole rings of **19-21**, caused a 3 to 30-fold decrease in potency. In contrast, for the imidazole-based propynamides (**2**, **26**, and **27**), potency was improved by 15 to 60% over the pyrrole-based inhibitor **16**. This indicates that the imidazole ring is more desirable for the propynamide-based oxindole scaffold in general. The imidazole-based chloromethylketone and propynamide compounds **2** and **21** also demonstrated greater than 25-fold selectivity for WT over C22V Nek2, and showed specific alkylation of Cys22 by mass spectrometry, confirming that they are irreversible cysteine-reactive Nek2 inhibitors (Figure 1-3).

As the kinase activity assay provides an apparent IC₅₀ value (Table 1-1^a), we cannot distinguish what component of inhibition explains the changes in potency for the imidazole-based compounds: the reversible binding affinity or the rate of covalent bond formation. Because the rate of covalent bond formation is a time-dependent factor contributing to the IC₅₀, we strictly standardize the duration of the assay. This method provides meaningfully comparable apparent IC₅₀ values encompassing both contributing factors. It is possible for the imidazole ring to be affecting either or both of these factors to cause the loss or gain in potency.

Further examination of the imidazole-based inhibitors revealed that small alkyl substituents on the imidazole ring are tolerated or desirable for Nek2 inhibition. The most potent compounds of the series were the 3'-methyl-imidazole substituted inhibitors **20** and **27**. The dialkyl-imidazole substituted chloromethylketone inhibitor **21**, containing an

ethyl group at the 5' position, was 6-fold less potent than the corresponding unsubstituted-imidazole analog **20**. The fact that Nek2 tolerates substituents at the 5' position is an important observation despite the loss of potency. Out of the tunable positions presented in Figure 1-1E, substituents at the 5' position are predicted to form the tightest contacts with the kinase active site. Therefore 5' substituents, are the most likely to destabilize binding to off target kinases through steric occlusion. For the propynamide-imidazole series the presence of the 5'-ethyl group of **2** showed only a 2-fold loss in potency compared to the corresponding unsubstituted-imidazole analog **27**. This modest loss of potency demonstrates that alkyl groups in the 5' position are tolerated to a greater extent when paired with the propynamide electrophile.

Table 1-1. Activity of inhibitors against Nek2 *in vitro*^a, Nek2 in cells^b, as inducers of mitotic exit^c, and against Cdk1 *in vitro*^d



Compound	R1	R2	R3	<i>In Vitro</i> ^a Nek2 IC ₅₀ (nM)	<i>In Cell</i> ^b Nek2 % Inhib. (5 μM)	% mitotic ^c exit (5 μM)	<i>In Vitro</i> ^d Cdk1 IC ₅₀ (nM)
4			H	<6	90	98	10
19			H	52	73	92	<1
20			H	16	75	100	<1
21			H	99	89	50	2250
34			Me	4730	12	0.9	>20000
36			H	>20000	14	27	4000
16			H	910	94	78	86
26			H	625	95	80	<1
27			H	372	95	99	<1
2			H	772	92	4	>20000
31			Me	>20000	19	0	>20000
35			H	18800	26	33	>20000

^a*In vitro* kinase assay IC₅₀ values for Nek2 presented as the mean of triplicate measurements. ^bPercent inhibition of endogenous Nek2 in A549 cells by 5 μM of the indicated compounds for 45 min, presented as a single measurement. ^cPercentage of monastrol arrested cells induced to undergo mitotic exit presented as the mean of N >75 total cells. Note: 2.6% of DMSO treated cells exhibited the mitotic exit phenotype. ^d*In vitro* kinase assay IC₅₀ values for Cdk1 presented as the mean of triplicate measurements.

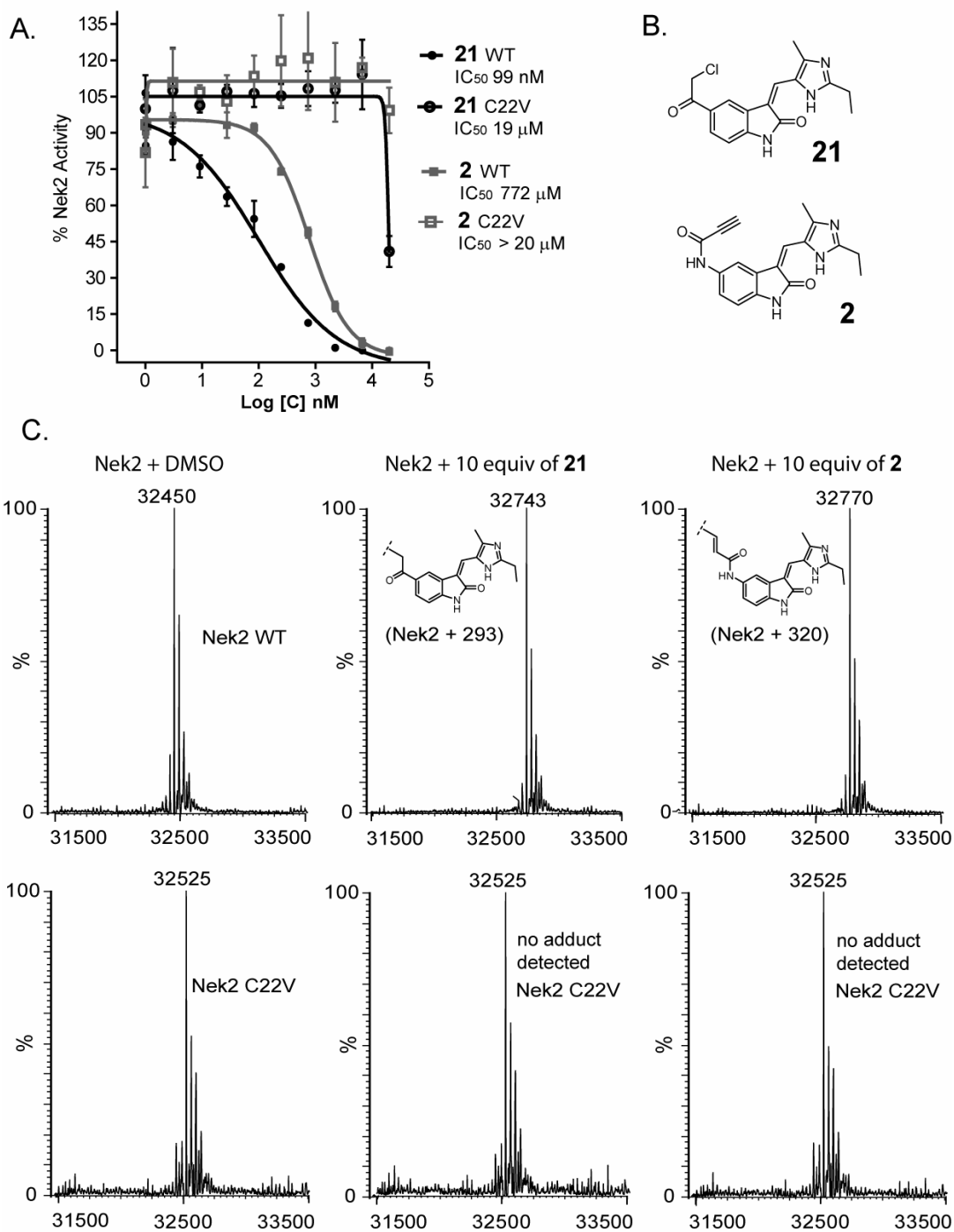


Figure 1-3. *In vitro* characterization of compounds **2** and **21**. (A) Kinase assay showing the dependence on Cys22 for potent Nek2 inhibition by **2** and **21**. (B) Chemical structure of **2** and **21**. (C) Mass spectrometry-based covalent binding assay showing specific alkylation of Cys22 by **2** and **21**.

1.6 Synthesis and *in vitro* characterization of negative control compounds

We next synthesized several negative control compounds to validate the binding mode and electrophilic mechanism of action of our chloromethylketone and propynamide inhibitors. We envisioned that these compounds would be especially useful for ruling out off-target effects in cell-based assays including the cellular assays for Nek2 kinase activity described below. The first set of compounds was designed to control for non-specific reactions of the electrophile. These compounds are methylated at the oxindole nitrogen to destabilize binding to the kinase active site by eliminating hydrogen bonding to the hinge region (**31** and **34**, Scheme 1-3). In the second set, the electrophiles were replaced by isosteric groups with greatly decreased or no intrinsic reactivity toward thiols³⁰ (**35** and **36**, Scheme 1-4). These compounds could be used to rule out reversible non-covalent inhibition of off-target kinases lacking the critical cysteine corresponding to Cys22 of Nek2.

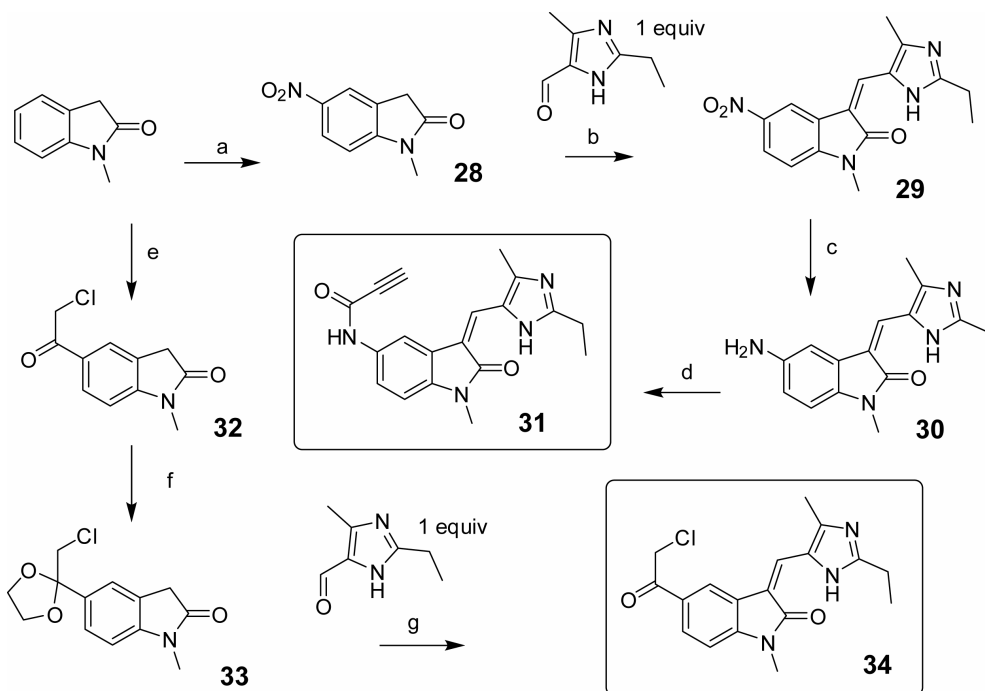
Synthesis of the electrophilic control compounds began with nitration of *N*-methyl-oxindole under standard conditions to give intermediate **28** in good yield. This was followed by Knoevenagel condensation of **28** with the appropriate aldehyde to provide the imidazole-substituted nitro-oxindole **29**. An initial attempt to reduce the nitro group on **29** through catalytic-hydrogenation over Pd/C led to competing reduction of the olefin linkage between the oxindole and imidazole rings. Specific reduction of the nitro group was achieved using a mildly-acidic zinc condition to provide free amine **30**. Carbodiimide amide bond forming chemistry was then used to give the propynamide-based control compound **31**. Friedel-Crafts acylation of *N*-methyl-oxindole to give intermediate **32**, followed by 1,3-dioxolane protection of the chloromethylketone

carbonyl gave intermediate **33** in excellent overall yield. A one-pot condensation/deprotection strategy then provided the chloromethylketone **34**.

The reversible binding control compounds were made in one step from intermediates on hand. The butynamide-based control compound **35**, predicted to be less electrophilic than propynamide **2** and hence inactive toward Nek2, was synthesized from amine intermediate **25** using carbodiimide amide bond forming chemistry. Finally the methylketone **36**, predicted to be inert toward Nek2, was made from 5-acetyl-oxindole through Knoevenagel condensation onto the appropriate imidazole-carboxaldehyde.

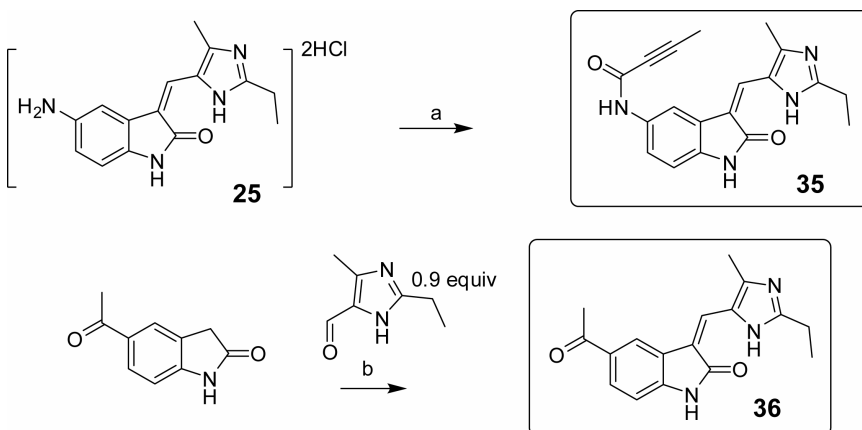
In vitro kinase assays with the negative control compounds (**31**, and **34-36**) against Nek2 all resulted in a greater than 24-fold loss of potency over their active analogs **2** and **21** (Table 1-1^a). This reduction in potency, consistent with our inhibitor-design model, verifies the importance of both the hinge-binding moiety and electrophile for potent inhibition of Nek2 *in vitro*.

Scheme 1-3. Synthesis of negative control compounds **31** and **34**.^a



^aReagents and conditions: (a) HNO₃ (1.7 equiv), H₂SO₄, 0 °C, 30 min (88%); (b) piperidine (0.3 equiv), THF, 75 °C, 18 h (73%); (c) Zn⁰ (excess), NH₄Cl (excess), THF, H₂O, rt, 10 min (71%); (d) propiolic acid (1.5 equiv), EDC (2 equiv), DMF, 0 °C, 2 h (23%); (e) AlCl₃ (6 equiv), ClCH₂COCl (1.7 equiv), CS₂, reflux, 2 h (88%); (f) ethylene glycol (2 equiv), pTSA·H₂O (0.2 equiv), benzene, reflux Dean Stark, 5 h (100%); (g) one pot: piperidine (0.3 equiv), THF, 75 °C, 18 h, then aq. HCl (excess), THF, 18 h (60%).

Scheme 1-4. Synthesis of negative control compounds **35** and **36**.^a



^aReagents and conditions: (a) 2-butynoic acid (6 equiv), EDC (4 equiv), HOBT (1 equiv), DIPEA (3 equiv), DMF, rt, 2 h (51%); (b) piperidine (0.3 equiv), THF, 75 °C, 16 h (34%).

1.7 Cell-based evaluation of Nek2 inhibitors

We next tested the activity of our inhibitors against endogenous Nek2 in human A549 lung cancer cells. This was accomplished by measuring the kinase activity of Nek2 immunoprecipitates from cells that were treated with inhibitors for 45 min at a concentration of 5 μM (Table 1-1^b, Figure 1-8). Inhibitors that were potent ($\text{IC}_{50} < 1 \mu\text{M}$) against Nek2 *in vitro* gave 73-95% inhibition of cellular Nek2, whereas the negative control compounds (**31**, **34**, **35**, and **36**) inhibited Nek2 by <26%. It is important to note that the immunoprecipitation process, which includes several washes, provides time for the dissociation of reversibly-bound inhibitors. The activity of our inhibitors in this assay suggests that they irreversibly inhibit Nek2 in live cells, consistent with our *in vitro* mass spectrometry data showing irreversible alkylation (Figure 1-2, and 1-3).

Despite being at least 4-fold more potent *in vitro* than the propynamides (**2**, **16**, **26**, and **27**) the chloromethylketones (**4**, **19**, **20**, and **21**) were less efficacious against Nek2 in cells. Poor stability of the chloromethylketones (e.g. toward cellular glutathione) in tissue culture conditions most likely explains this loss of potency. Compared to the propynamides, the chloromethylketones are ~15-fold more reactive toward thiols as measured by reaction with 2-mercaptoethanol in pH 7.5 PBS (data not shown). However, our data does not exclude other mechanisms that could explain the lower potency of the chloromethylketones (or kinase inhibitors³¹) in cells.

To gain more understanding of the specific mechanism of Nek2 inhibition in cells, we generated Hek293 cell lines expressing HA-tagged WT or C22V Nek2A (full-length) under the control of a tetracycline inducible promoter. Using these cell lines and IP kinase assay methodology similar to that used for endogenous Nek2, we found that

compound **2** selectively inhibited WT Nek2 ($IC_{50} = 1.3 \mu\text{M}$) and not the C22V mutant (Figure 1-4). These data suggest that inhibition of Nek2 in cells occurs via alkylation of Cys22 and is not likely due to inhibition of upstream kinases that activate Nek2.

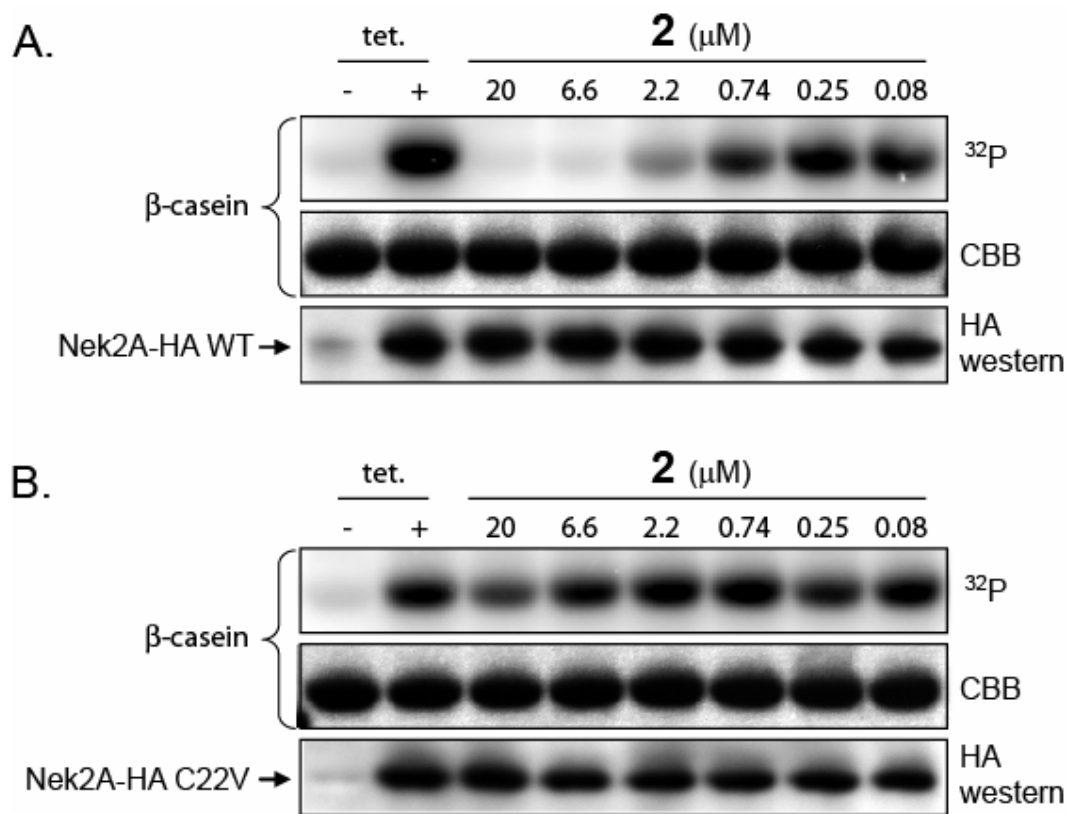


Figure 1-4. Kinase assays of HA-tagged Nek2A immunoprecipitates from cells treated with compound **2** demonstrate inhibition of Nek2 in live Hek293 cells through alkylation of active site Cys22. (A) WT Nek2. (B) C22V Nek2.

1.8 Inhibition of Nek2 in monastrol-arrested cells

Small-molecule inhibition of kinases that are required for maintenance of the SAC has been shown to trigger rapid mitotic exit without cell division in cells subjected to SAC-dependent cell-cycle arrest. For example, inhibitors of Cdk1 and AurB induce this phenotype.^{32,33} The small molecule, monastrol, inhibits the mitotic kinesin Eg5 (a microtubule motor protein), thereby preventing bi-polar spindle-assembly and triggering SAC-dependent metaphase arrest.³⁴ Because Nek2A has been implicated, by RNAi knockdown experiments, in regulation of the SAC, we tested whether our inhibitors would induce mitotic exit in monastrol-arrested cells.

We treated monastrol-arrested A549 cells with 5 μ M of our inhibitors for 45 minutes (Table 1-1^c). Following treatment with our compounds, the cells were fixed and stained for analysis by immunofluorescence. We included the well-characterized Cdk1 inhibitor **37** (RO3306, Figure 1-5) as a positive control for inducing mitotic exit.³⁵ Representative images from this experiment are presented in Figure 1-5. The mitotic exit phenotype is characterized by decondensation of chromatin, loss of histone-H3 phosphorylation at Ser10, and reorganization of microtubules. We relied on staining of phospho-histone-H3 (a common mitosis marker) to count cells that exhibited this phenotype (Table 1-1^c). Strikingly, every cell-active Nek2 inhibitor with a proton in the 5' position (**4**, **16**, **19**, **20**, **26** and **27**), triggered mitotic exit in 78-99% of the monastrol-arrested cells. In contrast, compounds **2** and **21** with ethyl groups in the 5' position were far less efficient inducers of mitotic exit, despite being equally active inhibitors of Nek2 in cells. Compounds **2** and **21** triggered mitotic exit in 4% and 50% of the arrested cells, respectively. However, the effect of compound **2** is negligible, since 2.6% of DMSO

treated cells underwent mitotic exit in these conditions. This discrepancy between Nek2 inhibition and induction of mitotic exit, most notably for compound **2**, suggests that Nek2 kinase activity is not essential for maintenance of the SAC in monastrol-arrested cells. Furthermore, these data demonstrate that compound **2** does not inhibit other kinases required for SAC-dependent arrest such as Cdk1, AurB, and Mps1, since inhibitors of these kinases have been shown to trigger mitotic exit under similar conditions.^{32,33,36}

Because efficient induction of mitotic exit by our compounds depends on a proton in the 5' position, and not Nek2 inhibition, this raises the possibility that compounds **4**, **16**, **19**, **20**, **26** and **27**, may be acting through inhibition of another kinase. Previously published studies show that similar oxindole compounds are potent reversible, inhibitors of Cdk1.³⁷ Because Cdk1 inhibitors are known to induce mitotic exit, we tested our compounds *in vitro* against Cdk1 in kinase assays (Table 1-1^d). Strikingly, compounds **4**, **16**, **19**, **20**, **26** and **27**, all proved to be low nanomolar inhibitors of Cdk1. A subset of these compounds, **19**, **20**, **26**, and **27**, performed at the limit of resolution for this assay, and are predicted to have picomolar affinity for Cdk1. This strong correlation between Cdk1 inhibition and induction of mitotic exit suggests that Cdk1 is a relevant target of these compounds in cells. Inhibition of Cdk1 may also explain the morphological similarity of cells induced to undergo mitotic exit by these compounds with that of the known Cdk1 inhibitor **37** (Figure 1-5).

Examination of our compounds that have little to no activity against Cdk1 supports the correlation between Cdk1 inhibition and mitotic exit. For example, negative control compound **34** was inactive against Cdk1 at 20 μ M and did not induce mitotic exit. The only compound that deviates from this trend is negative control compound **35**.

Compound **35** (Cdk1 $IC_{50} = 19 \mu\text{M}$) still triggered mitotic exit in 33% of monastrol arrested cells. However, the possibility still remains that compound **35** could be inhibiting other SAC kinases. Compound **21** induced mitotic exit in 50% of the arrested cells, and proved to have moderate activity against Cdk1 ($IC_{50} = 2.3 \mu\text{M}$). Most importantly, as predicted from its activity as a negligible inducer of mitotic exit (Table 1-1^c), one of our most potent Nek2 inhibitors, compound **2**, was inactive against Cdk1 at 20 μM .

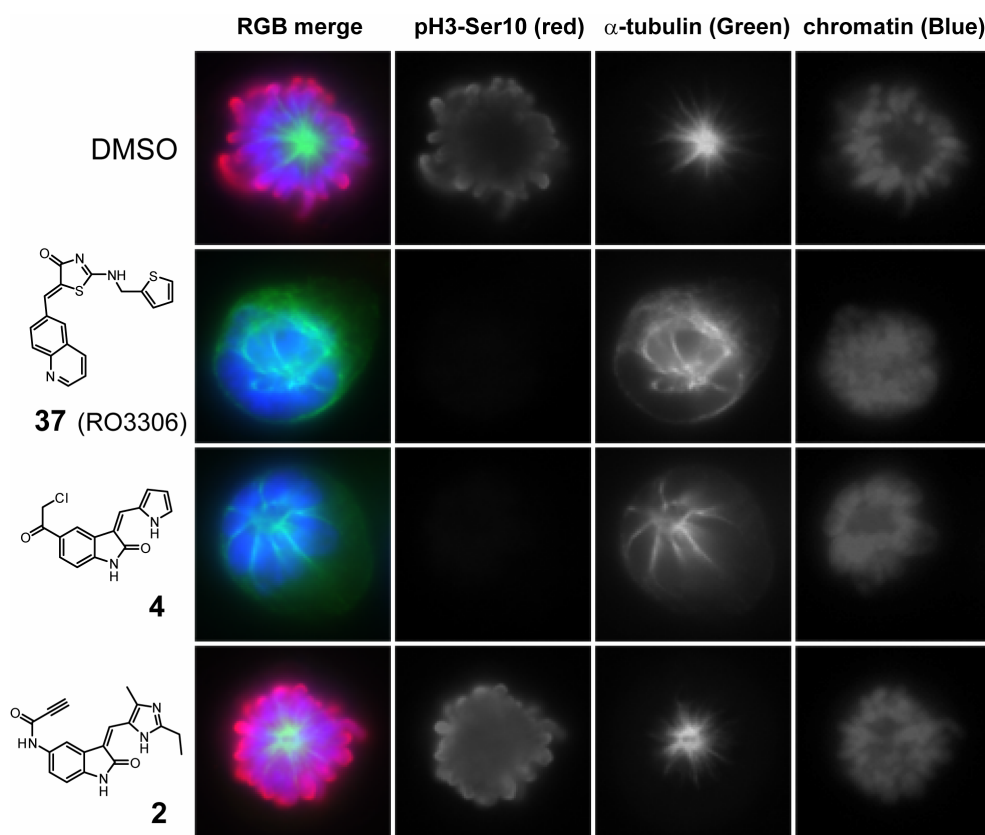


Figure 1-5. Representative images of the induction of mitotic exit in monastrol-arrested A549 cells by 5 μM of the indicated compounds. Compounds **2** and **4** both inhibit ~90% of Nek2 activity in cells at this concentration (Table 1-1^b), demonstrating that inhibition of Nek2 does not correlate with induction of this phenotype. The morphology of the cell associated with compound **4** is representative of all cells quantified in Table 1-1^c. This morphology closely resembles that of the cell associated with the known Cdk1 inhibitor **37**.

1.9 Further analysis of our most selective Nek2 inhibitor

The 5'-ethyl group of compound **2** is an essential feature for selective Nek2 inhibition (Table 1-1). Compound **2** is greater than 26-fold selective for Nek2 over Cdk1 (Nek2 IC_{50} = 0.772 μ M, Cdk1 IC_{50} >20 μ M). In contrast, compound **27** lacks the 5'-ethyl group and demonstrates inverse selectivity, being 372-fold selective for Cdk1 over Nek2 (Cdk1 IC_{50} = <1 nM, Nek2 IC_{50} = 372 nM). Direct comparison of compounds **2** and **27** against Cdk1 demonstrates how the 5'-ethyl group confers greater than 20000-fold decrease in potency (Table 1-1^d).

We also tested compound **2** for activity against kinases with the same active site cysteine as Nek2. We conducted *in vitro* kinase assays against Rsk2 and Plk1 as they represent the two largest kinase families with this cysteine (Figure 1-1C). To produce meaningfully comparable IC_{50} values we used 30 min inhibitor treatment times identical to that used for Nek2. In these assays, compound **2** was ~5-fold selective for Nek2 over Rsk2 (Rsk2 IC_{50} = 4.0 μ M), and greater than 26-fold selective for Nek2 over Plk1 (Plk1 IC_{50} = >20 μ M, Figure 1-7). Plk1 is an essential regulator of bi-polar spindle assembly, and other mitotic functions.^{38,39} If compound **2** cross-reacted with Plk1 its utility as a tool to study Nek2-specific biology would be compromised.

1.10 Inhibition of Nek2 at the G2/M transition

Nek2A has been implicated in the regulation of bi-polar spindle assembly and metaphase chromosome congression.^{12,40} To test whether our most specific Nek2 inhibitor (**2**) would have any effect on these processes, we arrested A549 cells at the G2/M border with the Cdk1 inhibitor **37**. We then treated the arrested cells with 5 μ M of **2** for 30 minutes to inhibit Nek2 (Figure 1-6A). Following treatment with **2**, the inhibitors were washed out to release the cells from arrest. The cells were then allowed to progress into mitosis for one hour in the presence of 10 μ M of proteasome inhibitor MG132, followed by formaldehyde-fixing and staining for immunofluorescence analysis. MG132 prevents the degradation of cyclin-B, causing cells to arrest in metaphase with bipolar-spindles.³³ By preventing mitotic progression at this stage we are able to accurately account for bi-polar spindle assembly, chromosomes that have failed to congress to the metaphase plate, and for the number of cells that have entered mitosis (Figure 1-6B). Representative images of this assay are shown in Figure 1-6C. We employed compound **31** as a control for non-specific effects of the propynamide electrophile.

In the presence of Nek2 inhibition, we observed no defects in bi-polar spindle assembly, chromosome congression, or in the total number of mitotic cells (Figure 1-6). Considering the roles mentioned for Nek2 in these processes, this result may appear contradictory, as does our result with compound **2** in monastrol arrested cells (Figure 1-4). However, our observations of small molecule inhibition of Nek2 at the G2/M transition, and in monastrol arrested cells, are the first of their kind. Furthermore this lack of function suggests that compound **2** does not inhibit Plk1 at doses that give full inhibition of Nek2. Small-molecule inhibition of Plk1 inhibits cell-cycle progression

causing cells to arrest in early metaphase with mono-polar mitotic spindles,³⁹ a phenotype that was not observed in this assay. The inactivity of **2** against Plk1 is also consistent with our *in vitro* kinase assay data (Figure 1-7).

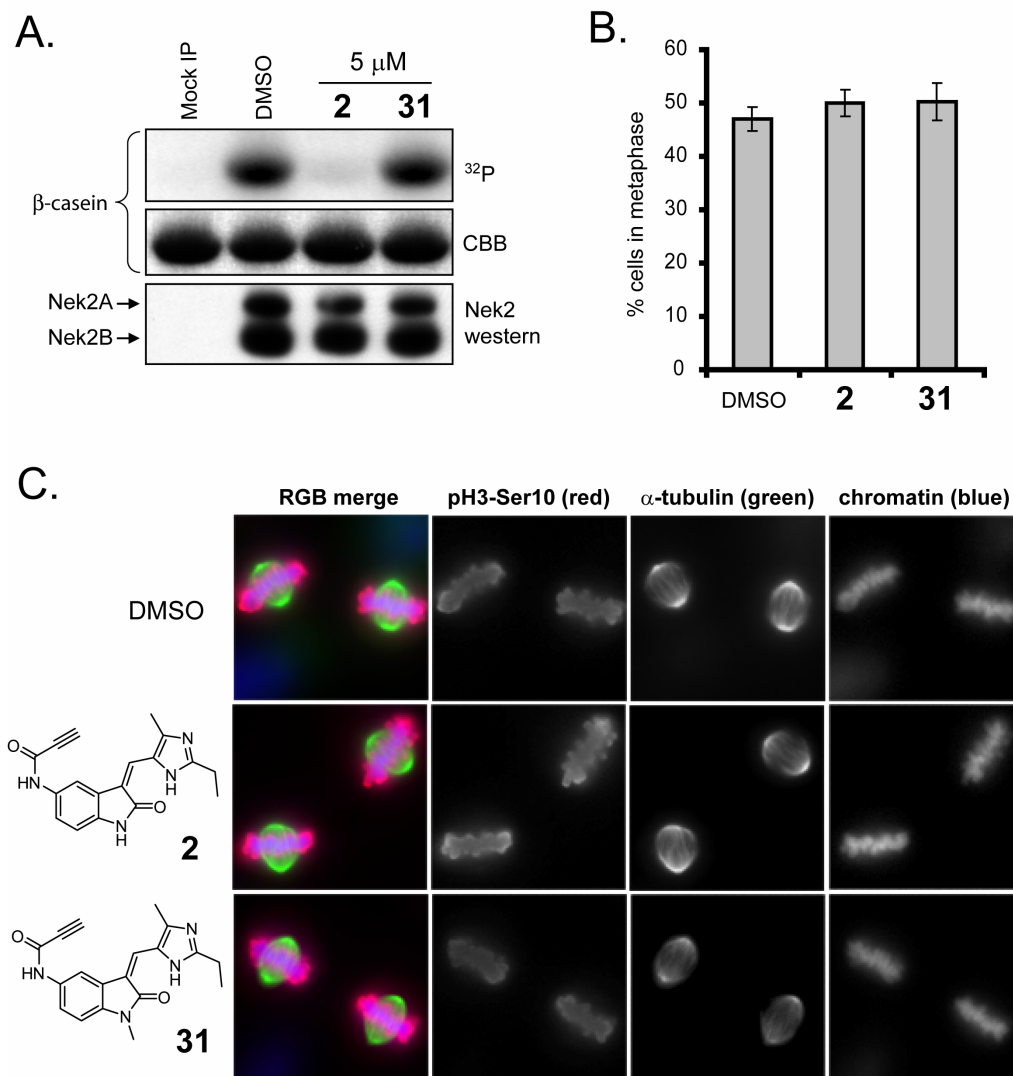


Figure 1-6. The effects Nek2 of inhibition on the G2/M transition and mitotic spindle assembly. (A) Endogenous Nek2 IP kinase assay showing inhibition of Nek2 by 5 μ M of **2** in A549 cells arrested at the G2/M border with the Cdk1 inhibitor **37**. (B) MG132-arrested A549 cells following treatment with 5 μ M of **2** or **31** at the G2/M transition, then progression into mitosis for 1 h. Mitotic entry, spindle assembly, and chromosome congression take place in the presence of Nek2 inhibition by **2**. (C) The total quantified mitotic index of cells from panel B, represented as the mean of triplicate biological replicates of N = >160 cells each, error bars represent standard deviation.

Due to the unavailability of cell-active Nek2 inhibitors, all prior studies have had to rely on traditional genetic techniques to study the function of Nek2 in cells. Examples include: ectopic overexpression of Nek2A leading to interphase centrosome separation,⁴⁰ siRNA against Nek2 leading to formation of mono polar mitotic spindles⁴⁰ and compromised SAC function,^{9,41} or the ectopic overexpression of non-phosphorylatable Nek2 substrates leading to chromosome congression defects.^{11,12} Because these approaches rely on overexpression or removal of proteins from the cell (siRNA), they can not specifically replicate the effects of inhibiting endogenous Nek2 kinase activity by small molecules. Supporting our observations, no prior study has shown Nek2 to be required for the G2/M transition, or to be *essential* for any of the aforementioned mitotic processes. We are not trying to imply that Nek2 is not involved in mitotic regulation. Our data simply suggests that Nek2 kinase activity is not *essential* for mitotic-entry, and spindle-assembly in A549 cells. It is possible that other cell types, including cancer cell lines that have been shown to overexpress Nek2, may respond differently to Nek2 inhibition. A more thorough investigation of Nek2 inhibition, beyond the scope of this communication, will be required to further unravel the subtle nuances, and cell-type specificity of Nek2 function. However, we do want to stress that our negative results relating Nek2 inhibition to mitotic-entry and spindle assembly, suggest that compound **2** does not inhibit essential mitotic kinases at concentrations that give full inhibition of Nek2.

1.11 Conclusions

Herein, we presented the optimization of a oxindole scaffold into cell-active, irreversible inhibitors of Nek2 (Table 1-1). A model describing the essential features of these compounds as Nek2 inhibitors is presented in Figure 1-1. These compounds inhibit Nek2 through specific alkylation of active-site Cys22 both *in vitro* (Figure 1-2), and in cells (Table 1-1^b, Figure 1-4). Many of these compounds were also potent reversible inhibitors of Cdk1 (Table 1-1^d). Consistent with their activity as Cdk1 inhibitors, these compounds triggered rapid mitotic exit in monastrol arrested cells (Table 1-1^c, Figure 1-5). In contrast, while giving 92% inhibition of Nek2 in cells, compound **2** (Figure 1-1B), did not trigger the mitotic exit phenotype, and proved to be inactive against Cdk1 (Table 1-1^d, Figure 1-5). These results suggest that Nek2 kinase activity is not essential for maintenance of the SAC in A549 cells. The lack of activity of compound **2** as an inducer of mitotic exit also suggests that it does not inhibit other kinases known to be essential for maintenance of the SAC. Compound **2** also proved to selectively inhibit Nek2 over other kinases with the same active-site cysteine, including the mitotic regulator Plk1 (Figure 1-7). Further examination of compound **2** in A549 cells showed that Nek2 kinase activity is also not essential for the G2/M transition or mitotic spindle-assembly (Figure 1-6). These results support recent findings that endogenous Nek2 is involved in but not essential for these processes.⁵ Furthermore, these results suggest that compound **2** does not inhibit Plk1 in cells, a structurally related kinase that is essential for bipolar spindle assembly.³⁹

1.12 Experimental methods

Note: chemical synthesis is presented in Chapter 2

Mutagenesis and protein expression

Bacterial expression plasmids (pET22b, Invitrogen) containing N-terminally His6-tagged Nek2-T175A kinase domain (aa 1-271) and full length Nek2A-T175A, were previously reported.²² Expression plasmids for Nek2-C22V-T175A kinase domain, and full length Nek2A-C22V-T175A were prepared by performing quick change mutagenesis on the parent pET22b vectors using the following oligonucleotide primers: 5'-ggctctacggccgctccagaagatccggag-3' and 5'-ctccggatcttctggacgcgccgtaggagcc-3' (Operon). Expression and purification of all Nek2 protein constructs was carried out according to a previously reported procedure.²²

In vitro Nek2, Cdk1, Rsk2, and Plk1 kinase assays

Inhibitors were incubated for 30 min at room temperature with either Nek2A-T175A (15 nM), or Nek2A-C22V-T175A (15 nM), in 20 μ L of kinase reaction buffer (100 μ M ATP, 20 mM HEPES pH 7.5, 5 mM MgCl₂, 0.1 mM EDTA, 0.08 mg/mL BSA) with 3% DMSO. Then 5 μ L of kinase reaction buffer containing 0.5 mg/mL β -casein (Sigma), and 2 μ Ci of [γ -³²P]ATP (PerkinElmer) was added. Kinase reactions were allowed to proceed for 30 min at room temperature. Then 5 μ L of the mixture was blotted onto nitrocellulose membrane (Bio-Rad) that had been pre-washed with wash buffer (1 M NaCl, 0.1 % H₃PO₄) and dried. The membrane was washed three times with wash buffer and then dried under a heat lamp. The dry blots were exposed to a storage-phosphor screen (GE Healthcare), imaged using a Typhoon Scanner (GE Healthcare), quantified using Image Quant software (GE Healthcare), then processed and plotted using Excel

(Microsoft) and GraphPad (Prism) software. Reactions were run in triplicate, and reactions lacking the kinase were used for background control.

Cdk1 assays were conducted using the method for Nek2 with the following substitutions: Cdk1/Cyclin-B complex (2 nM, Millipore), 38 μ M ATP, 0.2 mg/mL histone-H1 (Millipore) as the substrate (Sigma), and 4 μ Ci of [γ -³²P]ATP.

Plk1 assays were conducted using the method for Nek2 with the following substitutions: Plk1 (8.5 nM, Millipore), 3.75% DMSO, 2.5 mg/mL dephosphorylated α -casein as the substrate (Sigma), and 0.75 μ Ci of [γ -³²P]ATP.

Rsk2 assays were conducted as follows. Inhibitors were incubated for 30 min at room temperature with 5 nM of active Rsk2 C-term kinase domain²³ in 15 μ L of kinase reaction buffer (100 μ M ATP, 20 mM HEPES pH 7.5, 5 mM MgCl₂, 0.02 mg/mL BSA) with 5% DMSO. Then 10 μ L of kinase reaction buffer containing 0.2 mg/mL BSA, 417 μ M of substrate peptide (RRQLFRGFSFVAK), and 3 μ Ci of [γ -³²P]ATP was added. Kinase reactions were allowed to proceed for 30 min at room temperature, then 5 μ L of the mixture was blotted onto P81 filtermat (Whatman). The filtermat was washed once with 10% acetic acid, then twice with 0.1% phosphoric acid, then dried under a heat lamp, and further processed exactly as for Nek2 kinase assays.

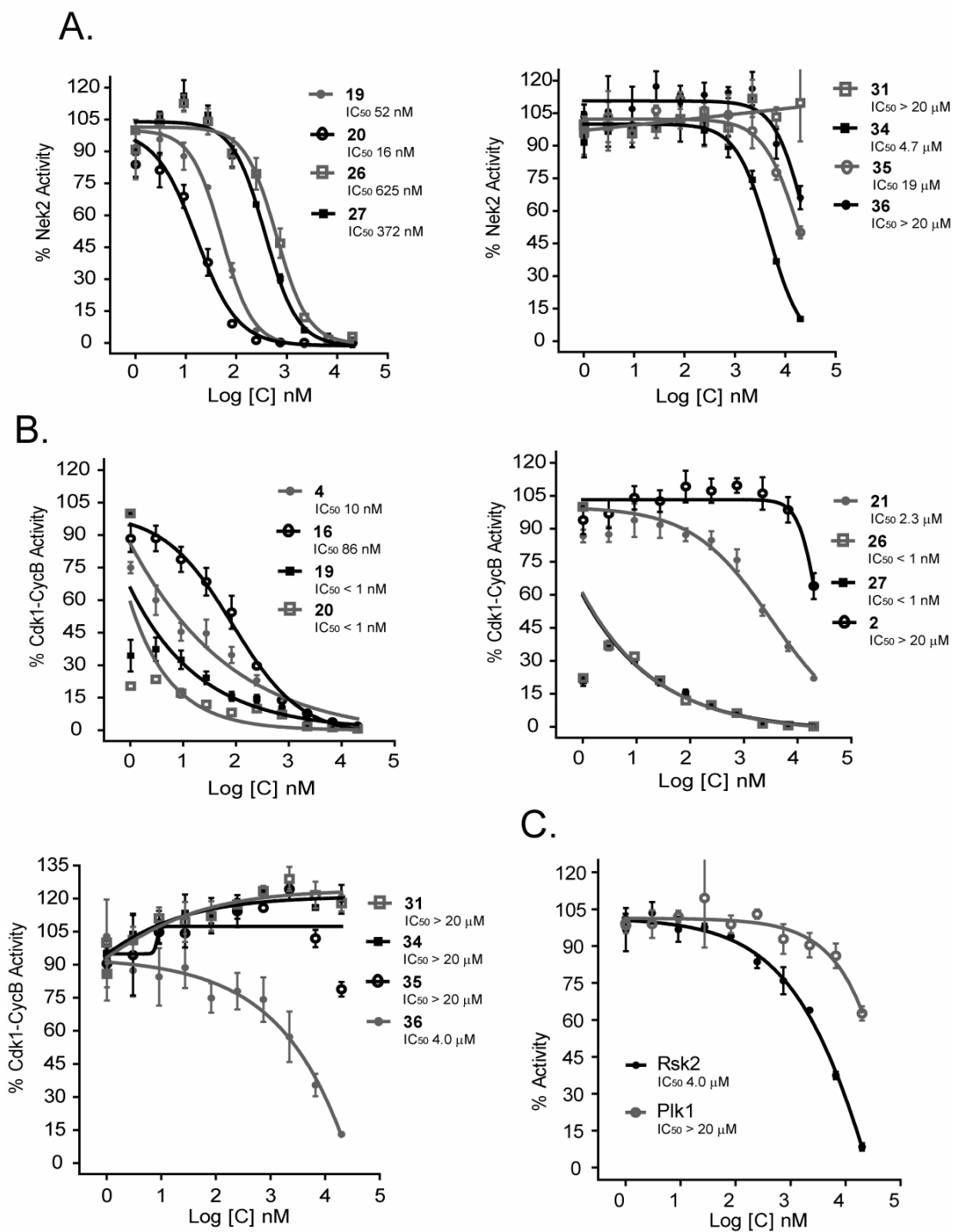


Figure 1-7. *In vitro* kinase assay dose response curves. (A) Nek2. (B) Cdk1/CyclinB. (C) Compound 2 against Rsk2 and Plk1.

Mass spectrometry-based covalent binding assays

Inhibitors (500 nM) were incubated with 50 nM of Nek2-T175A kinase domain, or Nek2-C22V-T175A kinase domain in pH 7.4 PBS (0.9 mM CaCl₂, 0.5 mM MgCl₂, 2.67 mM KCl, 1.47 mM KH₂PO₄, 138 mM NaCl, 8.06 mM NaH₂PO₄) with 5% DMSO for 5 h at room temperature, then quenched to pH 3 with 0.5 M HCl. The samples were then analyzed by LC-MS using linear gradient elution (5% to 95% acetonitrile with 0.2% formic acid over 3 min) on a Microtrap C18 protein column (Michrom Bioresources), with a Waters 1525 μ solvent delivery system, and a Waters LCT Premier ESI mass spectrometer for detection. The proteins or protein-adducts were detected as multiply charged ions, and computationally deconvoluted to provide a single mass for each species using MassLynx software (Waters).

General tissue culture

All cells were grown in growth media (high glucose DMEM, Gibco 11965) containing 10% fetal bovine serum (Culture Pure, Axenia Biologix), and penicillin/streptomycin (Gibco 15140) at 37 °C, in an atmosphere of 10% CO₂.

Preparation of poly-L-lysine coated cover slips

Poly-L-lysine coated cover slips were prepared by treating cover glass slips (Fisherbrand) with 1 M HCl at 40 °C for 4 h. The acid etched slips were then washed three times with water, rocked in 0.1% poly-L-lysine solution (Sigma) at room temperature for 1 h, washed three times with water, and then once with ethanol. The ethanol washed slips were then air dried and stored at 4 °C. These coated cover slips were sterilized under a germicidal lamp and washed with tissue culture media prior to use.

Generation of stable cell lines

Tetracycline-inducible Hek293 cell lines expressing C-terminal triple HA-tagged Nek2A (WT Nek2A-3HA or Nek2A-C22V-3HA), were made using the Invitrogen Flp-in HEK293 T-REx in-cell FRT recombination system. This was achieved according to the manufacturers instructions by co-transfecting Flp-in HEK293 T-REx cells (Invitrogen) with pOG44 (Invitrogen), and the expression plasmid pCDNA5/FRT/TO (Invitrogen) containing the Nek2A-3HA or Nek2A-C22V-3HA constructs, followed by hygromycin selection. The expression plasmids were generated from a Gateway donor vector (pDONR221, Invitrogen) that contained WT Nek2A-3HA or Nek2A-C22V-3HA. This was made using PCR to amplify WT or C22V Nek2A, and install Gateway recombination sequences and a C-terminal triple HA-tag. The PCR reaction used the following three oligonucleotide primers together: Nek2 N-terminal primer, 5'-
ggggacaagttgtacaaaaagcaggtgcggccgcaccatgccttccgggctgagg-3'; Nek2 C-terminal primer, 5'-
cgcatagtcagggacgtcataaggatatccagcgtaatctggaacatcataaggatatccgcgatgccaggatctgtc-3';
C-terminal-primer primer, 5'-
ggggaccactttgtacaagaaagctgggtggggatcctaagcgtaatctggaacatcgtatggtagcccgcgatagtcaggga
cgtcacat-3'. BP-clonase (Invitrogen) mediated recombination was then used to install the Nek2-3HA PCR product into pDONR221. LR-clonase (Invitrogen) mediated recombination was then used to transfer the Nek2A-3HA constructs from pDONR221 to a version of pCDNA5/FRT/TO (Invitrogen) that had previously been modified to contain the appropriate Gateway recombination sequences.

Immunoprecipitation kinase assays

For endogenous Nek2 IP kinase assays (Table 1-1^b, Figure 1-8), A549 cells were plated at 400000/well in six well plates (Nunc) and grown for 20 h. Three wells per condition were treated with 5 μ M of our Nek2 inhibitors in 2 mL/well of media for 45 min, washed twice with DPBS (Gibco), then immediately stored at -80 °C as dry mono-layers. Alternately: three wells per condition were arrested at the G2/M border for 20 h with 5 μ M of RO3306, then treated with 5 μ M of our Nek2 inhibitors plus 5 μ M of RO3306 in 2 mL/well of media for 30 min, washed twice with DPBS (Gibco), and immediately stored at -80 °C as dry mono-layers. Plates of cells were then thawed at room temperature for 5 minutes, treated with 200 μ L/well of ice cold lysis buffer (50 mM HEPES pH 7.6, 150 mM NaCl, 0.1% Triton X100, 1 mM DTT, 1x Roche PhosSTOP phosphatase inhibitors) containing protease inhibitors (Complete, Roche), then sonicated for 30 sec by floating the plate on a room temperature water bath. The three lysates from a single condition were combined and clarified for 30 min (20000 g's) at 4 °C. Samples of the clarified lysates were analyzed for total protein concentration by Bradford (Bio-Rad), and normalized for protein content with lysis buffer. Then 600 μ L of normalized lysate was incubated with 0.4 μ g of anti-Nek2 antibody (H-235, Santa Cruz) with rocking for 1.5h at 4 °C. Then 30 μ L of protein-A Dynabeads (Invitrogen) were added and rocking was continued for an additional 1.5 h at 4 °C. The beads were then washed (200 μ L per wash for 5 min with rocking at 4 °C) with lysis buffer, lysis buffer containing 0.5 M NaCl, then twice with kinase buffer (20 mM HEPES pH 7.5, 5 mM MgCl₂, 0.1 mM EDTA, 1 mM DTT, 1x PhoshSTOP). The beads were suspended in the last wash buffer and divided in half. One half was used for Nek2 western blot analysis, and the other half

was used for a kinase assay. For the kinase assay, after removal of the wash buffer the beads were incubated in 30 μ L of kinase buffer containing 0.5 mg/mL β -casein (Sigma), 100 μ M ATP, and 0.4 μ Ci of [γ - 32 P]ATP for 1 h at room temperature, then quenched with 8 μ L of 5x sample buffer (300 mM TRIS pH 6.8, 10% SDS, 50% glycerol, 0.01% bromophenol blue, 0.5 M DTT). Substrate proteins were resolved by SDS-PAGE then analyzed by coomassie staining, and autoradiography. Coomassie-stained gel images were captured using an Alpha-Imager (Alpha Innotech), and autoradiography was performed exactly as for *in vitro* kinase assays.

IP kinase assays of overexpressed HA-tagged Nek2A from tetracycline inducible Hek293 cell lines were carried out exactly as for endogenous Nek2 with the following changes. Tetracycline inducible Hek293 cell lines expressing either WT Nek2A-3HA or Nek2A-C22V-3HA were plated at 630000 cells per well in six well plates (Nunc) grown for 20 h, then treated with 1 μ g/mL for tetracycline for 7 h. One well per condition was then treated with compound **2** in 2 mL of media for 45 min, washed twice with DPBS (Gibco), then immediately stored at -80 $^{\circ}$ C a dry mono-layer. A single well of cells and 200 μ L of total normalized lysate was used for the IP process. The IP process used 1.6 μ g of 12CA5 anti-HA antibody (Roche).

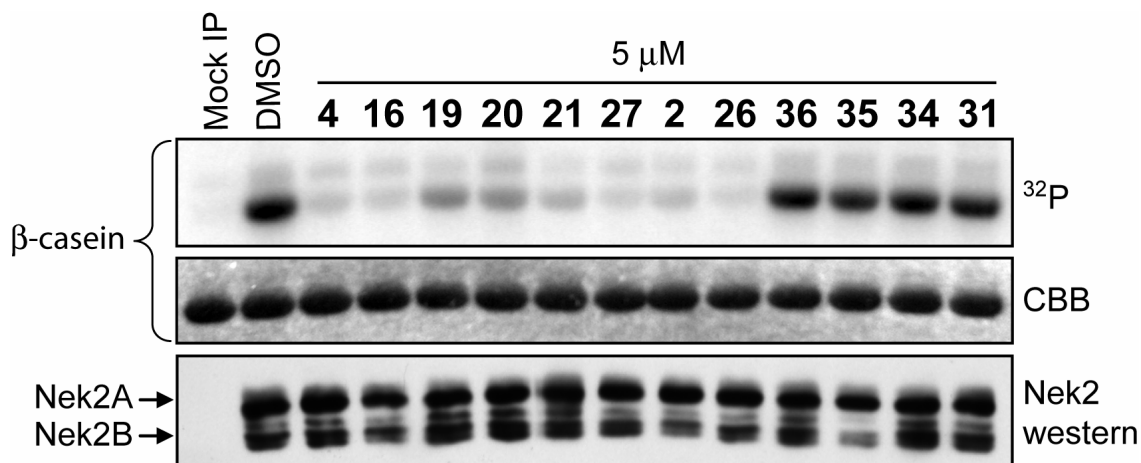


Figure 1-8. Endogenous Nek2 IP kinase assays from A549 cells that were treated with the indicated compounds for 45 minutes.

Western blot analysis

After removal of the wash buffer, beads from the immunoprecipitation were suspended in 30 μ L of kinase buffer (20 mM HEPES pH 7.5, 5 mM MgCl₂, 0.1 mM EDTA, 1 mM DTT, 1x PhoshSTOP). The bead suspension was then treated with 8 μ L of sample buffer (300 mM TRIS pH 6.8, 10% SDS, 50% glycerol, 0.01% bromophenol blue, 0.5 M DTT) containing NuPAGE Antioxidant (Invitrogen), and heated to 65 °C for 5 min. Samples were resolved on NuPAGE Novex Bis-Tris 4-12% gradient gels (Invitrogen), transferred to nitrocellulose membrane (Bio-Rad), blocked with 5% milk in TBST (50 mM Tris pH 7.6, 150 mM NaCl, 0.05% tween 20) for 1 h at room temperature, then washed three times with TBST.

For endogenous Nek2 westerns, membranes were then treated with 1:500 anti-Nek2 antibody (610593, BD Biosciences) in AB-Dil (50 mM Tris pH 7.6, 150 mM NaCl, 0.05% tween 20, 0.1% NaN₃, 2% BSA) for 1 h at room temperature, washed three times with TBST, then treated with 1:1000 anti-mouse-HRP antibody (Santa Cruz Biotech) in

5% milk-TBST for 30 minutes at room temperature. Blots were then washed three times with TBST, and detected using Supersignal West Femto Substrate (Thermo Scientific) and autoradiography film (Lab Scientific).

For Nek2-3HA westerns, membranes were then treated with 1:2000 anti-HA antibody (SAB4300603, Sigma) in AB-Dil for 1 h at room temperature, washed three times with TBST, then treated with 1:1000 anti-rabbit-HRP antibody (Santa Cruz Biotech) in 5% milk-TBST for 30 minutes at room temperature. Blots were then washed three times with TBST, and detected using Supersignal West Pico Substrate (Thermo Scientific) and autoradiography film (Lab Scientific). Images of all western blots were captured using a Alpha-Imager (Alpha Innotech).

Mitosis assays in A549 cells

For mitotic exit during monastrol-arrest assays, A549 cells (180000 cells in 1 mL media) were plated on 18 mm round poly-lysine coated cover slips in 12-well plates (Nunc), grown for 24 h, then treated with 100 μ M of monastrol in 1 mL of media for 18 h. The monastrol arrested cells were then treated with 5 μ M of our Nek2 inhibitors in the presence of 100 μ M monastrol in 1 mL of media for 45 min. The cells were then processed for immunofluorescence microscopy.

For inhibition of Nek2 at the G2/M transition, A549 cells (180000 cells in 1 mL media) were plated on 18 mm round poly-L-lysine coated cover slips in 12-well plates (Nunc), grown for 24 h, then treated with 5 μ M of RO3306 for 20 h. These RO3306 arrested cells were treated with 5 μ M of our Nek2 inhibitors for 30 min in the presence of 5 μ M RO3306, washed twice with plain media, then treated with 10 μ M of MG132 for 1 h. The cells were then processed for immunofluorescence microscopy.

Immunofluorescence microscopy

After removal of growth media, cells were formaldehyde-fixed for 10 min at room temperature with fixing buffer (80 mM PIPES pH 6.8, 1 mM MgCl₂, 1 mM EGTA, 0.1% Triton X100, 4% formaldehyde), and then blocked for 30 min with blocking buffer (20 mM TRIS pH 7.4, 150 mM NaCl, 0.1% Triton X100, 2% BSA, 0.1% sodium azide). Cells were then stained with 1:200 anti-phospho-Ser10 histone-H3 antibody (Millipore) in blocking buffer for 1h, washed with TBS-TX100 (20 mM TRIS pH 7.4, 150 mM NaCl, 0.1% Triton X100), and then stained with a mixture of 1:500 Alexa Flour-A594 conjugated anti-rabbit antibody (Molecular Probes) and 1:500 anti- α -tubulin FITC-conjugated antibody (Sigma), in blocking buffer for 1 h. The cells were then washed with TBS-TX100 and stained with 500 ng/ μ L of DAPI (Sigma) in TBS-TX100. Following DAPI staining the cells were washed with TBS-TX100 and mounted in Vectashield mounting media (Vector Labs). Images were captured using a Axiovert 200 inverted fluorescence microscope (Carl Zeiss) equipped with a C4742-98 CCD camera (Hamamatsu). Images were acquired and processed using Slide Book (Intelligent Imaging Innovations), and Photoshop software (Adobe).

Chapter 2

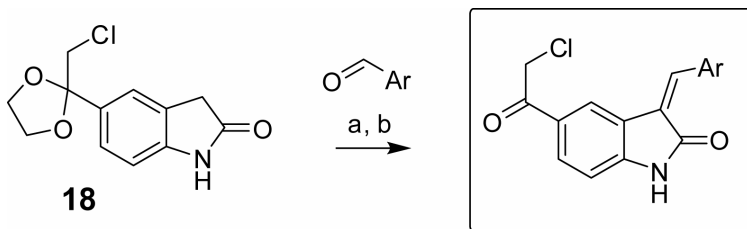
Synthesis of additional Nek2 inhibitors and oxindole scaffolds

2.1 Abstract

This chapter covers the synthesis of all novel organic compounds in this manuscript. Synthetic schemes and discussions for compounds **1-36** are presented in Chapter 1. Synthetic schemes for compounds **38-144**, and the experimental details for the synthesis of compounds **2-144** are presented in this chapter. The actual ^1H NMR spectra of compounds **2-144** are presented in Appendix B.

2.2 Synthesis of 5-chloromethylketone oxindole Nek2 inhibitors

Scheme 2-1. Synthesis of 5-chloromethylketone oxindole Nek2 inhibitors.^a



^aReagents and conditions: (a) Ar-CHO (0.9 to 1.5 equiv), piperidine (0.3 equiv), THF, 75 °C; (b) aq. HCl (excess), THF, rt. Reaction times for (a) and (b) are presented in Table 2.

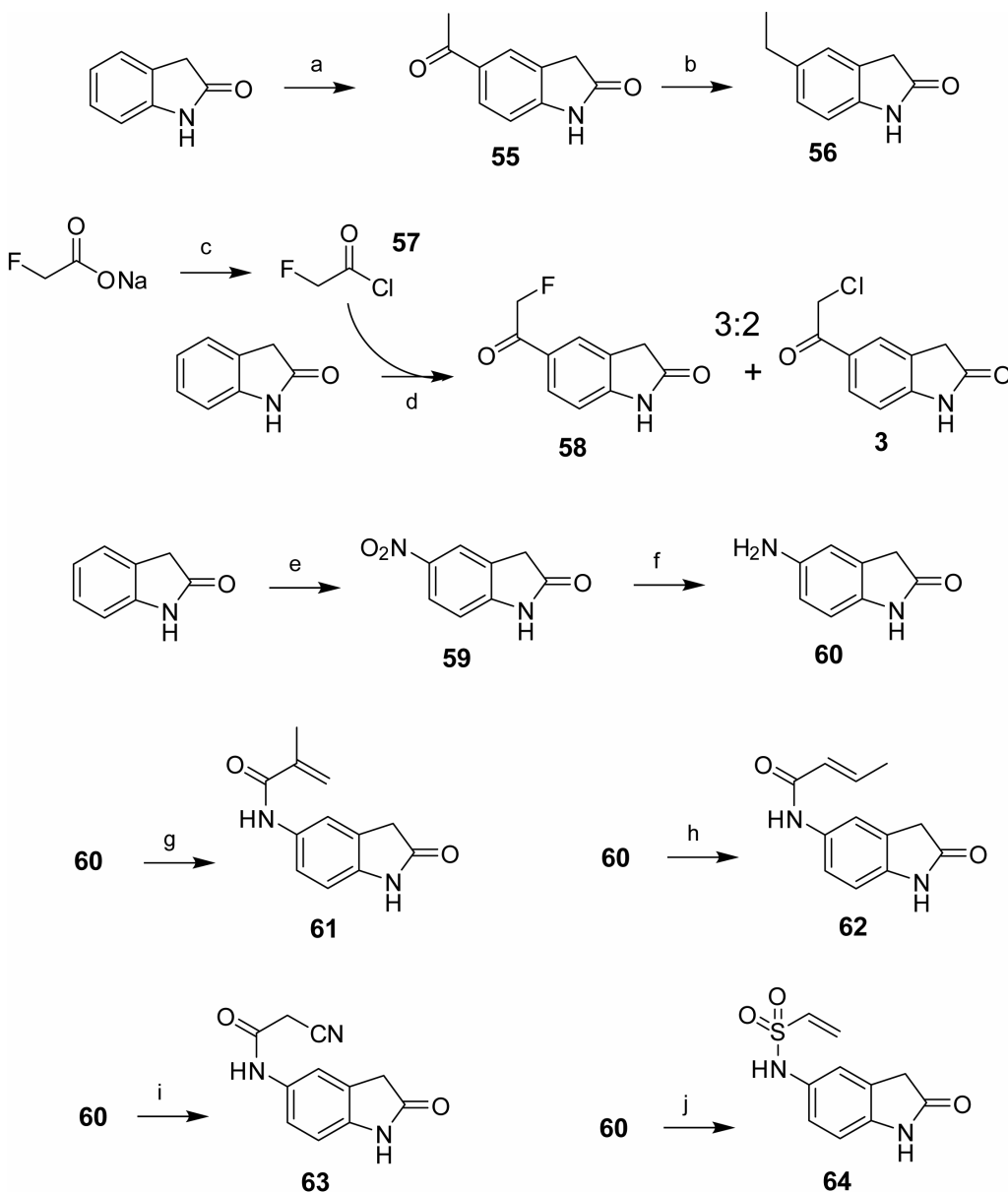
Table 2-1. 5-Chloromethylketone inhibitors synthesized according to Scheme 2-1.

Compound	Ar	Number of E/Z isomers	Reaction time a, b (h)	Yield (%)	Compound	Ar	Number of E/Z isomers	Reaction time a, b (h)	Yield (%)
38		1	7, 5	12 ^c	47		2 ^{f,g}	37, 20	27
39		1	40, 20	28	48		1 ^f	37, 18	14
40		1	40, 20	46 ^d	49		2 ^{h,g}	37, 18	45
41		1	21, 2	45	50		2 ^{h,g}	18, 18	32
42		1	20, 3	37 ^d	51		1 ^h	18, 18	43
43		2	17, 22	22 ^e	52		1 ^h	18, 18	9
44		1	17, 23	43	53		1	17, 23	17
45		1	17, 23	38	54		1	1, 18	42 ⁱ
46		2	17, 23	16 ^e					

Reaction times (a, b) refer to Scheme 5. ^cIsolated as the free base by washing with 1 N NaOH. ^dIsolated directly as the HCl salt. ^eCombined yield, isolated directly as a mixture of E and Z isomers. ^fIsolated as the more polar (slower running) isomer by silica gel chromatography prior to hydrolysis of the protecting group. ^gAfter isolation of a single isomer, the compound equilibrated back to a mixture of E/Z isomers. ^hIsolated as the less polar (faster running) isomer by silica gel chromatography prior to hydrolysis of the protecting group. ⁱ1.8 Equiv of piperidine was used.

2.3 Synthesis of 5-substituted oxindoles

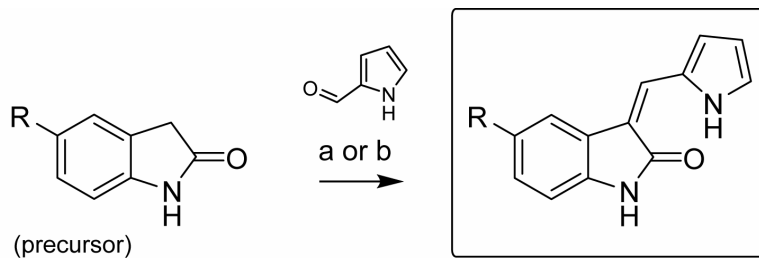
Scheme 2-2. Synthesis of 5-substituted oxindoles.^a



^aReagents and conditions: (a) AlCl_3 (6 equiv), acetyl chloride (1.3 equiv), CS_2 , reflux 4 h (85%); (b) triethylsilane (1.9 equiv), neat TFA, 0 °C to rt, 21 h (65%); (c) PCl_5 (1.1 equiv), reflux, 1 h (89%); (d) AlCl_3 (5 equiv), fluoroacetyl chloride (1.5 equiv), CS_2 , rt, 5 min (total yield of mixed products 61%); (e) HNO_3 (excess), H_2SO_4 , 0 °C, 30 min (69%); (f) cat. Pd/C, 1 atm H_2 , methanol, rt, 19 h (80%); (g) 2-methacryloyl chloride (2 equiv), pyridine (1.5 equiv), THF, 0 °C to rt, 1 h (15%); (h) crotonoyl chloride (1.3 equiv), 0 °C to rt, 20 min (35%); (i) cyanoacetic acid (1.1 equiv), EDC (2 equiv), acetonitrile, rt, 30 min (62%); (j) 2-chloroethanesulfonyl chloride (2.5 equiv), DIPEA (3 equiv), THF, 0 °C, 1 h (56%).

2.4 Synthesis of oxindole inhibitors substituted at the 5-position

Scheme 2-3. Synthesis of oxindole inhibitors substituted at the 5-position.^a

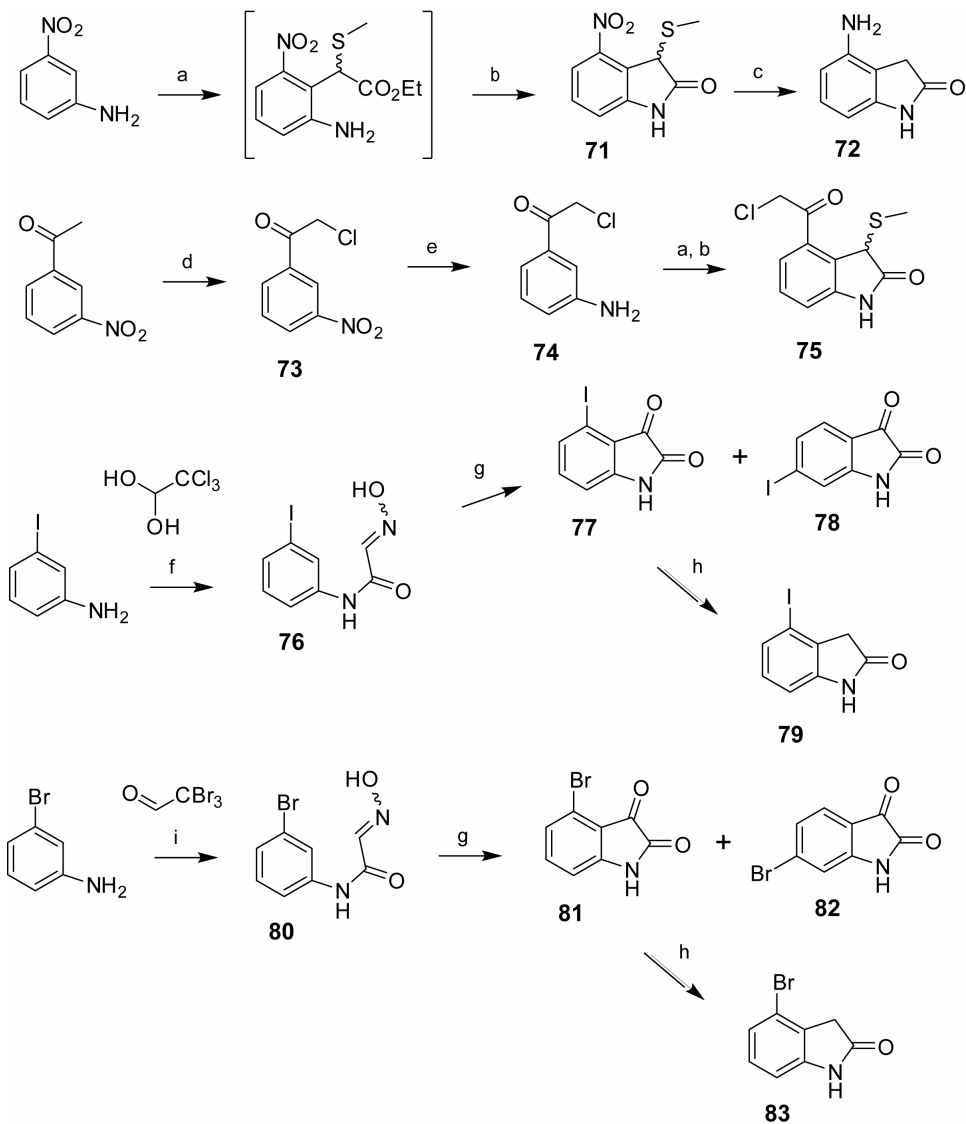


Compound	R	Method	Precursor	Reaction time (h)	Yield (%)
65		a	56	2	37
66		a	55	4	60
67		a	58	3	19
68		b	61	2	47
69		b	62	2	90
70		b	64	2	47

^aReagents and conditions: (a) Pyrrole-2-CHO (1.3 to 5 equiv), piperidine (0.1 to 0.2 equiv), EtOH, reflux; (b) pyrrole-2-CHO (10 equiv), piperidine (0.2 equiv), THF, 75 °C.

2.5 Synthesis of 4-substituted oxindoles

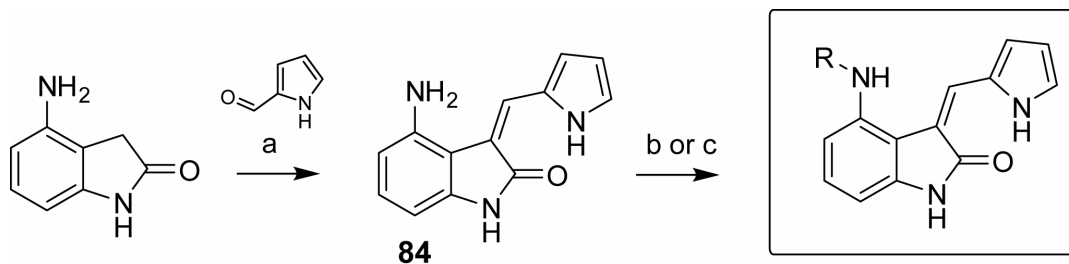
Scheme 2-4. Synthesis of 4-substituted oxindoles.^a



^aReagents and conditions: (a) one pot: $t\text{BuOCl}$ (1 equiv), DCM, $-60\text{ }^\circ\text{C}$, 10 to 30 min, then $\text{CH}_3\text{SCH}_2\text{CO}_2\text{Et}$ (1 equiv), DCM, $-50\text{ }^\circ\text{C}$, 1 h, then Et_3N (1 equiv), DCM, $-50\text{ }^\circ\text{C}$ to rt, 1.5 to 5 h; (b) aq. HCl , Et_2O , rt, 14 to 18 h (yield **71** 54%, yield **75** 20% over four steps, both gave single regioisomers); (c) Zn^0 (excess), glacial acetic acid and HCl , rt, 1.5 h (29%); (d) N -chlorosuccinimide (1.4 equiv), $p\text{TSA}\cdot\text{H}_2\text{O}$ (1.4 equiv), acetonitrile, 18 h (100%); (e) SnCl_2 (4 equiv), EtOH , 22 h (87%); (f) chloral hydrate (1.1 equiv), hydroxylamine hydrochloride (2.6 equiv), HCl (1.04 equiv), water / Na_2SO_4 , reflux, 45 min (carried on crude); (g) neat H_2SO_4 , $80\text{ }^\circ\text{C}$, 10 min (yield **77** 10%, yield **78** 2%, yield **81** 47%, yield **82** 25%); (h) neat hydrazine- H_2O (23 to 47 equiv), $125\text{ }^\circ\text{C}$, 15 min (yield **79** 72%, yield **83** 65%); (i) CBr_3CHO (1.3 equiv), hydroxylamine hydrochloride (3.8 equiv), HCl (1.06 equiv), water / Na_2SO_4 , reflux, 10 min (100%).

2.6 Synthesis of oxindole inhibitors with electrophiles at the 4-position

Scheme 2-5. Synthesis of oxindole inhibitors with electrophiles at the 4-position.^a

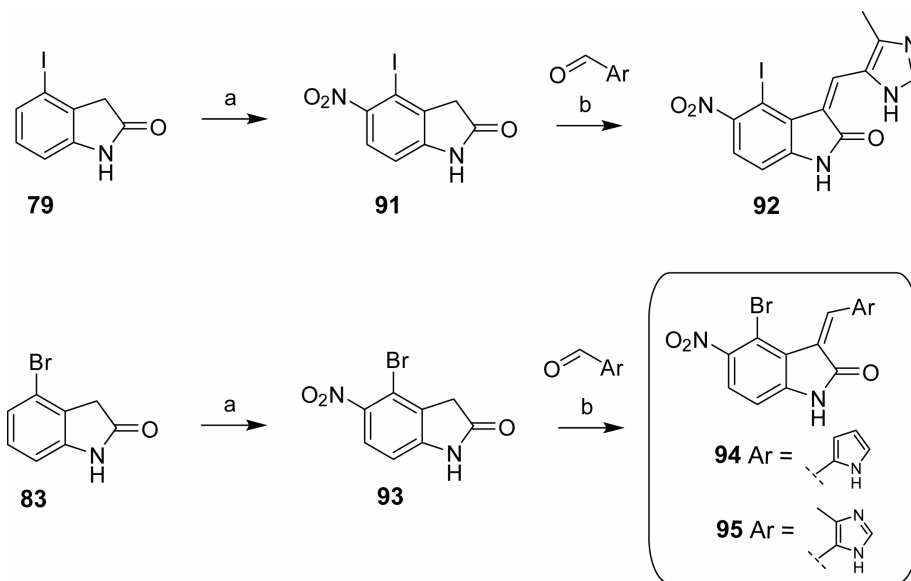


Compound	R	Method	Reaction time (min)	Yield (%)
85		b	30	65
86		b	60	59
87		b	120	low
88		b	30	90
89		c	15	62
90		b	30	67

^aReagents and conditions: (a) Pyrrole-2-CHO (1.1 equiv), piperidine (0.2 equiv), mol. sieves, THF, 75 °C, 46 h (66%); (b) R-Cl (1.2 to 2 equiv), pyridine (1.2 to 2 equiv), THF, 0 °C; (c) cyanoacetic acid (1.1 equiv), EDC (2 equiv), acetonitrile, rt, 15 min.

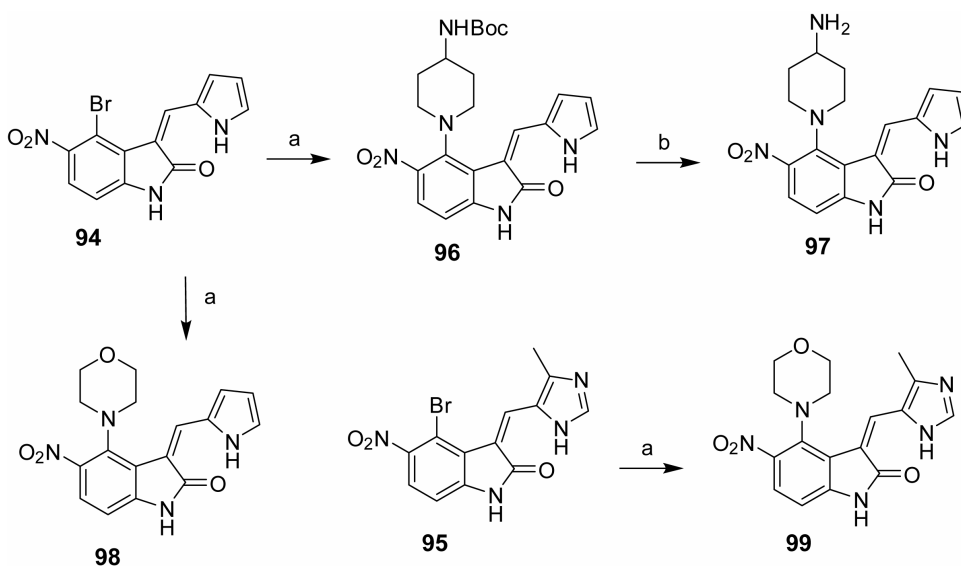
2.7 Synthesis of 4,5-di-substituted oxindole inhibitor scaffolds

Scheme 2-6. Synthesis of 4,5-di-substituted oxindole inhibitor scaffolds.^a



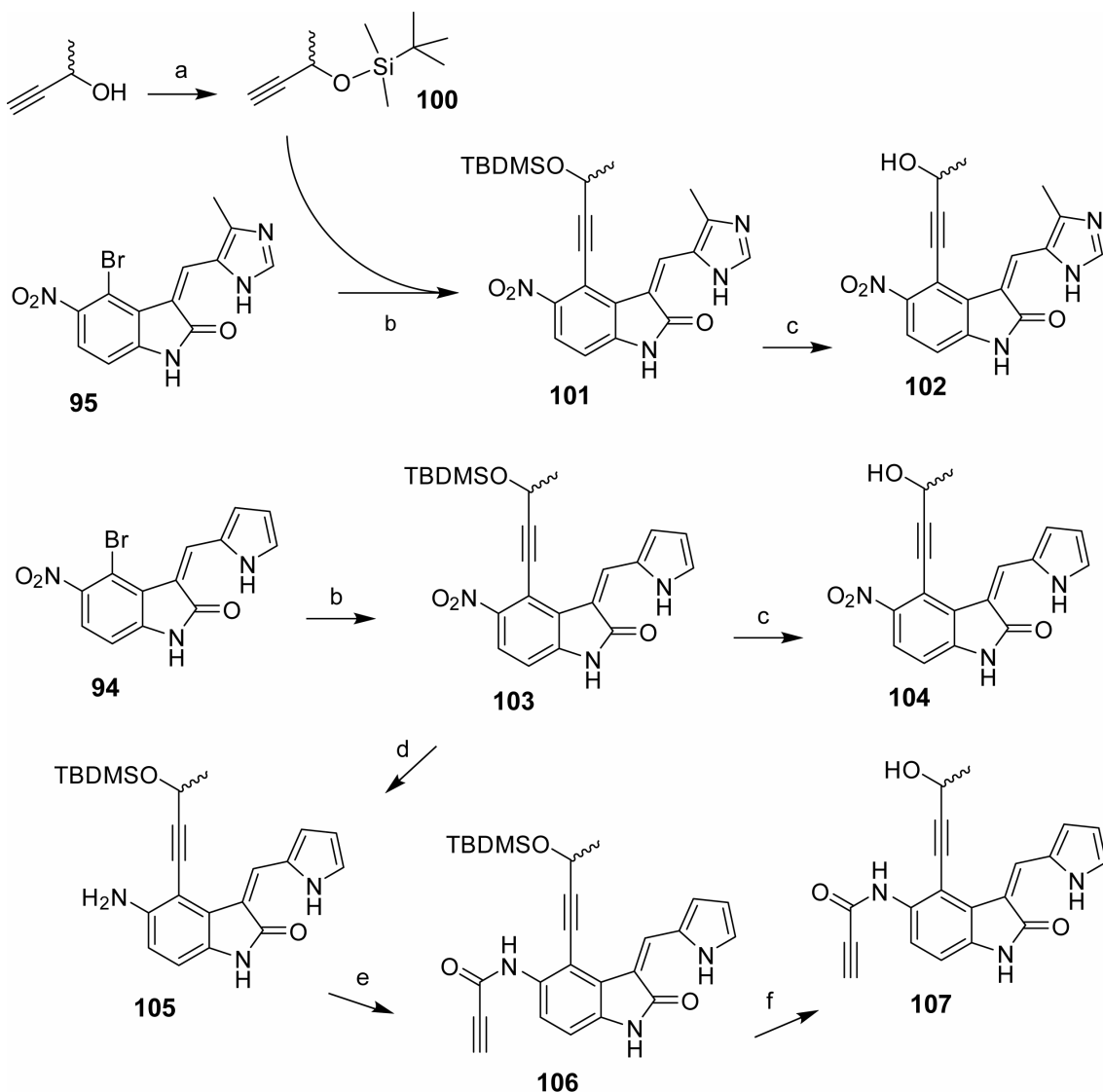
^aReagents and conditions: (a) HNO₃ (excess), H₂SO₄, -5 °C, 30 to 45 min (yield **91** 82%, yield **93** 76%); (b) Ar-CHO (1.2 equiv), piperidine (0.2 equiv), THF, 75 °C, 4 to 30 h (yield **92** 52%, yield **94** 63%, yield **95** 81%).

Scheme 2-7. Synthesis of oxindole inhibitor scaffolds with tertiary amines in the 4-position.^a



^aReagents and conditions: (a) DIPEA (23 equiv), NHR₂ (10 equiv), DMF or dioxane, 120 °C, 7 to 18 h (yield **96** 60%, yield **98** 15%, yield **99** 24%). (b) anhydrous HCl (excess), methanol, rt, 2 h (100%).

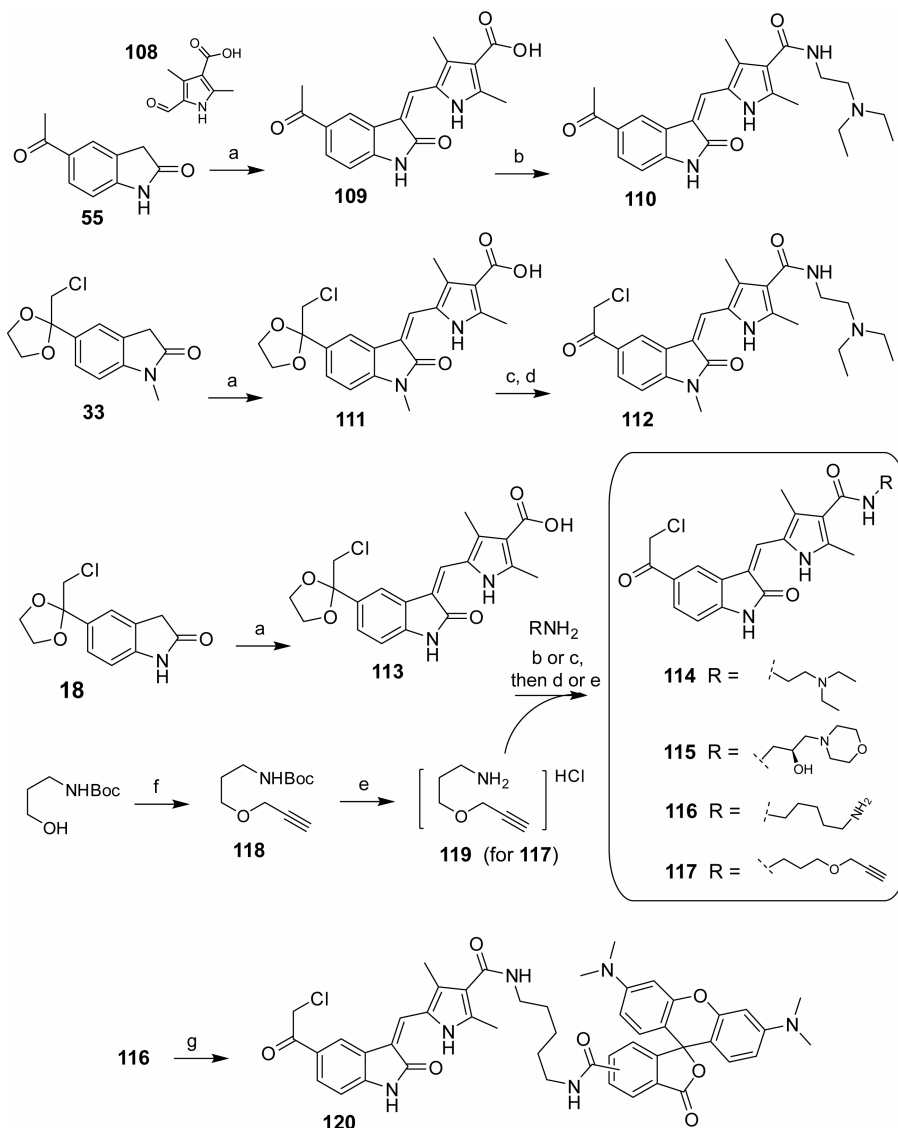
Scheme 2-8. Synthesis of oxindole inhibitor scaffolds with an alkyne in the 4-position.^a



^aReagents and conditions: (a) TBDMS-Cl (1 equiv), imidazole (2 equiv), DMF, rt, 5 h (68%); (b) **100** (2.5 equiv), (Ph₃P)₄Pd (0.01 to 0.1 equiv), CuI (0.1 equiv), Et₃N (70 to 140 equiv), DMF, 85 °C, 3 to 5 h (yield **101** 49%, yield **103** 20%); (c) HCl (excess), THF, rt, 2 h (yield **102** 49%, yield **104** 28%); (d) Zn⁰ (excess), sat. aq NH₄Cl, THF, 80 °C, 30 min (100%); (e) EDC (4 equiv), propionic acid (6 equiv), HOBt (1 equiv), DMF/acetonitrile, rt, 30 min (25%); (f) HCl (excess), THF, rt, 4 h (26%).

2.8 Synthesis of 5-acyl sunitinib analogs and chloromethylketone Nek2 active site-directed probes

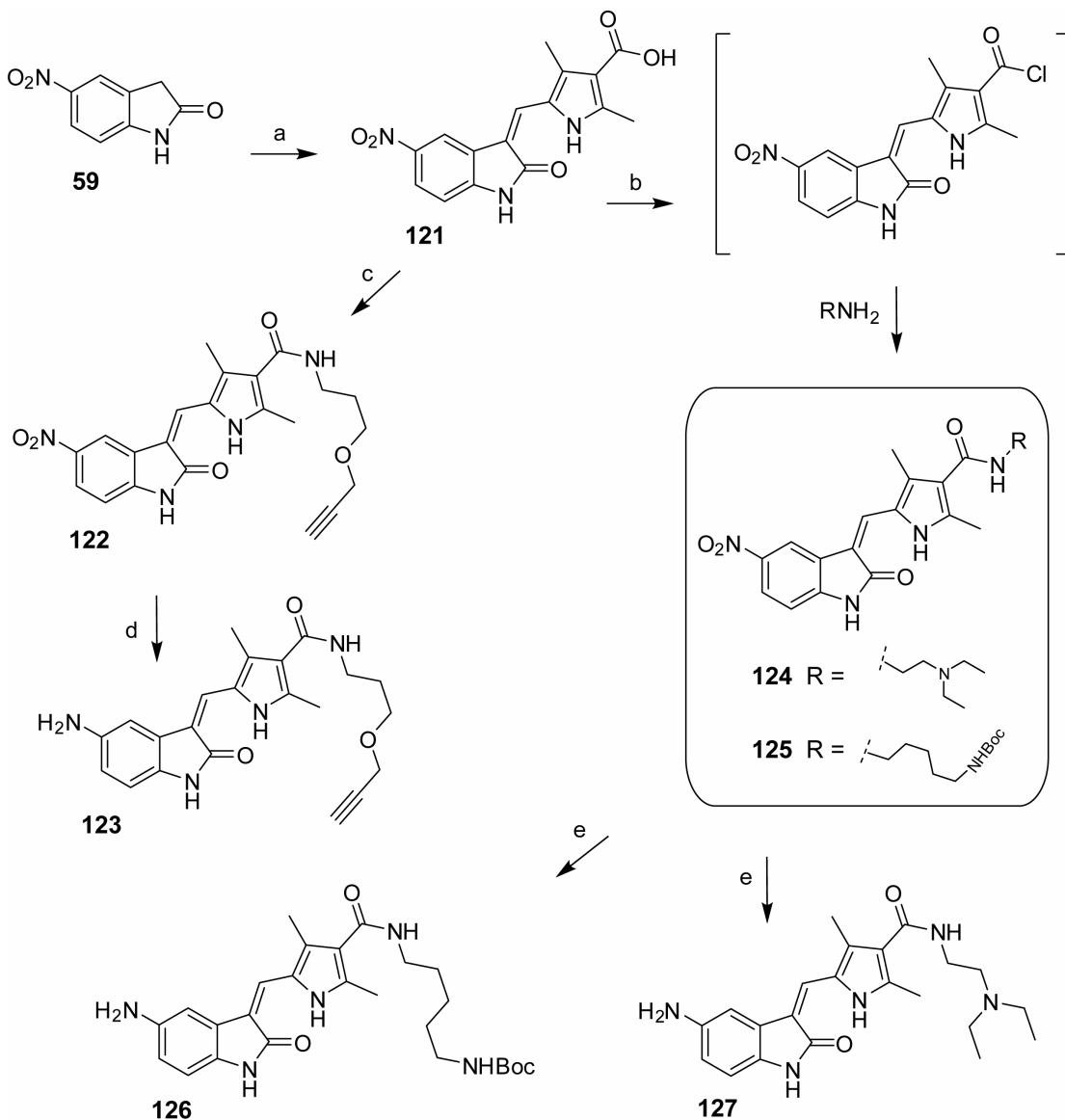
Scheme 2-9. Synthesis of 5-acyl sunitinib analogs and chloromethylketone Nek2 active site-directed probes.^a



^aReagents and conditions: (a) **108** (1 to 1.5 equiv), piperidine (1.2 to 1.8 equiv), THF, 75 °C, 2 to 24 h, (yield **109** 78%, yield **111** 53%, yield **113** 52%); (b) EDC (3 equiv), R-NH₂ (3 equiv), HOBT (1.5 equiv), DIPEA (3 equiv) DMF, rt, 2 to 13 h (yield **110** 51%); (c) EDC (2 equiv), R-NH₂ (1.2 to 2 equiv), HOBT (1 equiv), Et₃N (3 equiv) DMF, rt, 16 to 18 h; (d) aq HCl (excess), THF, rt, 2 to 18 h (for two steps, yield **112** 62%, yield **114** 76%, yield **115** 45%, yield **117** 53%); (e) anhydrous HCl, methanol, 2 h, rt, (yield for two steps **116** 75%, yield **119** 60%); (f) NaH (1.1 equiv), propargyl bromide (1.1 equiv), THF, rt, 24 h (53%); (g) rhodamine-NHS ester (1 equiv), DIPEA (3 equiv), DMF, 3 h.

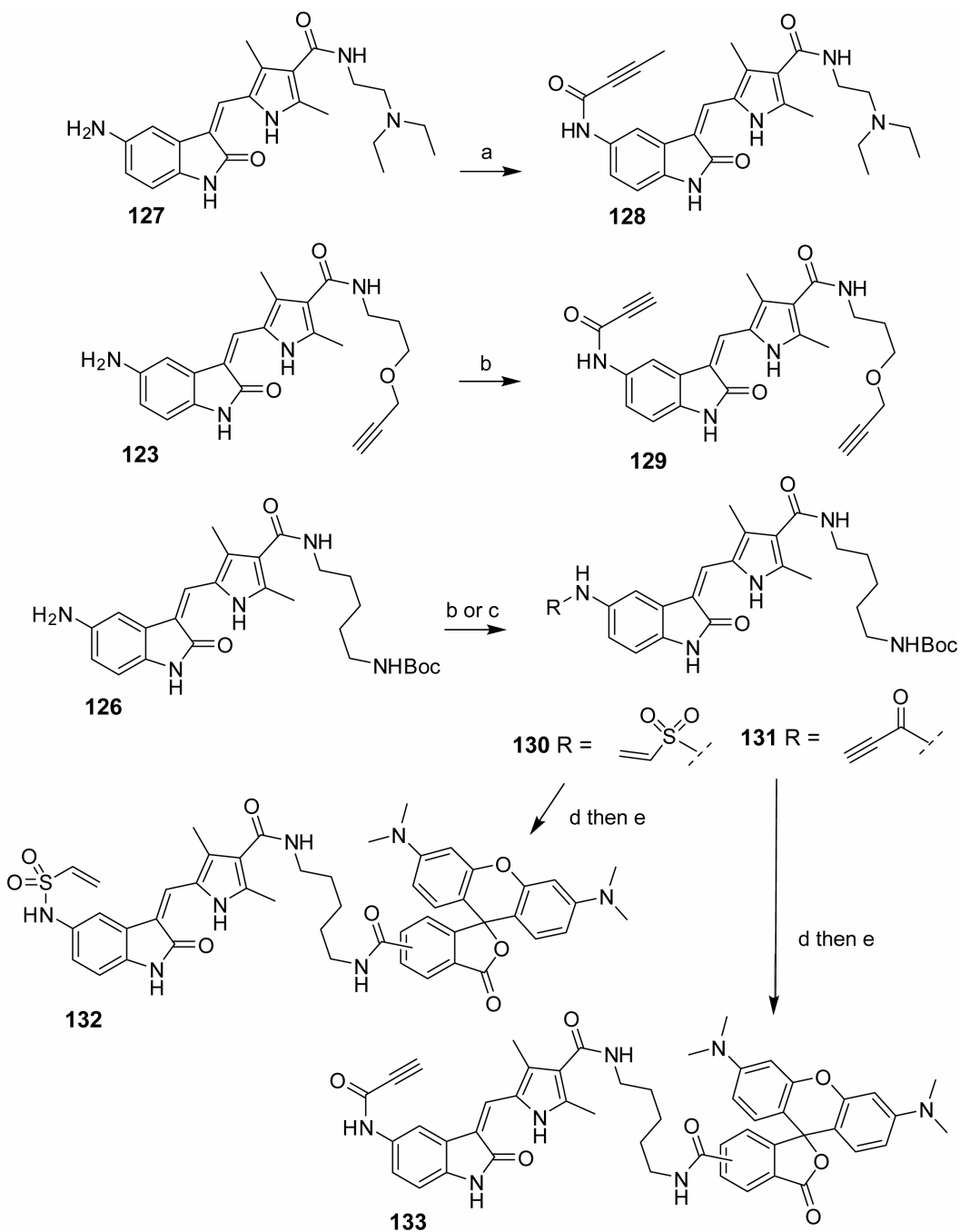
2.9 Synthesis of propynamide and vinyl sulfonamide-based Nek2 probes, and sunitinib analogs

Scheme 2-10. Synthesis of 5-amino sunitinib analogs.^a



^aReagents and conditions: (a) **108** (1.1 equiv), piperidine (1.4 equiv), THF, 75 °C, 18 h, (85%); (b) SOCl_2 (45 equiv), THF, reflux, 2 h, then RNH_2 (4.6 equiv), DIPEA (for **125** only, 2.5 equiv), THF, rt, 2 to 4 h (yield **124** 74%, yield **125** 64%); (c) EDC (3 equiv), $\text{R-NH}_3\text{Cl}$ (4 equiv), HOBT (1 equiv), DIPEA (3 equiv) DMF, rt, 20 h (53% \rightarrow 40); (d) Zn^0 (excess), sat. aq NH_4Cl , THF, rt, 18 h (97%); (e) cat. Pd/C, 1 atm H_2 , methanol, rt, 19 h (yield **126** 90%, yield **127** 96%).

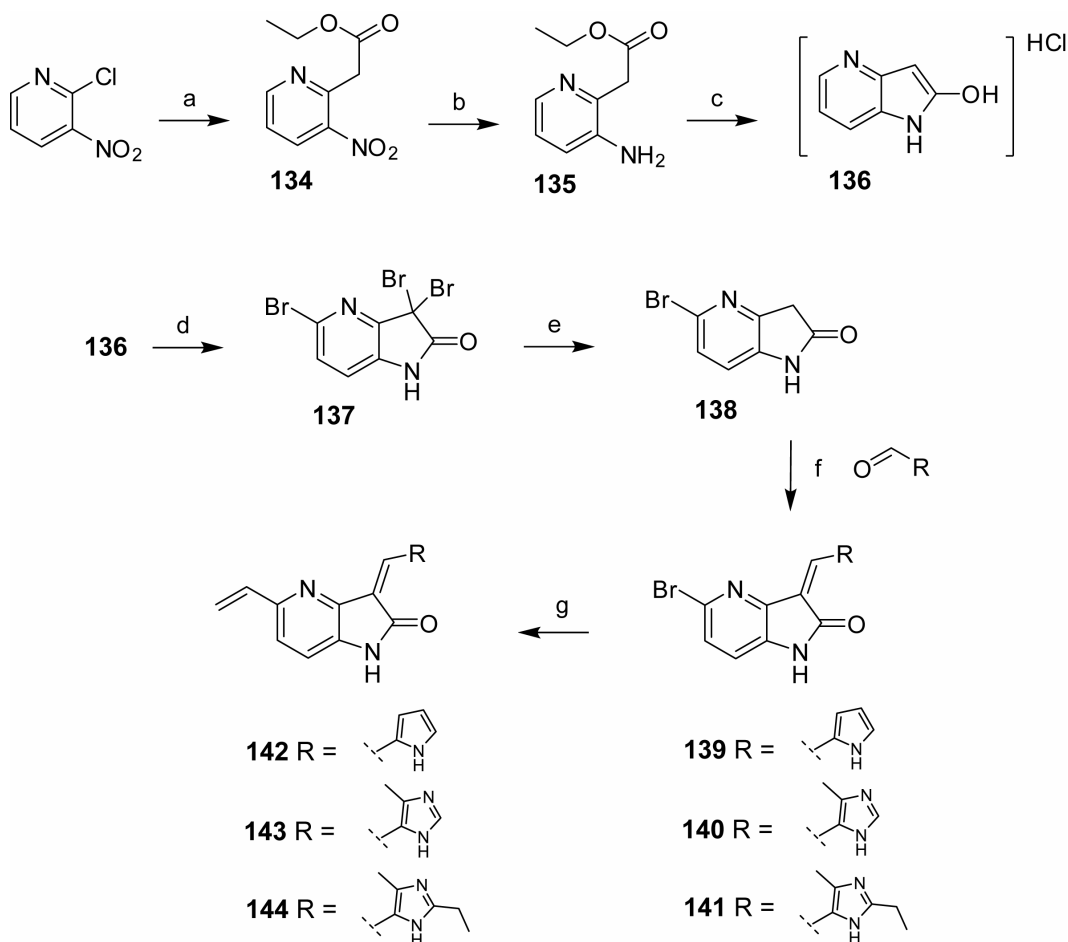
Scheme 2-11. Synthesis of propynamide and vinyl sulfonamide Nek2 probes, and sunitinib analogs.^a



^aReagents and conditions: (a) 2-Butynoic acid (6 equiv), EDC (4 equiv), HOBT (1 equiv), DIPEA (3 equiv), DMF/acetonitrile, rt, 2 h (34%); (b) propionic acid (1.2 to 6 equiv), EDC (2 to 4 equiv), HOBT (for **129** only, 1 equiv), DMF/acetonitrile, rt, 2 to 3 h (yield **129** 53%, yield **131** 49%); (c) 2-chloroethanesulfonyl chloride (2.5 equiv), DIPEA (3 equiv), THF, 0 °C to rt, 18 h (61%); (d) TFA (excess), DCM, rt, 2 h; (e) rhodamine-NHS ester (0.9 to 1.1 equiv), DIPEA (3 equiv), DMF, 5 to 30 h.

2.10 Synthesis of the 5-substituted 4-azaoxindole inhibitor scaffold

Scheme 2-12. Synthesis of the 5-substituted 4-azaoxindole inhibitor scaffold.^a



^aReagents and conditions: (a) Ethylacetate (2 equiv), NaH (2 equiv), DMF, rt to 70 °C, 2.5 h (36%); (b) cat. Pd/C, 1 atm H₂, ethanol, rt, 24 h (77%); (c) aq HCl (excess), rt, 5 days (95%); (d) Br₂ (10 equiv), t-BuOH, rt, 6 days (75%); (e) Zn⁰ (excess), sat. aq NH₄Cl, THF, rt, 24 h (80%); (f) R-CHO (1.2 equiv), piperidine (0.2 to 0.3 equiv), THF, 75 °C, 16 h (yield **139** 35%, yield **140** 70%, yield **141** 52%); (g) CH₂=CH-SnBu₃ (1.2 equiv), (Ph₃P)₄Pd (0.1 equiv), 2,6-di-tert-butyl-4-methylphenol (0.0005 equiv), toluene/DMF, reflux, 4 to 16 h (yield **142** 40%, yield **143** 35%, yield **144** 47%).

2.11 Experimental methods for the synthesis of all compounds

General chemical synthesis methodology

All reactions were conducted in oven-dried glassware under an atmosphere of air unless otherwise noted. Reagent grade reaction solvents DCM, DMF, and THF were dried over molecular sieves prior to use. Reagent grade solvents carbon disulfide, EtOAc, Et₂O, hexanes, methanol, and acetonitrile were used commercially pure as purchased. The organic bases Et₃N and DIPEA were dried over solid NaOH prior to use. All other reagents and starting materials were purchased commercially pure and used as obtained. Reactions were monitored by TLC using K65 250 μm glass-backed silica gel plates with a fluorescent indicator (Whatman). Flash column chromatography was carried out on 140-400 mesh silica gel as the solid phase (Fisher Scientific). Preparative reverse phase HPLC was performed on a Peeke Scientific Combi-A 5 μm preparative C18 column (50 x 22 mm, flow rate 10 mL/min) using a Varian Prostar 210 solvent delivery system equipped with a Varian Prostar 335 full spectrum UV/VIS detector. Analytical HPLC was performed using the same system equipped with a Varian Pursuit XRs 5 C18 column (150 x 4.6 mm, flow rate 1 mL/min), using acetonitrile/water linear gradient elution, 5% to 80% acetonitrile over 20 min. ¹H NMR spectra were obtained using a Varian Inova 400 MHz spectrometer. Spectral data is reported as follows: chemical shift (as ppm referenced to the residual DMSO solvent signal at 2.50 ppm, or the residual CHCl₃ solvent signal at 7.26 ppm), multiplicity (s=singlet, d=doublet, dd=doublet of doublets, dt=doublet of triplets, dq=doublet of quartets, p=pentet, t=triplet, q=quartet, m=multiplet), coupling constant, and integration value. High resolution mass spectra (HRMS) were recorded on a Thermo Electron Corporation LTQFT using electrospray

ionization with FT resolution set to 30000. The following compounds were synthesized according to published procedures: (S)-1-amino-3-morpholinopropan-2-ol hydrochloride,⁴⁶ t-butyl hypochlorite,⁴³ monastrol,⁴⁴ **37** (RO3306),⁴⁵ **55** (5-acetyl-oxindole),⁴² **57** (fluoroacetyl chloride),⁴⁷ **60** (5-amino-oxindole),⁴² **76** 2-(hydroxyimino)-N-(3-iodophenyl)acetamide,⁴⁸ **77** (4-iodoindoline-2,3-dione),⁴⁸ **78** (6-iodoindoline-2,3-dione),⁴⁸ **91** (4-iodo-5-nitroindolin-2-one),⁴⁹ **93** (4-bromo-5-nitroindolin-2-one),⁴⁹ **108** (5-formyl-2,4-dimethyl-1*H*-pyrrole-3-carboxylic acid),⁵⁰⁻⁵¹ **134** (ethyl 2-(3-nitropyridin-2-yl)acetate),⁵² **137** (3,3,5-tribromo-1*H*-pyrrolo[3,2-*b*]pyridin-2(3*H*)-one),⁵³ **138** (5-bromo-1*H*-pyrrolo[3,2-*b*]pyridin-2(3*H*)-one).⁵³

Synthesis of compounds 2-144

(Z)-N-(3-((2-ethyl-4-methyl-1*H*-imidazol-5-yl)methylene)-2-oxindolin-5-yl)propiolamide (2) JH295. DIPEA (45.5 mg, 0.352 mmol, 2 equiv) was added to a suspension of indolinone **25** (60.0 mg, 0.176 mmol, 1 equiv) in DMF (5 mL) at 0 °C with stirring. The resulting red solution was treated with propiolic acid (18.5 mg, 0.264 mmol, 1.5 equiv), then EDC (67.5 mg, 0.352 mmol, 2 equiv). Stirring was continued for 2.5 h, then the mixture was allowed to warm to room temperature for 1.5 h. The mixture was then diluted with 5% NaHCO₃ (50 mL), and extracted three times with EtOAc (50 mL). The combined EtOAc extract was washed with water, then saturated NaCl, and concentrated under vacuum. The resulting residue was triturated in EtOAc, recovered by filtration, washed with EtOAc, and dried under vacuum to give pure **2** (25 mg, 44%) as a yellow/orange solid. ¹H NMR (DMSO-*d*₆): δ 1.27 (t, *J* = 7.5 Hz, 3H), 2.40 (s, 3H), 2.76 (q, *J* = 7.6 Hz, 2H), 4.36 (s, 1H), 6.85 (d, *J* = 8.4 Hz, 1H), 7.24 (dd, *J* = 8.4, 1.5 Hz, 1H),

7.56 (s, 1H), 7.92 (d, $J = 1.8$ Hz, 1H), 10.6 (s, 1H), 10.9 (bs, 1H), 13.8 (bs, 1H); HRMS calcd for $C_{18}H_{17}N_4O_2$ 321.1352; found (ESI⁺) (M + H) 321.1368.

5-(2-Chloroacetyl)indolin-2-one (3) JH093. Chloroacetyl chloride (21.7 g, 192 mmol, 1.7 equiv) was added dropwise to a stirred suspension of anhydrous $AlCl_3$ (90.0 g, 675 mmol, 6 equiv) in carbon disulfide (420 mL). Stirring was allowed to continue at room temperature for 15 min. Indolin-2-one (15.0 g, 113 mmol, 1 equiv) was then added, and the mixture was brought to reflux for 2.5 h, then cooled on ice. After removal of the solvent by decantation the remaining thick brown residue was treated with ice cold water (500 mL). The resulting precipitate was recovered by filtration, washed with water, and dried under vacuum to provide pure **3** (21.6 g, 92%) as a white solid. ¹H NMR (DMSO-*d*₆): δ 3.57 (s, 2H), 5.08 (s, 2H), 6.93 (d, $J = 8.4$ Hz, 1H), 7.83 (s, 1H), 7.88 (d, $J = 8.1$ Hz, 1H), 10.8 (bs, 1H); HRMS calcd for $C_{10}H_9ClNO_2$ 210.0316; found (ESI⁺) (M + H) 210.0319.

(Z)-3-((1H-Pyrrol-2-yl)methylene)-5-(2-chloroacetyl)indolin-2-one (4) JH099. Indolinone **3** (750 mg, 3.58 mmol, 1 equiv) was added to a solution of pyrrole-2-carboxaldehyde (3.42 g, 36.3 mmol, 10 equiv), and piperidine (61.0 mg, 0.716 mmol, 0.2 equiv) in THF (125 mL). The resulting mixture was heated to 60 °C in a sealed jar for 45 min. After cooling to room temperature the THF was removed under vacuum to give a thick red oil that was dissolved in EtOAc. Treating this solution with hexanes (30 mL) produced a tarry red precipitate that was removed by filtration and discarded. The filtrate was then cooled on ice to produce an orange precipitate that was collected by filtration. This crude product was further purified by flash chromatography on silica gel (hexanes/EtOAc 3:1) followed by recrystallization from EtOAc to give **4** (200 mg, 20%)

as a crystalline orange solid. ^1H NMR (DMSO- d_6): δ 5.16 (s, 2H), 6.40-6.42 (m, 1H), 6.92-6.93 (m, 1H), 7.01 (d, J = 8.1 Hz, 1H), 7.42-7.44 (m, 1H), 7.84 (dd, J = 8.3, 1.7 Hz, 1H), 7.99 (s, 1H), 8.34 (d, J = 1.5 Hz, 1H), 11.3 (s, 1H), 13.2 (bs, 1H); HRMS calcd for $\text{C}_{15}\text{H}_{12}\text{ClN}_2\text{O}_2$ 287.0587; found (ESI $^+$) (M + H) 287.0584.

5-Iodo-3-(methylthio)indolin-2-one (5) JH058. Under an atmosphere of argon and protection from strong light, a solution of t-butyl hypochlorite (4.78 g, 44.0 mmol, 1 equiv) in DCM (20 mL) was added dropwise over 5 min to a stirred solution of 4-iodoaniline (9.64 g, 44.0 mmol, 1 equiv) in DCM (150 mL) at $-60\text{ }^\circ\text{C}$. Care was taken to keep the internal temperature of the mixture below $-50\text{ }^\circ\text{C}$ during the addition. The resulting mixture was allowed to stir for 15 min, then a solution of ethyl (methylthio)acetate (5.91 g, 44.0 mmol, 1 equiv) in DCM (20 mL) was added over the course of 8 min, keeping the internal temperature of the reaction below $-60\text{ }^\circ\text{C}$. The resulting mixture was allowed to stir for 1 h, then a solution of Et_3N (4.45 g, 44.0 mmol, 1 equiv) in DCM (20 mL) was added over the course of 5 min, again keeping the internal temperature of the reaction below $-60\text{ }^\circ\text{C}$. The reaction was then allowed to come to room temperature over the course of 45 min. The mixture was then washed with water, and concentrated under vacuum to give a red/black residue that was treated with Et_2O (150 mL) and 2 N HCl (20 mL) for 4 h at room temperature. The insoluble product was recovered by filtration, and washed with Et_2O to give pure **5** (6.3 g, 47%) as a grayish solid. ^1H NMR (DMSO- d_6): δ 1.95 (s, 3H), 4.55 (s, 1H), 6.69 (d, J = 8.1 Hz, 1H), 7.53 (s, 1H), 7.54-7.58 (m, 1H), 10.6 (s, 1H); HRMS calcd for $\text{C}_9\text{H}_9\text{INOS}$ 305.9450; found (ESI $^+$) (M + H) 305.9442.

5-Iodoindolin-2-one (6) JH069. Zinc powder (268 mg, 4.10 mmol, 5 equiv) was added to a suspension of indolinone **5** (250 mg, 0.819 mmol, 1equiv) in glacial acetic

acid (2 mL). The resulting mixture was heated to 60 °C for 30 min. After cooling to room temperature the mixture was diluted with water (8 mL), filtered to remove excess zinc, and extracted with EtOAc. The EtOAc extract was washed with dilute NaOH, water, then saturated NaCl, and concentrated under vacuum to give pure **6** (169 mg, 80%) as a white solid. ¹H NMR (DMSO-*d*₆): δ 3.63 (s, 2H), 6.98 (d, *J* = 8.4 Hz, 1H), 8.09 (s, 1H), 8.15 (dd, *J* = 8.4, 2.2 Hz, 1H), 11.0 (s, 1H); HRMS calcd for C₈H₇INO 259.9567; found (ESI⁺) (M+H) 259.9567.

(Z)-3-((1H-Pyrrol-2-yl)methylene)-5-iodoindolin-2-one (7) JH139. Indolinone **6** (150 mg, 0.579 mmol, 1 equiv) was added to a solution of pyrrole-2-carboxaldehyde (63.0 mg, 0.664 mmol, 1.1 equiv), and piperidine (9.9 mg, 0.17 mmol, 0.2 equiv) in THF (6 mL). The resulting mixture was heated to 75 °C in a sealed jar for 4 h. After cooling to room temperature the THF was removed under vacuum. The residue was then triturated in 1:1 hexanes/EtOAc, recovered by filtration, and dried under vacuum to give pure **7** (130 mg, 67%) as a yellow/orange solid. ¹H NMR (DMSO-*d*₆): δ 6.36-6.39 (m, 1H), 6.72 (d, *J* = 8.1 Hz, 1H), 6.83-6.85 (m, 1H), 7.38-7.40 (m, 1H), 7.45 (dd, *J* = 8.1, 1.5 Hz, 1H), 7.88 (s, 1H), 8.01 (d, *J* = 1.5 Hz, 1H), 11.0 (bs, 1H), 13.3 (bs, 1H); HRMS calcd for C₁₃H₁₀IN₂O 336.9838; found (ESI⁺) (M + H) 336.9838.

(Z)-3-((1H-Pyrrol-2-yl)methylene)-5-((E)-3-oxobut-1-enyl)indolin-2-one (8) JH142. Under an atmosphere of argon, indolinone **7** (50.0 mg, 0.149 mmol, 1 equiv), triphenylphosphine (23.0 mg, 0.0876 mmol, 0.6 equiv), triethylamine (75.0 mg, 0.741 mmol, 5 equiv), methyl vinyl ketone (42.0 mg, 0.599 mmol, 4 equiv), and palladium(II) acetate (10.0 mg, 0.0445 mmol, 0.3 equiv) were added to anhydrous DMF (2 mL). The mixture was sparged with dry argon, then heated to 85 °C for 2 h. After cooling to room

temperature the mixture was diluted with water (50 mL), and then extracted four times with EtOAc (40 mL). The combined EtOAc extract was washed with water, then saturated NaCl, and concentrated under vacuum to give a crude orange solid. This material was further purified by flash chromatography on silica gel (hexanes/EtOAc 1:1) to give **8** (20 mg, 48%) as a yellow solid. A small amount of this material was further purified by preparative HPLC (acetonitrile/water, linear gradient elution, 5% to 80% acetonitrile over 20 min) for use in bioassays. ¹H NMR (DMSO-*d*₆): δ 2.33 (s, 3H), 6.38-6.40 (m, 1H), 6.80 (d, *J* = 16 Hz, 1H), 6.84-6.86 (m, 1H), 6.93 (d, *J* = 8.1 Hz, 1H), 7.39-7.41 (m, 1H), 7.47 (dd, *J* = 8.2, 1.6 Hz, 1H), 7.61 (d, *J* = 16 Hz, 1H), 7.91 (s, 1H), 8.15 (d, *J* = 1.5 Hz, 1H), 11.1 (s, 1H), 13.2 (bs, 1H); HRMS calcd for C₁₇H₁₅N₂O₂ 279.1134; found (ESI⁺) (M + H) 279.1130.

(Z)-3-((1H-Pyrrol-2-yl)methylene)-5-((E)-2-(methylsulfonyl)vinyl)indolin-2-one (9) JH146. Under an atmosphere of argon, indolinone **7** (50.0 mg, 0.149 mmol, 1 equiv), triphenylphosphine (23.0 mg, 0.0876 mmol, 0.6 equiv), triethylamine (75.0 mg, 0.741 mmol, 5 equiv), methyl vinyl sulfone (63.0 mg, 0.594 mmol, 4 equiv), and palladium(II) acetate (10.0 mg, 0.0445 mmol, 0.3 equiv) were added to anhydrous DMF (2 mL). The mixture was sparged with dry argon, then heated to 85 °C for 2 h. After cooling to room temperature the DMF was removed under vacuum, and the remaining black residue was purified by flash chromatography on silica gel (hexanes/EtOAc 2:1 then hexanes/EtOAc 1:1) to give pure **9** (16 mg, 34%) as a yellow solid. ¹H NMR (DMSO-*d*₆): δ 3.09 (s, 3H), 6.39-6.41 (m, 1H), 6.84-6.86 (m, 1H), 6.94 (d, *J* = 8.1 Hz, 1H), 7.34 (d, *J* = 15 Hz, 1H), 7.40-7.42 (m, 1H), 7.47 (d, *J* = 15 Hz, 1H), 7.49 (dd, *J* = 8.1, 1.5 Hz, 1H), 7.84 (s, 1H),

8.14 (d, $J = 1.1$ Hz, 1H), 11.2 (s, 1H), 13.2 (s, 1H); HRMS calcd for $C_{16}H_{15}N_2O_3S$ 315.0803; found (ESI⁺) (M + H) 315.0798.

2-Chloro-*N*-(2-oxoindolin-5-yl)acetamide (10) JH081. Pyridine (120 mg, 1.52 mmol, 1.5 equiv) was added to a solution of 5-aminoindolin-2-one (150 mg, 1.01 mmol, 1 equiv) in anhydrous THF (50 mL). The mixture was cooled to 0 °C, then chloroacetyl chloride (148 mg, 1.31 mmol, 1.3 equiv) was added dropwise over the course of 5 min. The mixture was allowed to come to room temperature for 30 min, then water (10 mL) was added, and most of the THF was removed under vacuum. The resulting precipitate was recovered by filtration, and washed with water to give pure **10** (102 mg, 45%) as a white solid. ¹H NMR (DMSO-*d*₆): δ 3.47 (s, 2H), 4.20 (s, 2H), 6.76 (d, $J = 8.4$ Hz, 1H), 7.33 (dd, $J = 8.4, 1.8$ Hz, 1H), 7.49 (bs, 1H), 10.1 (s, 1H), 10.3 (s, 1H); HRMS calcd for $C_{10}H_{10}ClN_2O_2$ 225.0425; found (ESI⁺) (M + H) 225.0429.

***N*-(2-Oxoindolin-5-yl)acrylamide (11) JH060.** Acryloyl chloride (191 mg, 2.11 mmol, 1.2 equiv) was added dropwise over the course of 5 min to a solution of 5-aminoindolin-2-one (261 mg, 1.76 mmol, 1 equiv) in anhydrous THF (100 mL) at 0 °C. The mixture was allowed to warm to room temperature for 5 min, then filtered to remove some insoluble material. The filtrate was then concentrated under vacuum, and the remaining residue dissolved in EtOAc. This solution was washed with 5% NaHCO₃, then water, and concentrated under vacuum to give pure **11** (147 mg, 41%) as a white solid. ¹H NMR (DMSO-*d*₆): δ 3.47 (s, 2H), 5.71 (dd, $J = 9.9, 2.2$ Hz, 1H), 6.21 (dd, $J = 17, 2.2$ Hz, 1H), 6.40 (dd, $J = 17, 10$ Hz, 1H), 6.75 (d, $J = 8.4$ Hz, 1H), 7.41 (dd, $J = 8.4, 2.2$ Hz, 1H), 7.59 (d, $J = 1.8$ Hz, 1H), 9.98 (s, 1H), 10.3 (bs, 1H); HRMS calcd for $C_{11}H_{11}N_2O_2$ 203.0821; found (ESI⁺) (M + H) 203.0818.

***N*-(2-Oxoindolin-5-yl)propiolamide (12) JH079.** A solution of propiolic acid (114 mg, 1.63 mmol, 1.2 equiv) in acetonitrile (10 mL) was added dropwise over 10 min to a stirred solution of 5-aminoindolin-2-one (200 mg, 1.35 mmol, 1 equiv), and EDC (518 mg, 2.70 mmol, 2 equiv) in acetonitrile (70 mL) at room temperature. Stirring was continued for 30 min, then water (20 mL) was added, and most of the acetonitrile removed under vacuum. The resulting precipitate was recovered by filtration, washed with water, and dried under vacuum to give pure **12** (108 mg, 40%) as a white solid. ¹H NMR (DMSO-*d*₆): δ 3.46 (s, 2H), 4.35 (s, 1H), 6.75 (d, *J* = 8.4 Hz, 1H), 7.37 (dd, *J* = 8.4, 1.8 Hz, 1H), 7.49 (d, *J* = 1.8 Hz, 1H), 10.3 (s, 1H), 10.7 (s, 1H); HRMS calcd for C₁₁H₉N₂O₂ 201.0659; found (ESI⁺) (M + H) 201.0661.

***(E)*-Ethyl 4-oxo-4-(2-oxoindolin-5-ylamino)but-2-enoate (13) JH098.** A solution of mono-ethyl fumarate (175 mg, 1.21 mmol, 1.2 equiv) in acetonitrile (3 mL) was added dropwise over 10 min to a stirred solution of 5-aminoindolin-2-one (150 mg, 1.01 mmol, 1 equiv), and EDC (387 mg, 2.02 mmol, 2 equiv) in acetonitrile (50 mL) at room temperature. Stirring was continued for 105 min, then water (5 mL) was added, and most of the acetonitrile removed under vacuum. The resulting precipitate was recovered by filtration, washed with water, and dried under vacuum to give pure **13** (153 mg, 55%) as a white solid. ¹H NMR (DMSO-*d*₆): δ 1.26 (t, *J* = 7.1 Hz, 3H), 3.48 (s, 2H), 4.21 (q, *J* = 7.2 Hz, 2H), 6.67 (d, *J* = 15 Hz, 1H), 6.78 (d, *J* = 8.4 Hz, 1H), 7.19 (d, *J* = 15 Hz, 1H), 7.45 (dd, *J* = 8.2, 2.0 Hz, 1H), 7.61 (s, 1H), 10.3 (s, 1H), 10.4 (s, 1H); HRMS calcd for C₁₄H₁₅N₂O₄ 275.1032; found (ESI⁺) (M + H) 275.1029.

***(Z)*-*N*-(3-((1*H*-Pyrrol-2-yl)methylene)-2-oxoindolin-5-yl)-2-chloroacetamide (14) JH091.** Indolinone **10** (40.0 mg, 0.178 mmol, 1 equiv) was added to a solution of

pyrrole-2-carboxaldehyde (84.7 mg, 0.891 mmol, 5 equiv), and piperidine (1.5 mg, 0.018 mmol, 0.1 equiv) in THF (6 mL). The resulting mixture was heated to 75 °C in a sealed jar for 5 h. After cooling to room temperature the THF was removed under vacuum. The residue was then triturated in EtOAc, recovered by filtration, and dried under vacuum to give pure **14** (34 mg, 63%) as a yellow/orange solid. ¹H NMR (DMSO-*d*₆): δ 4.24 (s, 2H), 6.34-6.37 (m, 1H), 6.85 (d, *J* = 8.4 Hz, 1H), 6.91-6.94 (m, 1H), 7.20 (d, *J* = 8.4 Hz, 1H), 7.35-7.38 (m, 1H), 7.65 (s, 1H), 7.92 (s, 1H), 10.2 (s, 1H), 10.9 (s, 1H), 13.3 (bs, 1H); HRMS calcd for C₁₅H₁₃ClN₃O₂ 302.0696; found (ESI⁺) (M + H) 302.0694.

(Z)-N-(3-((1H-Pyrrol-2-yl)methylene)-2-oxoindolin-5-yl)acrylamide (15) JH089.

Indolinone **11** (40.0 mg, 0.198 mmol, 1 equiv) was added to a solution of pyrrole-2-carboxaldehyde (94.2 mg, 0.990 mmol, 5 equiv), and piperidine (1.7 mg, 0.020 mmol, 0.1 equiv) in THF (6 mL). The resulting mixture was heated to 75 °C in a sealed jar for 4 h. After cooling to room temperature the THF was removed under vacuum. The residue was then triturated in EtOAc, recovered by filtration, and dried under vacuum to give pure **15** (31 mg, 56%) as a yellow/orange solid. ¹H NMR (DMSO-*d*₆): δ 5.74 (d, *J* = 10 Hz, 1H), 6.25 (d, *J* = 17 Hz, 1H), 6.34-6.37 (m, 1H), 6.44 (dd, *J* = 17, 10 Hz, 1H), 6.84 (d, *J* = 8.4 Hz, 1H), 6.91-6.94 (m, 1H), 7.26 (d, *J* = 8.1 Hz, 1H), 7.34-7.38 (m, 1H), 7.62 (s, 1H), 8.04 (s, 1H), 10.1 (s, 1H), 10.9 (s, 1H), 13.3 (bs, 1H); HRMS calcd for C₁₆H₁₄N₃O₂ 280.1086; found (ESI⁺) (M + H) 280.1083.

(Z)-N-(3-((1H-Pyrrol-2-yl)methylene)-2-oxoindolin-5-yl)propiolamide (16)

JH100. Indolinone **12** (40.0 mg, 0.200 mmol, 1 equiv) was added to a solution of pyrrole-2-carboxaldehyde (190 mg, 2.00 mmol, 10 equiv), and piperidine (3.3 mg, 0.039 mmol, 0.2 equiv) in THF (6 mL). The resulting mixture was heated to 75 °C in a sealed

jar for 18 h. After cooling to room temperature the THF was removed under vacuum. The residue was purified by flash chromatography on silica gel (hexanes/EtOAc 2:1) to give **16** (16 mg, 29%) as an orange solid. A small amount of this material was further purified by preparative HPLC (acetonitrile/water, linear gradient elution, 5% to 80% acetonitrile over 20 min) for use in bioassays. ¹H NMR (DMSO-*d*₆): δ 4.37 (s, 1H), 6.35-6.37 (m, 1H), 6.84 (d, *J* = 8.4 Hz, 1H), 6.93-6.95 (m, 1H), 7.22 (dd, *J* = 8.2, 2.0 Hz, 1H), 7.35-7.38 (m, 1H), 7.61 (s, 1H), 7.91 (d, *J* = 1.8 Hz, 1H), 10.7 (s, 1H), 10.9 (s, 1H), 13.3 (bs, 1H); HRMS calcd for C₁₆H₁₁N₃O₂ 277.0851; found (ESI⁺) (M +) 277.0848.

(E)-Ethyl 4-((Z)-3-((1H-pyrrol-2-yl)methylene)-2-oxoindolin-5-ylamino)-4-oxobut-2-enoate (17) JH106. Indolinone **13** (40.0 mg, 0.198 mmol, 1 equiv) was added to a solution of pyrrole-2-carboxaldehyde (188 mg, 1.98 mmol, 10 equiv), and piperidine (3.5 mg, 0.041 mmol, 0.2 equiv) in THF (6 mL). The resulting mixture was heated to 75 °C in a sealed jar for 20 h. After cooling to room temperature the THF was removed under vacuum. The residue was then triturated in 1:1 hexanes/EtOAc, recovered by filtration, and dried under vacuum. This crude product was further purified by dissolving in THF (2 mL), and treating with hexanes (2.5 mL). The resulting precipitate was recovered by filtration, washed with hexanes, and dried under vacuum to give pure **17** (35 mg, 50%) as an orange solid. ¹H NMR (DMSO-*d*₆): δ 1.27 (t, *J* = 7.1 Hz, 3H), 4.22 (q, *J* = 7.1 Hz, 2H), 6.35-6.38 (m, 1H), 6.7 (d, *J* = 15 Hz, 1H), 6.87 (d, *J* = 8.1 Hz, 1H), 6.94-6.97 (m, 1H), 7.24 (d, *J* = 15 Hz, 1H), 7.27 (dd, *J* = 8.2, 1.6 Hz, 1H), 7.35-7.38 (m, 1H), 7.65 (s, 1H), 8.08 (d, *J* = 1.8, 1H), 10.5 (s, 1H), 10.9 (s, 1H), 13.3 (bs, 1H); HRMS calcd for C₁₉H₁₈N₃O₄ 352.1297; found (ESI⁺) (M + H) 352.1296.

5-(2-(Chloromethyl)-1,3-dioxolan-2-yl)indolin-2-one (18) JH154. Ethylene glycol (11.8 g, 190 mmol, 2 equiv) and pTSA·H₂O (3.36 g, 0.0177 mmol, 0.2 equiv) were added to a suspension of indolinone **3** (20.0 g, 95.4 mmol, 1 equiv) in toluene (2.5 L). The mixture was brought to reflux using a Dean Stark trap, and strong stirring for 12 h. After cooling to room temperature the mixture was washed with 5% NaHCO₃ (500 mL), then saturated NaCl (500 mL), and concentrated under vacuum to give **18** (24.2 g, 100%) as a tan solid. This material contained a small amount of impurity by ¹H NMR but was used without further purification. ¹H NMR (DMSO-*d*₆): δ 3.47 (s, 2H), 3.80-3.84 (m, 2H), 3.85 (s, 2H), 4.06-4.09 (m, 2H), 6.79 (d, *J* = 8.1 Hz, 1H), 7.28 (d, *J* = 8.1 Hz, 1H), 7.29 (s, 1H), 10.4 (s, 1H); HRMS calcd for C₁₂H₁₃ClNO₃ 254.0579; found (ESI⁺) (M + H) 254.0578.

(Z)-3-((1H-Imidazol-5-yl)methylene)-5-(2-chloroacetyl)indolin-2-one (19) JH176. Indolinone **18** (50.0 mg, 0.197 mmol, 1 equiv) was added to a suspension of 1*H*-imidazole-5-carbaldehyde (20.8 mg, 0.216 mmol, 1.1 equiv), and piperidine (5.0 mg, 0.059 mmol, 0.3 equiv) in THF (4 mL). The resulting mixture was heated to 75 °C in a sealed jar for 7 h. After cooling to room temperature conc. HCl (300 μL) was added, and stirring continued for 4.5 h. The mixture was treated with EtOAc (5 mL), and the resulting precipitate collected by filtration, triturated in 2 N NaOH, washed with water, and dried under vacuum to give pure **19** (23 mg, 41%) as a yellow solid. ¹H NMR (DMSO-*d*₆): δ 5.16 (s, 2H), 7.03 (d, *J* = 8.4 Hz, 1H), 7.72 (s, 1H), 7.89 (d, *J* = 8.4 Hz, 1H), 8.06 (s, 1H), 8.09 (s, 1H), 8.37 (s, 1H), 11.4 (s, 1H), 13.5 (bs, 1H); HRMS calcd for C₁₄H₁₁ClN₃O₂ 288.0540; found (ESI⁺) (M + H) 288.0532.

(Z)-5-(2-Chloroacetyl)-3-((4-methyl-1H-imidazol-5-yl)methylene)indolin-2-one (20) JH180. Indolinone **18** (50.0 mg, 0.197 mmol, 1 equiv) was added to a suspension of 4-methyl-1H-imidazole-5-carbaldehyde (23.9 mg, 0.216 mmol, 1.1 equiv), and piperidine (5.0 mg, 0.059 mmol, 0.3 equiv) in THF (3 mL). The resulting mixture was heated to 75 °C in a sealed jar for 9 h. After cooling to room temperature conc. HCl (300 µL) was added, and stirring continued for 24 h. The resulting precipitate was collected by filtration, washed with EtOAc, triturated in 2 N NaOH, washed with water, and dried under vacuum to give pure **20** (29 mg, 49%) as a yellow solid. ¹H NMR (DMSO-*d*₆): δ 2.51 (s, 3H), 5.18 (s, 2H), 7.02 (d, *J* = 8.4 Hz, 1H), 7.86 (dd, *J* = 8.3, 1.7 Hz, 1H), 7.97 (s, 1H), 7.99 (s, 1H), 8.52 (d, *J* = 1.8 Hz, 1H), 11.4 (s, 1H), 13.7 (bs, 1H); HRMS calcd for C₁₅H₁₃ClN₃O₂ 302.0696; found (ESI⁺) (M + H) 302.0693.

(Z)-5-(2-Chloroacetyl)-3-((2-ethyl-4-methyl-1H-imidazol-5-yl)methylene)indolin-2-one (21) JH249. Indolinone **18** (50.0 mg, 0.197 mmol, 1 equiv) was added to a suspension of 2-ethyl-4-methyl-1H-imidazole-5-carbaldehyde (33.0 mg, 0.239 mmol, 1.2 equiv), and piperidine (5.0 mg, 0.059 mmol, 0.3 equiv) in THF (5 mL). The resulting mixture was heated to 75 °C in a sealed jar for 20 h. After cooling to room temperature conc. HCl (300 µL) was added, and stirring continued for 20 h. The resulting precipitate was collected by filtration, triturated in 1 N NaOH, washed with water, and dried under vacuum to give pure **21** (32 mg, 49%) as a yellow solid. ¹H NMR (DMSO-*d*₆): δ 1.28 (t, *J* = 7.5 Hz, 3H), 2.47 (s, 3H), 2.78 (q, *J* = 7.6 Hz, 2H), 5.18 (s, 2H), 7.02 (d, *J* = 8.4 Hz, 1H), 7.84 (dd, *J* = 8.2, 1.6 Hz, 1H), 7.94 (s, 1H), 8.49 (d, *J* = 1.6 Hz, 1H), 11.4 (s, 1H), 13.7 (bs, 1H); HRMS calcd for C₁₇H₁₇ClN₃O₂ 330.1009; found (ESI⁺) (M + H) 330.1000.

tert-Butyl 2-oxindolin-5-ylcarbamate (22) JH275. DIPEA (5.19 g, 40.2 mmol, 4 equiv) and di-*tert*-butyl dicarbonate (6.20 g, 28.4 mmol, 2.8 equiv) were added to a solution of 5-aminoindolin-2-one (1.50 g, 10.1 mmol, 1 equiv) in anhydrous THF (500 mL). The resulting mixture was stirred at room temperature for 25 h, then concentrated under vacuum. The residue was purified by triturating in 1:1 hexanes/EtOAc, washing with hexanes, and drying under vacuum to give pure **22** (2.3 g, 92%) as a white solid. ¹H NMR (DMSO-*d*₆): δ 1.46 (s, 9H), 3.42 (s, 2H), 6.68 (d, *J* = 8.4 Hz, 1H), 7.20 (d, *J* = 8.1 Hz, 1H), 7.34 (s, 1H), 9.13 (s, 1H), 10.2 (s, 1H); HRMS calcd for C₁₃H₁₇N₂O₃ 249.1239; found (ESI⁺) (M + H) 249.1235.

(Z)-3-((1H-Imidazol-5-yl)methylene)-5-aminoindolin-2-one dihydrochloride (23) JH280. Indolinone **22** (750 mg, 3.02 mmol, 1 equiv) was added to a suspension of 1*H*-imidazole-5-carbaldehyde (320 mg, 3.33 mmol, 1.1 equiv), and piperidine (50.4 mg, 0.592 mmol, 0.2 equiv) in THF (45 mL). The resulting mixture was heated to 75 °C in a sealed jar for 20 h, then concentrated under vacuum. The residue was triturated in EtOAc, collected by filtration, washed with 1:1 hexanes/EtOAc, and then treated with a fresh solution of 4% v/v acetyl chloride in methanol (80 mL) for 23 h at room temperature with stirring. The mixture was concentrated to dryness under vacuum to give pure **23** (750 mg, 83%) as a yellow solid. ¹H NMR (DMSO-*d*₆): δ 7.02 (d, *J* = 8.1 Hz, 1H), 7.26 (d, *J* = 8.4 Hz, 1H), 7.59 (s, 1H), 7.94 (s, 1H), 8.36 (s, 1H), 8.99 (s, 1H), 11.4 (s, 1H); HRMS (free base) calcd for C₁₂H₁₁N₄O 227.0933; found (ESI⁺) (M + H) 227.0926.

(Z)-5-Amino-3-((4-methyl-1H-imidazol-5-yl)methylene)indolin-2-one dihydrochloride (24) JH281. Indolinone **22** (750 mg, 3.02 mmol, 1 equiv) was added to a suspension of 4-methyl-1*H*-imidazole-5-carbaldehyde (366 mg, 3.32 mmol, 1.1 equiv),

and piperidine (50.4 mg, 0.592 mmol, 0.2 equiv) in THF (45 mL). The resulting mixture was heated to 75 °C in a sealed jar for 20 h, then concentrated under vacuum. The residue was triturated in EtOAc, collected by filtration, washed with 1:1 hexanes/EtOAc, and then treated with a fresh solution of 4% v/v acetyl chloride in methanol (80 mL) for 48 h at room temperature with stirring. The mixture was concentrated to dryness under vacuum to give pure **24** (781 mg, 83%) as a yellow solid. ¹H NMR (DMSO-*d*₆): δ 2.63 (s, 3H), 7.02 (d, *J* = 8.1 Hz, 1H), 7.30 (dd, *J* = 8.1, 1.6 Hz, 1H), 7.86 (d, *J* = 1.8 Hz, 1H), 8.00 (s, 1H), 9.01 (s, 1H), 11.5 (bs, 1H); HRMS (free base) calcd for C₁₃H₁₃N₄O 241.1089; found (ESI⁺) (M + H) 241.1081.

(Z)-5-Amino-3-((2-ethyl-4-methyl-1*H*-imidazol-5-yl)methylene)indolin-2-one (25)
JH282. Indolinone **22** (750 mg, 3.02 mmol, 1 equiv) was added to a suspension of 2-ethyl-4-methyl-1*H*-imidazole-5-carbaldehyde (459 mg, 3.32 mmol, 1.1 equiv), and piperidine (50.4 mg, 0.592 mmol, 0.2 equiv) in THF (45 mL). The resulting mixture was heated to 75 °C in a sealed jar for 20 h, then concentrated under vacuum. The residue was triturated in EtOAc, collected by filtration, washed with 1:1 hexanes/EtOAc, and then treated with a fresh solution of 4% v/v acetyl chloride in methanol (80 mL) for 48 h at room temperature with stirring. The mixture was concentrated to dryness under vacuum to give pure **25** (740 mg, 72%) as a yellow solid. ¹H NMR (DMSO-*d*₆): δ 1.36 (t, *J* = 7.5 Hz, 3H), 2.60 (s, 3H), 3.04 (q, *J* = 7.6 Hz, 2H), 7.01 (d, *J* = 8.4 Hz, 1H), 7.23 (d, *J* = 8.4 Hz, 1H), 7.78 (bs, 1H), 7.99 (s, 1H), 11.5 (s, 1H); HRMS (free base) calcd for C₁₅H₁₇N₄O 269.1402; found (ESI⁺) (M + H) 269.1394.

(Z)-*N*-(3-((1*H*-Imidazol-5-yl)methylene)-2-oxoindolin-5-yl)propiolamide (26)
JH299. Under an atmosphere of argon DIPEA (45.5 mg, 0.352 mmol, 2.1 equiv) was

added to a stirred suspension of indolinone **23** (50.0 mg, 0.167 mmol, 1 equiv) in DMF (5 mL). The resulting red solution was cooled to 0 °C, treated with propiolic acid (70.2 mg, 1.00 mmol, 6 equiv), then EDC (67.5 mg, 0.352 mmol, 2.1 equiv). Stirring was continued for 2 h, then the mixture was diluted with EtOAc (150 mL), washed three times with water (50 mL), then with saturated NaCl, and concentrated under vacuum to give a crude orange solid. This material was further purified by preparative HPLC (acetonitrile/water, linear gradient elution, 5% to 80% acetonitrile over 20 min) to give pure **26** (3.8 mg, 8.2%) as a yellow/orange solid. ¹H NMR (DMSO-*d*₆): δ 4.38 (s, 1H), 6.86 (d, *J* = 8.4 Hz, 1H), 7.27 (d, *J* = 8.4 Hz, 1H), 7.74 (s, 1H), 7.74 (s, 1H), 7.96 (s, 1H), 8.02 (s, 1H), 10.7 (s, 1H), 11.0 (bs, 1H), 13.7 (bs, 1H); HRMS calcd for C₁₅H₁₁N₄O₂ 279.0882; found (ESI⁺) (M + H) 279.0876.

(Z)-N-(3-((4-Methyl-1H-imidazol-5-yl)methylene)-2-oxoindolin-5-yl)propiolamide (27) JH289. DIPEA (41.4 mg, 0.320 mmol, 2 equiv) was added to a suspension of indolinone **24** (50.0 mg, 0.160 mmol, 1 equiv) in DMF (5 mL) at 0 °C with stirring. The resulting red solution was treated with propiolic acid (16.8 mg, 0.240 mmol, 1.5 equiv), then EDC (61.3 mg, 0.320 mmol, 2 equiv). Stirring was continued for 2.5 h, then the mixture was diluted with 5% NaHCO₃ (50 mL), and extracted three times with EtOAc (50 mL). The combined EtOAc extract was washed with water, then saturated NaCl, and concentrated under vacuum. The residue was triturated in 1:1 hexanes/EtOAc, recovered by filtration, and washed with EtOAc, to give **27** (15 mg, 32%) as an orange solid. A small amount of this material was further purified by preparative HPLC (acetonitrile/water, linear gradient elution, 5% to 80% acetonitrile over 20 min) for use in bioassays. ¹H NMR (DMSO-*d*₆): δ 2.44 (s, 3H), 4.36 (s, 1H), 6.85 (d, *J* = 8.4 Hz, 1H),

7.27 (dd, $J = 8.4, 2.2$ Hz, 1H), 7.62 (s, 1H), 7.93 (s, 1H), 7.94 (d, $J = 1.8$ Hz, 1H), 10.7 (s, 1H), 11.0 (s, 1H), 13.8 (bs, 1H); HRMS calcd for $C_{16}H_{12}N_4O_2$ 292.0960; found (ESI⁺) (M +) 292.0965.

1-Methyl-5-nitroindolin-2-one (28) JH397. HNO_3 (70% aqueous, 1.41 g, 22.4 mmol, 1.7 equiv) was slowly added to a solution of 1-methylindolin-2-one (2.00 g, 13.6 mmol, 1 equiv) in conc. H_2SO_4 (8 mL) at 0 °C with stirring. Stirring was allowed to continue for 30 min, then the reaction was poured onto a water/ice mixture (200 mL). The resulting precipitate was collected by filtration, and washed with water (250 mL) to give pure **28** (2.3g, 88%) as a tan solid. 1H NMR (DMSO- d_6): δ 3.19 (s, 3H), 3.70 (s, 2H), 7.19 (d, $J = 8.4$ Hz, 1H), 8.14 (s, 1H), 8.26 (d, $J = 8.8$ Hz, 1H); HRMS calcd for $C_9H_7N_2O_3$ 191.0462; found (ESI⁻) (M - H) 191.0464.

(Z)-3-((2-Ethyl-4-methyl-1H-imidazol-5-yl)methylene)-1-methyl-5-nitroindolin-2-one (29) JH398. Indolinone **28** (100 mg, 0.520 mmol, 1 equiv) was added to a suspension of 2-ethyl-4-methyl-1H-imidazole-5-carbaldehyde (68.3 mg, 0.494 mmol, 0.95 equiv), and piperidine (13.3 mg, 0.156 mmol, 0.3 equiv) in THF (7 mL). The resulting mixture was heated to 75 °C in a sealed jar for 18 h. After cooling to room temperature the resulting precipitate was collected by filtration, and washed with EtOAc to give pure **29** (113 mg, 73%) as an orange solid. 1H NMR (DMSO- d_6): δ 1.43 (t, $J = 7.5$ Hz, 3H), 2.45 (s, 3H), 2.75 (q, $J = 7.6$ Hz, 2H), 3.29 (s, 3H), 7.16 (d, $J = 8.4$ Hz, 1H), 7.55 (s, 1H), 8.15 (dd, $J = 8.8, 2.6$ Hz, 1H), 10.6 (d, $J = 2.6$ Hz, 1H), 12.5 (bs, 1H); HRMS calcd for $C_{16}H_{17}N_4O_3$ 313.1301; found (ESI⁺) (M + H) 313.1293.

(Z)-5-Amino-3-((2-ethyl-4-methyl-1H-imidazol-5-yl)methylene)-1-methylindolin-2-one (30) JH402. Zinc dust (1.02 g, 15.6 mmol, 47 equiv) was added to a suspension of

indolinone **29** (105 mg, 0.336 mmol, 1 equiv) in THF (40 mL) and saturated aqueous NH₄Cl (20 mL) at room temperature. The resulting mixture was vigorously stirred for 10 min, then diluted with EtOAc (150 mL), washed with water, then saturated NaCl, and concentrated under vacuum to give pure **30** (67 mg, 71%) as a red/orange solid. ¹H NMR (DMSO-*d*₆): δ 1.32 (t, *J* = 7.7 Hz, 3H), 2.38 (s, 3H), 2.75 (q, *J* = 7.6 Hz, 2H), 3.11 (s, 3H), 4.50 (bs, 2H), 6.50 (dd, *J* = 8.1, 2.6 Hz, 1H), 6.62 (d, *J* = 8.1 Hz, 1H), 7.32 (s, 1H), 8.81 (d, *J* = 2.2 Hz, 1H), 12.2 (bs, 1H); HRMS calcd for C₁₆H₁₉N₄O 283.1553; found (ESI⁺) (M + H) 283.1552.

(Z)-N-(3-((2-Ethyl-4-methyl-1*H*-imidazol-5-yl)methylene)-1-methyl-2-oxoindolin-5-yl)propiolamide (31) JH404. EDC (80.3mg, 0.419 mmol, 2 equiv) was added to a solution of indolinone **30** (59.1 mg, 0.209 mmol, 1 equiv) and propiolic acid (22.2 mg, 0.317 mmol, 1.5 equiv) in DMF (4 mL) at 0 °C. The resulting mixture was allowed to stir for 2 h, then diluted with EtOAc (100 mL), washed with water, then saturated NaCl, and concentrated under vacuum to give a crude orange solid. This material was further purified by preparative HPLC (acetonitrile/water, linear gradient elution, 5% to 80% acetonitrile over 20 min) to give pure **31** (16 mg, 23%) as an orange solid. ¹H NMR (DMSO-*d*₆): δ 1.30 (t, *J* = 7.7 Hz, 3H), 2.41 (s, 3H), 2.76 (q, *J* = 7.7 Hz, 2H), 3.18 (s, 3H), 4.29 (s, 1H), 6.89 (d, *J* = 8.4 Hz, 1H), 7.24 (dd, *J* = 8.4, 2.2 Hz, 1H), 7.43 (s, 1H), 9.70 (d, *J* = 1.8 Hz, 1H), 10.5 (s, 1H), 12.3 (bs, 1H); HRMS calcd for C₁₉H₁₉N₄O₂ 335.1508; found (ESI⁺) (M + H) 335.1493.

5-(2-Chloroacetyl)-1-methylindolin-2-one (32) JH396. Chloroacetyl chloride (1.95g, 17.3 mmol, 1.7 equiv) was added dropwise to a stirred suspension of anhydrous AlCl₃ (8.10 g, 60.9 mmol, 6 equiv) in carbon disulfide (40 mL). Stirring was allowed to

continue at room temperature for 15 min. 1-Methylindolin-2-one (1.50 g, 10.2 mmol, 1 equiv) was then added, and the mixture was brought to reflux for 2 h, then cooled on ice. After removal of the solvent by decantation the remaining thick brown residue was treated with ice cold water. The resulting precipitate was recovered by filtration, washed with water, and dried under vacuum to provide pure **32** (2.0 g, 88%) as a white solid. ¹H NMR (DMSO-*d*₆): δ 3.17 (s, 3H), 3.64 (s, 2H), 5.11 (s, 2H), 7.12 (d, *J* = 8.4 Hz, 1H), 7.86 (d, *J* = 1.1 Hz, 1H), 7.99 (dd, *J* = 8.4, 1.8 Hz, 1H); HRMS calcd for C₁₁H₁₁ClNO₂ 224.0478; found (ESI⁺) (M + H) 224.0475.

5-(2-(Chloromethyl)-1,3-dioxolan-2-yl)-1-methylindolin-2-one (33) JH399.

Ethylene glycol (555 mg, 8.94 mmol, 2 equiv) and pTSA·H₂O (170 mg, 0.894 mmol, 0.2 equiv) were added to a suspension of indolinone **32** (1.00 g, 4.47 mmol, 1 equiv) in benzene (200 mL). The mixture was brought to reflux using a Dean Stark trap, and vigorous stirring for 5 h. After cooling to room temperature the mixture was washed with 5% NaHCO₃, then saturated NaCl, and concentrated under vacuum to give **3** (1.2 g, 100%) as a tan solid. ¹H NMR (DMSO-*d*₆): δ 3.06 (s, 3H), 3.50 (s, 2H), 3.76-3.80 (m, 2H), 3.82 (s, 2H), 4.02-4.06 (m, 2H), 6.91 (d, *J* = 8.1 Hz, 1H), 7.31 (s, 1H), 7.33 (d, *J* = 8.4 Hz, 1H); HRMS calcd for C₁₃H₁₅ClNO₃ 268.0740; found (ESI⁺) (M + H) 268.0737.

(Z)-5-(2-Chloroacetyl)-3-((2-ethyl-4-methyl-1*H*-imidazol-5-yl)methylene)-1-methylindolin-2-one hydrochloride (34) JH400. Indolinone **33** (50.0 mg, 0.187 mmol, 1 equiv) was added to a suspension of 2-ethyl-4-methyl-1*H*-imidazole-5-carbaldehyde (25.0 mg, 0.181 mmol, 0.97 equiv), and piperidine (4.8 mg, 0.056 mmol, 0.3 equiv) in THF (6 mL). The resulting mixture was heated to 75 °C in a sealed jar for 18 h. After cooling to room temperature conc. HCl (300 μL) was added, and stirring was allowed to

continue for an additional 18 h. The resulting precipitate was collected by filtration, washed with THF, and dried under vacuum to give pure **34** (40 mg, 60%) as an orange solid. ¹H NMR (DMSO-*d*₆): δ 1.30 (t, *J* = 7.7 Hz, 3H), 2.41 (s, 3H), 2.76 (q, *J* = 7.7 Hz, 2H), 3.18 (s, 3H), 4.29 (s, 1H), 6.89 (d, *J* = 8.4 Hz, 1H), 7.24 (dd, *J* = 8.4, 2.2 Hz, 1H), 7.43 (s, 1H), 9.70 (d, *J* = 1.8 Hz, 1H), 10.5 (s, 1H), 12.3 (bs, 1H); HRMS calcd for C₁₈H₁₉ClN₃O₂ 344.1166; found (ESI⁺) (M + H) 344.1153.

(Z)-N-(3-((2-Ethyl-4-methyl-1*H*-imidazol-5-yl)methylene)-2-oxoindolin-5-yl)but-2-ynamide (35) JH387. DMF (6 mL) was added to a solid mixture of indolinone **25** (50.0 mg, 0.147 mmol, 1 equiv), EDC (112 mg, 0.584 mmol, 4 equiv), HOBt (20.0 mg, 0.148 mmol, 1 equiv), and 2-butyric acid (74.0 mg, 0.880 mmol, 6 equiv), followed by DIPEA (57.0 mg, 0.441 mmol, 3 equiv). The resulting mixture was allowed to stir at room temperature for 2 h, then diluted with 5% NaHCO₃ (20 mL), and extracted with EtOAc. The EtOAc extract was washed with water, then saturated NaCl, then concentrated to dryness to give pure **35** (25 mg, 51%) as an orange solid. ¹H NMR (DMSO-*d*₆): δ 1.27 (t, *J* = 7.7 Hz, 3H), 2.04 (s, 3H), 2.40 (s, 3H), 2.75 (q, *J* = 7.6 Hz, 2H), 6.83 (d, *J* = 8.4 Hz, 1H), 7.22 (dd, *J* = 8.2, 2.0 Hz, 1H), 7.53 (s, 1H), 7.92 (d, *J* = 1.8 Hz, 1H), 10.4 (s, 1H), 10.9 (bs, 1H), 13.8 (s, 1H); HRMS calcd for C₁₉H₁₉N₄O₂ 335.1503; found (ESI⁺) (M + H) 335.1496.

(Z)-5-Acetyl-3-((2-ethyl-4-methyl-1*H*-imidazol-5-yl)methylene)indolin-2-one (36) JH379. 5-Acetylidolin-2-one (**55**) (100 mg, 0.571 mmol, 1 equiv) was added to a suspension of 2-ethyl-4-methyl-1*H*-imidazole-5-carbaldehyde (71.0 mg, 0.514 mmol, 0.9 equiv), and piperidine (14.0 mg, 0.164 mmol, 0.3 equiv) in THF (8 mL). The resulting mixture was heated to 75 °C in a sealed jar for 16 h. After cooling to room temperature

the product was collected by filtration, washed with THF, then EtOAc, to give **36** (57 mg, 34%) as an orange solid. A small amount of this material was further purified by preparative HPLC (acetonitrile/water, linear gradient elution, 5% to 80% acetonitrile over 20 min) for use in bioassays. ^1H NMR (DMSO- d_6): δ 1.28 (t, $J = 7.7$ Hz, 3H), 2.46 (s, 3H), 2.59 (s, 3H), 2.78 (q, $J = 7.6$ Hz, 2H), 6.98 (d, $J = 8.4$ Hz, 1H), 7.82 (dd, $J = 8.2$, 1.6 Hz, 1H), 7.94 (s, 1H), 8.46 (d, $J = 1.8$ Hz, 1H), 11.3 (bs, 1H), 13.7 (bs, 1H); HRMS calcd for $\text{C}_{17}\text{H}_{18}\text{N}_3\text{O}_2$ 296.1394; found (ESI $^+$) (M + H) 296.1396.

(38-54). This is a general procedure for the parallel synthesis of these 5-chloromethylketone-based inhibitors. A stock solution (2 mL) of indolinone **18** (50 mg/mL, 0.0985 mmol/mL, 1 equiv) in THF, and a stock solution (4 mL) of piperidine (1.25 mg/mL, 0.0147 mmol/mL, 0.3 equiv) in THF were added to an 8 mL glass jar. An aromatic aldehyde was then added. For well-soluble aldehydes 1.05 to 1.5 equivalents were used. For aldehydes that were not completely soluble 0.9 to 0.95 equivalents were used. This method helped to ensure that the leftover starting materials remained in solution at the end of the reaction. The jar was then capped with a Teflon lined lid and heated to 75 °C for 1 to 40 h in a sand bath. The progress of the reaction was monitored by TLC (all products are visibly yellow). After completion of the reaction the mixture was allowed to cool to room temperature. Next, to hydrolyze the 1,3-dioxolane protecting group the reactions were treated with 4 to 6 drops of concentrated HCl for 2 to 23 h. After the hydrolysis precipitated products were collected by filtration and washed with THF. For products that did not precipitate, the THF was removed under vacuum and the residue purified by trituration in EtOAc or EtOAc/Hexanes. Optionally, prior to hydrolysis, for reactions that yielded a mixture of E and Z isomers, the THF was removed

under vacuum and the residue purified by silica gel chromatography to resolve the isomers, using hexanes/EtOAc as the mobile phase. Following silica gel chromatography these products were hydrolyzed in THF/HCl, and purified as described above. A complete listing of reaction times, yields of isomers, and chemical yields for these compounds are presented in Table 2. The ^1H NMR data for compounds **38-54** are listed below.

(Z)-3-((1H-Imidazol-2-yl)methylene)-5-(2-chloroacetyl)indolin-2-one (38) JH177.

^1H NMR (DMSO- d_6): δ 5.18 (s, 2H), 7.07 (d, $J = 8.1$ Hz, 1H), 7.40 (s, 1H), 7.60 (d, $J = 2.2$ Hz, 1H), 7.91 (dd, $J = 8.1, 1.8$ Hz, 1H), 8.04 (s, 1H), 8.58 (d, $J = 1.8$ Hz, 1H), 11.6 (bs, 1H), 13.9 (bs, 1H).

(Z)-5-(2-Chloroacetyl)-3-(furan-2-ylmethylene)indolin-2-one (39) JH181.

^1H NMR (DMSO- d_6): δ 5.17 (s, 2H), 6.86 (dd, $J = 3.3, 1.8$ Hz, 1H), 7.01 (d, $J = 8.4$, 1H), 7.37 (d, $J = 3.7$ Hz, 1H), 7.45 (s, 1H), 7.95 (dd, $J = 8.1, 1.8$ Hz, 1H), 8.25 (d, $J = 1.8$ Hz, 1H), 8.98 (d, $J = 1.5$ Hz, 1H), 11.1 (bs, 1H).

(Z)-5-(2-Chloroacetyl)-3-(pyridin-2-ylmethylene)indolin-2-one hydrochloride

(40) JH182. ^1H NMR (DMSO- d_6): δ 5.19 (s, 2H), 7.06 (d, $J = 8.4$ Hz, 1H), 7.72-7.77 (m, 1H), 8.00 (dd, $J = 8.1, 1.5$ Hz, 1H), 8.18 (s, 1H), 8.24-8.29 (m, 1H), 8.51 (d, $J = 1.5$ Hz, 1H), 8.74 (d, $J = 8.4$ Hz, 1H), δ 8.93-8.97 (m, 1H), 11.6 (bs, 1H).

(Z)-3-((1H-Indol-3-yl)methylene)-5-(2-chloroacetyl)indolin-2-one (41) JH184.

^1H NMR (DMSO- d_6): δ 5.23 (s, 2H), 6.98 (d, $J = 8.1$ Hz, 1H), 7.25-7.29 (m, 2H), 7.53-7.57 (m, 1H), 7.84 (dd, $J = 8.1, 1.5$ Hz, 1H), 8.26-8.30 (m, 1H), 8.38 (s, 1H), 8.56 (d, $J = 1.5$ Hz, 1H), 9.48 (d, $J = 2.9$ Hz, 1H), 11.0 (s, 1H), 12.1 (bs, 1H).

(Z)-5-(2-Chloroacetyl)-3-(thiazol-2-ylmethylene)indolin-2-one hydrochloride (42)
JH185. ^1H NMR (DMSO- d_6): δ 5.19 (s, 2H), 7.05 (d, $J = 8.4$ Hz, 1H), 7.95 (dd, $J = 8.1$, 1.5 Hz, 1H), 8.10 (dd, $J = 3.3$, 1.1 Hz, 1H), 8.18 (d, $J = 2.9$ Hz, 1H), 8.38 (s, 1H), 8.62 (d, $J = 1.8$ Hz, 1H), 11.3 (s, 1H).

5-(2-Chloroacetyl)-3-(thiophen-2-ylmethylene)indolin-2-one (43) JH186. Isolated as a 3:1 mixture of E/Z isomers. This is the spectrum of the major isomer. ^1H NMR (DMSO- d_6): δ 5.16 (s, 2H), 6.98 (d, $J = 8.1$ Hz, 1H), 7.28 (dd, $J = 5.1$, 3.7 Hz, 1H), 7.90 (dd, $J = 8.4$, 1.5 Hz, 1H), 7.97 (d, $J = 5.1$ Hz, 1H), 8.02 (d, $J = 3.7$ Hz, 1H), 8.37 (s, 1H), 8.40 (d, $J = 1.5$ Hz, 1H), 11.1 (s, 1H).

(Z)-5-(2-Chloroacetyl)-3-(2-hydroxybenzylidene)indolin-2-one (44) JH187. ^1H NMR (DMSO- d_6): δ 4.95 (s, 2H), 6.90-6.98 (m, 3H), 7.31-7.35 (m, 1H), 7.64 (d, $J = 7.7$ Hz, 1H), 7.76 (s, 1H), 7.88 (dd, $J = 8.4$, 1.8 Hz, 1H), 8.11 (d, $J = 1.5$ Hz, 1H), 10.3 (s, 1H), 11.0 (s, 1H).

(Z)-5-(2-Chloroacetyl)-3-(2-hydroxy-3-methoxybenzylidene)indolin-2-one (45) JH188. ^1H NMR (DMSO- d_6): δ 3.88 (s, 3H), 5.00 (s, 2H), 6.94 (t, $J = 8.1$ Hz, 1H), 6.99 (d, $J = 8.1$ Hz, 1H), 7.14 (d, $J = 8.1$ Hz, 1H), 7.27 (d, $J = 7.7$ Hz, 1H), 7.81 (s, 1H), 7.92 (dd, $J = 8.4$, 1.8 Hz, 1H), 8.16 (d, $J = 1.8$ Hz, 1H), 9.53 (s, 1H), 11.1 (s, 1H).

5-(2-Chloroacetyl)-3-(2-hydroxy-3-nitrobenzylidene)indolin-2-one (46) JH189. Isolated as a clean 1:1 mixture of E/Z isomers. There was too much overlap in spectra to accurately assign chemical shifts.

5-(2-Chloroacetyl)-3-(2-hydroxy-5-nitrobenzylidene)indolin-2-one (47) JH191B. Isolated as a 1.3:1 mixture of E/Z isomers. This is the spectrum of the major isomer. ^1H NMR (DMSO- d_6): δ 4.91 (s, 2H), 6.98 (d, $J = 8.4$ Hz, 1H), 7.15 (d, $J = 9.2$ Hz, 1H), 7.66

(s, 1H), 7.90 (dd, $J = 8.4, 1.8$ Hz, 1H), 7.99 (d, $J = 1.5$ Hz, 1H), 8.24 (dd, $J = 9.2, 2.9$ Hz, 1H), 8.52 (d, $J = 2.9$ Hz, 1H), 11.1 (s, 1H), 12.0 (s, 1H).

(Z)-3-(5-tert-Butyl-2-hydroxybenzylidene)-5-(2-chloroacetyl)indolin-2-one (48)

JH192B. ^1H NMR (DMSO- d_6): δ 1.28 (s, 9H), 5.03 (s, 2H), 6.98 (d, $J = 8.9$, Hz, 1H), 6.99 (d, $J = 8.1$, Hz, 1H), 7.43 (dd, $J = 8.4, 2.6$ Hz, 1H), 7.65 (d, $J = 2.6$, Hz, 1H), 7.84 (s, 1H), 7.95 (dd, $J = 8.4, 1.8$ Hz, 1H), 8.22 (d, $J = 1.5$ Hz, 1H), 10.1 (s, 1H), 11.1 (s, 1H).

3-(3-tert-Butyl-2-hydroxybenzylidene)-5-(2-chloroacetyl)indolin-2-one (49)

JH193A. Isolated as a clean 3:1 mixture of E/Z isomers. There was too much overlap in spectra to accurately assign chemical shifts.

5-(2-Chloroacetyl)-3-(thiophen-3-ylmethylene)indolin-2-one (50) JH194A.

Isolated as a 2:1 mixture of E/Z isomers. This is the spectrum of the major isomer. ^1H NMR (DMSO- d_6): δ 5.16 (s, 2H), 6.97 (d, $J = 8.4$ Hz, 1H), 7.66 (dd, $J = 5.1, 2.9$ Hz, 1H), 7.90 (dd, $J = 8.4, 1.8$ Hz, 1H), 8.10 (s, 1H), 8.14 (dd, $J = 5.1, 1.1$ Hz, 1H), 8.35 (d, $J = 1.5$ Hz, 1H), 8.85 (d, $J = 2.6$ Hz, 1H), 11.1 (s, 1H).

(Z)-5-(2-Chloroacetyl)-3-(furan-3-ylmethylene)indolin-2-one (51) JH195A.

^1H NMR (DMSO- d_6): δ 5.15 (s, 2H), 6.97 (d, $J = 8.4$ Hz, 1H), 7.46 (d, $J = 1.8$ Hz, 1H), 7.83 (t, $J = 1.8$ Hz, 1H), 7.89 (dd, $J = 8.1, 1.5$ Hz, 1H), 7.93 (s, 1H), 8.31 (d, $J = 1.5$ Hz, 1H), 8.69 (d, $J = 1.1$ Hz, 1H), 11.1 (s, 1H).

(Z)-5-(2-Chloroacetyl)-3-(3-hydroxybenzylidene)indolin-2-one (52) JH196A.

^1H NMR (DMSO- d_6): δ 5.02 (s, 2H), 6.93 (dd, $J = 8.1, 2.2$ Hz, 1H), 7.00 (d, $J = 8.1$ Hz, 1H), 7.13 (s, 1H), 7.17 (d, $J = 7.7$ Hz, 1H), 7.36 (t, $J = 7.7$ Hz, 1H), 7.67 (s, 1H), 7.97 (dd, $J = 8.1, 1.5$ Hz, 1H), 8.23 (d, $J = 1.2$ Hz, 1H), 9.76 (s, 1H), 11.1 (s, 1H).

(Z)-5-(2-Chloroacetyl)-3-((5-(hydroxymethyl)furan-2-yl)methylene)indolin-2-one (53) JH198. ^1H NMR (DMSO- d_6): δ 4.72 (s, 2H), 5.25 (s, 2H), 6.69 (d, $J = 3.3$ Hz, 1H), 7.02 (d, $J = 8.4$, Hz, 1H), 7.31 (d, $J = 3.3$, Hz, 1H), 7.42 (s, 1H), 7.94 (dd, $J = 8.4$, 1.8 Hz, 1H), 9.03 (d, $J = 1.5$, Hz, 1H), 11.0 (s, 1H).

(Z)-5-((5-(2-Chloroacetyl)-2-oxoindolin-3-ylidene)methyl)-2,4-dimethyl-1H-pyrrole-3-carboxylic acid (54) JH156. ^1H NMR (DMSO- d_6): δ 2.55 (s, 3H), 2.56 (s, 3H), 5.20 (s, 2H), 7.02 (d, $J = 8.1$, Hz, 1H), 7.82 (d, $J = 8.4$, Hz, 1H), 7.90 (s, 1H), 8.50 (s, 1H), 11.4 (s, 1H), 13.7 (s, 1H).

5-Acetylundolin-2-one⁴² (55) JH008. Acetyl chloride (766 mg, 9.76 mmol, 1.3 equiv) was added dropwise to a stirred suspension of anhydrous AlCl_3 (6.11 g, 45.8 mmol, 6.1 equiv) in carbon disulfide (26 mL). Stirring was then allowed to continue at room temperature for 10 min. Indolin-2-one (1.0 g, 7.51 mmol, 1 equiv) was then added. The mixture was then brought to reflux for 4 h, and cooled on ice. After removal of the solvent by decantation the remaining thick brown residue was treated with ice cold water (100 mL). The resulting precipitate was recovered by filtration, washed with water, and dried under vacuum to provide pure **55** (1.12 g, 85%) as a white solid. ^1H NMR (DMSO- d_6): δ 2.50 (s, 3H), 3.55 (s, 2H), 6.90 (dd, $J = 8.1$, 3.7 Hz, 1H), 7.80 (s, 1H), 7.85 (d, $J = 8.1$ Hz, 1H), 10.8 (bs, 1H).

5-Ethylundolin-2-one⁴² (56) JH018. Triethylsilane (451 mg, 3.88 mmol, 1.36 equiv) was added dropwise to a stirred solution of **55** (500 mg, 2.85 mmol, 1 equiv) in trifluoroacetic acid (3.75 mL) on an ice bath. Stirring was allowed to continue for 5 h then more triethylsilane (182 mg, 1.56 mmol, 0.55 equiv) was added. Stirring was allowed to continue for an additional 16 h at room temperature then the reaction was

dumped onto crushed ice (200 mL). After the ice had melted the mixture was extracted with EtOAc. The EtOAc extract was washed with brine, dried over sodium sulfate, and concentrated under vacuum to give the crude product as a cream-colored solid. This material was added to boiling hexanes (30 mL) and treated with DCM (~3-4 mL) until a clear solution formed. The DCM was then removed by distillation, and the remaining liquid cooled. The resulting precipitate was collected by filtration, washed with hexanes, and dried under vacuum to give pure **56** (300 mg, 65%) as a pale yellow solid. ¹H NMR (DMSO-*d*₆): δ 1.22 (t, *J* = 7.7 Hz, 3H), 2.61 (q, *J* = 7.7 Hz, 2H), 3.52 (s, 2H), 6.80 (d, *J* = 8.1 Hz, 1H), 7.05 (d, *J* = 7.3 Hz, 1H), 7.08 (s, 1H), 8.77 (bs, 1H).

Fluoroacetyl chloride⁴⁷ (**57**) **JH040**. Sodium fluoroacetate ([Poison! lethal in humans at 2–10 mg/kg], 5.25 g, 52.4 mmol, 1 equiv) was added to solid PCl₅ (12 g, 57.6 mmol, 1.1 equiv) in a 50 mL round bottom flask. A distillation head and condenser were immediately placed on the flask. The flask was then swirled to mix the solids and initiate an exothermic reaction that produced HCl (Note: don't breathe the fumes as the final product is volatile and toxic!). The mixture was then heated on an oil bath (100 °C), and stirred until it became a refluxing liquid. Reflux was allowed to continue for 45 min then the bath temperature was increased to 130 °C. With this amount of heating the product was collected by distillation to give **57** (4.5 g, 89%, *d* = 1.45 g/mL) as a clear liquid.

5-(2-Fluoroacetyl)indolin-2-one (58) JH044. Fluoroacetyl chloride (**57**) ([Poison!], 544 mg, 5.67 mmol, 1.5 equiv) was added dropwise to a stirred suspension of anhydrous AlCl₃ (2.5 g, 18.8 mmol, 5 equiv) in carbon disulfide (20 mL). Stirring was then allowed to continue at room temperature for 10 min. Indolin-2-one (0.5 g, 3.76 mmol, 1 equiv) was then added, and the mixture was shaken with venting due to the formation of HCl for

a little over 1 min (longer reaction times promote fluorine to chlorine halogen exchange on the desired product). The solvent was then removed by decantation, and the remaining thick brown residue treated with ice cold water (100 mL). The resulting precipitate was recovered by filtration, washed with water, and dried under vacuum to provide a 3:2 mixture of **58** and **3** (461 mg total for the mixture, ~61% combined yield). The desired product, **58**, was separated by preparative HPLC on a C18 column. ^1H NMR (DMSO- d_6): δ 3.56 (s, 2H), 5.73 (d, $J = 46$ Hz, 2H), 6.93 (d, $J = 8.1$ Hz, 1H), 7.74 (s, 1H), 7.78 (d, $J = 8.1$ Hz, 1H), 10.8 (bs, 1H).

5-Nitroindolin-2-one⁴² (**59**) **JH054**. Concentrated HNO_3 (2.5 mL) was added to a stirred solution of indolin-2-one (6.5 g, 48.9 mmol, 1 equiv) in conc. H_2SO_4 (25 mL) at -10 °C. The resulting mixture was stirred at 0 °C for 30 min then poured into ice water. The resulting precipitate was recovered by filtration, washed with water, and air dried to give pure **59** as a light tan solid (6.0 g, 69%). ^1H NMR (DMSO- d_6): δ 3.63 (s, 2H), 6.98 (d, $J = 8.8$ Hz, 1H), 8.09 (s, 1H), 8.14 (d, $J = 8.4$ Hz, 1H), 11.0 (bs, 1H).

5-Aminoindolin-2-one⁴² (**60**) **JH056**. A suspension of **59** (1.0 g, 5.61 mmol, 1 equiv) and 10% Pd/C (500 mg) in methanol (50 mL) was placed under 1 atm of hydrogen with stirring for 19 h. The catalyst was then removed by filtration, followed by the methanol under reduced pressure to give pure **60** (661 mg, 80%) as an off white solid. ^1H NMR (DMSO- d_6): δ 3.31 (s, 2H), 4.63 (s, 2H), 6.37 (d, $J = 8.4$ Hz, 1H), 6.49 (d, $J = 8.4$ Hz, 1H), 6.50 (s, 1H), 9.91 (s, 1H).

N-(2-Oxoindolin-5-yl)methacrylamide (**61**) **JH082**. 2-Methacryloyl chloride (211 mg, 2.02 mmol, 2 equiv) was added dropwise over the course of 5 min to a solution of **60** (150 mg, 1.01 mmol, 1 equiv) and pyridine (120 mg, 1.52 mmol, 1.5 equiv) in anhydrous

THF (50 mL) at 0 °C. The mixture was allowed to warm to room temperature and stir for 1 h. Then water (10 mL) was added, and most of the THF removed under vacuum. After standing overnight the resulting precipitate was collected by filtration to give pure **61** (25 mg, 15%) as a white solid. ¹H NMR (DMSO-*d*₆): δ 1.93 (s, 3H), 3.46 (s, 2H), 5.46 (s, 1H), 5.75 (s, 1H), 6.74 (d, *J* = 8.4 Hz, 1H), 7.42 (d, *J* = 8.4 Hz, 1H), 7.55 (s, 1H), 9.62 (s, 1H), 10.3 (s, 1H).

(E)-N-(2-oxoindolin-5-yl)but-2-enamide (62) JH080. Crotonoyl chloride (275 mg, 2.63 mmol, 1.3 equiv) was added dropwise over the course of 5 min to a solution of **60** (300 mg, 2.02 mmol, 1 equiv) in anhydrous THF (115 mL) at 0 °C. The mixture was then allowed to warm to room temperature and stir for 15 min. After filtration to remove some insoluble material, water (20 mL) was added and most of the THF removed under vacuum. The resulting precipitate was collected by filtration to give pure **62** (142 mg, 35%) as a white solid. ¹H NMR (DMSO-*d*₆): δ 1.85 (d, *J* = 7.0 Hz, 3H), 3.46 (s, 2H), 6.09 (d, *J* = 15 Hz, 1H), 6.73 (d, *J* = 8.1 Hz, 1H), 6.74 (dd, *J* = 15, 7.0 Hz, 1H), 7.38 (d, *J* = 8.4 Hz, 1H), 7.57 (s, 1H), 9.77 (s, 1H), 10.3 (s, 1H).

2-Cyano-N-(2-oxoindolin-5-yl)acetamide (63) JH078. To a stirred solution of **60** (150 mg, 1.01 mmol, 1 equiv) and EDC (387 mg, 2.02 mmol, 2 equiv) in acetonitrile (40 mL) was added cyanoacetic acid (95 mg, 1.11 mmol, 1.1 equiv) in acetonitrile (4 mL) over the course of 5 min. The resulting mixture was allowed to stir for 30 minutes at room temperature. Water (25 mL) was then added, followed by removal of most of the acetonitrile under reduced pressure. The resulting precipitate was collected by filtration to give pure **63** (134 mg, 62%) as a white solid. ¹H NMR (DMSO-*d*₆): δ 3.47 (s, 2H), 3.84

(s, 2H), 6.76 (d, $J = 8.4$ Hz, 1H), 7.29 (d, $J = 8.4$ Hz, 1H), 7.44 (s, 1H), 10.1 (s, 1H), 10.3 (s, 1H).

***N*-(2-Oxoindolin-5-yl)ethanesulfonamide (64) JH083.** 2-Chloroethanesulfonyl chloride (412 mg, 2.53 mmol, 2.5 equiv) was added dropwise to a solution of **60** (150 mg, 1.01 mmol, 1 equiv) and DIPEA (392 mg, 3.03 mmol, 3 equiv) in anhydrous THF (50 mL) at 0 °C. The mixture was allowed stir for 1 h. Then water (5 mL) was added, and most of the THF removed under vacuum. The resulting precipitate was collected by filtration to give pure **64** (135 mg, 56%) as a white solid. ¹H NMR (DMSO-*d*₆): δ 3.45 (s, 2H), 5.97 (d, $J = 8.9$ Hz, 1H), 6.00 (d, $J = 17$ Hz, 1H), 6.70 (dd, $J = 17, 8.9$ Hz, 1H), 6.73 (d, $J = 8.1$ Hz, 1H), 6.97 (d, $J = 8.4$ Hz, 1H), 7.03 (s, 1H), 9.61 (s, 1H), 10.3 (s, 1H).

***(Z)*-3-((1*H*-Pyrrol-2-yl)methylene)-5-ethylindolin-2-one (65) JH048.** Indolinone **56** (100 mg, 0.620 mmol, 1 equiv) was added to a solution of pyrrole-2-carboxaldehyde (76.7 mg, 0.806 mmol, 1.3 equiv), and piperidine (5.3 mg, 0.062 mmol, 0.1 equiv) in EtOH (2 mL). The resulting mixture was refluxed for 4 h. After cooling to room temperature EtOH (3 mL) was added. The precipitated product was recovered by filtration, washed with EtOH, and dried under vacuum to give pure **65** (55 mg, 37%) as a yellow solid. ¹H NMR (DMSO-*d*₆): δ 1.20 (t, $J = 7.7$ Hz, 3H), 2.60 (q, $J = 7.7$ Hz, 2H), 6.32-6.35 (m, 1H), 6.78 (d, $J = 7.7$ Hz, 1H), 6.78-6.83 (m, 1H), 6.99 (d, $J = 7.7$ Hz, 1H), 7.31-7.35 (m, 1H), 7.49 (s, 1H), 7.73 (s, 1H), 10.8 (s, 1H), 13.3 (bs, 1H).

***(Z)*-3-((1*H*-Pyrrol-2-yl)methylene)-5-acetylindolin-2-one (66) JH049.** Indolinone **55** (200 mg, 1.14 mmol, 1 equiv) was added to a solution of pyrrole-2-carboxaldehyde (542 mg, 5.7 mmol, 5 equiv), and piperidine (9.7 mg, 0.114 mmol, 0.1 equiv) in EtOH (11 mL). The resulting mixture was refluxed for 5.5 h, then stirred at room temperature

for 18 h. The resulting precipitate was recovered by filtration, washed with EtOH, and dried under vacuum to give pure **66** (170 mg, 60%) as a yellow solid. ¹H NMR (DMSO-*d*₆): δ 2.58 (s, 3H), 6.37-6.41 (m, 1H), 6.90-6.94 (m, 1H), 6.98 (d, *J* = 8.1 Hz, 1H), 7.39-7.43 (m, 1H), 7.82 (d, *J* = 8.1 Hz, 1H), 8.0 (s, 1H), 8.30 (s, 1H), 11.3 (s, 1H), 13.2 (bs, 1H).

(Z)-3-((1H-Pyrrol-2-yl)methylene)-5-(2-fluoroacetyl)indolin-2-one 67 (JH050).

Indolinone **58** (13 mg, 0.067 mmol, 1 equiv) was added to a solution of pyrrole-2-carboxaldehyde (32 mg, 0.34 mmol, 5 equiv), and piperidine (0.9 mg, 0.01 mmol, 0.2 equiv) in EtOH (2.6 mL). The resulting mixture was heated to 60 °C in a sealed jar for 3 h. After cooling to room temperature the volume of the mixture was reduced under vacuum. The resulting precipitate was recovered by filtration, washed with EtOH, and dried under vacuum to give pure **67** (3.5 mg, 19%) as a green-yellow solid. The NMR of this material contained too much water accurately assign chemical shifts.

(Z)-N-(3-((1H-Pyrrol-2-yl)methylene)-2-oxoindolin-5-yl)methacrylamide (68)

JH094. Indolinone **61** (16 mg, 0.074 mmol, 1 equiv) was added to a solution of pyrrole-2-carboxaldehyde (70.4 mg, 0.74 mmol, 10 equiv), and piperidine (1.3 mg, 0.015 mmol, 0.2 equiv) in THF (2.5 mL). The resulting mixture was heated to 75 °C in a sealed jar for 2 h. After cooling to room temperature the mixture was concentrated to dryness under vacuum. The residue was then purified by triturating in 4:1 EtOAc:hexanes overnight. The product was then recovered by filtration and dried under vacuum to give pure **68** (170 mg, 60%) as a yellow solid. ¹H NMR (DMSO-*d*₆): δ 1.96 (s, 3H), 5.49 (s, 1H), 5.81 (s, 1H), 6.33-6.37 (m, 1H), 6.83 (d, *J* = 8.1 Hz, 1H), 6.89-6.92 (m, 1H), 7.30 (dd, *J* = 8.4,

1.8 Hz, 1H), 7.34-7.38 (m, 1H), 7.61 (s, 1H), 7.96 (d, $J = 1.5$ Hz, 1H), 9.68 (s, 1H), 10.8 (s, 1H), 13.3 (bs, 1H).

(E)-N-((Z)-3-((1H-Pyrrol-2-yl)methylene)-2-oxoindolin-5-yl)but-2-enamide (69)

JH095. Indolinone **62** (40 mg, 0.185 mmol, 1 equiv) was added to a solution of pyrrole-2-carboxaldehyde (176 mg, 1.85 mmol, 10 equiv), and piperidine (3.2 mg, 0.037 mmol, 0.2 equiv) in THF (2.5 mL). The resulting mixture was heated to 75 °C in a sealed jar for 2 h. After cooling to room temperature the mixture was concentrated to dryness under vacuum. The residue was then purified by triturating in 4:1 EtOAc:hexanes overnight. The product was then recovered by filtration and dried under vacuum to give pure **69** (49 mg, 90%) as a yellow solid. ^1H NMR (DMSO- d_6): δ 1.87 (d, $J = 5.9$ Hz, 3H), 6.12 (d, $J = 15$ Hz, 1H), 6.33-6.38 (m, 1H), 6.78 (dd, $J = 16, 7.3$ Hz, 1H), 6.82 (d, $J = 8.4$ Hz, 1H), 6.91-6.95 (m, 1H), 7.24 (dd, $J = 8.1, 1.5$ Hz, 1H), 7.34-7.37 (m, 1H), 7.60 (s, 1H), 8.02 (s, 1H), 9.85 (s, 1H), 10.8 (s, 1H), 13.3 (bs, 1H).

(Z)-N-(3-((1H-Pyrrol-2-yl)methylene)-2-oxoindolin-5-yl)ethanesulfonamide (70)

JH096. Indolinone **64** (40 mg, 0.168 mmol, 1 equiv) was added to a solution of pyrrole-2-carboxaldehyde (160 mg, 1.68 mmol, 10 equiv), and piperidine (2.9 mg, 0.034 mmol, 0.2 equiv) in THF (2.5 mL). The resulting mixture was heated to 75 °C in a sealed jar for 2 h. After cooling to room temperature the mixture was concentrated to dryness under vacuum. The residue was dissolved in EtOAc and filtered to remove some tar. The soluble product was then purified by silica gel chromatography using 2:1 hexanes:EtOAc as the mobile phase to give pure **70** (25 mg, 47%) as a yellow solid. ^1H NMR (DMSO- d_6): δ 5.98 (d, $J = 9.9$ Hz, 1H), 6.03 (d, $J = 17$ Hz, 1H), 6.34-6.39 (m, 1H), 6.75 (dd, $J = 17, 9.9$ Hz, 1H), 6.82 (d, $J = 8.1$ Hz, 1H), 6.91-6.94 (m, 1H), 6.95 (dd, $J = 8.4, 2.2$ Hz,

1H), 7.35-7.38 (m, 1H), 7.41 (d, $J = 1.8$ Hz, 1H), 7.68 (s, 1H), 9.65 (s, 1H), 10.9 (s, 1H), 13.3 (s, 1H).

3-(Methylthio)-4-nitroindolin-2-one (71) JH117. Under an atmosphere of argon and protection from strong light, a solution of t-butyl hypochlorite (15.7 g, 145 mmol, 1 equiv) in DCM (70 mL) was added dropwise over 10 min to a stirred solution of 3-nitroaniline (20 g, 145 mmol, 1 equiv) in DCM (1000 mL) at -65 °C. Care was taken to keep the internal temperature of the mixture below -50 °C during the addition. The resulting mixture was allowed to stir for 10 min, then a solution of ethyl (methylthio)acetate (19.5 g, 145 mmol, 1 equiv) in DCM (60 mL) was added over the course of 5 min, keeping the internal temperature of the reaction below -60 °C. The resulting mixture was allowed to stir for 1 h, then a solution of Et_3N (14.7 g, 145 mmol, 1 equiv) in DCM (60 mL) was added over the course of 7 min, again keeping the internal temperature of the reaction below -60 °C. The reaction was then allowed to come to room temperature, and stir for a total of 5 h. The mixture was then washed with water (100 mL), and concentrated under vacuum to give a red/black residue that was treated with Et_2O (420 mL) and 2 N HCl (70 mL) for 18 h at room temperature. The insoluble product was recovered by filtration, and washed with Et_2O to give pure **71** (17.8 g, 54%) as a grayish-brown solid. ^1H NMR (DMSO- d_6): δ 1.90 (s, 3H), 4.86 (s, 1H), 7.24 (d, $J = 7.7$ Hz, 1H), 7.52 (d, $J = 7.7$ Hz, 1H), 7.72 (d, $J = 7.7$ Hz, 1H), 11.0 (s, 1H).

4-Aminoindolin-2-one (72) JH118. Indolinone **71** (17.6 g, 68.8 mmol, 1 equiv) was added to a solution of zinc dust (54 g, 826 mmol, 12 equiv) in glacial acetic acid (530 mL) at room temperature. Concentrated HCl (31.6 mL) was then added dropwise over the course of 15 min, using an external ice bath to keep the temperature of the reaction below

60 °C (40 °C may be a better ceiling). The reaction was allowed to stir at room temperature for 105 min, then filtered through celite to remove solids. The acetic acid was removed by vacuum distillation to give an off-white slurry. This slurry was suspended in 800 mL of water and treated with solid NaOH to bring the pH to 13. The resulting mixture was extracted with warm EtOAc (2.2 L) in 500 mL portions. The combine EtOAc extracts were washed with water, then brine, and reduced in volume under vacuum to precipitate the product. The product was collected by filtration and washed with EtOAc to give pure **72** (6.5 g, 64%) as a grey solid. ¹H NMR (DMSO-*d*₆): δ 3.12 (s, 2H), 4.97 (s, 2H), 6.01 (d, *J* = 7.3 Hz, 1H), 6.17 (d, *J* = 8.4 Hz, 1H), 6.79 (t, *J* = 7.7 Hz, 1H), 10.1 (s, 1H).

2-Chloro-1-(3-nitrophenyl)ethanone (73) JH086. *N*-Chlorosuccinimide (11.3 g, 84.3 mmol, 1.4 equiv) was added to a solution of pTSA·H₂O (16.03 g, 84.3 mmol, 1.4 equiv) and 3-nitro-acetophenone (10 g, 60.2 mmol, 1 equiv) in acetonitrile (300 mL) at room temperature. The resulting mixture was allowed to stir at room temperature for 18 h, then concentrated to dryness under vacuum. The resulting residue was dissolved in EtOAc (300 mL) and washed with sat. NaHCO₃, then water, then brine. The EtOAc was then removed under reduced pressure to give pure **73** (10.2 g, 100%) as a white solid. ¹H NMR (DMSO-*d*₆): δ 5.33 (s, 2H), 7.87 (t, *J* = 8.1 Hz, 1H), 8.39 (dt, *J* = 7.7, 1.5 Hz, 1H), 8.51 (dd, *J* = 8.1, 2.2 Hz, 1H), 8.68 (t, *J* = 1.8 Hz, 1H).

1-(3-Aminophenyl)-2-chloroethanone (74) JH097. Compound **73** (16.0 g, 30.0 mmol, 1 equiv) was suspended in EtOH (250 mL). The resulting mixture was treated with SnCl₂ (22.8 g, 120 mmol, 4 equiv) and stirred at room temperature for 22 h. Most of the EtOH was then removed under reduced pressure. The residual suspension was then added

to 5% NaHCO₃ (1 L). The resulting mixture was extracted with EtOAc (1.5 L) in 500 mL portions. The combined EtOAc extracts were then concentrated under reduced pressure to give pure **74** (4.4g, 87%) as a white solid. ¹H NMR (DMSO-*d*₆): δ 5.08 (s, 2H), 6.83-6.86 (m, 1H), 7.11-7.18 (m, 3H).

4-(2-Chloroacetyl)-3-(methylthio)indolin-2-one (75) JH110. Under an atmosphere of argon and protection from strong light, a solution of t-butyl hypochlorite (2.94 g, 0.027 mmol, 1.05 equiv) in DCM (12 mL) was added dropwise over 5 min to a stirred solution of **74** (4.37 g, 0.026 mmol, 1 equiv) in DCM (120 mL) at -65 °C. Care was taken to keep the internal temperature of the mixture below -50 °C during the addition. The resulting mixture was allowed to stir for 10 min, then a solution of ethyl (methylthio)acetate (3.64 g, 0.027 mmol, 1.05 equiv) in DCM (12 mL) was added over the course of 5 min, keeping the internal temperature of the reaction below -60 °C. The resulting mixture was allowed to stir for 1 h, then a solution of Et₃N (2.74 g, 0.027 mmol, 1.05 equiv) in DCM (12 mL) was added over the course of 5 min, again keeping the internal temperature of the reaction below -60 °C. The reaction was then allowed to come to room temperature and stir for a total of 80 min. The mixture was then concentrated under vacuum to give a red/black residue that was treated with Et₂O (100 mL) and 2 N HCl (12 mL) for 20 h at room temperature. The insoluble material was then recovered by filtration. This material was purified by extracting with boiling methanol, filtering to remove solids. The methanol extract was then cooled to room temperature. The resulting precipitate was collected by filtration and washed with methanol to give pure **75** (1.3 g, 20%) as a grayish-brown solid. ¹H NMR (DMSO-*d*₆): δ 1.90 (s, 3H), 4.68 (s, 1H), 5.03 (d, *J* = 16 Hz, 1H), 5.21 (d,

$J = 16$ Hz, 1H), 7.08 (d, $J = 7.7$ Hz, 1H), 7.40 (t, $J = 8.1$ Hz, 1H), 7.50 (d, $J = 8.1$ Hz, 1H), 10.7 (s, 1H).

2-(Hydroxyimino)-*N*-(3-iodophenyl)acetamide (76) JH221.⁴⁸ A solution of 3-iodoaniline (24.4 g, 111 mmol, 1 equiv) and conc HCl (9.63 mL) in water (436 mL), was added to a mixture of chloral hydrate (20.3 g, 123 mmol, 1.1 equiv), water (261 mL), and Na₂SO₄ (290 g, 2.04 mol, 18.4 equiv), followed by a solution of hydroxylamine hydrochloride (20 g, 288 mmol, 2.6 equiv) in water (72 mL). The resulting mixture was heated to reflux for 45 min, then immediately cooled on ice. The resulting precipitate was removed by filtration, washed with water, and dried under vacuum. The resulting residue was triturated in DCM (80 mL), recovered by filtration, washed with DCM (50 mL), and dried under vacuum to give **76** (18.3 g, 57%). This material was used as is in the synthesis of **78** and **79**.

4-Iodoindoline-2,3-dione⁴⁸ (**77**) JH227, and **6-iodoindoline-2,3-dione**⁴⁸ (**78**) JH227B. Compound **76** (18.3 g, 63 mmol) was added to concentrated H₂SO₄ (83 g) at 50 °C. The addition was done in small portions to keep the temperature of the reaction below 55 °C using an ice bath when needed. The resulting mixture was then heated to 80 °C for 10 min, then immediately cooled to 25 °C, and poured onto crushed ice (450 g). Once the ice had melted the resulting red-precipitate was collected by filtration, washed with water, and dissolved in 2 N NaOH (150 mL). This solution was filtered to remove some insoluble material, washed with DCM (25 mL), cooled to 0 °C, then acidified to pH 4 with glacial acetic acid (~70 mL). The resulting precipitate was recovered by filtration, washed with water (250 mL), and dried under vacuum to give pure **77** (7.5g, 10%). The filtrate was allowed to stand for 15 days. The resulting precipitate was recovered by

filtration, washed with water and dried under vacuum to give pure **78** (1.9 g, 2%). **77** ^1H NMR (DMSO- d_6): δ 6.90 (d, $J = 8.1$ Hz, 1H), 7.25 (t, $J = 8.1$ Hz, 1H), 7.48 (d, $J = 8.1$ Hz, 1H), 11.0 (s, 1H).

78 ^1H NMR (DMSO- d_6): δ 7.25 (d, $J = 7.7$ Hz, 1H), 7.27 (d, $J = 1.5$ Hz, 1H), 7.47 (dd, $J = 7.7, 1.5$ Hz, 1H), 11.1 (s, 1H).

4-Iodoindolin-2-one (79) JH321. Compound **77** (6.0 g, 22 mmol, 1 equiv) was added to hydrazine monohydrate (25.8 g, 506 mmol, 23 equiv). The resulting mixture was heated using a 125 °C oil bath for 15 min. During this time a precipitate formed and re-dissolved. This precipitate was probably the intermediate hydrazone, as it stained with p-anise aldehyde on TLC (the final product does not stain). After heating, the reaction was cooled to 25 °C, diluted with water (100 mL), and made strongly acidic with concentrated HCl. The resulting mixture was cooled on ice. The resulting precipitate was recovered by filtration, washed with water (250 mL), and dried under vacuum to give pure **79** (4.1 g, 72%). ^1H NMR (DMSO- d_6): δ 3.29 (s, 2H), 6.77 (d, $J = 7.7$ Hz, 1H), 6.92 (t, $J = 7.7$ Hz, 1H), 7.25 (d, $J = 8.1$ Hz, 1H), 10.6 (s, 1H).

N-(3-Bromophenyl)-2-(hydroxyimino)acetamide (80) JH311. A solution of 3-bromo-aniline (47 g, 273 mmol, 1 equiv) and conc HCl (24.2 mL) in water (280 mL), was added to a mixture of tri-bromo-acetaldehyde (100 g, 356 mmol, 1.3 equiv), water (745 mL), and Na_2SO_4 (82 g, 573 mmol, 2.1 equiv), followed by a solution of hydroxylamine hydrochloride (71.2 g, 1.02 mol, 3.75 equiv) in water (317 mL). The resulting mixture was heated to reflux for 10 min, then immediately cooled on ice. The resulting precipitate was removed by filtration, washed with water (5 L), and dried under

vacuum to give **80** (67.5 g, 100%). ^1H NMR (DMSO- d_6): δ 7.28-7.31 (m, 2H), 7.62-7.65 (m, 2H), 8.02 (s, 1H), 10.3 (s, 1H), 12.2 (s, 1H).

4-Bromoindoline-2,3-dione (81) JH312, and 6-bromoindoline-2,3-dione (82)

JH312B. Compound **80** (67.5 g, 280 mmol) was added to concentrated H_2SO_4 (800 mL). The addition was done in small portions to keep the temperature of the reaction below 40 $^\circ\text{C}$ using an ice bath when needed. The resulting mixture was then heated to 83 $^\circ\text{C}$ for 10 min (it took 30 min to reach 80 $^\circ\text{C}$) then immediately cooled to 25 $^\circ\text{C}$, and poured onto crushed ice (3500 mL). Once the ice melted, the resulting red-precipitate was collected by filtration and washed with water (1.5 L). The filter cake was suspended in water (700 mL) and treated with 50% w/v NaOH (50 mL: this is probably more than required). The resulting solution was filtered to remove some insoluble material then acidified to pH 4 with concentrated HCl and cooled on an ice bath. The resulting precipitate was recovered by filtration, washed with water (2 L), and dried under vacuum to give pure **81** (14.1 g, 23 %). The filtrate was then made strongly acidic with concentrated HCl. The resulting precipitate was recovered by filtration, washed with water and dried under vacuum to give a 1:1 mixture of **81** and **82** (31 g, 49% combined yield). **81** ^1H NMR (DMSO- d_6): δ 6.89 (d, $J = 7.7$ Hz, 1H), 7.23 (d, $J = 8.1$ Hz, 1H), 7.46 (d, $J = 8.1$ Hz, 1H), 11.2 (s, 1H). **82** ^1H NMR (DMSO- d_6): δ 7.08 (s, 1H), 7.27 (d, $J = 7.7$ Hz, 1H), 7.44 (d, $J = 7.7$ Hz, 1H), 11. (s, 1H).

4-Bromoindolin-2-one (83) JH316. Compound **81** (4.0 g, 17.7 mmol, 1 equiv) was added to hydrazine monohydrate (20.6 g, 404 mmol, 23 equiv). The resulting mixture was heated using a 125 $^\circ\text{C}$ oil bath for 25 min. Note: the intermediate hydrazone runs on top of the product by TLC however it stains with p-anise aldehyde (the final product does

not stain). After heating, the reaction was cooled to 25 °C, diluted with water (50 mL), and made strongly acidic with concentrated HCl. The resulting mixture was cooled on ice and extracted with EtOAc (750 mL) in five 150 mL portions. The combined EtOAc extracts were washed with water, then brine, then clarified with activated carbon, and concentrated under vacuum to give pure **83** (3 g, 80%) as a orange solid. ¹H NMR (DMSO-*d*₆): δ 3.44 (s, 1H), 6.81 (d, *J* = 6.6 Hz, 1H), 7.06-7.16 (m, 2H), 10.6 (s, 1H).

(Z)-3-((1H-Pyrrol-2-yl)methylene)-4-aminoindolin-2-one (84) JH119. Indolinone **72** (1.5 g, 10.1 mmol, 1 equiv) was added to a solution of pyrrole-2-carboxaldehyde (1.01 g, 10.6 mmol, 1.05 equiv), and piperidine (172 mg, 2.02 mmol, 0.2 equiv) in THF (60 mL). The resulting mixture was heated to 75 °C in a sealed jar for 24 h. Some molecular sieves were then added and heating continued for 21.5 h. After cooling to room temperature the molecular sieves were removed by filtration. The filtrate was concentrated to dryness under vacuum. The residue was then purified by recrystallization from methanol to give pure **84** (1.7 g, 66%) as a yellow solid. ¹H NMR (DMSO-*d*₆): δ 5.52 (s, 2H), 6.19 (d, *J* = 7.3 Hz, 1H), 6.27-6.30 (m, 1H), 6.39 (d, *J* = 8.1 Hz, 1H), 6.72-6.75 (m, 1H), 6.87 (t, *J* = 7.7 Hz, 1H), 7.21-7.30 (m, 1H), 7.59 (s, 1H), 10.7 (s, 1H), 13.3 (s, 1H).

(Z)-N-(3-((1H-Pyrrol-2-yl)methylene)-2-oxoindolin-4-yl)acrylamide (85) JH120. Pyridine (63.2 mg, 0.799 mmol, 1.2 equiv) was added to a solution of **84** (150 mg, 0.666 mmol, 1 equiv) in anhydrous THF (50 mL). The mixture was cooled to 0 °C then a solution of acryloyl chloride (72.3 mg, 0.799 mmol, 1.2 equiv) in THF (5 mL) was added dropwise. The resulting mixture was allowed stir at 0 °C for 15 min, then allowed to come to room temperature and stir for 15 min. Water (6 mL) was then added and most of

the THF was removed under vacuum. The resulting precipitate was recovered by filtration, washed with water, and dried under vacuum to give pure **85** (104 mg, 65%) as a yellow solid. ¹H NMR (DMSO-*d*₆): δ 5.83 (d, *J* = 9.9 Hz, 1H), 6.20-6.38 (m, 2H), 6.51-6.69 (m, 2H), 6.74-6.96 (m, 2H), 7.14 (t, *J* = 8.1 Hz, 1H), 7.36 (s, 1H), 7.54 (s, 1H), 10.1 (s, 1H), 11.0 (s, 1H), 13.4 (s, 1H).

(E)-N-((Z)-3-((1H-Pyrrol-2-yl)methylene)-2-oxoindolin-4-yl)but-2-enamide (86)
JH121. Pyridine (65.9 mg, 0.833 mmol, 1.25 equiv) was added to a solution of **84** (150 mg, 0.666 mmol, 1 equiv) in anhydrous THF (50 mL). The mixture was cooled to 0 °C then crotonoyl chloride (87.0 mg, 0.833 mmol, 1.25 equiv) was added dropwise. The mixture was allowed to come to room temperature and stir for 1 h. Water (10 mL) was then added and most of the THF was removed under vacuum. The resulting precipitate was recovered by filtration, washed with water, and dried under vacuum to give pure **86** (115 mg, 59%) as a yellow solid. ¹H NMR (DMSO-*d*₆): δ 1.91 (d, *J* = 6.6 Hz, 3H), 6.19-6.38 (m, 2H), 6.63-6.68 (m, 1H), 6.74-6.92 (m, 3H), 7.12 (t, *J* = 8.1 Hz, 1H), 7.35 (s, 1H), 7.54 (s, 1H), 9.86 (s, 1H), 11.0 (s, 1H), 13.4 (s, 1H).

(Z)-N-(3-((1H-Pyrrol-2-yl)methylene)-2-oxoindolin-4-yl)methacrylamide (87)
JH122. Pyridine (79.0 mg, 0.999 mmol, 1.5 equiv) was added to a solution of **84** (150 mg, 0.666 mmol, 1 equiv) in anhydrous THF (50 mL). The mixture was cooled to 0 °C then 2-methacryloyl chloride (104 mg, 0.999 mmol, 1.5 equiv) was added dropwise. The mixture was allowed to stir at 0 °C for 2 h. Water (10 mL) was then added and most of the THF was removed under vacuum. The resulting precipitate was recovered by filtration, washed with water, and dried under vacuum. This material was purified by dissolving in THF, concentrating to saturation under vacuum, then diluting with one

volume of EtOAc. The resulting precipitate was collected by filtration, and subjected to the same purification procedure again to give **87** (small amount) as a yellow solid. ¹H NMR (DMSO-*d*₆): δ 2.02 (s, 3H), 5.61 (s, 1H), 5.94 (s, 1H), 6.33-6.37 (m, 1H), 6.57-6.60 (m, 1H), 6.80 (d, *J* = 7.7 Hz, 1H), 6.84 (d, *J* = 8.1 Hz, 1H), 7.14 (t, *J* = 8.1 Hz, 1H), 7.34-7.38 (m, 1H), 7.49 (s, 1H), 9.90 (s, 1H), 11.0 (s, 1H), 13.3 (s, 1H).

(Z)-N-(3-((1H-Pyrrol-2-yl)methylene)-2-oxoindolin-4-yl)-2-chloroacetamide (88)

JH123. Pyridine (63.2 mg, 0.799 mmol, 1.2 equiv) was added to a solution of **84** (150 mg, 0.666 mmol, 1 equiv) in anhydrous THF (50 mL). The mixture was cooled to 0 °C then chloroacetyl chloride (90.2 mg, 0.799 mmol, 1.2 equiv) was added dropwise. The mixture was allowed to come to room temperature and stir for 30 min. Water (10 mL) was then added and most of the THF was removed under vacuum. The resulting precipitate was recovered by filtration, washed with water, and dried under vacuum to give pure **88** (180 mg, 90%) as a yellow solid. ¹H NMR (DMSO-*d*₆): δ 4.38 (s, 2H), 6.35-6.37 (m, 1H) 6.80 (d, *J* = 7.7 Hz, 1H), 6.80-6.83 (m, 1H), 6.87 (d, *J* = 8.1 Hz, 1H), 7.14 (t, *J* = 8.1 Hz, 1H), 7.35-7.38 (m, 1H), 7.67 (s, 1H), 10.3 (s, 1H), 11.0 (s, 1H), 13.4 (bs, 1H).

(Z)-N-(3-((1H-Pyrrol-2-yl)methylene)-2-oxoindolin-4-yl)-2-cyanoacetamide (89)

JH126. To a stirred solution of **84** (150 mg, 0.666 mmol, 1 equiv) and EDC (255 mg, 1.33 mmol, 2 equiv) in acetonitrile (50 mL) was added cyanoacetic acid (62.3 mg, 1.11 mmol, 1.1 equiv) in acetonitrile (3 mL) over the course of 5 min. The resulting mixture was allowed to stir for 15 minutes at room temperature. Water (25 mL) was then added, followed by removal of most of the acetonitrile under reduced pressure. The resulting precipitate was collected by filtration to give pure **89** (120 mg, 62%) as a yellow solid. ¹H

NMR (DMSO- d_6): δ 3.99 (s, 2H), 6.30-6.33 (m, 1H), 6.75 (d, $J = 8.4$ Hz, 1H), 6.84 (d, $J = 8.1$ Hz, 1H), 6.92-6.94 (m, 1H), 7.09 (t, $J = 7.7$ Hz, 1H), 7.31-7.33 (m, 1H), 7.60 (s, 1H), 10.2 (s, 1H), 11.0 (s, 1H), 13.3 (s, 1H).

(E)-Ethyl 4-((Z)-3-((1H-pyrrol-2-yl)methylene)-2-oxoindolin-4-ylamino)-4-oxobut-2-enoate (90) JH130. Monoethyl fumarate (128 mg, 0.888 mmol, 2 equiv) was added to a solution of thionyl chloride (119 mg, 0.888 mmol, 2 equiv) in THF (20 mL). The resulting mixture was refluxed for 1h then concentrated to dryness under vacuum. The residue from this reaction was dissolved in THF (2 mL) then added dropwise to a solution of pyridine (70.2 mg, 0.888 mmol, 2 equiv) and **84** (100 mg, 0.444 mmol, 1 equiv) in anhydrous THF (40 mL) at 0 °C. The resulting mixture was allowed to stir at 0 °C for 15 min, then at room temperature for 15 min. Water (15 mL) was then added and most of the THF was removed under vacuum. The resulting mixture was then treated with sat. NaHCO₃ (2 mL). The resulting precipitate was recovered by filtration, washed with 1 N HCl, then water, and dried under vacuum to give pure **90** (105 mg, 67%) as a yellow solid. ¹H NMR (DMSO- d_6): δ 1.29 (t, $J = 7.7$ Hz, 3H), 4.25 (q, $J = 7.3$ Hz, 2H), 6.32-6.36 (m, 1H), 6.72-6.75 (m, 1H), 6.75 (d, $J = 15$ Hz, 1H), 6.80 (d, $J = 7.3$ Hz, 1H), 6.96 (d, $J = 8.1$ Hz, 1H), 7.15 (t, $J = 7.7$ Hz, 1H), 7.35-7.38 (m, 1H), 7.37 (d, $J = 15$ Hz, 1H), 7.55 (s, 1H), 10.5 (s, 1H), 11.0 (s, 1H), 13.4 (bs, 1H).

4-Iodo-5-nitroindolin-2-one (91) JH331.⁴⁹ A solution of concentrated HNO₃ (700 μ L) in concentrated H₂SO₄ (3.6 mL) was slowly added dropwise over the course of 10 minutes to a solution of **79** (2.5 g, 9.7 mmol, 1 equiv) in concentrated H₂SO₄ (30 mL) at -5 °C. The resulting mixture was allowed to stir for 20 min at -5 °C then added to crushed ice (300 mL). After the ice melted the resulting precipitate was collected by filtration,

washed with water, and dried under vacuum to give pure **91** (2.4 g, 82%) as a solid. ¹H NMR (DMSO-*d*₆): δ 3.51 (s, 2H), 6.93 (d, *J* = 8.8 Hz, 1H), 7.94 (d, *J* = 8.4 Hz, 1H), 11.2 (s, 1H).

(Z)-4-Iodo-3-((4-methyl-1H-imidazol-5-yl)methylene)-5-nitroindolin-2-one (92) JH334. Indolinone **91** (195 mg, 0.641 mmol, 1 equiv) was added to a suspension of 4-methyl-1H-imidazole-5-carbaldehyde (81.2 mg, 0.737 mmol, 1.2 equiv), and piperidine (11 mg, 0.13 mmol, 0.2 equiv) in THF (6 mL). The resulting mixture was heated to 75 °C in a sealed jar for 30 h. After cooling to room temperature the resulting precipitate was collected by filtration, washed with EtOAc, and dried under vacuum to give pure **92** (130 mg, 52%) as a yellow solid. ¹H NMR (DMSO-*d*₆): δ 2.47 (s, 3H), 7.03 (d, *J* = 8.4 Hz, 1H), 7.69 (d, *J* = 8.1 Hz, 1H), 8.05 (s, 1H), 9.19 (s, 1H), 11.5 (s, 1H), 13.6 (bs, 1H).

4-Bromo-5-nitroindolin-2-one (93) JH355.⁴⁹ A solution of concentrated HNO₃ (2.37 mL) in concentrated H₂SO₄ (12 mL) was slowly added dropwise over the course of 10 minutes to a solution of **83** (6.6 g, 31 mmol, 1 equiv) in concentrated H₂SO₄ (67 mL) at -5 °C. The resulting mixture was allowed to stir for 45 min at -5 °C then added to a mixture of crushed ice (150 mL) and water (60 mL). After the ice melted the resulting precipitate was collected by filtration, washed with water, and dried under vacuum to give pure **99** (7.2 g, 90%) as a tan solid. ¹H NMR (DMSO-*d*₆): δ 3.59 (s, 2H) 6.94 (d, *J* = 8.4 Hz, 1H), 8.01 (d, *J* = 8.4 Hz, 1H), 11.1 (bs, 1H).

(Z)-3-((1H-Pyrrol-2-yl)methylene)-4-bromo-5-nitroindolin-2-one (94) JH319. Indolinone **93** (100 mg, 0.394 mmol, 1 equiv) was added to a solution of pyrrole-2-carboxaldehyde (43 mg, 0.453 mmol, 1.2 equiv), and piperidine (6.7 mg, 0.079 mmol, 0.2 equiv) in THF (6 mL). The resulting mixture was heated to 75 °C in a sealed jar for

24 h. After cooling to room temperature the mixture was decanted from some precipitated tar and concentrated under reduced pressure. The resulting residue was triturated in EtOAc, recovered by filtration, washed with 1:1 hexanes:EtOAc, and dried under vacuum to give pure **94** (82 mg, 63%) as a yellow solid. ¹H NMR (DMSO-*d*₆): δ 6.45-6.47 (m, 1H), 7.04 (d, *J* = 8.4 Hz, 1H), 7.09-7.11 (m, 1H), 7.52-7.54 (m, 1H), 7.79 (d, *J* = 8.4 Hz, 1H), 8.79 (s, 1H), 11.6 (bs, 1H), 13.4 (bs, 1H).

(Z)-4-Bromo-3-((4-methyl-1H-imidazol-5-yl)methylene)-5-nitroindolin-2-one (95) JH318. Indolinone **93** (100 mg, 0.394 mmol, 1 equiv) was added to a suspension of 4-methyl-1H-imidazole-5-carbaldehyde (49.9 mg, 0.453 mmol, 1.2 equiv), and piperidine (6.7 mg, 0.079 mmol, 0.2 equiv) in THF (5 mL). The resulting mixture was heated to 75 °C in a sealed jar for 3.5 h. After cooling to room temperature the resulting precipitate was collected by filtration, washed with EtOAc, and dried under vacuum to give pure **95** (109 mg, 81%) as a yellow solid. ¹H NMR (DMSO-*d*₆): δ 2.39 (s, 3H), 7.00 (d, *J* = 8.4 Hz, 1H), 7.78 (d, *J* = 8.4 Hz, 1H), 7.99 (s, 1H), 8.79 (s, 1H), 13.5 (bs, 1H).

(Z)-tert-Butyl 1-(3-((1H-pyrrol-2-yl)methylene)-5-nitro-2-oxoindolin-4-yl)piperidin-4-ylcarbamate (96) JH320. A mixture of **94** (75 mg, 0.225 mmol, 1 equiv), tert-butyl piperidin-4-ylcarbamate (450 mg, 2.25 mmol, 10 equiv), DIPEA (725 mg, 5.61 mmol, 25 equiv), and dioxane (7 mL) was heated to 120 °C for 6.5 h in a sealed jar. The resulting mixture was then concentrated to dryness under reduced pressure. The resulting residue was extracted with EtOAc (5 mL). The EtOAc extract was then concentrated to a volume of 1.5 mL and purified by silica gel chromatography, using 2.5:1 hexanes:EtOAc as the mobile phase, to give almost pure **96** (70 mg, 68%) as a thick red semi-solid. ¹H NMR (CDCl₃) note: the cyclohexyl protons are not assigned: δ 1.49 (s, 9H), 6.37-6.46

(m, 1H), 6.73 (d, $J = 8.4$ Hz, 1H), 6.83-6.87 (m, 1H), 7.19-7.23 (m, 1H), 7.45 (d, $J = 8.4$ Hz, 1H), 8.62 (s, 1H), 9.32 (s, 1H), 13.2 (bs, 1H).

(Z)-3-((1H-Pyrrol-2-yl)methylene)-4-(4-aminopiperidin-1-yl)-5-nitroindolin-2-one hydrochloride (97) JH346. To a solution of acetyl chloride (24 mg, 0.4 mmol, 20 equiv) in methanol (1 mL) was added **96** (7 mg, 0.02 mmol, 1 equiv). The resulting mixture was allowed to stir at room temperature for 2 h, then concentrated to dryness to give pure **97** (6 mg, 100%). ^1H NMR (DMSO- d_6): δ note: the cyclohexyl protons are not assigned: δ 6.42-6.46 (m, 1H), 6.83 (d, $J = 8.4$ Hz, 1H), 7.37-7.40 (m, 1H), 7.46-7.49 (m, 1H), 7.55 (d, $J = 8.4$ Hz, 1H), 8.38 (s, 1H), 11.4 (s, 1H), 13.3 (bs, 1H).

(Z)-3-((1H-pyrrol-2-yl)methylene)-4-morpholino-5-nitroindolin-2-one (98) JH336. A mixture of **94** (100 mg, 0.299 mmol, 1 equiv), morpholine (261 mg, 2.99 mmol, 10 equiv), DIPEA (890 mg, 6.88 mmol, 23 equiv), and DMF (2.7 mL) was heated to 125 °C for 18 h in a sealed jar. After cooling to room temperature water (50 mL) was added. The resulting mixture was extracted with EtOAc (250 mL) in five 50 mL portions. The combined EtOAc extracts were washed with water, then brine, and concentrated to dryness under vacuum. The residue was purified by trituration in methanol to give pure **98** (15 mg, 15%). ^1H NMR (DMSO- d_6): δ 2.94-3.2 (m, 4H), 3.84 (bs, 4H), 6.41-6.45 (m, 1H), 6.83 (d, $J = 8.4$ Hz, 1H), 7.00-7.03 (m, 1H), 7.45-7.48 (m, 1H), 7.57 (d, $J = 8.4$ Hz, 1H), 8.59 (s, 1H), 11.4 (s, 1H), 13.3 (bs, 1H).

(Z)-3-((4-Methyl-1H-imidazol-5-yl)methylene)-4-morpholino-5-nitroindolin-2-one (99) JH335. A mixture of **95** (123 mg, 0.352 mmol, 1 equiv), morpholine (307 mg, 3.52 mmol, 10 equiv), DIPEA (1.05 g, 8.1 mmol, 23 equiv), and DMF (3 mL) was heated to 125 °C for 18 h in a sealed jar. After cooling to room temperature water (50 mL) was

added. The resulting mixture was extracted with EtOAc (250 mL) in five 50 mL portions. The combined EtOAc extracts were washed with water, then brine, and concentrated to dryness under vacuum. The residue was purified by trituration in methanol to give pure **99** (30 mg, 24%). ¹H NMR (DMSO-*d*₆): δ 2.52 (s, 3H), 3.05-3.18 (m, 4H), 3.81-3.88 (m, 4H), 6.85 (d, *J* = 8.4 Hz, 1H), 7.58 (d, *J* = 8.4 Hz, 1H), 8.00 (s, 1H), 8.70 (s, 1H), 11.5 (s, 1H), 13.8 (bs, 1H).

(But-3-yn-2-yloxy)(tert-butyl)dimethylsilane (100) JH343. A mixture of 3-butyn-2-ol (6.94 g, 99 mmol, 1.4 equiv), TBDMS-Cl (11 g, 73 mmol, 1 equiv), and imidazole (10 g, 147 mmol, 2 equiv) in DMF (25 mL) was allowed to stir at room temperature for 5 h. The resulting mixture was then dumped into water (250 mL) and extracted with hexanes (150 mL) in three 50 mL portions. The combine hexanes extract was washed with water, then brine, and concentrated under reduced pressure to give pure **100** (12.3 g, 68%) as a clear liquid (volatile under strong vacuum). ¹H NMR (CDCl₃): δ 0.117 (s, 3H), 0.131 (s, 3H), 0.905 (s, 9H), 1.42 (d, *J* = 6.6 Hz, 3H), 2.35 (d, *J* = 2.2 Hz, 1H), 4.52 (dq, *J* = 6.6, 2.2 Hz, 1H).

(Z)-4-(3-(tert-Butyldimethylsilyloxy)but-1-ynyl)-3-((4-methyl-1*H*-imidazol-5-yl)methylene)-5-nitroindolin-2-one (101) JH351. To an oven-dried, argon-purged Schlenk flask was added **95** (50 mg, 0.143 mmol, 1 equiv), (Ph₃P)₄Pd (16.5 mg, 0.014 mmol, 0.1 equiv), CuI (3 mg, 0.014 mmol, 0.1 equiv), DMF (1.5 mL), Et₃N (2 g, 19 mmol, 138 equiv), and **100** (66 mg, 0.358 mmol, 2.5 equiv). The flask was further purged with argon then heated to 85 °C for 3 h. After cooling to room temperature the resulting mixture was diluted with EtOAc (20 mL) and washed with 10% aq NH₄Cl (100 mL). The NH₄Cl wash was back-extracted with EtOAc. The combine EtOAc extracts were then

washed with 5% NaHCO₃, then water, then brine, and concentrated to dryness under vacuum. The resulting residue was purified by silica gel chromatography using 2:1 hexanes:EtOAc as the mobile phase, followed by preparative silica gel TLC, to give pure **101** (12.5 mg, 20%). ¹H NMR (CDCl₃): δ 0.133 (s, 3H), 0.156 (s, 3H), 0.898 (s, 9H), 1.62 (d, *J* = 6.6 Hz, 3H), 2.63 (s, 3H), 4.96 (q, *J* = 6.6 Hz, 1H), 6.94 (d, *J* = 8.4 Hz, 1H), 7.26 (s, 1H), 7.86 (s, 1H), 7.92 (d, *J* = 8.8 Hz, 1H), 9.02 (s, 1H), 13.8 (bs, 1H).

(Z)-4-(3-Hydroxybut-1-ynyl)-3-((4-methyl-1*H*-imidazol-5-yl)methylene)-5-nitroindolin-2-one (102) JH357. Concentrated HCl (10 μL) was added to a solution of **101** (12.5 mg, 0.028 mmol, 1 equiv) in THF (2 mL). The resulting mixture was allowed to stir at room temperature for 2 h (during this time a yellow precipitate formed) then concentrated to dryness. The resulting residue was triturated in EtOAc, recovered by filtration, washed with EtOAc, and dried under vacuum to give pure **102** (5.1 mg, 49%) as a yellow solid. ¹H NMR (DMSO-*d*₆): δ 1.49 (d, *J* = 6.6 Hz, 3H), 2.61 (s, 3H), 4.85 (q, *J* = 6.6 Hz, 1H), 7.13 (d, *J* = 8.8 Hz, 1H), 8.08 (d, *J* = 8.8 Hz, 1H), 8.68 (s, 1H), 8.98 (s, 1H), 12.1 (s, 1H), 13.8 (bs, 1H).

(Z)-3-((1*H*-Pyrrol-2-yl)methylene)-4-(3-(tert-butyldimethylsilyloxy)but-1-ynyl)-5-nitroindolin-2-one (103) JH359. To an oven-dried, argon-purged Schlenk flask was added **94** (700 mg, 2.1 mmol, 1 equiv), (Ph₃P)₄Pd (25 mg, 0.021 mmol, 0.01 equiv), CuI (38 mg, 0.2 mmol, 0.1 equiv), DMF (20 mL), Et₃N (14.9 g, 147 mmol, 70 equiv), and **100** (968 mg, 5.3 mmol, 2.5 equiv). The flask was further purged with argon then heated to 85 °C for 5 h. After cooling to room temperature the resulting mixture was diluted with EtOAc (275 mL) then washed with 20% aq NH₄Cl (800 mL) in four 200 mL portions, then water, then brine, and concentrated to dryness under vacuum. The resulting residue

was purified by silica gel chromatography, using 3:1 hexanes:EtOAc as the mobile phase, to give pure **103** (430 mg, 49%) as a orange solid (this material could probably be purified by recrystallization from chloroform). This material was used as is in following reactions.

(Z)-3-((1H-Pyrrol-2-yl)methylene)-4-(3-hydroxybut-1-ynyl)-5-nitroindolin-2-one (104) JH361. Concentrated HCl (10 μ L) was added to a solution of **103** (20 mg, 0.046 mmol, 1 equiv) in THF (1 mL). The resulting mixture was allowed to stir at room temperature for 18 h then 3 drops of concentrated HCl were added and stirring was allowed to continue for an additional 24 h. The mixture was then concentrated to dryness under vacuum. The resulting residue was purified by silica gel chromatography, using 2:1 hexanes:EtOAc as the mobile phase, to give pure **104** (5 mg, 28%) as a yellow solid. ^1H NMR (DMSO- d_6): δ 1.46 (d, $J = 6.6$ Hz, 3H), 4.77-4.83 (m, 1H), 5.87 (d, $J = 5.9$ Hz, 1H), 6.40-6.43 (m, 1H), 6.97-7.00 (m, 1H), 7.47-7.50 (m, 1H), 7.91 (d, $J = 8.9$ Hz, 1H), 8.90 (s, 1H), 11.6 (s, 1H), 13.3 (bs, 1H).

(Z)-3-((1H-Pyrrol-2-yl)methylene)-5-amino-4-(3-(tert-butyl dimethylsilyloxy)but-1-ynyl)indolin-2-one (105) JH368. Zinc dust (1.12 g, 17.5 mmol, 68 equiv) was added to a suspension of indolinone **103** (112 mg, 0.256 mmol, 1 equiv) in THF (22 mL) and saturated aqueous NH_4Cl (11.2 mL). The resulting mixture was vigorously stirred and heated to 80 $^\circ\text{C}$ for 30 min. The THF layer was then separated, diluted with EtOAc (100 mL), washed with water, then saturated NaCl, and concentrated under vacuum to give pure **105** (105 mg, 100%) as a red solid. ^1H NMR (DMSO- d_6): δ 0.181 (s, 3H), 0.194 (s, 3H), 0.94 (s, 9H), 1.68 (d, $J = 6.6$ Hz, 3H), 4.95 (q, $J = 6.6$ Hz, 1H), 6.37-6.40 (m, 1H),

6.55 (d, $J = 8.4$ Hz, 1H), 6.69 (d, $J = 8.4$ Hz, 1H), 6.77-9.79 (m, 1H), 7.19-7.21 (m, 1H), 7.26 (s, 1H), 8.62 (s, 1H), 13.4 (bs, 1H).

(Z)-N-(3-((1H-Pyrrol-2-yl)methylene)-4-(3-(tert-butyldimethylsilyloxy)but-1-ynyl)-2-oxoindolin-5-yl)propiolamide (106) JH374. A solution of propiolic acid (32.15 mg, 0.456 mmol, 6 equiv) in acetonitrile (1 mL) was added to a solution of **105** (31 mg, 0.076 mmol, 1 equiv), EDC (58.2 mg, 0.30 mmol, 4 equiv), and HOBt (11 mg, 0.080 mmol, 1.05 equiv) in 1:1 DMF:acetonitrile (10 mL). The resulting mixture was allowed to stir at room temperature for 30 min then 1 N HCl (50 mL) was added. The resulting mixture was extracted with EtOAc. The EtOAc extract was washed with water, then saturated NaCl, then concentrated to dryness. The resulting residue was purified by preparative TLC to give pure **106** (8.4 mg, 25%) as an orange solid. ^1H NMR (DMSO- d_6): δ 0.206 (s, 3H), 0.216 (s, 3H), 0.951 (s, 9H), 1.73 (d, $J = 6.6$ Hz, 3H), 2.95 (s, 1H), 4.98 (q, $J = 6.6$ Hz, 1H), 6.40-6.43 (m, 1H), 6.80-6.83 (m, 1H), 6.87 (d, $J = 8.8$ Hz, 1H), 7.21-7.25 (m, 1H), 7.91 (s, 1H), 8.16 (d, $J = 8.4$ Hz, 1H), 8.19 (s, 1H), 8.56 (s, 1H), 13.4 (bs, 1H).

(Z)-N-(3-((1H-Pyrrol-2-yl)methylene)-4-(3-hydroxybut-1-ynyl)-2-oxoindolin-5-yl)propiolamide (107) JH375. Aqueous HCl (1 N, 400 μL) was added to a solution of **106** (7.6 mg, 0.017 mmol, 1 equiv) in THF (800 μL). The resulting mixture was allowed to stir at room temperature for 4 h then filtered to remove some insoluble material. The filtrate was then concentrated to dryness under vacuum. The resulting residue was suspended in chloroform (1.5 mL) and filtered to remove some insoluble material. The filtrate was concentrated to dryness to give pure **107** (1.5 mg, 26%) as a yellow solid. ^1H NMR (DMSO- d_6): δ 1.51 (d, $J = 6.6$ Hz, 3H), 4.34 (s, 1H), 4.79 (q, $J = 6.6$ Hz, 1H), 6.38-

6.42 (m, 1H), 6.86-6.92 (m, 1H), 6.89 (d, $J = 8.1$ Hz, 1H), 7.20 (d, $J = 8.4$ Hz, 1H), 7.43 (s, 1H), 8.67 (s, 1H), 10.1 (s, 1H), 11.1 (s, 1H), 13.4 (bs, 1H).

(Z)-5-((5-Acetyl-2-oxoindolin-3-ylidene)methyl)-2,4-dimethyl-1H-pyrrole-3-carboxylic acid (109) JH152. Indolinone **55** (100 mg, 0.571 mmol, 1 equiv) was added to a solution of **108** (143 mg, 0.856 mmol, 1.5 equiv), and piperidine (87 mg, 0.861 mmol, 1.8 equiv) in THF (7 mL). The resulting mixture was heated to 75 °C in a sealed jar for 2 h. After cooling to room temperature the mixture was treated with 1.3 N HCl (3 mL) and EtOAc (5 mL). The resulting mixture was reduced in volume by 50% under reduced pressure. The resulting precipitate was collected by filtration then dried under vacuum to give pure **109** (144 mg, 78%) as a greenish-brown solid. ¹H NMR (DMSO-*d*₆): δ 2.54 (s, 3H), 2.55 (s, 3H), 2.60 (s, 3H), 6.98 (d, $J = 8.4$ Hz, 1H), 7.80 (dd, $J = 8.4, 1.8$ Hz, 1H), 7.88 (s, 1H), 8.85 (d, $J = 1.5$ Hz, 1H), 11.3 (bs, 1H), 13.7 (bs, 1H).

(Z)-5-((5-Acetyl-2-oxoindolin-3-ylidene)methyl)-N-(2-(diethylamino)ethyl)-2,4-dimethyl-1H-pyrrole-3-carboxamide (110) JH381. *N*¹,*N*¹-Diethylethane-1,2-diamine (69.5 mg, 0.555 mmol, 3 equiv) was added to a solution of **109** (60 mg, 0.185 mmol, 1 equiv), EDC (106.4 mg, 0.555 mmol, 3 equiv), HOBT (37.5 mg, 0.278 mmol, 1.5 equiv), and DIPEA (71.9 mg, 0.555 mmol, 3 equiv) in DMF (6 mL). The resulting mixture was allowed to stir at room temperature for 13 h then 0.5 N HCl (24mL) was added. The resulting mixture was washed with EtOAc then made basic with 1N NaOH. The resulting mixture was then extracted with EtOAc. The EtOAc extract was washed with water, then saturated NaCl, then concentrated to dryness to give pure **110** (40 mg, 51%). ¹H NMR (DMSO-*d*₆) note: due to overlap with the DMSO peak the four internal methylene protons could not be assigned: δ 0.977 (t, $J = 7.0$ Hz, 6H), 2.45 (s, 3H), 2.47 (s, 3H), 2.60

(s, 3H), 3.28 (q, $J = 7.0$ Hz, 4H), 6.98 (d, $J = 8.1$ Hz, 1H), 7.44 (t, $J = 5.9$ Hz, 1H), 7.79 (dd, $J = 8.4, 1.8$ Hz, 1H), 7.85 (s, 1H), 8.43 (d, $J = 1.5$ Hz, 1H), 11.3 (bs, 1H), 13.6 (bs, 1H).

(Z)-5-((5-(2-(Chloromethyl)-1,3-dioxolan-2-yl)-1-methyl-2-oxoindolin-3-ylidene)methyl)-2,4-dimethyl-1H-pyrrole-3-carboxylic acid (111) JH401. Indolinone **33** (100 mg, 0.374 mmol, 1.05 equiv) was added to a solution of **108** (59.4 mg, 0.355 mmol, 1 equiv), and piperidine (39.3 mg, 0.462 mmol, 1.3 equiv) in THF (7 mL). The resulting mixture was heated to 75 °C in a sealed jar for 24 h. After cooling to room temperature the resulting precipitate was collected by filtration, washed with 0.1 N HCl, then water, then methanol, then EtOAc, and dried under vacuum to give pure **111** (82 mg, 53%). ¹H NMR (DMSO-*d*₆): δ 2.54 (s, 3H), 2.55 (s, 3H), 3.32 (s, 3H), 3.86-3.90 (m, 2H), 3.96 (s, 2H), 4.10-4.13 (m, 2H), 7.05 (d, $J = 8.4$ Hz, 1H), 7.36 (dd, $J = 8.1, 1.8$ Hz, 1H), 7.79 (s, 1H), 8.00 (d, $J = 1.5$ Hz, 1H), 12.2 (s, 1H), 13.7 (bs, 1H).

(Z)-5-((5-(2-Chloroacetyl)-1-methyl-2-oxoindolin-3-ylidene)methyl)-N-(2-(diethylamino)ethyl)-2,4-dimethyl-1H-pyrrole-3-carboxamide (112) JH405. *N*¹,*N*¹-Diethylethane-1,2-diamine (27.9 mg, 0.24 mmol, 2 equiv) was added to a suspension of **111** (50 mg, 0.12 mmol, 1 equiv), EDC (46 mg, 0.24 mmol, 2 equiv), HOBt (16.2 mg, 0.12 mmol, 1 equiv), and Et₃N (36.4 mg, 0.38 mmol, 3 equiv) in DMF (6 mL). The resulting mixture was allowed to stir at room temperature for 18 h then 5% NaHCO₃ (50 mL) was added. The resulting mixture was then extracted with EtOAc. The EtOAc extract was washed with water, then saturated NaCl, then concentrated to dryness. The resulting residue was dissolved in THF (4 mL) and treated with 4 drops of concentrated HCl. The resulting mixture was allowed to stir at room temperature for 18 h then

concentrated to dryness under vacuum to give pure **111** (35 mg, 62%) as a yellow solid.

¹H NMR (DMSO-*d*₆) note: due to overlap with the DMSO peak the four internal methylene protons could not be assigned: δ 0.984 (t, *J* = 7.0 Hz, 6H), 2.47 (s, 3H), 2.48 (s, 3H), 3.37 (s, 3H), 5.20 (s, 2H), 7.22 (d, *J* = 8.4 Hz, 1H), 7.49 (bs, 1H), 7.87 (s, 1H), 7.88 (d, *J* = 8.1 Hz, 1H), 8.49 (s, 1H), 13.5 (bs, 1H).

(Z)-5-((5-(2-(Chloromethyl)-1,3-dioxolan-2-yl)-2-oxoindolin-3-ylidene)methyl)-2,4-dimethyl-1H-pyrrole-3-carboxylic acid (113) JH155. Indolinone **18** (1.14 g, 4.51 mmol, 1 equiv) was added to a solution of **108** (905 mg, 5.41 mmol, 1.2 equiv), and piperidine (576 mg, 6.77 mmol, 1.5 equiv) in THF (70 mL). The resulting mixture was heated to 75 °C in a sealed jar for 4 h. After cooling to room temperature for 18 h, 1 N HCl (20 mL) and EtOAc (70 mL) were added. The resulting precipitate was collected by filtration (from the two phase mixture), washed with water, and dried under vacuum to give pure **113** (950 mg, 52%). ¹H NMR (DMSO-*d*₆): δ 2.52 (s, 3H), 2.54 (s, 3H) 3.86-3.89 (m, 2H), 3.94 (s, 2H), 4.09-4.12 (m, 2H), 6.87 (d, *J* = 8.1 Hz, 1H), 7.27 (dd, *J* = 8.1, 1.5 Hz, 1H), 7.75 (s, 1H), 7.94 (d, *J* = 1.1 Hz, 1H), 11.0 (s, 1H), 12.1 (s, 1H), 13.8 (s, 1H).

(Z)-5-((5-(2-Chloroacetyl)-2-oxoindolin-3-ylidene)methyl)-N-(2-(diethylamino)ethyl)-2,4-dimethyl-1H-pyrrole-3-carboxamide (114) JH175. *N*¹,*N*¹-Diethylethane-1,2-diamine (17.3 mg, 0.149 mmol, 1.2 equiv) was added to a solution of **113** (50 mg, 0.124 mmol, 1 equiv), EDC (47.5 mg, 0.25 mmol, 2 equiv), HOBT (16.8 mg, 0.12 mmol, 1 equiv), and Et₃N (37.6 mg, 0.37 mmol, 3 equiv) in DMF (5 mL). The resulting mixture was allowed to stir at room temperature for 16 h then 1 N HCl (50 mL) was added. After 10 minutes the resulting mixture was washed with EtOAc then made

basic with 5% NaHCO₃. The resulting mixture was then extracted with EtOAc. The EtOAc extract was washed with water, then saturated NaCl, then concentrated to dryness to give pure **114** (43 mg, 76%) as a yellow solid. ¹H NMR (DMSO-*d*₆): δ 0.983 (t, *J* = 6.6 Hz, 6H), 2.46 (s, 3H), 2.48 (s, 3H), 2.50-2.58 (m, 4H), 3.24-3.32 (m, 4H), 5.20 (s, 2H), 7.02 (d, *J* = 8.1 Hz, 1H), 7.48 (bs, 1H), 7.81 (dd, *J* = 8.1, 1.5 Hz, 1H), 7.85 (s, 1H), 8.47 (d, *J* = 1.5 Hz, 1H), 11.4 (s, 1H), 13.5 (s, 1H).

(S,Z)-5-((5-(2-Chloroacetyl)-2-oxoindolin-3-ylidene)methyl)-N-(2-hydroxy-3-morpholinopropyl)-2,4-dimethyl-1H-pyrrole-3-carboxamide hydrochloride (115) JH386. (S)-1-Amino-3-morpholinopropan-2-ol hydrochloride (80 mg, 0.327 mmol, 3 equiv) was added to a solution of **113** (50 mg, 0.125 mmol, 1 equiv), EDC (71.3 mg, 0.372 mmol, 3 equiv), HOBt (25 mg, 0.186 mmol, 1.5 equiv), and DIPEA (48 mg, 0.372 mmol, 3 equiv) in DMF (6 mL). The resulting mixture was allowed to stir at room temperature for 13 h then 0.5 N HCl (24mL) was added. The resulting mixture was washed with EtOAc then made basic with 1N NaOH. The resulting mixture was then extracted with EtOAc. The EtOAc extract was washed with water, then saturated NaCl, then concentrated to dryness. The residue was dissolved in THF (50 mL) and treated with 10 drops of concentrated HCl. The resulting mixture was allowed to stir at room temperature for 18 h then concentrated to dryness under reduced pressure to give pure **115** (30 mg, 45%). ¹H NMR (DMSO-*d*₆) note: the aliphatic methylene protons are not assigned: δ 2.50 (s, 3H), 2.51 (s, 3H), 5.21 (s, 2H), 7.03 (d, *J* = 8.1 Hz, 1H), 7.82 (d, *J* = 9.1 Hz, 1H), 7.84 (bs, 1H), 7.87 (s, 1H), 8.49 (s, 1H), 11.4 (s, 1H), 13.6 (s, 1H).

(Z)-N-(5-Aminopentyl)-5-((5-(2-chloroacetyl)-2-oxoindolin-3-ylidene)methyl)-2,4-dimethyl-1H-pyrrole-3-carboxamide hydrochloride (116) JH165. tert-Butyl 5-

aminopentylcarbamate (75.4 mg, 0.373 mmol, 1.1 equiv) was added to a solution of **113** (137 mg, 0.339 mmol, 1 equiv), EDC (130 mg, 0.678 mmol, 2 equiv), HOBT (45.8 mg, 0.339 mmol, 1 equiv), and Et₃N (68.6 mg, 0.678 mmol, 2 equiv) in DMF (12 mL). The resulting mixture was allowed to stir at room temperature for 6 h then water (150 mL) was added. The resulting mixture was then extracted with EtOAc. The EtOAc extract was washed with water then concentrated to dryness. The residue was purified by silica gel chromatography, using 3:1 hexanes:EtOAc as the mobile phase, to give pure **116** (148 mg, 75%). ¹H NMR (DMSO-*d*₆): δ 1.35-1.41 (m, 2H), 1.49-1.57 (m, 2H), 1.57-1.65 (m, 2H), 2.45 (s, 3H), 2.46 (s, 3H), 2.73-2.79 (m, 2H), 3.20-3.25 (m, 2H), 5.21 (s, 2H), 7.03 (d, *J* = 8.1 Hz, 1H), 7.72 (t, *J* = 5.5 Hz, 1H), 7.81 (dd, *J* = 8.1, 1.5 Hz, 1H), 7.86 (s, 1H), 8.48 (d, *J* = 1.5 Hz, 1H), 11.4 (s, 1H), 13.5 (s, 1H).

(Z)-5-((5-(2-Chloroacetyl)-2-oxoindolin-3-ylidene)methyl)-2,4-dimethyl-N-(3-(prop-2-ynoxy)propyl)-1H-pyrrole-3-carboxamide (117) JH391. Compound **119** (84 mg, 0.558 mmol, 3 equiv) was added to a solution of **113** (75 mg, 0.188 mmol, 1 equiv), EDC (107 mg, 0.558 mmol, 3 equiv), HOBT (37.5 mg, 0.279 mmol, 1.5 equiv), and DIPEA (72 mg, 0.558 mmol, 3 equiv) in DMF (8 mL). The resulting mixture was allowed to stir at room temperature for 20 h then 1 N HCl (40 mL) and water (100 mL) were added. The resulting mixture was then extracted with EtOAc. The EtOAc extract was washed with 5% NaHCO₃, then water, then brine, and concentrated to dryness under reduced pressure. The residue was suspended in THF (4 mL) and treated with concentrated HCl (160 μL). The resulting mixture was allowed to stir at room temperature for 20 h then concentrated to dryness under reduced pressure to give pure **117** (30 mg, 53%). ¹H NMR (DMSO-*d*₆): δ 1.78 (p, *J* = 6.6 Hz, 2H), 2.45 (s, 3H), 2.46 (s,

3H), 3.29 (dt, $J = 6.6, 5.6$ Hz, 2H), 3.42 (t, $J = 2.6$ Hz, 1H), 3.52 (t, $J = 2.5$ Hz, 2H), 4.14 (d, $J = 2.2$ Hz, 2H), 5.20 (s, 2H), 7.02 (d, $J = 8.4$ Hz, 1H), 7.66 (t, $J = 5.5$ Hz, 1H), 7.81 (dd, $J = 8.4, 1.8$ Hz, 1H), 7.85 (s, 1H), 8.46 (d, $J = 1.1$ Hz, 1H), 11.3 (s, 1H), 13.5 (s, 1H).

tert-Butyl 3-(prop-2-ynyloxy)propylcarbamate (118) JH389. A solution of tert-butyl 3-hydroxypropylcarbamate (2.5 g, 14.3 mmol, 1 equiv) in THF (5 mL) was added dropwise to a suspension of NaH (377 mg, 15.7 mmol, 1.1 equiv) in THF (5 mL) at 0 °C. The resulting mixture was allowed to stir for 1h then propargyl bromide (1.88 g, 15.7 mmol, 1.1 equiv) was added dropwise. The resulting mixture was allowed to stir at room temperature for 24 h then water (50 mL) was added. The resulting mixture was extracted with hexanes. The hexanes extract was concentrated to dryness under reduced pressure. The residue was purified by vacuum distillation to give pure **118** (1.6 g, 53%) as a clear viscous liquid. $^1\text{H NMR}$ (DMSO- d_6): δ 1.44 (s, 9H), 1.78 (p, $J = 6.2$ Hz, 2H), 2.43 (t, $J = 2.6$ Hz, 1H), 3.20-3.26 (m, 2H), 3.59 (t, $J = 6.2$ Hz, 2H), 4.14 (d, $J = 2.6$ Hz, 2H).

3-(Prop-2-ynyloxy)propan-1-amine hydrochloride (119) JH390. To a solution of acetyl chloride (1.4 g, 17.8 mmol, 2 equiv) in methanol (20 mL) was added **118** (1.25 g, 8.7 mmol, 1 equiv). The resulting mixture was allowed to stir at room temperature for 3 h, then concentrated to dryness to give pure **119** (950 mg, 80%) as a white solid. $^1\text{H NMR}$ (DMSO- d_6): δ 1.82 (p, $J = 7.3$ Hz, 2H), 2.76-2.84 (m, 2H), 3.45 (t, $J = 2.2$ Hz, 1H), 3.50 (t, $J = 5.9$ Hz, 2H), 4.13 (d, $J = 2.6$ Hz, 2H), 8.06 (bs, 3H).

120 (JH168). A solution of 5(6)-rhodamine NHS ester (4.6 mg, 0.0087 mmol, 1 equiv) in DMF (200 μL) was added to a solution of **116** (5 mg, 0.010 mmol, 1.2 equiv), and DIPEA (4.0 mg, 0.031 mmol, 3 equiv) in DMF (200 μL). The resulting mixture was allowed to stir at room temperature for 2.5 h then concentrated to dryness under reduced

pressure. The residue was purified by preparative HPLC on a C18 column using 10-60% acetonitrile with 0.1% TFA. The isomer with a longer retention time was isolated, and dissolved in DMSO. The concentration of this stock solution (1.2 mM) was determined by diluting into methanol with 0.1% TFA, and comparing of the absorbance at 551 nm to that of a rhodamine stock solution. ESI MS, found (M +1) 855.1.

(Z)-2,4-Dimethyl-5-((5-nitro-2-oxoindolin-3-ylidene)methyl)-1H-pyrrole-3-carboxylic acid (121) JH235. Indolinone **59** (100 mg, 0.561 mmol, 1 equiv) was added to a solution of **108** (103 mg, 0.617 mmol, 1.1 equiv), and piperidine (67 mg, 0.785 mmol, 1.4 equiv) in THF (7 mL). The resulting mixture was heated to 75 °C in a sealed jar for 18 h. After cooling to room temperature 1 N HCl (2 mL) and methanol (14 mL) were added. The resulting precipitate was collected by filtration and dried under vacuum to give pure **121** (152 mg, 85%) as an orange brown solid. ¹H NMR (DMSO-*d*₆): δ 2.50 (s, 3H), 2.51 (s, 3H), 7.00 (d, *J* = 8.9 Hz, 1H), 8.01 (s, 1H), 8.02 (dd, *J* = 8.8, 2.2 Hz, 1H), 8.83 (d, *J* = 2.2 Hz, 1H), 11.5 (s, 1H), 12.2 (s, 1H), 13.6 (a, 1H).

(Z)-2,4-Dimethyl-5-((5-nitro-2-oxoindolin-3-ylidene)methyl)-N-(3-(prop-2-ynyloxy)propyl)-1H-pyrrole-3-carboxamide (122) JH393. Compound **119** (214 mg, 1.43 mmol, 4 equiv) was added to a solution of **121** (117 mg, 0.357 mmol, 1 equiv), EDC (205 mg, 1.07 mmol, 3 equiv), HOBt (46.1 mg, 0.357 mmol, 1 equiv), and DIPEA (139 mg, 1.07 mmol, 3 equiv) in DMF (8 mL). The resulting mixture was allowed to stir at room temperature for 20 h then EtOAc (200 mL) was added. The resulting mixture was washed with 1 N HCl, then 5% NaHCO₃, then water, then brine, and concentrated to dryness under reduced pressure to give pure **122** (80 mg, 53%). ¹H NMR (DMSO-*d*₆): δ 1.78 (p, *J* = 6.6 Hz, 2H), 2.45 (s, 3H), 2.47 (s, 3H), 3.28 (dt, *J* = 6.2, 6.2 Hz, 2H), 3.42 (t,

$J = 2.6$ Hz, 1H), 3.52 (t, $J = 6.2$ Hz, 2H), 4.14 (d, $J = 2.2$ Hz, 2H), 7.05 (d, $J = 8.4$ Hz, 1H), 7.69 (t, $J = 5.9$ Hz, 1H), 8.03 (s, 1H), 8.07 (dd, $J = 8.4, 2.2$ Hz, 1H), 8.86 (d, $J = 2.2$ Hz, 1H), 11.5 (s, 1H), 13.5 (bs, 1H).

(Z)-5-((5-Amino-2-oxoindolin-3-ylidene)methyl)-2,4-dimethyl-N-(3-(prop-2-ynyloxy)propyl)-1H-pyrrole-3-carboxamide (123) JH394. Zinc dust (1g) was added to a suspension of indolinone **122** (90 mg, 0.213 mmol, 1 equiv) in THF (50 mL) and saturated aqueous NH_4Cl (10 mL) at room temperature. The resulting mixture was vigorously stirred for 18 h, then diluted with EtOAc (200 mL), washed with water, then saturated NaCl, and concentrated under vacuum to give pure **123** (65 mg, 97%) as a red solid. ^1H NMR ($\text{DMSO}-d_6$): δ 1.76 (p, $J = 6.6$ Hz, 2H), 2.35 (s, 3H), 2.41 (s, 3H), 3.27 (dt, $J = 6.6, 5.9$ Hz, 2H), 3.42 (t, $J = 2.2$ Hz, 1H), 3.52 (t, $J = 6.2$ Hz, 2H), 4.13 (d, $J = 2.6$ Hz, 2H), 4.62 (bs, 2H), 6.41 (dd, $J = 8.4, 2.2$ Hz, 1H), 6.57 (d, $J = 8.4$ Hz, 1H), 6.94 (d, $J = 1.8$ Hz, 1H), 7.36 (s, 1H) 7.57 (t, $J = 5.9$ Hz, 1H), 10.5 (s, 1H), 13.7 (bs, 1H).

(Z)-N-(2-(Diethylamino)ethyl)-2,4-dimethyl-5-((5-nitro-2-oxoindolin-3-ylidene)methyl)-1H-pyrrole-3-carboxamide (124) JH230. Compound **121** (300 mg, 0.917 mmol, 1 equiv) was added to a solution of SOCl_2 (4.91 g, 41 mmol, 45 equiv) in THF (300 mL). The resulting mixture was heated to reflux for 2 h then concentrated to dryness under reduced pressure. The residue was then dissolved in THF (300 mL) and treated with N^1,N^1 -Diethylethane-1,2-diamine (491 mg, 4.23 mmol, 5 equiv). The resulting mixture was allowed to stir at room temperature for 4 h then concentrated to dryness under vacuum. The residue was partitioned between 1 N NaOH (10 mL) and EtOAc (120 mL). From this two-phase mixture a solid was recovered by filtration to give pure **124** (148 mg) as an orange solid. The EtOAc layer was separated and concentrated

under vacuum to 20 mL. The resulting precipitate was recovered by filtration to give more pure **124** (139 mg, total yield 287 mg, 74%) as an orange solid. ¹H NMR (DMSO-*d*₆): δ 0.977 (t, *J* = 7.0 Hz, 6H), 2.46 (s, 3H), 2.48 (s, 3H), 2.48-2.56 (m, 4H), 3.29 (q, *J* = 7.0 Hz, 4H), 7.05 (d, *J* = 8.8 Hz, 1H), 7.49 (t, *J* = 5.5 Hz, 1H), 8.03 (s, 1H), 8.06 (dd, *J* = 8.4, 2.2 Hz, 1H), 8.85 (d, *J* = 2.2 Hz, 1H), 11.5 (bs, 1H), 13.5 (bs, 1H).

(Z)-tert-Butyl 5-(2,4-dimethyl-5-((5-nitro-2-oxoindolin-3-ylidene)methyl)-1H-pyrrole-3-carboxamido)pentylcarbamate (125) JH248. Compound **121** (400 mg, 1.22 mmol, 1 equiv) was added to a solution of SOCl₂ (4.91 g, 41 mmol, 34 equiv) in THF (500 mL). The resulting mixture was heated to reflux for 2 h then concentrated to dryness under reduced pressure. The resulting residue was dissolved in THF (300 mL) then treated with DIPEA (394 mg, 3.05 mmol, 2.5 equiv), and tert-butyl 5-aminopentylcarbamate (494 mg, 2.44 mmol, 2 equiv). The resulting mixture was allowed to stir at room temperature for 4 h then concentrated to dryness under vacuum. The residue was dissolved in EtOAc (300 mL) and methanol (30 mL). The resulting solution was washed with 0.5 N HCl (150 mL), then 0.5 N NaOH (100 mL), then water, then brine, and concentrated to dryness under reduced pressure to give pure **125** (400 mg, 64%) as an orange solid. ¹H NMR (DMSO-*d*₆): δ 1.23-1.29 (m, 2H), 1.33 (s, 9H), 1.33-1.40 (m, 2H), 1.40-1.49 (m, 2H), 2.40 (s, 3H), 2.42 (s, 3H), 2.84-2.89 (m, 2H), 3.13-3.18 (m, 2H), 6.73 (t, *J* = 7.0 Hz, 1H), 7.02 (d, *J* = 8.8 Hz, 1H), 7.65 (t, *J* = 5.5 Hz, 1H), 8.00 (s, 1H), 8.02 (dd, *J* = 8.4, 2.1 Hz, 1H), 8.82 (d, *J* = 2.6 Hz, 1H), 11.5 (s, 1H), 13.5 (s, 1H)

(Z)-tert-Butyl 5-(5-((5-amino-2-oxoindolin-3-ylidene)methyl)-2,4-dimethyl-1H-pyrrole-3-carboxamido)pentylcarbamate (126) JH251. A suspension of **125** (300 mg, 0.587 mmol, 1 equiv) and 10% Pd/C (100 mg) in methanol (125 mL) was placed under 1

atm of hydrogen with stirring for 18 h. The catalyst was then removed by filtration, followed by the methanol under reduced pressure. The residue was purified by trituration in EtOAc/DCM to give pure **126** (254 mg, 90%) as a red solid. ^1H NMR (DMSO- d_6): δ 1.22-1.56 (m, 6H), 1.37 (s, 9H), 2.35 (s, 3H), 2.40 (s, 3H), 2.85-2.95 (m, 2H), 3.13-3.23 (m, 2H), 4.66 (bs, 2H), 6.41 (d, $J = 8.1$ Hz, 1H), 6.58 (d, $J = 8.1$ Hz, 1H), 6.77 (t, $J = 6.6$ Hz, 1H), 6.94 (s, 1H), 7.36 (s, 1H), 7.56 (t, $J = 5.2$ Hz, 1H), 10.5 (s, 1H), 13.7 (s, 1H).

(Z)-5-((5-Amino-2-oxoindolin-3-ylidene)methyl)-N-(2-(diethylamino)ethyl)-2,4-dimethyl-1H-pyrrole-3-carboxamide (127) JH232. A suspension of **124** (250 mg, 0.585 mmol, 1 equiv) and 10% Pd/C (75 mg) in methanol (600 mL) was placed under 1 atm of hydrogen with stirring for 5 h. The catalyst was then removed by filtration, followed by the methanol under reduced pressure to give pure **127** (221 mg, 96%) as a red solid. ^1H NMR (DMSO- d_6): δ 0.972 (t, $J = 7.3$ Hz, 6H), 2.36 (s, 3H), 2.42 (s, 3H), 2.49-2.55 (m, 4H), 3.27 (q, $J = 6.6$ Hz, 4H), 4.61 (bs, 2H), 6.41 (dd, $J = 8.1, 2.2$ Hz, 1H), 6.57 (d, $J = 8.1$ Hz, 1H), 6.95 (d, $J = 2.2$ Hz, 1H), 7.36 (s, 1H), 10.5 (s, 1H), 13.7 (s, 1H).

(Z)-5-((5-But-2-ynamido-2-oxoindolin-3-ylidene)methyl)-N-(2-(diethylamino)ethyl)-2,4-dimethyl-1H-pyrrole-3-carboxamide (128) JH388. DMF (5 mL) was added to a solid mixture of indolinone **127** (50 mg, 0.127 mmol, 1 equiv), EDC (99 mg, 0.561 mmol, 4 equiv), HOBt (17 mg, 0.126 mmol, 1 equiv), and 2-butynoic acid (64 mg, 0.756 mmol, 6 equiv), followed by DIPEA (33 mg, 0.252 mmol, 2 equiv). The resulting mixture was allowed to stir at room temperature for 2 h, then diluted with 5% NaHCO_3 (20 mL), and extracted with EtOAc. The EtOAc extract was washed with water, then saturated NaCl, then concentrated to dryness. The resulting residue was purified by trituration in methanol to give pure **128** (20 mg, 34%) as an orange solid. ^1H NMR

(DMSO- d_6): δ 0.973 (t, J = 7.3 Hz, 6H), 2.04 (s, 3H), 2.39 (s, 3H), 2.44 (s, 3H), 2.46-2.56 (m, 4H), 3.28 (q, J = 6.6 Hz, 4H), 6.82 (d, J = 8.1 Hz, 1H), 7.22 (dd, J = 8.4, 2.2 Hz, 1H), 7.42 (t, J = 5.5 Hz, 1H), 7.45 (s, 1H), 7.89 (d, J = 1.8 Hz, 1H), 10.4 (s, 1H), 10.9 (s, 1H), 13.6 (s, 1H).

(Z)-2,4-Dimethyl-5-((2-oxo-5-propiolamidindolin-3-ylidene)methyl)-N-(3-(prop-2-ynyloxy)propyl)-1H-pyrrole-3-carboxamide (129) JH395. Propiolic acid (64 mg, 0.756 mmol, 6 equiv) was added to a suspension of indolinone **123** (50 mg, 0.127 mmol, 1 equiv), EDC (97.4 mg, 0.508 mmol, 4 equiv), and HOBt (18 mg, 0.127 mmol, 1 equiv), in DMF (4 mL) and acetonitrile (10 mL). The resulting mixture was allowed to stir on an ice bath for 2 h then diluted with 5 % NaHCO₃ (20 mL). The resulting suspension was extracted with EtOAc. The EtOAc extract was washed with water, then saturated NaCl, then concentrated to dryness to give **129** (30 mg, 53%) as an orange solid. ¹H NMR (DMSO- d_6): δ 1.76 (p, J = 6.6 Hz, 2H), 2.34 (s, 3H), 2.43 (s, 3H), 3.27 (dt, J = 6.2, 6.2 Hz, 2H), 3.42 (t, J = 2.5 Hz, 1H), 3.52 (t, J = 6.2 Hz, 2H), 4.14 (d, J = 2.2 Hz, 2H), 4.35 (s, 1H), 6.84 (d, J = 8.1 Hz, 1H), 7.25 (dd, J = 8.4, 1.8 Hz, 1H), 7.47 (s, 1H), 7.63 (t, J = 5.5 Hz, 1H), 7.88 (d, J = 1.5 Hz, 1H), 10.6 (s, 1H), 10.9 (s, 1H), 13.6 (s, 1H).

(Z)-tert-Butyl 5-(2,4-dimethyl-5-((2-oxo-5-(vinylsulfonamido)indolin-3-ylidene)methyl)-1H-pyrrole-3-carboxamido)pentylcarbamate (130) JH258. 2-Chloroethanesulfonyl chloride (21.2 mg, 0.13 mmol, 2.5 equiv) was added dropwise to a solution of **126** (25 mg, 0.052 mmol, 1 equiv) and DIPEA (20.2 mg, 0.156 mmol, 3 equiv) in anhydrous THF (8 mL) at 0 °C. The mixture was allowed stir for 20 min, then for 18 h at room temperature, then concentrated to dryness. The residue was then suspended in EtOAc (50 mL). This suspension was washed with 1 N HCl (20 mL), then

5% NaHCO₃ (50 ML), then water, then brine, and concentrated to dryness under reduced pressure to give pure **130** (18 mg, 61%). ¹H NMR (DMSO-*d*₆): δ 1.26-1.52 (m, 6H), 1.37 (s, 9H), 2.39 (s, 3H), 2.42 (s, 3H), 2.85-2.93 (m, 2H), 3.17-3.22 (m, 2H), 5.96-6.02 (m, 2H), 6.73-6.83 (m, 3H), 6.92-6.95 (m, 1H), 7.52 (bs, 2H), 7.61 (t, *J* = 6.5 Hz, 1H), 9.54 (s, 1H), 10.9 (s, 1H), 13.6 (s, 1H).

(Z)-tert-Butyl 5-(2,4-dimethyl-5-((2-oxo-5-propionlamidoindolin-3-ylidene)methyl)-1H-pyrrole-3-carboxamido)pentylcarbamate (131) JH268. Propiolic acid (18 mg, 0.725 mmol, 1.2 equiv) was added to a suspension of indolinone **126** (100 mg, 0.208 mmol, 1 equiv), and EDC (80 mg, 0.416 mmol, 2 equiv) in DMF (8 mL) and acetonitrile (40 mL). The resulting mixture was allowed to stir at room temperature for 2.5 h then concentrated to dryness under reduced pressure. The resulting residue was purified by silica gel chromatography, using EtOAc as the mobile phase, to give **131** (52 mg, 49%) as an orange solid. ¹H NMR (DMSO-*d*₆): δ 1.22-1.47 (m, 6H), 1.32 (s, 9H), 2.33 (s, 3H), 2.37 (s, 3H), 2.84-2.89 (m, 2H), 3.12-3.1. (m, 2H), 4.30 (s, 1H), 6.72 (t, *J* = 5.5 Hz, 1H), 6.79 (d, *J* = 8.1 Hz, 1H), 7.20 (dd, *J* = 8.4, 1.8 Hz, 1H), 7.42 (s, 1H), 7.57 (t, *J* = 5.9 Hz, 1H), 7.84 (d, *J* = 1.8 Hz, 1H), 10.6 (s, 1H), 10.9 (s, 1H), 13.6 (s, 1H).

132 (JH283). Dry TFA (0.5 mL) was added to a solution of Indolinone **130** (20 mg) in DCM (2 mL). The resulting mixture was allowed to stir at room temperature for 2 h then concentrated to dryness to give the TFA salt of the free amine. To a solution of this amine (13.8 mg, 0.024 mmol, 1.2 equiv), and DIPEA (7.8 mg, 0.06 mmol, 3 equiv) in DMF (1 mL) was added a solution of 5(6)-rhodamine NHS ester (10.6 mg, 0.02 mmol, 1 equiv) in DMF (200 μL). The resulting mixture was allowed to stir at room temperature for 18 h then concentrated to dryness under reduced pressure. The residue was purified

by preparative HPLC on a C18 column using a gradient of 10-60% acetonitrile over 30 min. The product was dissolved in DMSO. The concentration of this stock solution (2.0 mM) was determined by diluting into methanol with 0.1% TFA, and comparing of the absorbance at 551 nm to that of a rhodamine stock solution. ESI MS, found (M +1) 884.3.

133 (JH278). Dry TFA (2 mL) was added to Indolinone **131** (30 mg). The resulting mixture was allowed to stir at room temperature for 3.5 h then concentrated to dryness to give the TFA salt of the free amine. To a solution of this amine (15 mg, 0.027 mmol, 1 equiv), and DIPEA (10.6 mg, 0.08 mmol, 3 equiv) in DMF (1 mL) was added a solution of 5(6)-rhodamine NHS ester (16 mg, 0.035 mmol, 1.1 equiv) in DMF (200 μ L). The resulting mixture was allowed to stir at room temperature for 4.5 h then concentrated to dryness under reduced pressure. The residue was purified by preparative HPLC on a C18 column using a gradient of 20-100% acetonitrile over 30 min. The product was dissolved in DMSO. The concentration of this stock solution (2.6 mM) was determined by diluting into methanol with 0.1% TFA, and comparing of the absorbance at 551 nm to that of a rhodamine stock solution. ESI MS, found (M +1) 846.2.

Ethyl 2-(3-nitropyridin-2-yl)acetate (134) JH225.⁵² On an ice bath, ethyl acetoacetate (41.1 g, 316 mmol, 2 equiv) was added to a suspension of NaH (7.6 g, 316 mmol, 2 equiv) in DMF (125 mL) at a rate that kept the internal temperature of the reaction below 50 °C. The resulting mixture was allowed to stir for 45 minutes then 2-chloro-3-nitropyridine (25 g, 158 mmol, 1 equiv) was added in small portions. The resulting mixture was allowed to stir at room temperature for 1.5 h then heated to 70 °C for 1 h. The volume of the reaction was reduced by 110 mL under reduced pressure then

suspended in 10% acetic acid (800 mL). The resulting mixture was extracted with Et₂O (1250 mL) in five 250 mL portions. The combined Et₂O extracts were washed with water, then brine, and dried over solid MgSO₄. The resulting mixture was treated with HCl gas until acidic and then stirred overnight. During this time an oil separated then crystallized, and was collected by filtration. This material was suspended in 5% NaHCO₃ (120 mL) and stirred for 15 h at room temperature. The resulting mixture was extracted with EtOAc. The EtOAc extract was washed with water, then brine, and concentrated under reduced pressure to give pure **134** (11.8 g, 35%) as a yellow oil. ¹H NMR (DMSO-*d*₆): δ 1.17 (t, *J* = 7.0 Hz, 3H), 4.10 (q, *J* = 7.3 Hz, 2H), 4.25 (s, 2H), 7.69 (dd, *J* = 8.4, 4.7 Hz, 1H), 8.55 (dd, *J* = 8.4, 1.5 Hz, 1H), 8.85 (dd, *J* = 4.7, 1.5 Hz, 1H).

Ethyl 2-(3-aminopyridin-2-yl)acetate (135) JH228. A solution of **134** (11.8 g, 56 mmol, 1 equiv) and 10% Pd/C (1.9 g) in ethanol (475 mL) was placed under 1 atm of hydrogen with stirring for 24 h. The catalyst was then removed by filtration, followed by the ethanol under reduced pressure to give pure **135** (7.76 g, 77%) as an yellow-white solid. ¹H NMR (DMSO-*d*₆): δ 1.18 (t, *J* = 7.0 Hz, 3H), 3.67 (s, 2H), 4.07 (q, *J* = 7.3 Hz, 2H), 5.10 (bs, 2H), 6.96 (d, *J* = 2.9 Hz, 2H), 7.70 (t, *J* = 2.9 Hz, 1H).

1*H*-Pyrrolo[3,2-*b*]pyridin-2-ol hydrochloride (136) JH269. Compound **135** (5.6 g, 31 mmol, 1 equiv) was added to 1 M HCl (90 mL). The resulting mixture was allowed to stir at room temperature for 5 days, then clarified with activated carbon (1 g), and concentrated to dryness to give pure **136** (5 g, 95%) as an off-white solid. ¹H NMR (DMSO-*d*₆): δ 3.72 (bs, 1H), 5.83 (s, 1H), 7.18 (t, *J* = 7.3 Hz, 1H), 7.94 (d, *J* = 7.7 Hz, 1H), 8.16 (d, *J* = 5.9 Hz, 1H), 12.4 (s, 1H).

3,3,5-Tribromo-1*H*-pyrrolo[3,2-*b*]pyridin-2(3*H*)-one (137) JH274.⁵³ Bromine (14.9 g, 93 mmol, 10 equiv) was added to a solution of **136** (1.58 g, 9.3 mmol, 1 equiv) in 1:1 t-butanol:water (100 mL). The resulting mixture was allowed to stir at room temperature for 48 h, then 5% NaHCO₃ (100 mL) was added. The resulting precipitate was recovered by filtration. This material contained some of the 3,3-dibromo product, so it was treated with 2.5 mL of bromine in 1:1 t-butanol:water (80 mL) for 6 days at room temperature. The resulting mixture was then treated with 5% Na₂CO₃ (100 mL). The resulting precipitate was recovered by filtration, washed with water, and dried under vacuum to give pure **137** (2.73 g, 75%). ¹H NMR (DMSO-*d*₆): δ 7.34 (d, *J* = 8.4 Hz, 1H), 7.60 (d, *J* = 8.4 Hz, 1H), 11.6 (s, 1H).

5-Bromo-1*H*-pyrrolo[3,2-*b*]pyridin-2(3*H*)-one (138) JH290.⁵³ Zinc dust (6 g) was added to a solution of **137** (2.73 g, 7.4 mmol, 1 equiv) in THF (30 mL) and saturated aqueous NH₄Cl (30 mL) at room temperature. The resulting mixture was vigorously stirred for 24 h, then filtered to remove excess zinc. The resulting two-phase mixture was diluted with water and extracted with EtOAc. The EtOAc extract was washed with water, then brine, and concentrated under reduced pressure to give pure **138** (1.25 g, 78%) as a tan solid. ¹H NMR (DMSO-*d*₆): δ 3.63 (s, 2H), 7.10 (d, *J* = 8.1 Hz, 1H), 7.39 (d, *J* = 8.1 Hz, 1H), 10.6 (s, 1H).

(*Z*)-3-((1*H*-Pyrrol-2-yl)methylene)-5-bromo-1*H*-pyrrolo[3,2-*b*]pyridin-2(3*H*)-one (139) JH293. Compound **138** (100 mg, 0.47 mmol, 1 equiv) was added to a solution of pyrrole-2-carboxaldehyde (53.6 g, 0.56 mmol, 1.2 equiv), and piperidine (12 mg, 0.14 mmol, 0.3 equiv) in THF (6 mL). The resulting mixture was heated to 75 °C in a sealed jar for 16 h. After cooling to room temperature the reaction was diluted with EtOAc (6

mL). The resulting precipitate was collected by filtration to give pure **139** (48 mg, 35%) as an orange solid. Note: this reaction forms two isomers by TLC but solidifies as a single isomer. This single isomer will slowly convert back to two isomers after a few days in solution. ¹H NMR (DMSO-*d*₆): δ 6.47-6.50 (m, 1H), 7.24 (d, *J* = 8.1 Hz, 1H), 7.44 (d, *J* = 8.1 Hz, 1H), 7.58-7.62 (m, 1H), 7.64 (s, 1H), 10.7 (s, 1H).

(Z)-5-Bromo-3-((4-methyl-1H-imidazol-5-yl)methylene)-1H-pyrrolo[3,2-*b*]pyridin-2(3H)-one (140) JH301. Compound **138** (200mg, 0.939 mmol, 1 equiv) was added to a solution of 4-methyl-1H-imidazole-5-carbaldehyde (124 g, 1.12 mmol, 1.2 equiv), and piperidine (24 mg, 0.282 mmol, 0.3 equiv) in THF (8 mL). The resulting mixture was heated to 80 °C in a sealed jar for 1.5 h. After cooling to room temperature the resulting precipitate was collected by filtration and washed with EtOAc to give pure **140** (199 mg, 70%) as an orange solid. ¹H NMR (DMSO-*d*₆): δ 2.45 (s, 3H), 7.28 (d, *J* = 8.4 Hz, 1H), 7.49 (d, *J* = 8.1 Hz, 1H), 7.58 (s, 1H), 8.23 (s, 1H), 10.8 (s, 1H), 13.8 (bs, 1H).

(Z)-5-Bromo-3-((2-ethyl-4-methyl-1H-imidazol-5-yl)methylene)-1H-pyrrolo[3,2-*b*]pyridin-2(3H)-one (141) JH305. Compound **138** (200mg, 0.939 mmol, 1 equiv) was added to a solution of 2-ethyl-4-methyl-1H-imidazole-5-carbaldehyde (154 g, 1.12 mmol, 1.2 equiv), and piperidine (16 mg, 0.186 mmol, 0.2 equiv) in THF (8 mL). The resulting mixture was heated to 80 °C in a sealed jar for 5.5 h. After cooling to room temperature the resulting precipitate was collected by filtration then washed with EtOAc to give pure **141** (161 mg, 52%) as an orange solid. ¹H NMR (DMSO-*d*₆): δ 1.40 (t, *J* = 7.7 Hz, 3H), 2.40 (s, 3H), 2.84 (q, *J* = 7.7 Hz, 2H), 7.25 (d, *J* = 8.4 Hz, 1H), 7.45 (d, *J* = 8.4 Hz, 1H), 7.51 (s, 1H), 10.8 (s, 1H), 13.7 (bs, 1H).

(Z)-3-((1H-Pyrrol-2-yl)methylene)-5-vinyl-1H-pyrrolo[3,2-b]pyridin-2(3H)-one (142) JH297. A solution of **139** (50 mg, 0.17 mmol, 1 equiv) in toluene (10 mL) and DMF (1 mL) was sparged with argon. To this suspension was added a solution of 2,6-di-tert-butyl-4-methylphenol (0.2 mg, 0.0009 mmol, 0.005 eq) in toluene (150 μ L), followed by (PPh₃)₄Pd (20 mg, 0.017 mmol, 0.1 equiv), and CH₂=CH-SnBu₃ (65.6 mg, 0.20 mmol, 1.2 equiv). The resulting mixture was heated to reflux for 4 h then allowed to stir at room temperature overnight. The resulting mixture was diluted with EtOAc (125 mL), then washed with water, then brine, and concentrated under vacuum. The resulting residue was purified by triturating in EtOAc, then washing with 1:1 hexanes:EtOAc, to give pure **142** (18 mg, 40%). ¹H NMR (DMSO-*d*₆): δ 5.46 (d, *J* = 11 Hz, 1H), 6.09 (d, *J* = 17 Hz, 1H), 6.46-6.48 (m, 1H), 6.96 (dd, *J* = 18, 11 Hz, 1H), 7.08-7.12 (m, 1H), 7.27 (d, *J* = 8.1 Hz, 1H), 7.38 (d, *J* = 8.1 Hz, 1H), 7.60-7.63 (m, 1H), 7.62 (s, 1H), 10.7 (s, 1H).

(Z)-3-((4-Methyl-1H-imidazol-5-yl)methylene)-5-vinyl-1H-pyrrolo[3,2-b]pyridin-2(3H)-one (143) JH302. A solution of **140** (50 mg, 0.16 mmol, 1 equiv) in toluene (10 mL) and DMF (1 mL) was sparged with argon. To this suspension was added a solution of 2,6-di-tert-butyl-4-methylphenol (0.2 mg, 0.0009 mmol, 0.005 eq) in toluene (150 μ L), followed by (PPh₃)₄Pd (23 mg, 0.02 mmol, 0.1 equiv), and CH₂=CH-SnBu₃ (60.3 mg, 0.19 mmol, 1.2 equiv). The resulting mixture was heated to reflux for 4 h then allowed to stir at room temperature overnight. The resulting mixture was diluted with EtOAc (125 mL), then washed with water, then brine, and concentrated under vacuum. The resulting residue was purified by triturating in EtOAc, then washing with 1:1 hexanes:EtOAc, to give pure **143** (13 mg, 35%). ¹H NMR (DMSO-*d*₆): δ 2.44 (s, 3H), 5.47 (d, *J* = 11 Hz,

1H), 6.06 (d, $J = 18$ Hz, 1H), 6.99 (dd, $J = 18, 11$ Hz, 1H), 7.31 (d, $J = 8.1$ Hz, 1H), 7.45 (d, $J = 8.4$ Hz, 1H), 7.59 (s, 1H), 8.21 (s, 1H), 10.8 (s, 1H).

(Z)-3-((2-Ethyl-4-methyl-1H-imidazol-5-yl)methylene)-5-vinyl-1H-pyrrolo[3,2-*b*]pyridin-2(3H)-one (144) JH308. A solution of **141** (50 mg, 0.15 mmol, 1equiv) in toluene (10 mL) and DMF (1 mL) was sparged with argon. To this suspension was added a solution of 2,6-di-tert-butyl-4-methylphenol (0.2 mg, 0.0009 mmol, 0.005 eq) in toluene (150 μ L), followed by $(\text{PPh}_3)_4\text{Pd}$ (17.3 mg, 0.02 mmol, 0.1 equiv), and $\text{CH}_2=\text{CH-SnBu}_3$ (57.1 mg, 0.18 mmol, 1.2 equiv). The resulting mixture was heated to reflux for 4 h then allowed to stir at room temperature overnight. The resulting mixture was diluted with EtOAc (125 mL), then washed with water, then brine, and concentrated under vacuum. The resulting residue was purified by triturating in EtOAc, then washing with 1:1 hexanes:EtOAc, to give pure **144** (20 mg, 47%). $^1\text{H NMR}$ ($\text{DMSO-}d_6$): 1.31 (t, $J = 7.7$ Hz, 3H), 2.40 (s, 3H), 2.83 (q, $J = 7.7$ Hz, 2H), 5.48 (d, $J = 12$ Hz, 1H), 6.04 (d, $J = 18$ Hz, 1H), 6.92 (dd, $J = 18, 11$ Hz, 1H), 7.28 (d, $J = 8.1$ Hz, 1H), 7.40 (d, $J = 8.1$ Hz, 1H), 7.51 (s, 1H), 10.8 (s, 1H).

Chapter 3

Biochemical characterization of inhibitors and Nek2

3.1 Abstract

In vitro Nek2 kinase assays of electrophilic oxindole inhibitors that were not covered in Chapter 1 are presented. These assays provide new insights for the further design of irreversible Nek2 inhibitors. *In vitro* Nek2 kinase assays of reversible oxindole inhibitors, and a series of reversible pyrimidine inhibitors, provide new lead Nek2 inhibitor scaffolds. *In vitro* Aurora B kinase assays were used to further demonstrate the specificity of our irreversible Nek2 inhibitors. An immobilized kinase assay was developed to study the kinetics of irreversible Nek2 inhibition. Proof of concept experiments show the use of rhodamine-conjugated and “clickable” Nek2 inhibitors as active site-directed probes. Three new Nek2A autophosphorylation sites were discovered by mass spec analysis. One of these new phosphorylation sites (pT13) may participate in a conserved phosphorylation-controlled salt bridge that regulates kinase activity. Nek2A is also capable of phosphorylating the mitotic kinesin Eg5 *in vitro*.

3.2 Electrophilic inhibitors in Nek2 kinase assays

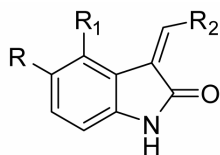
A full dose-response study will be required to fully elucidate the structure activity-relationships of the compounds listed in Table 3-1. However some important trends do emerge from examination of the compounds tested at single concentrations.

Examination of the compounds with a chloromethylketone in the oxindole 5-position (R, Table 3-1) reveals that many of the corresponding aromatic rings tested in the R₂ position produce Nek2 inhibitors with nanomolar potency. Nearly all of the chloromethylketone compounds listed in Table 3-1 were tested at the single concentration of 375 nM. The goal in this screen was to find aromatic rings that led to an increase in potency over compound **2** (80% inhibition at 350 nM) containing a 2-pyrrole ring in the R₂ position. None of the chloromethylketones presented in Table 3-1, besides compound **38**, met this constraint and were therefore not further studied. However, Chapter 1 discusses the shortcomings of Nek2 inhibitors with a hydrogen atom in the 5'-position like the 2-pyrrole-containing compound **2**, as they are all potent Cdk1 inhibitors. It is possible that, although they are not the most potent Nek2 inhibitors, some of the compounds in Table 3-1 may offer advantages in selectivity for Nek2 over other kinases. Also, most of the aromatic rings tested with chloromethylketones in the oxindole 5-position have never been explored with other electrophiles. For the aromatic rings that have been studied with other electrophiles, similar trends in potency to the corresponding chloromethylketone series were observed (Chapter 1, Table 1-1). This observation demonstrates the utility of the easily-synthesized chloromethylketones as a model system to study the use of alternate aromatic rings as Nek2 inhibitors.

None of the compounds tested with Michael acceptors in the oxindole 4-position (R_1 , Table 3-1) were potent Nek2 inhibitors. However, none of the compounds with the same Michael acceptors in the oxindole 5-position (R , Table 3-1) were potent Nek2 inhibitors either (Chapter 1, Figure 1-2 and Table 3-1). Based on these data, we cannot rule out the oxindole 4-position as a less-favorable place for the electrophilic moiety.

A series of vinyl aza-oxindoles that were designed to mimic the electrophilic cysteine-reactivity of 2-vinyl pyridine⁷³ proved to be inactive as Nek2 inhibitors at 10 μ M (Table 3-2). The reactivity of these compounds as electrophiles toward thiols has not yet been determined.

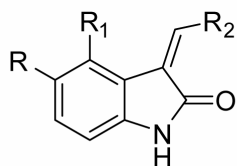
Table 3-1. Electrophilic oxindole inhibitors in Nek2 kinase assays.



Compound	R	R ₁	R ₂	Nek2 Inhibition	Assay Method
38		H		93%	375 nM WT Nek2A single concentration
39		H		23%	375 nM WT Nek2A single concentration
40		H		8%	375 nM WT Nek2A single concentration
41		H		32%	375 nM WT Nek2A single concentration
42		H		20%	375 nM WT Nek2A single concentration
43		H		54% ^a	375 nM WT Nek2A single concentration
44		H		24%	375 nM WT Nek2A single concentration
45		H		16%	375 nM WT Nek2A single concentration
46		H		0% ^a	375 nM WT Nek2A single concentration
47		H		---	not tested
48		H		8%	375 nM WT Nek2A single concentration

^a Assayed as a mixture of E/Z isomers.

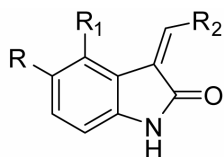
Table 3-1 (continued). Electrophilic oxindole-based inhibitors in Nek2 kinase assays.



Compound	R	R ₁	R ₂	Nek2 Inhibition		Assay Method
49		H		4% ^a	375 nM	WT Nek2A single concentration
50		H		47% ^a	375 nM	WT Nek2A single concentration
51		H		65%	375 nM	WT Nek2A single concentration
52		H		35%	375 nM	WT Nek2A single concentration
53		H		25%	375 nM	WT Nek2A single concentration
54		H		30%	150 nM	WT Nek2A single concentration
67		H		>10 μM	IC ₅₀	WT Nek2A dose response
68		H		0%	10 μM	WT Nek2A single concentration
69		H		0%	10 μM	WT Nek2A single concentration
70		H		1.7 μM	IC ₅₀	WT Nek2A dose response
85	H			15%	10 μM	WT Nek2A single concentration

^a Assayed as a mixture of E/Z isomers.

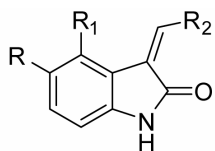
Table 3-1 (continued). Electrophilic oxindole-based inhibitors in Nek2 kinase assays.



Compound	R	R ₁	R ₂	Nek2 Inhibition	Assay Method
86	H			5%	10 μM WT Nek2A single concentration
87	H			15%	10 μM WT Nek2A single concentration
88	H			0%	10 μM WT Nek2A single concentration
89	H			0%	10 μM WT Nek2A single concentration
90	H			15%	10 μM WT Nek2A single concentration
106				>20 μM	IC ₅₀ WT Nek2A dose response
107				500 nM	IC ₅₀ WT Nek2A dose response
114		H		200 nM	IC ₅₀ WT Nek2A dose response
115		H		---	not tested
116		H		250 nM	IC ₅₀ WT Nek2A dose response

^a Assayed as a mixture of E/Z isomers.

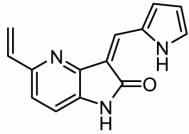
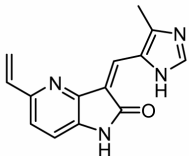
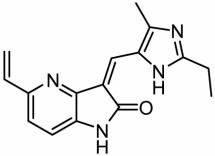
Table 3-1 (continued). Electrophilic oxindole-based inhibitors in Nek2 kinase assays.



Compound	R	R ₁	R ₂	Nek2 Inhibition	Assay Method
117		H		---	not tested
120		H		200 nM	IC ₅₀ WT Nek2A dose response
128		H		---	not tested
129		H		---	not tested
132		H		85%	5 μM WT Nek2A single concentration
133		H		70%	5 μM WT Nek2A single concentration

^a Assayed as a mixture of E/Z isomers.

Table 3-2. Nek2 kinase assays of 5-vinyl-4-aza-oxindoles.

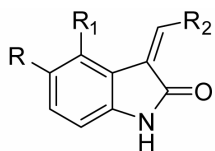
Compound	Structure	Nek2 Inhibition	Assay Method
142		0%	10 μ M WT Nek2A single concentration
143		0%	10 μ M WT Nek2A single concentration
144		0%	10 μ M WT Nek2A single concentration

3.3 Reversible inhibitors in Nek2 kinase assays

Our most potent oxindole-based reversible Nek2 inhibitor scaffolds were modeled after published Cdk2 inhibitors.^{54,55} These compounds contained tertiary amino or alkyne groups in the oxindole 4-position (R_1 , Table 3-3), substituted with hydrogen bond donating moieties (**97**, **102**, and **104**). Compounds of this class have been shown to form a hydrogen bond to the aspartate residue of the well-conserved kinase DFG motif in Cdk2.^{54,55} Because the potency of these compounds against Nek2 depends on the presence of a hydrogen bond donating group, as shown by comparison of compounds **97** and **98** (Table 3-3), they probably form a hydrogen bond to the DFG motif in Nek2 as well.

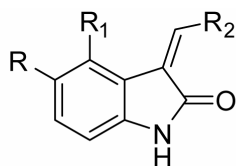
In theory, conversion of one of these scaffolds to an electrophilic inhibitor should make the most potent irreversible Nek2 inhibitor yet. A propynamide inhibitor based on scaffold **104** ($IC_{50} = 5 \mu\text{M}$, Table 3-3) was synthesized (compound **107**) and had an IC_{50} of 500 nM against Nek2 (Table 3-1). This represents a 10-fold increase in potency over the parent reversible scaffold **104**. A similar comparison of the reversible scaffold **25** ($IC_{50} = \sim 20 \mu\text{M}$, Table 3-3) and its corresponding irreversible propynamide analog **27** ($IC_{50} = 327 \text{ nM}$, Chapter 1, Table 1-1) shows a 60-fold increase in potency. These data demonstrate how inferring the potency of an irreversible inhibitor from the potency of an analogous reversible scaffold will not always lead to the design of the most potent compounds. The best way to design irreversible inhibitors based on structure-activity relationships would be to measure the reversible binding affinity (K_i) and the rate of enzyme alkylation (k_r) for the actual irreversible inhibitors (Figure 3-1), and use these parameters for further inhibitor design, rather than kinase assay IC_{50} values.

Table 3-3. Oxindole reversible inhibitors in Nek2 kinase assays



Compound	R	R ₁	R ₂	Nek2 Inhibition	Assay Method
sunitinib	F	H		10 μM	IC ₅₀ WT Nek2A dose response
24	NH ₂	H		40%	15 μM WT Nek2A single concentration
25	NH ₂	H		40%	15 μM WT Nek2A single concentration
65	Et	H		0%	15 μM WT Nek2A single concentration
66		H		35%	15 μM WT Nek2A single concentration
95	NO ₂	Br		>60 μM	IC ₅₀ WT Nek2A dose response
97	NO ₂			2.3 μM	IC ₅₀ WT Nek2A dose response
98	NO ₂			60 μM	IC ₅₀ WT Nek2A dose response

Table 3-3 (continued). Oxindole-based reversible inhibitors in Nek2 kinase assays



Compound	R	R ₁	R ₂	Nek2 Inhibition	Assay Method
99	NO ₂			>60 μM	IC ₅₀ WT Nek2A dose response
102	NO ₂			1.3 μM	IC ₅₀ WT Nek2A dose response
104	NO ₂			5.0 μM	IC ₅₀ WT Nek2A dose response
109		H		5.0 μM	IC ₅₀ WT Nek2A dose response
121	NO ₂	H		50%	15 μM WT Nek2A single concentration
124	NO ₂	H		55%	15 μM WT Nek2A single concentration
127	NH ₂	H		11 μM	IC ₅₀ WT Nek2A dose response

Table 3-4. Pyrimidine inhibitors in Nek2 kinase assays

These compounds were synthesized and provided by Dustin Maly (currently Assistant Professor of Chemistry at the University of Washington) in Kevan Shokat's lab here at UCSF.

Compound	Structure	Nek2 Inhibition	Assay Method
ASC65		0.80 μM	IC ₅₀ WT Nek2A dose response
ASC34 (GKI1198)		1.4 μM	IC ₅₀ WT Nek2A dose response
ASC56 (GKI1230)		1.4 μM	IC ₅₀ WT Nek2A dose response
ASC24 (GKI1168)		2.6 μM	IC ₅₀ WT Nek2A dose response
ASC58 (DJM1162)		2.7 μM	IC ₅₀ WT Nek2A dose response
ASC33 (GKI1196)		3.0 μM	IC ₅₀ WT Nek2A dose response
ASC43 (DJM1165)		3.1 μM	IC ₅₀ WT Nek2A dose response
ASC28 (GKI1178)		4.3 μM	IC ₅₀ WT Nek2A dose response
ASC49 (DJM1190)		5.3 μM	IC ₅₀ WT Nek2A dose response
ASC29 (GKI1182)		6.9 μM	IC ₅₀ WT Nek2A dose response

Table 3-4 (continued). Pyrimidine-based inhibitors in Nek2 kinase assays

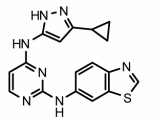
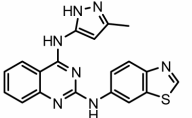
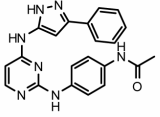
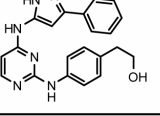
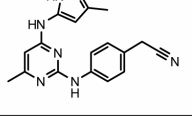
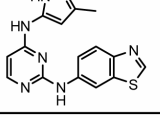
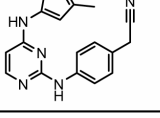
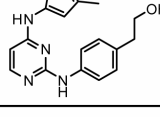
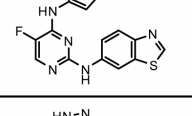
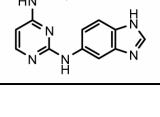
Compound	Structure	Nek2 Inhibition	Assay Method
ASC26 (GKI1174)		30%	5 μ M WT Nek2A single conc.
ASC1 (GKI162)		45%	5 μ M WT Nek2A single conc.
ASC10 (GKI1126)		40%	5 μ M WT Nek2A single conc.
ASC12 (GKI1130)		50%	5 μ M WT Nek2A single conc.
ASC13 (GKI1138)		25%	5 μ M WT Nek2A single conc.
ASC3 (GKI165)		10%	5 μ M WT Nek2A single conc.
ASC4 (GKI166)		2%	5 μ M WT Nek2A single conc.
ASC5 (GKI167)		0%	5 μ M WT Nek2A single conc.
ASC17 (GKI1148)		0%	5 μ M WT Nek2A single conc.
ASC21 (GKI1158)		20%	5 μ M WT Nek2A single conc.

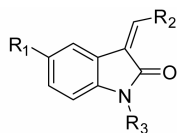
Table 3-4 (continued). Pyrimidine-based inhibitors in Nek2 kinase assays

Compound	Structure	Nek2 Inhibition	Assay Method
ASC41 (DJM1163)		25%	5 μ M WT Nek2A single conc.
ASC42 (DJM1164)		0%	5 μ M WT Nek2A single conc.
ASC23 (GKI1164)		0%	5 μ M WT Nek2A single conc.
ASC27 (GKI1176)		50%	5 μ M WT Nek2A single conc.
ASC52 (DJM1177)		25%	5 μ M WT Nek2A single conc.
ASC30 (GKI1186)		45%	5 μ M WT Nek2A single conc.
ASC48 (DJM1187)		45%	5 μ M WT Nek2A single conc.
ASC31 (GKI1188)		25%	5 μ M WT Nek2A single conc.
ASC53 (DJM2004)		35%	5 μ M WT Nek2A single conc.

3.4 Oxindole compounds in Aurora B kinase assays

Because many of the compounds in Table 3-5 were shown to be low nM inhibitors of Cdk1 and to induce mitotic exit in monastrol-arrested cells (Chapter 1, Table 1-1), we tested them for inhibition of AurB, since inhibition of this kinase has also been implicated in the induction of mitotic exit.³² In general, these compounds are much less efficient inhibitors of AurB than Cdk1. Importantly, compound **2**, our most selective Nek2 inhibitor (Nek2 IC₅₀ = 772 nM, Chapter 1, Table 1-1), shows 19-fold selectivity for Nek2 over AurB.

Table 3-5. Oxindole compounds in Aurora-B kinase assays



Compound	R1	R2	R3	<i>In Vitro</i> Aurora B IC ₅₀ (nM)
4			H	250
19			H	2200
20			H	2800
21			H	2200
34			Me	6000
36			H	5000
16			H	250
26			H	2800
27			H	3000
2			H	15000
31			Me	>20000
35			H	6000

3.5 The kinetics of irreversible Nek2 inhibition

An assay was developed to apply the kinetic analysis of irreversible inhibitors developed by Kitz and Wilson⁵⁶ to inhibitors of Nek2. This assay allows for the measurement of the reversible binding affinity (K_i) and the rate of covalent modification of Nek2 (k_r) by our irreversible inhibitors. The determination of these parameters for a series of irreversible inhibitors would provide the most valuable structure-activity relationship parameters for the further design of irreversible inhibitors.

To perform the Kitz-Wilson analysis, the amount of covalently-modified enzyme that forms as a function of inhibitor concentration and time must be measured. It is also important that the inhibitor concentration be in excess of the enzyme concentration to make the required pseudo-first order approximation. The immobilized-kinase assay provides a convenient platform to make these measurements for Nek2 (Figure 3-1).

The assay is conducted by coating the pure active kinase onto an ELISA-style protein binding plate. A Sypro Ruby (Invitrogen) stained gel can then be used to calculate the amount of Nek2 on the plate by comparing the amount of Nek2 in the coating buffer before and after coating of the plate (data not shown). The amount of Nek2 that binds to the plate is linearly proportional to the concentration of Nek2 in the coating buffer up to the concentration that saturates the plate (data not shown). The calculated amount of Nek2 on the plate can then be used to plot a theoretical inhibition curve based on the stoichiometry of Nek2 on the plate and the inhibitor in solution (Figure 3-1B). The volume of inhibitor solution can also be varied to alter this stoichiometry. Inhibitors can be added to the immobilized-kinase, then washed off with high temporal resolution, on a minute time scale, prior to measurement of the concentration of unbound enzyme as the

ratio of activities between treated and untreated samples. If the observed amount of inhibition converges over time to the calculated amount of inhibition as in Figure 3-1B, this indicates that all of the Nek2 that is bound to the plate is active and contributing to inhibitor binding. A dose-response plot as in Figure 3-1B also shows what inhibitor concentrations are in excess of the enzyme concentration and therefore can be used in the Kitz-Wilson analysis⁵⁶ (Figure 3-1C and Figure 3-1D).

The reversible binding affinity of compound **2** ($K_i = 4.8 \mu\text{M}$, Figure 3-1E) indicates how the presence of the propynamide electrophile confers a 4-fold increase in reversible binding affinity compared to the reversible oxindole-scaffold **25** ($\text{IC}_{50} = \sim 20 \mu\text{M}$, Table 3-3) with an amine in place of the propynamide. The contribution to potency from the reactivity of the propynamide electrophile towards Cys22 in Nek2 (0.0053 s^{-1} , Figure 3-1E) coupled with the reversible affinity of compound **2** results in an IC_{50} of 772 nM towards Nek2 (Chapter 1, Table 1-1), or a 26-fold increase in potency over compound **25**.

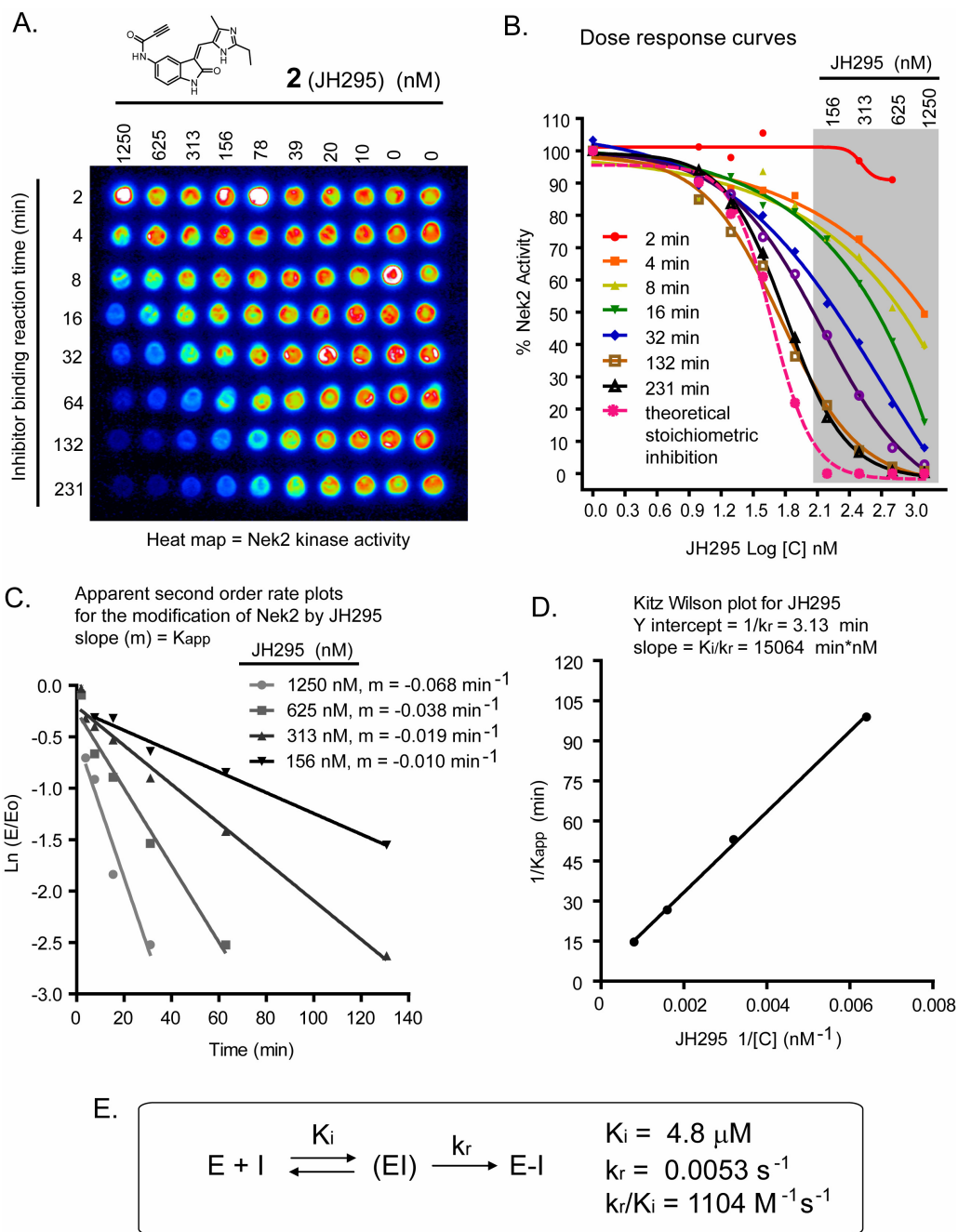


Figure 3-1. Immobilized Nek2 kinase assay at 25 °C. (A) Heat map of the raw kinase assay data showing the experimental layout as well as the dose and time dependence of inhibition. (B) Dose-response curves showing convergence over time to theoretical stoichiometric inhibition where half of the inhibitor concentration equals half of the enzyme concentration. The grey box highlights reactions where the inhibitor concentration is in excess of the enzyme concentration, a requirement for the pseudo first order approximation. (C) The apparent second-order rate plot for the modification of Nek2 by JH295 relating the free enzyme concentration, $\text{Ln}(E/E_0)$, to the inhibitor binding reaction time. (D) Kitz-Wilson plot for JH295. (E) Reaction diagram for irreversible inhibition and the constants determined for JH295.

3.6 Nek2 active site-directed probes

Rhodamine-conjugated Nek2 inhibitors (**120**, **132**, and **133**) can be used as Nek2 active site directed probes (Figure 3-2). All of these compounds label Nek2A in a dose-dependent manner, and are competed by pre-treatment of Nek2 with an unlabeled inhibitor at a concentration known to give full inhibition of Nek2 activity (Figure 3-2). This competition indicates that these probes label the active site of Nek2 at the lower concentrations tested. However at higher concentrations these compounds begin to label a second site on Nek2 that is not competed by the unlabeled compound. These data suggest that rhodamine conjugation promotes an off-target alkylation event. This propensity for off-target alkylation unfortunately limits the utility of these compounds as specific labeling reagents for the Nek2 active site.

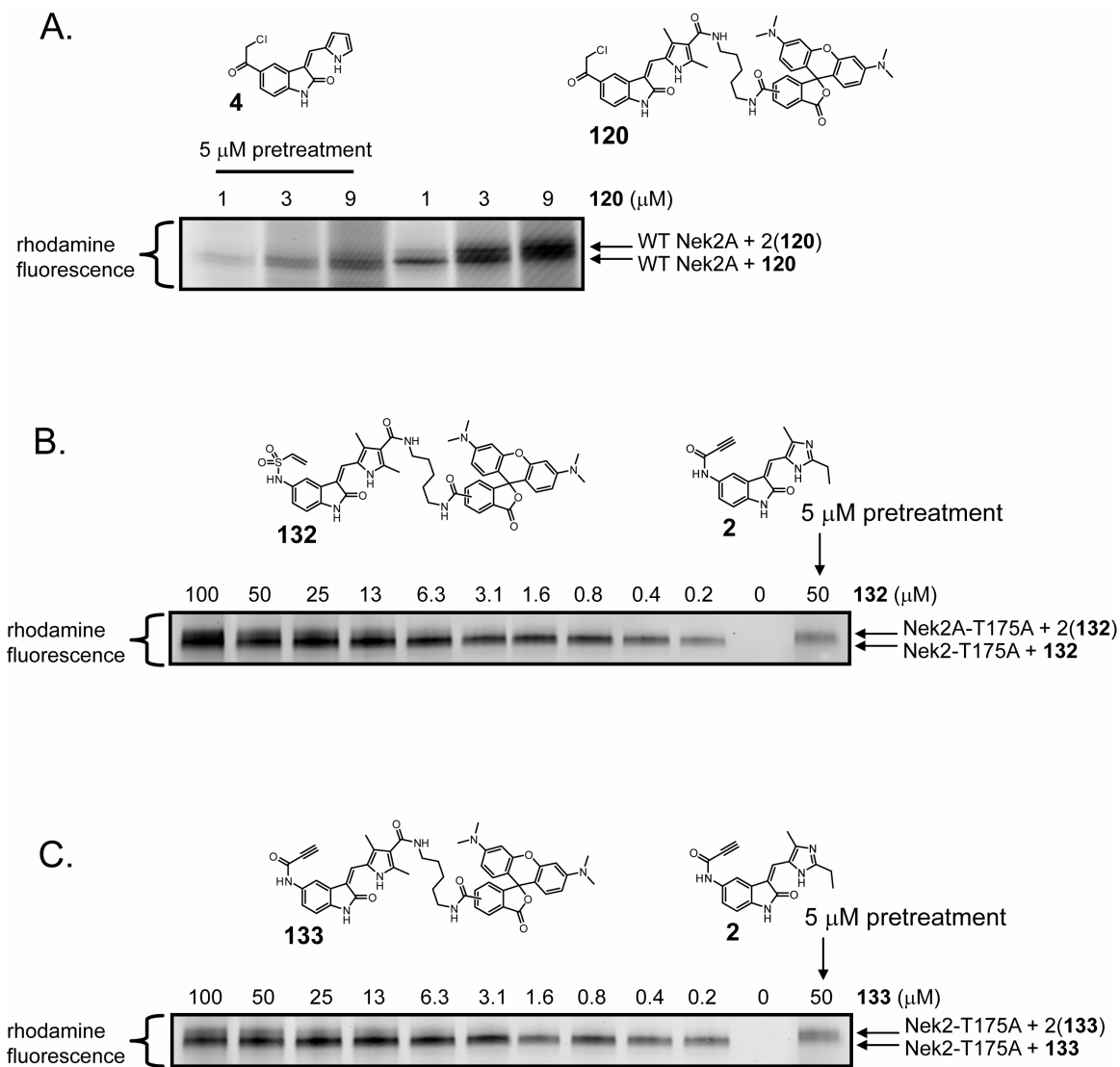


Figure 3-2. Rhodamine labeling of recombinant Nek2 with rhodamine-conjugated inhibitors. (A) Nek2 was treated with the indicated concentrations of **120** for 30 min at room temperature then visualized by rhodamine fluorescence on a SDS-PAGE gel. Samples of Nek2 pretreated with **4** were used as a competition control for labeling of the active site. (B) Same experiment as in Panel A employing compound **132** as the probe and compound **2** as the competitor. (C) Same experiment as in Panel A employing compound **133** as the probe and compound **2** as the competitor. Note: at the higher concentrations tested, the rhodamine-conjugated inhibitors appear to label a second residue on Nek2 that does not compete with the unlabeled inhibitors.

Compounds **117** and **129** were designed to label the Nek2 active site through derivatization by click chemistry.⁵⁷ A proof of concept of this methodology is presented in Figure 3-3. Compound **117** was able to label Nek2 in a dose-dependent manner as detected by derivatization with a rhodamine azide (Figure 3-3A). Compound **117** also labeled Nek2 in a manner that competes with compound **21**, suggesting labeling of the Nek2 active site. At the higher concentrations tested, labeling of BSA was also detected. This is likely due to direct alkylation of BSA by compound **117**. Compound **129** also labeled Nek2 in a dose dependent manner as detected by derivatization with a rhodamine azide (Figure 3-3B). However, this compound failed to compete with compound **2**, suggesting that it modifies Nek2 in a non-specific manner. The labeling of BSA by compound **129** also indicates that there is non-specific activity of compound **129**.

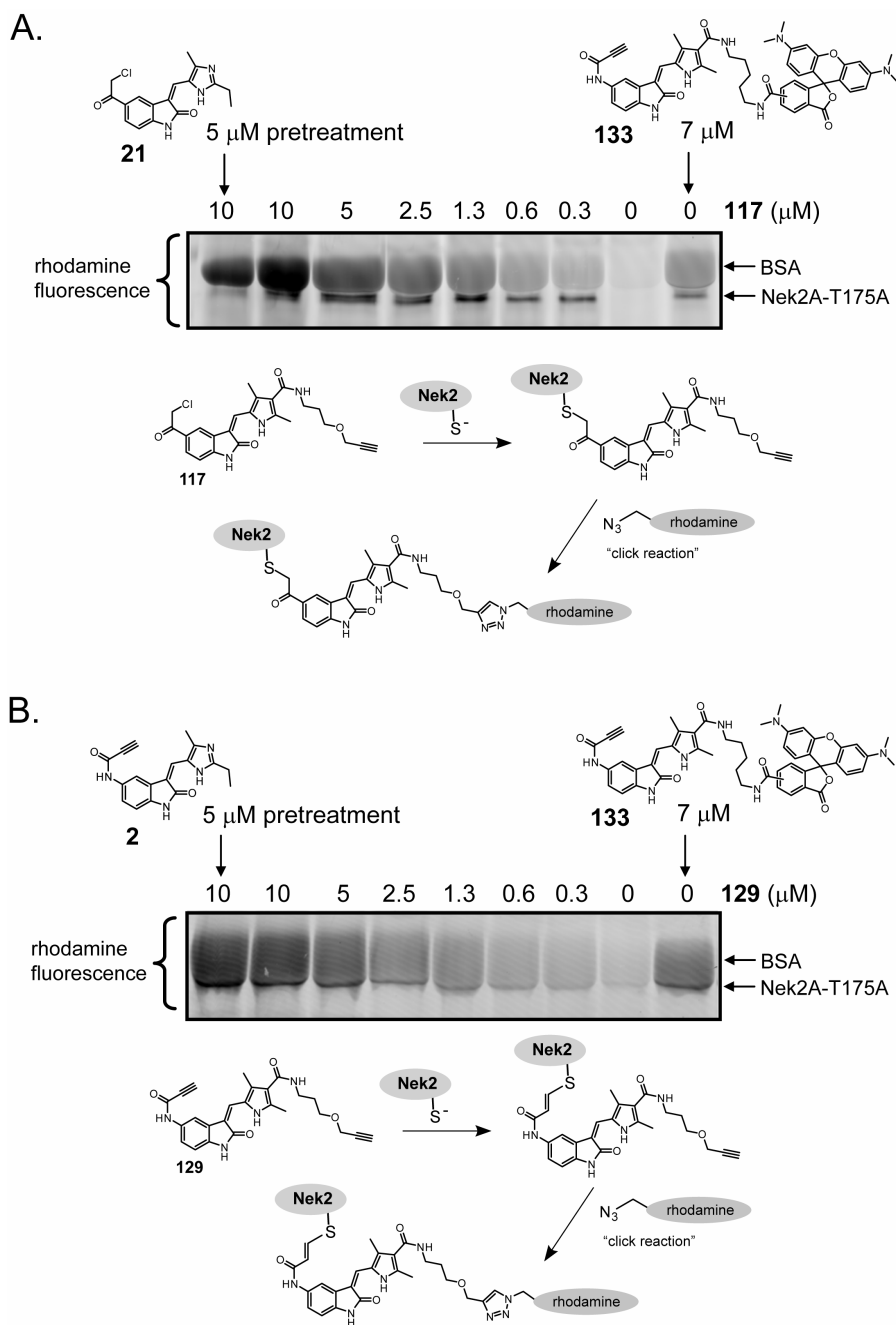


Figure 3-3. Rhodamine labeling of recombinant Nek2 with “clickable” inhibitors. (A) Nek2 was treated with the indicated concentrations of **117**, denatured with SDS, labeled with a rhodamine-conjugated azide through click chemistry, and then visualized by rhodamine fluorescence on a SDS-PAGE gel. A sample of Nek2 pretreated with compound **21** was used to demonstrate specific labeling of the active site. A sample of Nek2 labeled with the rhodamine-conjugated active site probe **133** was used to show labeled Nek2 on the gel. (B) The same experiment as in Panel A employing compound **129** as the probe and compound **2** as the competitor. The lack of competition suggests that compound **129** labels Nek2 on a residue other than active site Cys22.

3.7 Autophosphorylation of recombinant Nek2

A previous study detected several autophosphorylation sites on recombinant Nek2A-T175A by mass spectrometry (Figure 3-4A) and characterized the effect of phosphorylation on Nek2 kinase activity.²² We were able to detect three new autophosphorylation sites on the same Nek2 construct through trypsin digest and LC-MS/MS (Figure 3-4A). One of these new phosphorylation sites (Thr13) was in the glycine-rich loop of the Nek2 kinase domain.

Roughly 50 human kinases have a positively or negatively charged residue in the same position as Thr13 in Nek2 that pairs with an oppositely charged residue downstream in the glycine rich loop (Lck, Figure 3-4B) to form a salt bridge.⁶⁰ This salt bridge effects enzymatic activity, as well as inhibitor and ATP binding in certain kinases.⁶⁰ We hypothesized that Nek2 may have a phosphorylation-controlled version of this salt bridge that regulates its kinase activity. Indeed, Nek2 has a positively charged arginine residue in the corresponding downstream position that could possibly form a salt bridge with phospho-Thr13 (Figure 3-4B).

A sequence alignment generated from the Shokat Lab Kinase Sequence Database⁶² revealed that roughly 10% of the human kinome contains a threonine, serine, or tyrosine, paired with an arginine or lysine, in positions analogous to the Nek2 threonine/arginine pair (Figure 3-5). Phosphorylation of these residues has been documented in several phosphoproteomic studies looking at cell extracts.^{59, 63-69} Despite this precedence for regulation of kinase activity by phosphorylation, the function of these phosphorylation events has not yet been studied.

The non-phosphorylatable T13A and the phosphomimetic T13E mutations on Nek2A-T175A were made to test whether phosphorylation of T13 may regulate Nek2 activity and ATP binding (Figure 3-4C). Both mutations resulted in decreased catalytic efficiency and ATP binding compared to WT Nek2A-T175A (Figure 3-4C). It is difficult to accurately interpret the meaning of these results, since many factors still exist that can affect the activity of recombinant Nek2A-T175A. This construct is phosphorylated on 11 other residues that may have dominant effects on its catalytic activity. Also, the T13E mutation may not accurately mimic the effects of T13 phosphorylation.⁷⁴ If the reduced catalytic activity of the T13A mutant is in fact a reflection of the non-phosphorylated state, this is an indication of the predicted outcome: the phosphorylated species would form a salt bridge enhancing ATP binding and catalytic activity. Perhaps this form of regulation would have more dramatic effects in other kinases or in the context of multi-protein complexes such as centrosomal Nek2 in cells.

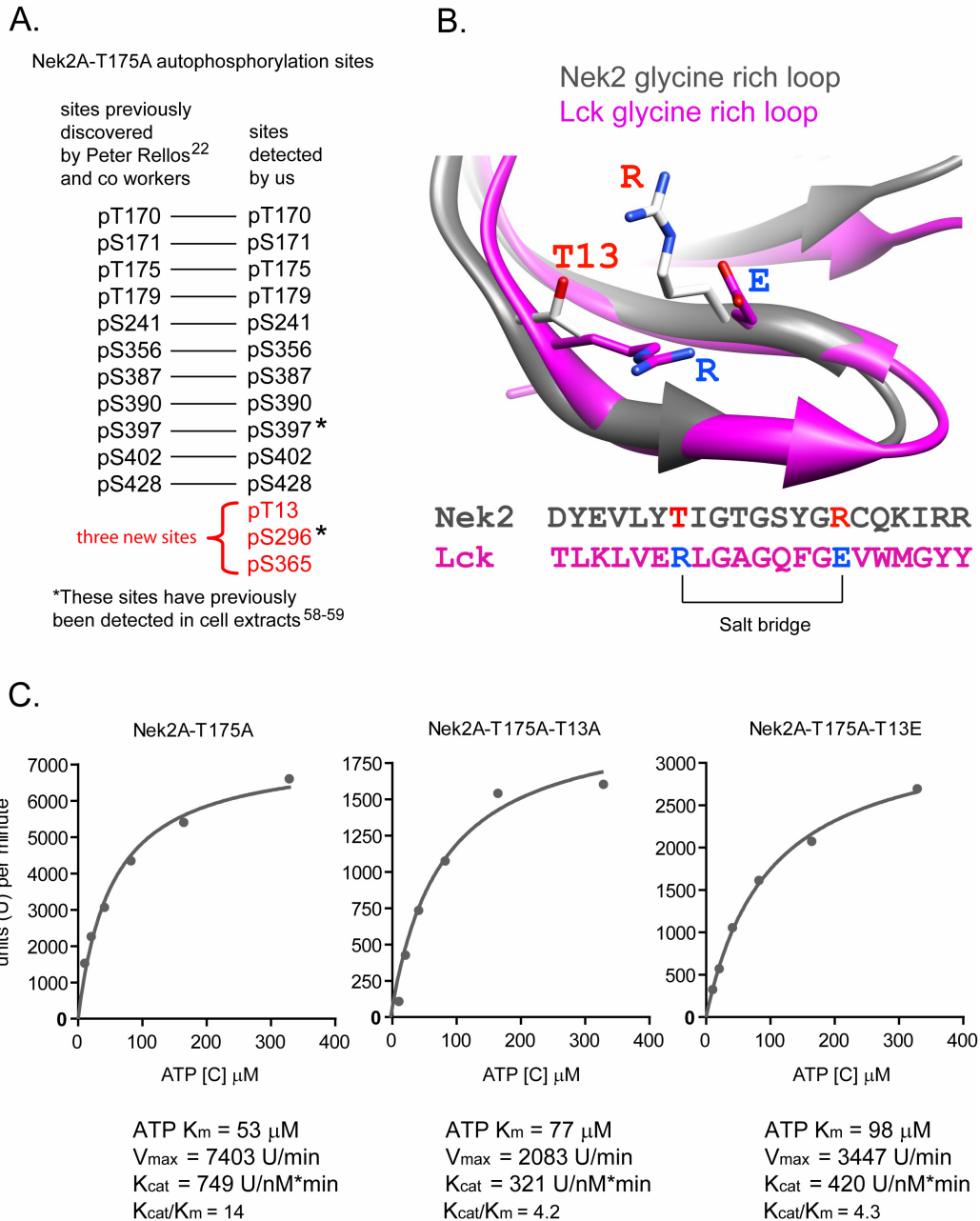


Figure 3-4. Discovery of new Nek2A autophosphorylation sites and the characterization of T13 phosphomimetic Nek2 mutants. (A) Discovery of three new Nek2A-T175A autophosphorylation sites by mass spec. (B) Overlay of Nek2 (PDB ID 2JAV)²² and Lck (PDB ID 2OF2)⁶¹ crystal structures showing residues forming a constitutive salt bridge (Lck) found in 10% of the kinome.⁶⁰ This salt bridge has been shown to increase catalytic activity and enhance ATP binding.⁶⁰ We hypothesized that Nek2 may contain a phosphorylation-controlled version of this salt bridge that forms between pT13 and R21. (C) Measurement of the catalytic efficiency and ATP binding of phosphomimetic and non-phosphorylatable T13 Nek2 mutants.

Potential kinases with a “Nek2 polarized” phosphorylation controlled salt bridge

Family #	Annotation	1	2
family6	FGFR-I	-----LVLGK TL GGEG EF G VK VKATAFH-----LKGRRGGYTT VA VKMLKENASPS-----	
family12	NimA-I	-----MPSRAENYEVLY TL IGT SG CR CG QKIQRKSDG-----KIL VW KELHYGSMTE-----	
family14	US3-I	DDDDCLIPSKEKAREVAASFGYTVIK TL TPG SE GR VM VVATKDGQPE-----P VV LKIGQKGTTL-----	
family16	FGFR-II	-----PRKNLVLGK TL GGEG EF G VK VKATAFH-----LKGRA--GYTT VA VKMLKENAS-----	
family17	PKC/PKA	-----FDTLA TV GTG TF GR VL VVHLVKEKTAK-----H FF A LK VMSIPDVIRL-----	
family32	LAMMER	-----YEIVD TL GGEG AF G KV VECIDHKAGG-----R HV AV KIVKNVDRYCE-----	
family37	KIN1/SN	-----YRLLR TL IGK GN F AK VKLARHILTG-----RE VA IK IID-----	
family41	PDGFR	-----LSFGK TL GAG AF G KV VEATAYGLIKSDAA-----M TV AV KMLKPS-----	
family101	NinaC	-----WEIE TL IGK GY G KV YKVINKRDG-----S LA AV KILDPVSD-----	
family105	cAMP-I	-----CDAL VM GTG TF GR VL VVHLV-KEK-----TAK HH FA LK VMS IPDVIRK-----	
family218	Kin2	-----YEFLE TL GK GY G KV KA-RES-SG-----R LV AI K SIR -----KDK	
family222	PKC	-----LEI IA TLGV GG F RV ELVVKVKNEN-----V AF AM K CIR KKHIVDTKQ-----	
family230	cAMP-I	-----CADEQPHIGNYRL LL TK IGK GN F AK VKLA-RHILTG-----RE VA IK IIDKTQLNP-----	
family269	No ann	-----MSGDKLLSELGYK LR TL IGEG SY G KV VATSKKYK-----T VA IK VVD-----RRRAPP	
family269	No ann	-----MEDFLLSNGYQLG K IGEG TY S KV KEAFSKKHQR-----K VA IK VID-----KMGGPE	

Potential kinases with a phosphorylation-controlled salt bridge opposite of Nek2 polarity

Family #	Annotation	1	2
family5	CDC7	-----FKIED K IGEG TF S SV YLATAQLQVGP-----E KI AL KHLIPTSHP-----	
family19	Wee1	-----FHELE K IGSG EF G SF VKCVKRLDG-----C IV AI KRSKPLAGSV-----	
family24	GC Kina	-----FDVLE K GGEG SY G SV YKAIHK-----ETGQ IV AI KQVPVES-----	
family40	Unc-51	-----FILTE RL GG TY A TV KAYAKDTR-----E VV AI KCVAKKSLNK-----	
family43	CDK	-----YIKLE K GGEG TY A TV YKGRSKL-----TEN LV AL KEI-----	
family43	CDK	PLSRMSRRASLSDIGFGKLETYVK LD K GGEG TY A TV FYKGRSKL-----MEN LV AL KEI-----	
family53	KKIALRE	-----YETLG V GGEG SY G TV MCKCHKNTGQ-----I V AI KIFYE-----	
family59	Raf	-----VML STR IGSG SF G TV YK-KWHG-----D V AV KILKVVDPPTP-----	
family69	Mos	-----VCLLQ RL GAG GF G SV YKATYRGVP-----V AI KQVKNCTKNR-----	
family111	DICTY	-----RAGPFILG PL GN SP VP SI --V-QCLARKDG-TDDFY QL KI LTLLEERGQDGIES---Q-----	
family133	PAK/ST	-----LRSIVSVGDPKKYTR FE K IGQ AS G TV YTA-MDVATGQ-----E V AI RQMN LQ -----	
family141	CDC15	-----FDVLE K GGEG SY G SF VKFA-IHKESG-----Q VV AI KQVPVESD-----	
family223	SRPK1	-----YHVIR K LGW GH F TV WLS-WDIQ GK -----K FV AM KVVKSA-----	
family229	CDK2	-----YEKLE K GGEG SY A TV YK-KSKVNW-----K LV AL KVIR LQ -----	
family236	KIS	-----WQVQS RL SG SS A SV YRVRCGNP-----G SP PA L KQ FLPPGTG-----AAA-----	
family238	CDK5	-----MQKYEKLE K IGEG TY G TV FKAKNRETHE-----I V AL KRVRLDD-----	
family255	PKL12	-----YLF I Q L GGEG FS Y VDLVEGLHDGH-----F Y AL KRIL CHE -----	
family260	p21	-----YTRYE K IGQ AS G TV FATDVALGQ-----E V AI KQIN L -----Q KQ PK KEL II	

Figure 3-5. Partial glycine-rich-loop sequence alignment generated from the UCSF Shokat Lab Kinase Sequence Database⁶² showing kinases that may have a phosphorylation-controlled salt bridge. The family numbers and annotations of representative kinases correspond to the Shokat Kinase Sequence Database. Annotations with a yellow highlight represent sequences with multiple kinase entries. Positions 1 and 2 (red) show the residues that may form a salt bridge upon phosphorylation. Residues shown in green are predicted to contact ATP in the kinase active site.

3.8 Phosphorylation of Eg5 by Nek2A

Recombinant WT Nek2A will phosphorylate recombinant full length Eg5, and both proteins play a role in establishing bipolar mitotic spindles.⁵ Perhaps Nek2A regulates Eg5 in cells through phosphorylation, but further studies are required to map the phosphorylation sites and establish their functional relevance by mutagenesis. Regulation of Eg5 by Nek2 is intriguing given the recent demonstration that Nek2 contributes to bipolar spindle assembly and that Nek2 knockdown sensitizes cells to low doses of the Eg5 inhibitor monastrol (a “synthetic-lethal” type interaction).⁵

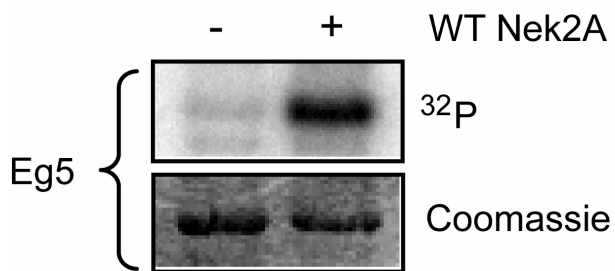


Figure 3-6. WT Nek2A was used to phosphorylate recombinant full length Eg5.

3.9 Experimental methods

WT Nek2A Kinase assays

Inhibitors were incubated for 30 min at room temperature with 11.6 nM of WT Nek2A (Invitrogen, or expressed in house from insect cells) in 15 μ L of kinase reaction buffer (150 μ M ATP, 20 mM HEPES pH 7.5, 5 mM MgCl₂, 0.1 mM EDTA, 0.3 mg/mL BSA) with 1.6% DMSO. Next, 10 μ L of kinase reaction buffer containing 1.2 mg/mL of myelin basic protein (Upstate), and 2 μ Ci of [γ -³²P]ATP (PerkinElmer) was added. Kinase reactions were allowed to proceed for 30 min at room temperature. Then, 5 μ L of the mixture was blotted onto P81 filtermat (Whatman). The filtermat was washed once with 10% acetic acid, then twice with 0.1% phosphoric acid, then once with methanol, and then dried under a heat lamp (Bio-Rad). The dry blots were exposed to a storage-phosphor screen (GE Healthcare), imaged using a Typhoon Scanner (GE Healthcare), quantified using Image Quant software (GE Healthcare), then processed and plotted using Excel (Microsoft) and GraphPad (Prism) software. Reactions were run in duplicate, and reactions lacking the kinase were used for background control.

Aurora B kinase assays

Inhibitors were incubated for 30 min at room temperature with 15 ng of AurB/INCENP complex (Millipore) in 20 μ L of kinase reaction buffer (13 μ M ATP, 20 mM HEPES pH 7.5, 5 mM MgCl₂, 0.1 mM EDTA, 0.2 mg/mL BSA) with 3% DMSO. Next, 5 μ L of kinase reaction buffer containing 0.75 mg/mL of Histone-H1 (Millipore), and 4 μ Ci of [γ -³²P]ATP (PerkinElmer) was added. Kinase reactions were allowed to proceed for 30 min at room temperature. Then, 5 μ L of the reaction mixture was blotted

onto nitrocellulose membrane (Bio-Rad) that had been pre-washed with wash buffer (1 M NaCl, 0.1 % H₃PO₄) and dried. The membrane was washed three times with wash buffer, and then dried under a heat lamp. The dry blots were exposed to a storage-phosphor screen (GE Healthcare), imaged using a Typhoon Scanner (GE Healthcare), quantified using Image Quant software (GE Healthcare), then processed and plotted using Excel (Microsoft) and GraphPad (Prism) software. Reactions were run in triplicate, and reactions lacking the kinase were used for background control.

Immobilized Nek2 kinase assay

Into a Nunc Maxisorb ELISA style protein binding 96-well plate was placed 50 μ L/well of a 300 nM solution of full length Nek2A-T175A (Chapter 1) in PBS (0.9 mM CaCl₂, 0.5 mM MgCl₂, 2.67 mM KCl, 1.47 mM KH₂PO₄, 138 mM NaCl, 8.06 mM NaH₂PO₄). The plate was then rocked at 4 °C for 2.5 h, taking care to keep the solution in the bottom of the wells. The Nek2 solution was removed and the plate was then washed twice at 4 °C with 250 μ L/well of kinase reaction buffer (20 mM HEPES pH 7.5, 5 mM MgCl₂, 0.1 mM EDTA). The washes were conducted for 10 min each, taking care to minimize “dry time” between washes. The buffer from the last wash was then removed (one row at a time, taking care to minimize “dry time”) and a solution of **2** (75 μ L/well) in kinase reaction buffer containing 2% DMSO was added at room temperature. After the desired incubation time, the inhibitor solution was removed and 250 μ L/well of holding buffer (kinase reaction buffer containing 2% DMSO) was added. To measure the activity of the unbound Nek2, the holding buffer was removed (again minimizing “dry time!”) and 50 μ L/well of kinase reaction mix (kinase reaction buffer containing 100 μ M ATP, 1 mg/mL β -casein, and 0.08 μ Ci/ μ L of [γ -³²P]ATP) was added. The plate was then rocked

at room temperature for 60 min, and then 5 μ L of the reaction mixture was blotted onto nitrocellulose membrane (Bio-Rad) that had been pre-washed with wash buffer (1 M NaCl, 0.1 % H_3PO_4) and dried. The membrane was washed three times with wash buffer and then dried under a heat lamp. The dry blot was exposed to a storage-phosphor screen (GE Healthcare), imaged using a Typhoon Scanner (GE Healthcare), quantified using Image Quant software (GE Healthcare), then processed and plotted using Excel (Microsoft) and GraphPad (Prism) software. Reactions lacking the kinase were used for a background control.

Labeling of Nek2 with rhodamine-conjugated inhibitors

Rhodamine-conjugated compounds **120**, **132**, or **133** were incubated with either Nek2A-T175A (75 nM), or 69 nM of WT Nek2A (Upstate), in PBS (0.9 mM CaCl_2 , 0.5 mM MgCl_2 , 2.67 mM KCl, 1.47 mM KH_2PO_4 , 138 mM NaCl, 8.06 mM NaH_2PO_4), containing 8% DMSO for 30 min at room temperature. Samples were then analyzed by SDS-PAGE. Rhodamine fluorescence was detected in the gel using a Typhoon Scanner (GE Healthcare). Identical reactions using Nek2 that had been pre-treated with compound **2** or **4** for 30 minutes at room temperature were used as competition controls for specific labeling of the active site.

Labeling of Nek2 with “clickable” inhibitors

For labeling of Nek2, compound **117** or **129** was incubated with 80 nM of Nek2A-T175A (Chapter 1) in PBS (0.9 mM CaCl_2 , 0.5 mM MgCl_2 , 2.67 mM KCl, 1.47 mM KH_2PO_4 , 138 mM NaCl, 8.06 mM NaH_2PO_4), containing BSA (0.5 mg/mL) and DMSO (10%) at room temperature for 20 min. For click reactions, SDS (1.25 μ L 20% w/v), rhodamine-azide (0.5 μ L, 5 mM), TCEP (0.5 μ L, 0.3 M, pH 7.5), TBTA (1.5 μ L,

1.2 mM in t-butanol), and CuSO₄ (0.5 μL, 50 mM) were added in that order to 20 μL of the labeled Nek2 solution. Click reactions were allowed to proceed at room temperature for 1 h, then samples were analyzed by SDS-PAGE. Rhodamine fluorescence was detected in the gel using a Typhoon Scanner (GE Healthcare). Identical reactions using Nek2 that had been pre-treated with 5 μM of **2** or **21** for 30 minutes at room temperature were used as competition controls for specific labeling of the active site. Nek2 that had been labeled with 7 μM of **133** for 30 minutes at room temperature was used as a control for detection of rhodamine-labeled Nek2 on the gel.

Mass spectrometry for Nek2A-T175A autophosphorylation

Recombinant Nek2A-T175A (12 μg) was resolved on an SDS-PAGE gel and detected by Coomassie stain. The Coomassie stained band was excised and subjected to in-gel tryptic digestion as follows. The excised gel band was chopped into <1 mm³ pieces and placed into a 0.65 mL low protein-binding tube (PGC Scientific). The gel pieces were then washed with wash buffer (25 mM NH₄HCO₃, in 50% aq acetonitrile) until the Coomassie stain was removed (about 4 washes were required). Then, enough DTT solution (10 mM DTT, in 25 mM NH₄HCO₃) to cover the gel pieces was added, and the resulting mixture was incubated at 56 °C for 30 min. The DTT solution was then removed and the gel pieces were treated with iodoacetamide (55 mM iodoacetamide, in 25 mM NH₄HCO₃) for 30 min at room temperature. After removal of the iodoacetamide, the gel pieces were washed twice with wash buffer (10 min per wash with vortexing), then desiccated to complete dryness under reduced pressure in a centrifugal evaporator (Genevac). The gel pieces were then rehydrated with 25 μL of “side chain protected” porcine trypsin (Promega) solution (5 ng/μL in 25 mM NH₄HCO₃), and then covered

with 25 mM NH_4HCO_3 . The resulting mixture was incubated at 37 °C for 4 h before the supernatant was transferred to a new tube. The gel pieces were then extracted two times with extraction buffer (5 % v/v formic acid in 50% aq acetonitrile) for 15 minutes each with vortexing. The combined tryptic digest supernatant and formic acid extract was then concentrated to a volume of ~60 μL . This solution represents approximately 4.5 pmol/ μL of starting Nek2.

This tryptic digest solution was diluted and subjected to LC/MS/MS analysis using an LTQ Orbitrap XL (Thermo) mass spectrometer. Three 90 min LC/MS/MS analyses were performed. LC Conditions for a 90 minute run (NanoAcquity HPLC system (Waters) follow: 0.4 $\mu\text{L}/\text{min}$ flow, (Solvent A = 0.1% formic acid in water, Solvent B = 0.1% formic acid in acetonitrile), trap 5 min at 2% acetonitrile, then 2 to 30% acetonitrile in 65 min, then 2 min at 50% acetonitrile, then back to 2% acetonitrile for 20 minutes, using a NanoAcuity BEH130 C18 column (100 μm (ID) x 10 cm (length)).

For run T9102602, ~50 fmol were injected for a 90 min run (mass range monitored: m/z 320-1600). The 6 most abundant multiply charged ions were selected for linear trap CID.

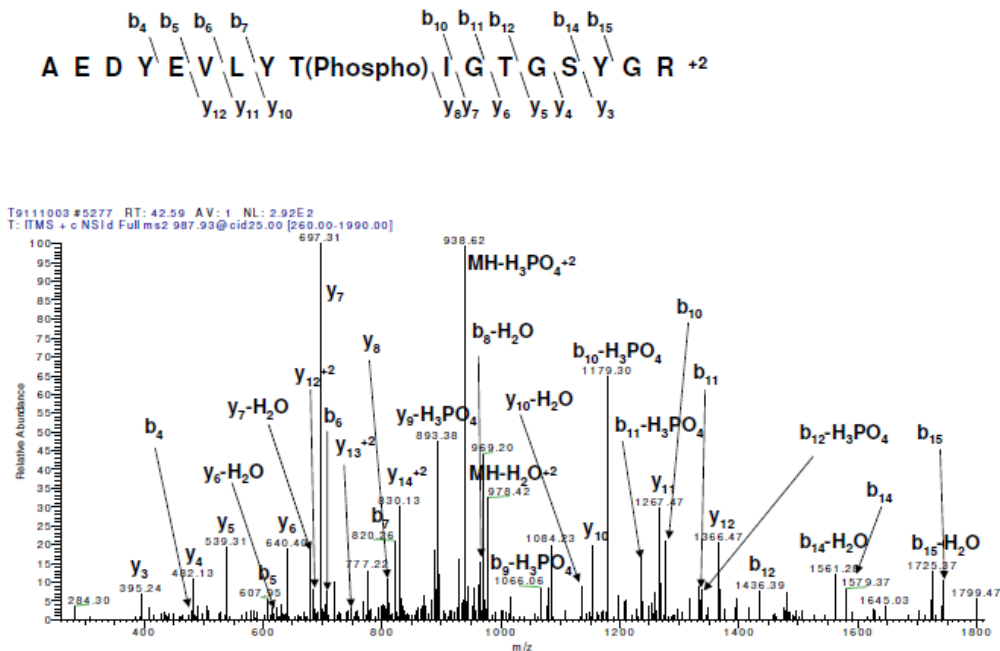
For run T9102903, ~850 fmol were injected, a narrower mass range was monitored, for a 90 min run (mass range monitored: m/z 600-1200). The 6 most abundant multiply charged ions were selected for linear trap CID.

For run T9102904, 850 fmol were injected for a 90 min run (mass range monitored: m/z 320-1600). The 6 most abundant multiply charged ions were selected for linear trap CID.

The precursor ions were measured in the Orbitrap, then CID experiments were performed in the linear trap on the 6 most abundant multiply charged ions. Dynamic exclusion was enabled. Then the raw data were transformed into peak-lists using an in-house script called PAVA. With these peak-lists and the following parameters database searches were performed by Protein Prospector. Search parameters: SwissProt, without species restriction, then *homo sapiens* only, precursor mass tolerance: 25 ppm, fragment tolerance: 0.8 Da, Met oxidation, cyclization of N-terminal Gln residues, protein acetylation and TYS (phosphorylation) were considered as variable modifications, Cys carbamidomethylation was considered as fixed modification, enzyme = trypsin, and 2 missed cleavages. Data and search results were merged from the 3 analyses and all phosphopeptide identifications and site assignments were manually validated. The annotated CID spectra for the three new autophosphorylation sites are presented below (Figure 3-8).

pT13

Saida Patricia Salas
11/12/2009



Determination of ATP K_m values for Nek2 mutants

Expression plasmids for full length His-tagged Nek2A-T175A-T13A and Nek2A-T175A-T13E were prepared by performing quick change mutagenesis on the parent pET22b Nek2A-T175A (Chapter 1) vector using the following oligonucleotide primers: 5'-gtgtgtacgccattggcacaggc-3' and 5'-gcctgtgccaatggcgtacaacac-3' for T13A; and 5'-gtgtgtacgagattggcacaggc-3' and 5'-gcctgtgccaatctcgtacaacac-3' for T13E (Operon). Expression and purification of all Nek2 protein constructs was carried out according to a previously reported procedure.²²

Kinase reactions were run at room temperature using Nek2A-T175A (9.98 nM), Nek2A-T175A-T13A (6.48 nM), or Nek2A-T175A-T13E (8.20 nM) in kinase reaction buffer (20 mM HEPES pH 7.5, 5 mM MgCl₂, 0.1 mM EDTA, 0.2 mg/mL BSA) containing a 12:1 ratio of ATP: [γ -³²P]ATP and 1 mg/mL β -casein as the substrate. Every 10 min, 5 μ L of the mixture was blotted onto nitrocellulose membrane (Bio-Rad) that had been pre-washed with wash buffer (1 M NaCl, 0.1 % H₃PO₄) and dried. After all of the time points were collected, the membrane was washed three times with wash buffer and then dried under a heat lamp. The dry blots were exposed to a storage-phosphor screen (GE Healthcare), imaged using a Typhoon Scanner (GE Healthcare), quantified using Image Quant software (GE Healthcare), then processed and plotted using Excel (Microsoft) and GraphPad (Prism) software. The Michaelis–Menten curve fitting algorithm in GraphPad was used to determine kinetic parameters.

Phosphorylation of Eg5 by Nek2A

Full length WT Nek2A (14 nM) was incubated with 0.12 mg/mL of full length recombinant Eg5 (a gift from Tarun Kapoor) in kinase reaction buffer (20 mM HEPES

pH 7.5, 5 mM MgCl₂, 0.1 mM EDTA, 100 μM ATP, 0.1 mg/mL BSA, 1% DMSO)

containing 2.5 μCi of [γ -³²P]ATP for 30 min at room temperature. The reaction was then analyzed by SDS-PAGE, and visualized by Coomassie stain and autoradiography.

Chapter 4

Cell-based characterization of inhibitors

4.1 Abstract

A Nek2 IP kinase assay employing a dot-blot readout was developed to study the potency and stability of our electrophilic inhibitors in cells. Select compounds were tested for inhibition of Rsk2 and Msk1 in cells since these kinases contain an active site cysteine analogous to Nek2. A more detailed analysis of the induction of mitotic exit by oxindole inhibitors with a hydrogen atom in the 5'-position further suggests that Cdk1 is a target of these compounds in cells. Oxindole compound **21** inhibits Plk1 in cells and induces the formation of monopolar spindles that resemble Plk1 inhibition. However, compound **21** also appears to induce the formation of monopolar spindles in a manner independent of Plk1 inhibition. Mitotic spindle assembly and cell proliferation assays suggest that high micromolar concentrations of our electrophilic oxindoles induce chromosome congression defects and inhibit cell proliferation due to non-specific effects of the electrophile.

4.2 Inhibition of Nek2 in Hek293 cells

To rapidly profile the potency of irreversible Nek2 inhibitors in cells, an IP-kinase assay method was developed to take advantage of the high signal-to-noise ratio achieved from the tetracycline-inducible Nek2A-3HA Hek293 cells, along with the higher throughput achieved from the dot blot readout used in all *in vitro* kinase assays. A representative image showing biological triplicate dose-response curves generated from this assay is presented in Figure 4-1A.

The most significant observations from this assay regarding the inhibition of Nek2 in cells are summarized in Figure 4-1. Importantly, the minimum dose (~ 5 μ M) required for full inhibition of Nek2 for compounds **2** and **21** correlates with that determined for endogenous Nek2 in IP kinase assays (Chapter 1, Figure 1-8). These data suggest that this assay will predict the same inhibitor potencies as endogenous Nek2 IP kinase assays with much less work. This assay also provides information about compound stability in tissue culture conditions. As addressed in Chapter 1 (Table 1-1), the chloromethylketone compounds are less efficient in cells than the propynamides due to poor stability. Comparison of the time dependence of inhibition for chloromethylketone compound **114** versus propynamide compound **2** (Figure 4-1B) shows that compound **114** achieves maximum potency within 5 min on cells, then loses potency after 2 h. The more stable propynamide **2** actually gains potency over this time, as would be expected for an irreversible inhibitor. These data indicate that compound **114** must be degraded within 2 h and that Nek2 activity begins to recover. Recovery of Nek2 activity is probably due to synthesis of new protein, as the “IC₁₀₀” for compound **114** shifts to a greater value between 30 min and 2 h. If all of the Nek2 were inhibited at 30

min, the only way that activity could recover would be through new protein synthesis. The poor stability of chloromethylketone compounds in tissue culture conditions can also be observed by the effect of cell density on inhibitor potency (Figure 4-1C). A 3-fold increase in cell density results in a 5-fold loss of inhibitor potency, indicating that chloromethylketone **21** is degraded by cells. This degradation can take place metabolically or simply by the alkylation of biological molecules (e.g. GSH) by **21**. Carefully controlling cell to inhibitor stoichiometry is an important factor for all cell biological assays comparing the effects of these compounds. The propynamides appear to be degraded about 20 times more slowly than the chloromethylketones in cells, but they too have limited stability (Figure 4-1D). For propynamide **2**, maximum potency is achieved after 2 h on cells, and then Nek2 activity begins to recover. Endogenous Nek2 activity also just begins to recover in 2 h after a single 5 μ M dose of propynamide **2** (data not shown).

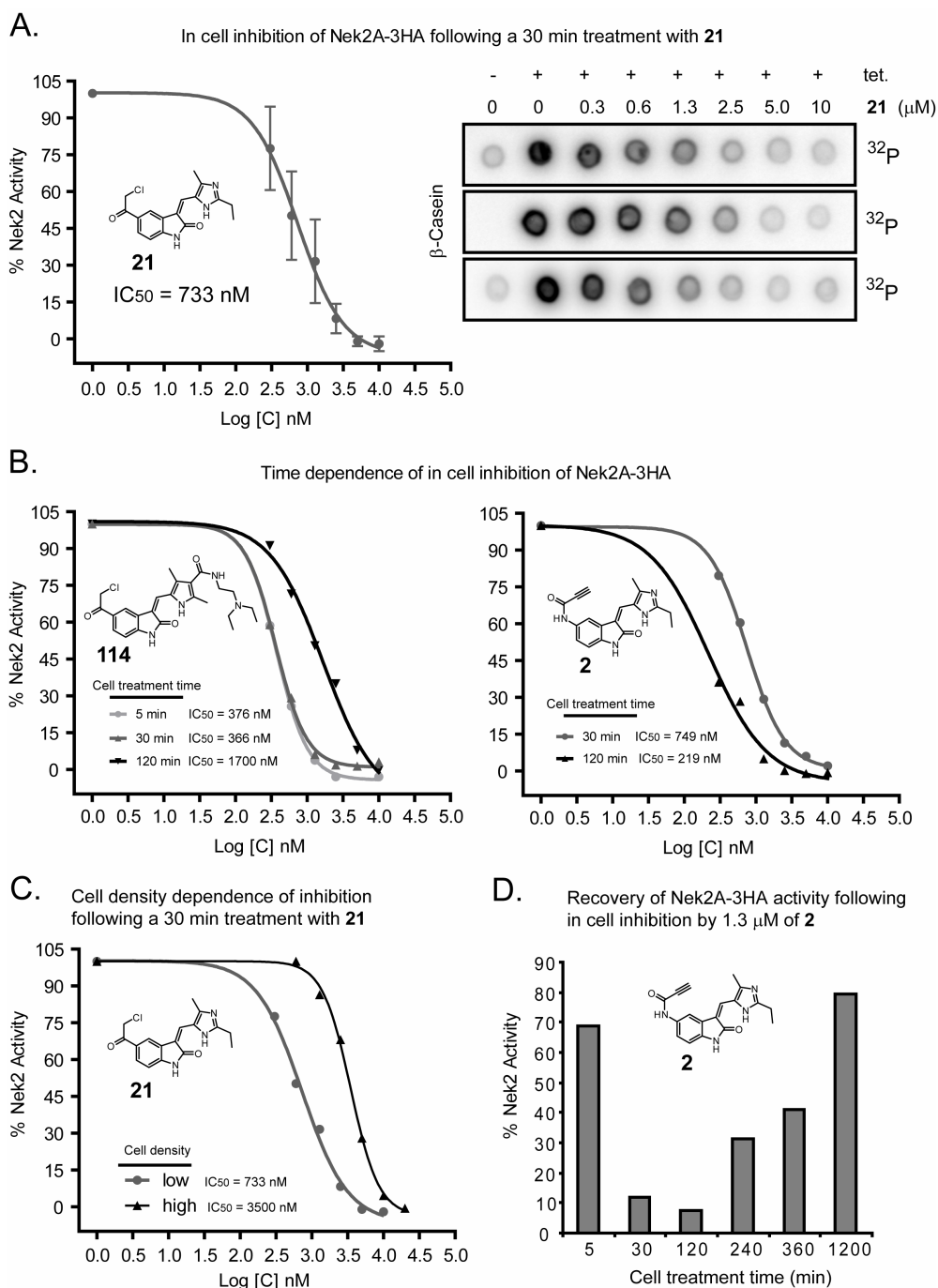


Figure 4-1. Inhibition of Nek2A-3HA in tetracycline inducible Hek293 cells using a dot blot IP kinase assay readout. (A) IP kinase assay dose response curve and raw data for the inhibition of Nek2A-3HA by compound **21**. The curve is plotted as the mean of triplicate measurements and error bars represent the standard deviation. (B) Time dependence of inhibition showing how chloromethylketone **114** loses potency over 2 h, and how propynamide **2** gains potency over 2 h. (C) Dose response curves showing how chloromethylketone **21** loses potency as cell density increases. (D) Time dependence of inhibition by 1.3 μM of compound **2** showing recovery of Nek2 activity over 20 h.

4.3 Inhibition of Rsk2 and Msk1 in cells

Since the C-terminal kinase domains of Rsk2 and Msk1 contain active site cysteines analogous to that of Nek2 (Chapter 1, Figure 1-1C), we sought to see if our irreversible Nek2 inhibitors would inhibit these kinases in cells (Figure 4-2). Comparing assays from Figure 4-1 and Figure 4-2 that employed a 30 min treatment of cells, compound **2** (JH295) proved to be 5-fold selective for Nek2 over Rsk2, and 7-fold selective for Nek2 over Msk1. Because the Rsk2 and Msk1 assays (Figure 4-2) take place in serum-free media and the Nek2 assays use serum-containing media, the selectivity of compound **2** for Nek2 may be even greater given the possibility that serum could lower the effective inhibitor concentration in the Nek2 assay (Figure 4-1B). Again, comparing assays from Figure 4-1 and Figure 4-2, compound **114** was 7 and 30-fold selective for Nek2 over Rsk2 and Msk1, respectively, and compound **21** was 3-fold selective for Nek2 over both Rsk2 and Msk1. Compound **115** (Nek2 IP kinase assay $IC_{50} = 1.1 \mu\text{M}$, data not shown) was 11 and > 18-fold selective for Nek2 over Rsk2 and Msk1, respectively. The potency of the other compounds in Figure 4-2 against Nek2 in cells has not yet been determined.

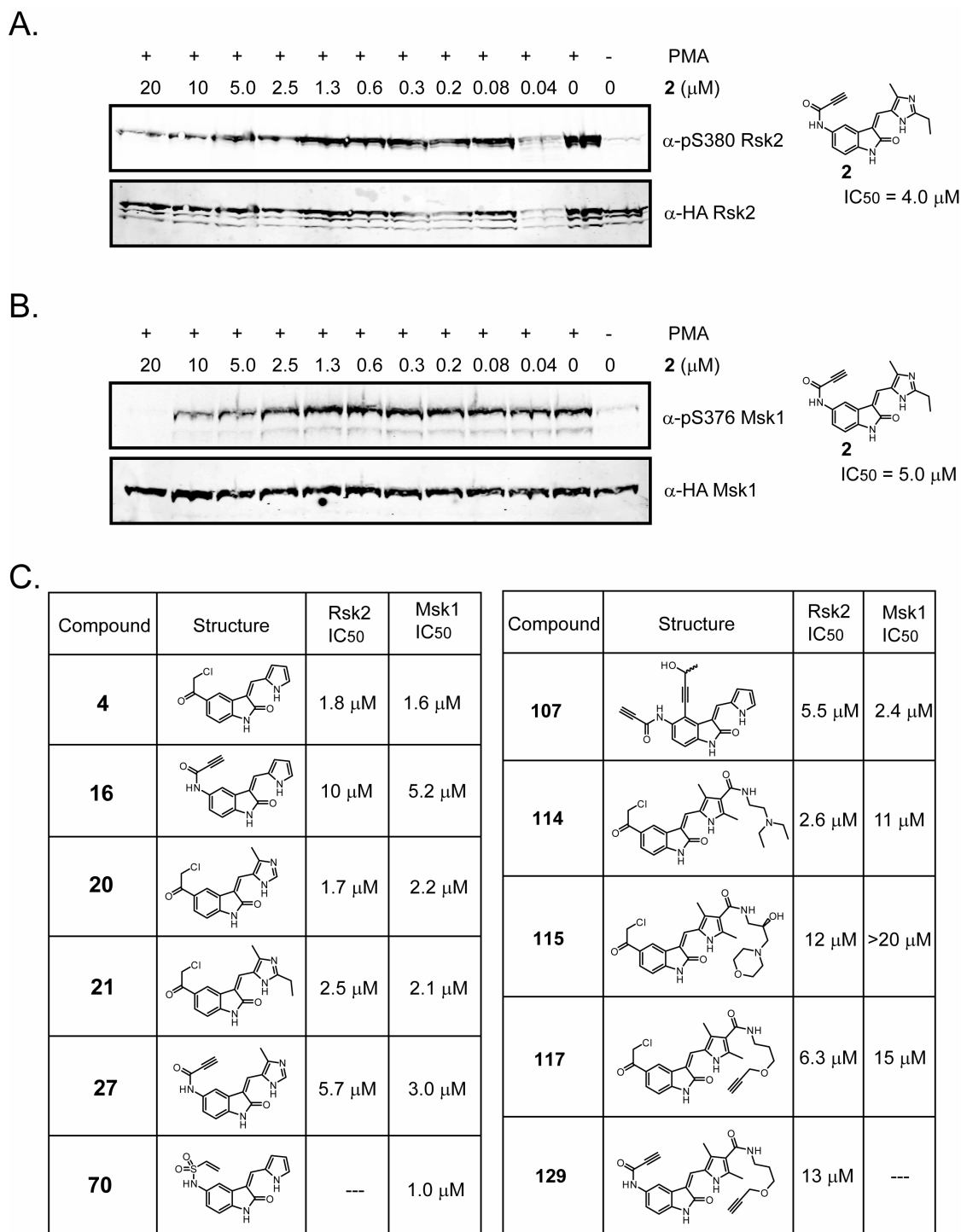


Figure 4-2. Inhibition of HA-tagged Rsk2 in Hek293 cells, and inhibition of HA-tagged Msk1 in Cos7 cells. (A) Representative Western blot showing inhibition of Rsk2 autophosphorylation in response to PMA stimulation. (B) Representative Western blot showing inhibition of Msk2 autophosphorylation in response to PMA stimulation. (C) IC₅₀ values for select compounds in these cell-based Rsk2 and Msk1 autophosphorylation assays.

4.4 Inhibitor-induced mitotic phenotypes

Chapter 1 discussed how all of our oxindole-based Nek2 inhibitors with a hydrogen atom in the 5'-position (Chapter 1, Figure 1-1E, and Figure 4-4A) efficiently triggered mitotic exit in monastrol-arrested cells at a concentration of 5 μ M (Chapter 1, Table 1-1). Chapter 1 also discussed how this is likely due to inhibition of Cdk1, and how these compounds are indeed potent inhibitors of Cdk1 *in vitro* (Chapter 1, Table 1-1). This section covers the mitotic exit phenotype in more detail and provides further evidence for the inhibition of Cdk1. This section also examines how oxindole **21** induces the formation of monopolar mitotic spindles similar to Plk1 inhibitors,³⁹ and how our compounds hinder chromosome alignment during metaphase.

For small-molecule kinase inhibitors, two mechanisms leading to the induction of mitotic exit from monastrol-arrested cells include inhibition of Cdk1³³ and inhibition of AurB.³² Figure 4-3 illustrates this mitotic exit phenotype and shows how the AurB-mediated pathway requires proteasome activity to ultimately inactivate Cdk1 in turn triggering mitotic exit. The only mechanism known by us to trigger mitotic exit in the presence of a proteasome inhibitor is through direct inhibition of Cdk1.³³ The kinetics of mitotic exit as triggered by our oxindole compounds (Figure 4-4A) resemble those published for inhibition of AurB.³² The morphology of cells that have undergone mitotic exit through the action of our compounds is also indistinguishable from that of cells that have been treated with the known Cdk1 and Aurora kinase inhibitors, RO3306³⁵ and VX680⁷⁰ (Figure 4-4B). The fact that oxindole **20** is capable of inducing mitotic exit from monastrol-arrested cells in the presence of the proteasome inhibitor MG132 suggests that Cdk1 is indeed a cellular target of our oxindole compounds (Figure 4-5). Compound **20** is

in fact a much more potent inhibitor of Cdk1 ($IC_{50} < 1 \text{ nM}$, Chapter 1, Table 1-1) than AurB ($IC_{50} \sim 2.8 \mu\text{M}$, Chapter 3, Table 3-5) *in vitro*.

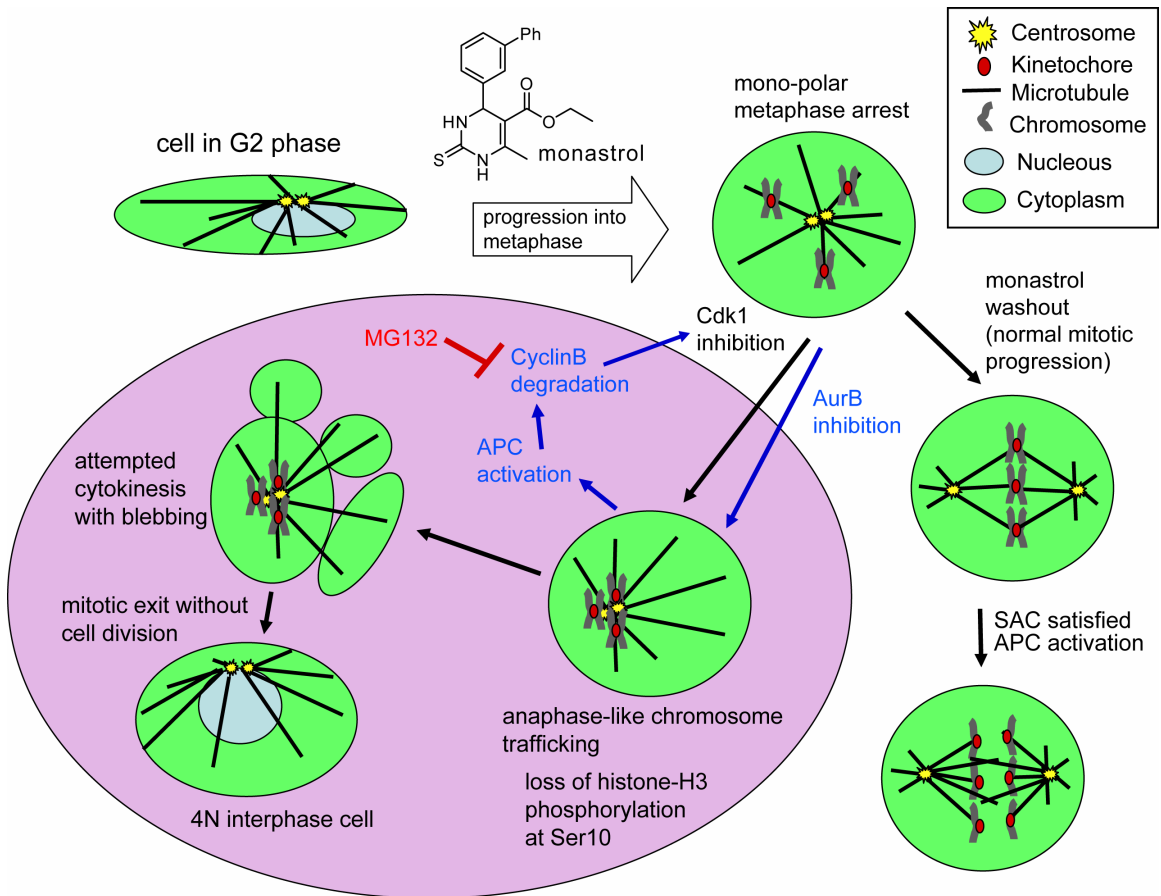


Figure 4-3. Cartoon depicting mitotic exit from monastrol-arrested cells due to AurB or Cdk1 inhibition. Inhibition of AurB bypasses the spindle assembly checkpoint (SAC), leading to activation of the anaphase promoting complex (APC). APC activation leads to proteasome-dependent degradation of CyclinB and in turn inactivation of Cdk1. Inactivation of Cdk1 ultimately triggers mitotic exit without cell division. The mitotic exit pathway triggered by inhibitors of AurB can be blocked by the proteasome inhibitor MG132 (Figure 4-5), although these cells will still exhibit “anaphase-like” movement of chromosomes toward the centrosomes.

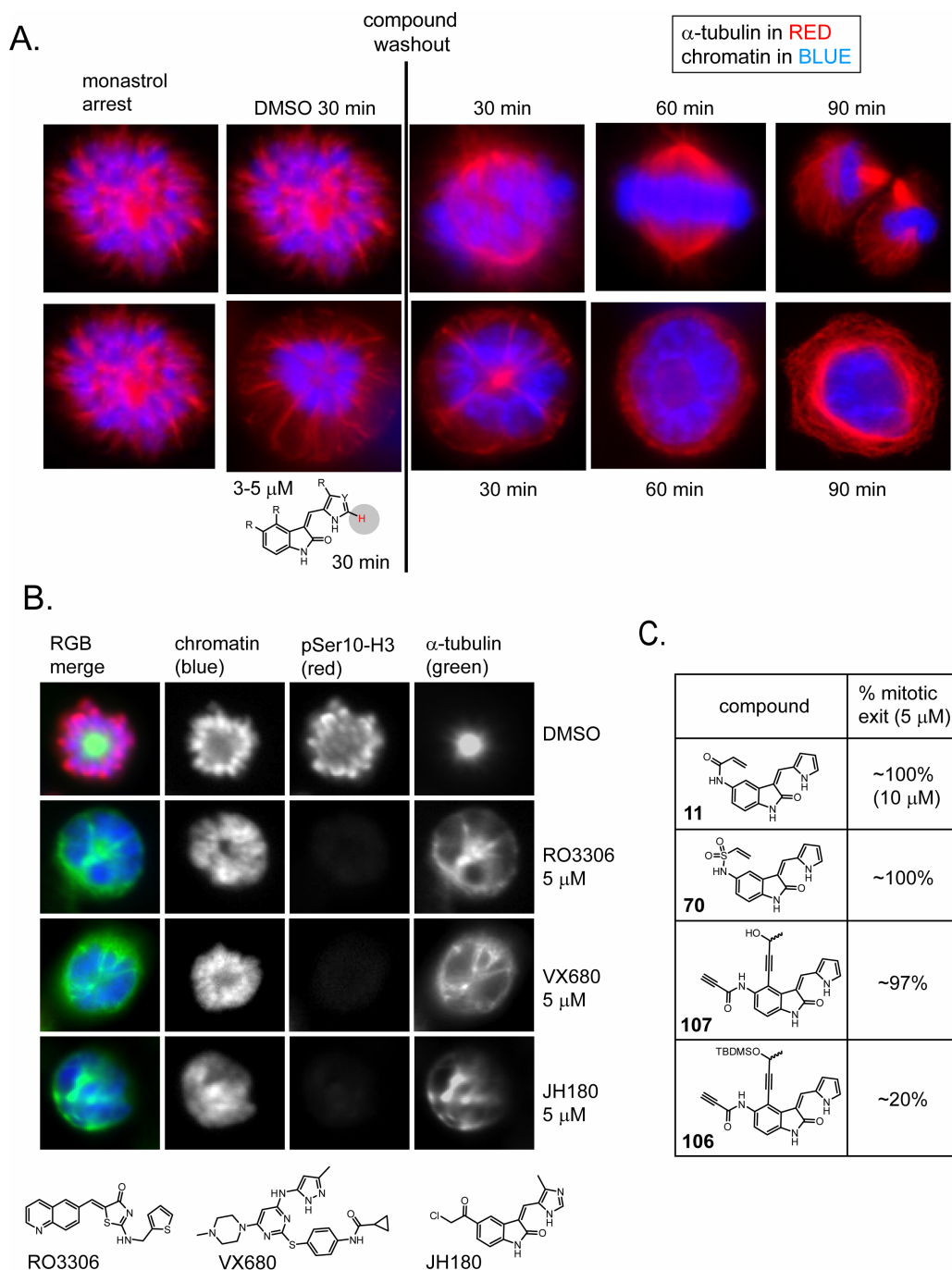


Figure 4-4. Compounds that trigger mitotic exit in monastrol-arrested cells. (A) Representative images of HeLa cells showing the kinetics and irreversibility of oxindole-induced mitotic exit compared to normal mitotic progression following release from monastrol arrest up to 90 min post-washout. All of our oxindole inhibitors with a hydrogen in the 5' position (red) induce this phenotype at 3-5 μ M, likely due to Cdk1 inhibition. (B) Morphology of A549 cells that have undergone mitotic exit from monastrol arrest in response to the Cdk1 inhibitor RO3306, the Aurora inhibitor VX680, or compound **20** (JH180). (C) Inhibitors not covered in Chapter 1 that induce mitotic exit from monastrol arrest.

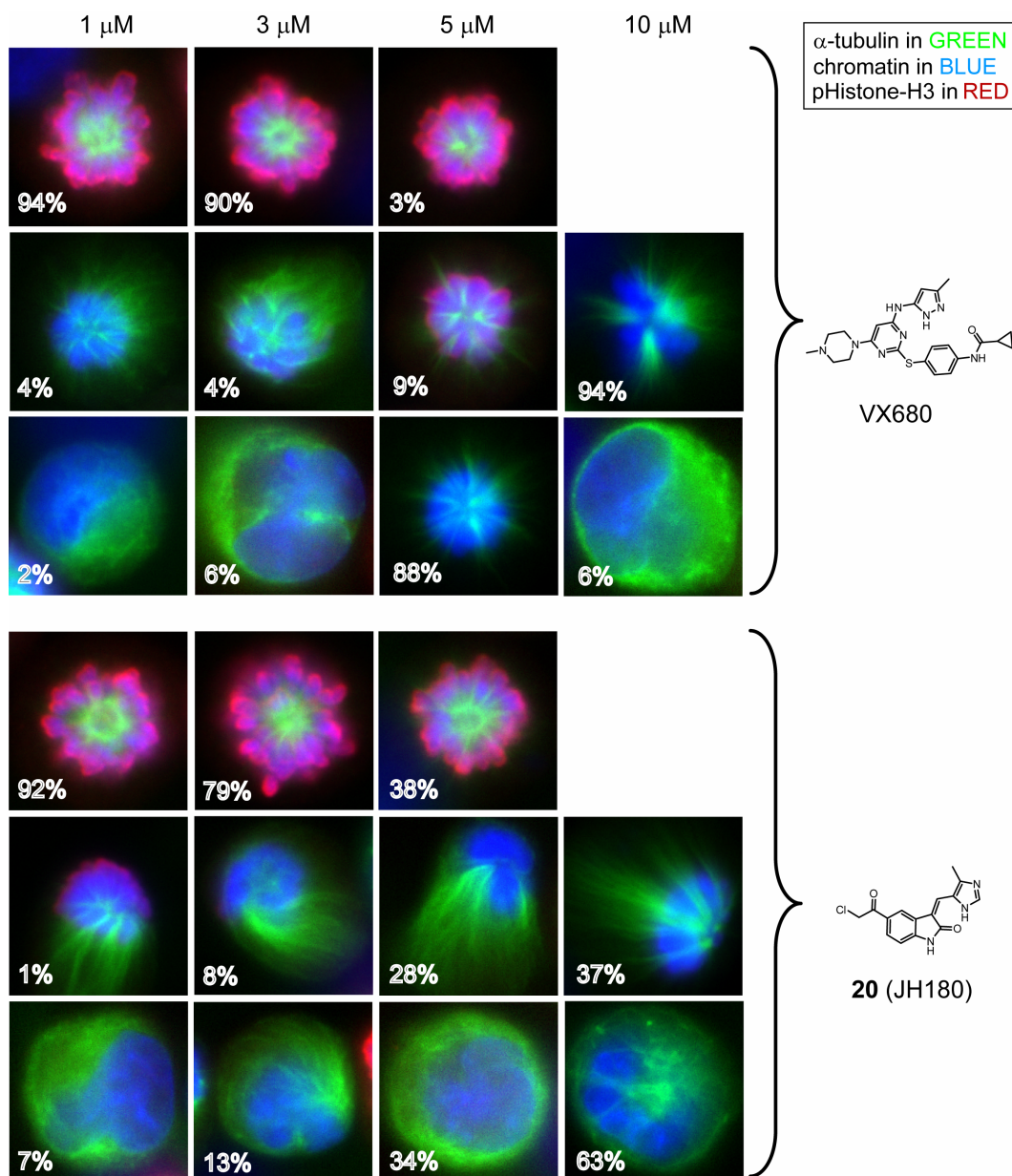


Figure 4-5. Representative images of monastrol-arrested A549 cells that have been treated with either VX680 or compound **20** for 80 min in the presence of the proteasome inhibitor MG132 (10 μ M). These images show how mitotic exit due to Aurora inhibition (VX680) can be blocked by proteasome inhibition. Note how the anaphase-like movement of chromosomes toward the centrosomes still takes place for VX680 despite the blockage of mitotic exit by MG132. Because compound **20** induces mitotic exit in the presence of proteasome inhibition, it likely targets Cdk1 in cells. Compound **20** is a picomolar inhibitor of Cdk1/Cyclin-B complex in vitro (Chapter 1, Table 1-1) and a micromolar inhibitor of AurB (Chapter 3, Table 3-5).

At concentrations higher than required to inhibit cellular Nek2 (full inhibition occurs in cells at 5 μ M, Chapter 1, Table 1-1, and Figure 4-1), compound **21** induces the formation of monopolar spindles. Similar to the Aurora inhibitor VX680 (Figure 4-5), treatment of monastrol-arrested A549 cells with 10 μ M of compound **21** triggers an anaphase-like movement of chromosomes toward the spindle pole (Figure 4-6A). In contrast to VX680, however, compound **21** does not cause the loss of histone-H3 phosphorylation at Ser10 or induce mitotic exit.

Plk1 inhibitors have been shown to induce monopolar spindles with metaphase cell-cycle arrest and trigger the collapse of bipolar spindles to form monopolar spindles in MG132-arrested cells.³⁹ The morphology of the monopolar spindles resulting from the action of compound **21** on both monastrol-arrested (Figure 4-6A) and MG132 arrested cells (Figure 4-6C) resembles that of the monopole documented for Plk1 inhibitors.³⁹ Compound **21** also appears to block cell-cycle progression after washout from monastrol-arrested cells (Figure 4-6A, and Figure 4-6D). One possibility is that compound **21** is irreversibly inhibiting Plk1 in cells at 10 μ M, as Plk1 has an active site cysteine analogous to Nek2 (Chapter 1, Figure 1-1). Indeed, compound **21** inhibits endogenous Plk1 activity at 10 μ M in monastrol-arrested A549 cells, as measured by IP kinase assays (Figure 4-6B). However, compound **21** is still capable of inducing monopolar spindles and blocking cell cycle progression in RPE cells that have been engineered to express either WT GFP-Plk1 or C67V GFP-Plk1, where the active site cysteine has been mutated to a valine, as the only copy of the Plk1 gene.⁷¹ In IP kinase assays of both of these cell lines, compound **21** does not inhibit Plk1 at concentrations that induce monopolar spindles in nearly 100% of the monastrol-arrested cells (Figure 4-6D and Figure 4-6E).

These data suggest that Plk1 may not be the target of compound **21** responsible for the induction of monopolar spindles. We do not think this phenotype is due to Nek2 inhibition either because overexpression of inhibitor-resistant Nek2A-C22V or Nek2B-C22V fails to rescue the effects of compound **21** (data not shown).

The fact that monopolar spindles persist after washout of compound **21** does not prove that the target of compound **21** is irreversibly inhibited. For example, once monastrol-arrested cells have been induced to undergo mitotic exit by the reversible Aurora inhibitor VX680, they continue to undergo mitotic exit even if VX680 is washed out (data not shown). This is a good example of a reversible kinase inhibitor triggering an irreversible cell-cycle transition that will persist in the absence of continued kinase inhibition once set in motion. It is possible that compound **21** may be inducing the formation of monopolar spindles through reversible inhibition of another kinase implicated in this phenotype, such as AurA⁷² or Mps1.³⁶

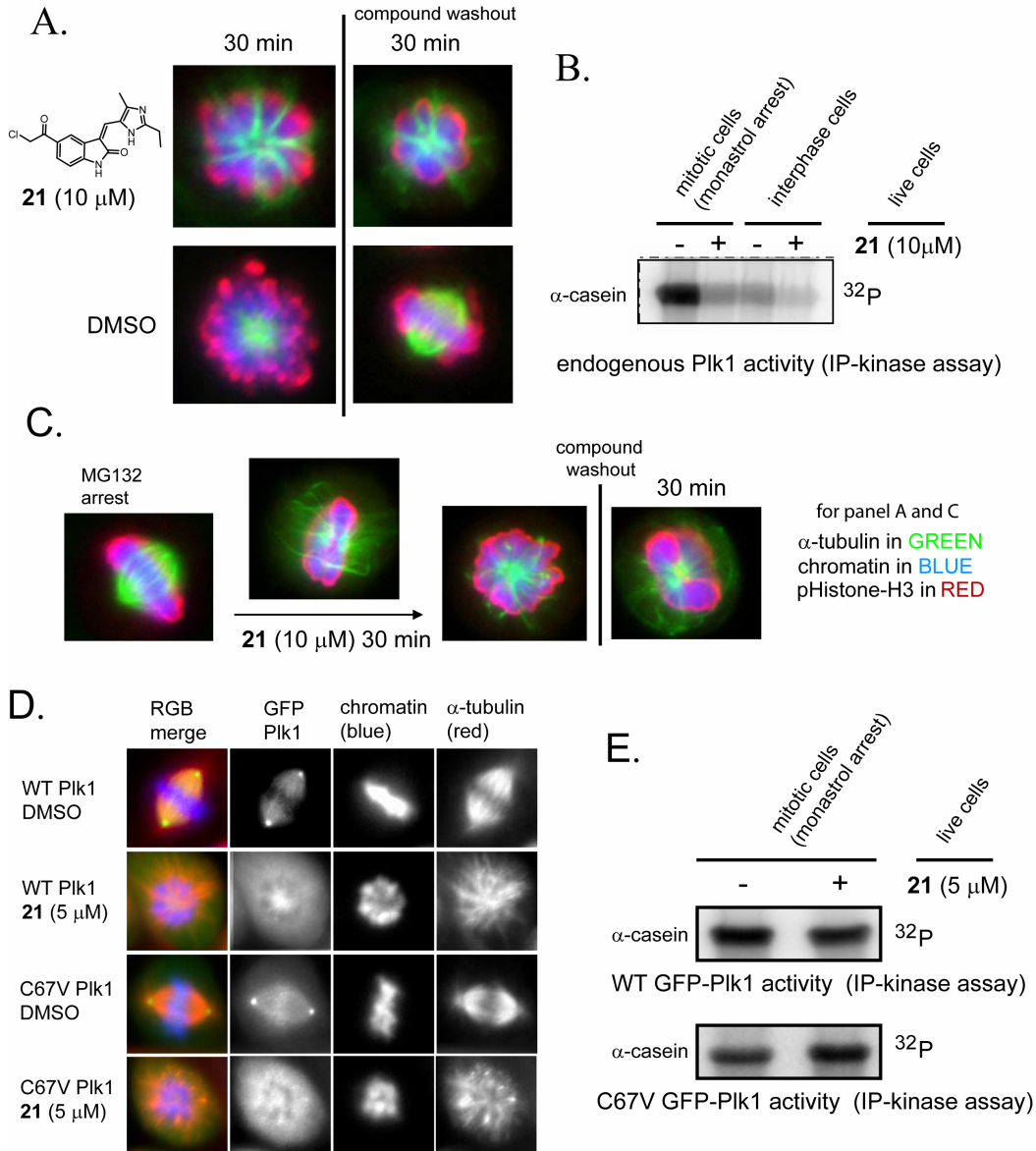
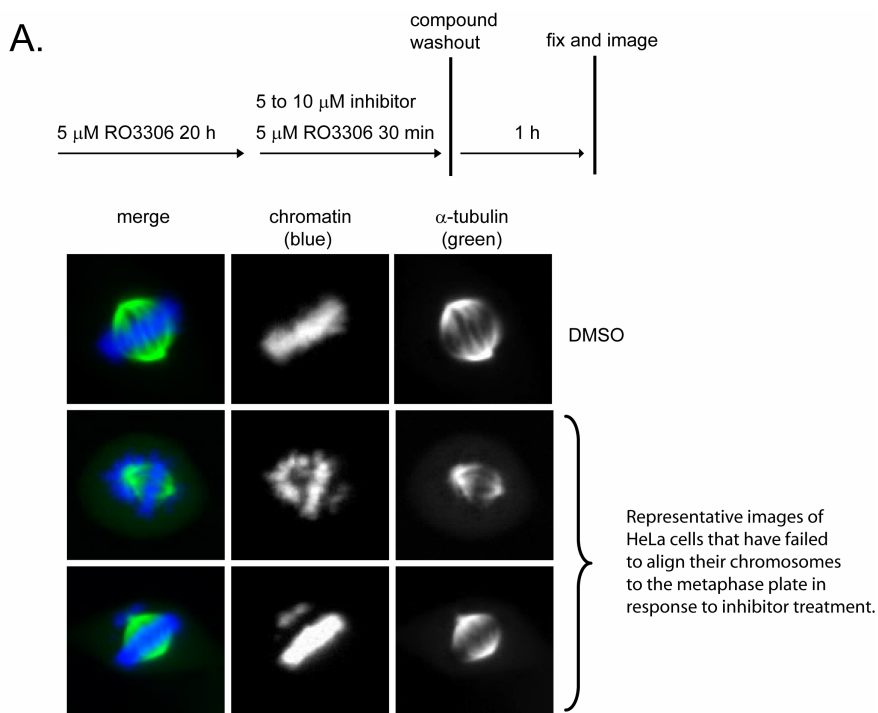


Figure 4-6. At concentrations higher than required to inhibit Nek2, compound **21** induces the formation of monopolar spindles. (A) Treatment of monastrol-arrested A549 cells with **21** (10 μ M) results in anaphase-like movement of chromosomes similar to that observed for Aurora inhibition (VX680, Figure 4-5) but without the loss of histone-H3 phosphorylation at Ser10 and mitotic exit. This phenotype resembles that of Plk1 inhibitors.³⁹ (B) Compound **21** (10 μ M) inhibits endogenous Plk1 in monastrol-arrested A549 cells at 10 μ M. (C) Compound **21** (10 μ M) causes the collapse of bipolar spindles, also similar to Plk1 inhibitors.³⁹ (D) Compound **21** (5 μ M) induces monopolar spindles in monastrol-arrested RPE cells expressing inhibitor-resistant Plk1. These images are presented 30 min after the washout of monastrol and compound **21** following 18 h of monastrol arrest, then a 30 min treatment with monastrol plus compound **21**. (E) Plk1 IP-kinase assays from stable RPE cells showing the lack of inhibition by compound **21** (5 μ M). Note: the contrast of the blots are normalized, C67V Plk1 has about 10-fold less total activity than WT Plk1.⁷¹

Our electrophilic oxindoles hinder the ability of cells to align their chromosomes at the metaphase plate (chromosome congression). Treatment of cells arrested at the G2/M border (RO3306 arrest) with electrophilic oxindoles causes a delay in the congression of chromosomes to the metaphase plate following release into mitosis by RO3306 washout (Figure 4-7). Although previous studies have implicated Nek2 in the regulation of chromosome congression by demonstrating congression defects in response to ectopic-overexpression of non-phosphorylatable Nek2 substrates,^{11,12} we do not believe that our inhibitors induce this phenotype by inhibition of Nek2. The primary reason for this is that the electrophilic negative-control compounds that do not inhibit Nek2 in cells are nearly as effective at inducing this congression-defect phenotype (Figure 4-7B). Nek2 IP kinase assays for negative-control compound **31** are presented in Chapter 1 Table 1-1, and negative-control compound **112** gives 50% inhibition of endogenous Nek2 at 5 μ M (data not shown).

The numbers for the percentage of cells showing chromosome congression defects (Figure 4-7B) are presented as a rough guideline. This is a difficult phenotype to pinpoint and there is considerable variance between experiments. For example, factors such as cell type, the duration of G2/M arrest, the exact time spent in mitosis prior to fixation, the temperature of cell fixation, and cell density all appear to modulate the induction of this phenotype by these compounds. The numbers presented in Figure 4-7B are a good approximation for HeLa, A549, and Hek293 cells. The current working model is that these chromosome congression defects are due to non-specific effects of the electrophile that slow down the rate of chromosome congression (data not shown) and not due to inhibition of Nek2.



B.

compound	[C] μ M	% cells with unaligned chromosomes
2 	5 to 10	50 to 90%
31 	5 to 10	25 to 80%
114 	5	~50%
112 	5	~30%

Figure 4-7. Representative images of HeLa cells that have failed to align their chromosomes at the metaphase plate following treatment with oxindole Nek2 inhibitors during G2/M arrest (RO3306) then release into mitosis for 1 h. (B) Compounds that have been shown to hinder the alignment of chromosomes in the context of Panel A. These numbers are given as a rough guideline only. In general this effect seems to be due to the electrophile and not Nek2 inhibition since compounds **34** and **112** do not inhibit Nek2 at the concentrations indicated. The exact number of cells that exhibit this phenotype at a given compound concentration is difficult to determine. Factors such as cell type, the duration of G2/M arrest, the exact time spent in mitosis prior to fixation, and cell density all appear to effect the induction of this phenotype by these compounds.

4.5 Inhibition of cell proliferation

Similar to the induction of chromosome congression defects (Figure 4-6), our electrophilic oxindole Nek2 inhibitors are cytotoxic in a manner dependent on the presence of the electrophile (Figure 4-8). Figure 4-8 shows EC₅₀ values for the inhibition of Hek293 cell proliferation in response to a single 16 h dose of the indicated compounds. To summarize, compounds containing electrophiles (**2**, **21**, **31**, **34**, **112**, and **114**) are at least 3-fold more potent than their non-electrophilic analogs (**35**, **36**, and **110**). The electrophilic compounds that have specifically been designed by methylation of the hinge-binding moiety not to inhibit kinases (**31**, **34**, and **112**) are as potent as the kinase-binding electrophilic compounds (**2**, **21**, and **114**). These data suggest that non-specific effects of the electrophile (and not kinase inhibition) are responsible for the inhibition of proliferation. The numbers presented in Figure 4-8 serve as a rough guideline only. The anti-proliferative effects of these compounds are very dependent on cell density (cell to compound stoichiometry).

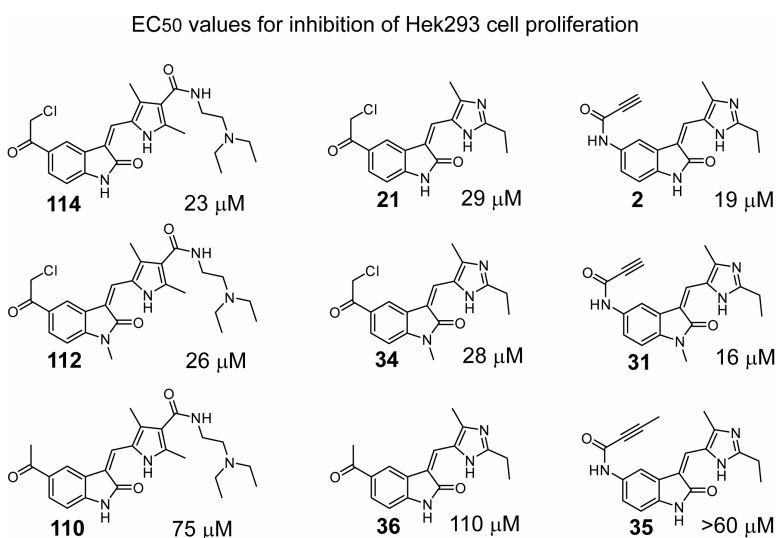


Figure 4-8. EC₅₀ values for the inhibition of Hek293 cell proliferation as measured by an Alamar Blue metabolism assay.

4.6 Experimental methods

Dot blot IP kinase assays of Nek2A-3HA

IP kinase assays of overexpressed HA-tagged Nek2A from tetracycline-inducible Hek293 cell lines (Chapter 1) were carried out exactly as presented in Chapter 1 with the following changes. For the high cell-density experiment (Figure 4-1C), cells were plated at 1.8 million cells per well. For all dot blot IP kinase assays, following the last wash of the beads (the sample was not divided for Western analysis as in Chapter 1), the wash buffer was removed, and the beads were incubated in 30 μ L of kinase buffer containing 0.5 mg/mL β -casein (Sigma), 100 μ M ATP, and 0.4 μ Ci of [γ - 32 P]ATP for 1 h at room temperature. Next, 5 μ L of the reaction mixture (including beads) was blotted onto nitrocellulose membrane (Bio-Rad) that had been pre-washed with wash buffer (1 M NaCl, 0.1 % H_3PO_4) and dried. The membrane was washed three times with wash buffer, and then dried under a heat lamp. The dry blots were exposed to a storage-phosphor screen (GE Healthcare), imaged using a Typhoon Scanner (GE Healthcare), quantified using Image Quant software (GE Healthcare), then processed and plotted using Excel (Microsoft) and GraphPad (Prism) software. IP's from cells that had not been treated with tetracycline were used as a background control. Alternately, the reactions can be blotted at various time intervals to test the linearity of the kinase assay readout (for example 15, 30, and 60 min).

Cell-based Rsk2 and Msk1 autophosphorylation assays

Cos7 cells and tetracycline-inducible Hek293-Frt HA-Rsk2 cells (a gift from Iana Serafimova in our lab) were grown and propagated according to the general tissue culture conditions presented in Chapter 1.

For Rsk2 autophosphorylation assays, tetracycline-inducible Hek293 cells (Iana Serafimova) expressing full-length HA-Rsk2 were plated at 300,000 cells/well in 12-well tissue culture plates (Nunc) with media containing 1 $\mu\text{g}/\text{mL}$ of tetracycline. The cells were allowed to grow for 24 h then treated with serum-free media for 2 h. After incubation in serum free media, the cells were treated with inhibitors in 1 mL/well of serum-free media for 30 min. The inhibitor-containing media was then removed, and the cells were treated with serum-free media containing 100 ng/mL of PMA for 30 min. After the PMA treatment, the media was removed and the cells were immediately stored at $-80\text{ }^{\circ}\text{C}$ as dry monolayers. Plates of cells were then thawed at room temperature for 5 min, and then treated with 60 $\mu\text{L}/\text{well}$ of lysis buffer (50 mM HEPES pH 7.5, 150 mM NaCl, 0.5% Triton-X100, 1 mM DTT, 1x Roche complete protease inhibitors, 1X Roche PhosSTOP phosphatase inhibitor cocktail). Plates containing lysis buffer were sonicated by floating on a water bath for 30 sec. Lysates were then removed, transferred to a 0.6 mL tube, and clarified at 20,000 g for 10 min. The protein content of the clarified lysates was measured by Bradford assay (BioRad), and the lysates were then normalized with lysis buffer. The normalized lysates were resolved by SDS-PAGE, transferred to nitrocellulose membrane, and then analyzed by Western blot. For Western blots, the nitrocellulose membranes were blocked with Li-Cor Blocking buffer (Li-Cor) for 1 h at room temperature then washed three times with TBST. Membranes were then treated with a mixture of 1:500 anti-pS380 Rsk2 antibody (Cell Signaling), and 1:1000 anti-HA antibody (12CA5, Roche) in AB-Dil (50 mM Tris pH 7.6, 150 mM NaCl, 0.05% Tween 20, 0.1% NaN_3 , 2% BSA) for 1 h at room temperature. Membranes were then washed three times with TBST, and then treated with a mixture of 1:5000 anti-rabbit-IR800

antibody (Li-Cor) and 1:5000 anti-mouse-IR680 antibody (Li-Cor) in 5% milk-TBST for 30 minutes at room temperature. Blots were then washed three times with TBST, and then visualized and quantified using an infrared Odyssey Scanner (Li-Cor).

For Msk1 autophosphorylation assays, a confluent 10 cm dish of Cos7 cells was transfected with full length HA-tagged Msk1 in the pMT2 mammalian expression vector. The transfection was carried out as follows. To 1.5 mL of Opti-MEM reduced serum media (Gibco) was added 24 μ g of Msk1-HA pMT2. The resulting mixture was incubated at room temperature for 5 min, and then a solution of 60 μ L of Lipofectamine2000 (Invitrogen) in 1.5 mL of opti-MEM was added. The resulting mixture was incubated at room temperature for 20 min before being added to a confluent 10 cm dish of Cos7 cells in 15 mL of antibiotic-free media. The transfected cells were allowed to grow for 17 h then dislodged with trypsin. The resulting cell suspension was diluted to 40 mL with tissue culture media and then plated at 1 mL/well in 12-well tissue culture plates (Nunc). The transfected cells were allowed to grow for 3 h, and then changed to 1 mL/well of serum free media. At this point the cells were processed and analyzed exactly as for the Rsk2 assays with the following antibodies used for the Western analysis. For primary antibodies, a mixture of 1:1000 anti-pS376 Msk1 antibody (Cell Signaling), and 1:1000 anti-HA antibody (12CA5, Roche) in AB-Dil was used for 1 h at room temperature. For secondary antibodies, a mixture of 1:5000 anti-rabbit-IR800 antibody (Li-Cor) and 1:5000 anti-mouse-IR680 antibody (Li-Cor) in 5% milk-TBST for 30 minutes at room temperature was used.

Mitosis assays in A549, HeLa, and RPE cells

Immunofluorescence microscopy and mitotic exit during monastrol-arrest assays were done exactly as described in Chapter 1, with the exception of Figure 18A. The only difference for the cells in Figure 18A was that they were stained with a 1:1000 dilution of anti- α -tubulin antibody (Sigma, T6199) for 1h, followed by a mixture of anti-mouse-alexafuor-594 conjugated antibody (Molecular Probes) and 500 ng/mL DAPI for 45 minutes.

In general, monastrol was always used at 100 μ M for 6 to 18 h to arrest cells in metaphase. RO3306 was always used at 5 μ M for 16 to 20 h to arrest cells at the G2/M border. MG132 arrested cells were formed by releasing monastrol-arrested cells into 10 μ M of MG132 for 1h. RPE cells containing WT GFP-Plk1 and CV GFP-Plk1 were grown in DMEM-F12 (Gibco) media with 10% FBS.⁷¹

Plk1 IP kinase assays

For endogenous Plk1 IP kinase assays, two 150 cm² flasks of A549 cells were grown to confluency then treated with 100 μ M of monastrol for 6.5 h. One flask was then treated with 10 μ M of JH249 (**21**) plus 100 μ M of monastrol for 30 min. The other flask was treated with DMSO plus monastrol as a control. The mitotic cells from both flasks were then dislodged (“mitotic shake off”) by hitting the flask against a lab bench (rather forcefully). The media containing the mitotic cells was then removed and spun at 900 g to pellet the mitotic cells. The cell pellet was washed with 3 mL of PBS, re-pelleted, and then frozen in liquid N₂ after removal of the PBS supernatant. The adherent monolayers of interphase cells were scraped loose into PBS, pelleted, washed with PBS, and then also frozen in liquid N₂. The cell pellets were then thawed into 300 μ L of lysis buffer (PBS

containing 0.5% v/v triton-X100, 1 mM DTT, 1x Roche Complete protease inhibitor cocktail, and 1x Sigma Phosphatase inhibitor cocktails #1 and #2). The lysates were then clarified at 20000 g for 10 min, and normalized for total protein content. The normalized lysates were incubated with 2 µg of anti-Plk1 antibody (H135, Santa Cruz Biotech) for 2 h at 4 °C. Then, 50 µL of protein-A Dynabeads (Invitrogen) was added and the samples were rocked at 4 °C for another 2 h. The beads were then washed twice (5 min/wash) with 250 µL of lysis buffer then once with 250 µL of lysis buffer containing 0.5 M NaCl. The beads were then washed twice with kinase buffer (20 mM HEPES pH 7.5, 5 mM MgCl₂, 0.1 mM EDTA, 1 mM DTT, 1x Sigma phosphatase inhibitor cocktails #1 and #2). For the kinase assays, after removal of the wash buffer, the beads were incubated in 60 µL of kinase buffer containing 2 mg/mL of α-casein (Sigma), 50 µM ATP, and 0.6 µCi/µL of [γ -³²P]ATP for 1 h at room temperature, then quenched with 15 µL of 5x sample buffer (300 mM TRIS pH 6.8, 10% SDS, 50% glycerol, 0.01% bromophenol blue, 0.5 M DTT). The substrate protein was then resolved by SDS-PAGE, and then analyzed by Coomassie staining and autoradiography. Autoradiography was performed exactly as for *in vitro* kinase assays.

GFP-Plk1 IP kinase assays from the stable RPE cell lines⁷¹ were performed exactly as for endogenous Plk1 with the following exceptions. Three 10 cm dishes of cells were used per data point, and no mitotic shake-off was employed. The cell pellets were lysed into 640 µL of lysis buffer.

Inhibition of Hek293 cell proliferation

Un-induced Hek293-FRT (tetracycline-inducible Nek2A-HA) cells (Chapter 1) were plated at 30,000 cells/well in clear-bottom black-walled 96-well tissue culture plates

using 100 μL of media, and then grown for 24 h. Inhibitors were then added as 3x stocks in tissue culture media, and growth was allowed to proceed for another 16 h. A 10x stock of Alamar Blue (Invitrogen) was then added to produce a 1x final concentration. After 4.5 h of growth at 37 °C, the plate was scanned on a plate reader to measure Alamar Blue fluorescence (545 nm excitation, and 590 nm emission).

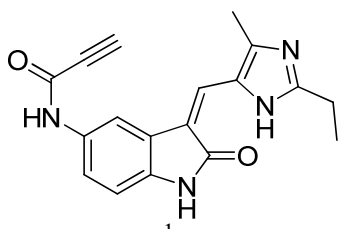
Appendix A

Abbreviations

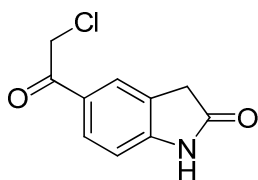
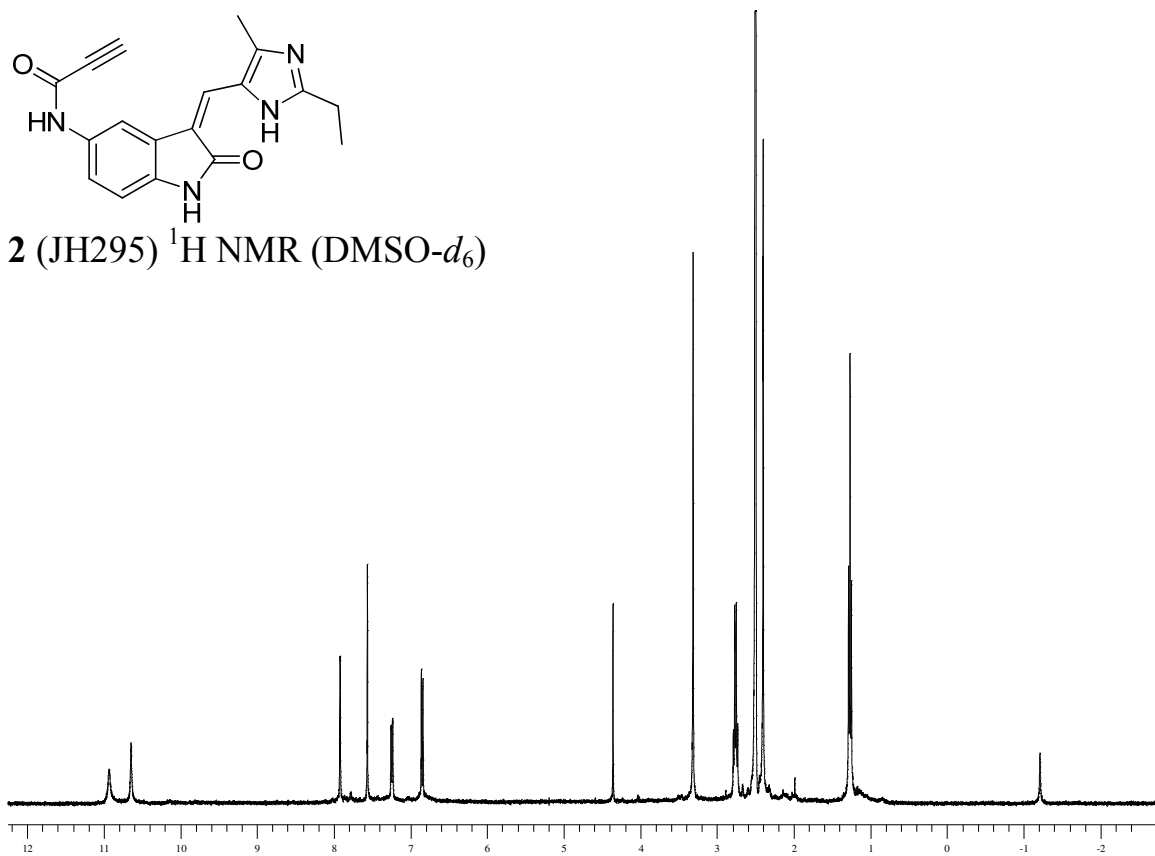
APC/C, anaphase promoting complex/cyclosome; ATP, adenosine triphosphate; AurB, Aurora kinase B; Boc, t-butyloxycarbonyl; BSA, bovine serum albumin; B-Raf, rapidly accelerated fibrosarcoma kinase B; CBB, Coomassie Brilliant Blue; Cdc20, cell-division cycle protein 20; Cdk1, cyclin dependent kinase 1; C-Nap1, centrosomal Nek2 associated protein 1; DCM, dichloromethane; DIPEA, *N,N*-diisopropylethylamine; DMF, dimethylformamide; DTT, dithiothreitol; EDC, 1-ethyl-3-(3-dimethylaminopropyl) carbodiimide hydrochloride; Eg5, kinesin family member 11; Et₂O, diethyl ether; Et₃N, triethylamine; EtOAc, ethyl acetate; H-Ras, Harvey rat sarcoma viral oncogene homolog; HA, hemagglutinin; Hec1, high expression in cancer-1; HOBt, hydroxybenzotriazole; Mad2, mitotic arrest deficient gene 2; Mps1, monopolar spindle kinase 1; Nek2, NIMA related kinase 2; p90Rsk2, p90 ribosomal S6 protein kinase 2; PBS, phosphate buffered saline; Plk1, polo-like kinase 1; PMA, phorbol 12-myristate 13-acetate; pTSA·H₂O, para-toluenesulfonic acid monohydrate; Pd/C, palladium on carbon; RNAi, RNA interference; SAC, spindle assembly checkpoint; shRNA, short hairpin RNA; siRNA, small interfering RNA; TBTA, tris[(1-benzyl-1*H*-1,2,3-triazol-4-yl)methyl] amine; THF, tetrahydrofuran; TLC, thin layer chromatography; WT, wild type.

Appendix B

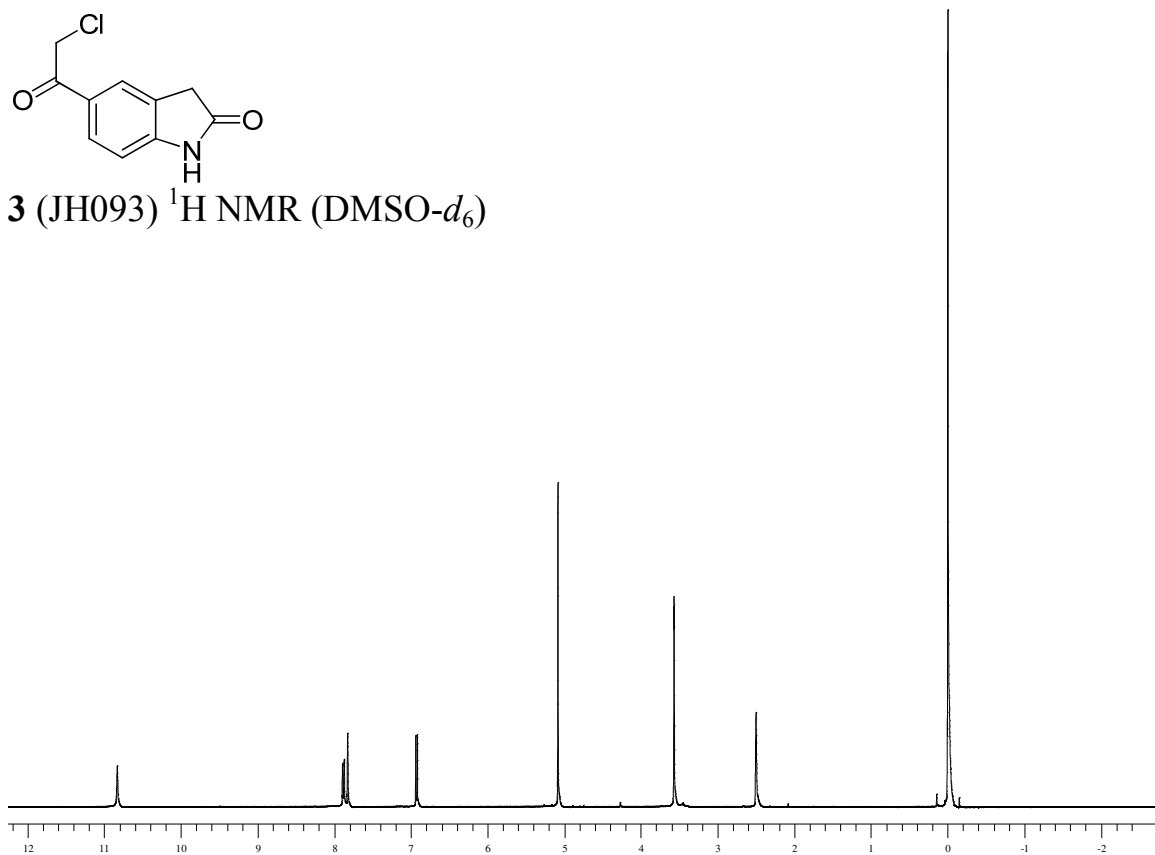
^1H NMR spectra of compounds 2-144

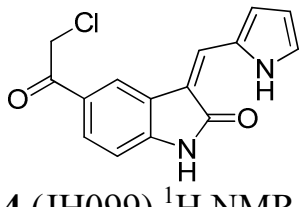


2 (JH295) ^1H NMR (DMSO- d_6)

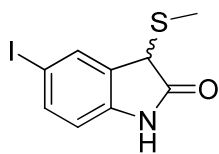
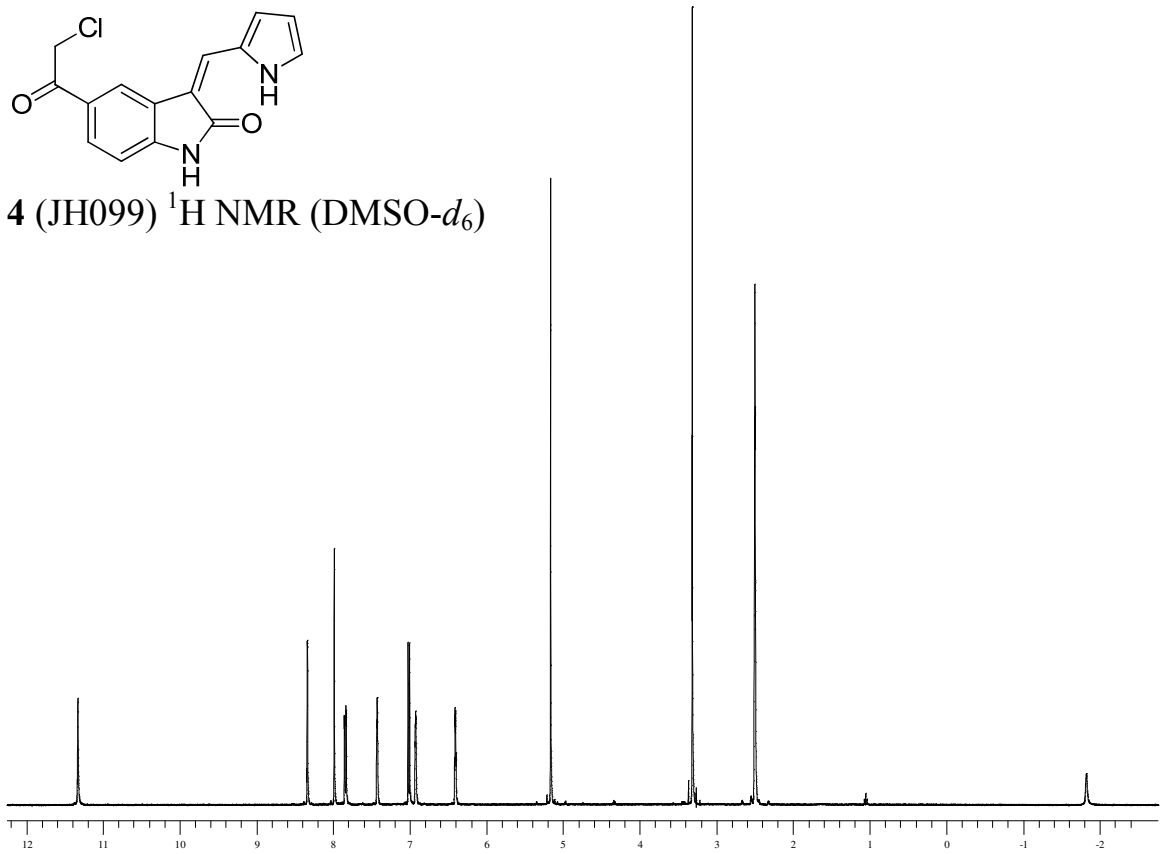


3 (JH093) ^1H NMR (DMSO- d_6)

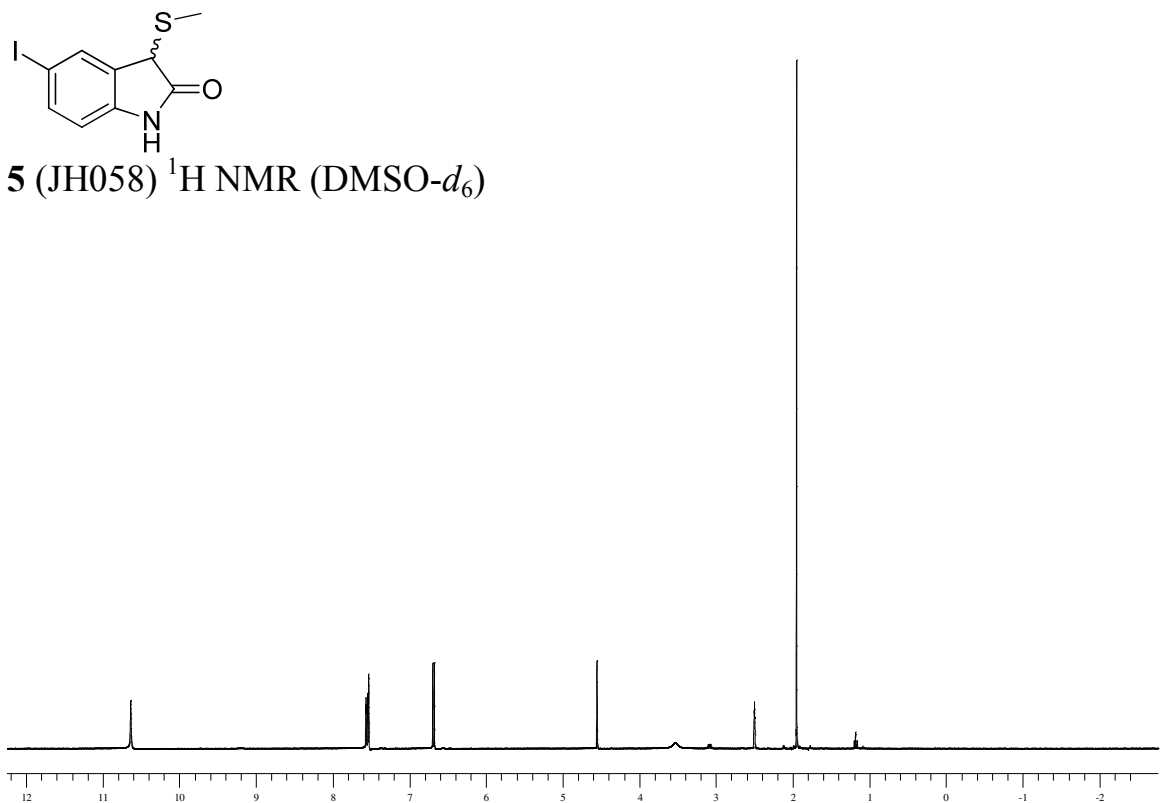


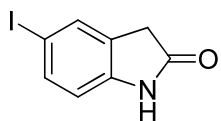


4 (JH099) ^1H NMR (DMSO- d_6)

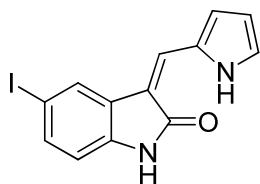
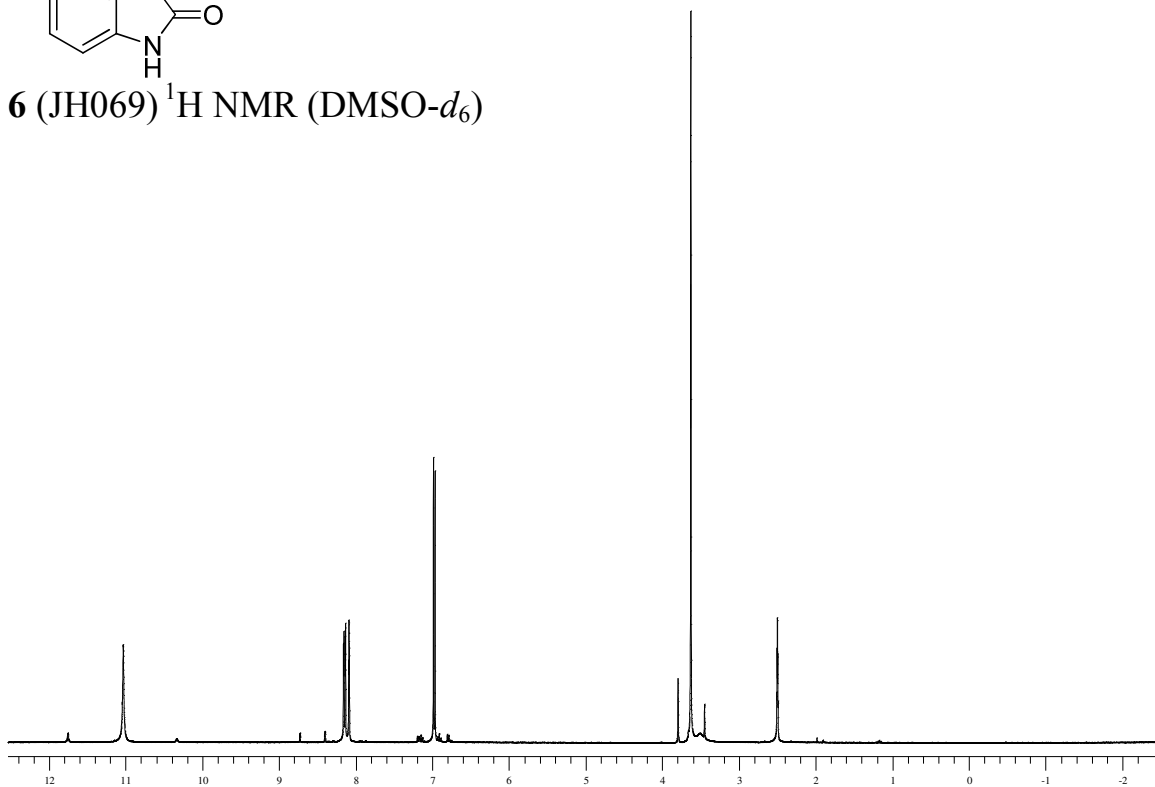


5 (JH058) ^1H NMR (DMSO- d_6)

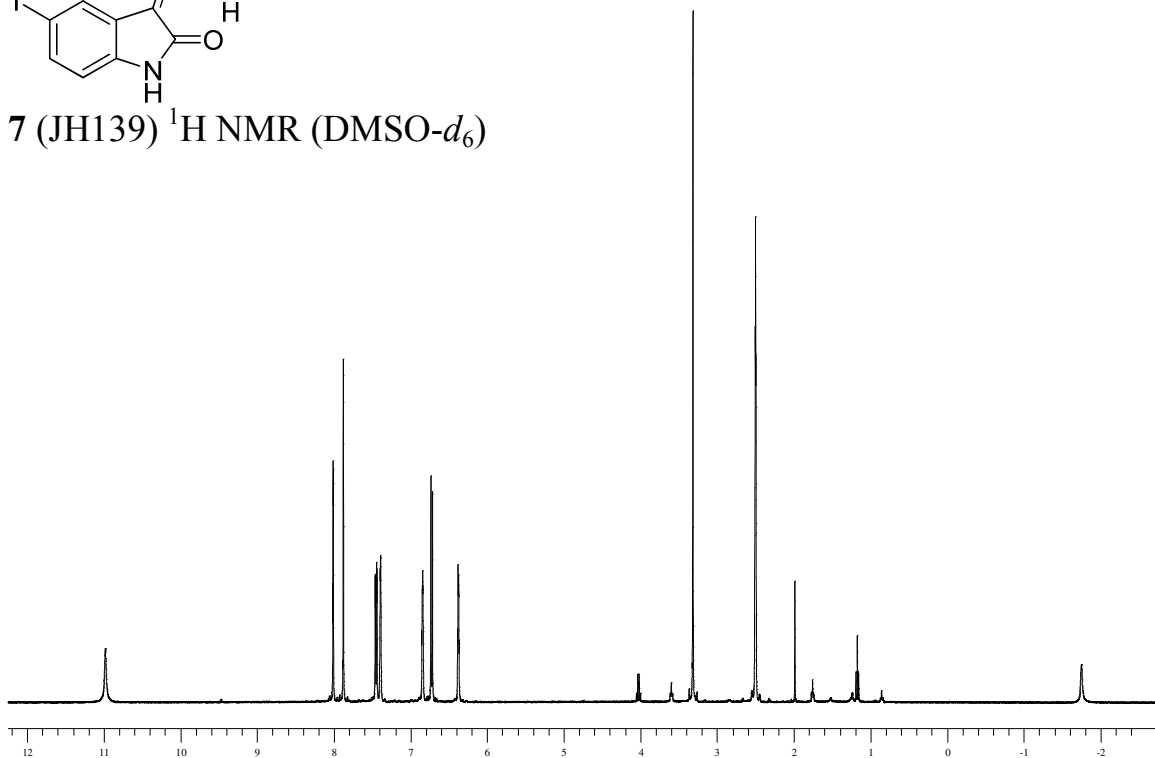


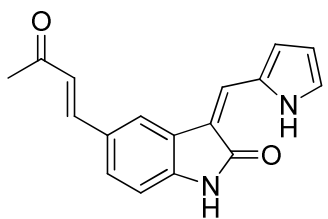


6 (JH069) ^1H NMR (DMSO- d_6)

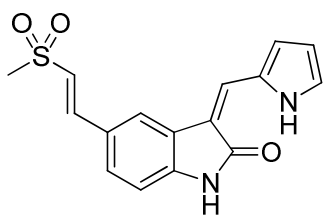
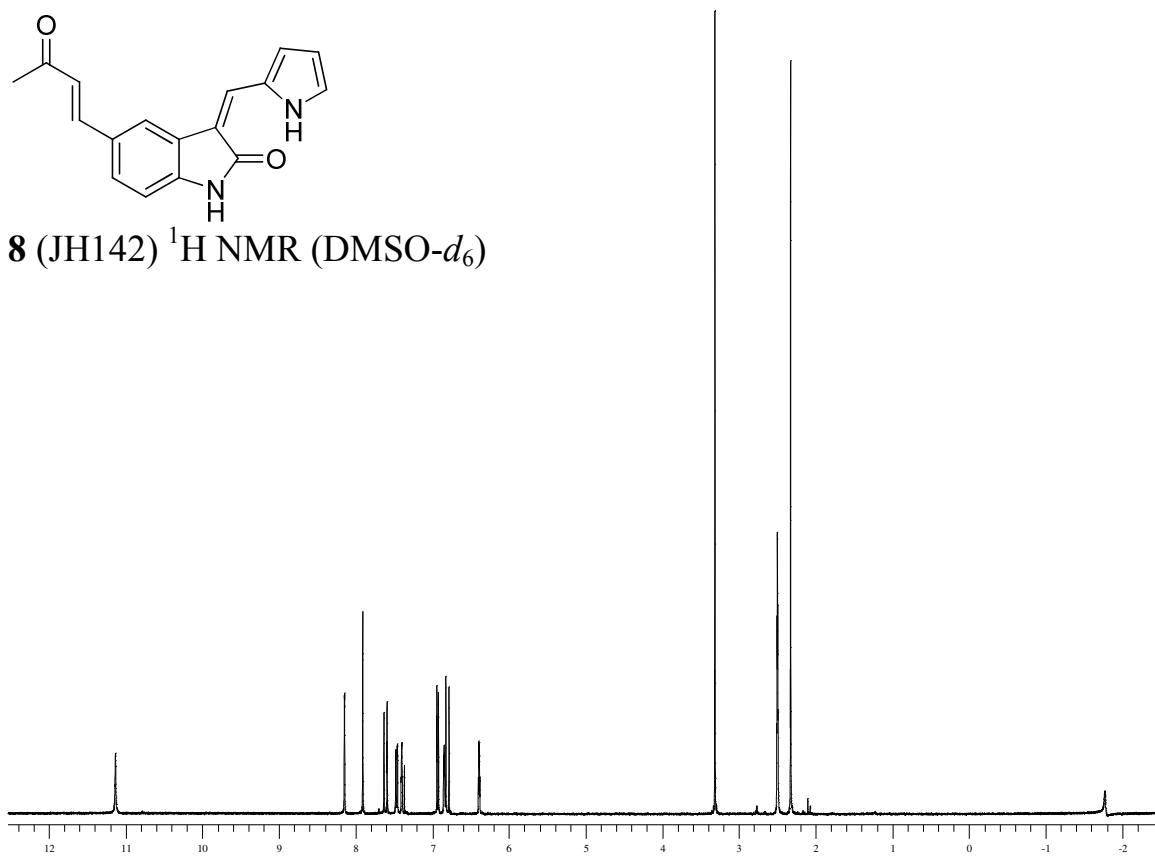


7 (JH139) ^1H NMR (DMSO- d_6)

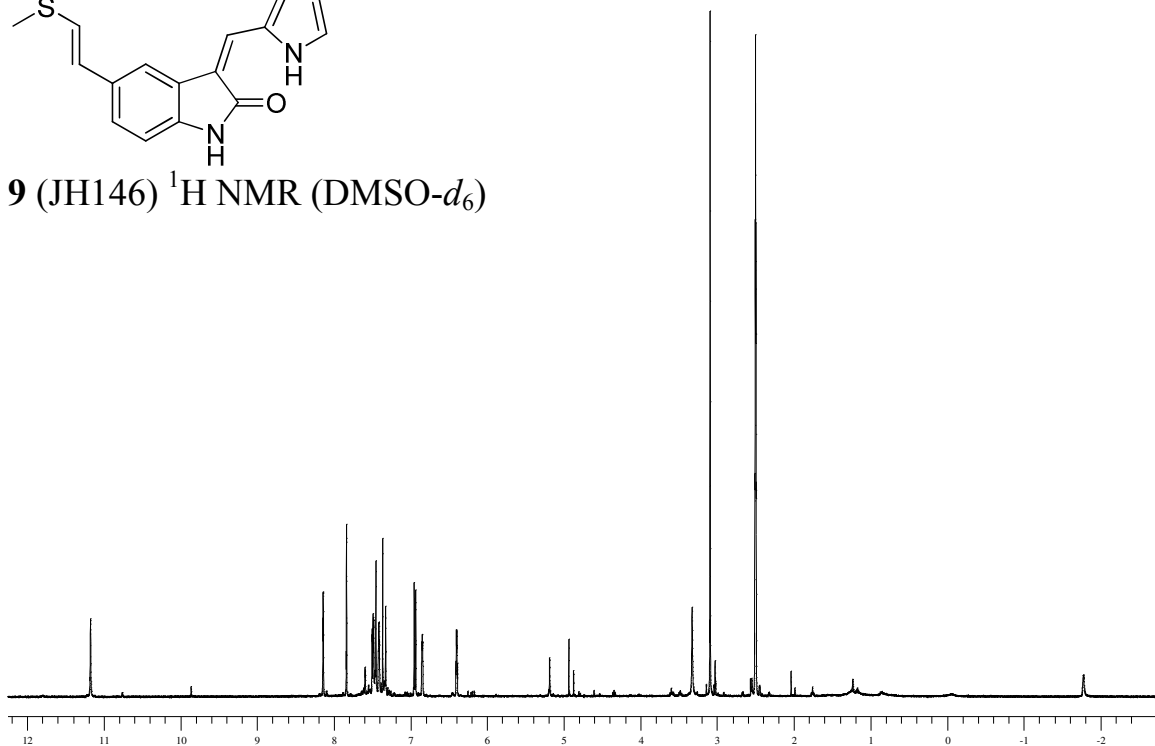


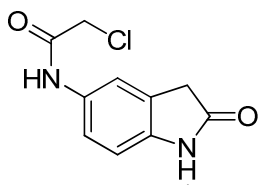


8 (JH142) ^1H NMR (DMSO- d_6)

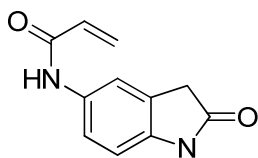
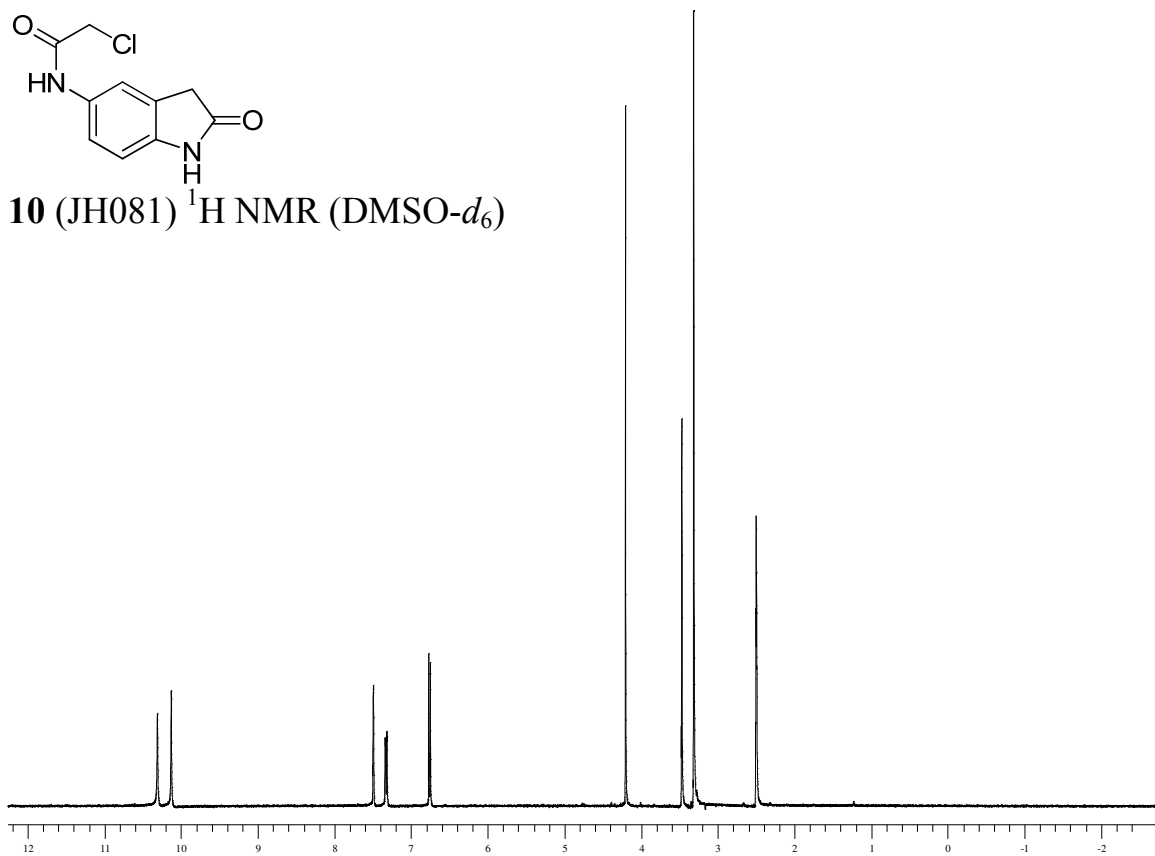


9 (JH146) ^1H NMR (DMSO- d_6)

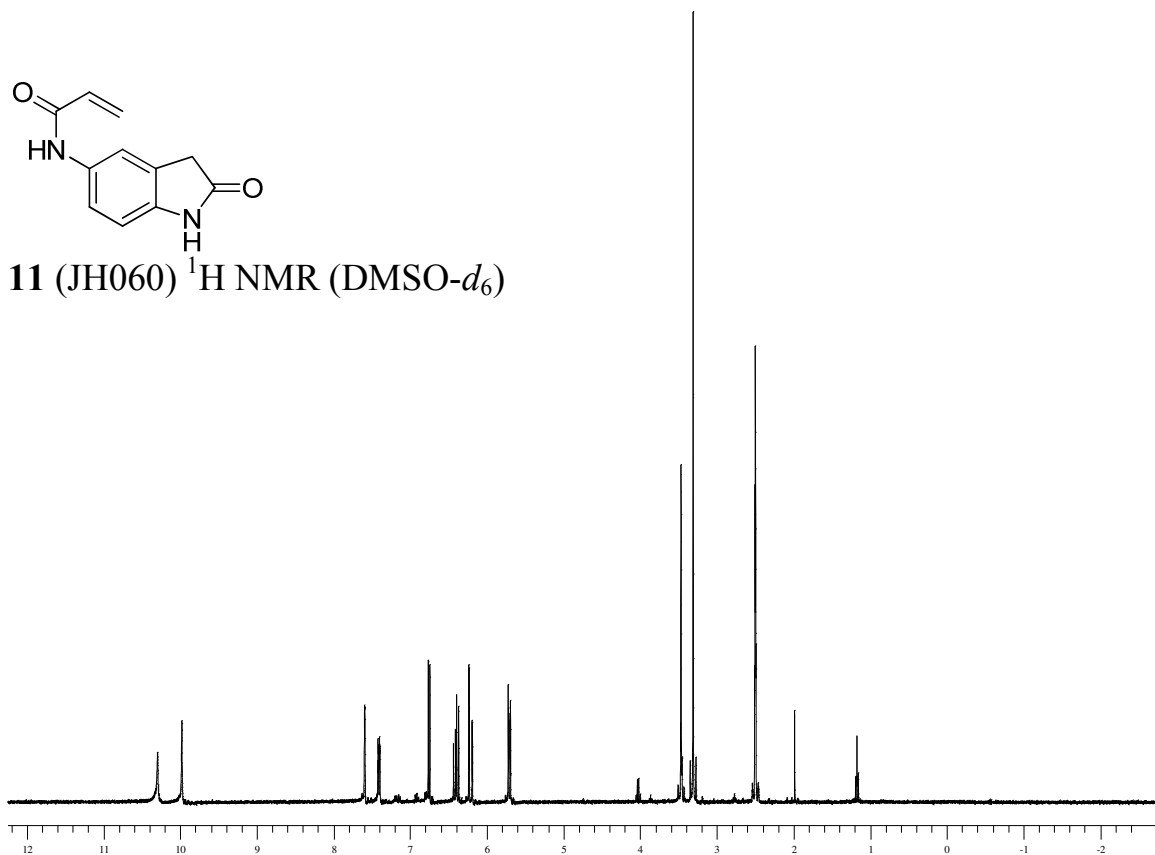


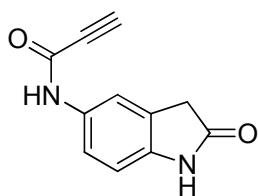


10 (JH081) ^1H NMR (DMSO- d_6)

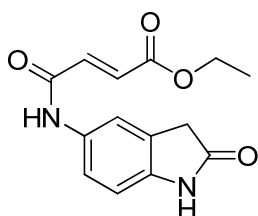
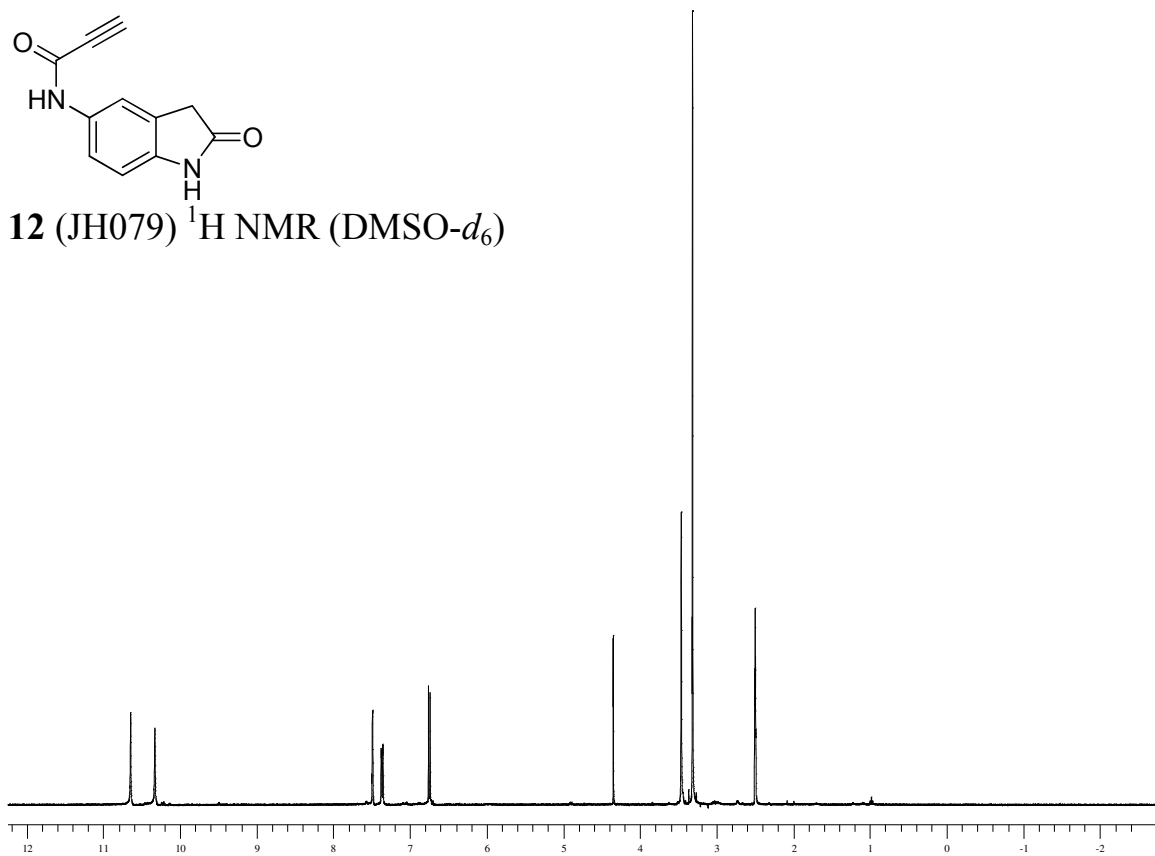


11 (JH060) ^1H NMR (DMSO- d_6)

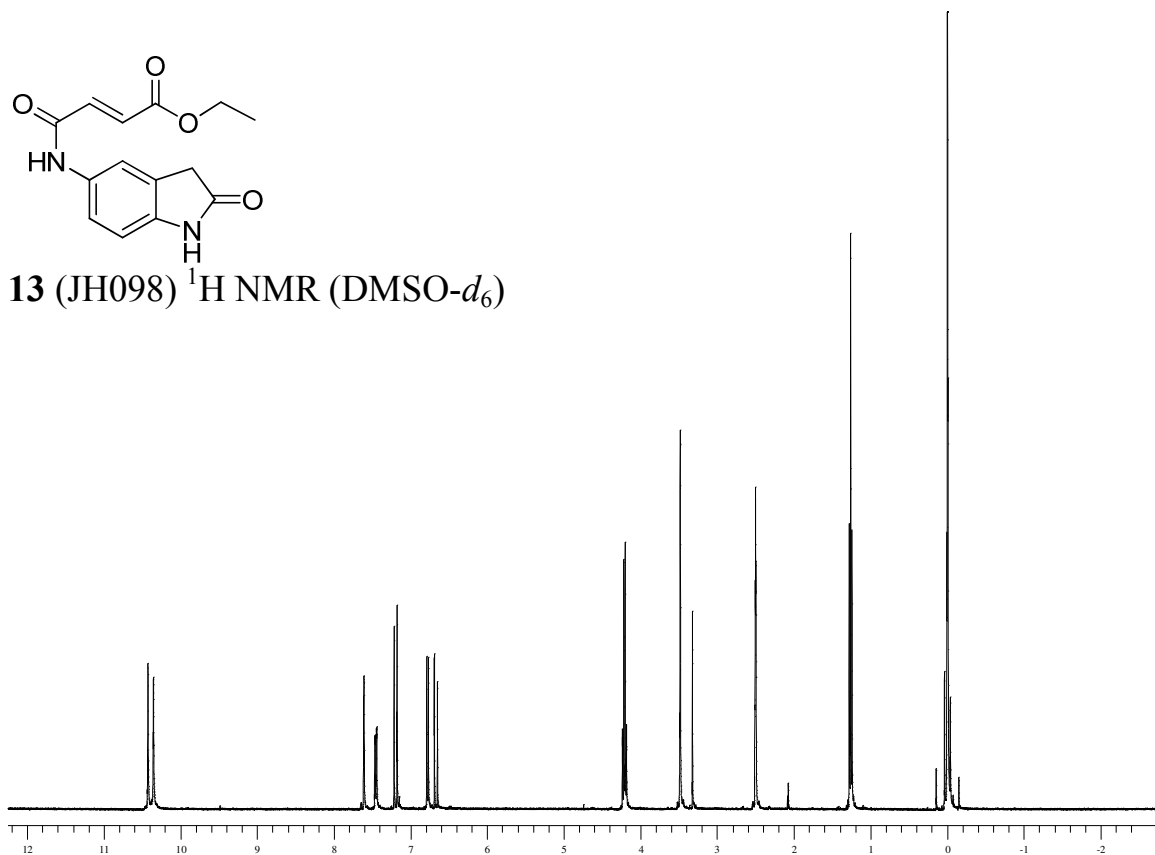


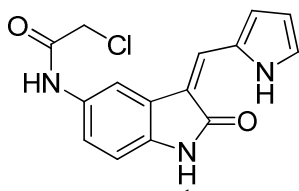


12 (JH079) ^1H NMR (DMSO- d_6)

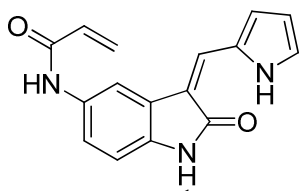
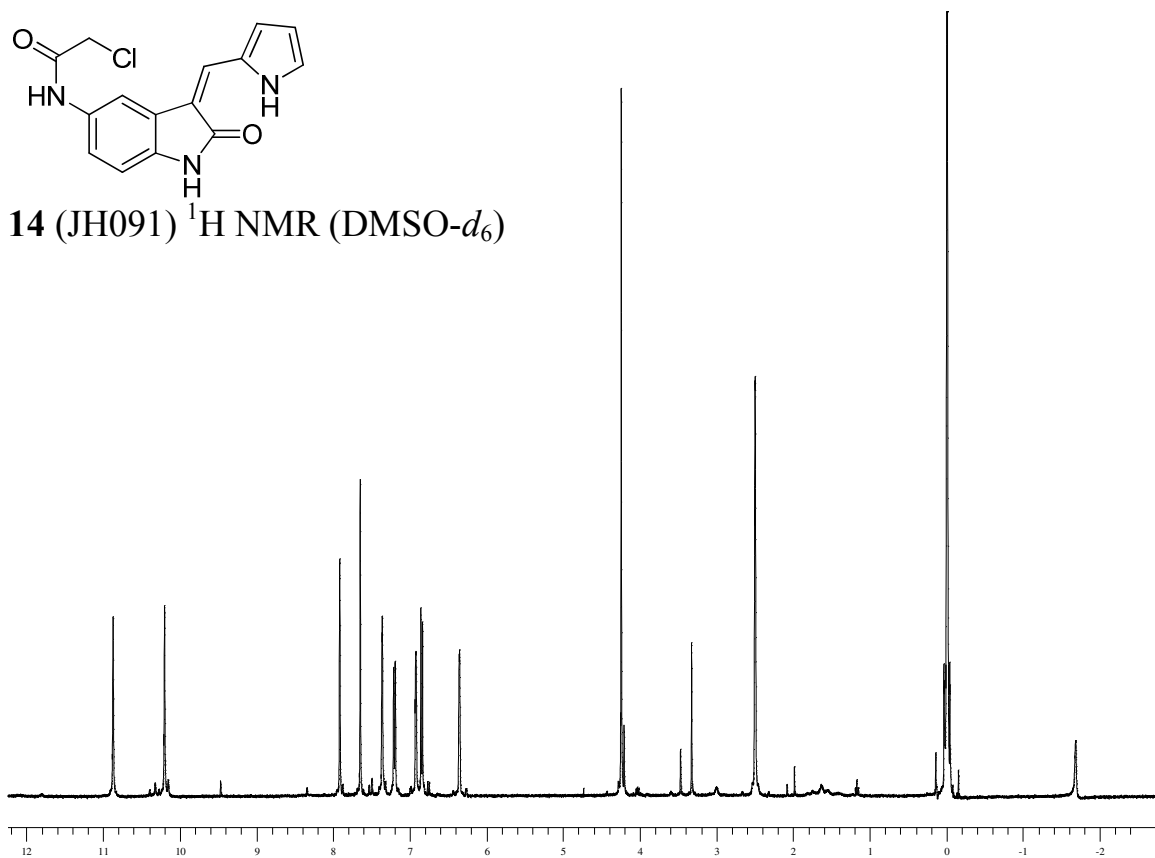


13 (JH098) ^1H NMR (DMSO- d_6)

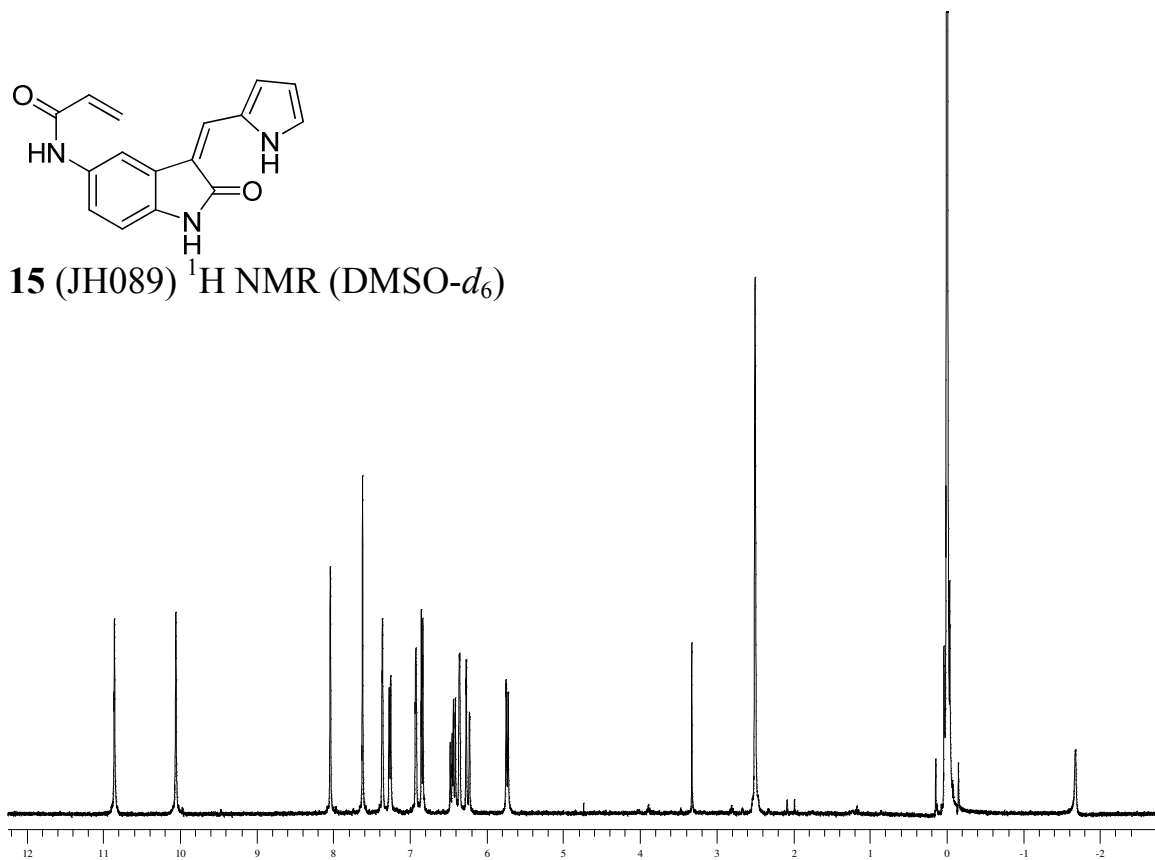


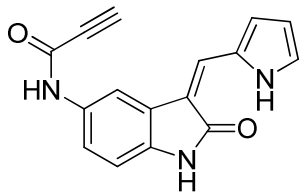


14 (JH091) ^1H NMR (DMSO- d_6)

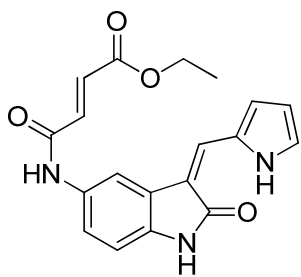
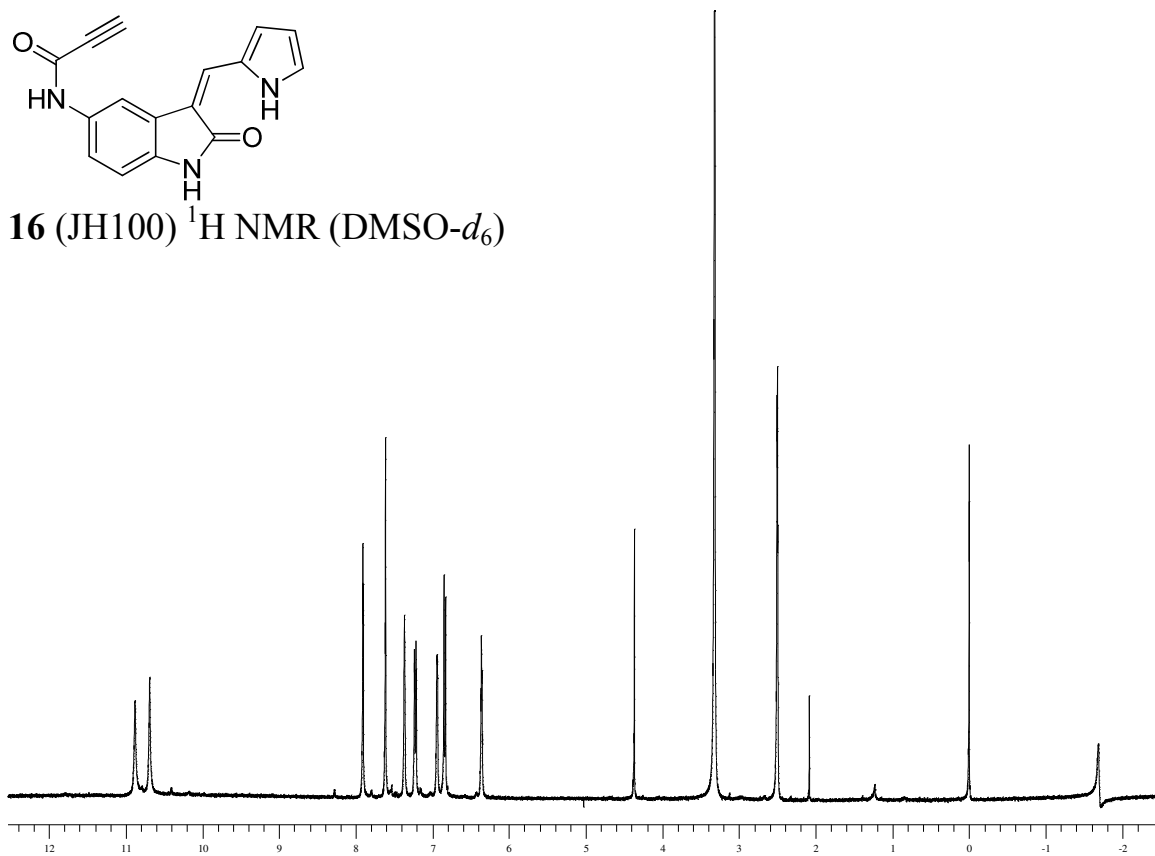


15 (JH089) ^1H NMR (DMSO- d_6)

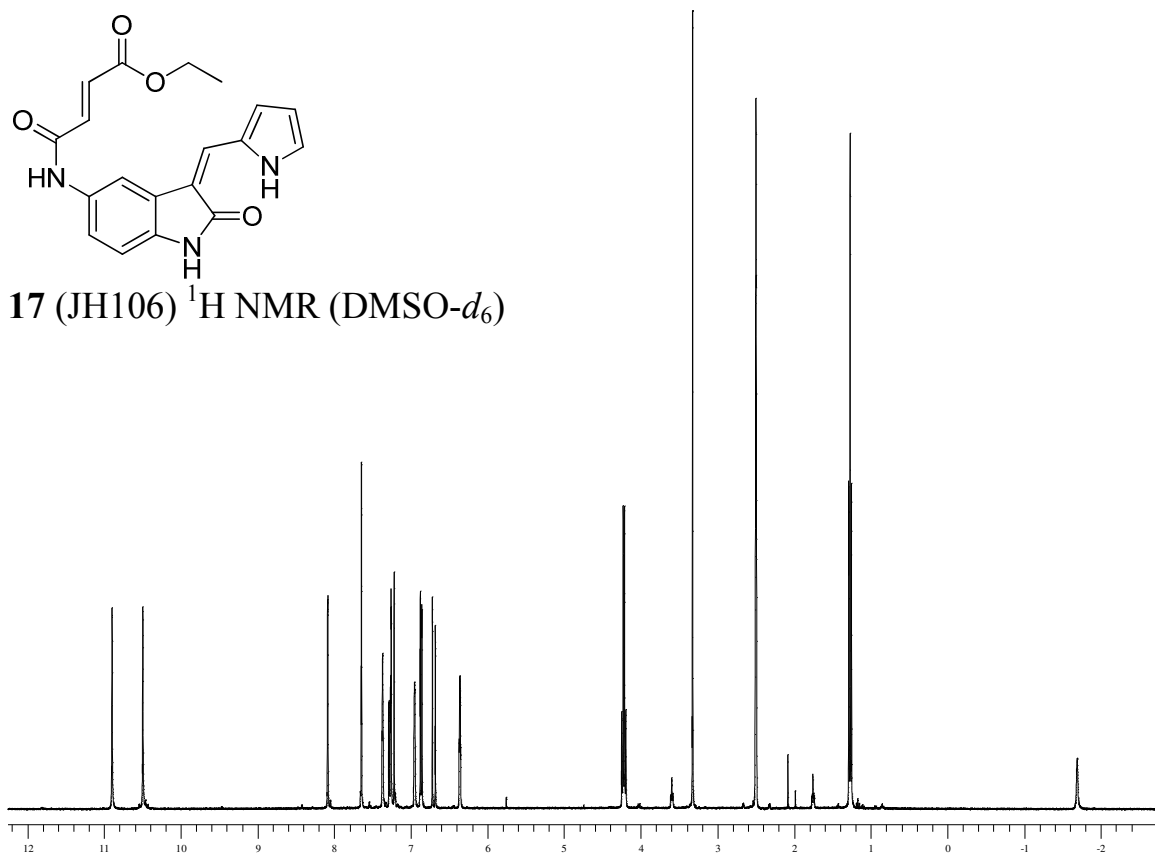


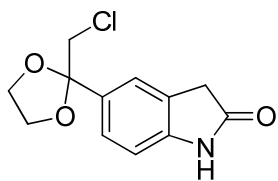


16 (JH100) ^1H NMR (DMSO- d_6)

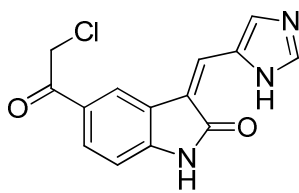
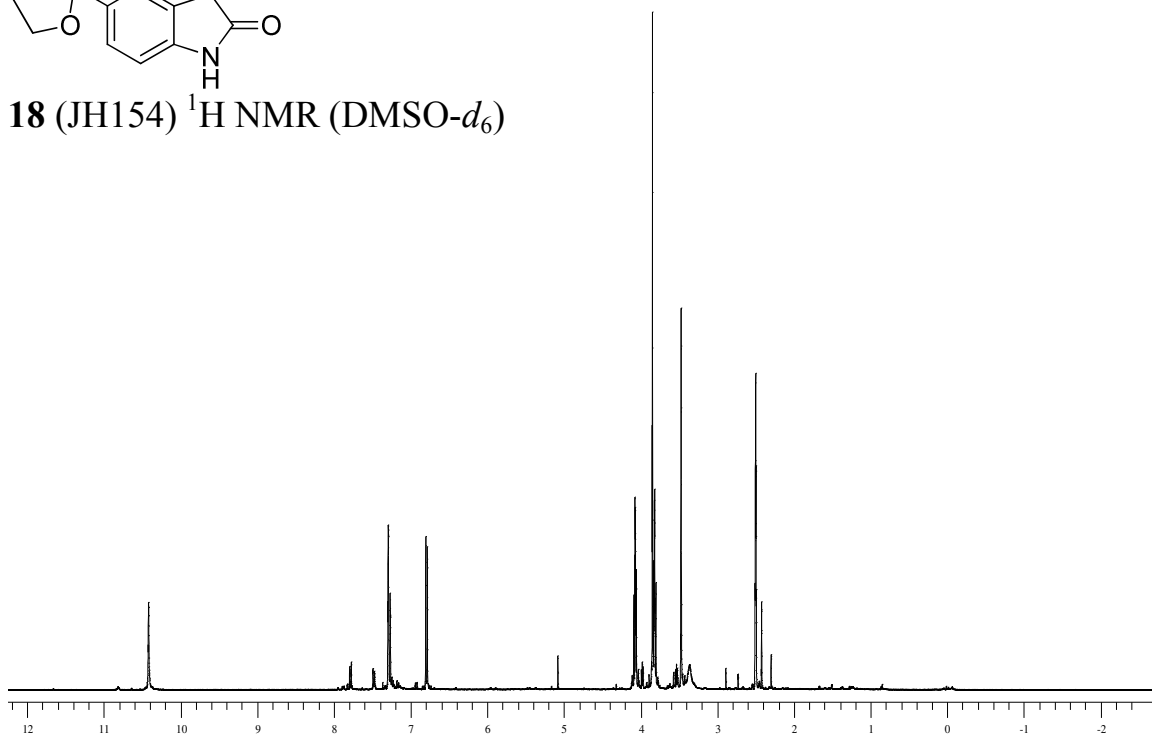


17 (JH106) ^1H NMR (DMSO- d_6)

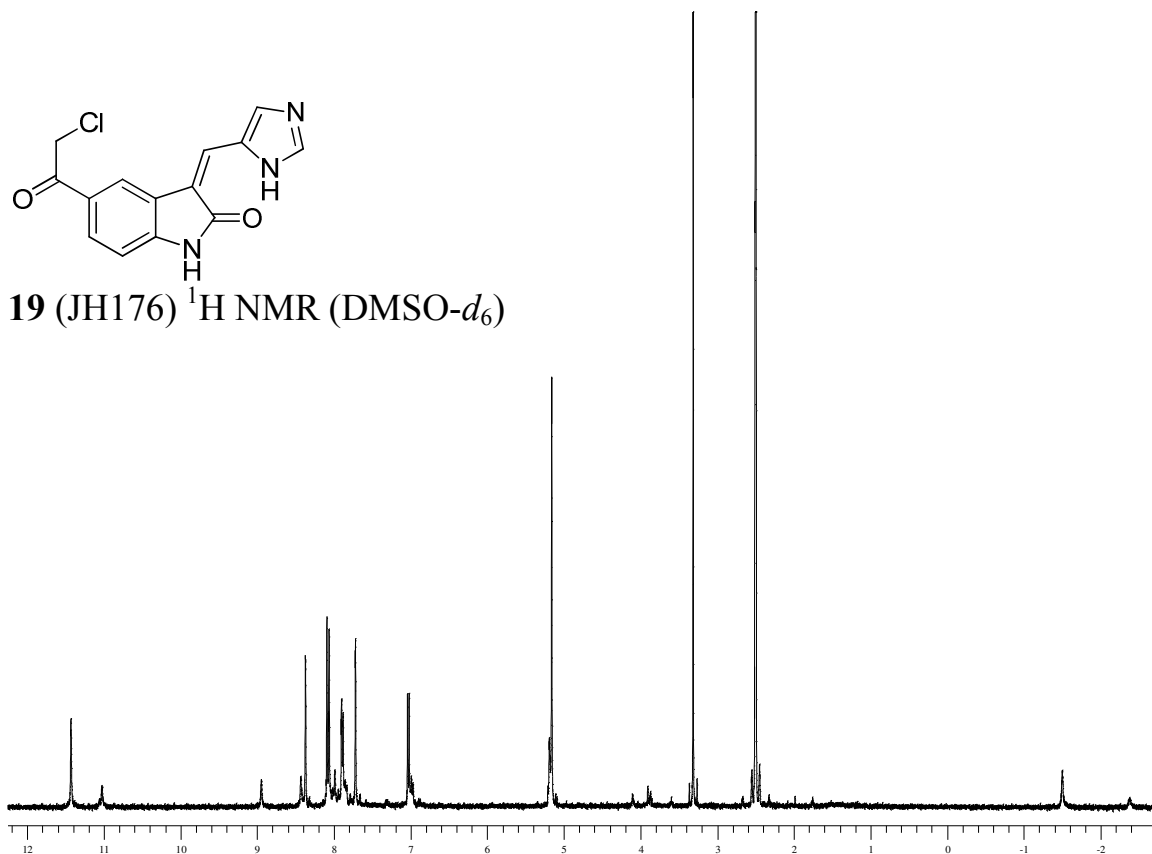


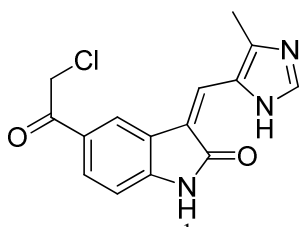


18 (JH154) ^1H NMR (DMSO- d_6)

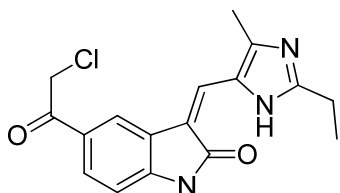
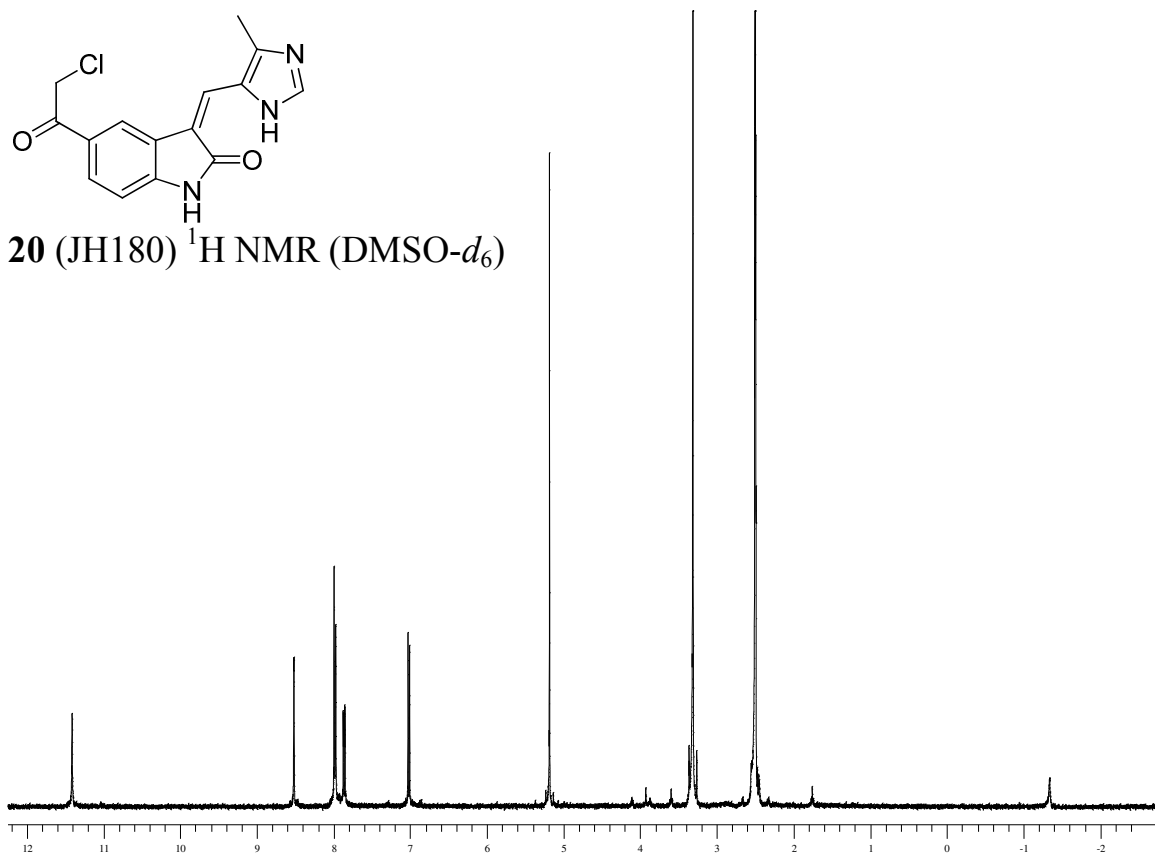


19 (JH176) ^1H NMR (DMSO- d_6)

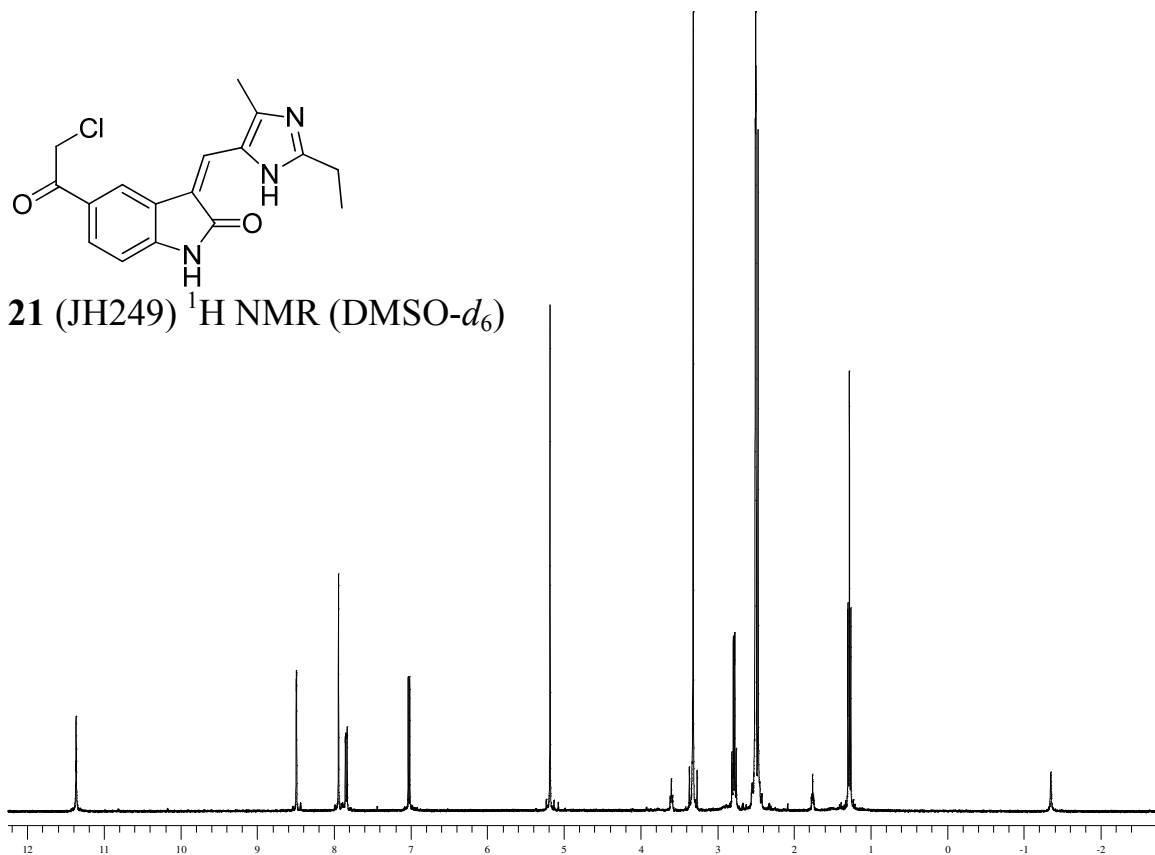


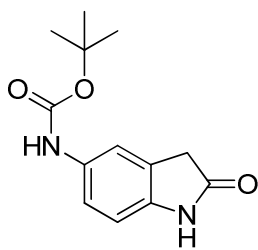


20 (JH180) ^1H NMR (DMSO- d_6)

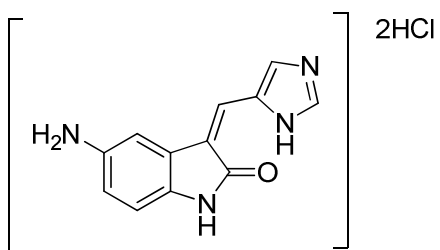
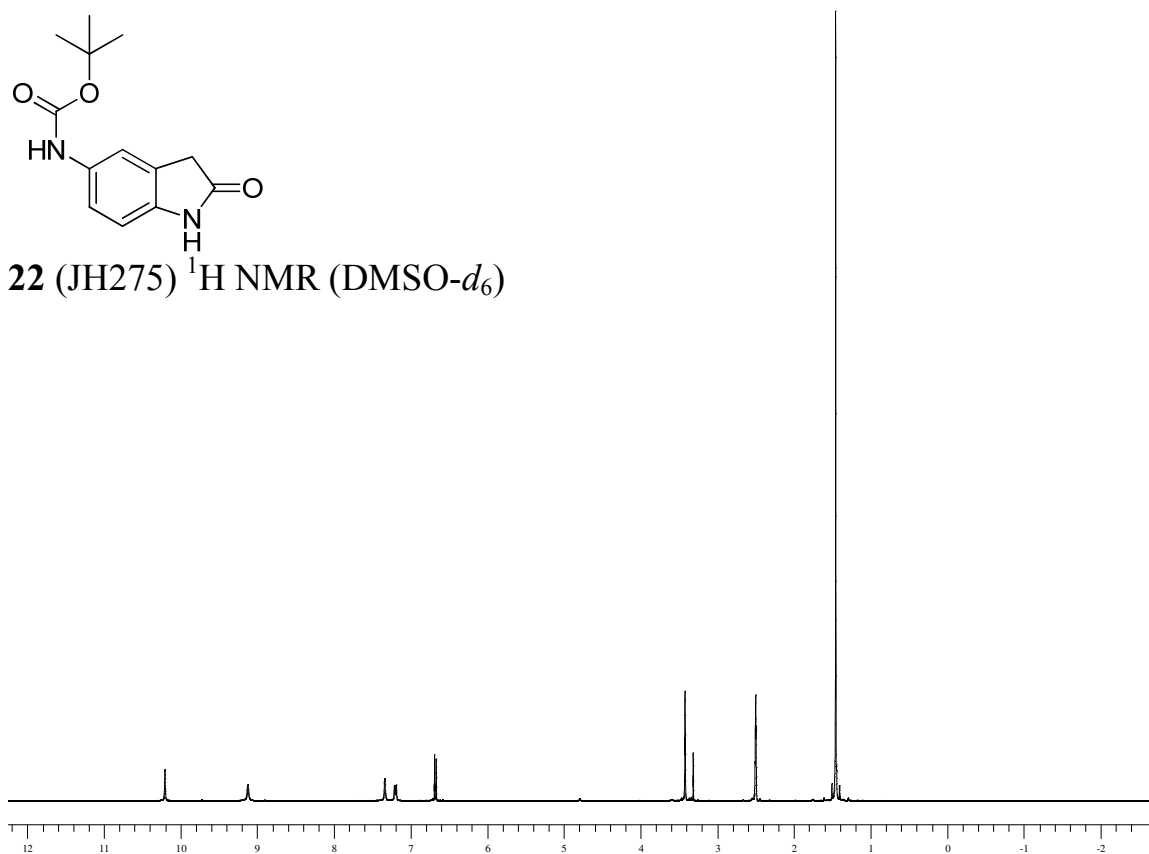


21 (JH249) ^1H NMR (DMSO- d_6)

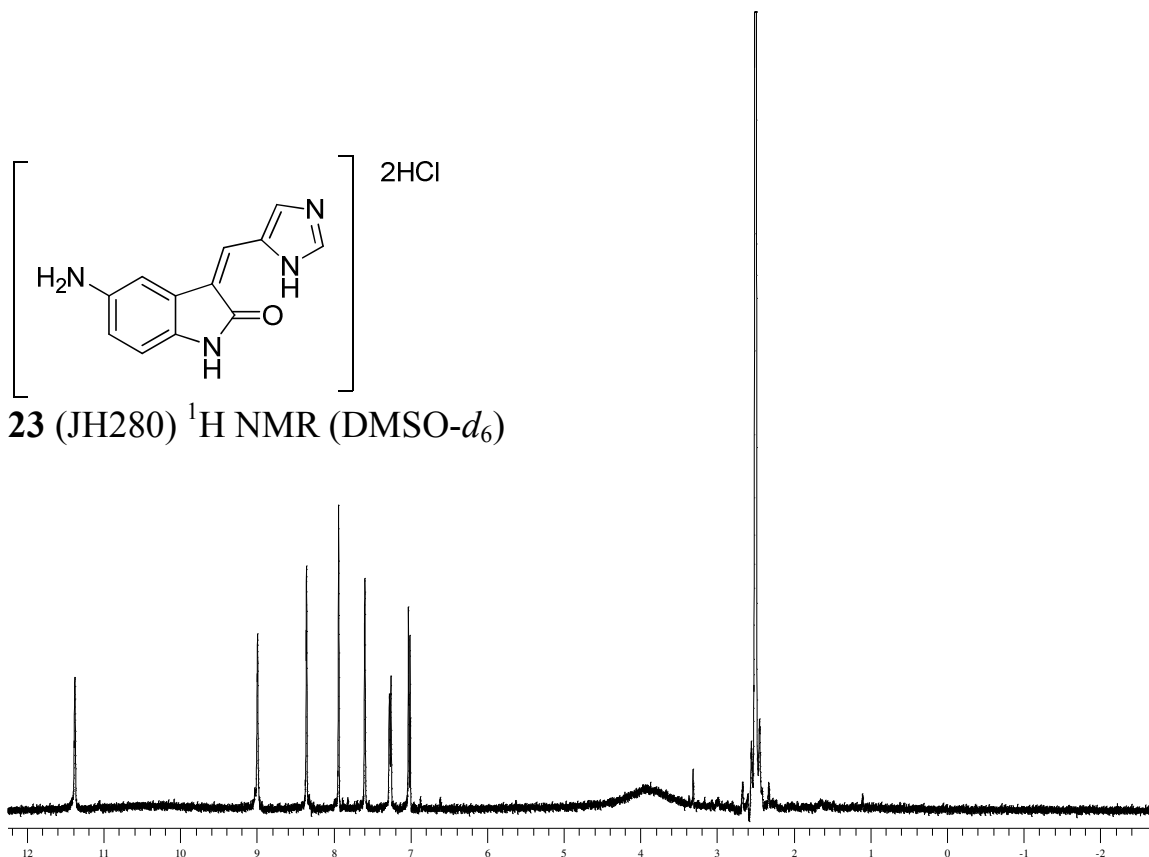


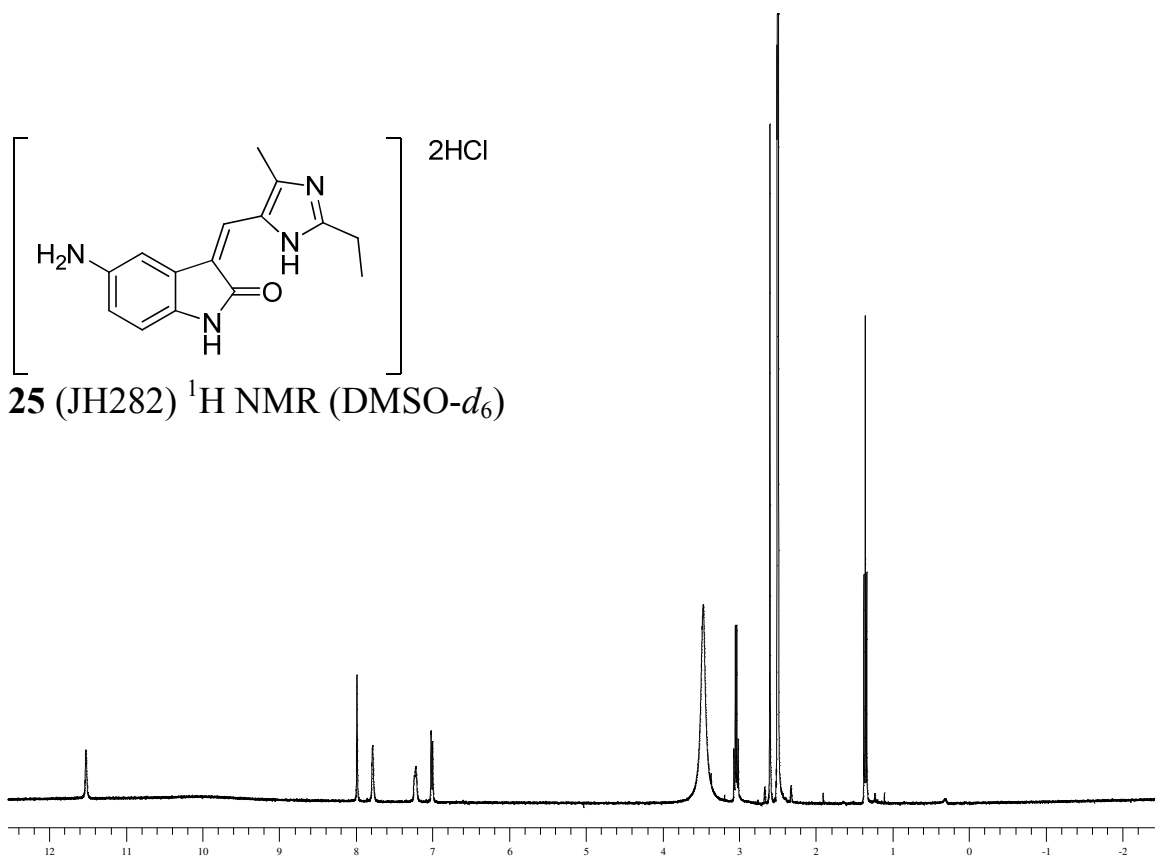
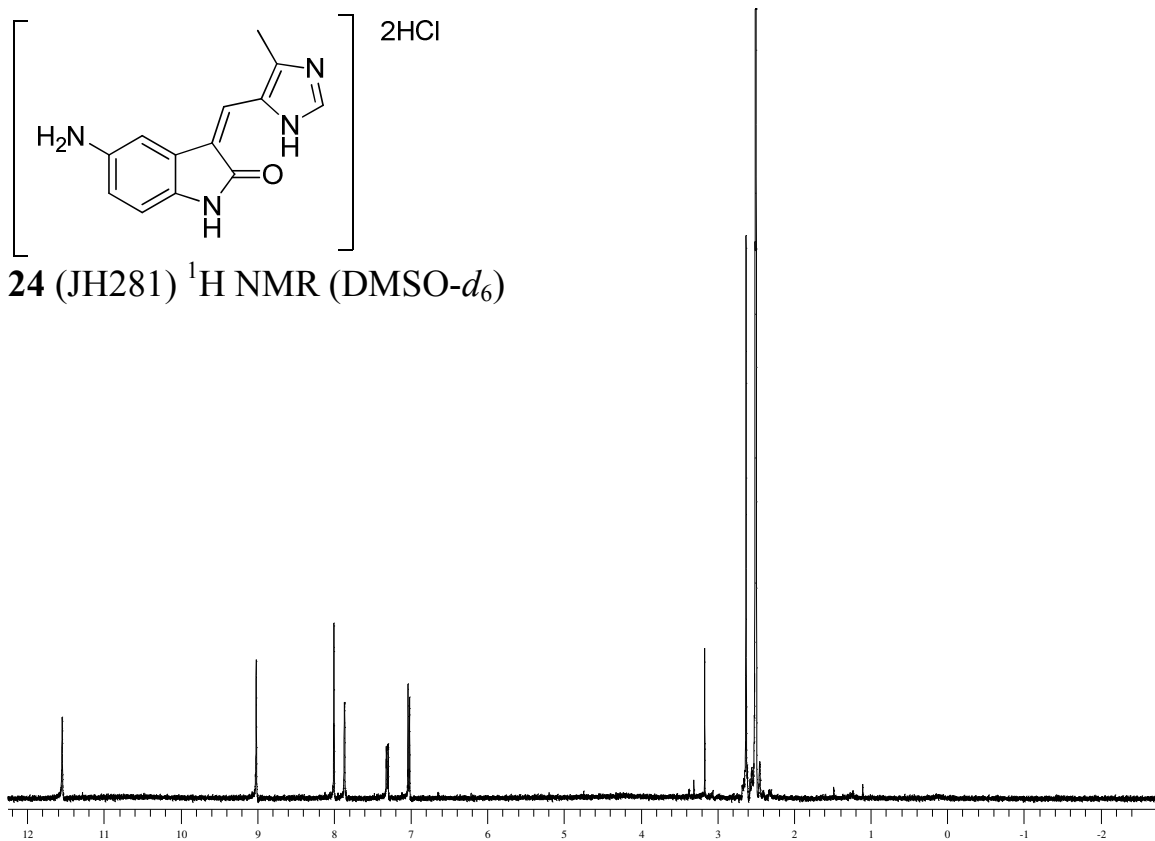


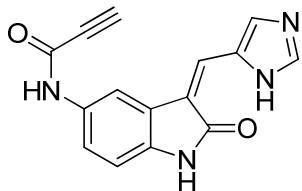
22 (JH275) ^1H NMR (DMSO- d_6)



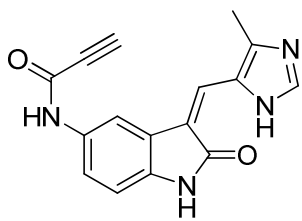
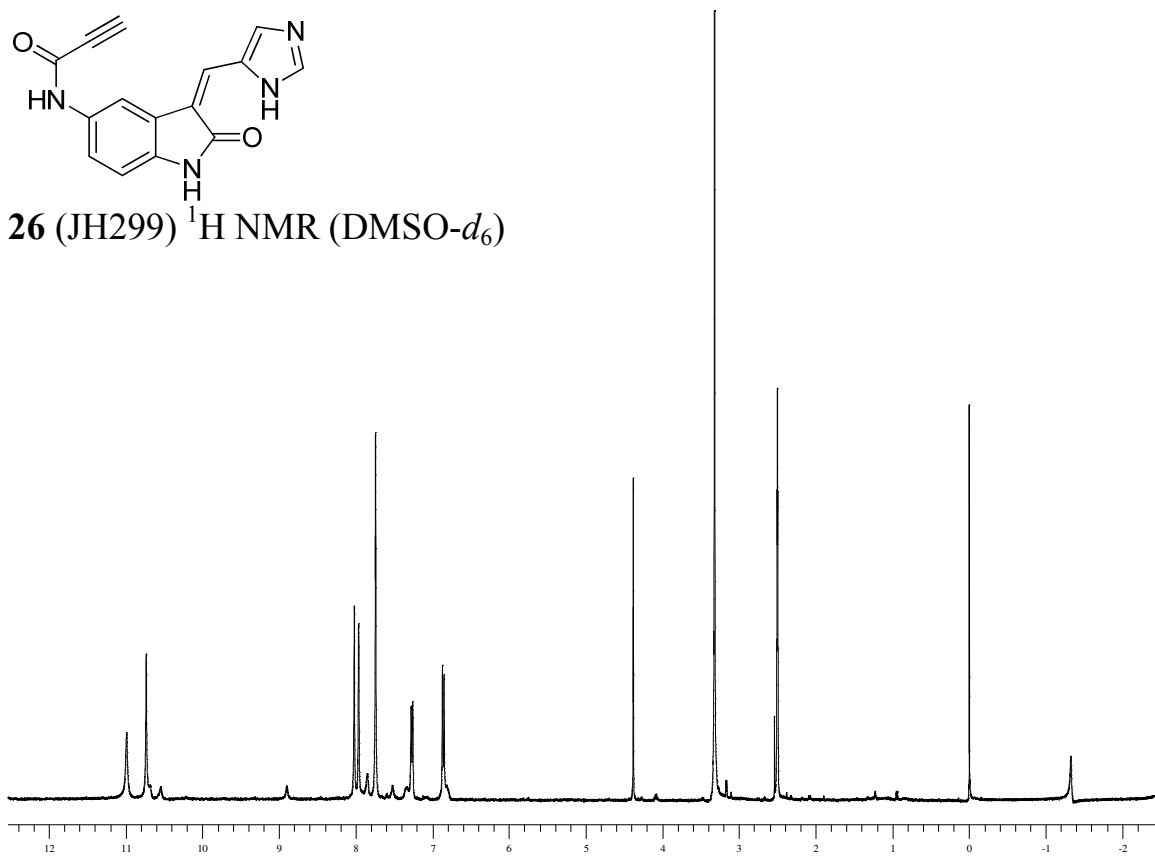
23 (JH280) ^1H NMR (DMSO- d_6)



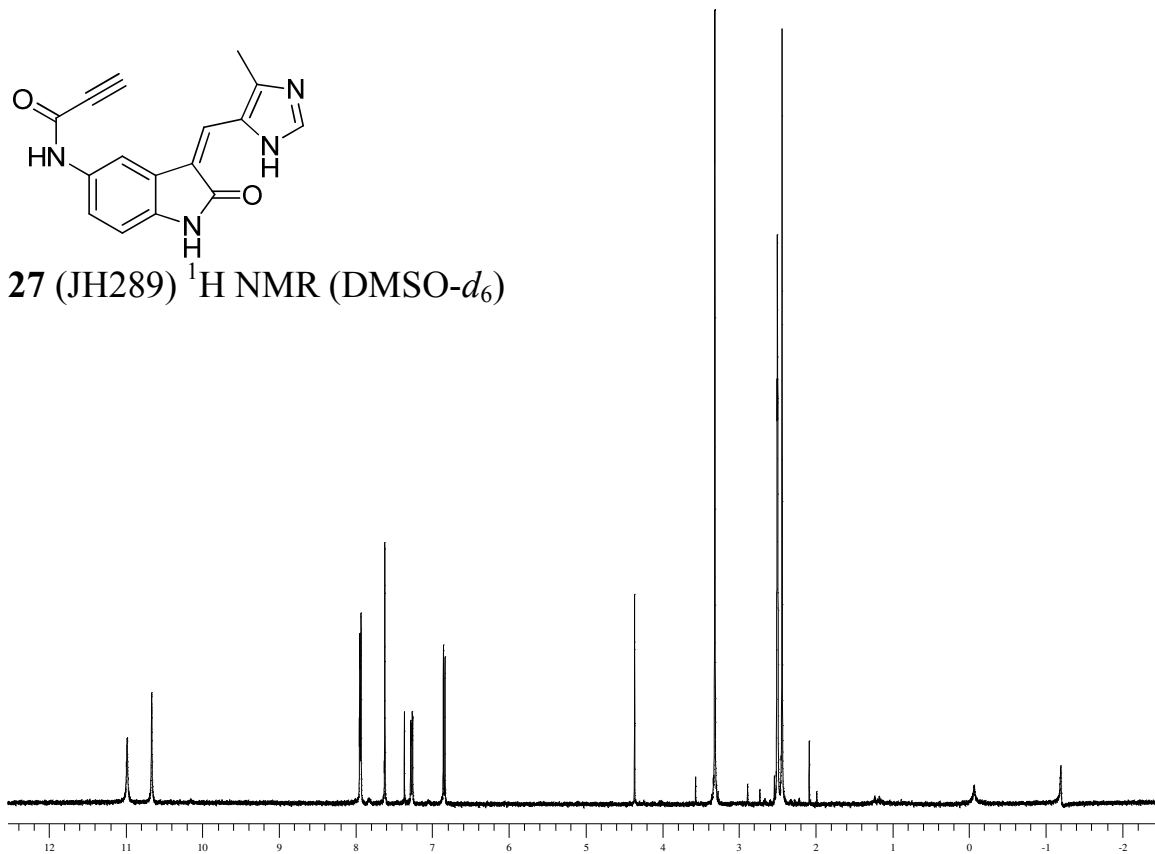


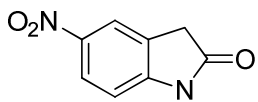


26 (JH299) ^1H NMR (DMSO- d_6)

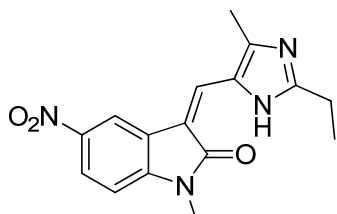
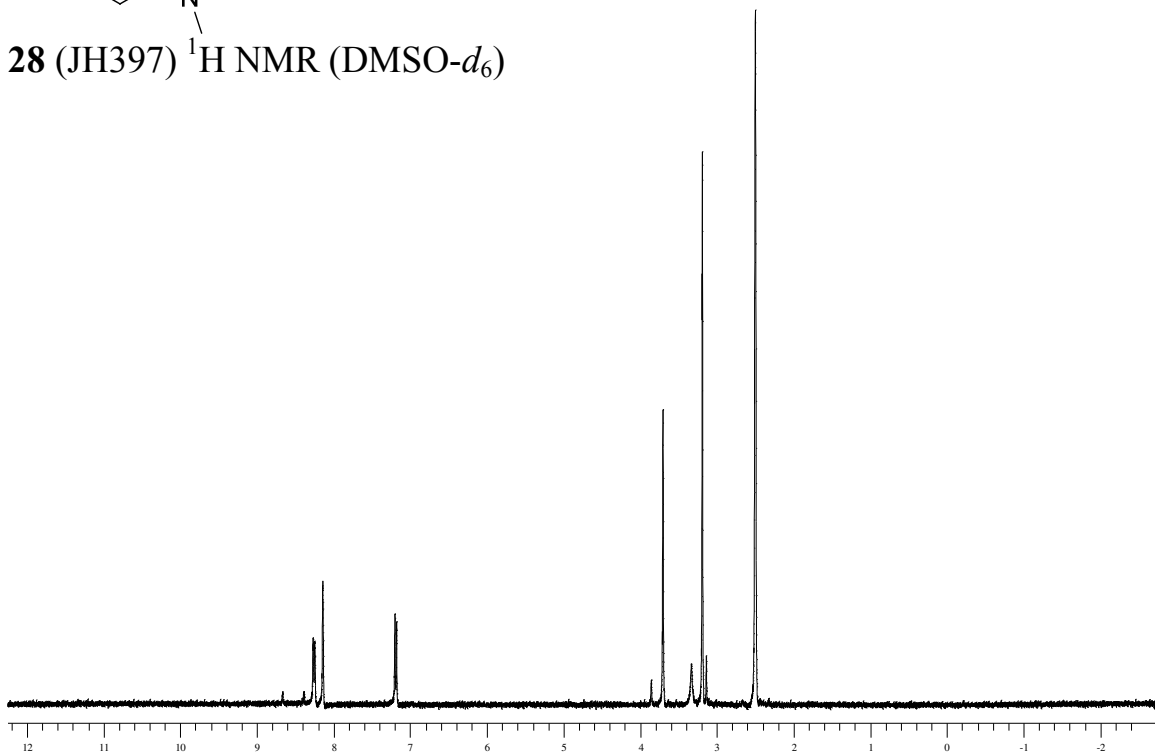


27 (JH289) ^1H NMR (DMSO- d_6)

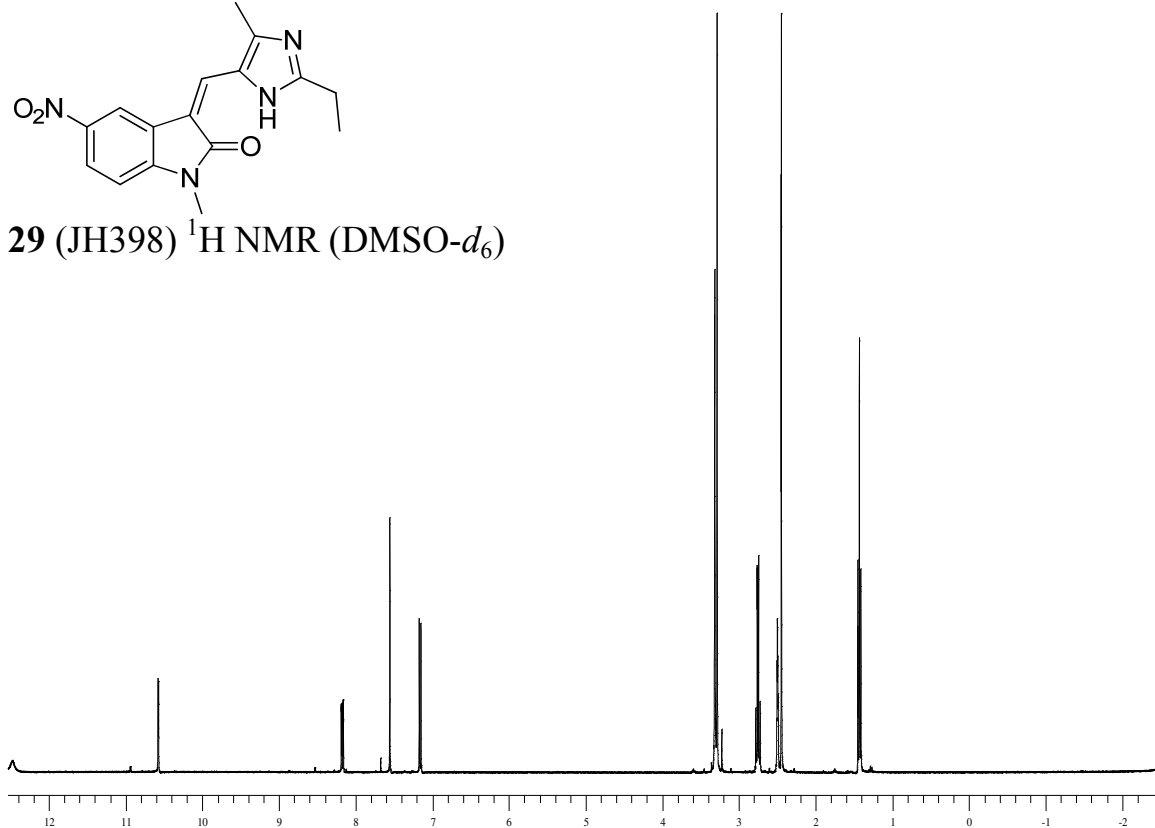


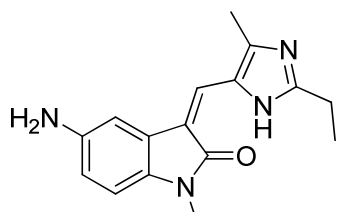


28 (JH397) ^1H NMR (DMSO- d_6)

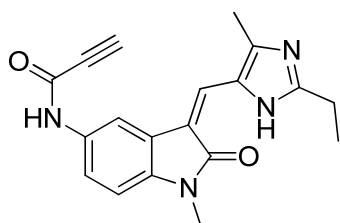
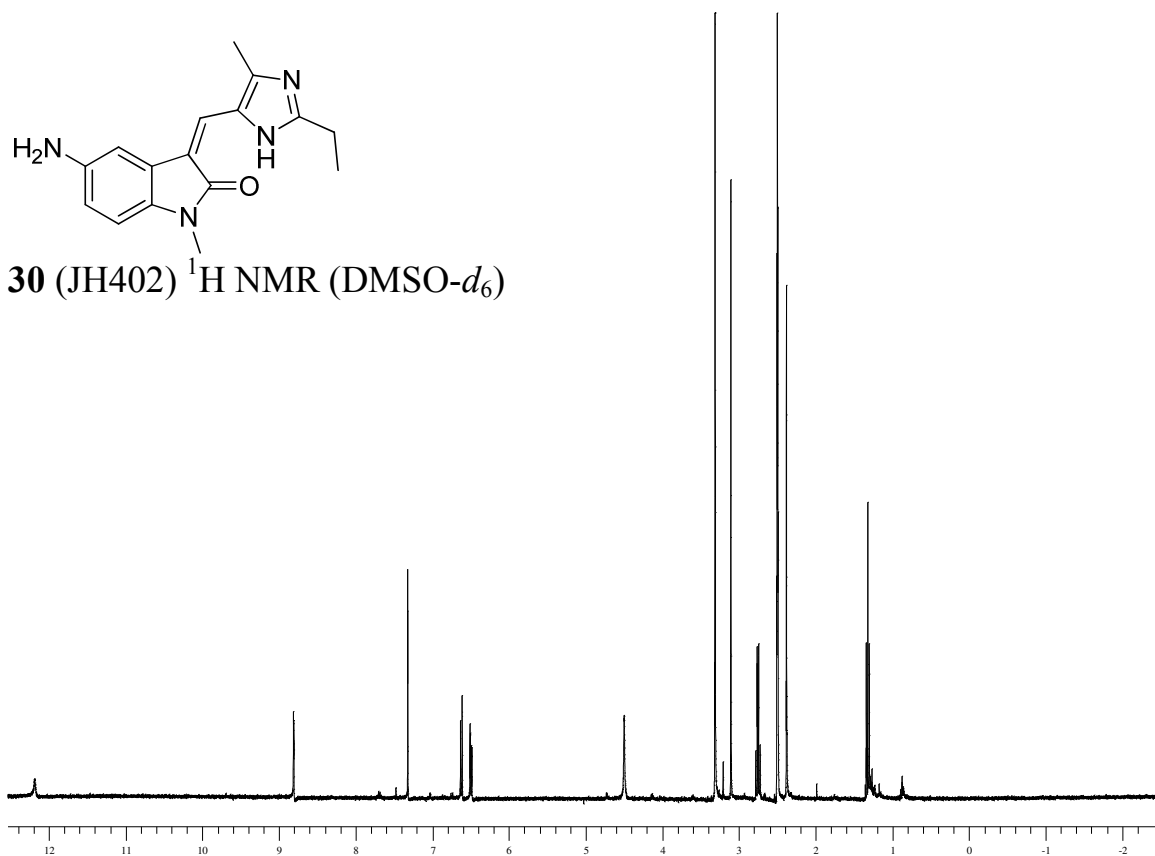


29 (JH398) ^1H NMR (DMSO- d_6)

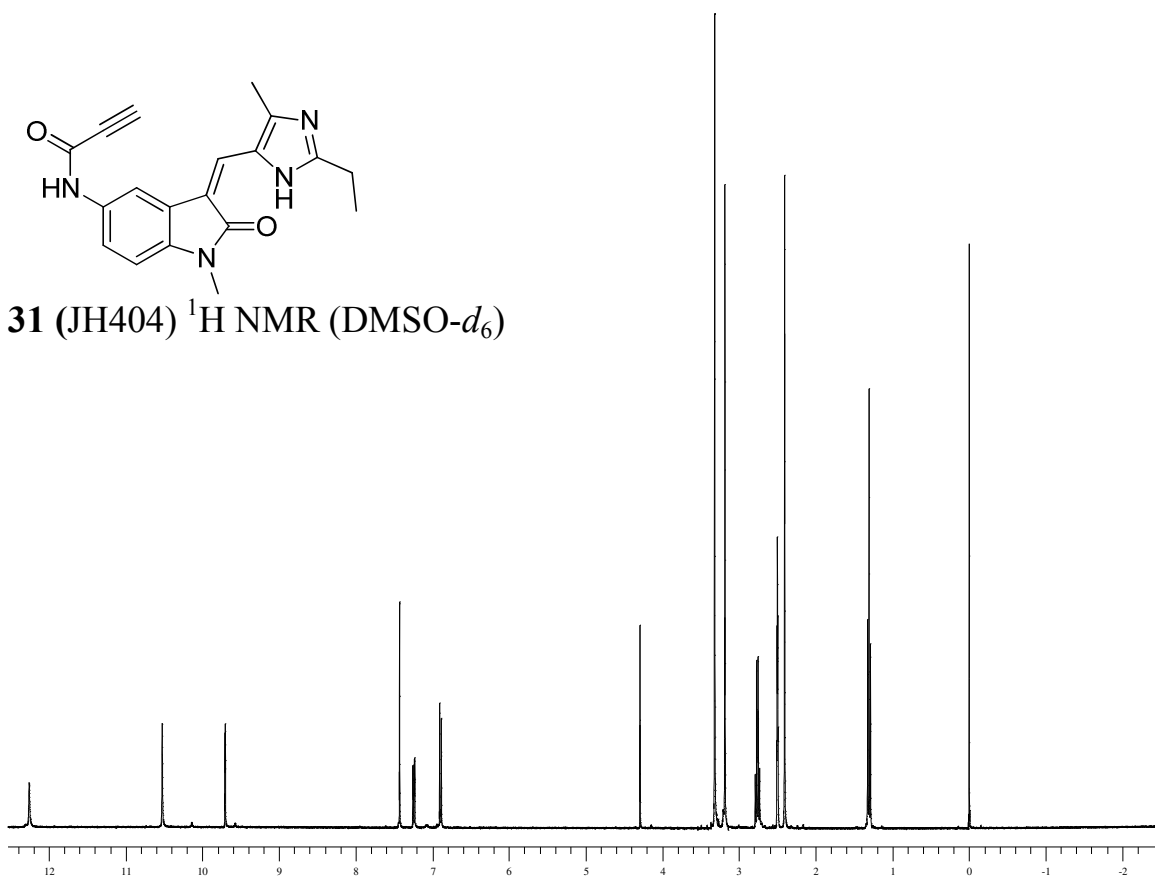


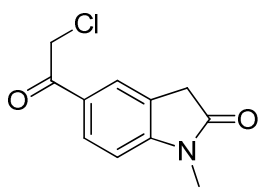


30 (JH402) ^1H NMR (DMSO- d_6)

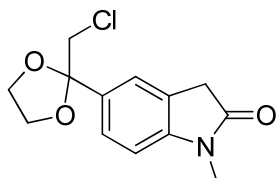
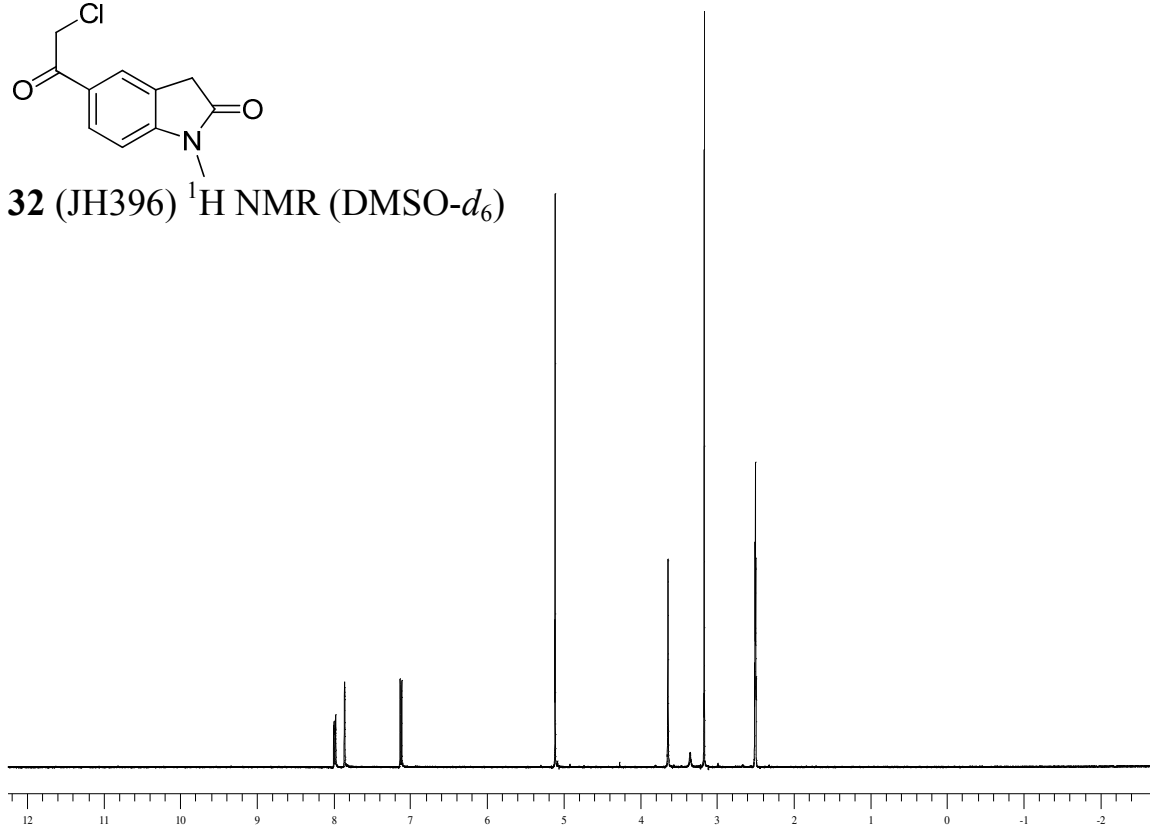


31 (JH404) ^1H NMR (DMSO- d_6)

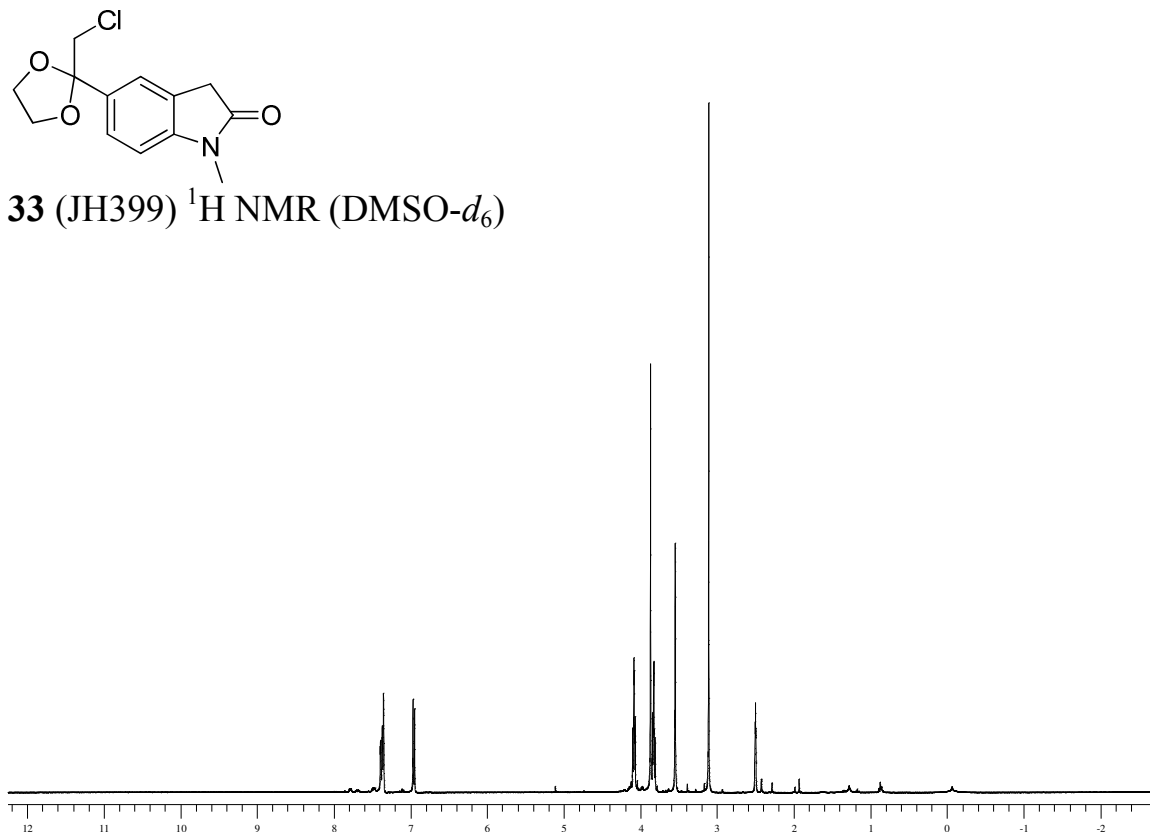


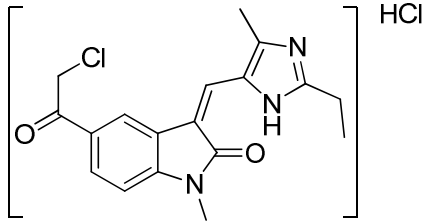


32 (JH396) ^1H NMR (DMSO- d_6)

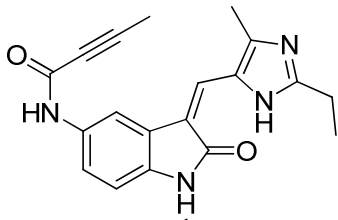
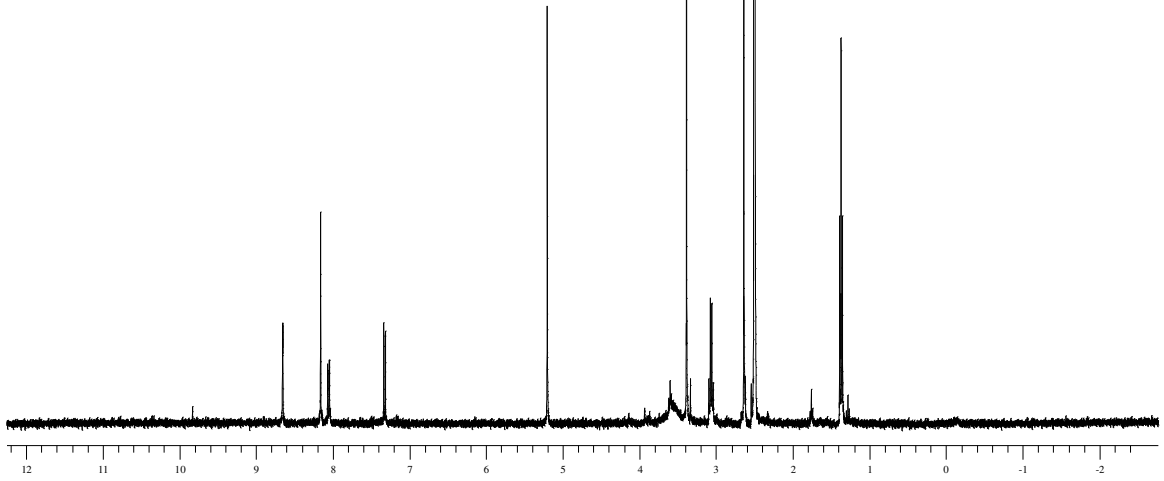


33 (JH399) ^1H NMR (DMSO- d_6)

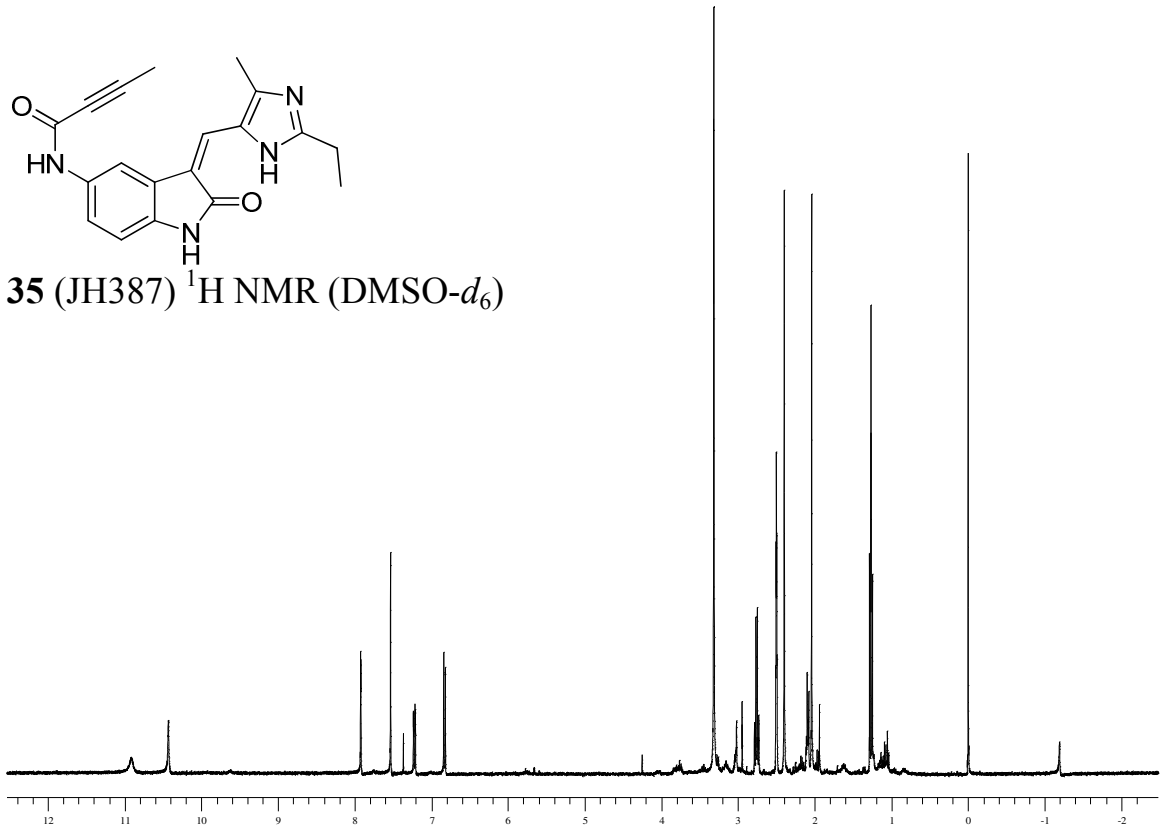


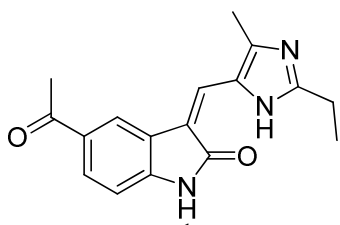


34 (JH400) ^1H NMR ($\text{DMSO-}d_6$)

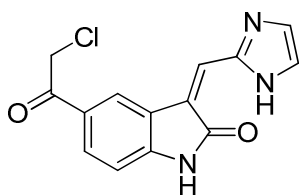
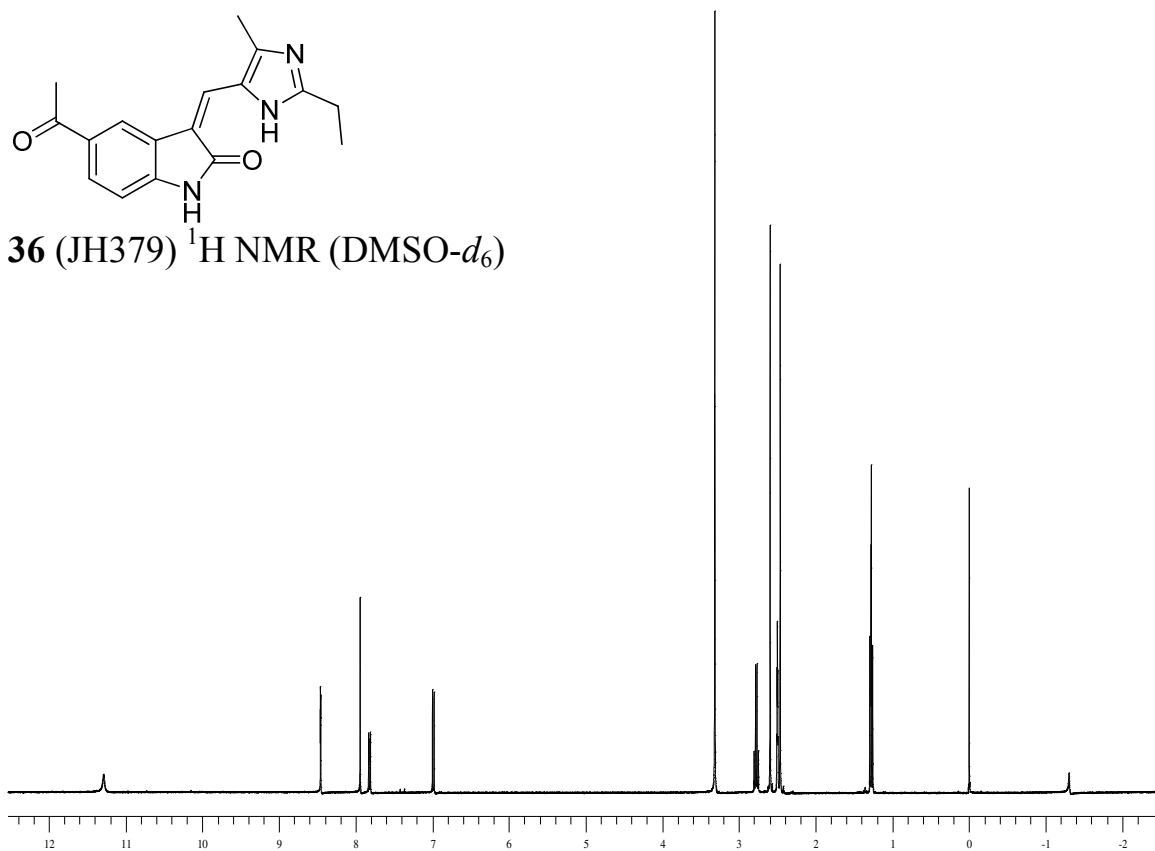


35 (JH387) ^1H NMR ($\text{DMSO-}d_6$)

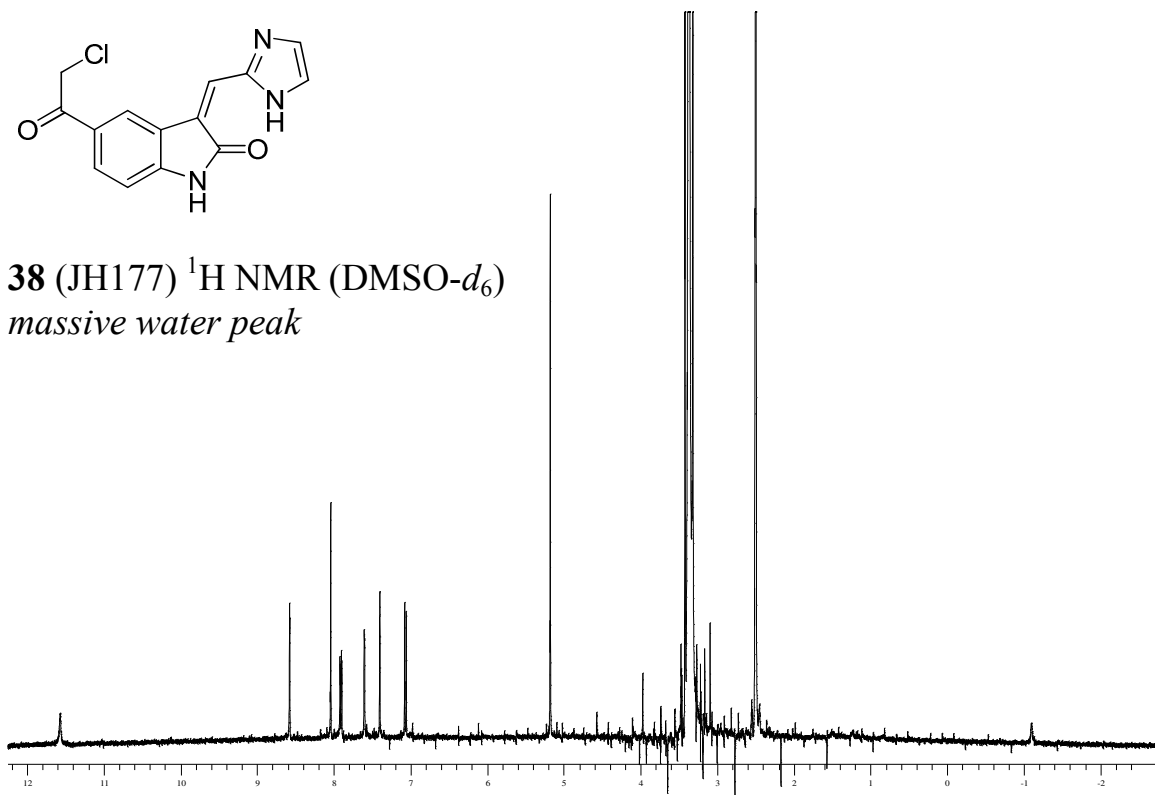


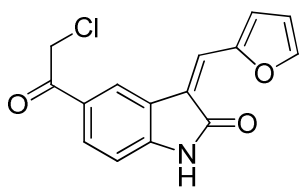


36 (JH379) ^1H NMR (DMSO- d_6)

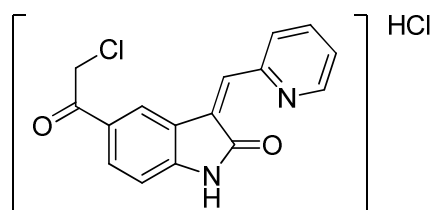
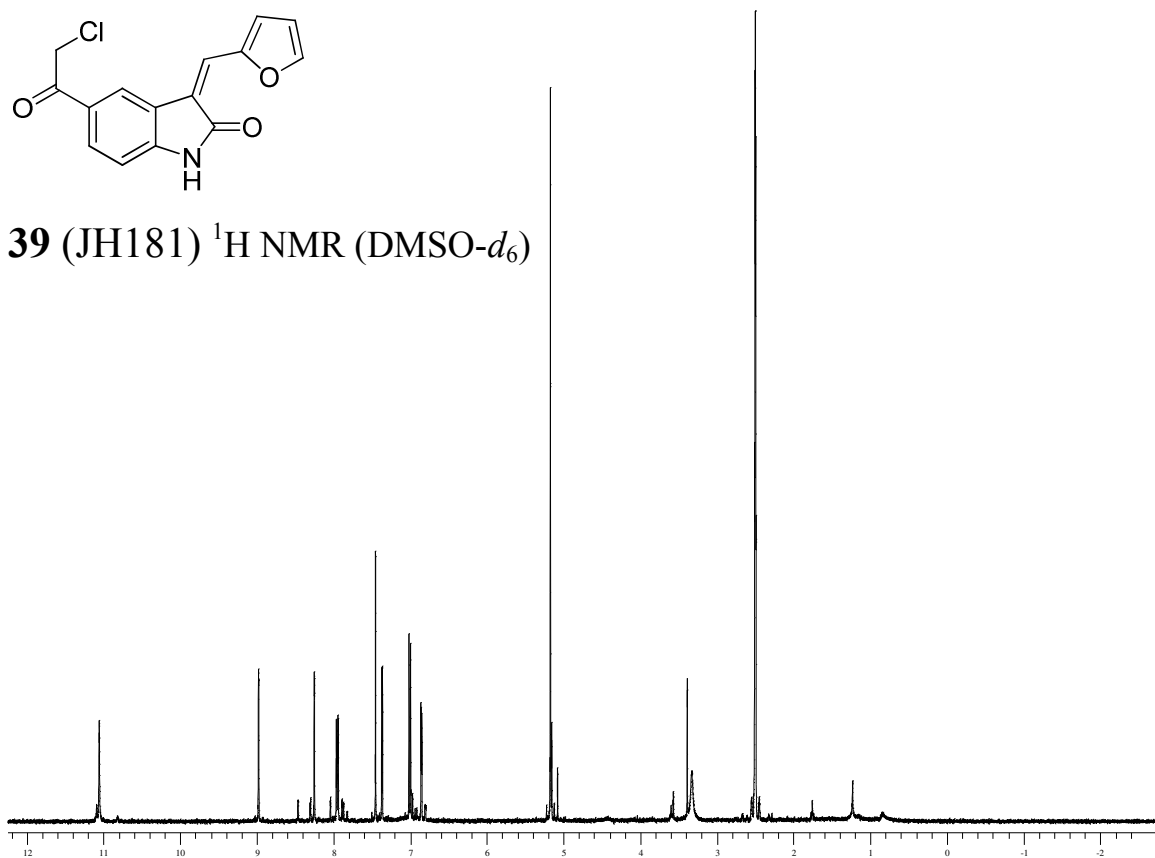


38 (JH177) ^1H NMR (DMSO- d_6)
massive water peak

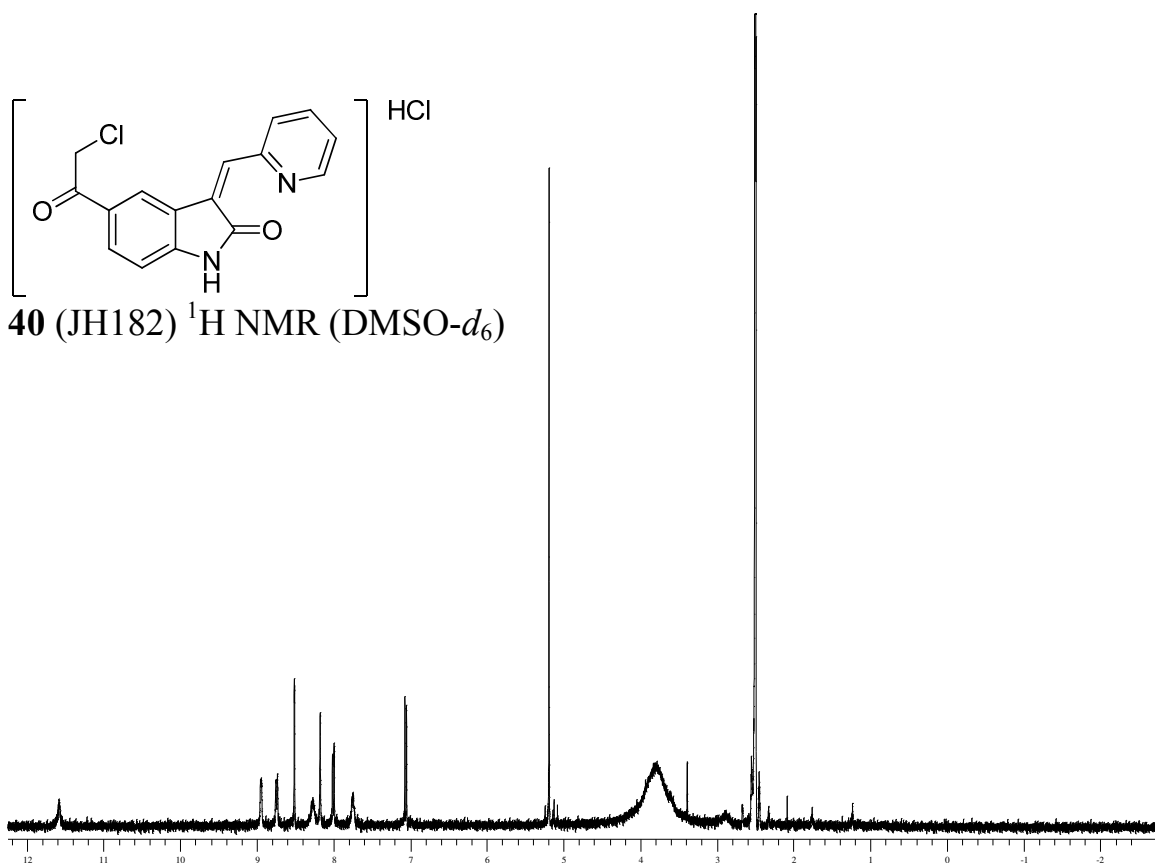


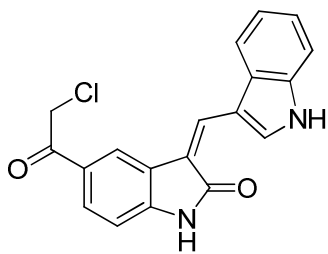


39 (JH181) ^1H NMR (DMSO- d_6)

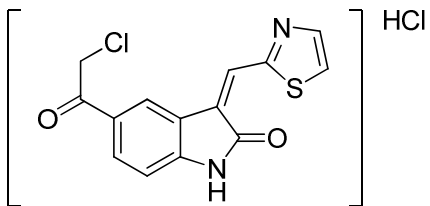
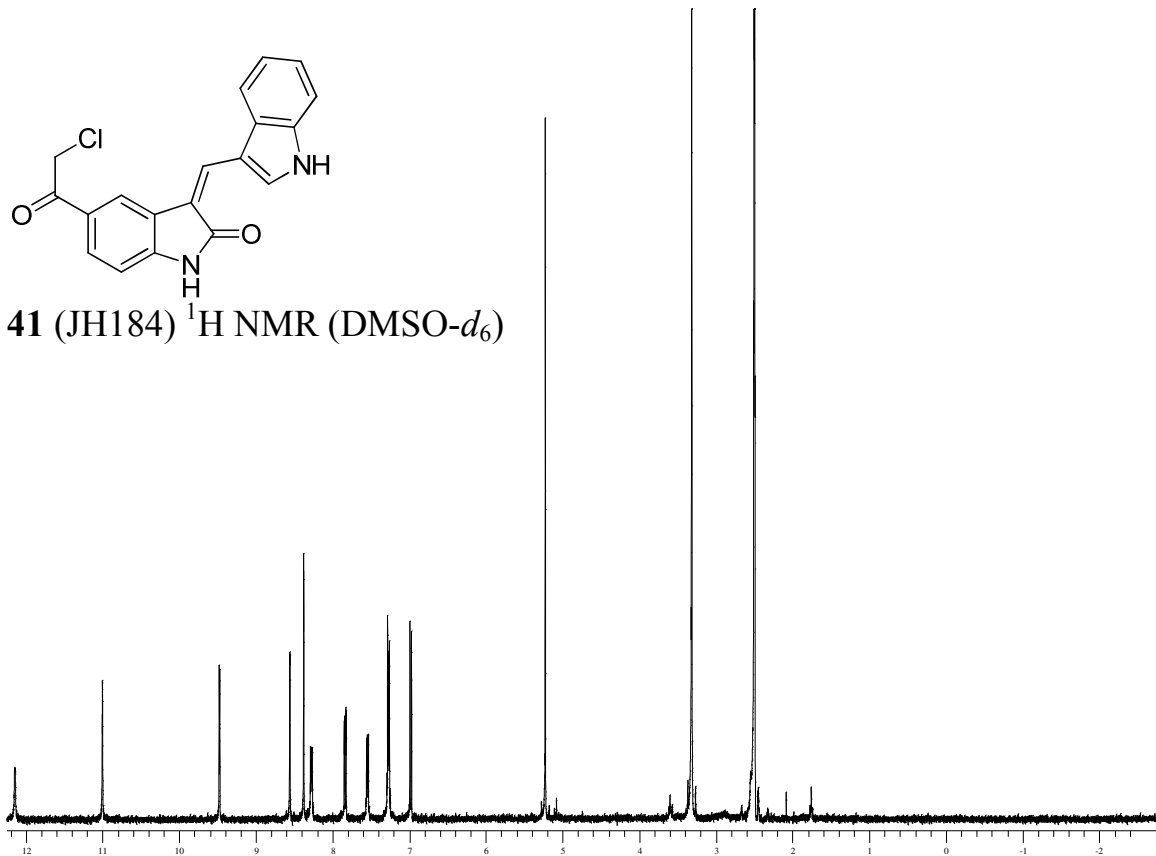


40 (JH182) ^1H NMR (DMSO- d_6)

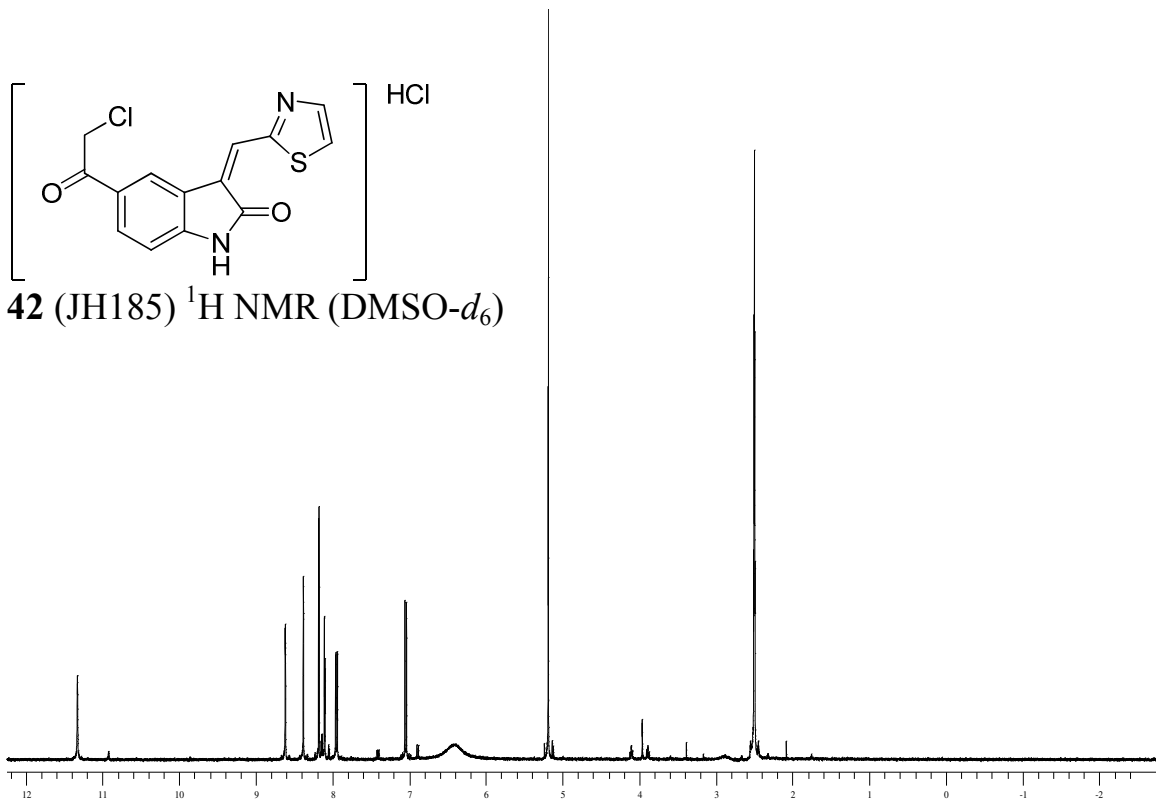


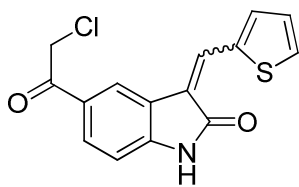


41 (JH184) ^1H NMR (DMSO- d_6)

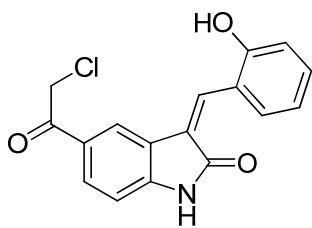
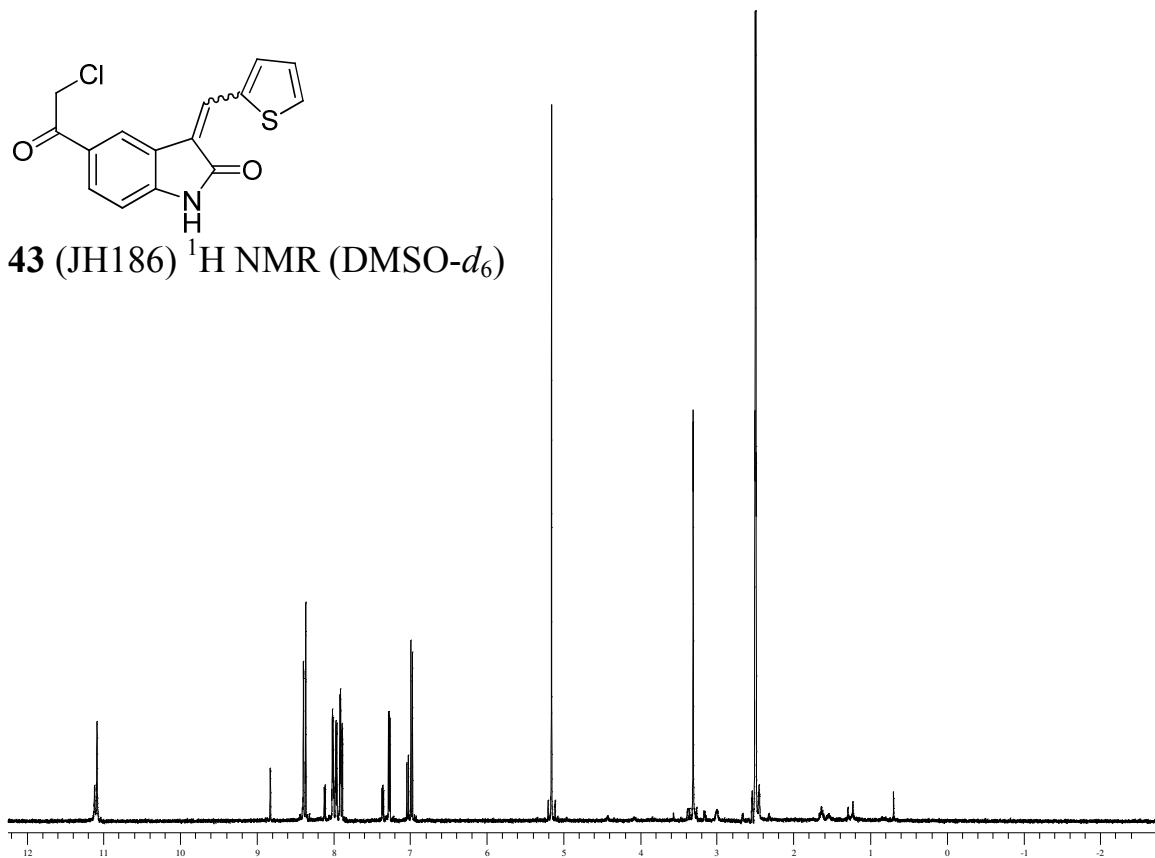


42 (JH185) ^1H NMR (DMSO- d_6)

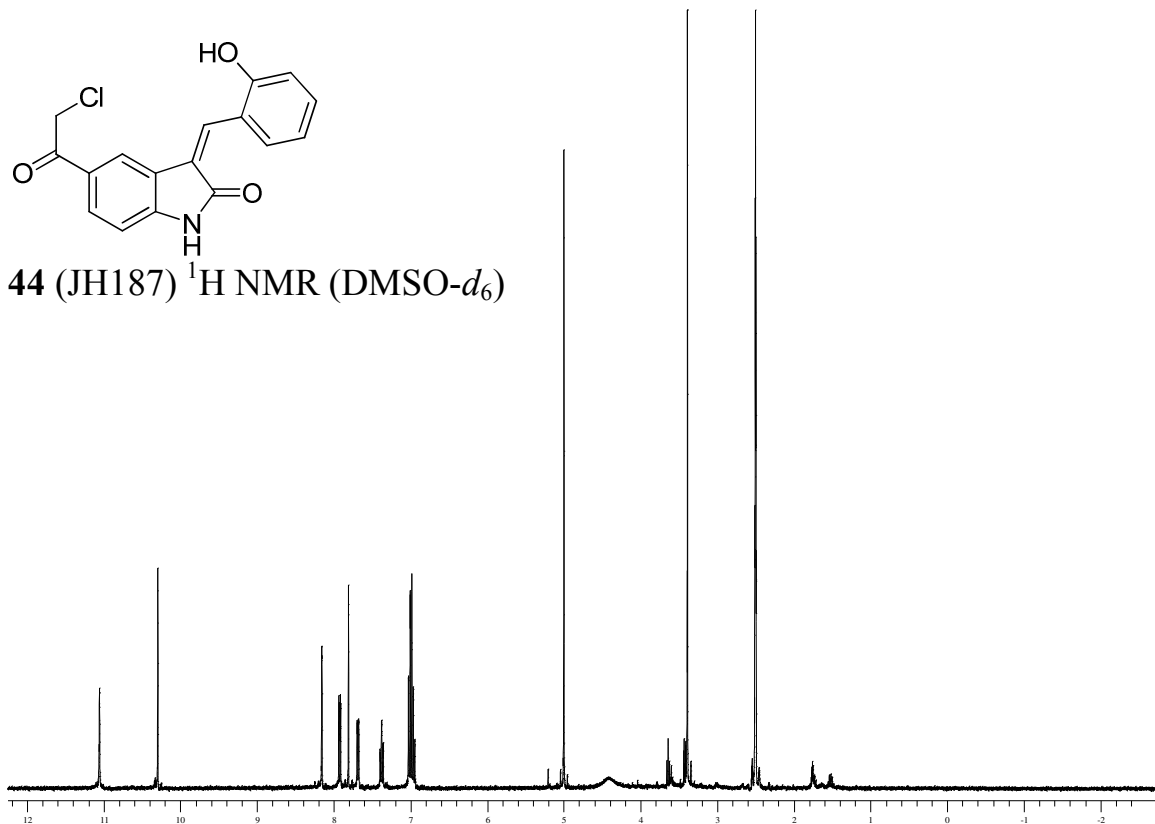


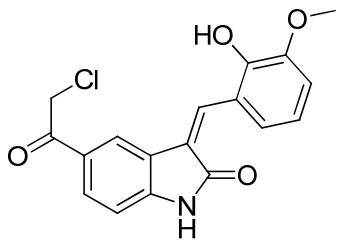


43 (JH186) ^1H NMR (DMSO- d_6)

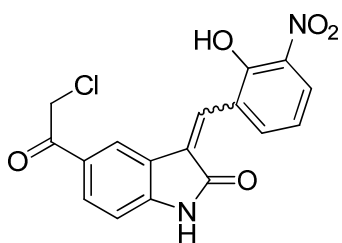
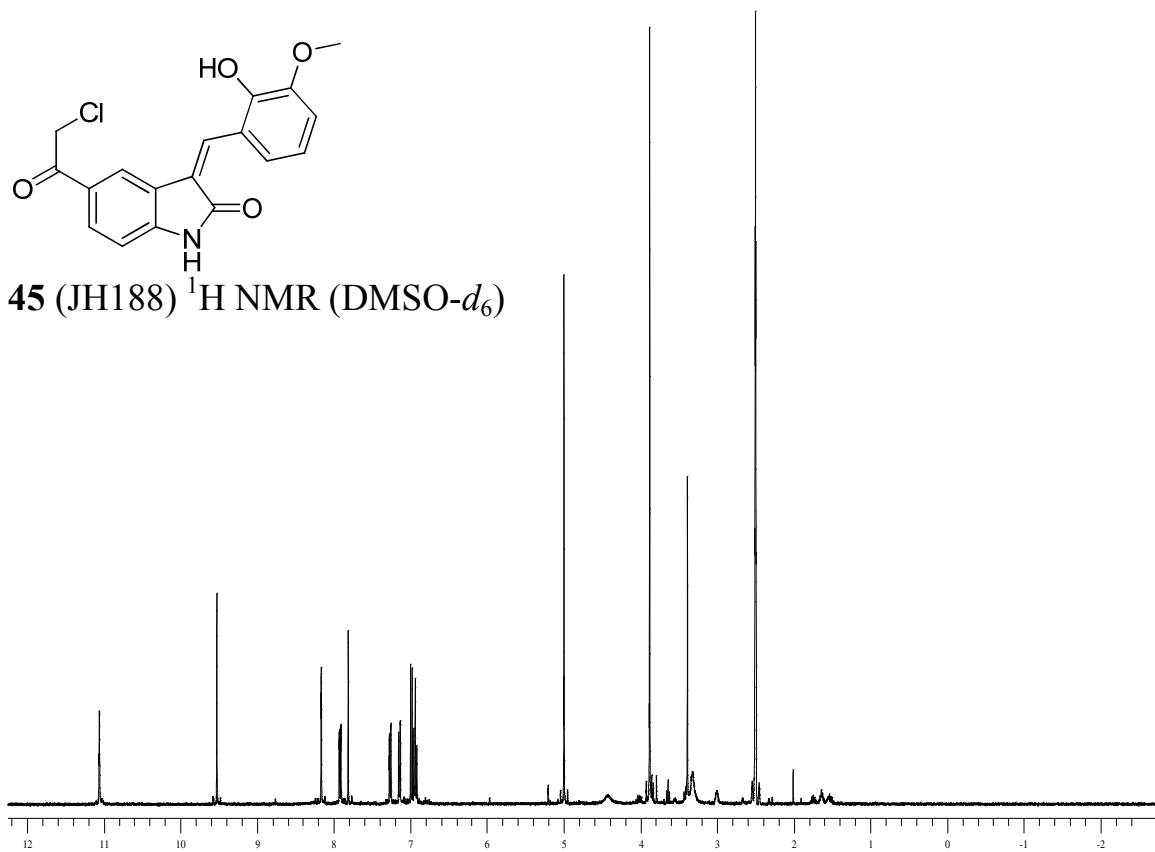


44 (JH187) ^1H NMR (DMSO- d_6)

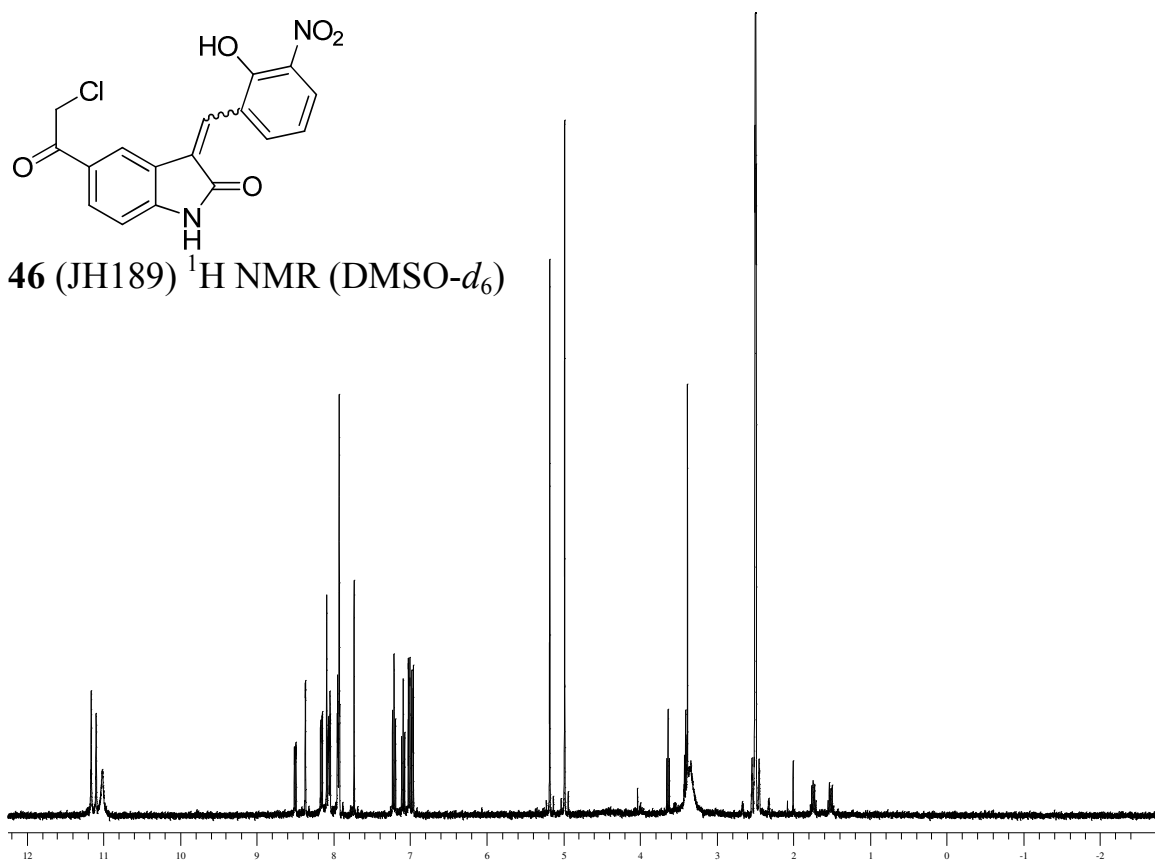


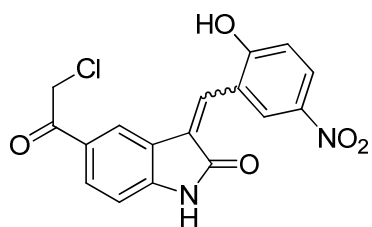


45 (JH188) ^1H NMR (DMSO- d_6)

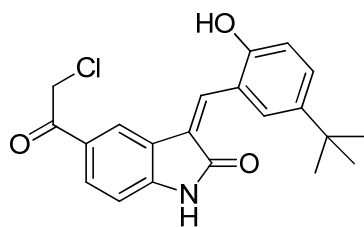
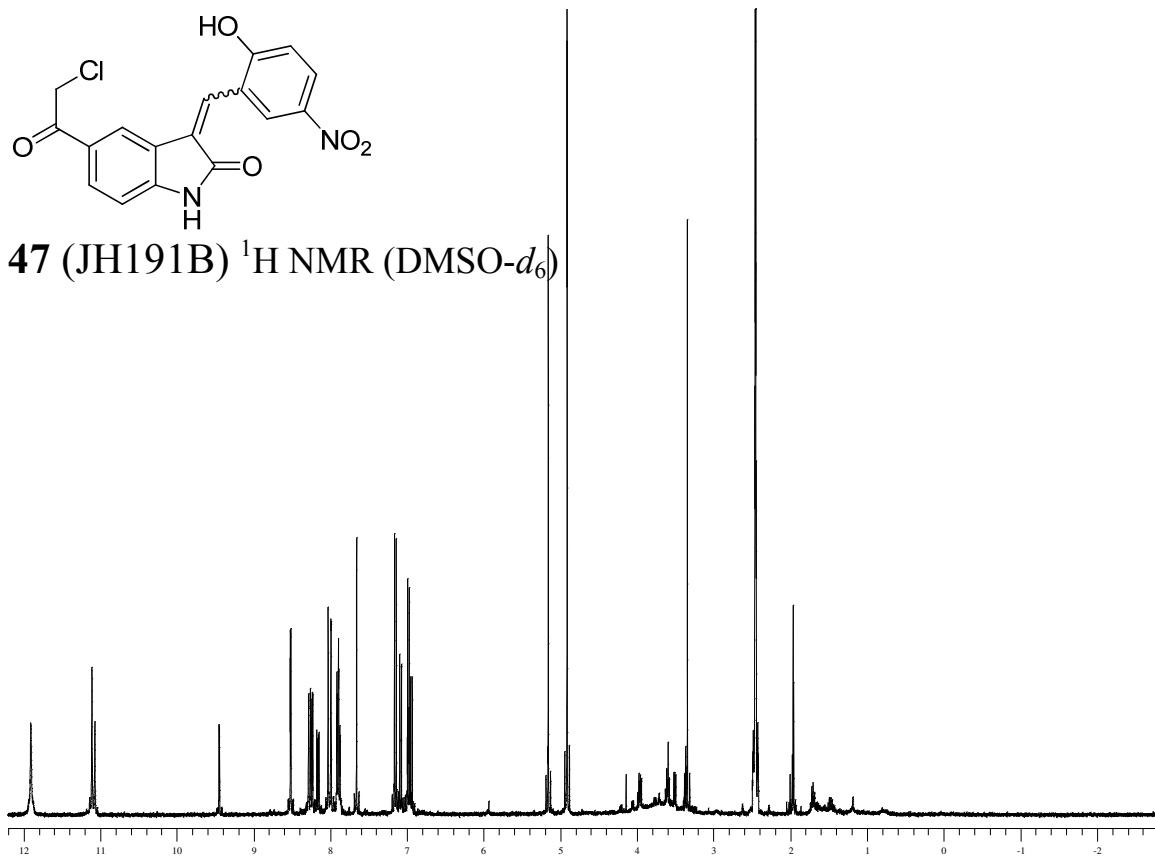


46 (JH189) ^1H NMR (DMSO- d_6)

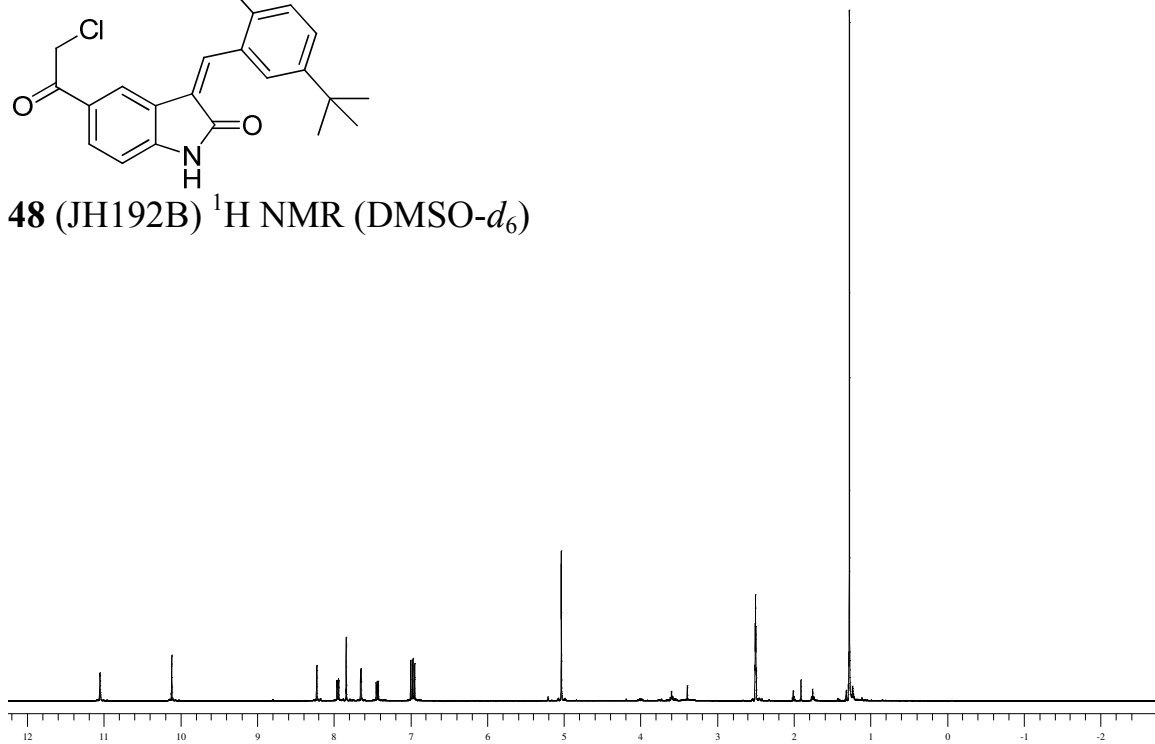


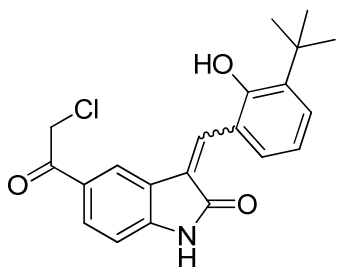


47 (JH191B) ^1H NMR (DMSO- d_6)

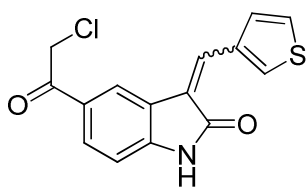
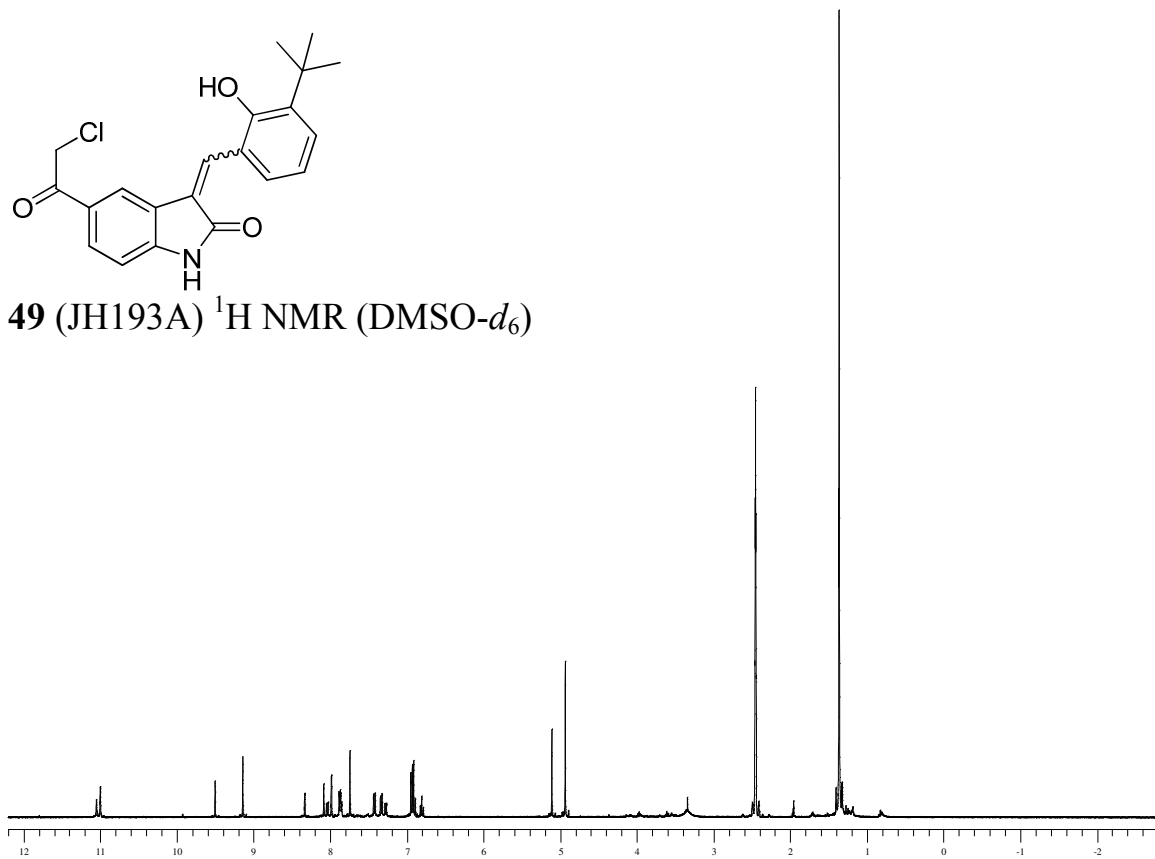


48 (JH192B) ^1H NMR (DMSO- d_6)

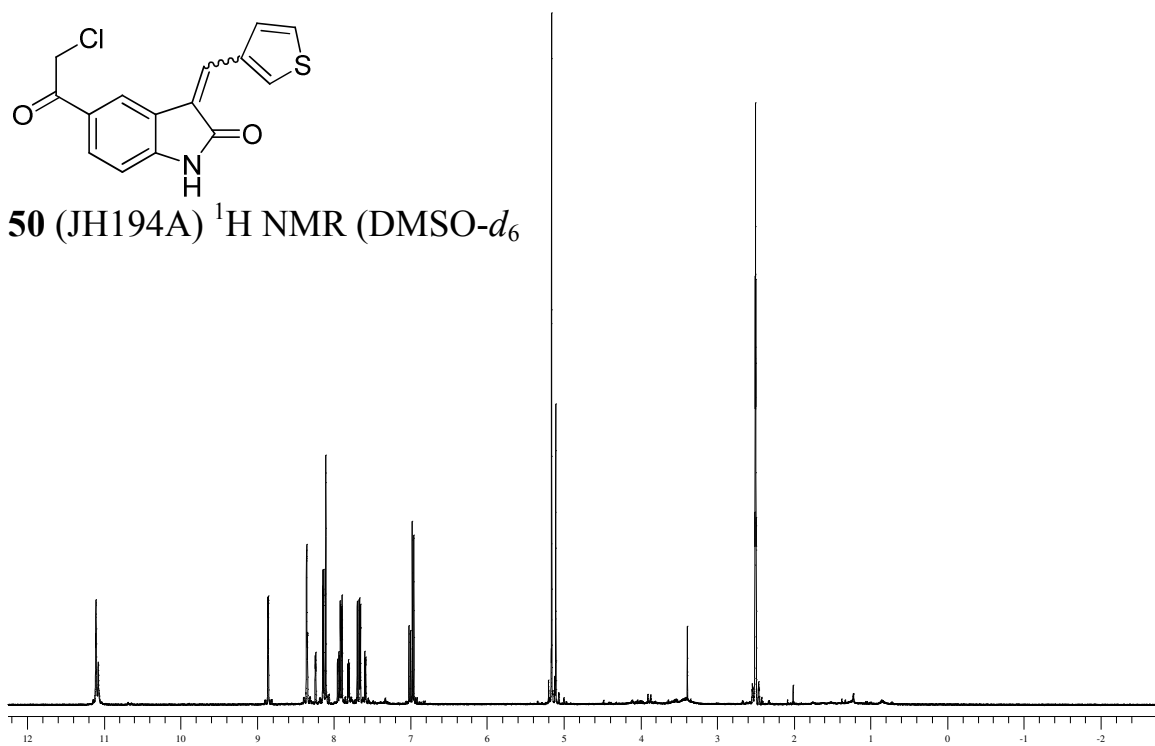


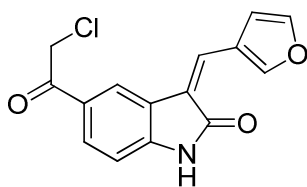


49 (JH193A) ^1H NMR (DMSO- d_6)

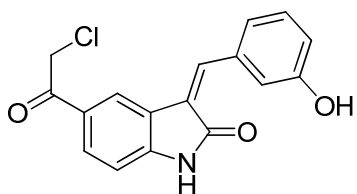
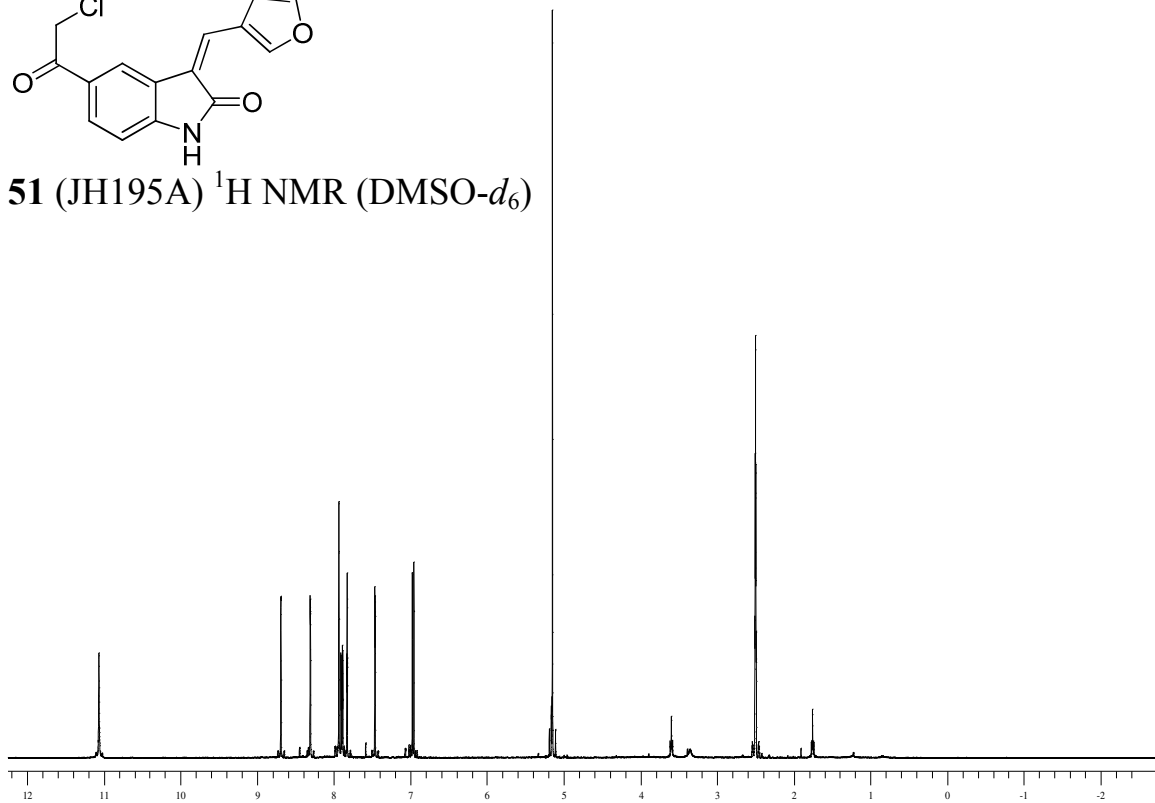


50 (JH194A) ^1H NMR (DMSO- d_6)

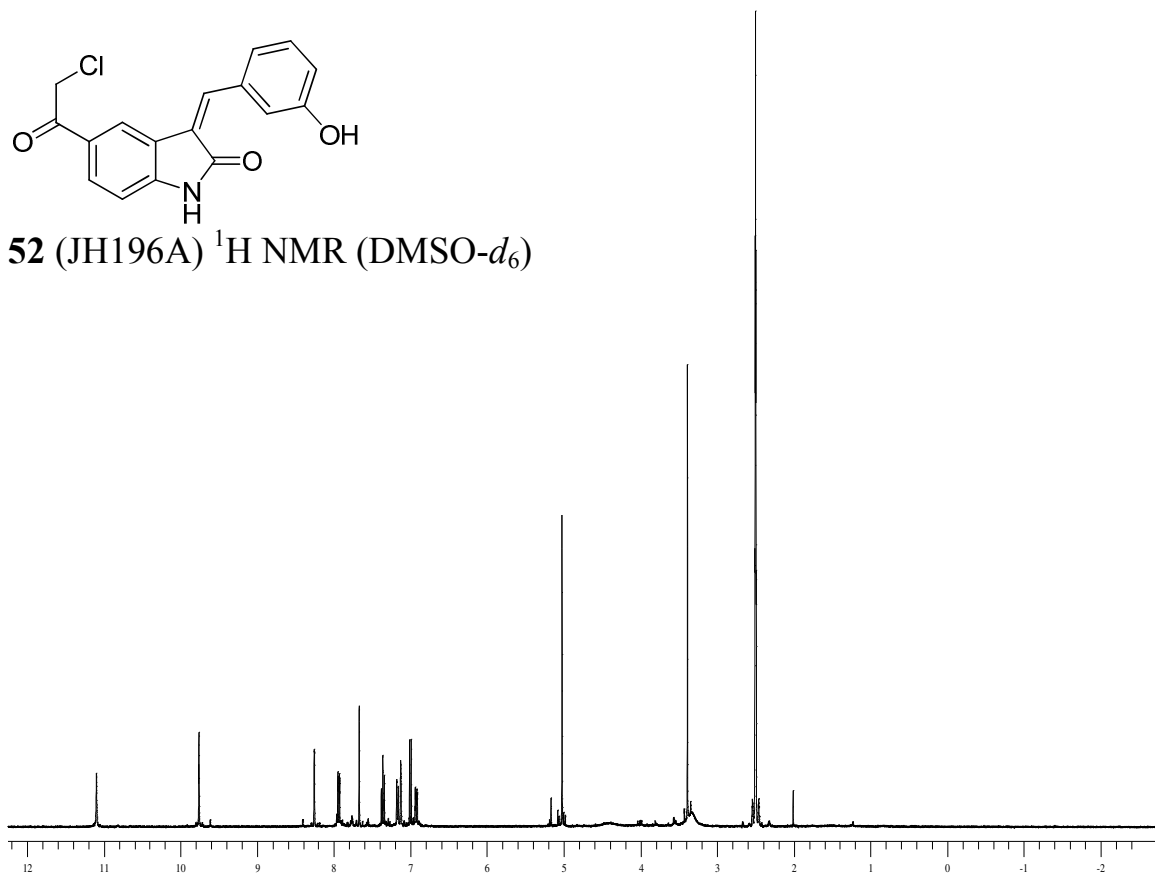


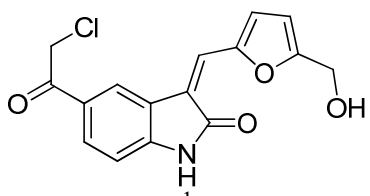


51 (JH195A) ^1H NMR (DMSO- d_6)

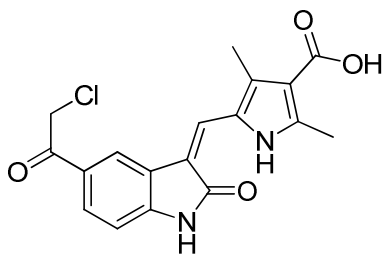
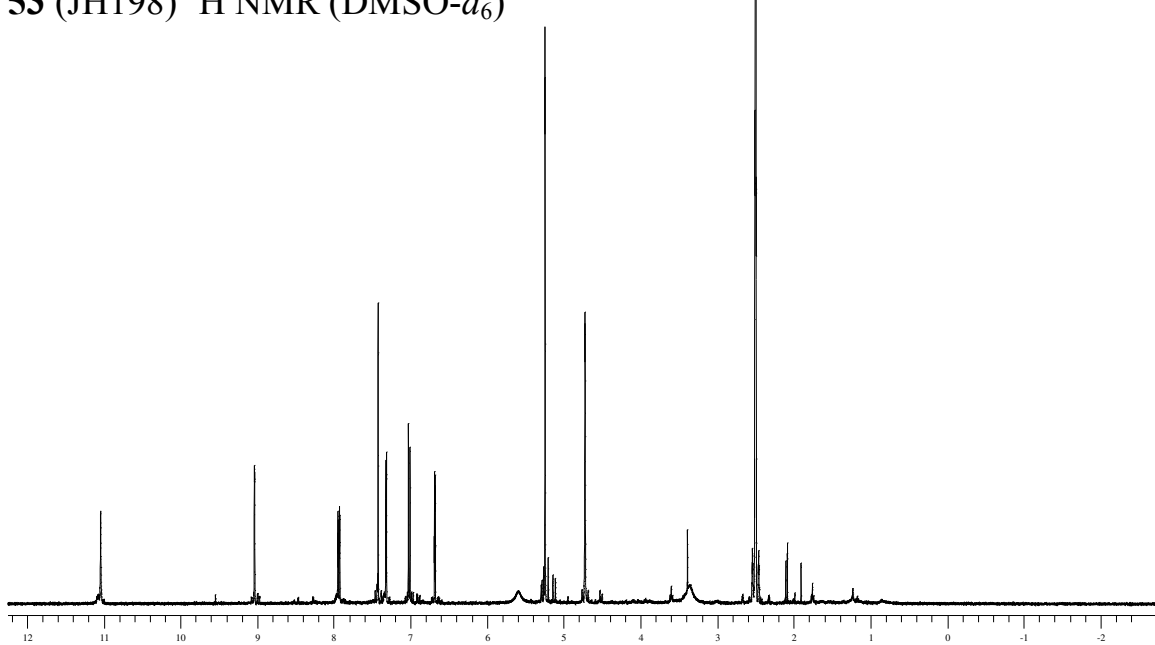


52 (JH196A) ^1H NMR (DMSO- d_6)

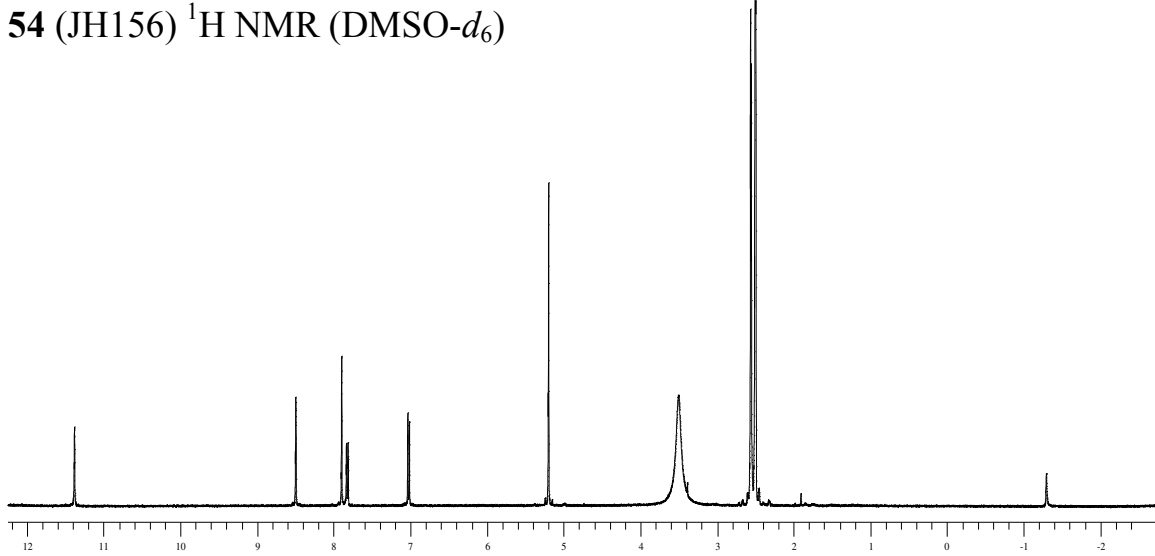


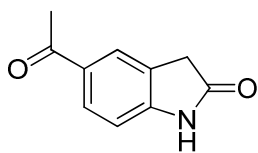


53 (JH198) ^1H NMR (DMSO- d_6)

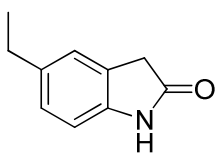
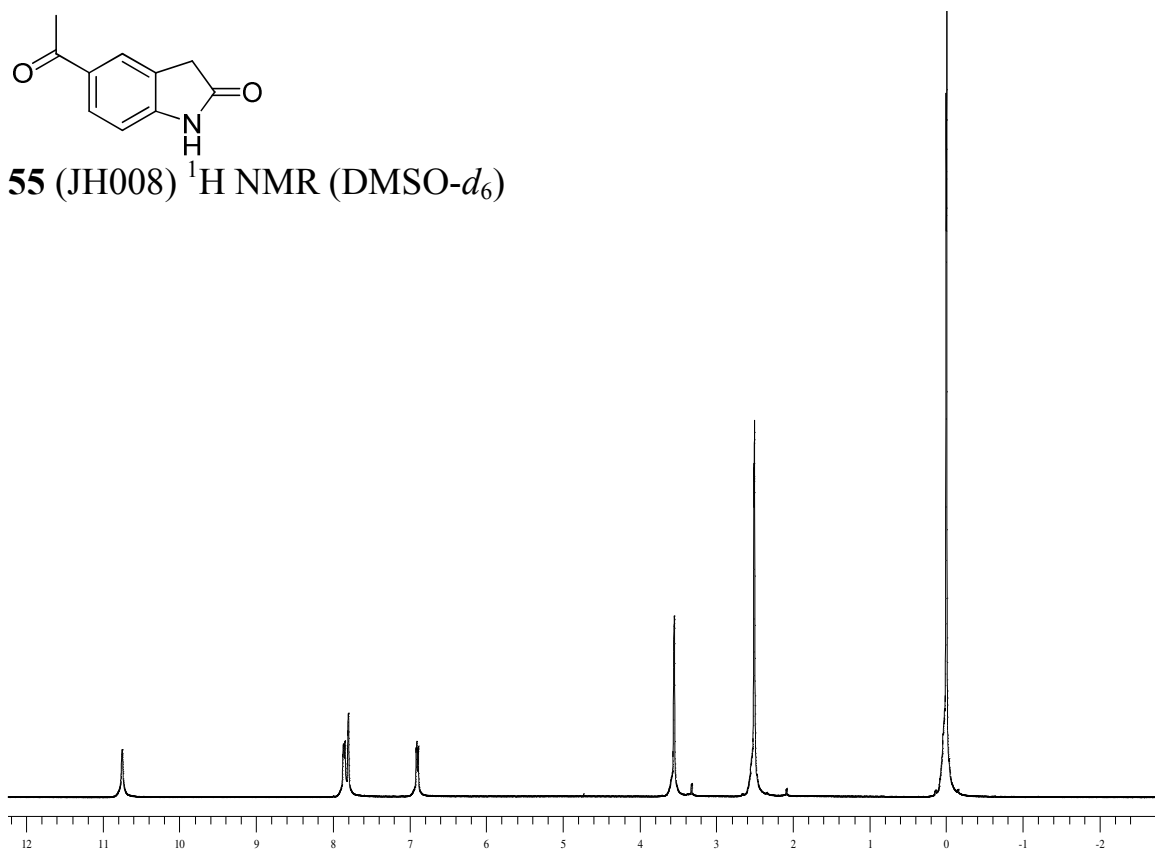


54 (JH156) ^1H NMR (DMSO- d_6)

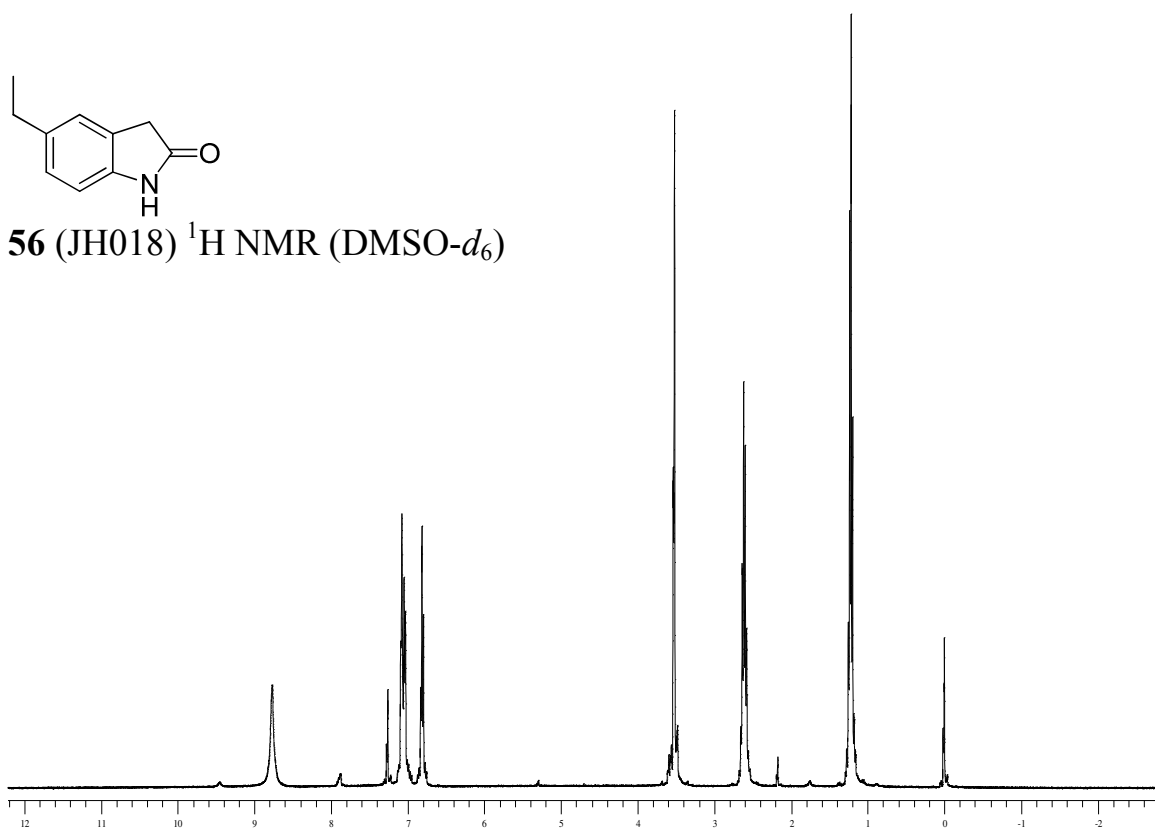


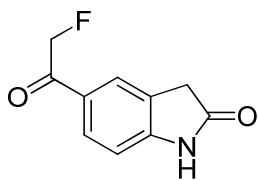


55 (JH008) ^1H NMR (DMSO- d_6)

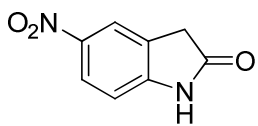
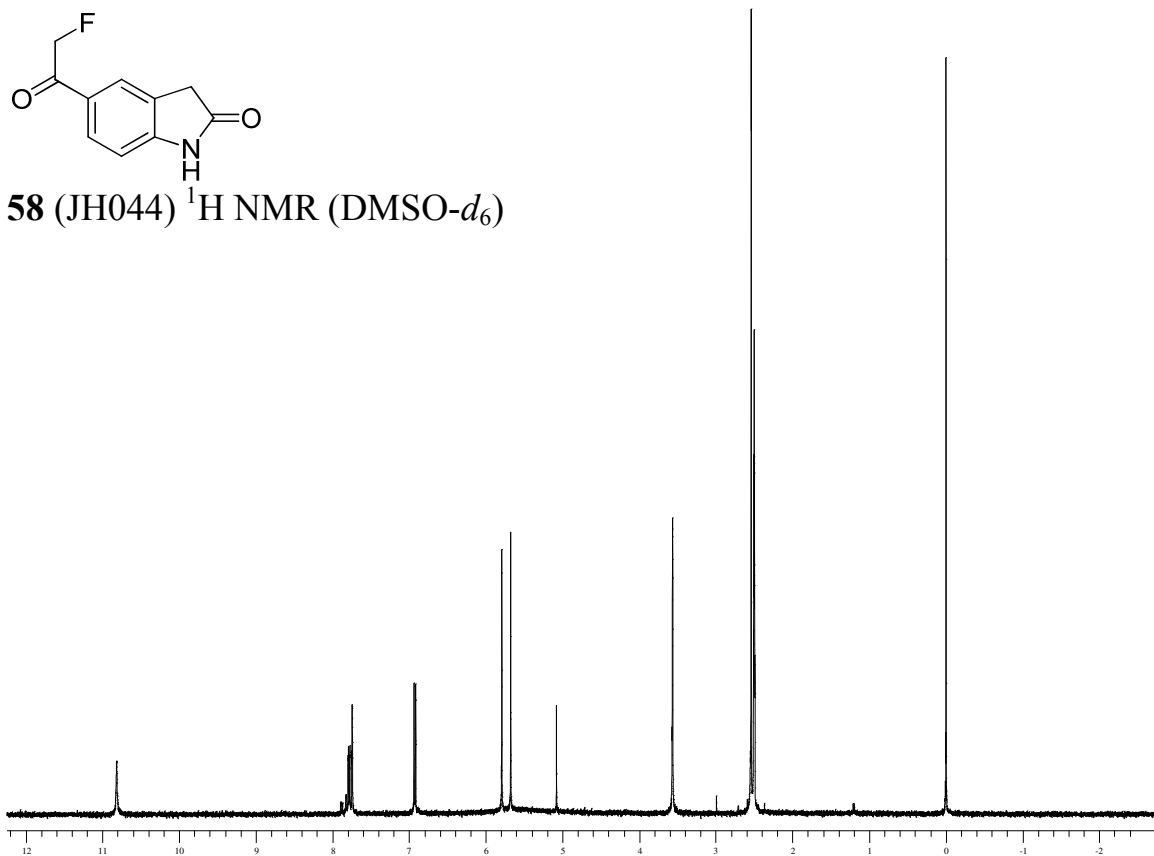


56 (JH018) ^1H NMR (DMSO- d_6)

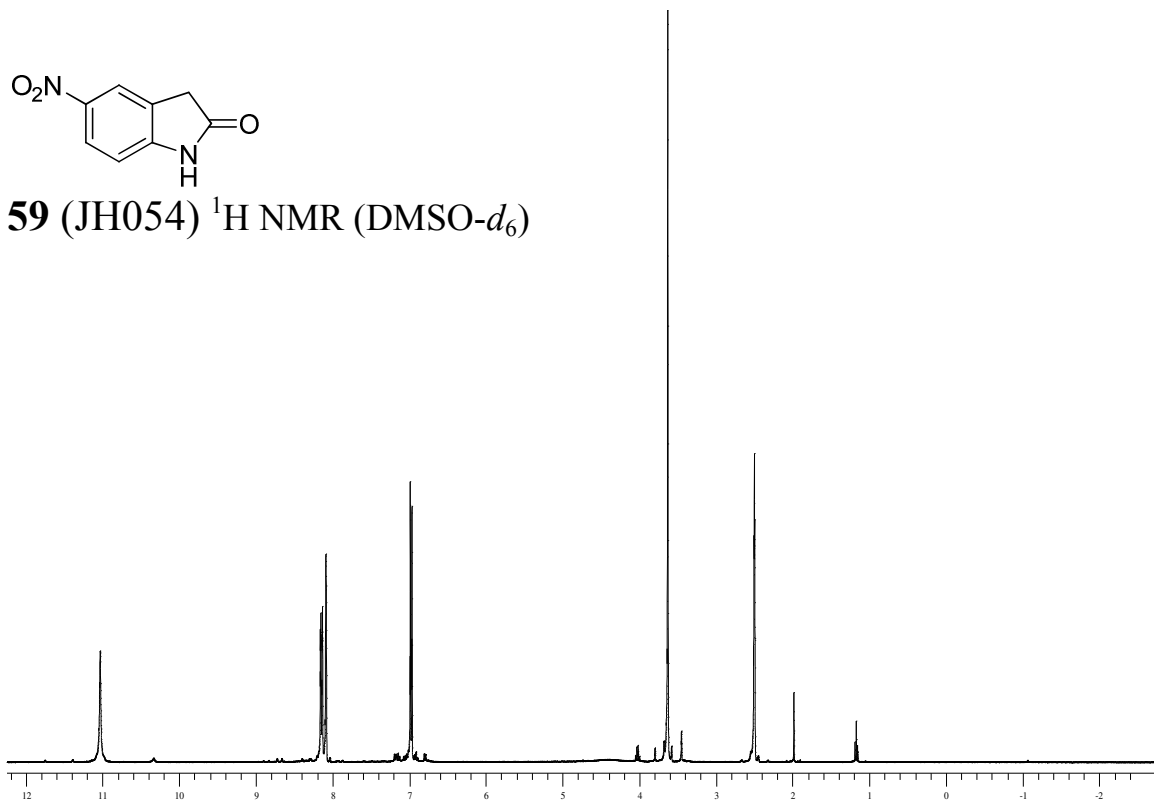


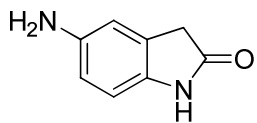


58 (JH044) ^1H NMR (DMSO- d_6)

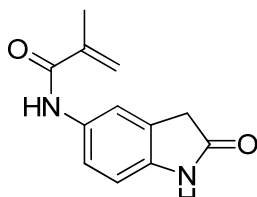
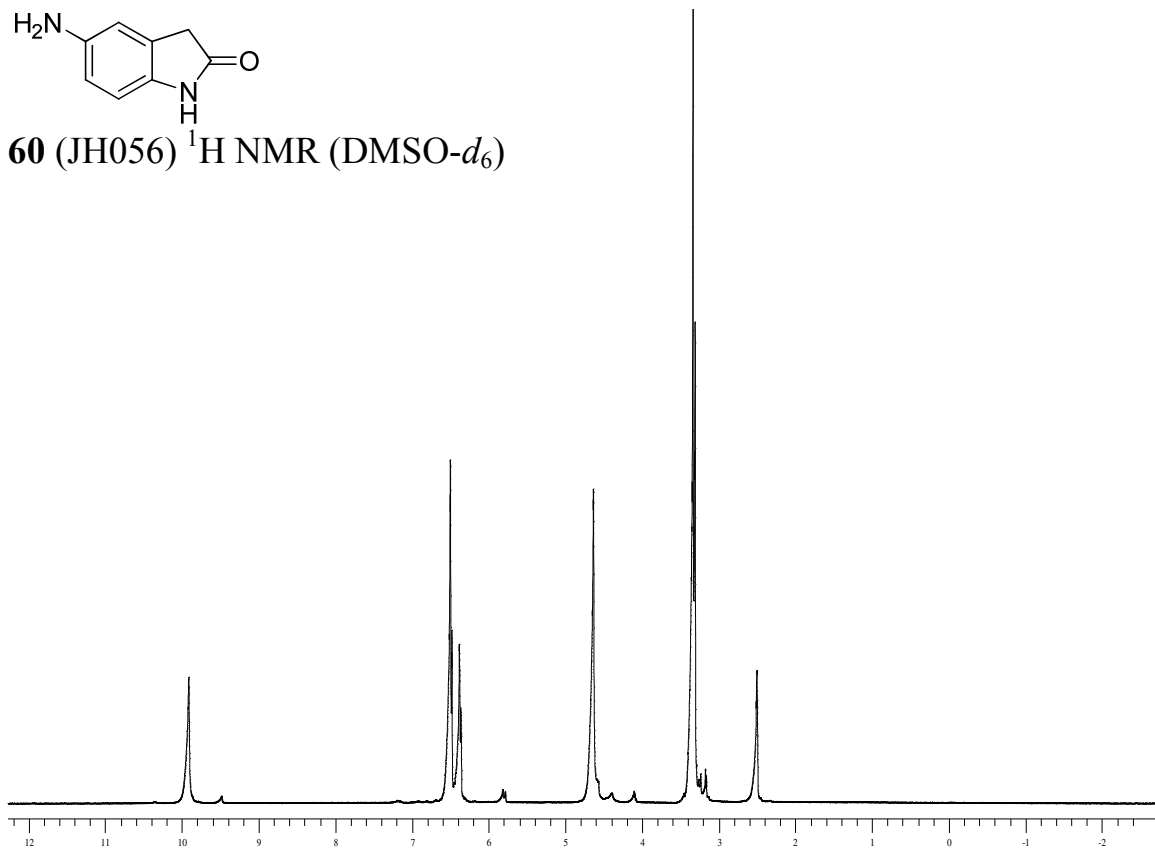


59 (JH054) ^1H NMR (DMSO- d_6)

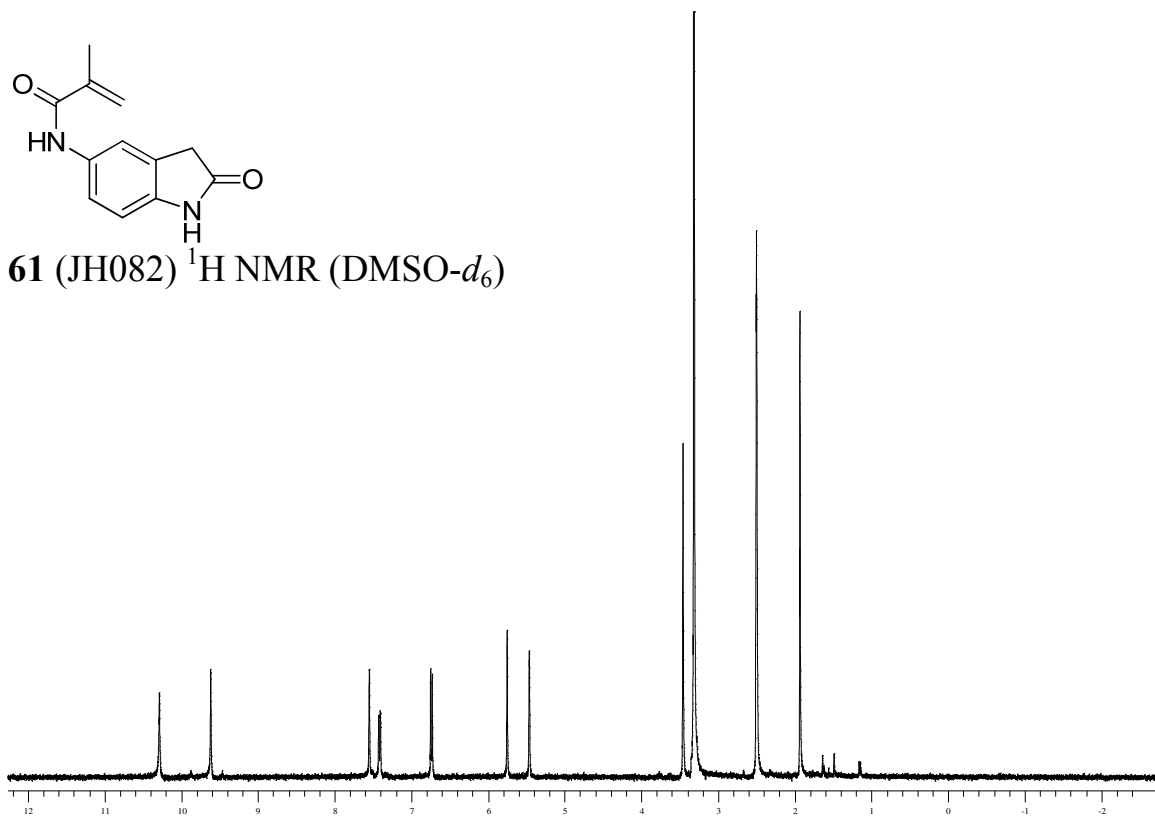


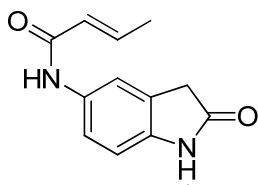


60 (JH056) ^1H NMR (DMSO- d_6)

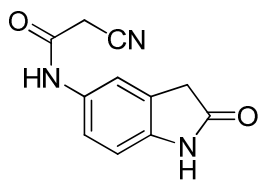
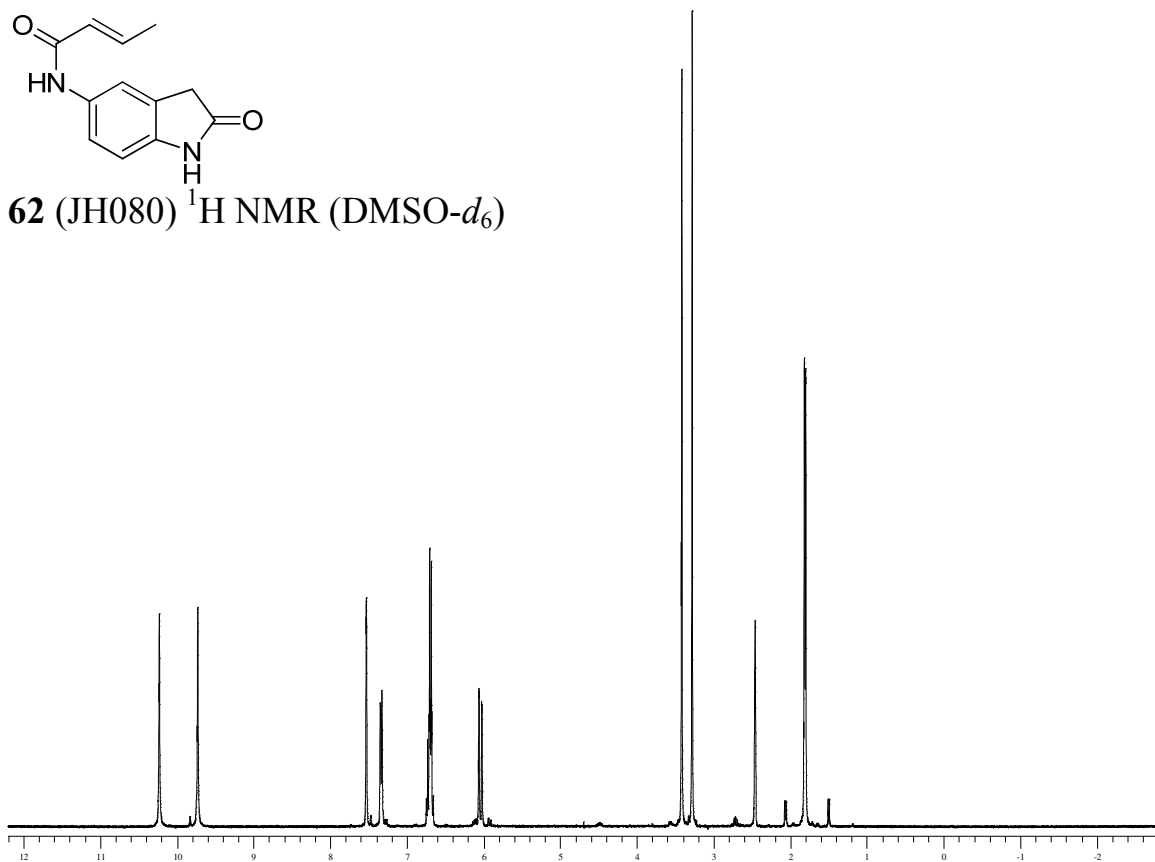


61 (JH082) ^1H NMR (DMSO- d_6)

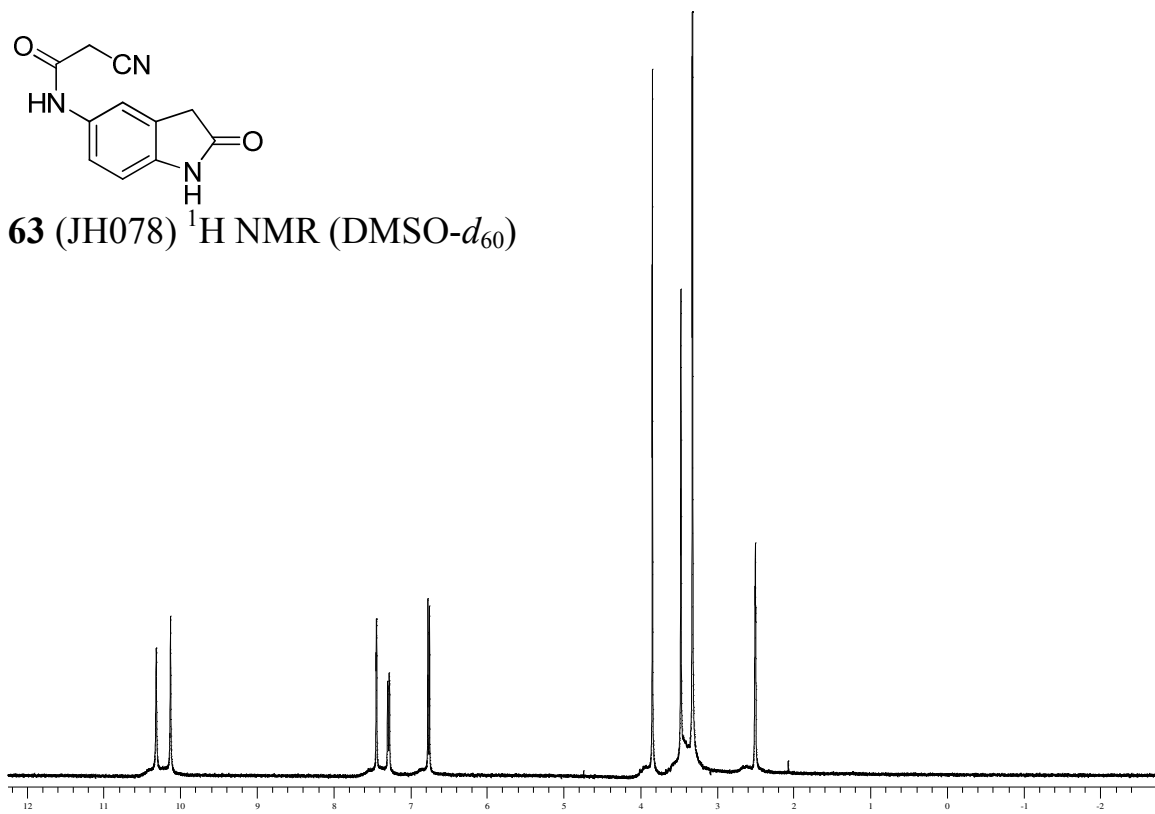


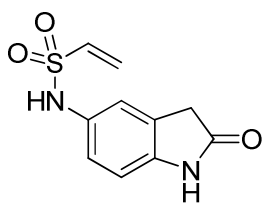


62 (JH080) ^1H NMR (DMSO- d_6)

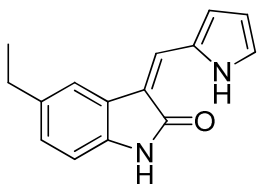
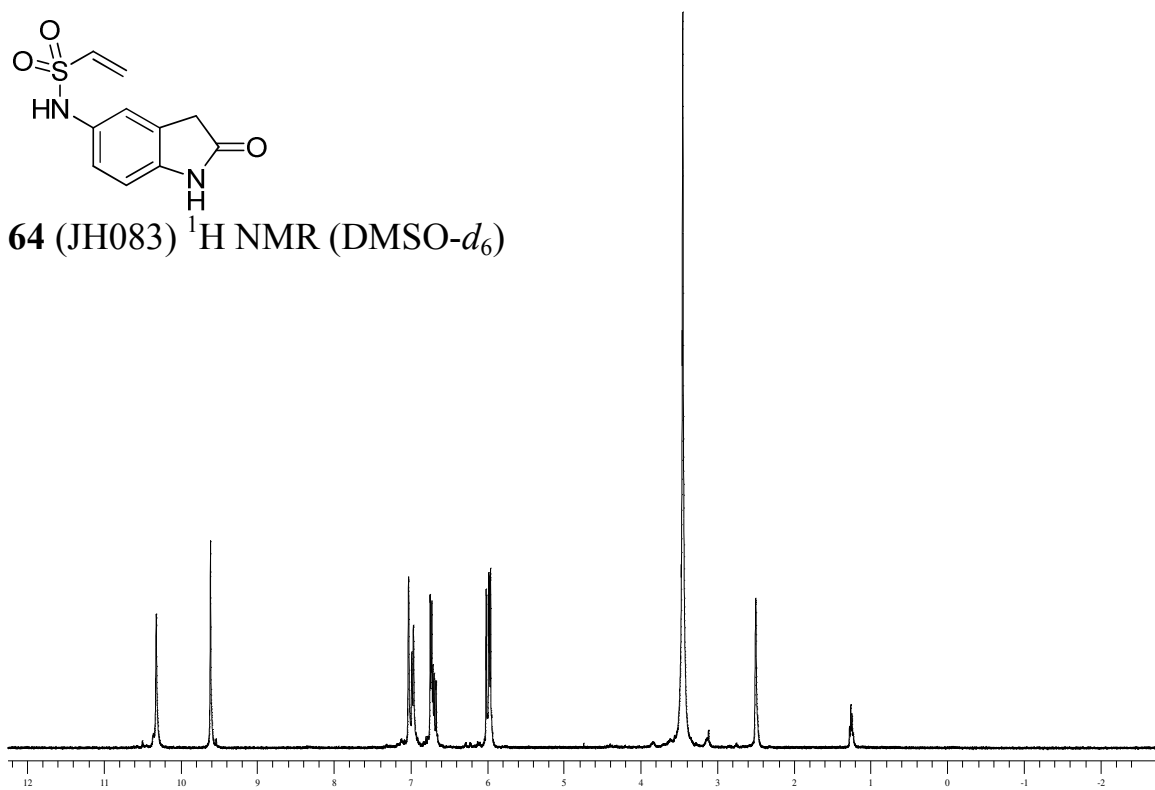


63 (JH078) ^1H NMR (DMSO- d_6)

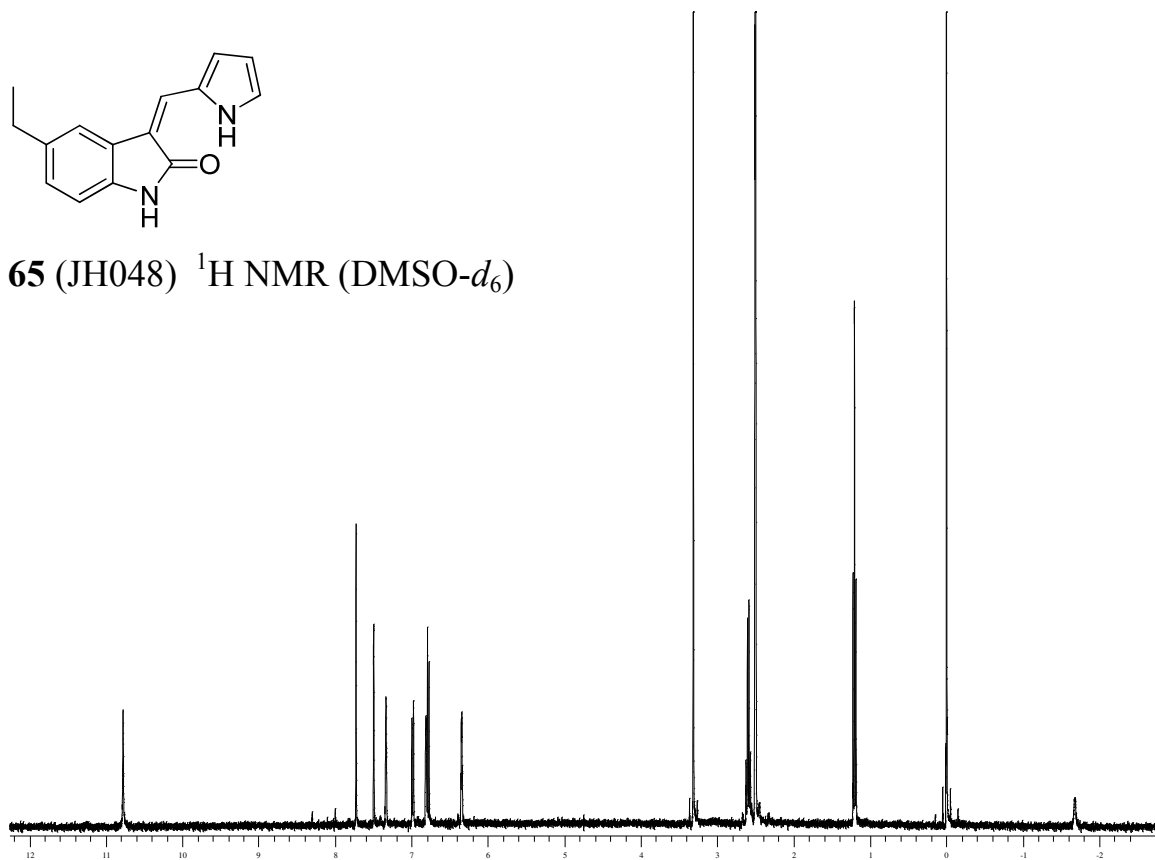


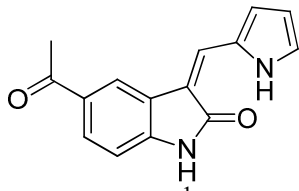


64 (JH083) ^1H NMR (DMSO- d_6)

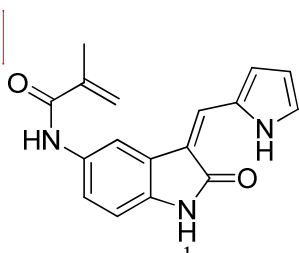
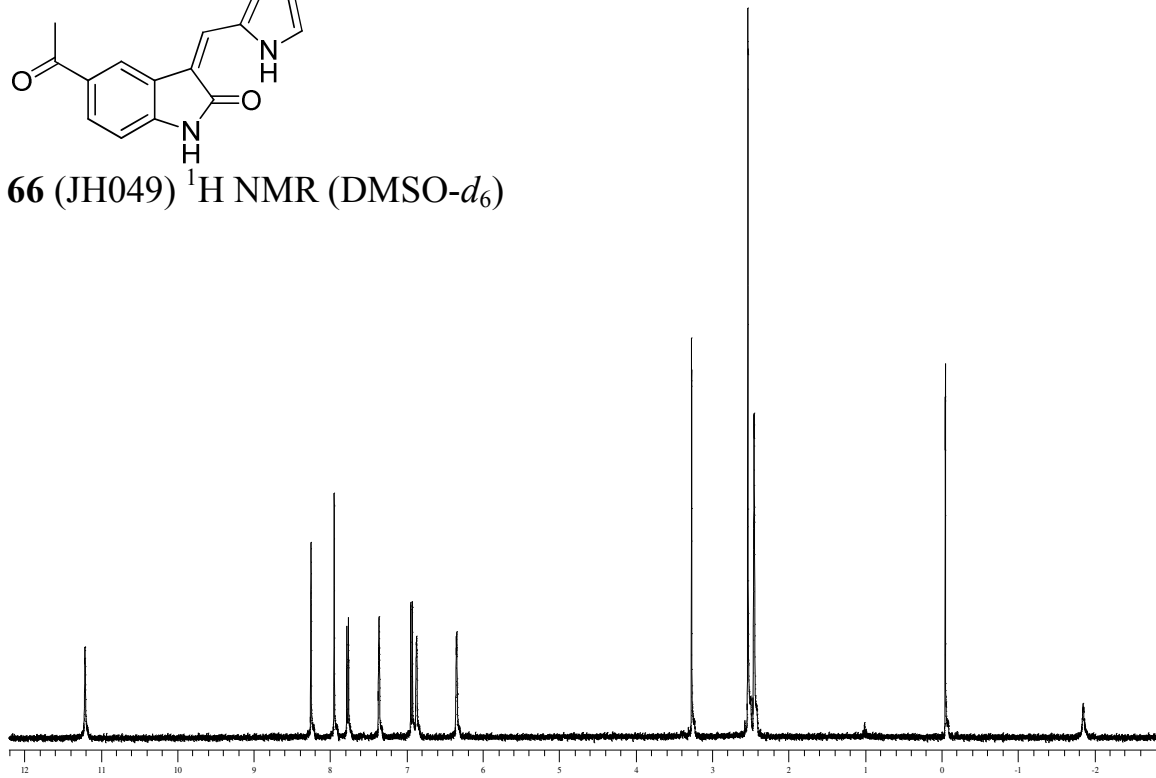


65 (JH048) ^1H NMR (DMSO- d_6)

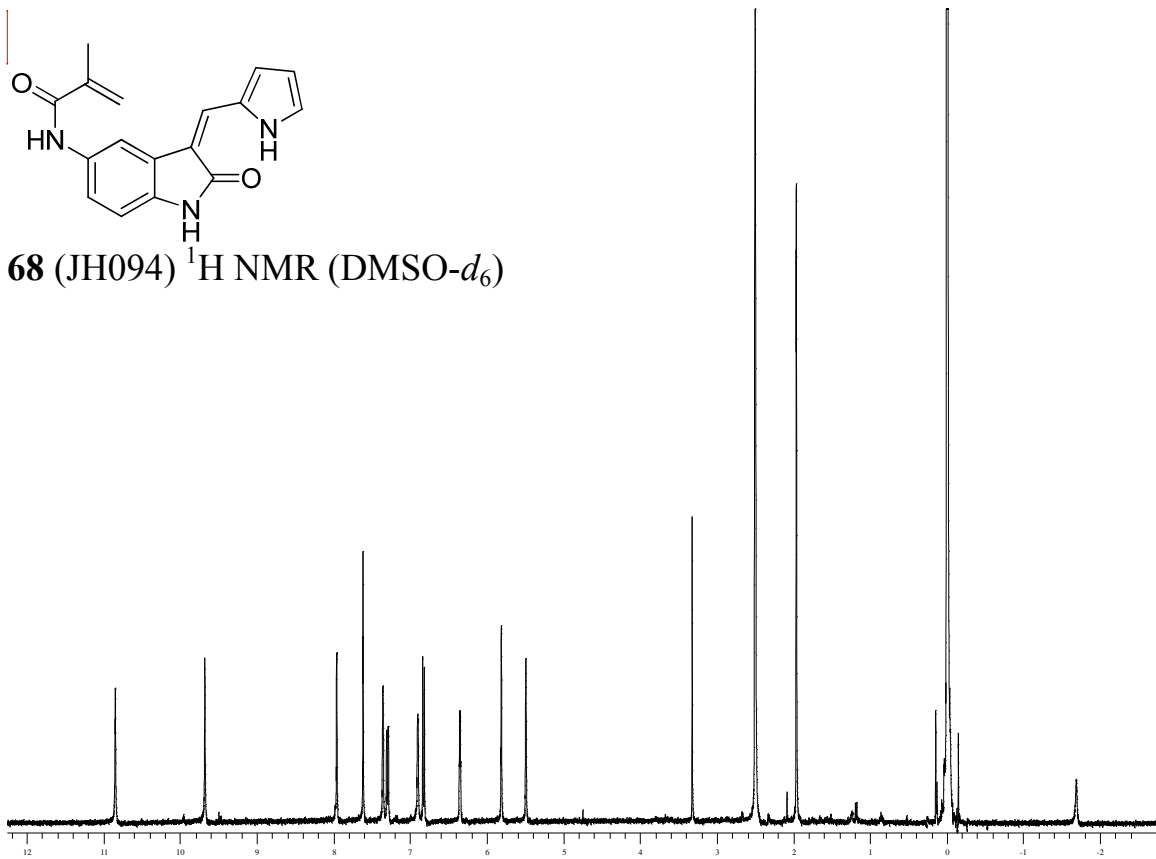


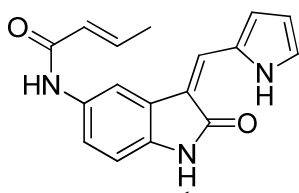


66 (JH049) ^1H NMR (DMSO- d_6)

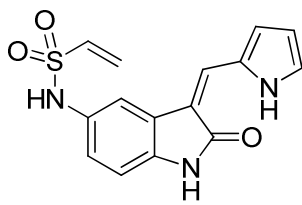
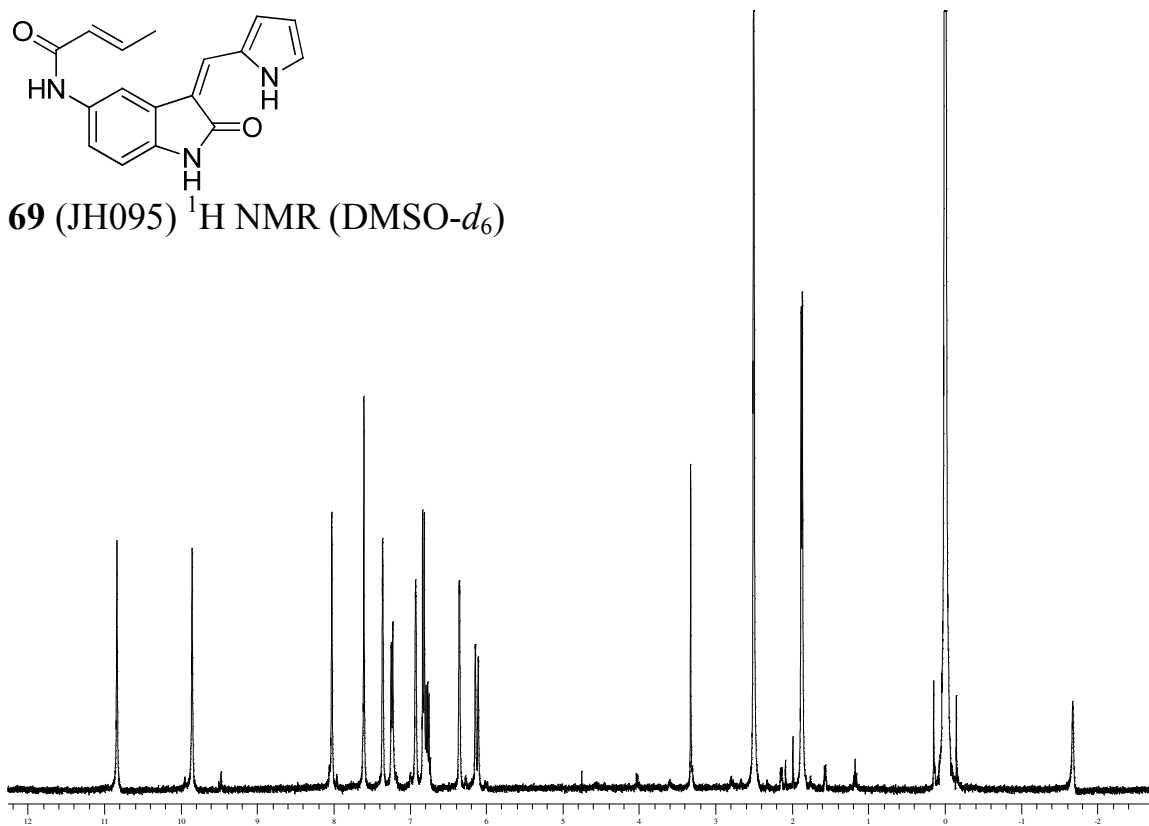


68 (JH094) ^1H NMR (DMSO- d_6)

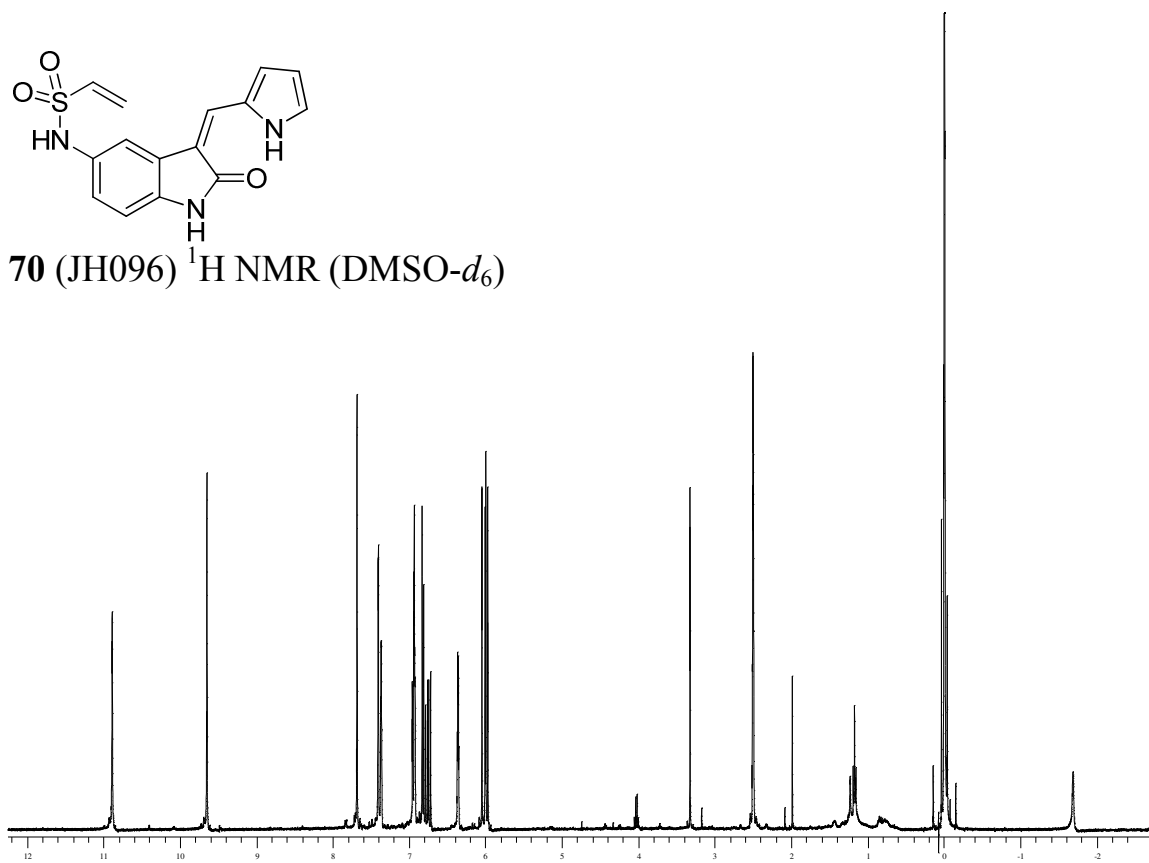


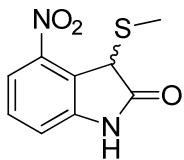


69 (JH095) ^1H NMR (DMSO- d_6)

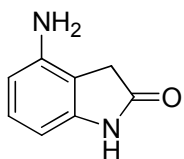
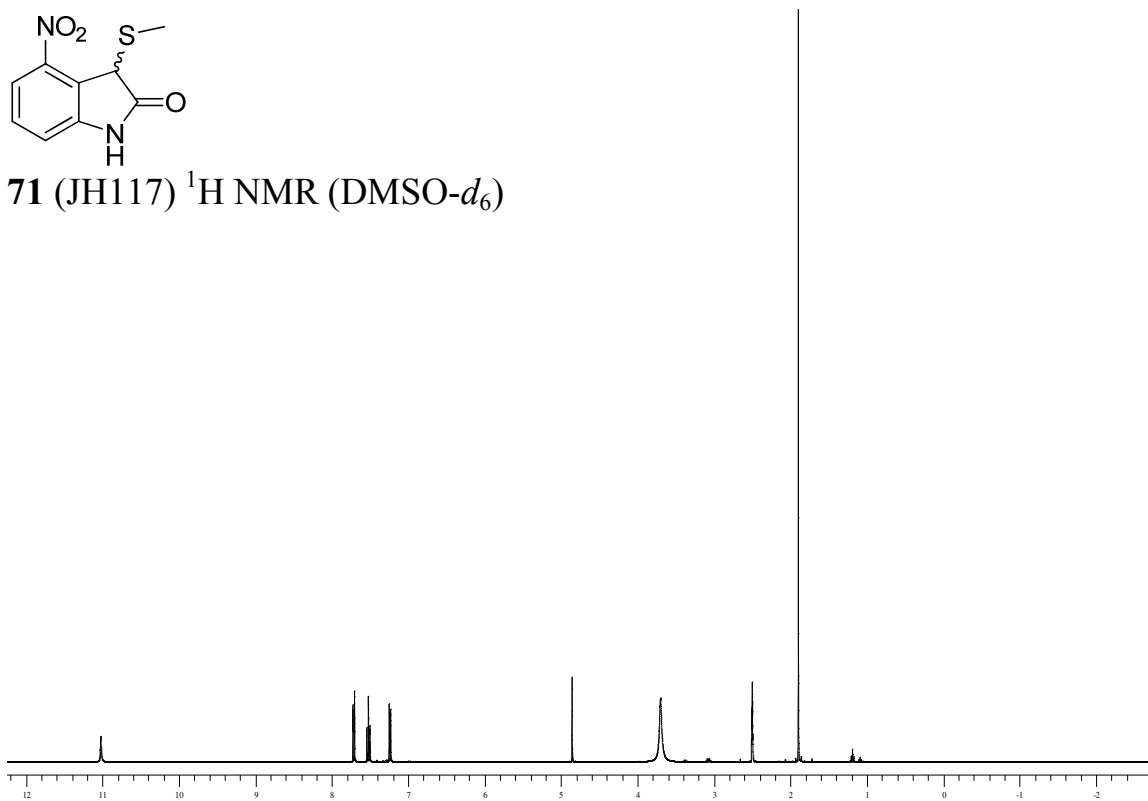


70 (JH096) ^1H NMR (DMSO- d_6)

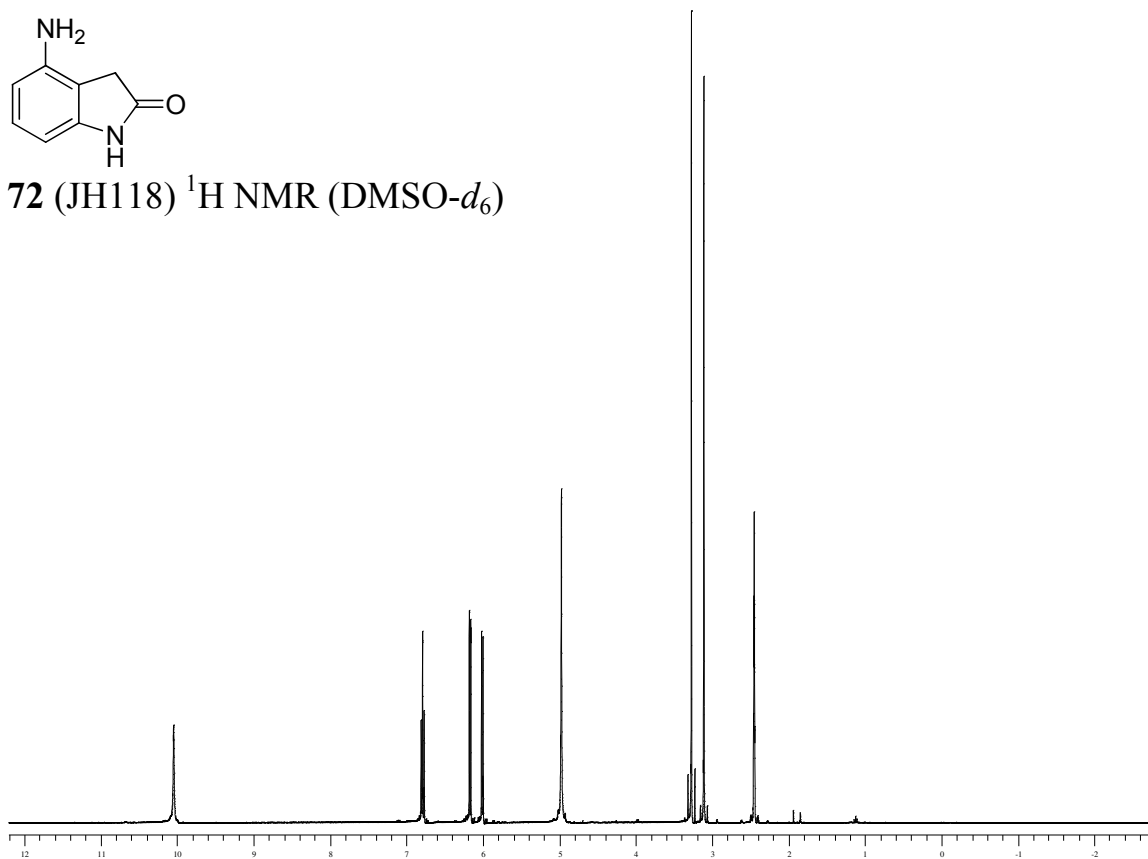


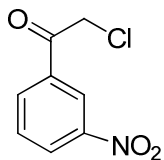


71 (JH117) ^1H NMR (DMSO- d_6)

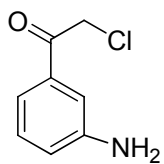
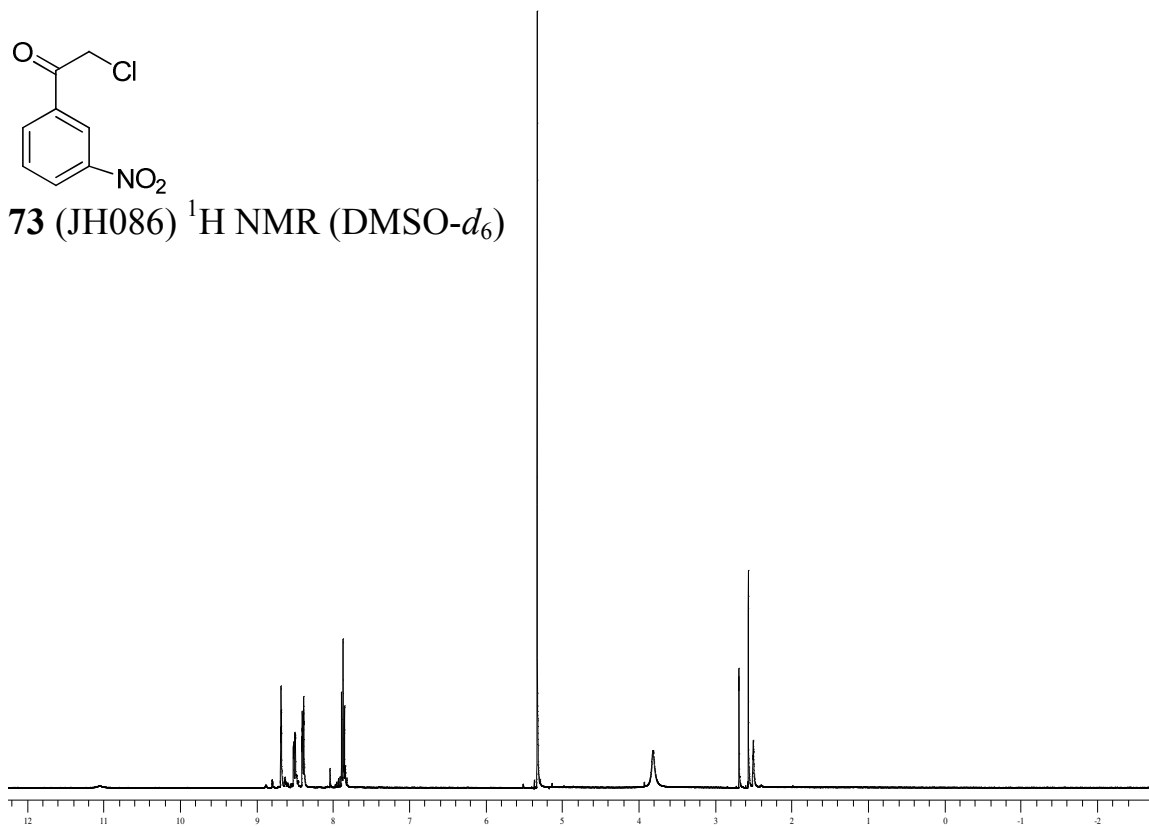


72 (JH118) ^1H NMR (DMSO- d_6)

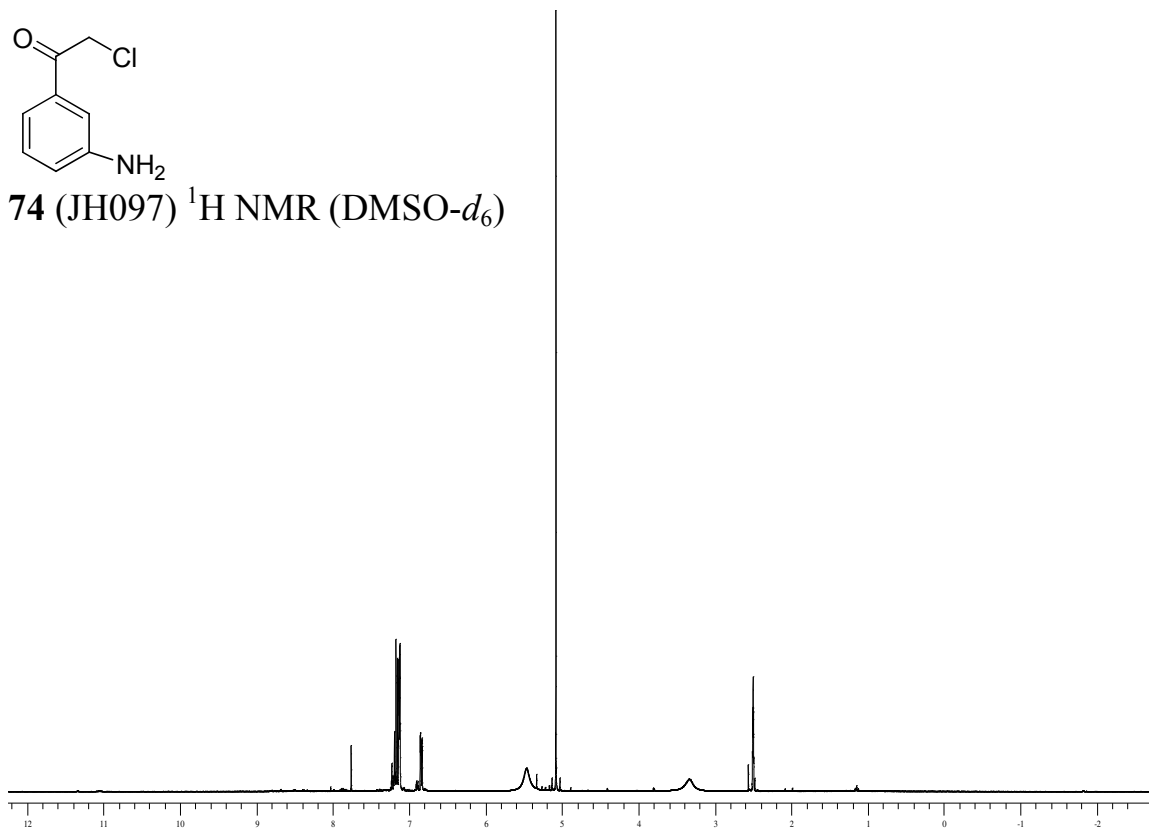


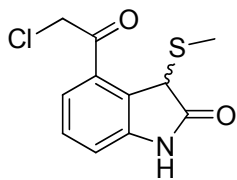


73 (JH086) ^1H NMR (DMSO- d_6)

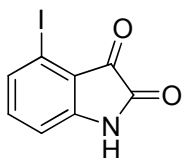
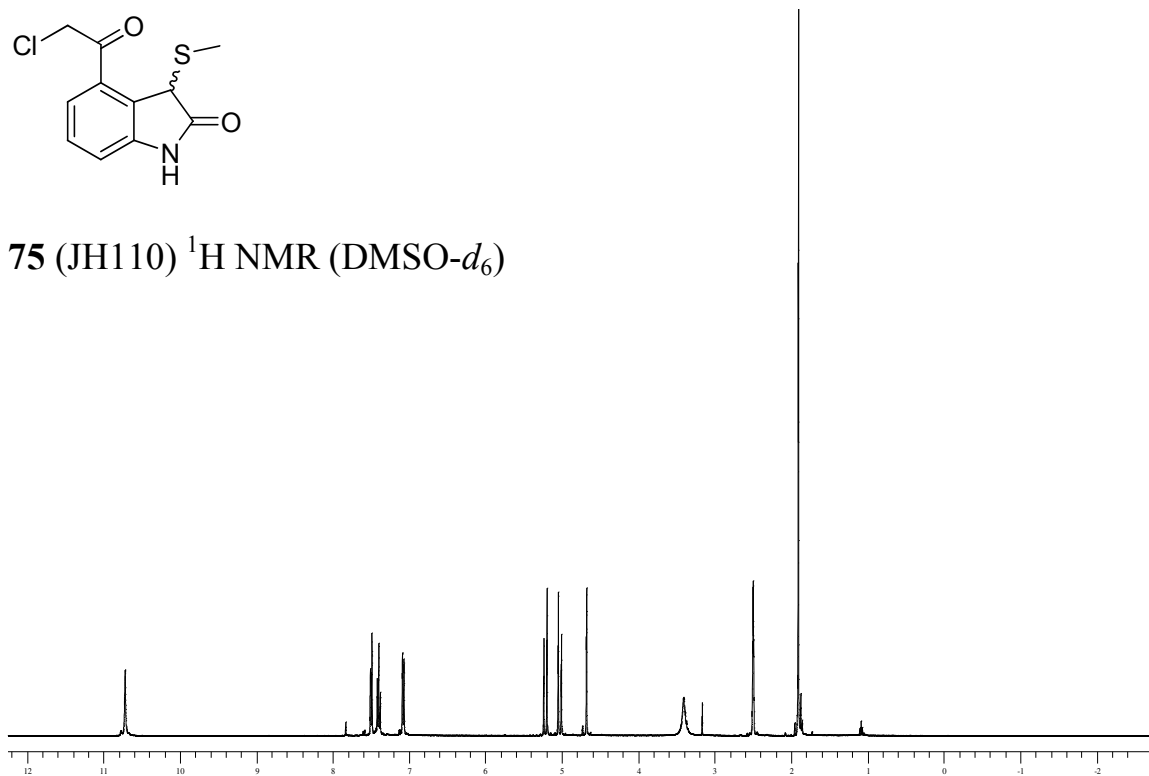


74 (JH097) ^1H NMR (DMSO- d_6)

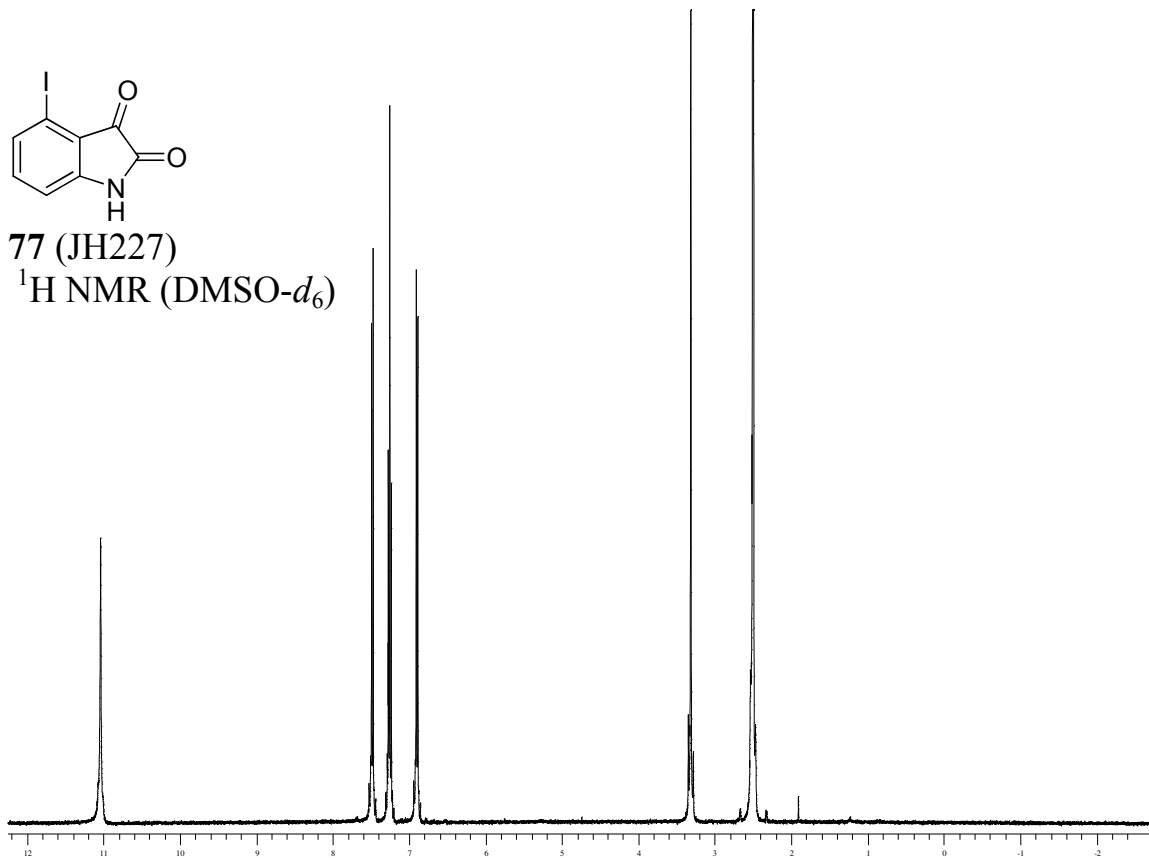


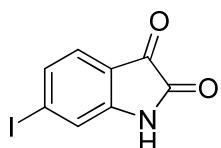


75 (JH110) ^1H NMR (DMSO- d_6)

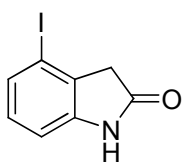
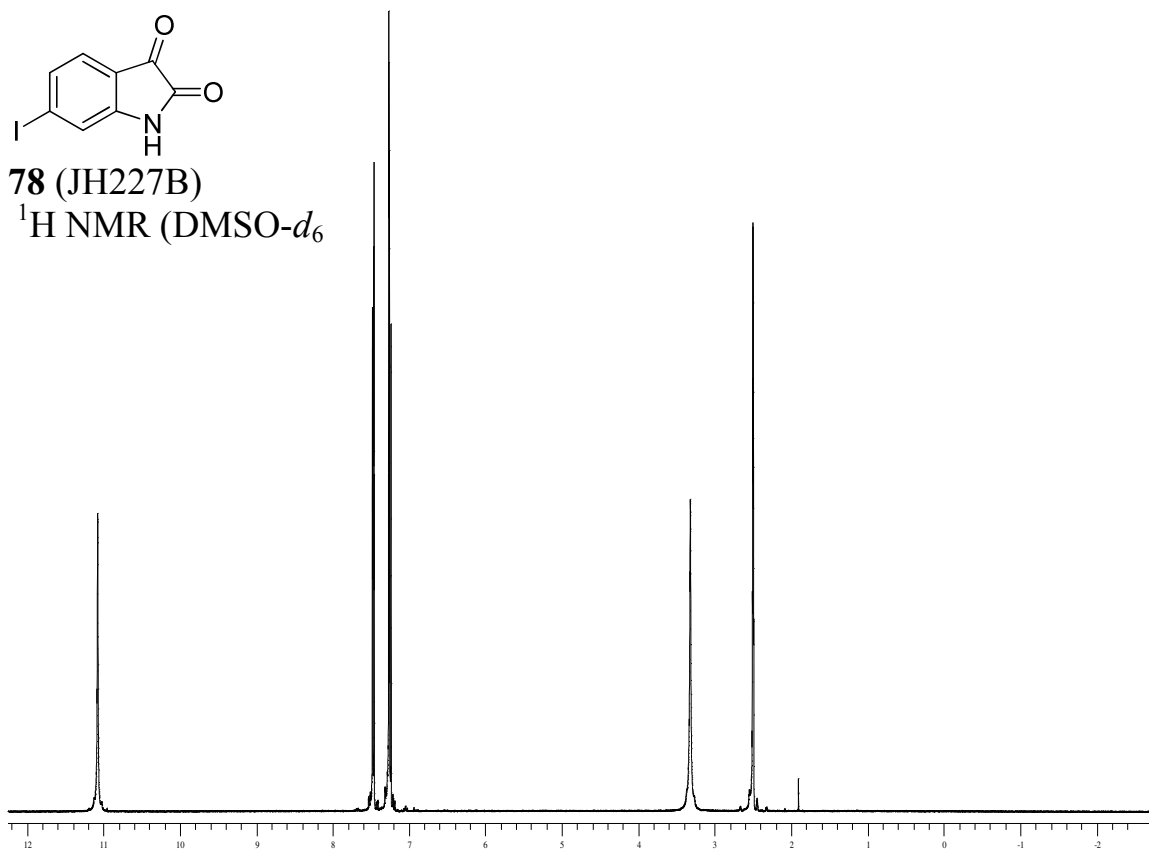


77 (JH227) ^1H NMR (DMSO- d_6)

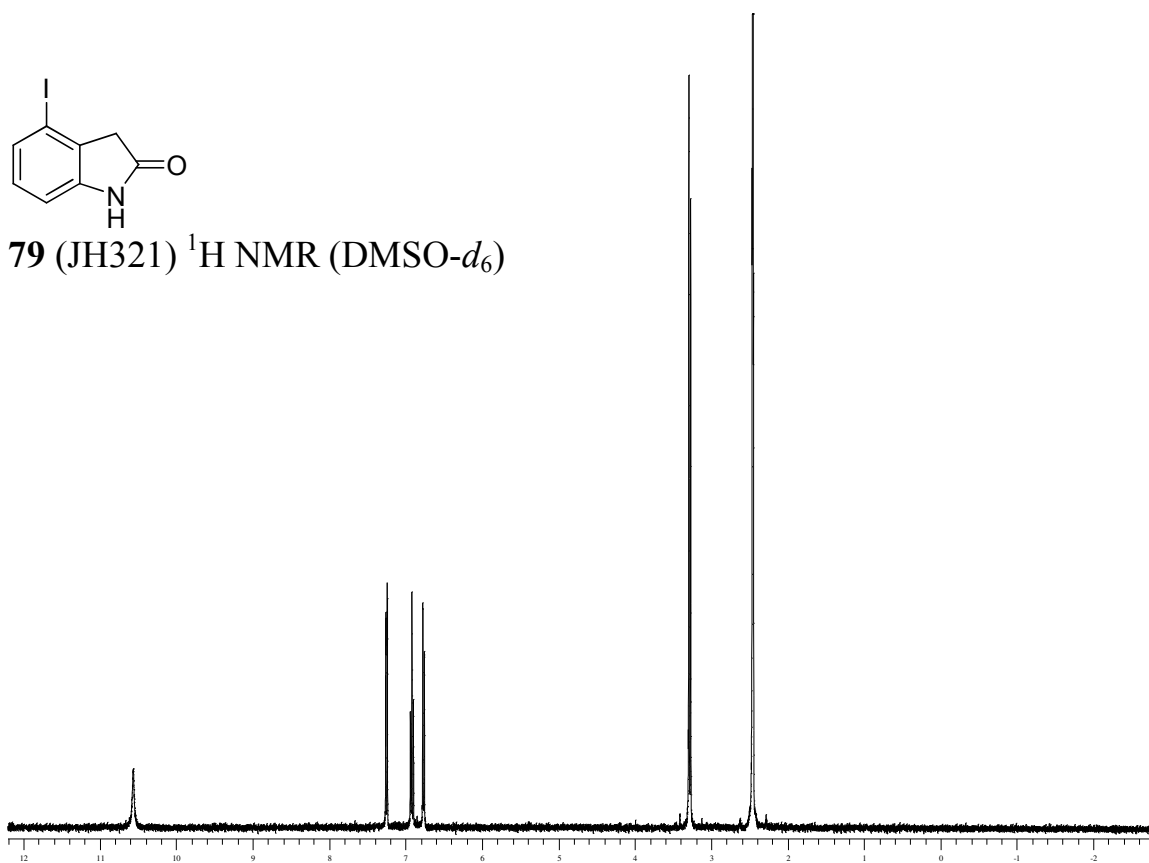


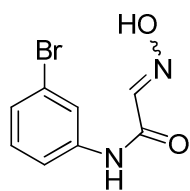


78 (JH227B)
 $^1\text{H NMR}$ (DMSO- d_6)

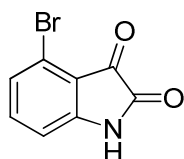
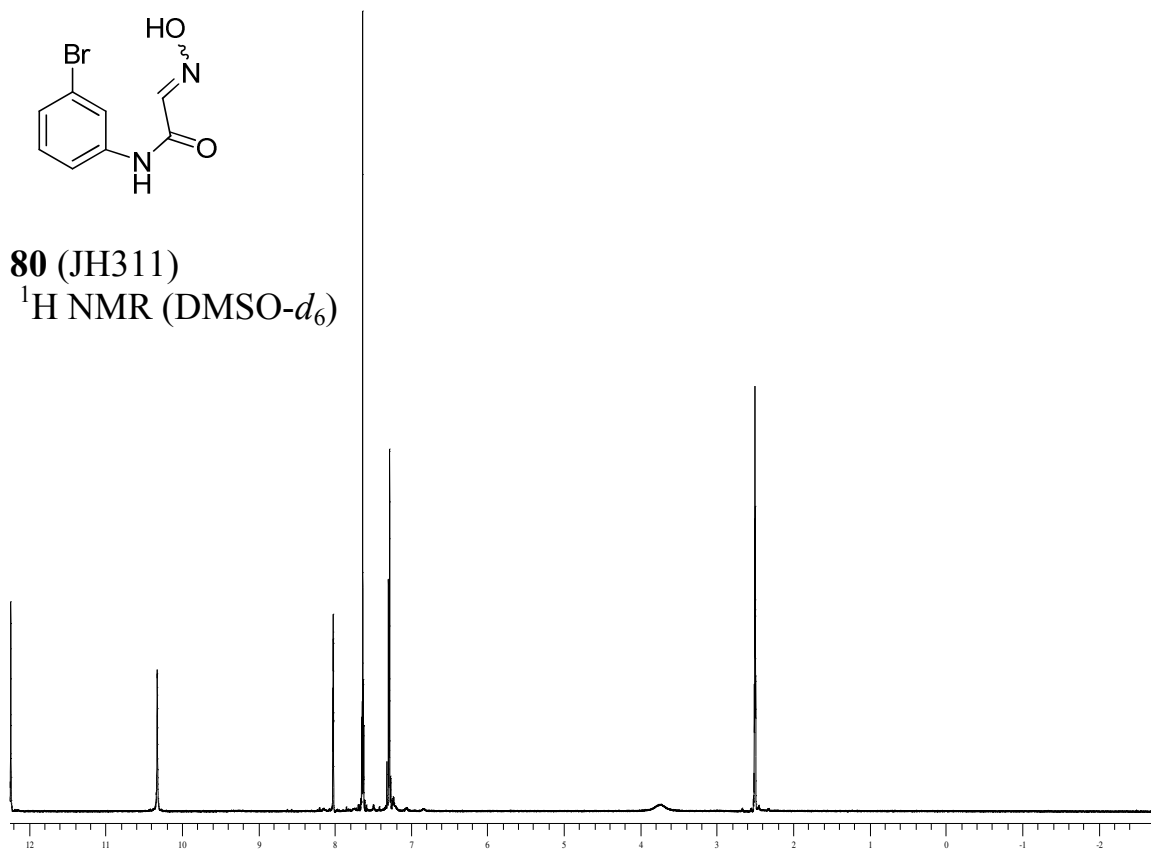


79 (JH321) $^1\text{H NMR}$ (DMSO- d_6)

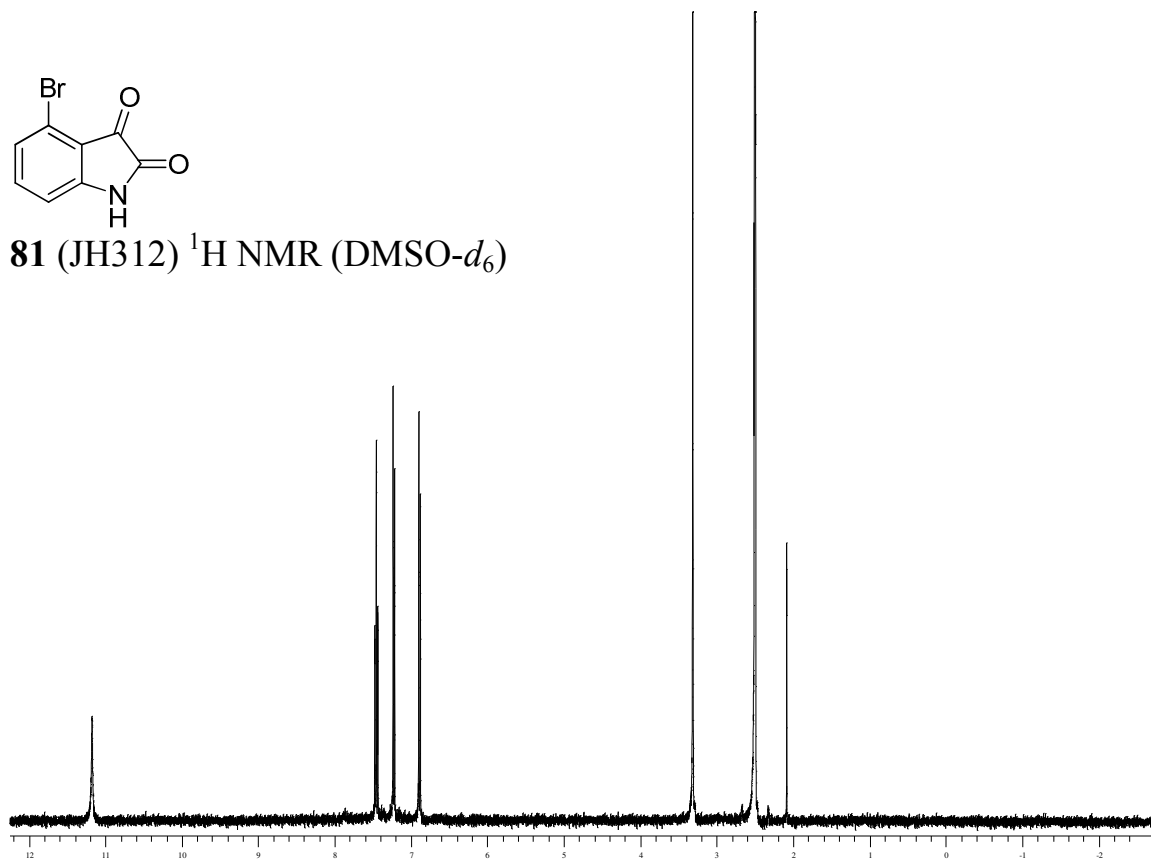


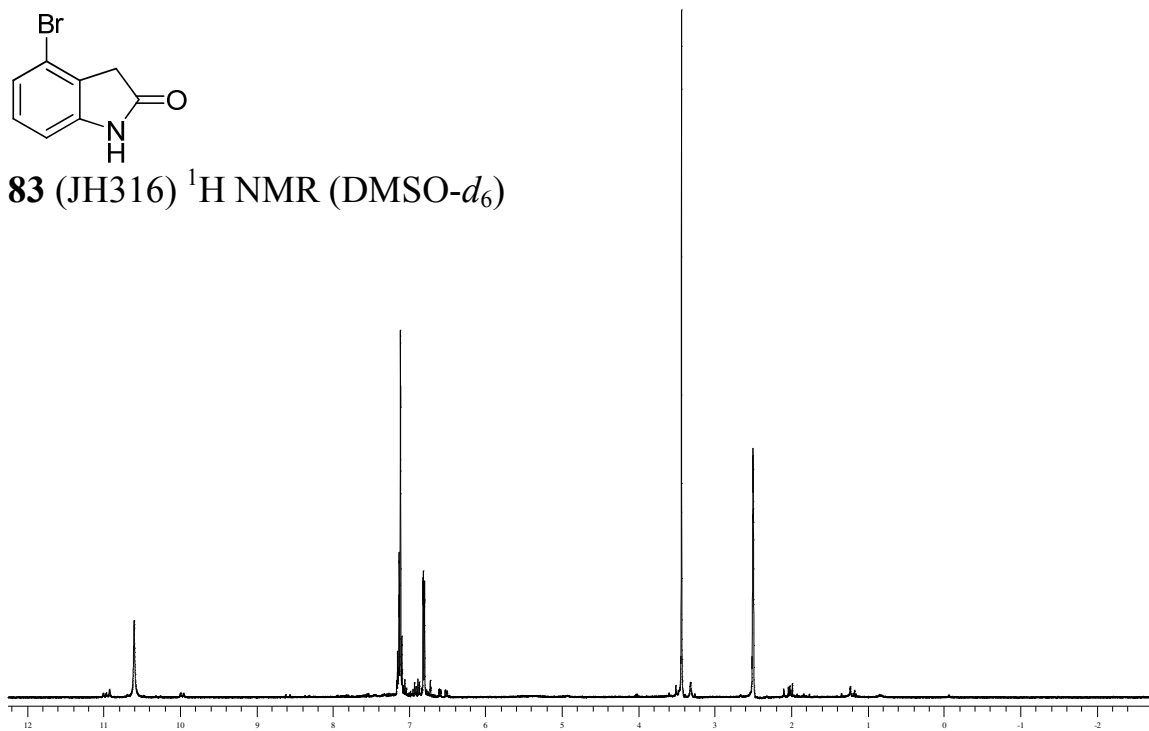
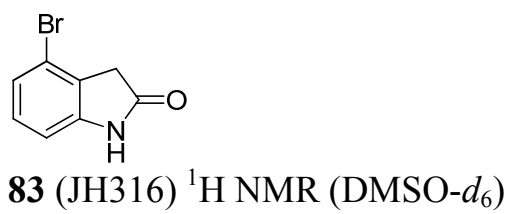
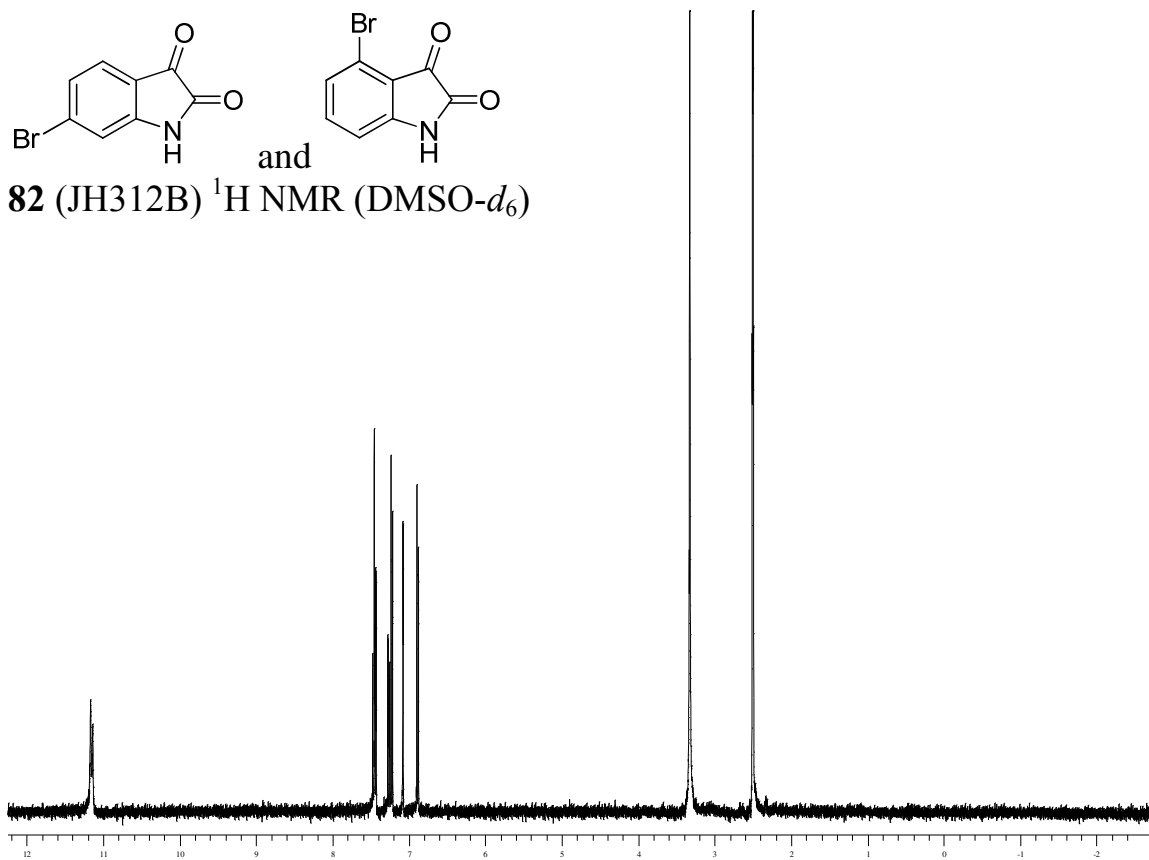
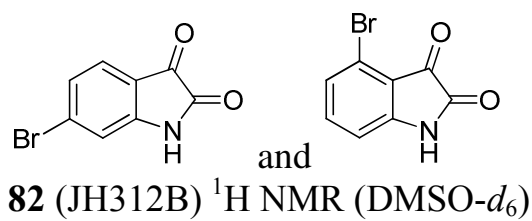


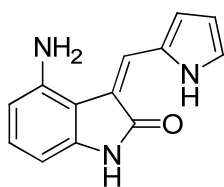
80 (JH311)
 $^1\text{H NMR}$ (DMSO- d_6)



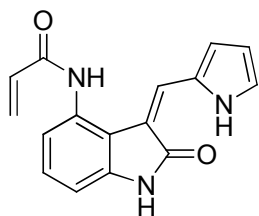
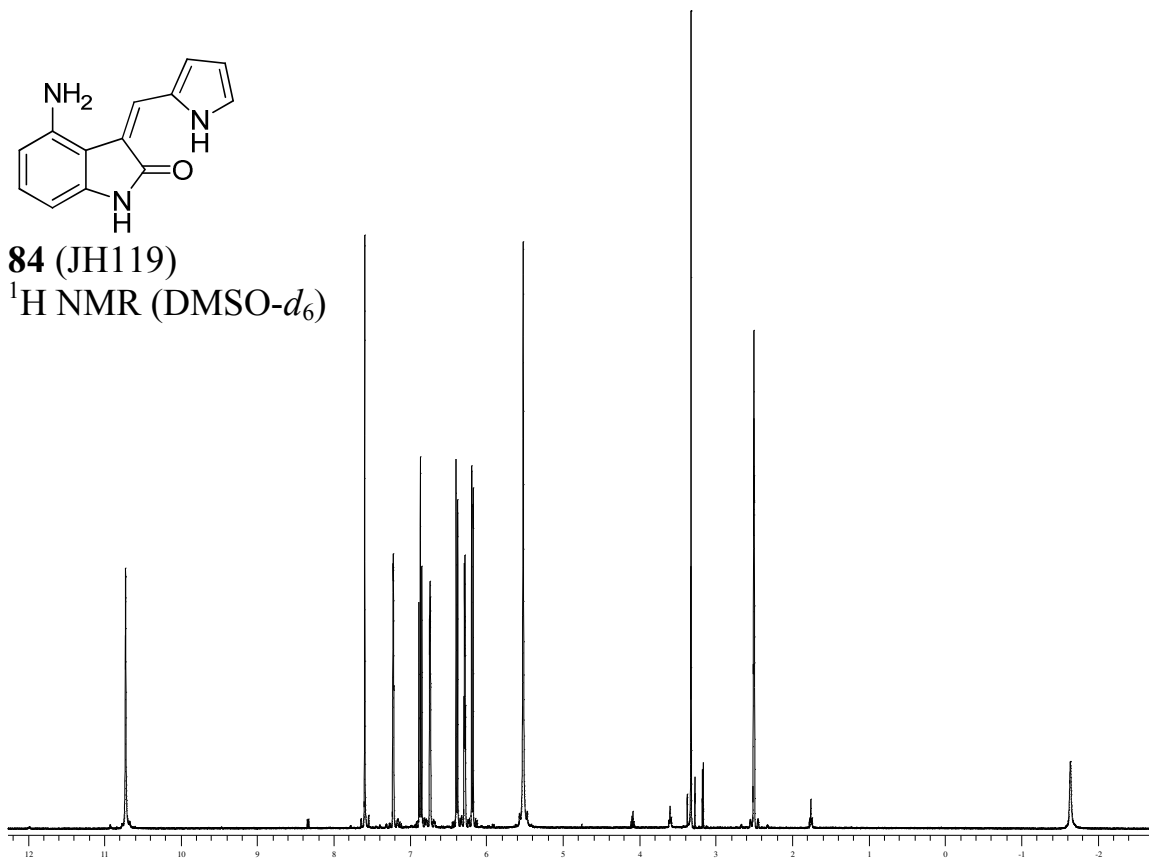
81 (JH312) $^1\text{H NMR}$ (DMSO- d_6)



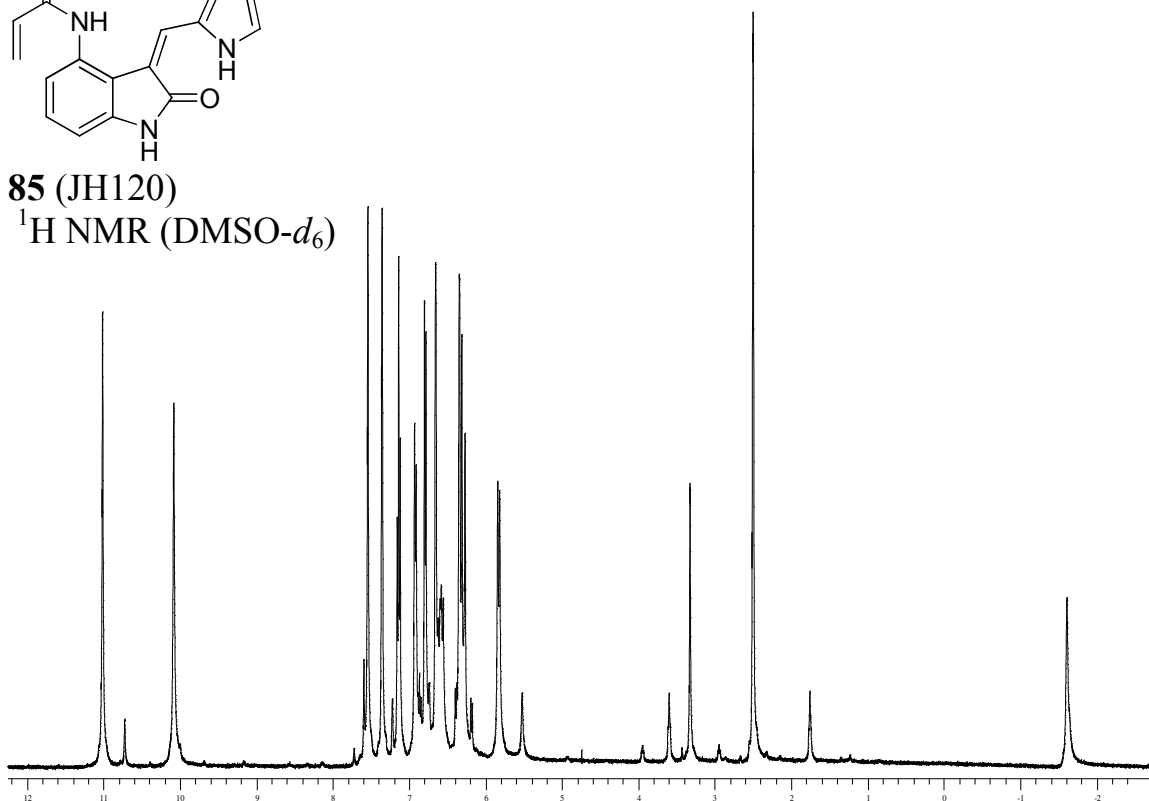


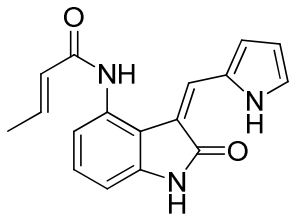


84 (JH119)
 $^1\text{H NMR}$ (DMSO- d_6)

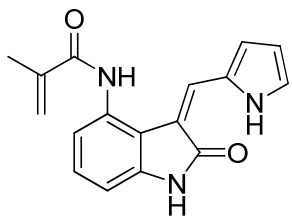
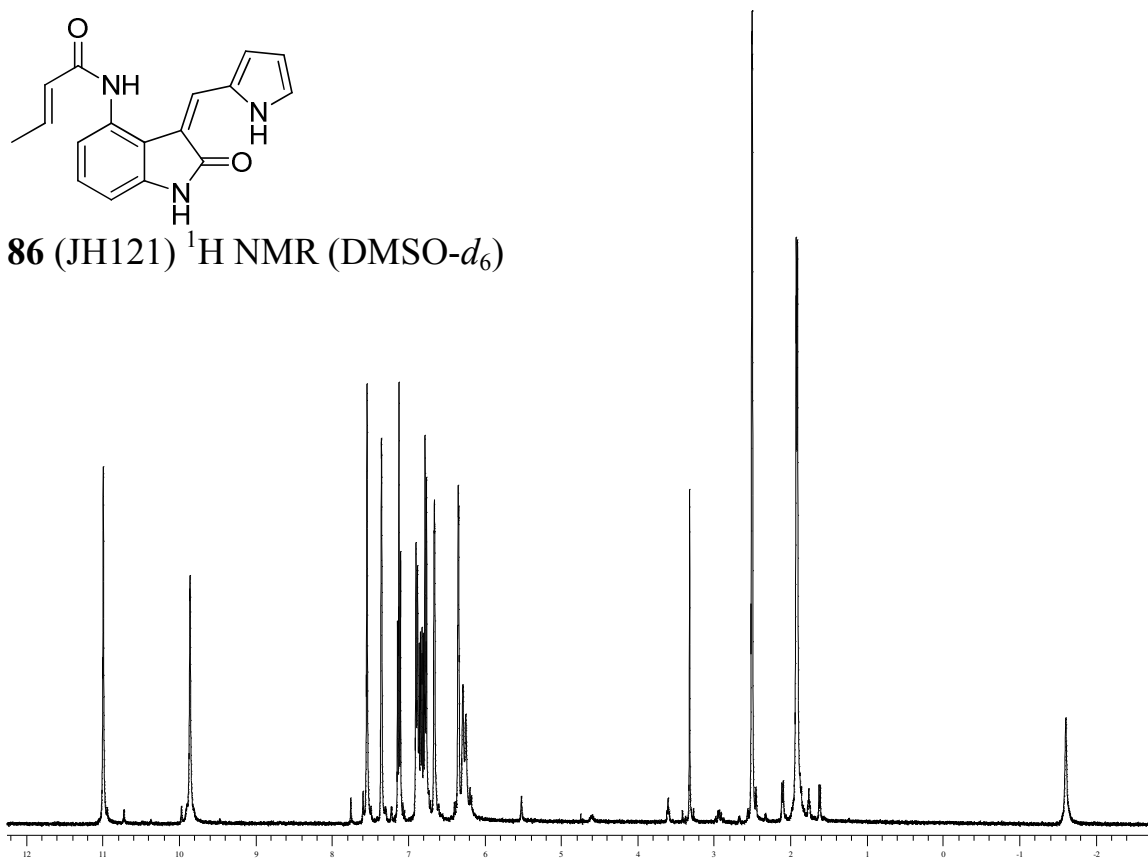


85 (JH120)
 $^1\text{H NMR}$ (DMSO- d_6)

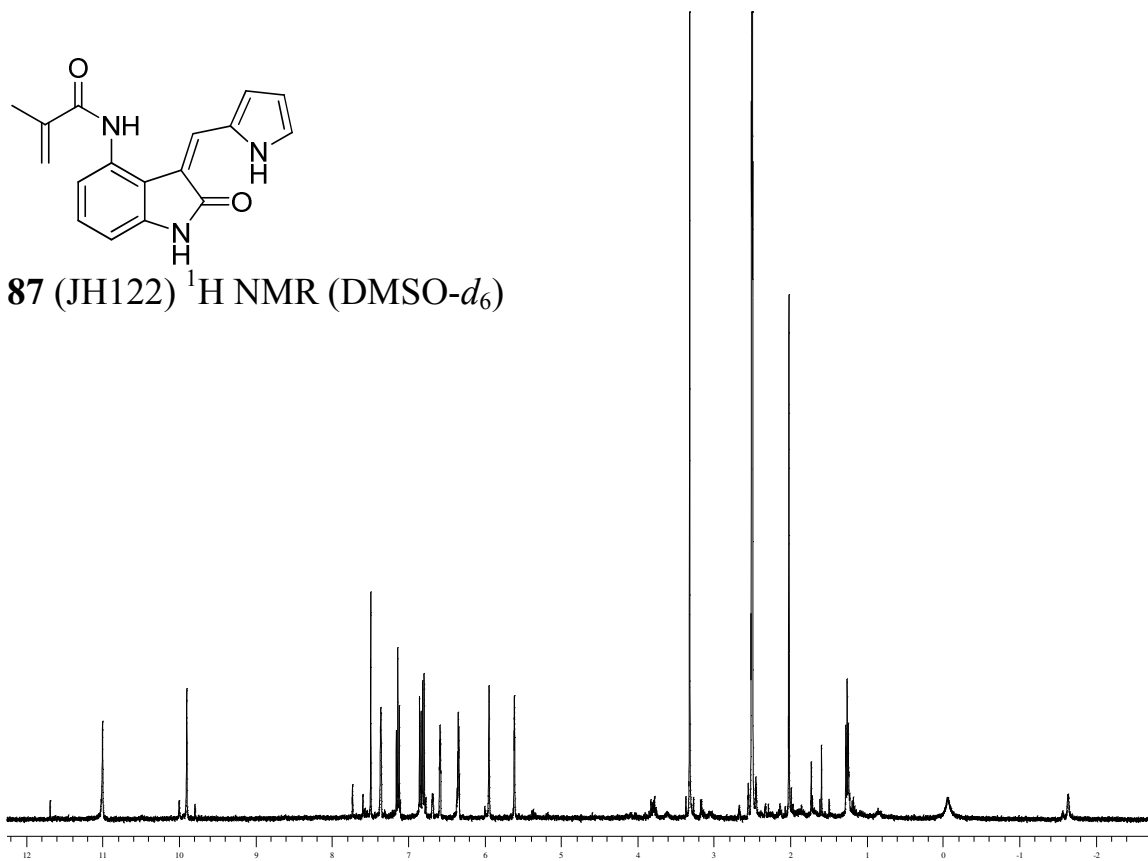


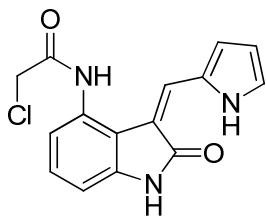


86 (JH121) ^1H NMR (DMSO- d_6)

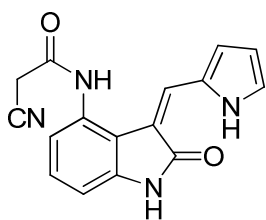
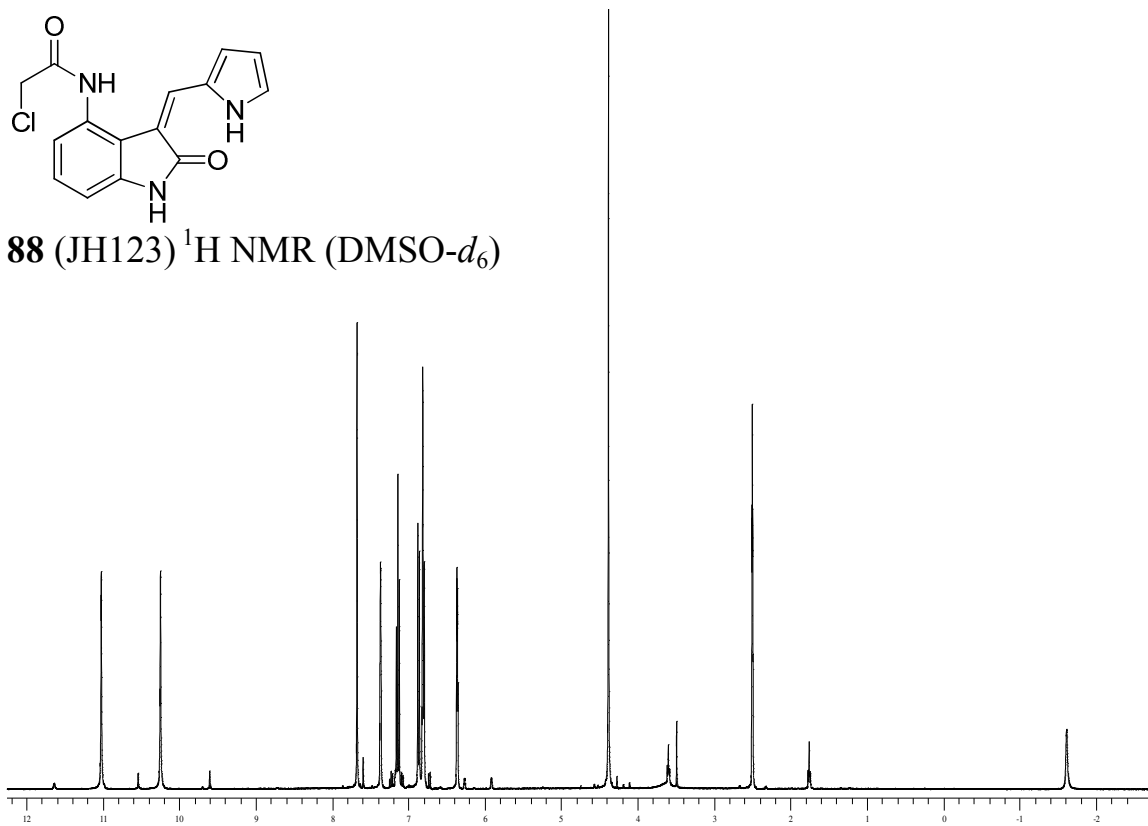


87 (JH122) ^1H NMR (DMSO- d_6)

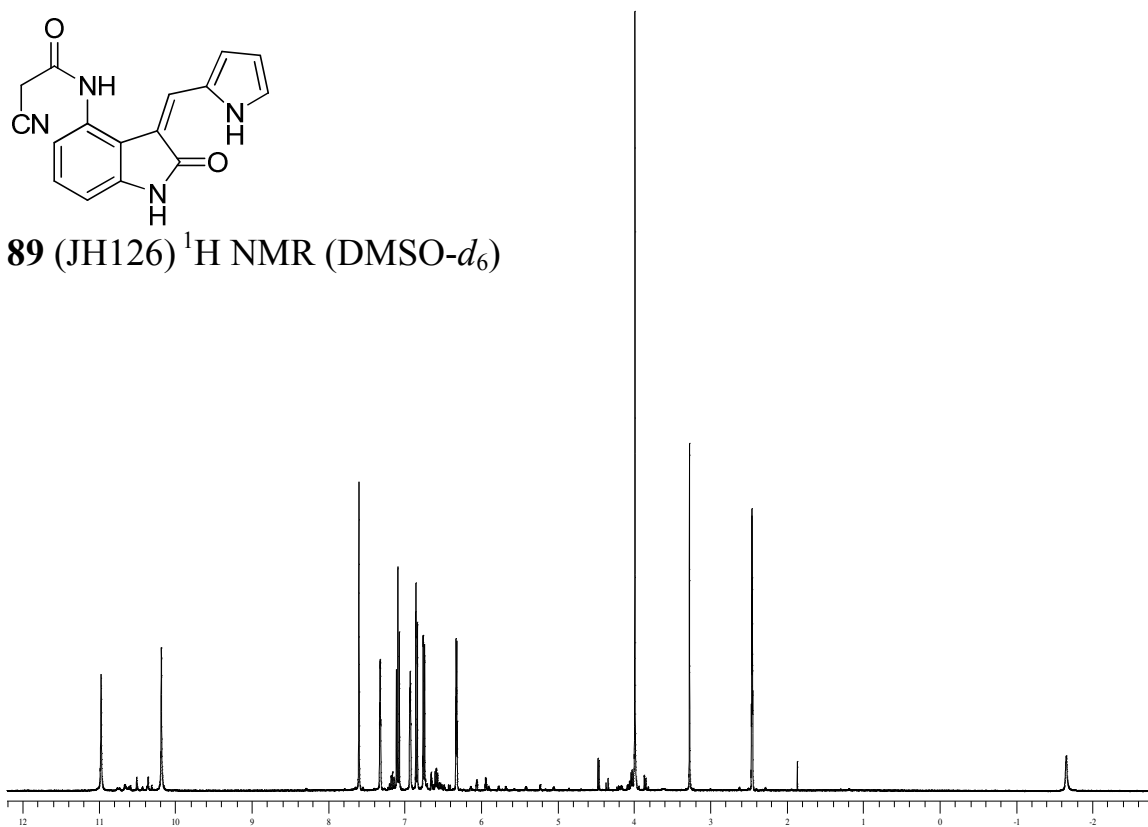


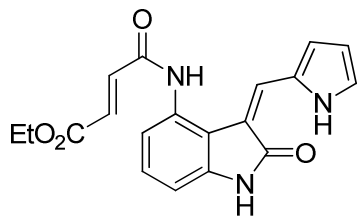


88 (JH123) ^1H NMR (DMSO- d_6)

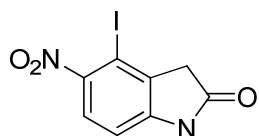
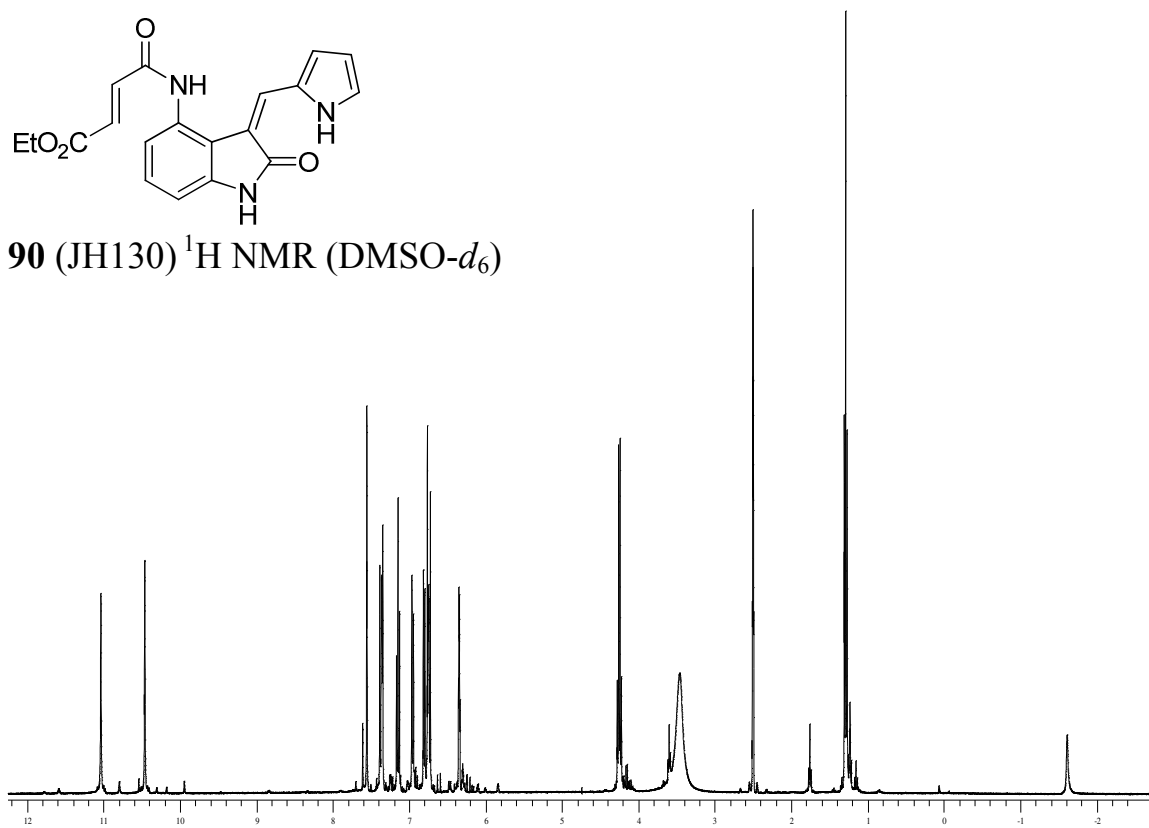


89 (JH126) ^1H NMR (DMSO- d_6)

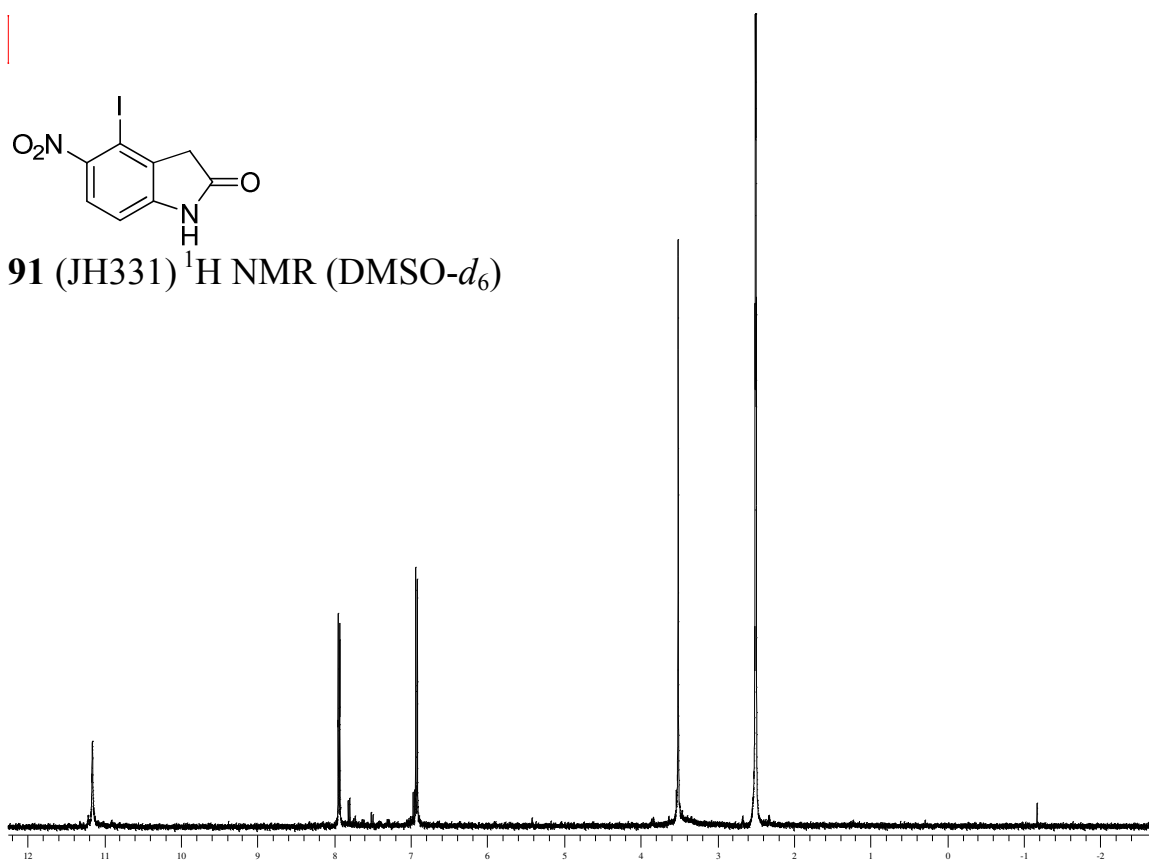


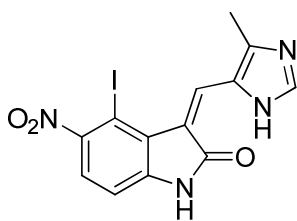


90 (JH130) ^1H NMR (DMSO- d_6)

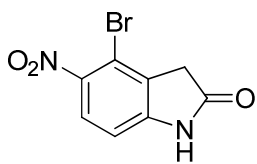
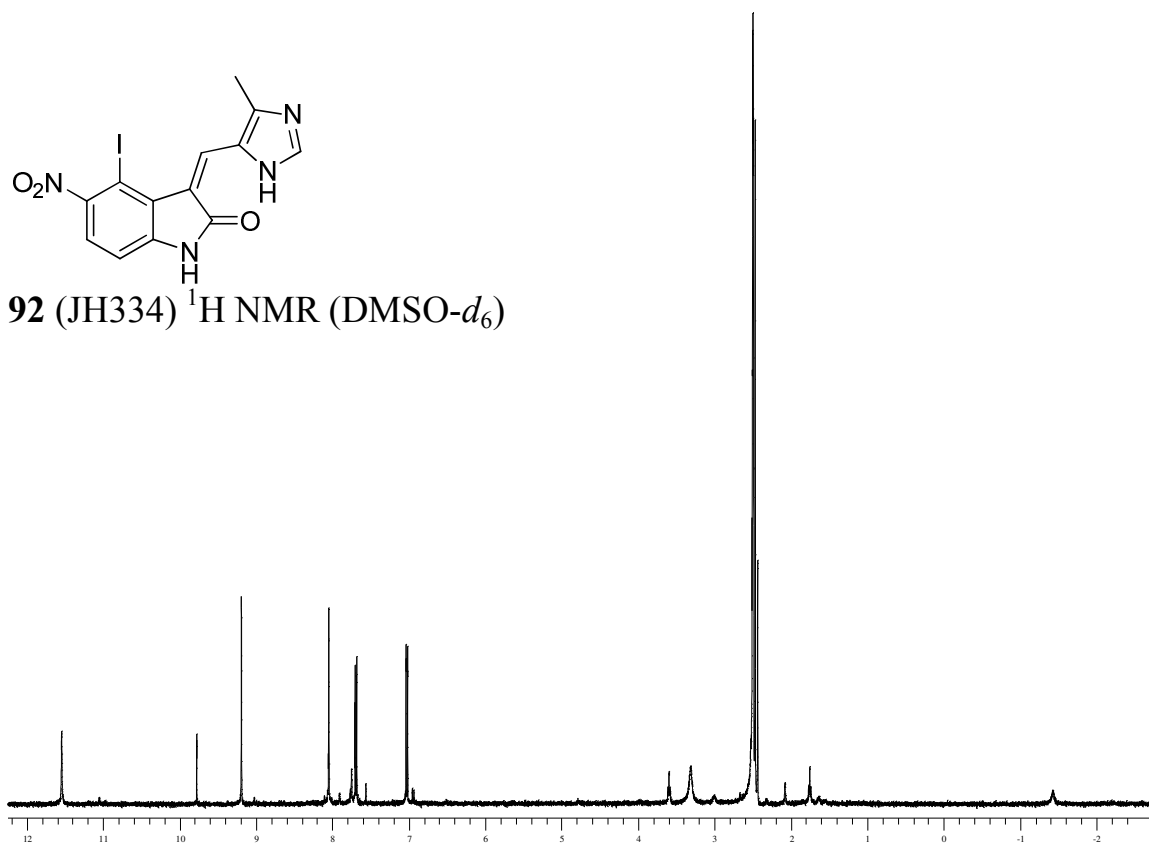


91 (JH331) ^1H NMR (DMSO- d_6)

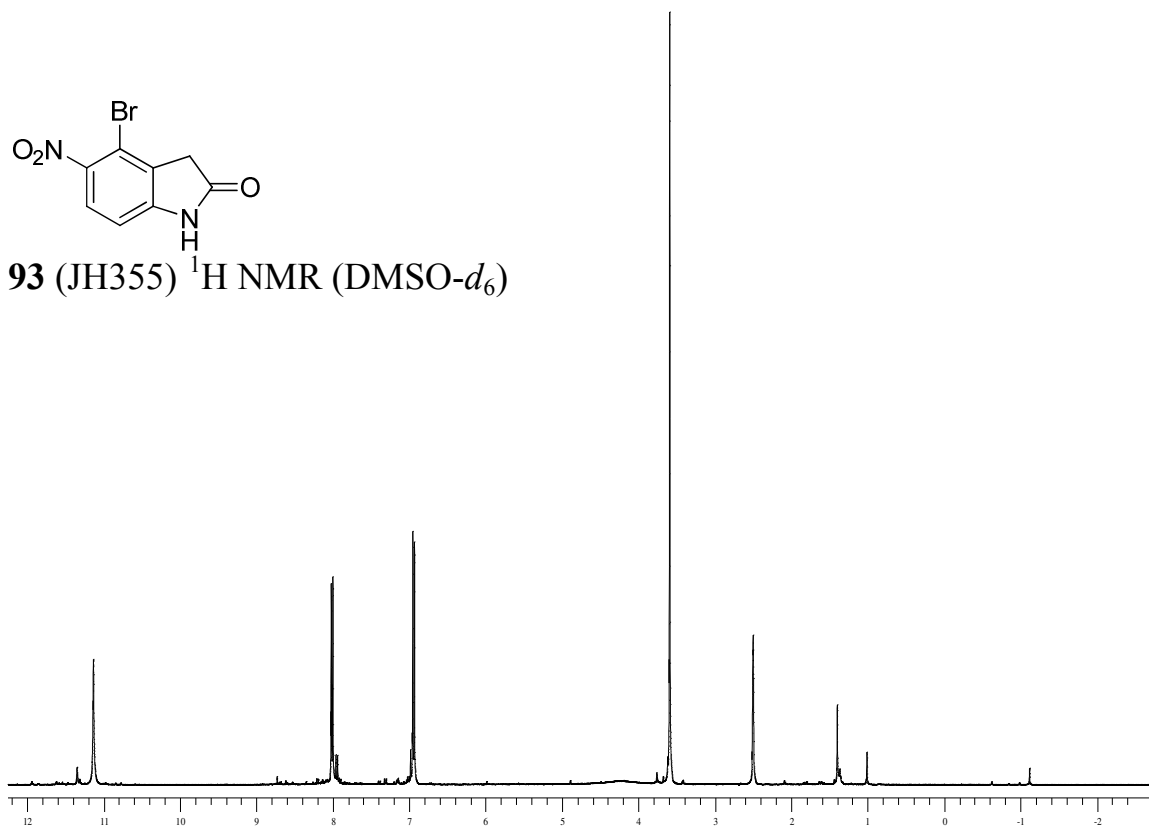


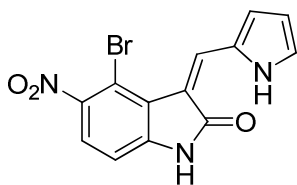


92 (JH334) ^1H NMR (DMSO- d_6)

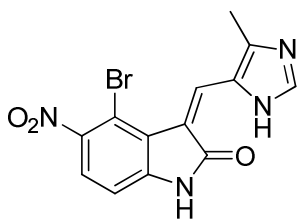
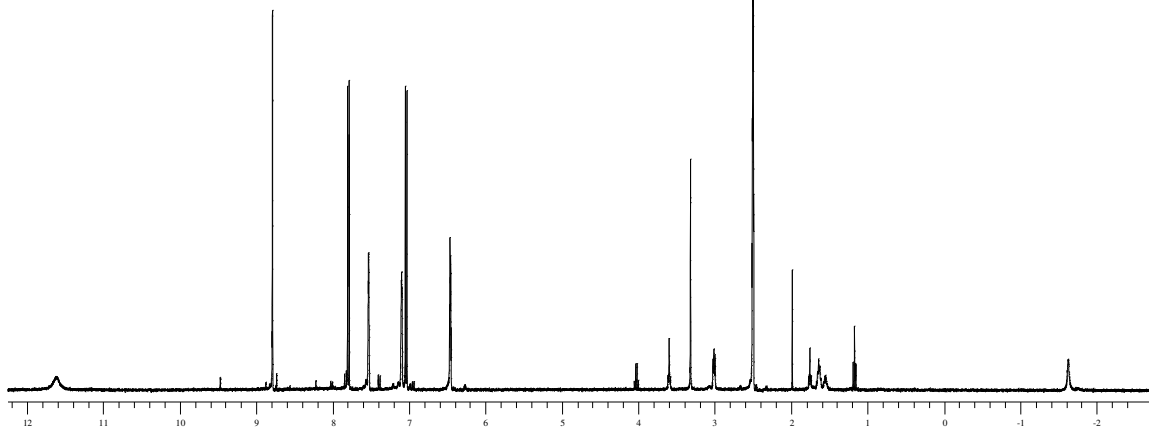


93 (JH355) ^1H NMR (DMSO- d_6)

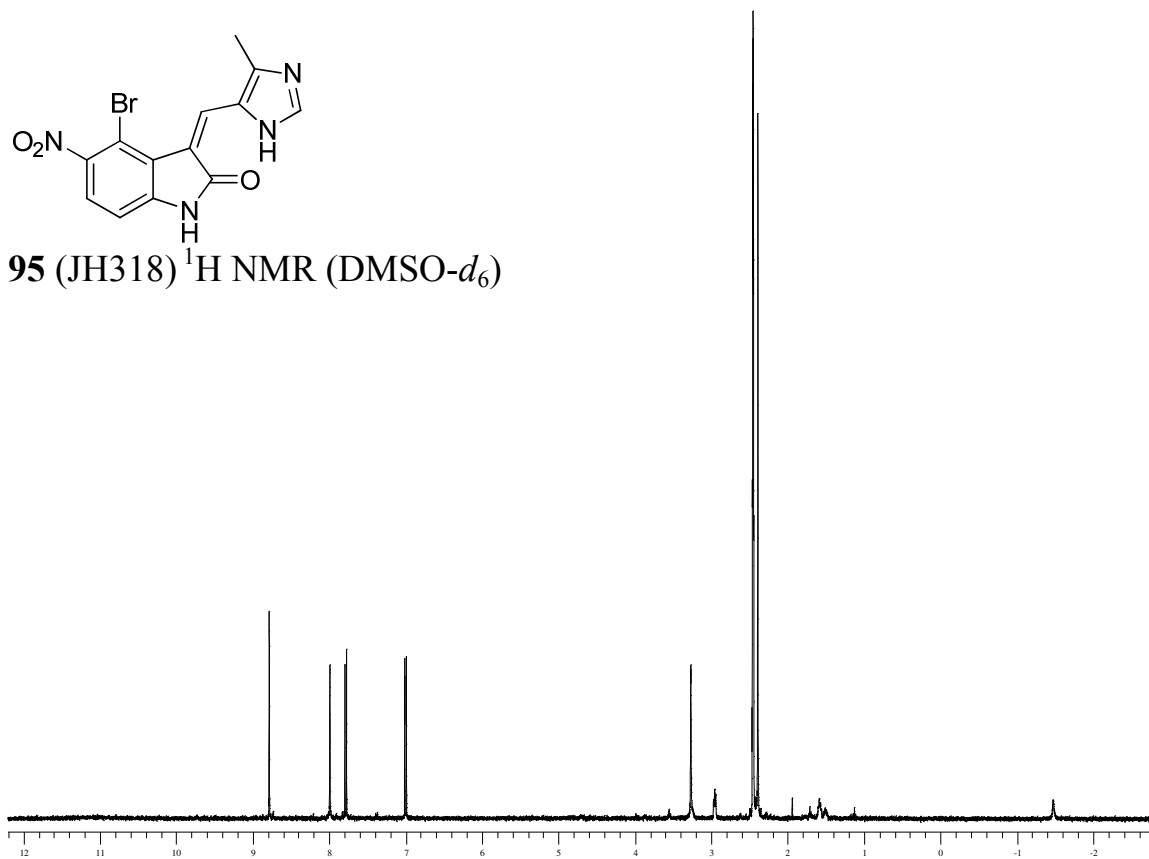


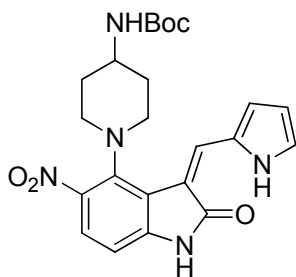


94 (JH319) ^1H NMR (DMSO- d_6)
EtOAc: 1.13 (t), 1.94 (s), 3.98 (q)

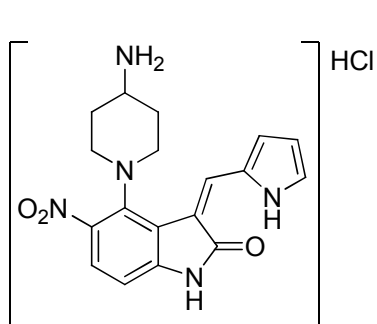
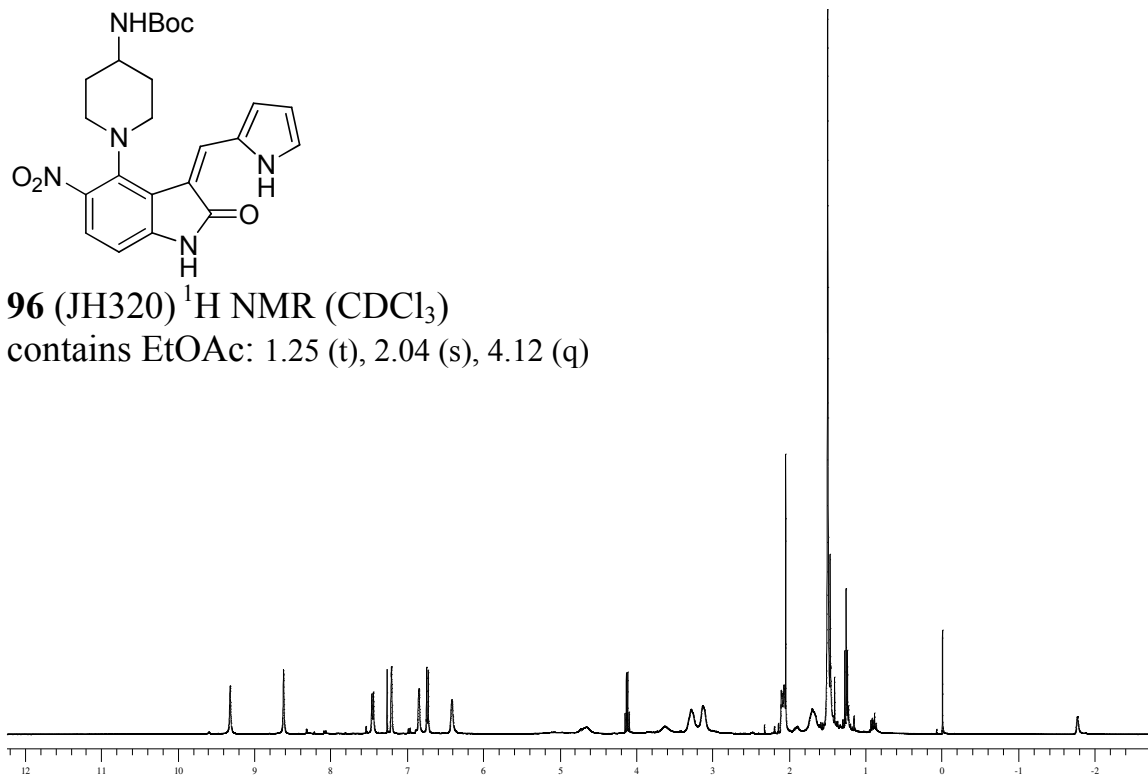


95 (JH318) ^1H NMR (DMSO- d_6)

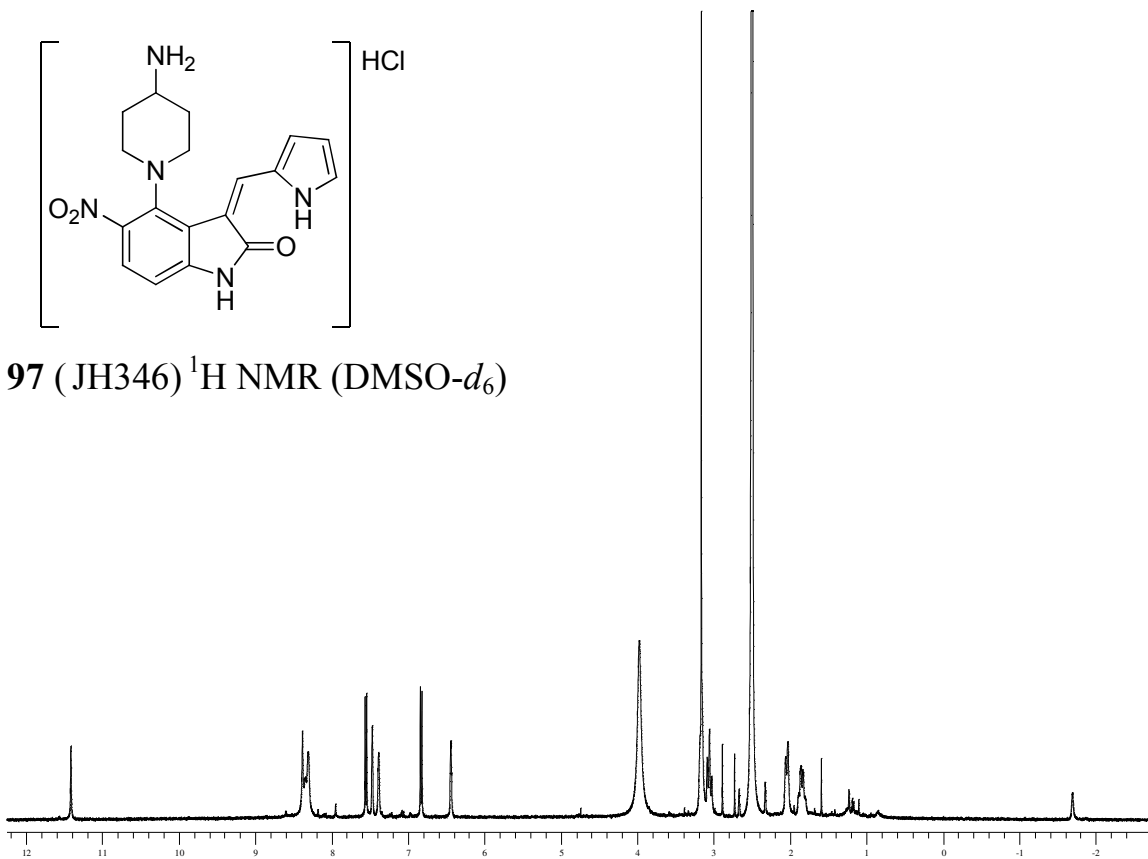


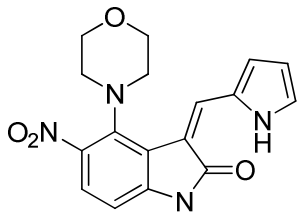


96 (JH320) ^1H NMR (CDCl_3)
contains EtOAc: 1.25 (t), 2.04 (s), 4.12 (q)

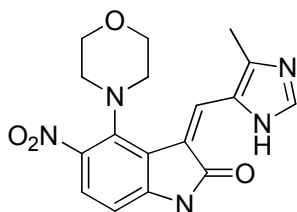
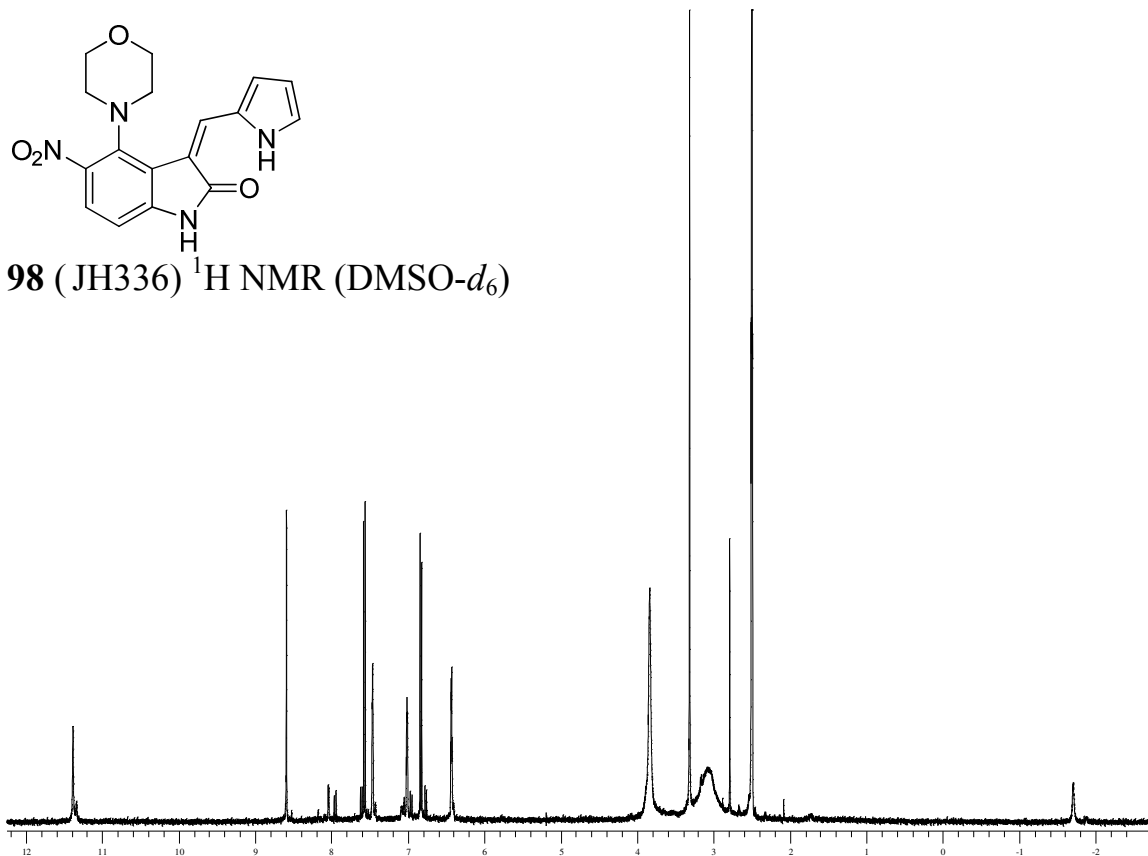


97 (JH346) ^1H NMR ($\text{DMSO}-d_6$)

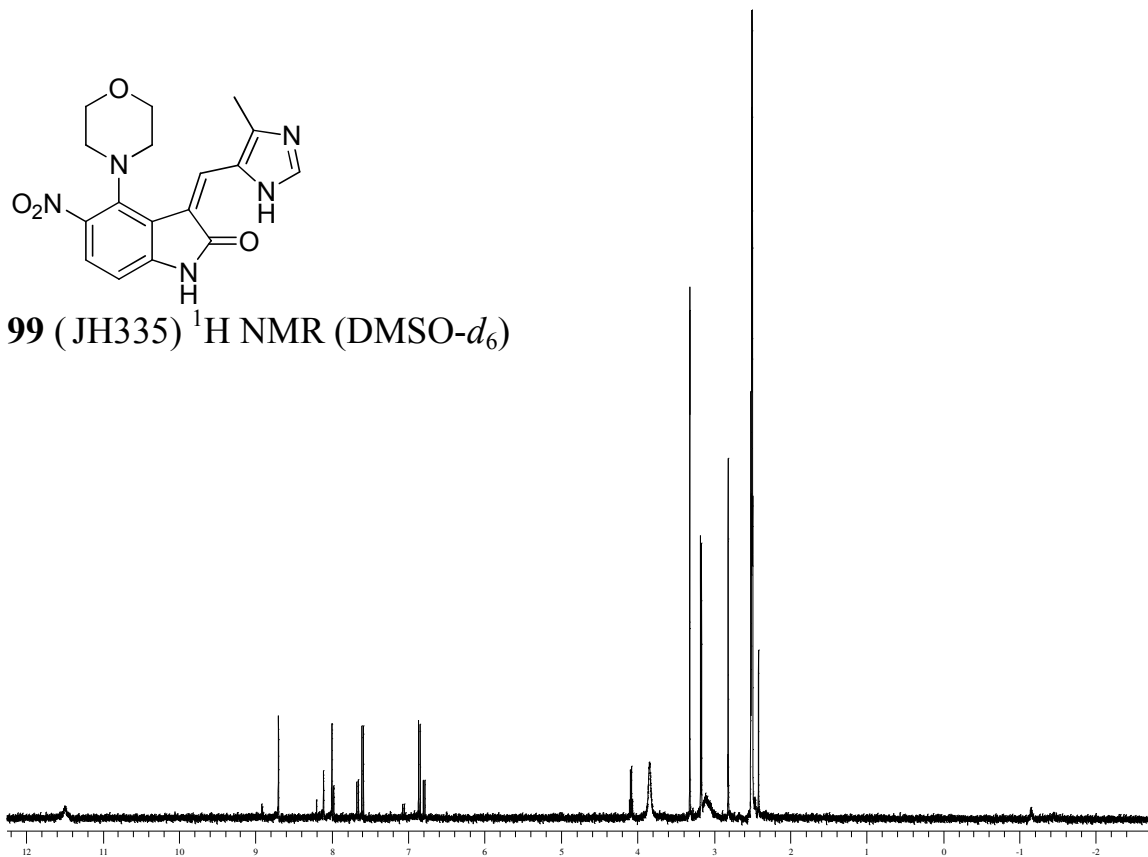


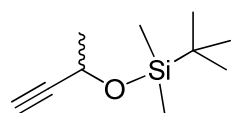


98 (JH336) ^1H NMR (DMSO- d_6)

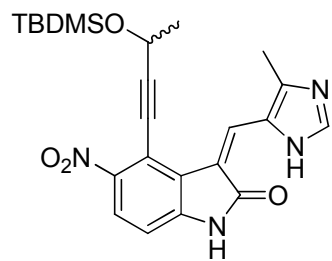
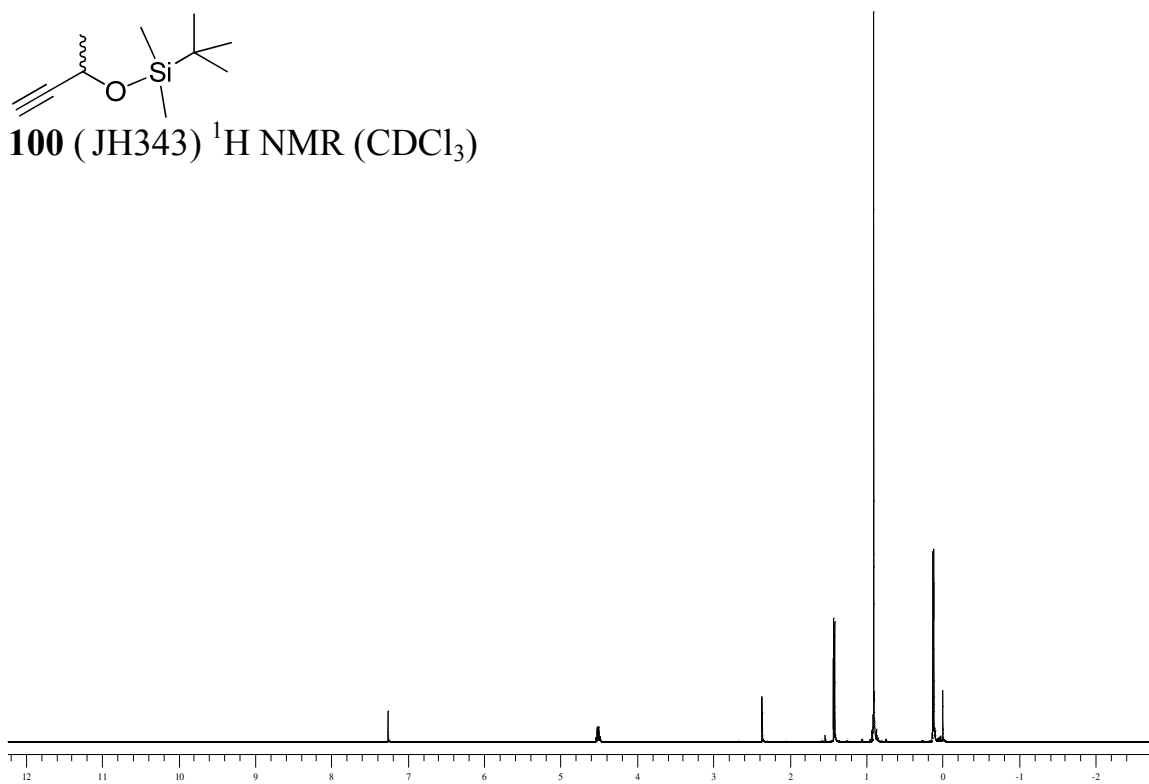


99 (JH335) ^1H NMR (DMSO- d_6)

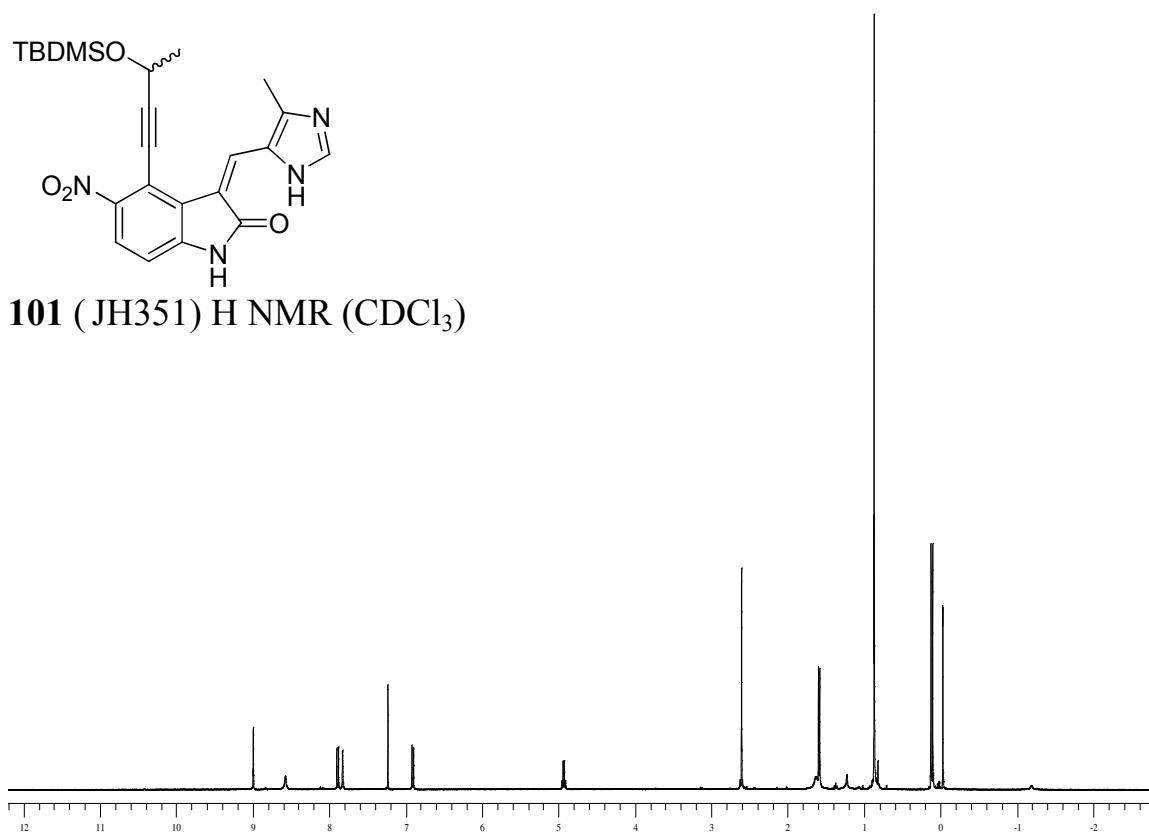


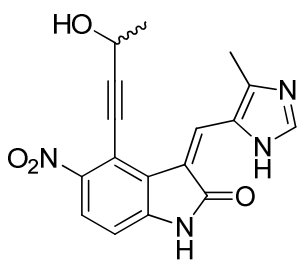


100 (JH343) ^1H NMR (CDCl_3)

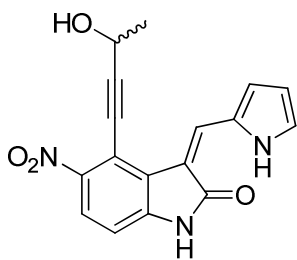
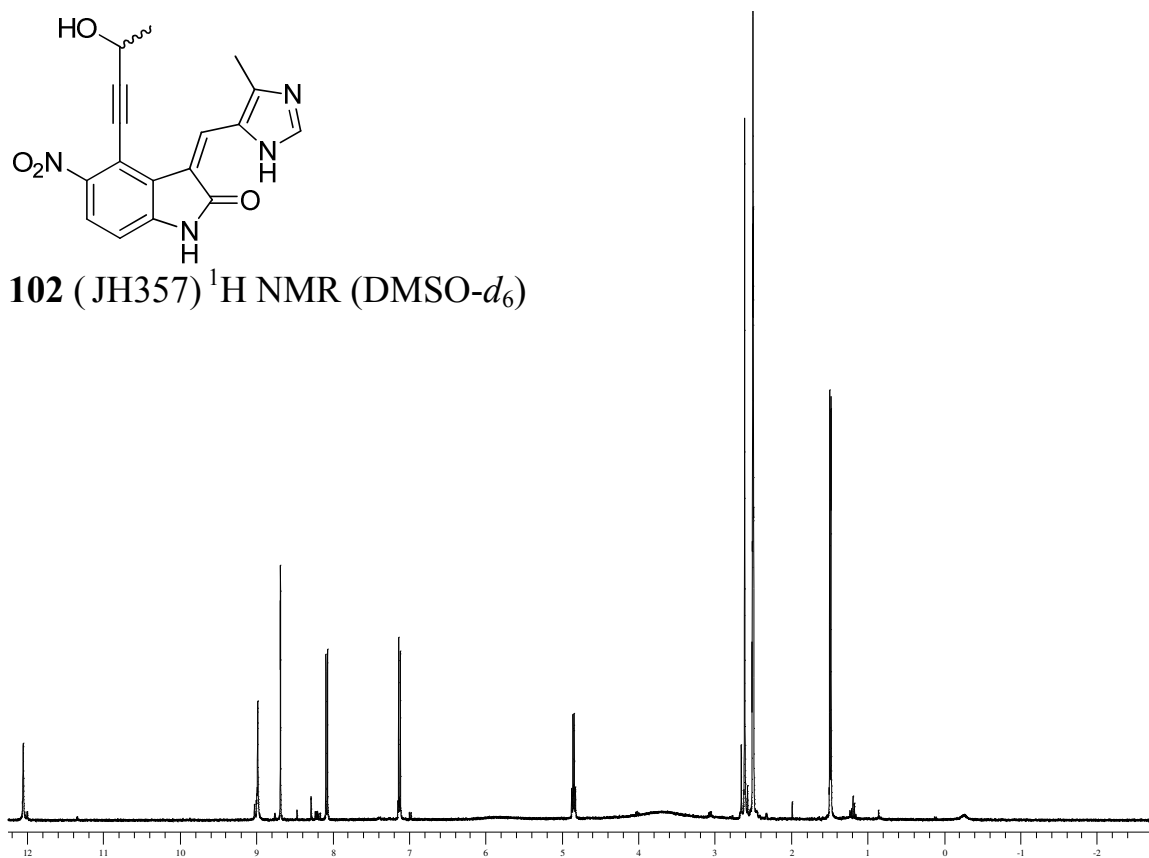


101 (JH351) ^1H NMR (CDCl_3)

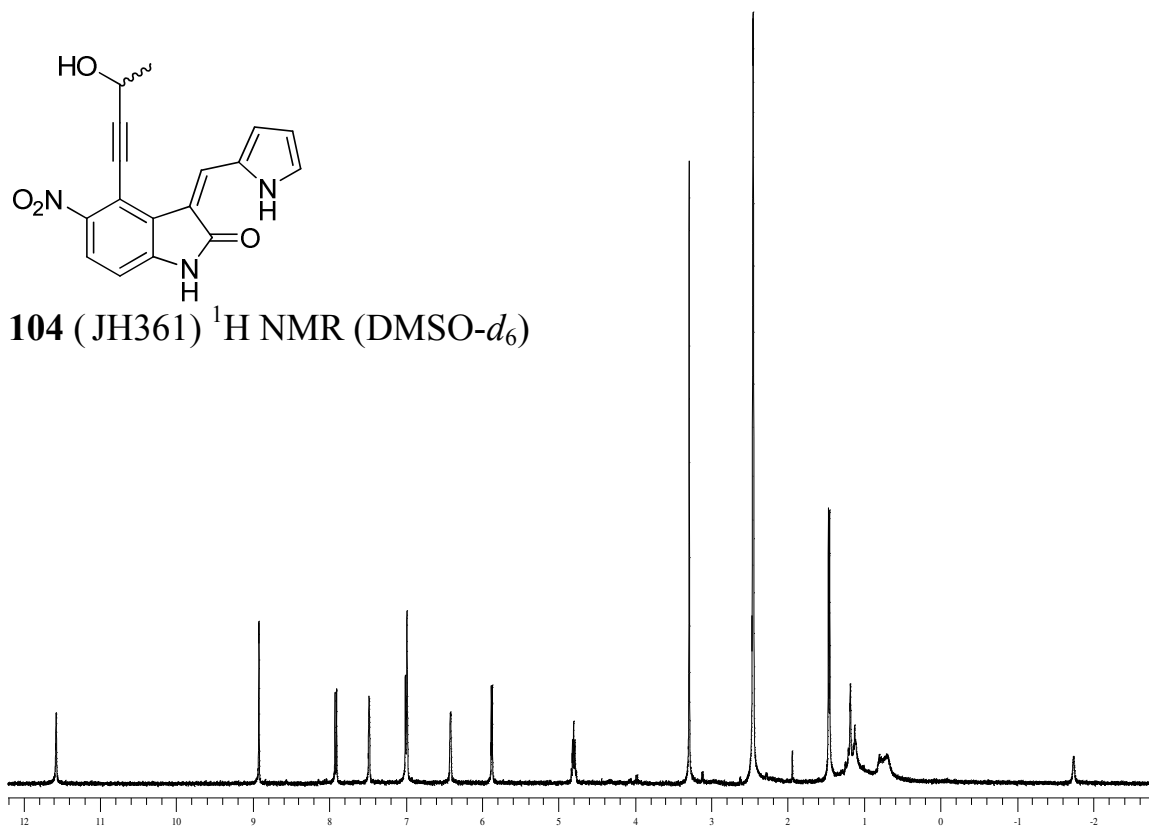


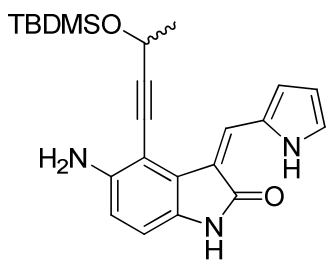


102 (JH357) ¹H NMR (DMSO-*d*₆)

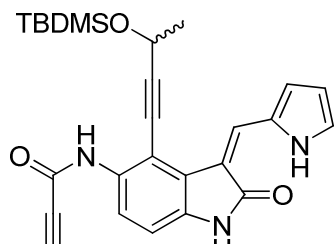
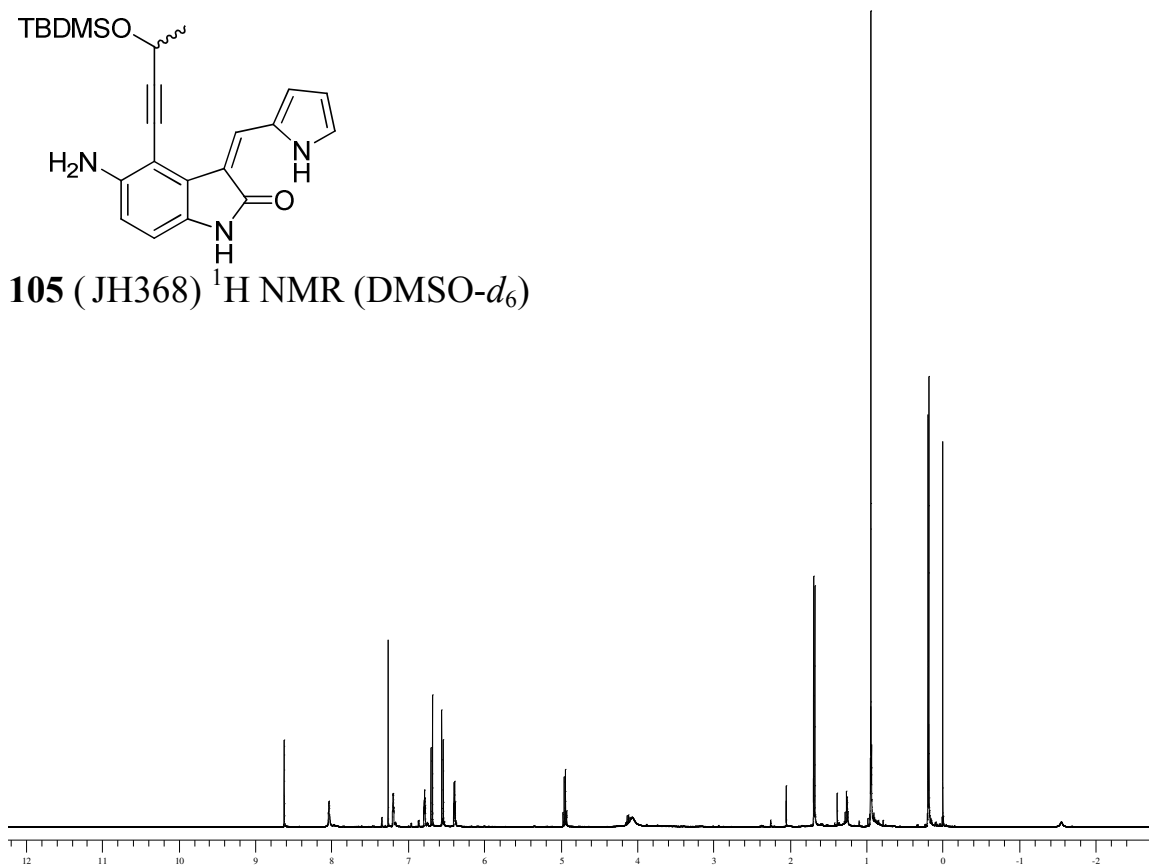


104 (JH361) ¹H NMR (DMSO-*d*₆)

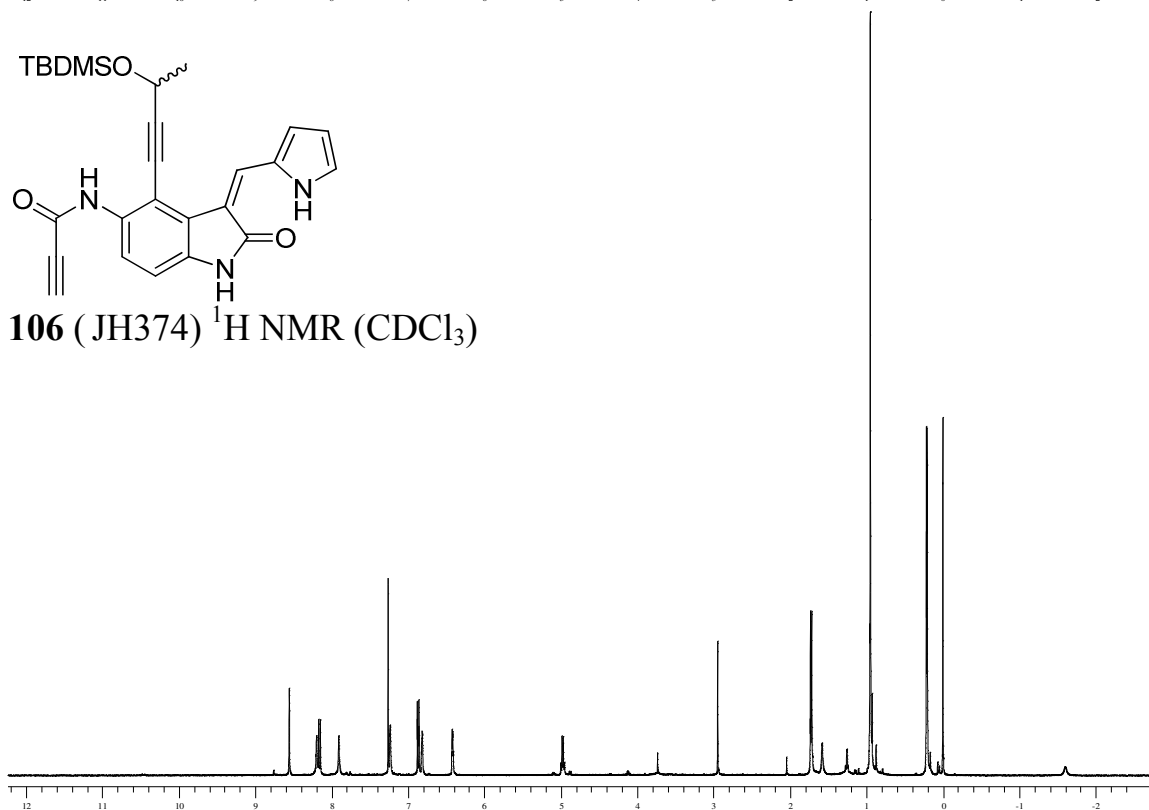


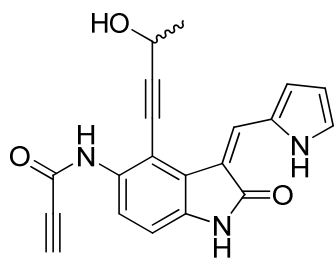


105 (JH368) ^1H NMR ($\text{DMSO}-d_6$)

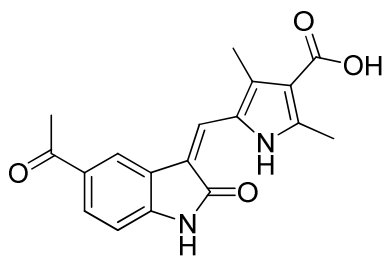
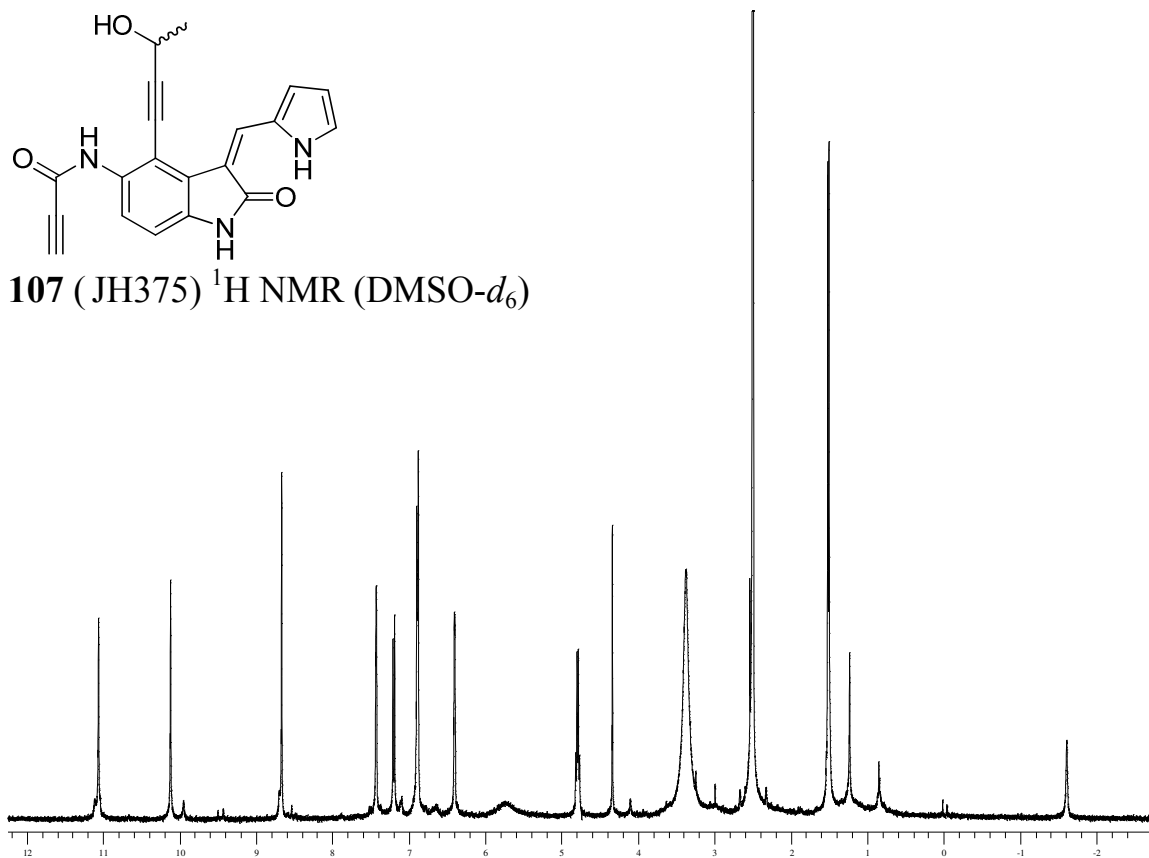


106 (JH374) ^1H NMR (CDCl_3)

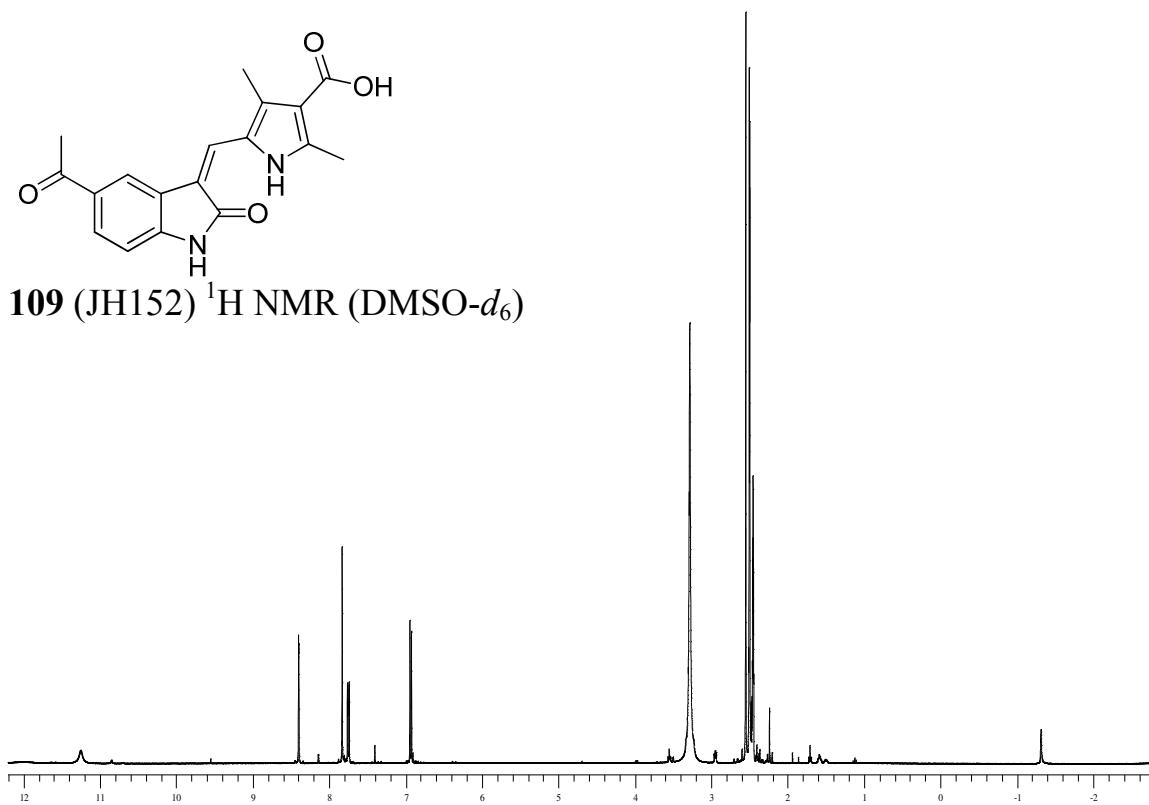


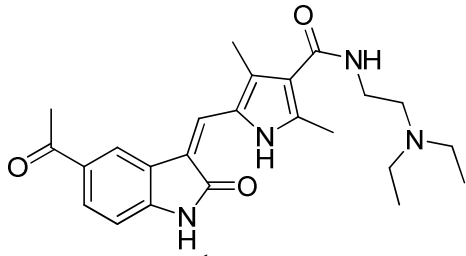


107 (JH375) ^1H NMR (DMSO- d_6)

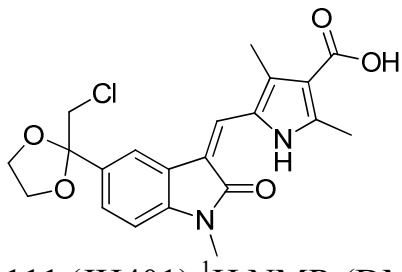
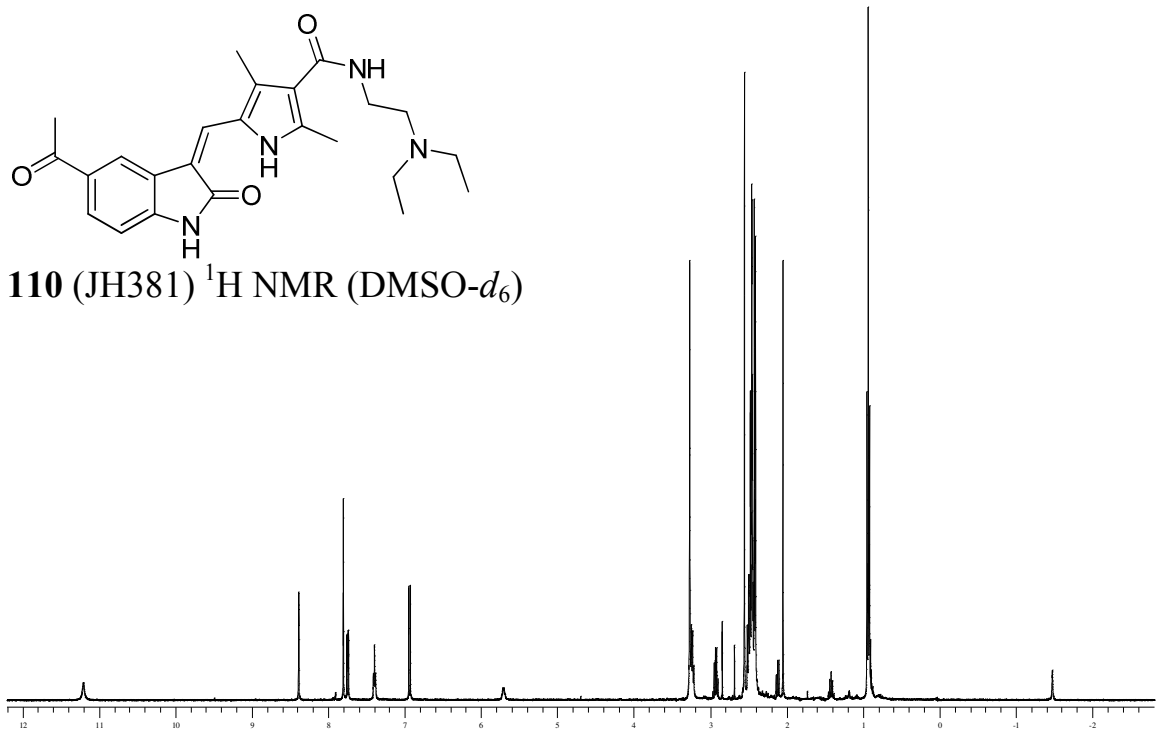


109 (JH152) ^1H NMR (DMSO- d_6)

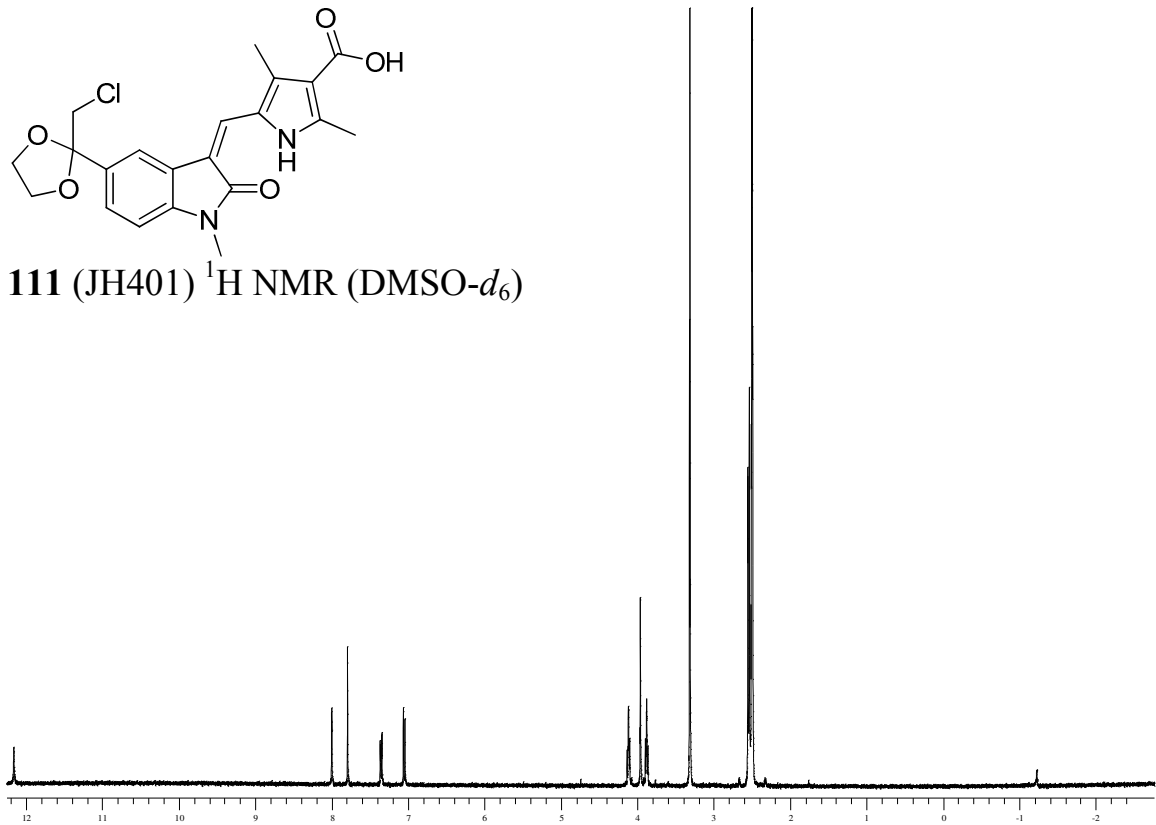


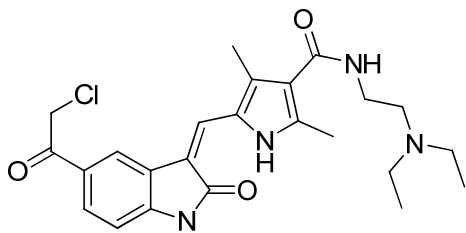


110 (JH381) ^1H NMR (DMSO- d_6)

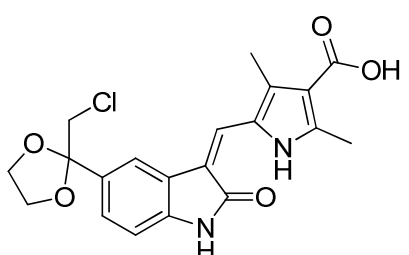
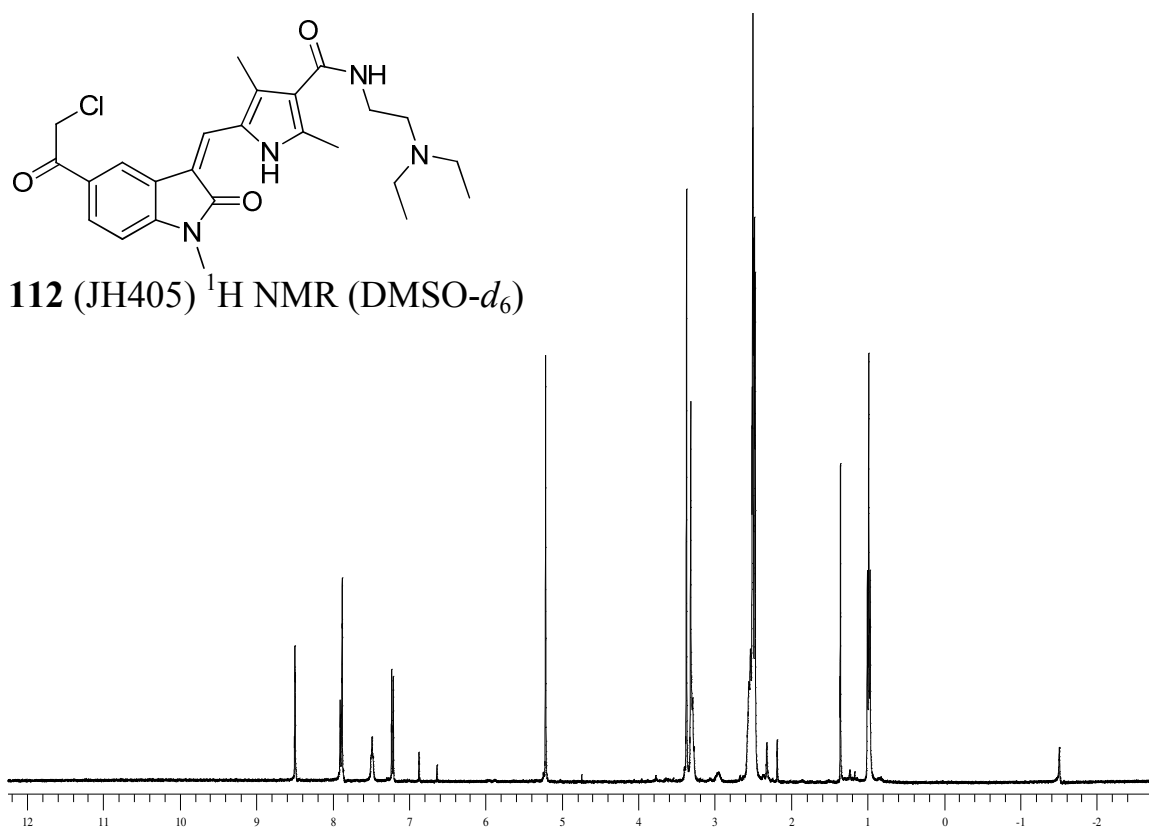


111 (JH401) ^1H NMR (DMSO- d_6)

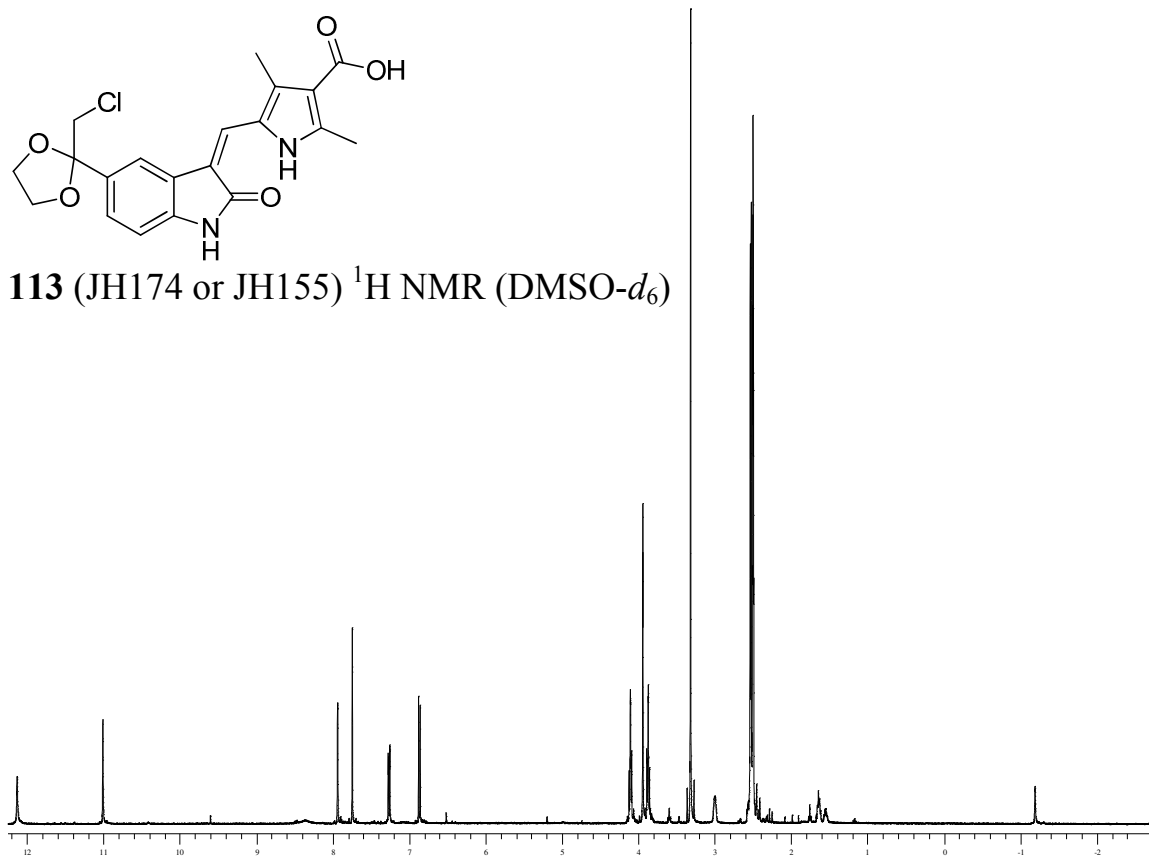


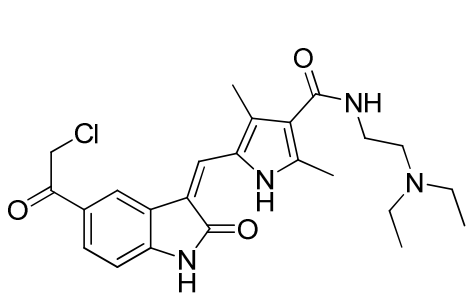


112 (JH405) ^1H NMR (DMSO- d_6)

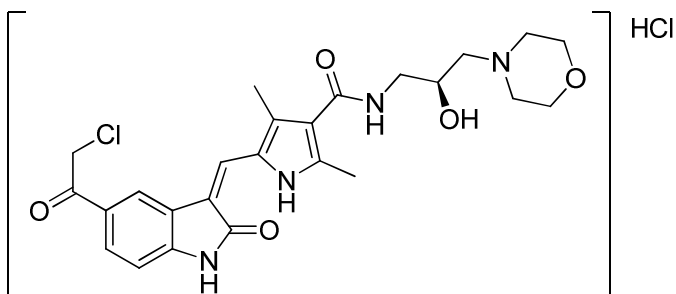
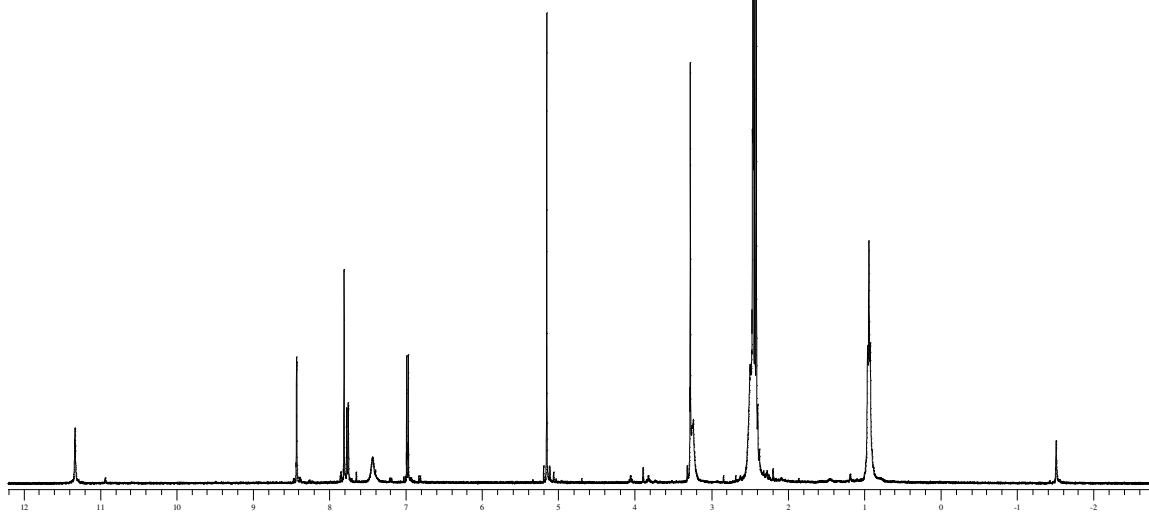


113 (JH174 or JH155) ^1H NMR (DMSO- d_6)

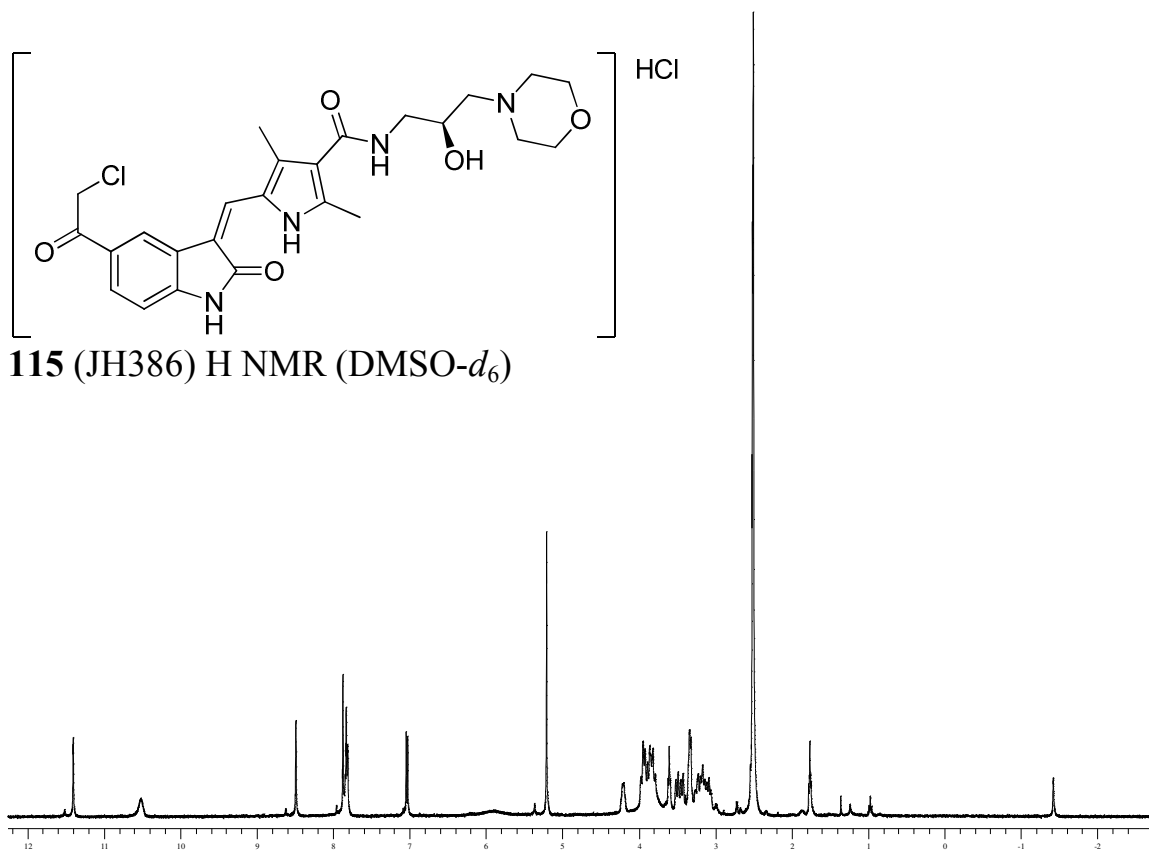


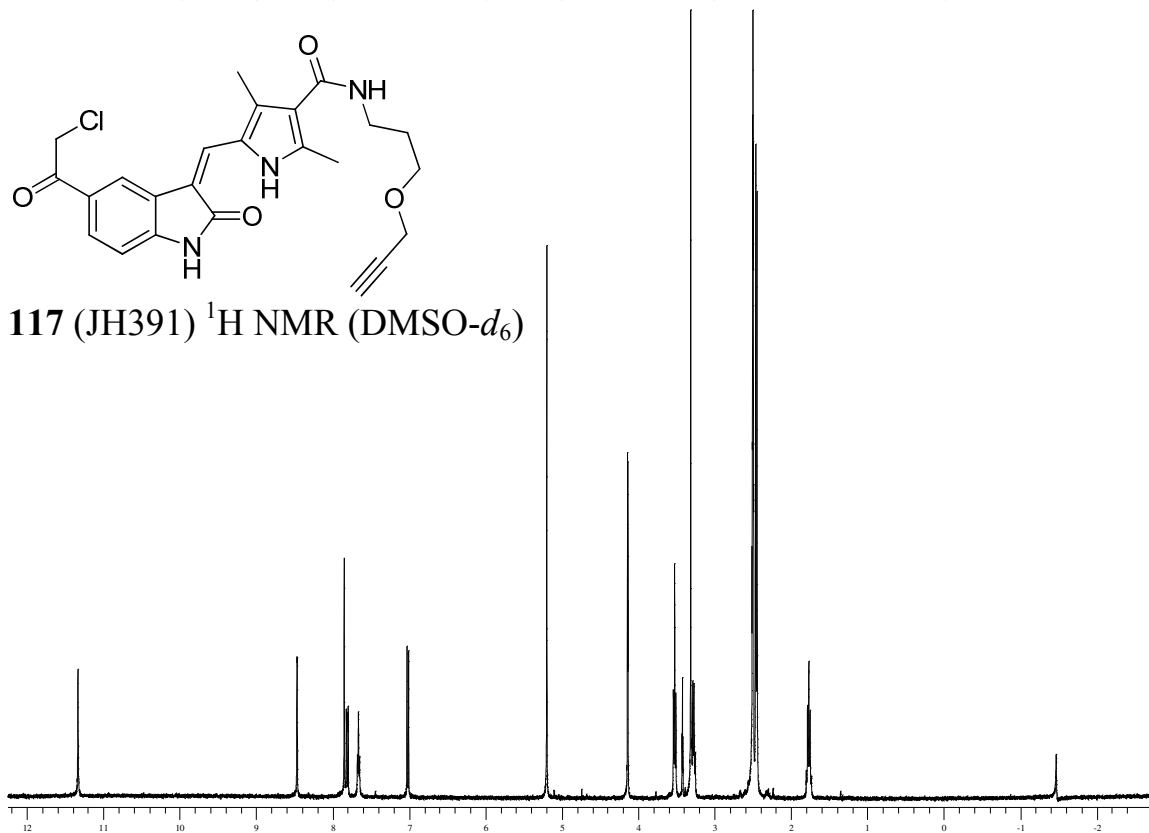
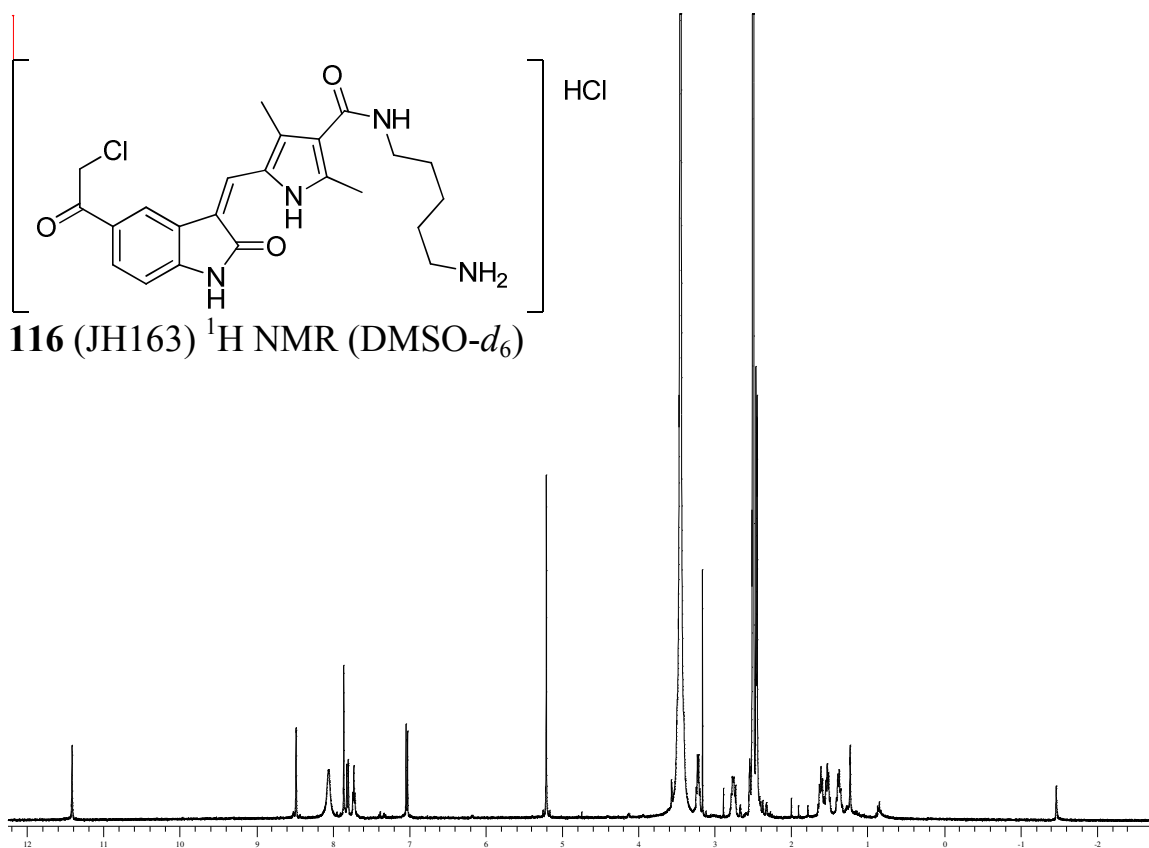


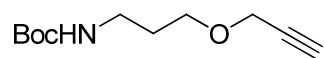
114 (JH175) ^1H NMR (DMSO- d_6)



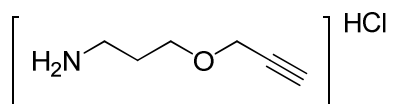
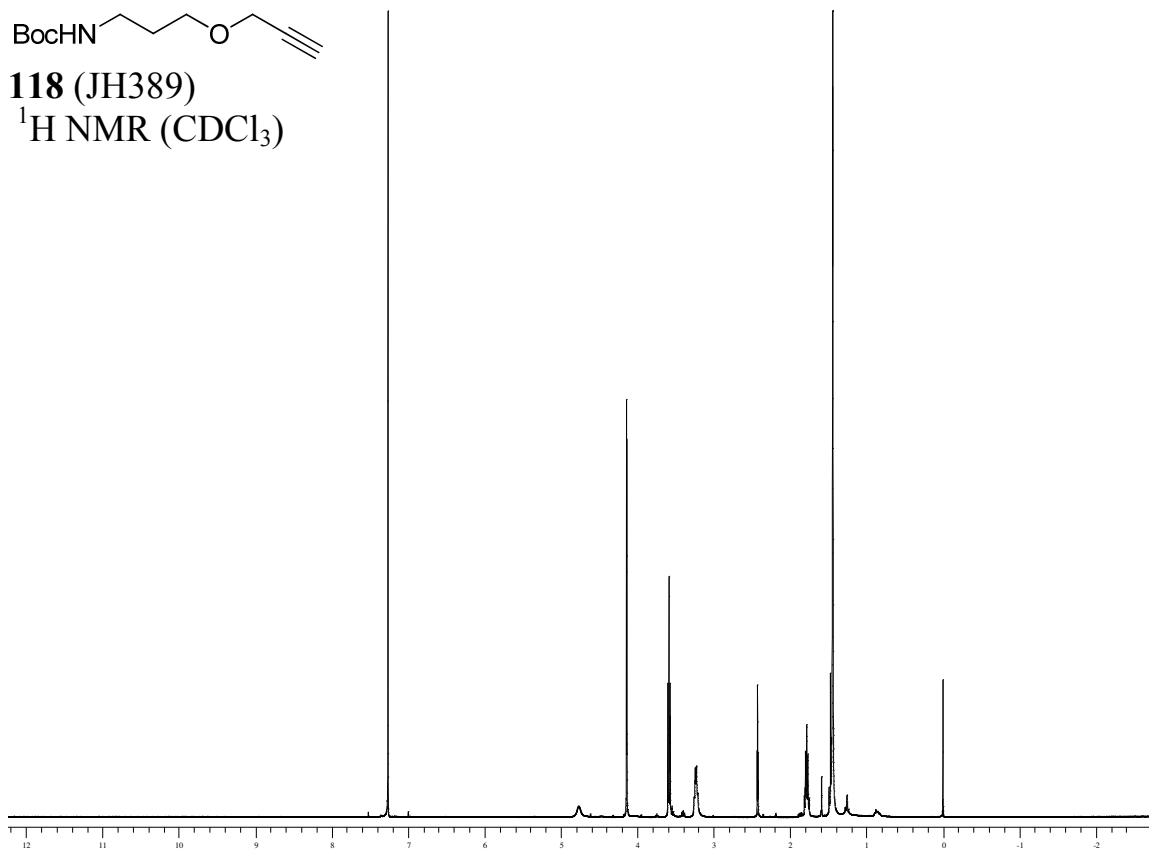
115 (JH386) ^1H NMR (DMSO- d_6)



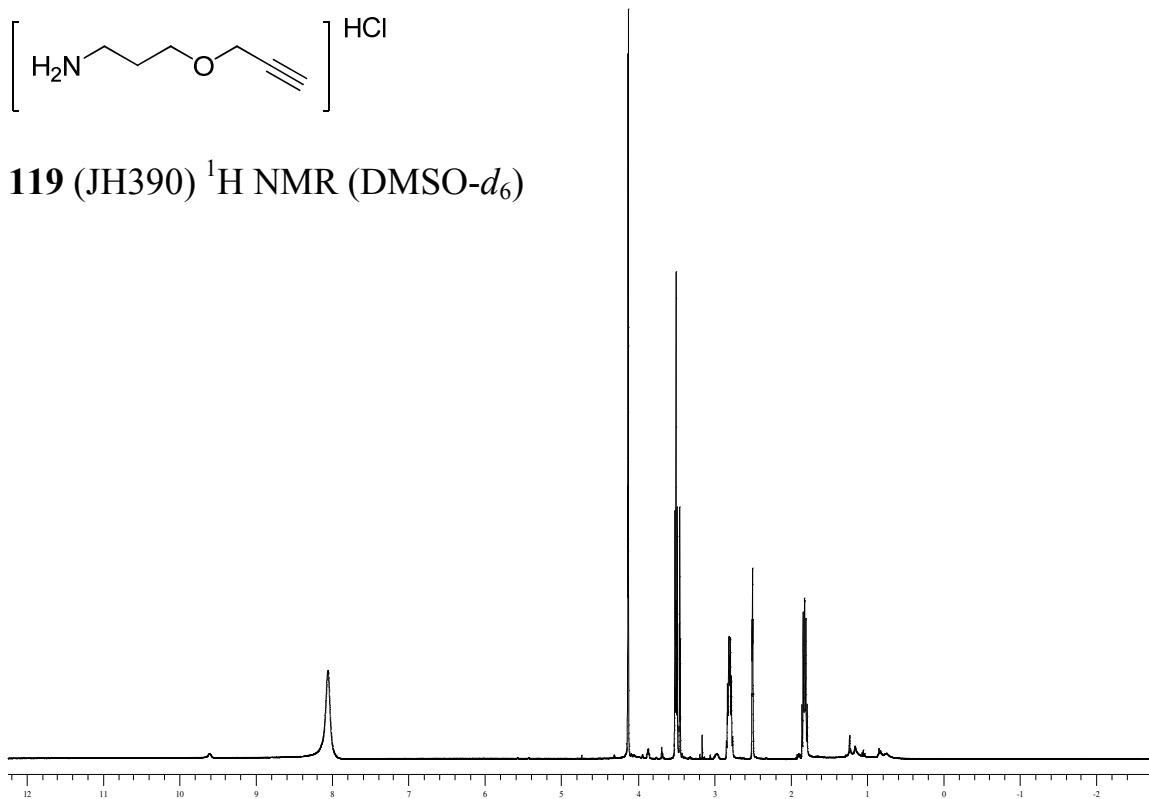


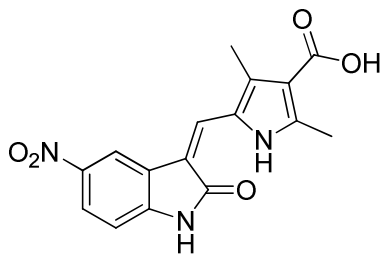


118 (JH389)
 ^1H NMR (CDCl_3)

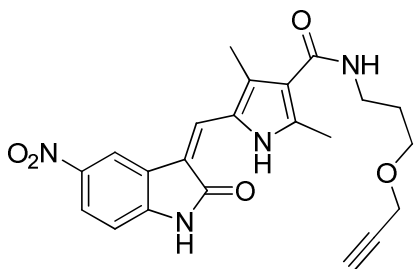
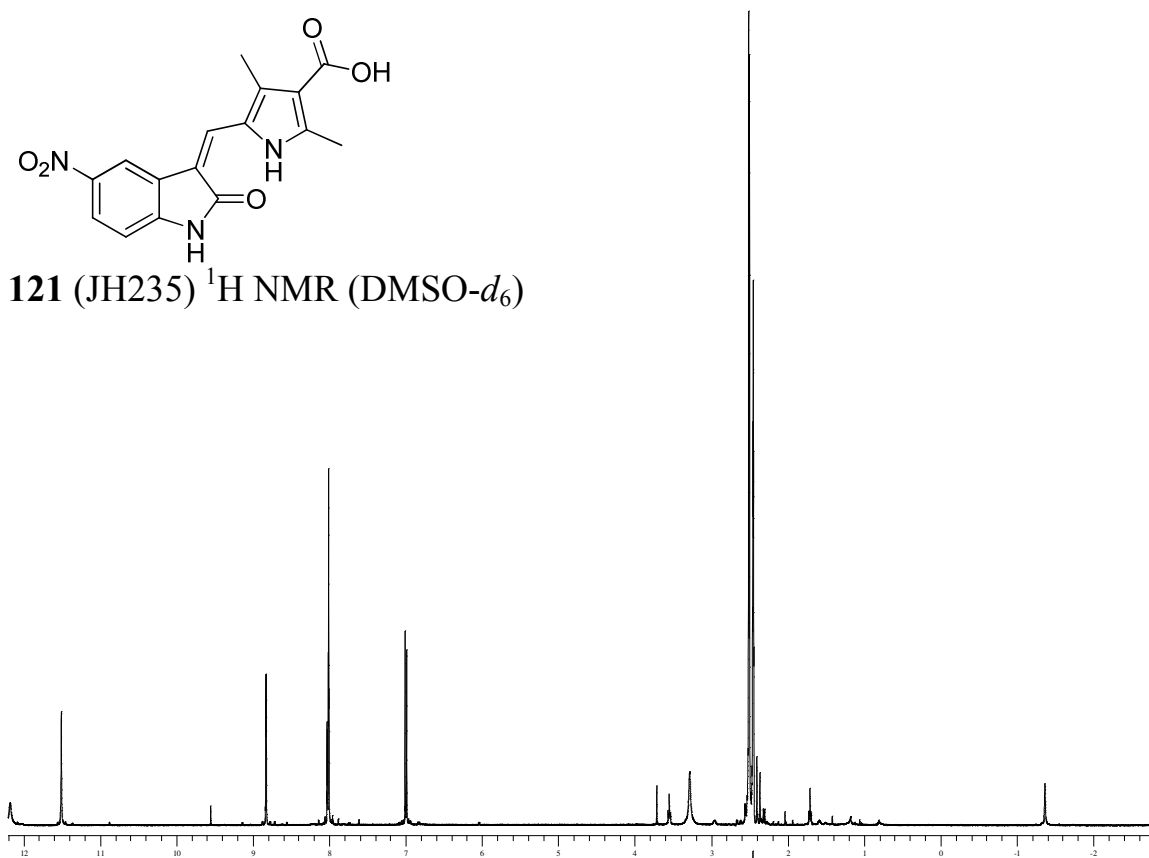


119 (JH390) ^1H NMR ($\text{DMSO}-d_6$)

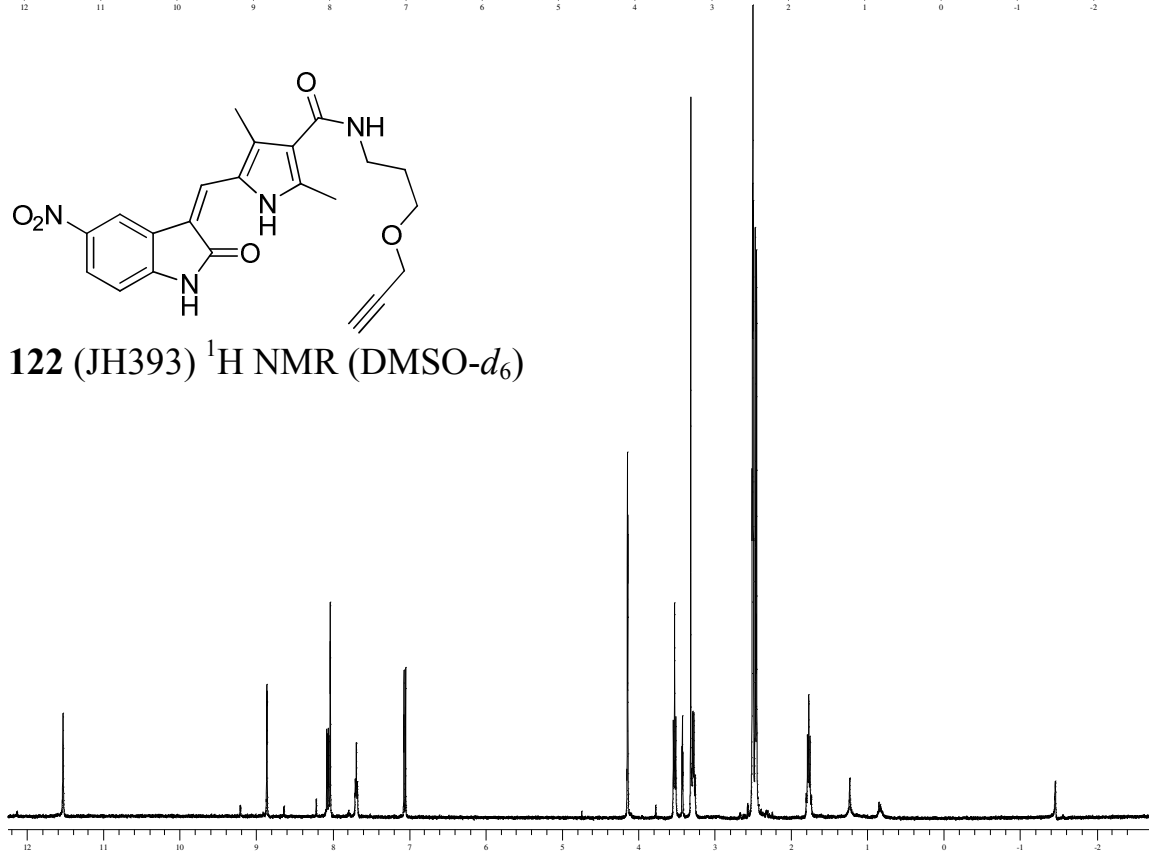


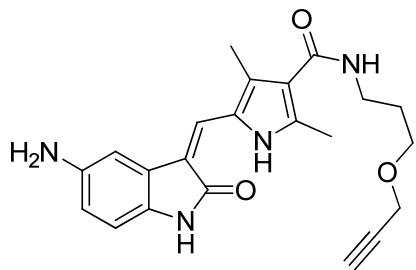


121 (JH235) ^1H NMR (DMSO- d_6)

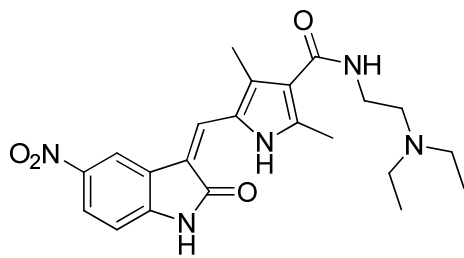
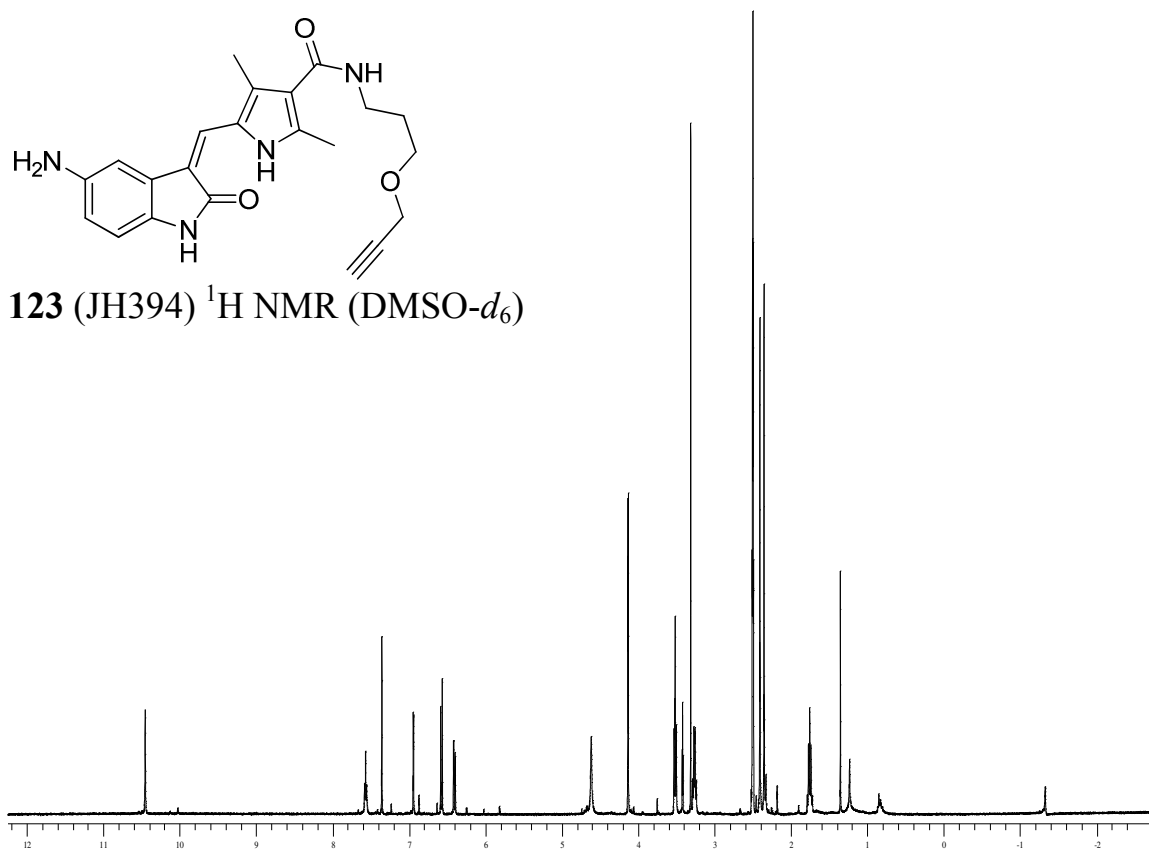


122 (JH393) ^1H NMR (DMSO- d_6)

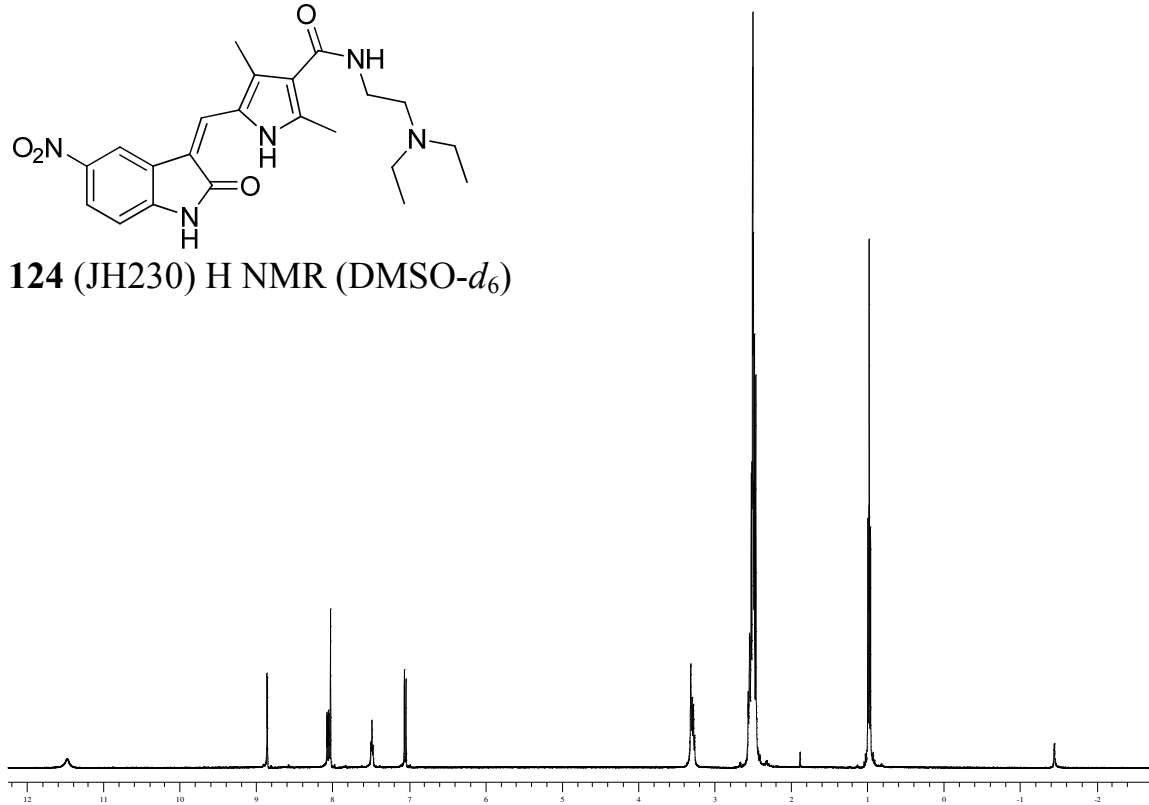


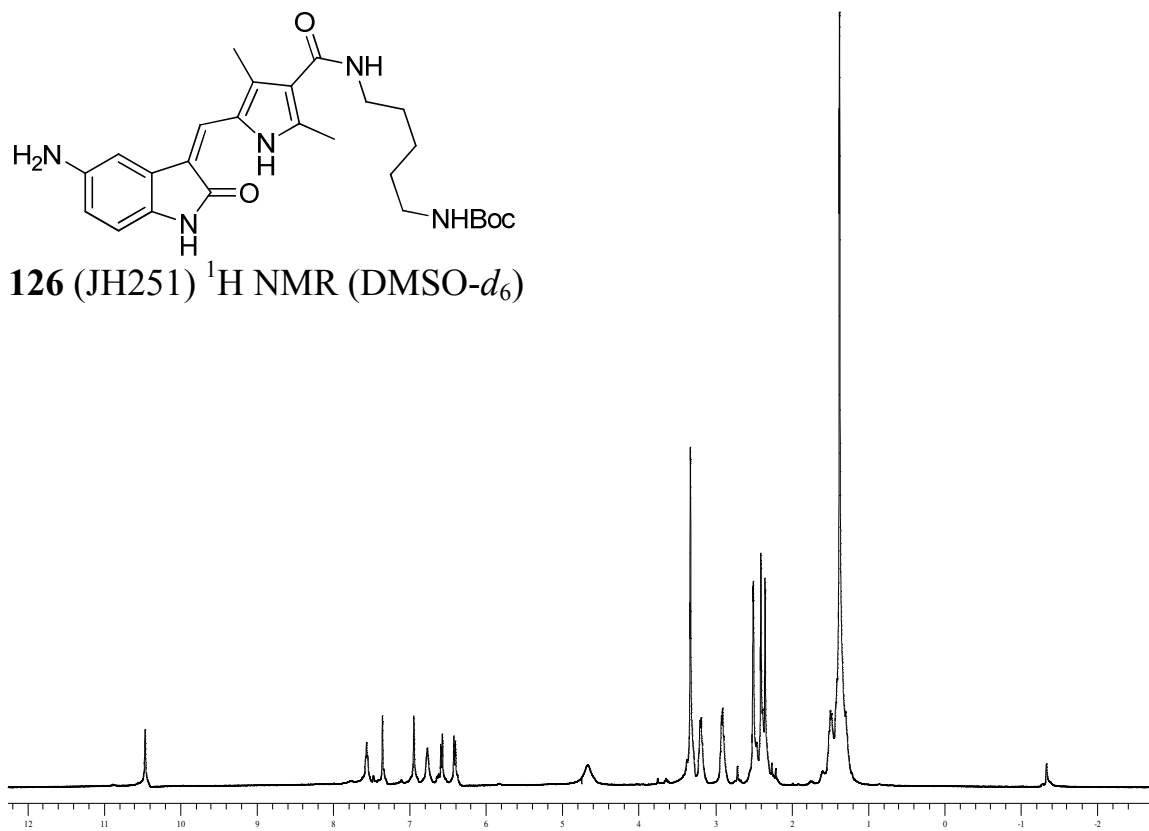
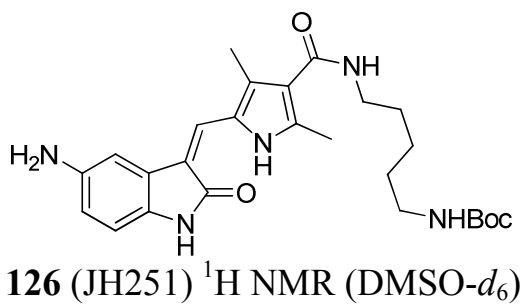
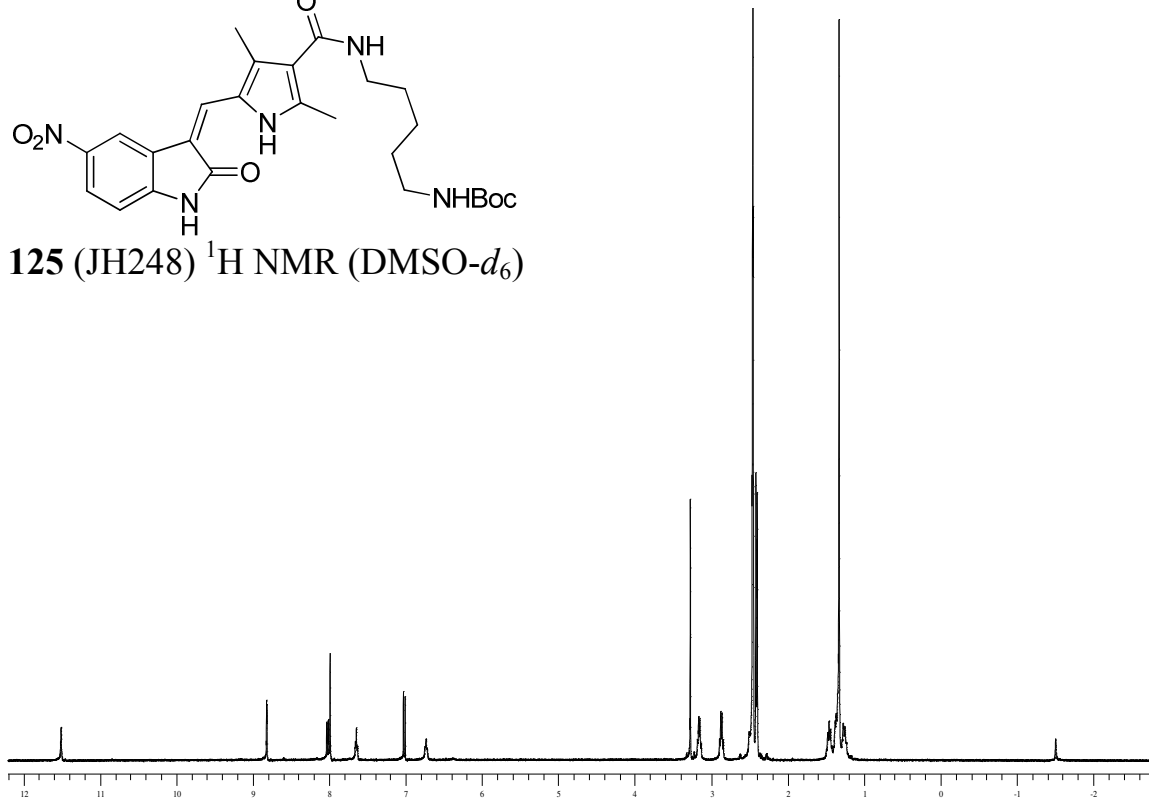
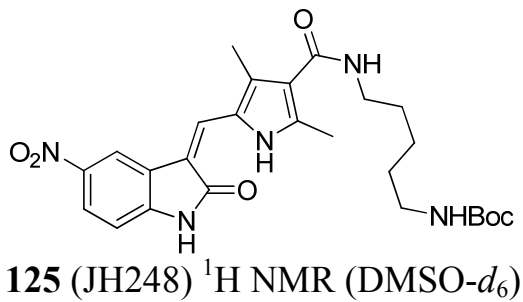


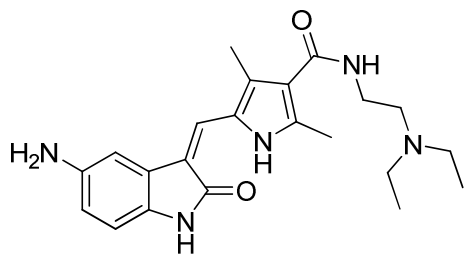
123 (JH394) ^1H NMR (DMSO- d_6)



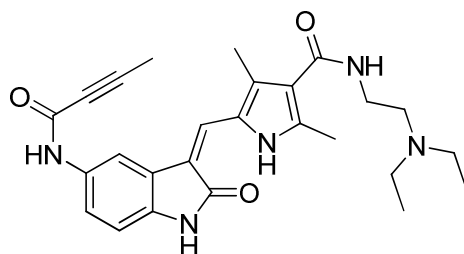
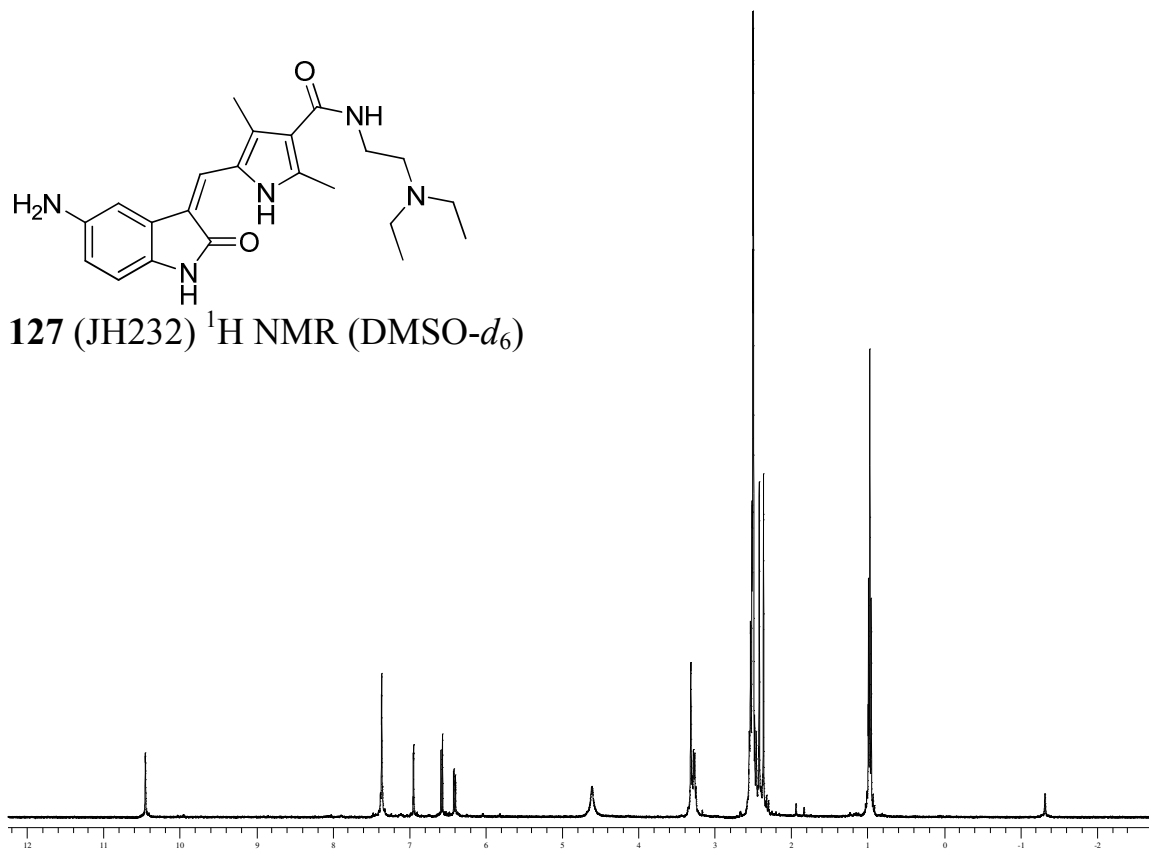
124 (JH230) ^1H NMR (DMSO- d_6)



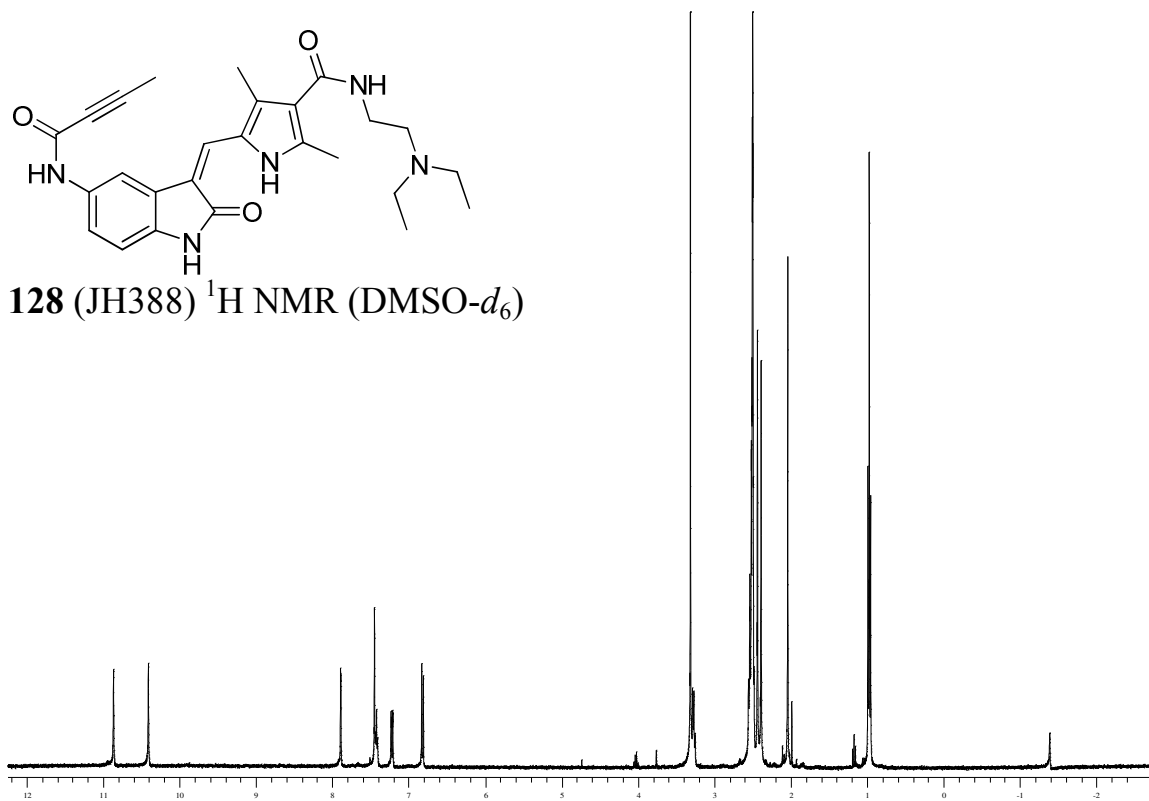


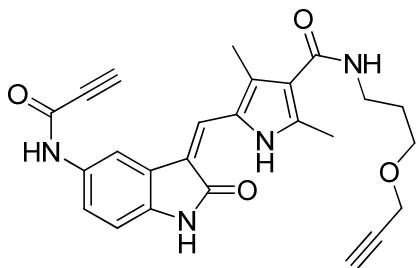


127 (JH232) ^1H NMR (DMSO- d_6)

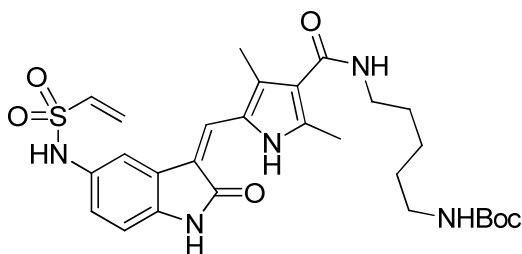
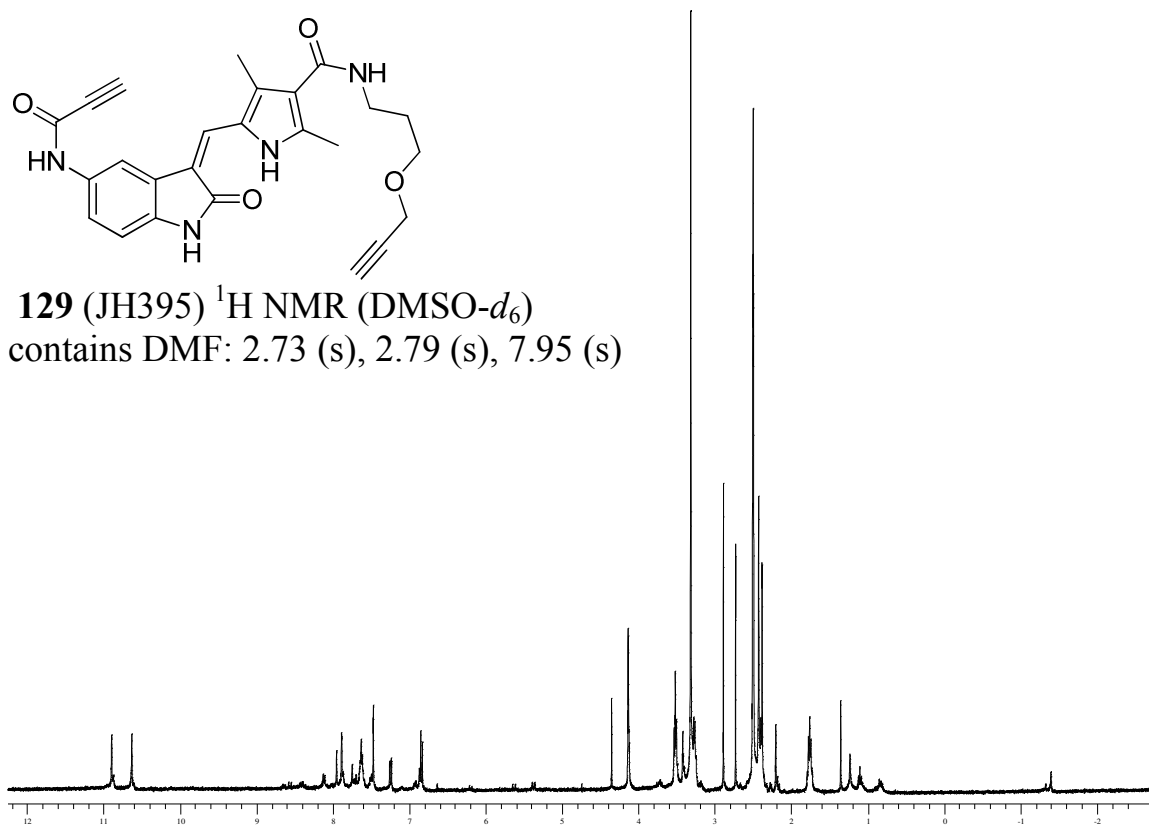


128 (JH388) ^1H NMR (DMSO- d_6)

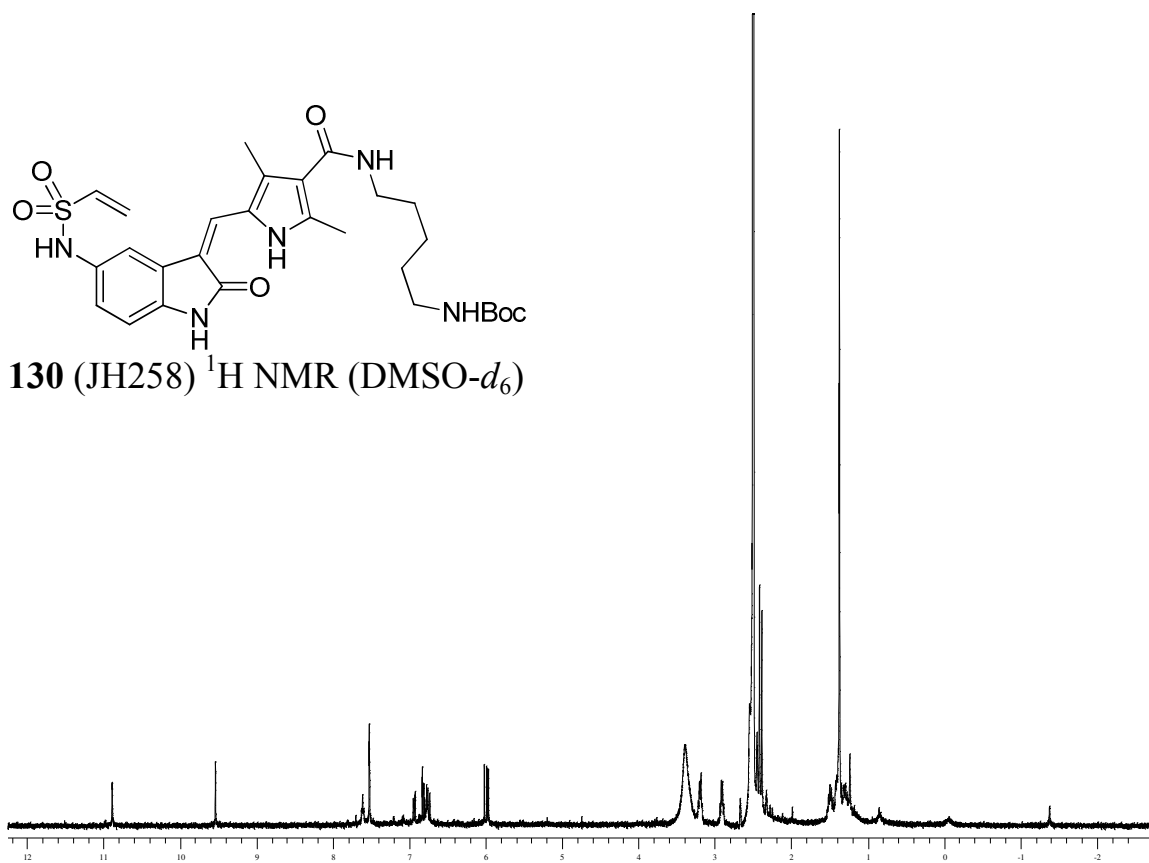


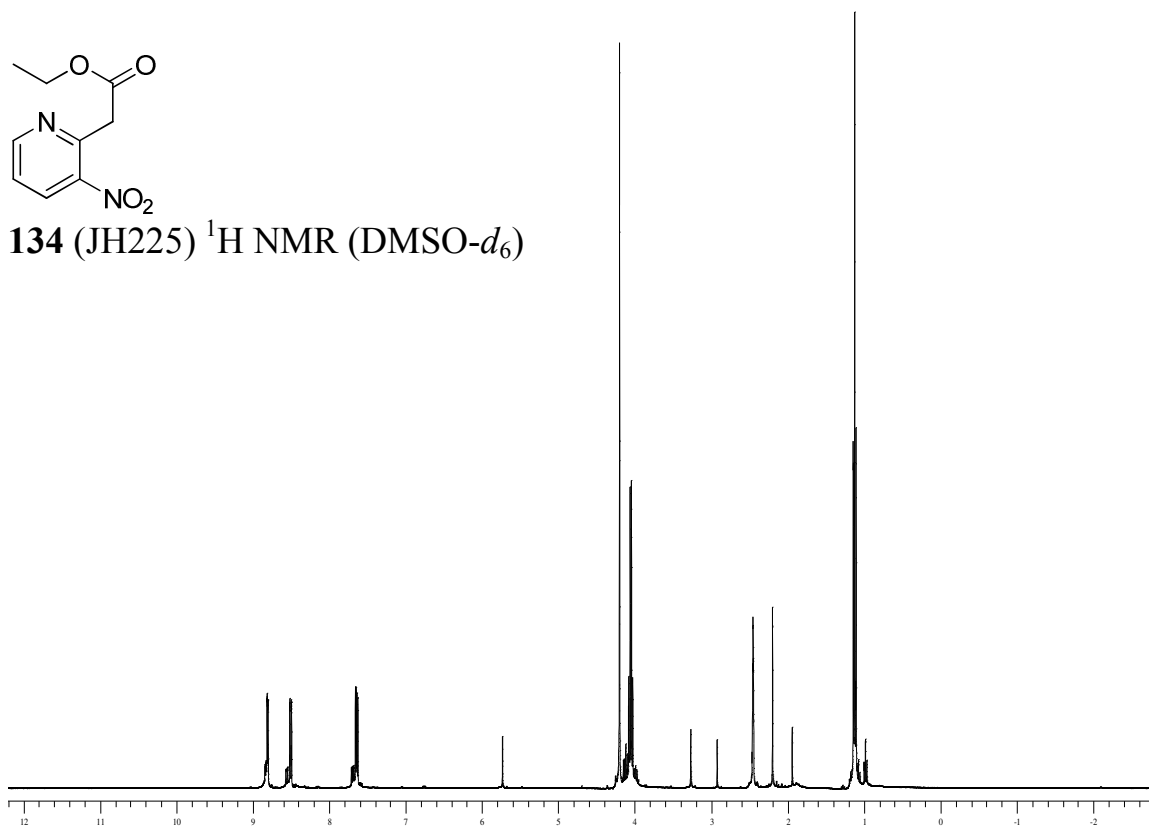
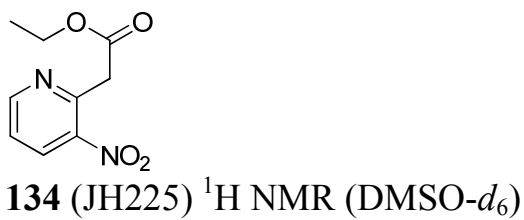
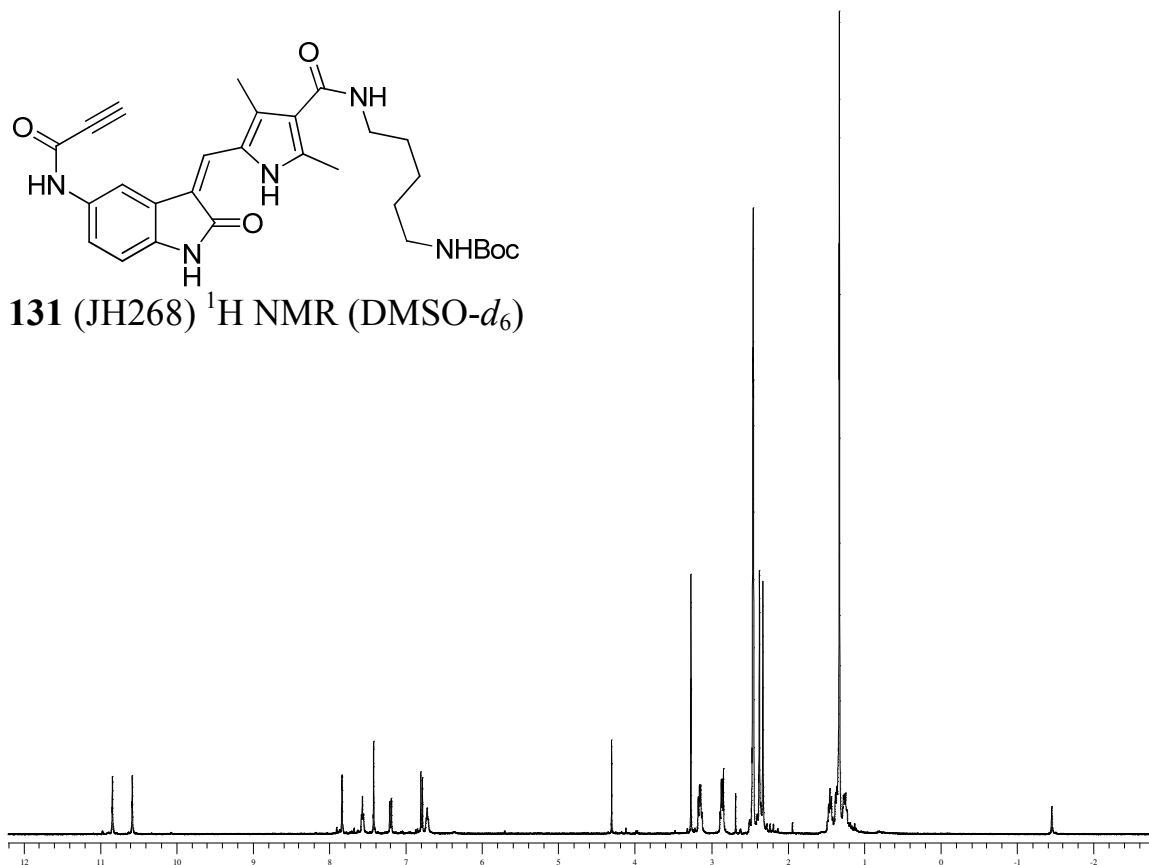
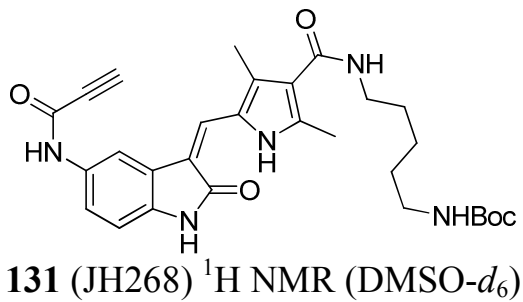


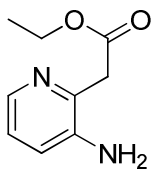
129 (JH395) ^1H NMR (DMSO- d_6)
contains DMF: 2.73 (s), 2.79 (s), 7.95 (s)



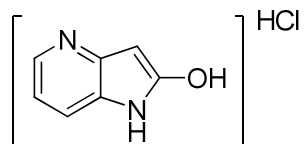
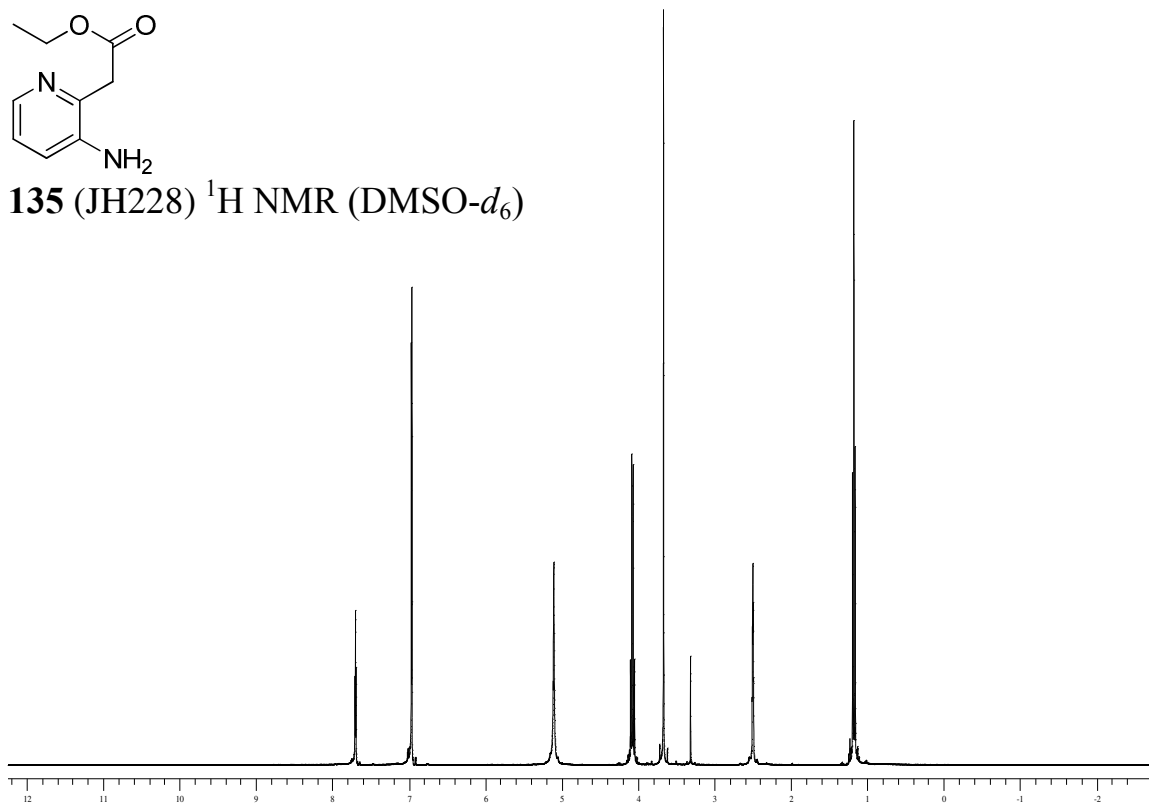
130 (JH258) ^1H NMR (DMSO- d_6)



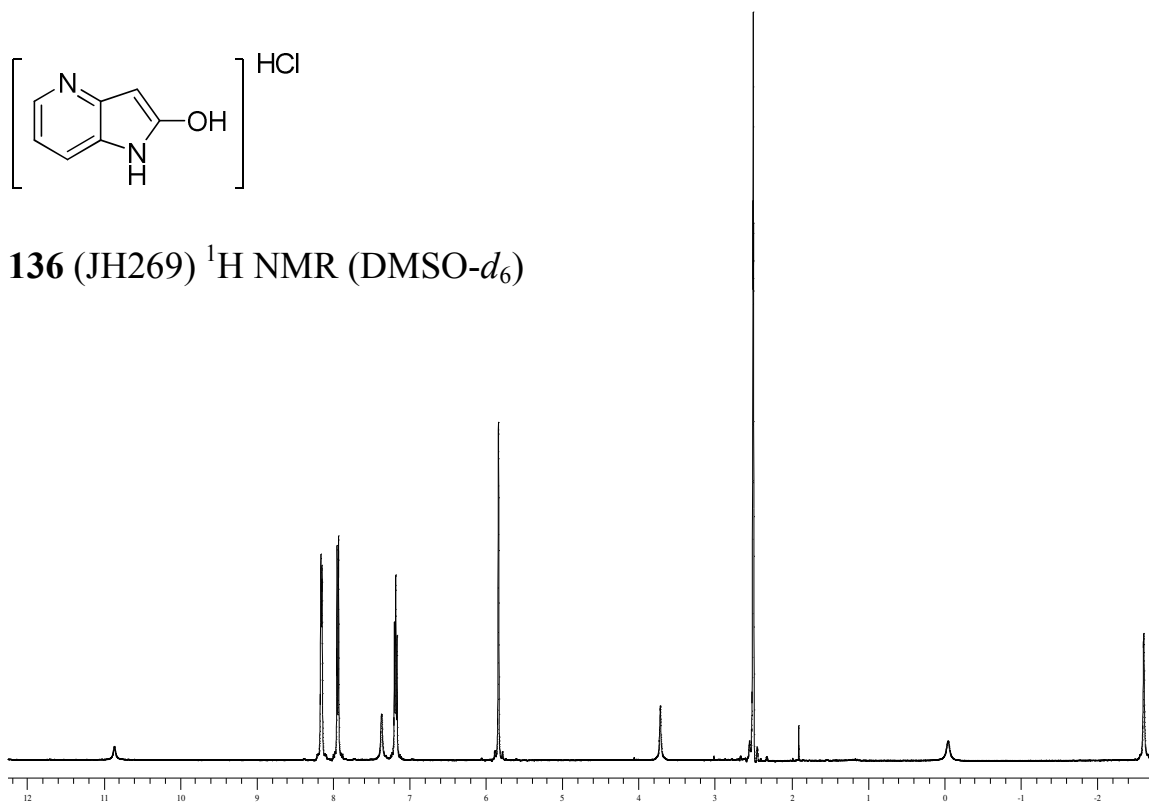


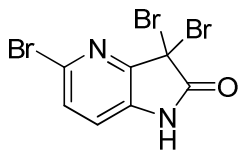


135 (JH228) ^1H NMR (DMSO- d_6)

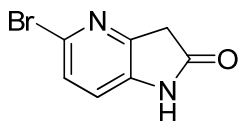
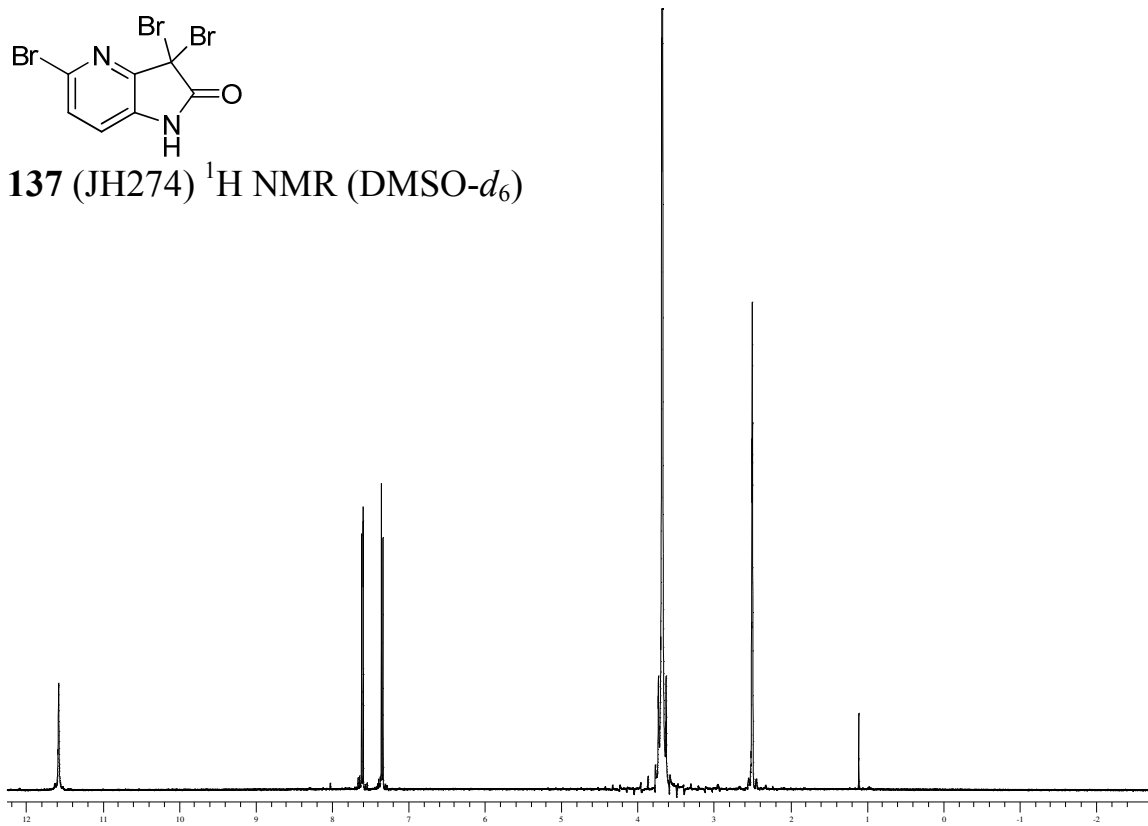


136 (JH269) ^1H NMR (DMSO- d_6)

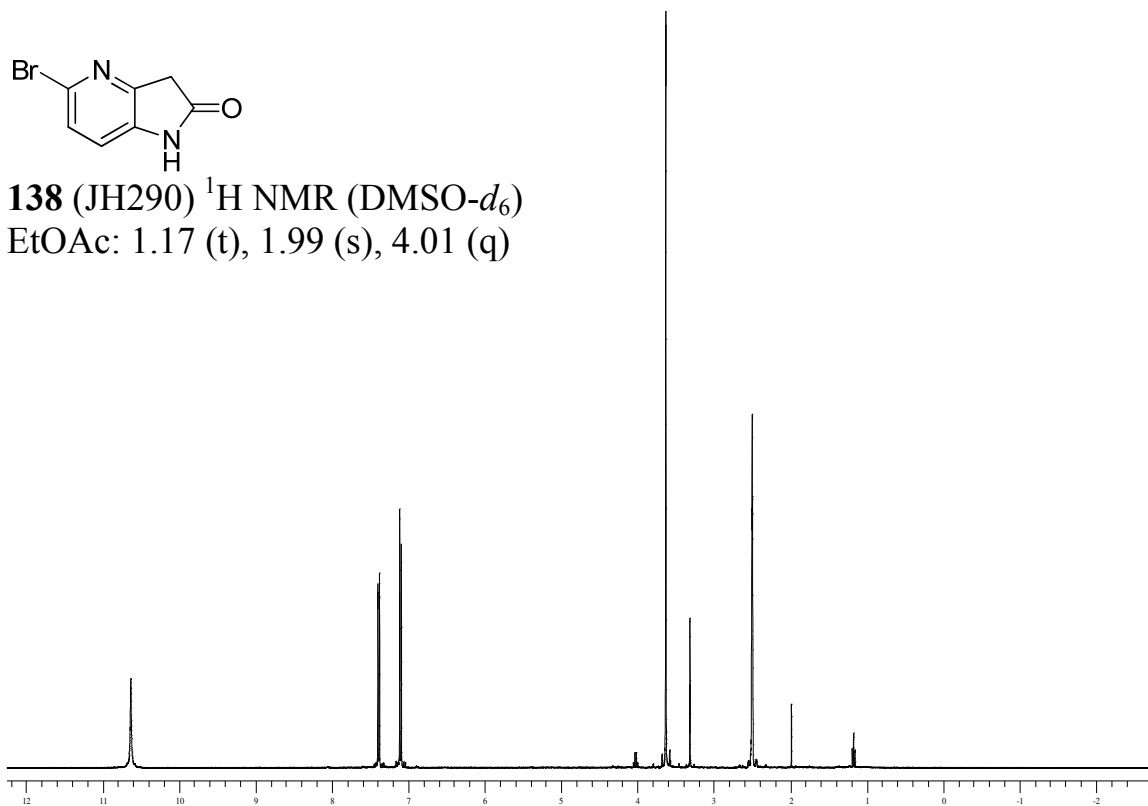


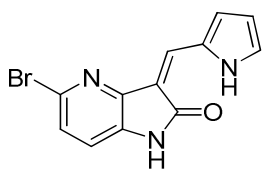


137 (JH274) ^1H NMR (DMSO- d_6)

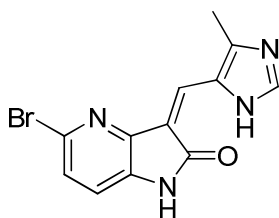
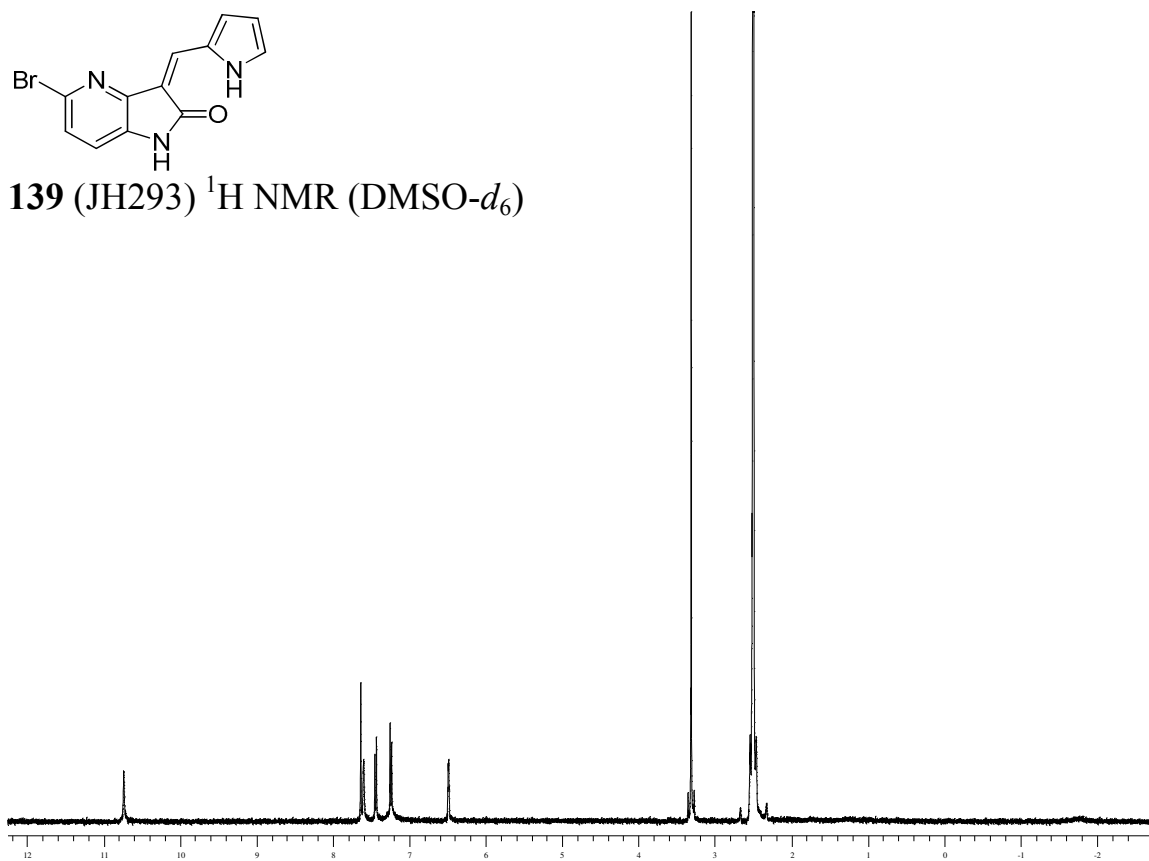


138 (JH290) ^1H NMR (DMSO- d_6)
EtOAc: 1.17 (t), 1.99 (s), 4.01 (q)

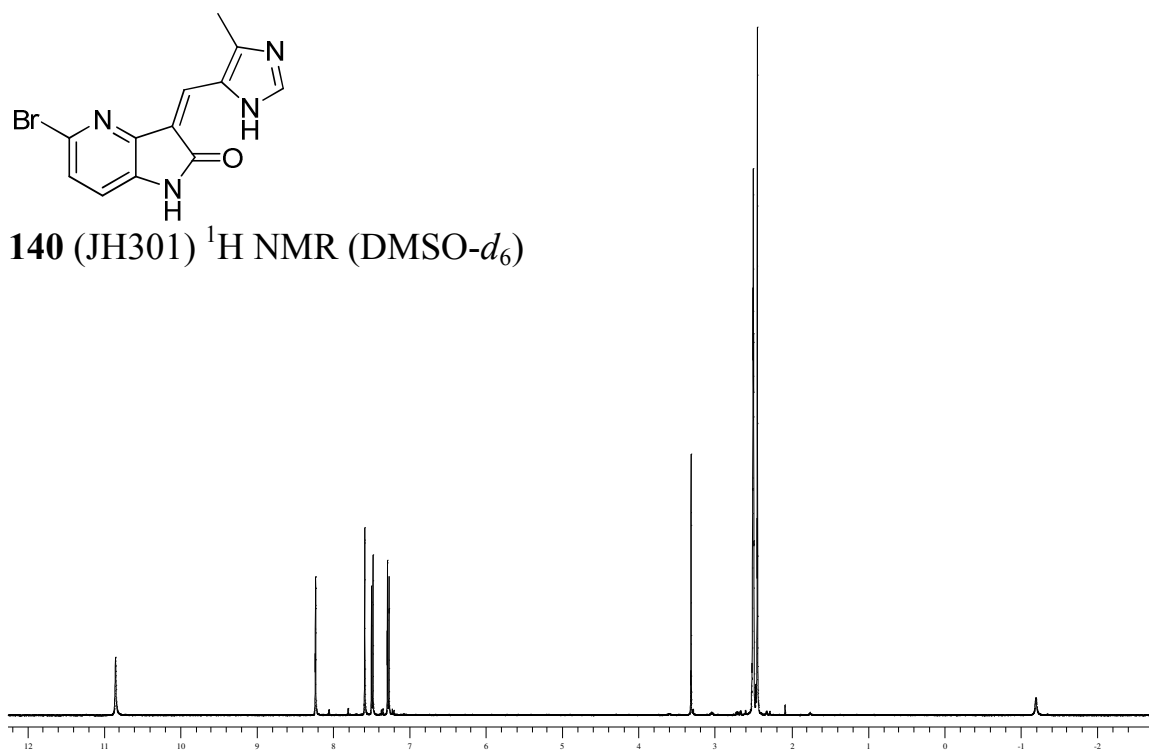


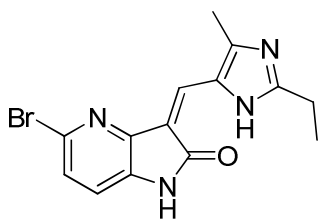


139 (JH293) ^1H NMR (DMSO- d_6)

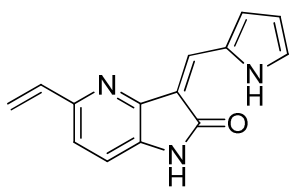
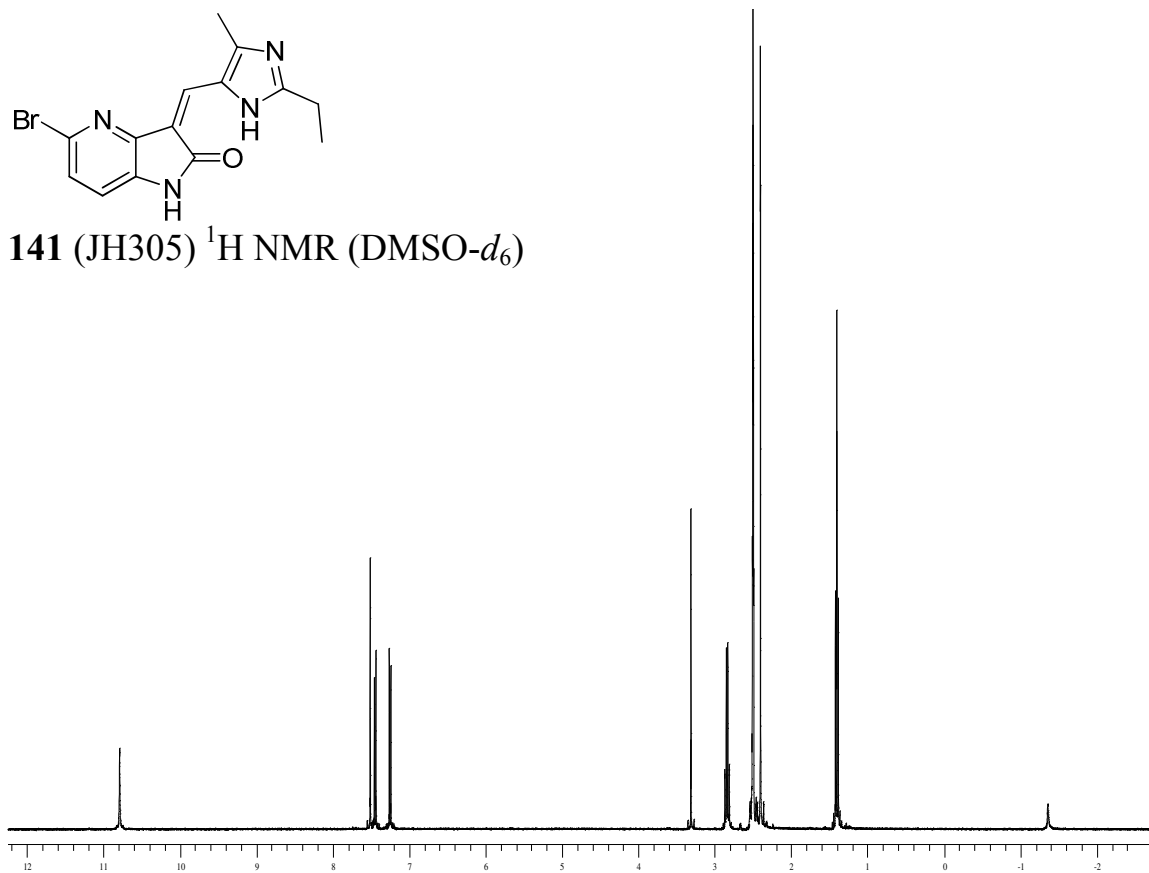


140 (JH301) ^1H NMR (DMSO- d_6)

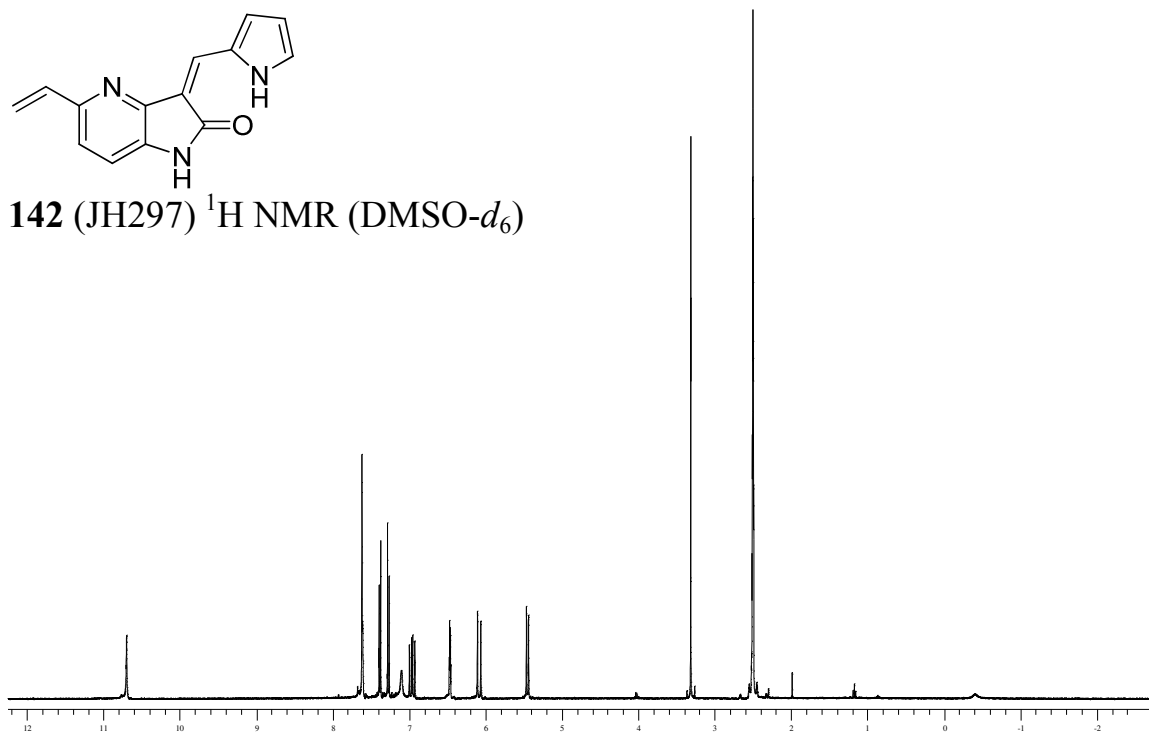


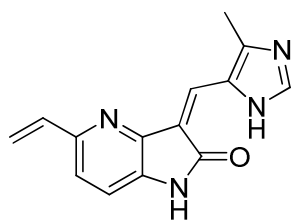


141 (JH305) ^1H NMR (DMSO- d_6)

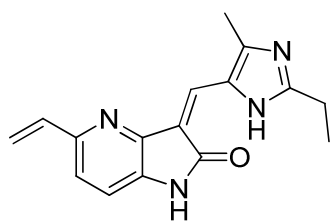
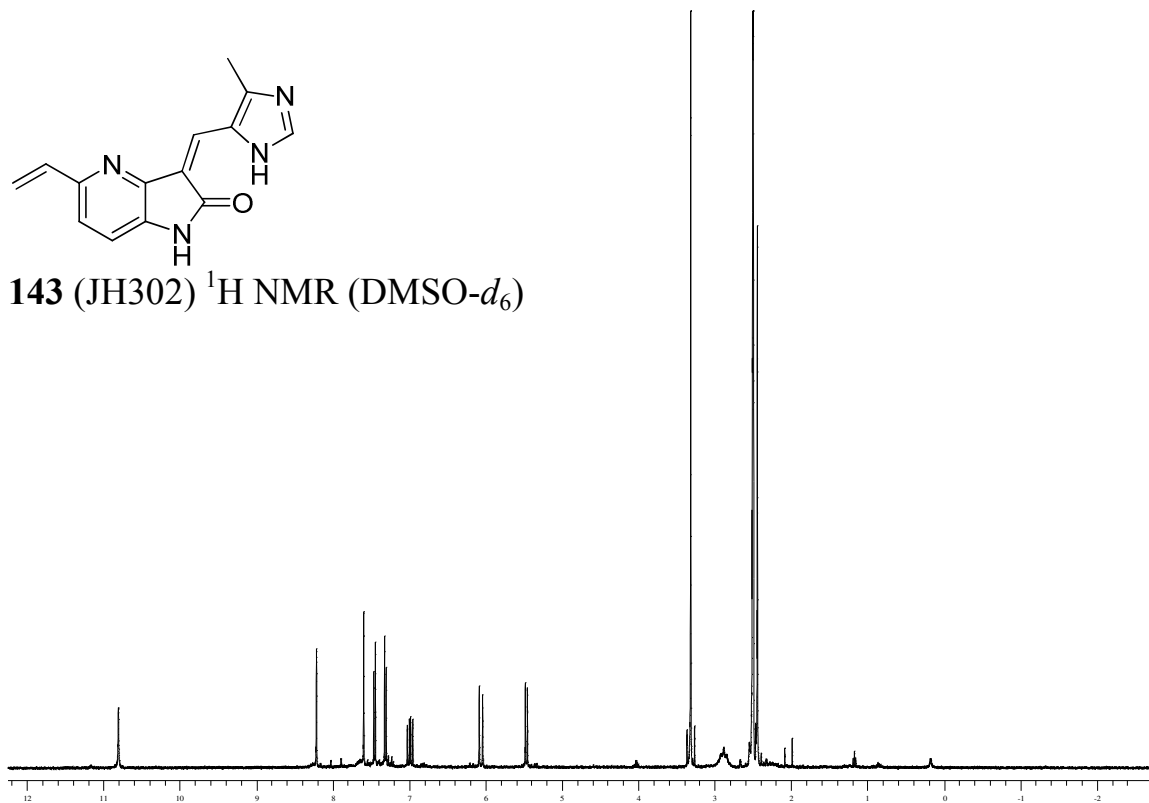


142 (JH297) ^1H NMR (DMSO- d_6)

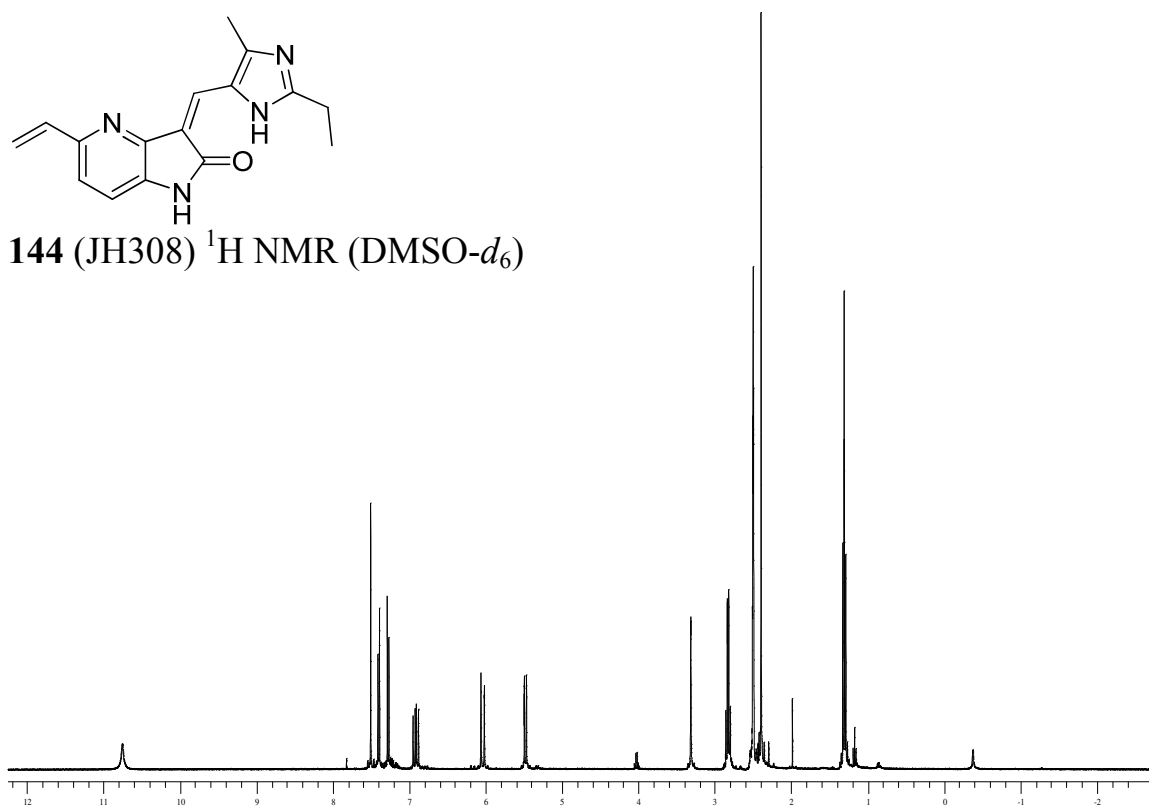




143 (JH302) ^1H NMR (DMSO- d_6)



144 (JH308) ^1H NMR (DMSO- d_6)



Appendix C

References

- (1) Hames, R. S.; Fry, A. M. Alternative splice variants of the human centrosome kinase Nek2 exhibit distinct patterns of expression in mitosis. *Biochem. J.* **2002**, *361*, 77–85.
- (2) Wu, W.; Baxter, J. E.; Wattam, S. L.; Hayward, D. G.; Fardilha, M.; Knebel, A.; Ford, E. F.; da Cruz e Silva, E. F.; Fry, A. M. Alternative splicing controls nuclear translocation of the cell cycle-regulated Nek2 kinase. *J. Biol. Chem.* **2007**, *282*, 26431–26440.
- (3) Hames, R. S.; Wattam, S. L.; Yamano, H.; Bacchieri, R.; Fry, A. M. APC/C-mediated destruction of the centrosomal kinase Nek2A occurs in early mitosis and depends upon a cyclin A-type D-box. *EMBO J.* **2001**, *20*, 7117–7127.
- (4) Eto, M.; Elliott, E.; Prickett, T. D.; Brautigan, D. L. Inhibitor-2 regulates protein phosphatase-1 complexed with NimA-related kinase to induce centrosome separation. *J. Biol. Chem.* **2002**, *277*, 44013–44020.
- (5) Mardin, B. R.; Lange, C.; Baxter, J. E.; Hardy, T.; Scholz, S. R.; Fry, A. M.; Schiebel, E. Components of the Hippo pathway cooperate with Nek2 kinase to regulate centrosome disjunction. *Nature Cell Biol.* **2010**, *12*, 1166–1176.
- (6) O'Regan, L.; Blot, J.; Fry, A. M. Mitotic regulation by NIMA-related kinases. *Cell Div.* **2007**, *2*, 25.
- (7) Bahe, S.; Stierhof, Y. D.; Wilkinson, C. J.; Leiss, F.; Nigg, E. A. Rootletin forms centriole-associated filaments and functions in centrosome cohesion. *J. Cell Biol.* **2005**, *171*, 27–33.
- (8) Fry, A. M.; Mayor, T.; Meraldi, P.; Stierhof, Y. D.; Tanaka, K.; Nigg, E. A. C-Nap1, a Novel centrosomal coiled-coil protein and candidate substrate of the cell cycle-regulated protein kinase Nek2. *J. Cell Biol.* **1998**, *141*, 1563–1574.

- (9) Draviam, V. M.; Stegmeier, F.; Nalepa, G.; Sowa, M. E.; Chen, J.; Liang, A.; Hannon, G. J.; Sorger, P. K.; Harper, J. W.; Elledge, S. J. A functional genomic screen identifies a role for TAO1 kinase in spindle-checkpoint signalling. *Nature Cell Biol.* **2007**, *9*, 556–564.
- (10) Liu, Q.; Hirohashi, Y.; Du, X.; Greene, M. I.; Wang, Q. Nek2 targets the mitotic checkpoint proteins Mad2 and Cdc20: A mechanism for aneuploidy in cancer. *Exp. Mol. Pathol.* **2010**, *88*, 225–233.
- (11) Du, J.; Cai, X.; Yao, J.; Ding, X.; Wu, Q.; Pei, S.; Jiang, K.; Zhang, Y.; Wang, W.; Shi, Y.; Lai, Y.; Shen, J.; Teng, M.; Huang, H.; Fei, Q.; Reddy, E. S.; Zhu, J.; Jin, C.; Yao, X. The mitotic checkpoint kinase Nek2A regulates kinetochore microtubule attachment stability. *Oncogene* **2008**, *27*, 4107–4114.
- (12) Fu, G.; Ding, X.; Yuan, K.; Aikhionbare, F.; Yao, J.; Cai, X.; Jiang, K.; Yao, X. Phosphorylation of human Sgo1 by NEK2A is essential for chromosome congression in mitosis. *Cell Res.* **2007**, *17*, 608–618.
- (13) Kokuryo, T.; Senga, T.; Yokoyama, Y.; Nagino, M.; Nimura, Y.; Hamaguchi, M. Nek2 as an effective target for inhibition of tumorigenic growth and peritoneal dissemination of cholangiocarcinoma. *Cancer Res.* **2007**, *67*, 9637–9642.
- (14) Tsunoda, N.; Kokuryo, T.; Oda, K.; Senga, T.; Yokoyama, Y.; Nagino, M.; Nimura, Y.; Hamaguchi, M. Nek2 as a novel molecular target for the treatment of breast carcinoma. *Cancer Sci.* **2009**, *100*, 111–116.
- (15) Hayward, D. G.; Clarke, R. B.; Faragher, A. J.; Pillai, M. R.; Hagan, I. M.; Fry, A. M. The centrosomal kinase Nek2 displays elevated levels of protein expression in human breast cancer. *Cancer Res.* **2004**, *64*, 7370–7376.

- (16) Barbagallo, F.; Paronetto, M. P.; Franco, R.; Chieffi, P.; Dolci, S.; Fry, A. M.; Geremia, R.; Sette, C. Increased expression and nuclear localization of the centrosomal kinase Nek2 in human testicular seminomas. *J. Pathol.* **2009**, *217*, 431–441.
- (17) Andréasson, U.; Dictor, M.; Jerkeman, M.; Berglund, M.; Sundström, C.; Linderöth, J.; Rosenquist, R.; Borrebaeck, C. A.; Ek, S. Identification of molecular targets associated with transformed diffuse large B cell lymphoma using highly purified tumor cells. *Am. J. Hematol.* **2009**, *84*, 803–808.
- (18) Zeng, X.; Shaikh, F. Y.; Harrison, M. K.; Adon, A. M.; Trimboli, A. J.; Carroll, K. A.; Sharma, N.; Timmers, C.; Chodosh, L. A.; Leone, G.; Saavedra, H. I. The Ras oncogene signals centrosome amplification in mammary epithelial cells through cyclin D1/Cdk4 and Nek2. *Oncogene* **2010**, *29*, 5103–5112.
- (19) Whelligan, D. K.; Solanki, S.; Taylor, D.; Thomson, D. W.; Cheung, K. M.; Boxall, K.; Mas-Droux, C.; Barillari, C.; Burns, S.; Grummitt, C. G.; Collins, I.; van Montfort, R. L.; Aherne, G. W.; Bayliss, R.; Hoelder, S. Aminopyrazine inhibitors binding to an unusual inactive conformation of the mitotic kinase Nek2: SAR and structural characterization. *J. Med. Chem.* **2010**, *53*, 7682–7698.
- (20) Emmitte, K. A.; Adjabeng, G. M.; Andrews, C. W.; Alberti, J. G.; Bambal, R.; Chamberlain, S. D.; Davis-Ward, R. G.; Dickson, H. D.; Hassler, D. F.; Hornberger, K. R.; Jackson, J. R.; Kuntz, K. W.; Lansing, T. J.; Mook, R. A. Jr.; Nailor, K. E.; Pobanz, M. A.; Smith, S. C.; Sung, C. M.; Cheung, M. Design of potent thiophene inhibitors of polo-like kinase 1 with improved solubility and reduced protein binding. *Bioorg. Med. Chem. Lett.* **2009**, *19*, 1694–1697.
- (21) Hayward, D. G.; Newbatt, Y.; Pickard, L.; Byrne, E.; Mao, G.; Burns, S.; Sahota, N. K.; Workman, P.; Collins, I.; Aherne, W.; Fry, A. M. Identification by high-

- throughput screening of viridian analogs as biochemical and cell-based inhibitors of the cell cycle-regulated Nek2 kinase. *J. Biomol. Screening* **2010**, *15*, 918–927.
- (22) Rellos, P.; Ivins, F. J.; Baxter, J. E.; Pike, A.; Nott, T. J.; Parkinson, D.-M.; Das, S.; Howell, S.; Fedorov, O.; Shen, Q. Y.; Fry, A. M.; Knapp, S.; Smerdon, S. J. Structure and regulation of the human Nek2 centrosomal kinase. *J. Biol. Chem.* **2006**, *282*, 6833–6842.
- (23) Cohen, M. S.; Zhang, C.; Shokat, K. M.; Taunton, J. Structural bioinformatics-based design of selective, irreversible kinase inhibitors. *Science* **2005**, *308*, 1318–1321.
- (24) Zhang, J.; Yang, P. L.; Gray, N. S. Targeting cancer with small molecule kinase inhibitors. *Nature Rev. Cancer* **2009**, *9*, 28–39.
- (25) Schirmer, A.; Kennedy, J.; Murli, S.; Reid, R.; Santi, D. V. Targeted covalent inactivation of protein kinases by resorcylic acid lactone polyketides. *PNAS* **2006**, *103*, 4234–4239.
- (26) Shen, Y.; Boivin, R.; Yoneda, N.; Du, H.; Schiller, S.; Matsushima, T.; Goto, M.; Shirota, H.; Gusovsky, F.; Lemelin, C.; Jiang, Y.; Zhang, Z.; Pelletier, R.; Ikemori-Kawada, M.; Kawakami, Y.; Inoue, A.; Schnaderbeck, M.; Wang, Y. Discovery of anti-inflammatory clinical candidate E6201, inspired from resorcylic lactone LL-Z1640-2, III. *Bioorg. Med. Chem. Lett.* **2010**, *20*, 3155–3157.
- (27) Honigberg, L. A.; Smith, A. M.; Sirisawad, M.; Verner, E.; Loury, D.; Chang, B.; Li, S.; Pan, Z.; Thamm, D. H.; Miller, R. A.; Buggy, J. J. The Bruton tyrosine kinase inhibitor PCI-32765 blocks B-cell activation and is efficacious in models of autoimmune disease and B-cell malignancy. *PNAS* **2010**, *107*, 13075–13080.

- (28) Noble, M. E.; Endicott, J. A.; Johnson, L. N. Protein kinase inhibitors: insights into drug design from structure. *Science* **2004**, *303*, 1800–1805.
- (29) Bishop, A. C.; Ubersax, J. A.; Petsch, D. T.; Matheos, D. P.; Gray, N. S.; Blethrow, J.; Shimizu, E.; Tsien, J. Z.; Schultz, P. G.; Rose, M. D.; Wood, J. L.; Morgan, D. O.; Shokat, K. M. Chemical switch for inhibitor-sensitive alleles of any protein kinase. *Nature* **2000**, *407*, 395–401.
- (30) Tsou, H-R.; Mamuya, N.; Johnson, B. D.; Reich, M. F.; Gruber, B. C.; Ye, F.; Nilakantan, R.; Shen, R.; Discafani, C.; DeBlanc, R.; Davis, R.; Koehn, F. E.; Greenberger, L. M.; Wang, Y-F.; Wissner, A. 6-Substituted-4-(3-bromophenylamino)quinazolines as putative irreversible inhibitors of the epidermal growth factor receptor (EGFR) and human epidermal growth factor receptor (HER-2) tyrosine kinases with enhanced antitumor activity. *J. Med. Chem.* **2001**, *44*, 2719–2734.
- (31) Knight, Z. A.; Shokat, K. M. Features of selective kinase inhibitors. *Chem. Biol.*, **2005**, *12*, 621–637.
- (32) Hauf, S.; Cole, R. W.; LaTerra, S.; Zimmer, C.; Schnapp, G.; Walter, R.; Heckel, A.; van Meel, J.; Rieder, C. L.; Peters, J-M. The small molecule Hesperadin reveals a role for Aurora B in correcting kinetochore–microtubule attachment and in maintaining the spindle assembly checkpoint. *J. Cell Biol.* **2003**, *161*, 281–294.
- (33) Potapova, T. A.; Daum, J. R.; Pittman, B. D.; Hudson, J. R.; Jones, T. N.; Satinover, D. L.; Stukenberg, P. T.; Gorbsky, G. J. The reversibility of mitotic exit in vertebrate cells. *Nature* **2006**, *440*, 954–958.
- (34) Kapoor, T. M.; Mayer, T. U.; Coughlin, M. L.; Mitchison, T. J. Probing spindle assembly mechanisms with monastrol, a small molecule inhibitor of the mitotic kinesin, Eg5. *J. Cell Biol.* **2000**, *150*, 975–988.

- (35) Vassilev, L. T.; Tovar, C.; Chen, S.; Knezevic, D.; Zhao, X.; Sun, H.; Heimbrook, D. C.; Chen, L. Selective small-molecule inhibitor reveals critical mitotic functions of human Cdk1. *PNAS* **2006**, *103*, 10660–10665.
- (36) Kwiatkowski, N.; Jelluma, N.; Filippakopoulos, P.; Soundararajan, M.; Manak, M. S.; Kwon, M.; Choi, H. G.; Sim, T.; Deveraux, Q. L.; Rottmann, S.; Pellman, D.; Shah, J. V.; Kops, G. J.; Knapp, S.; Gray, N. S. Small-molecule kinase inhibitors provide insight into Mps1 cell cycle function. *Nat. Chem. Biol.* **2010**, *6*, 359–368.
- (37) Moshinsky, D. J.; Bellamacina, C. R.; Boisvert, D. C.; Huang, P.; Hui, T.; Jancarik, J.; Kim, S. H.; Rice, A. G. SU9516: biochemical analysis of Cdk inhibition and crystal structure in complex with Cdk2. *Biochem. Biophys. Res. Commun.* **2003**, *310*, 1026–1031.
- (38) Barr, F. A.; Silljé, H. H.; Nigg, E. A. Polo-like kinases and the orchestration of cell division. *Nat. Rev. Mol. Cell Biol.* **2004**, *5*, 429–441.
- (39) Peters, U.; Cherian, J.; Kim, J. H.; Kwok, B. H.; Kapoor, T. M. Probing cell-division phenotype space and Polo-like kinase function using small molecules. *Nature Chem. Biol.* **2006**, *2*, 618–626.
- (40) Faragher, A. J.; Fry, A. M. Nek2A kinase stimulates centrosome disjunction and is required for formation of bipolar mitotic spindles. *Mol. Biol. Cell* **2003**, *14*, 2876–2889.
- (41) Lou, Y.; Yao, J.; Zereshki, A.; Dou, Z.; Ahmed, K.; Wang, H.; Hu, J.; Wang, Y.; Yao, X. NEK2A interacts with MAD1 and possibly functions as a novel integrator of the spindle checkpoint signaling. *J. Biol. Chem.* **2004**, *279*, 20049–20057.

- (42) Tang, P. C.; Sun, Li.; McMahon, G.; Blake, R. A. 3-(Cyclohexanoheteroarylidenyl)-2-indolinone protein tyrosine kinase inhibitors. *US Patent* 6114371, **2000**.
- (43) Mintz, M. J.; Walling, C. t-Butyl hypochlorite. *Org. Syn. Coll.* **1969**, *49*, 9.
- (44) Dallinger, D.; Kappe C. O. Rapid preparation of the mitotic kinesin Eg5 inhibitor monastrol using controlled microwave-assisted synthesis. *Nature Protoc.* **2007**, *2*, 317–321.
- (45) Chen, S.; Chen, L.; Le, N. T.; Zhao, C.; Sidduri, A.; Lou, J. P.; Michoud, C.; Portland, L.; Jackson, N.; Liu, J-J.; Konzelmann, F.; Chi, F.; Tovar, C.; Xiang, Q.; Chen, Y.; Wen, Y.; Vassilev, L. T. Synthesis and activity of quinolinyl-methylene-thiazolinones as potent and selective cyclin-dependent kinase 1 inhibitors. *Bioorg. Med. Chem. Lett.* **2007**, *17*, 2134–2138.
- (46) Tang, P. C.; Su, Y.; LI, Y.; Zhang, L.; Zhao, F.; Yang, J.; Zhou, Y.; Bie, P.; Qian, G.; Ju, M. Pyrrolo-nitrogenous heterocyclic derivatives, the preparation and the pharmaceutical use thereof. *International Patent* WO20081383232, **2008**.
- (47) Truce, W. E. The Preparation of fluoroacetyl chloride. *J. Am. Chem. Soc.* **1948**, *70*, 2828–2828.
- (48) Snow, R. A.; Cotrell, D. M.; Paquette, L. A. Demonstration and analysis of bridging regioselectivity operative during di- π -methane photorearrangement of ortho-substituted benzonorbornadines and *anti*-7,8-benzotricyclo[4.2.2.0^{2,5}]deca-3,7,9-trienes. *J. Am. Chem. Soc.* **1977**, *99*, 3734–3744.
- (49) Luk, K-C.; Mahaney, P. E.; Mischke, S. G. 4-and 5-Alkynyloxindoles and 4-and 5-alkenyloxindoles. *US Patent* 6313310, **2001**.
- (50) Sun, L.; Liang, C.; Shirazian, S.; Zhou, Y.; Miller, T.; Cui, J.; Fukuda, J. Y.; Chu J. Y.; Nematalla, A.; Wang, X.; Chen, H.; Sistla, A.; Luu, T. C.; Tang, F.; Wei, J.; Tang, C.

- Discovery of 5-[5-fluoro-2-oxo-1,2-dihydroindol-(3Z)-ylidenemethyl]-2,4-dimethyl-1H-pyrrole-3-carboxylic acid (2-diethylaminoethyl)amide, a novel tyrosine kinase inhibitor targeting vascular endothelial and platelet-derived growth factor receptor tyrosine kinase. *J. Med. Chem.* **2003** *46*, 1116–1119.
- (51) Manley, J. M.; Kalman, M. J.; Conway, B. G.; Ball, C. C.; Havens, J. L.; Vaidyanathan, R. Early Amidation Approach to 3-[(4-Amido)pyrrol-2-yl]-2-indolinones. *J. Org. Chem.* **2003**, *68*, 6447–6450.
- (52) Höfgen, N.; Kuss, H.; Olbrich, M.; Egerland, U.; Rundfeldt, C.; Steinike, K.; Schindler, R. 7-Azaindoles and the use thereof as therapeutic agents. *International Patent* WO9611929, **2007**.
- (53) Wood, E. R.; Kuyper, L.; Petrov, K. G.; Hunter, R. N. 3rd; Harris, P. A.; Lackey, K. Discovery and in vitro evaluation of potent TrkA kinase inhibitors: oxindole and aza-oxindoles. *Bioorg. Med. Chem. Lett.* **2004**, *14*, 953–957.
- (54) Dermatakis, A.; Luk, K. C.; DePinto, W.; Synthesis of potent oxindole Cdk2 inhibitors. *Bioorg. Med. Chem.* **2003**, *11*, 1873–1881.
- (55) Luk, K. C.; Simcox, M. E.; Schutt, A.; Rowan, K.; Thompson, T.; Chen, Y.; Kammlott, U.; DePinto, W.; Dunten, P.; Dermatakis, A. A new series of potent oxindole inhibitors of Cck2. *Bioorg. Med. Chem. Lett.* **2004**, *14*, 913–917.
- (56) Kitz, R.; Wilson, B. Esters of methanesulfonic acid as irreversible inhibitors of acetylcholinesterase. *J. Biol. Chem.* **1962**, *237*, 3245–3249.
- (57) Speers, A. E.; Cravatt, B. F. Profiling enzyme activities in vivo using click chemistry methods. *Chem. Biol.* **2004**, *11*, 535–546.
- (58) Zahedi, R. P.; Lewandrowski, U.; Wiesner, J.; Wortelkamp, S.; Moebius, J.; Schütz C.; Walter, U.; Gambaryan, S.; Sickmann, A. Phosphoproteome of resting human platelets. *J. Proteome. Res.* **2008**, *7*, 526–534.

- (59) Daub, H.; Olsen, J. V.; Bairlein, M.; Gnad, F.; Oppermann, F. S.; Körner, R.; Greff, Z.; Kéri, G.; Stemmann, O.; Mann, M. Kinase-selective enrichment enables quantitative phosphoproteomics of the kinome across the cell cycle. *Mol. Cell.* **2008**, *31*, 438–448.
- (60) Barouch-Bentov, R.; Che, J.; Lee, C. C.; Yang, Y.; Herman, A.; Jia, Y.; Velentza, A.; Watson, J.; Sternberg, L.; Kim, S.; Ziaee, N.; Miller, A.; Jackson, C.; Fujimoto, M.; Young, M.; Batalov, S.; Liu, Y.; Warmuth, M.; Wiltshire, T.; Cooke, MP.; Sauer, K. A conserved salt bridge in the G loop of multiple protein kinases is important for catalysis and for in vivo Lyn function. *Mol. Cell.* **2009**, *33*, 43–52.
- (61) Martin, M. W.; Newcomb, J.; Nunes, J. J.; Bemis, J. E.; McGowan, D. C.; White, R. D.; Buchanan, J. L.; DiMauro, E. F.; Boucher, C.; Faust, T.; Hsieh, F.; Huang, X.; Lee, J. H.; Schneider, S.; Turci, S. M.; Zhu, X. Discovery of novel 2,3-diarylfuro[2,3-b]pyridin-4-amines as potent and selective inhibitors of Lck: synthesis, SAR, and pharmacokinetic properties. *Bioorg. Med. Chem. Lett.* **2007**, *17*, 2299–22304.
- (62) Buzko, O.; Shokat, K. M. A kinase sequence database: sequence alignments and family assignment. *Bioinformatics* **2002**, *18*, 1274–1275.
- (63) Oppermann, F. S.; Gnad, F.; Olsen, J. V.; Hornberger, R.; Greff, Z.; Kéri, G.; Mann, M.; Daub, H. Large-scale proteomics analysis of the human kinome. *Mol. Cell Proteomics.* **2009**, *8*, 1751–1764.
- (64) Chen, R. Q.; Yang, Q. K.; Lu, B. W.; Yi, W.; Cantin, G.; Chen, Y. L.; Fearn, C.; Yates, J. R. 3rd; Lee, J. D. C25B mediates rapamycin-induced oncogenic responses in cancer cells. *Cancer Res.* **2009**, *69*, 2663–2668.
- (65) Göransson, O.; Deak, M.; Wullschleger, S.; Morrice, N. A.; Prescott, A. R.; Alessi, D. R. Regulation of the polarity kinases PAR-1/MARK by 14-3-3 interaction and phosphorylation. *J. Cell Sci.* **2006**, *119*, 4059–4070.

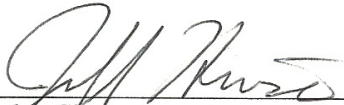
- (66) Seidler, J.; Adal, M.; Kübler, D.; Bossemeyer, D.; Lehmann, W. D.; Analysis of autophosphorylation sites in the recombinant catalytic subunit alpha of cAMP-dependent kinase by nano-UPLC-ESI-MS/MS. *Anal. Bioanal. Chem.* **2009**, *395*, 1713–1720.
- (67) Baljuls, A.; Schmitz, W.; Mueller, T.; Zahedi, R. P.; Sickmann, A.; Hekman, M.; Rapp, U. R. Positive regulation of A-Raf by phosphorylation of isoform-specific hinge segment and identification of novel phosphorylation sites. *J. Biol. Chem.* **2008**, *283*, 27239–27254.
- (68) Luo, W.; Slebos, R. J.; Hill, S.; Li, M.; Brábek, J.; Amanchy, R.; Chaerkady, R.; Pandey, A.; Ham, A. J.; Hanks, S. K. Global impact of oncogenic Src on a phosphotyrosine proteome. *J. Proteome. Res.* **2008**, *7*, 3447–3460.
- (69) Trinidad, J. C.; Thalhammer, A.; Specht, C. G.; Lynn, A. J.; Baker, P. R.; Schoepfer, R.; Burlingame, A. L. Quantitative analysis of synaptic phosphorylation and protein expression. *Mol. Cell Proteomics.* **2008**, *7*, 684–696.
- (70) Harrington, E. A.; Bebbington, D.; Moore, J.; Rasmussen, R. K.; Ajose-Adeogun, A. O.; Nakayama, T.; Graham, J. A.; Demur, C.; Hercend, T.; Diu-Hercend, A.; Su, M.; Golec, J. M.; Miller, K. M. VX-680, a potent and selective small-molecule inhibitor of the Aurora kinases, suppresses tumor growth in vivo. *Nat Med.* **2004**, *10*, 262–267.
- (71) Burkard, M. E.; Randall, C. L.; Larochele, S.; Zhang, C.; Shokat, K. M.; Fisher, R. P.; Jallepalli, P. V. Chemical genetics reveals the requirement for Polo-like kinase 1 activity in positioning RhoA and triggering cytokinesis in human cells. *PNAS* **2007**, *104*, 4383–4388.
- (72) Girdler, F.; Gascoigne, K. E.; Evers, P. A.; Hartmuth, S.; Crafter, C.; Foote, K. M.; Keen, N. J.; Taylor, S. S. Validating Aurora B as an anti-cancer drug target. *J. Cell Sci.* **2006**, *119*, 3664–3675.

- (73) Sebastiano, R.; Citterio, A.; Lapadula, M.; Righetti, P. G. A new deuterated alkylating agent for quantitative proteomics. *Rapid. Commun. Mass Spectrom.* **2003**, *17*, 2380–2386.
- (74) Mandell, D. J.; Chorny, I.; Groban, E. S.; Wong, S. E.; Levine, E.; Rapp, C. S.; Jacobson M. P. Strengths of hydrogen bonds involving phosphorylated amino acid side chains. *J. Am. Chem. Soc.* **2007**, *129*, 820–827.

Publishing Agreement

It is the policy of the University to encourage the distribution of all theses and dissertations. Copies of all UCSF theses and dissertations will be routed to the library via the Graduate Division. The library will make all theses and dissertations accessible to the public and will preserve these to the best of their abilities, in perpetuity.

I hereby grant permission to the Graduate Division of the University of California, San Francisco to release copies of my thesis or dissertation to the Campus Library to provide access and preservation, in whole or in part, in perpetuity.



Author Signature

1/11/2011
Date